# USER MANUAL

**(2nd Edition)**

**for a**

**THREE-DIMENSIONAL FINITE ELEMENT PROGRAM**

# UT3PC

**A Fundamental Approach to Design of**

**COAL MINE ENTRIES, BARRIER PILLARS, BLEEDER ENTRIES,**

**INTERPANEL BARRIER PILLARS,**

**PILLARS and ROOMS in ROOM and PILLAR MINES,**

**SHAFTS and TUNNELS**

**With Provision for Joint Effects**

William G. Pariseau
Emeritus Professor of Mining Engineering
University of Utah

April, 2023

CONTENTS

**USER-FRIENDLY THREE-DIMENSIONAL FINITE ELEMENT PROGRAMS for ANALYSIS OF COAL MINE ENTRIES, BARRIER PILLARS, BLEEDER ENTRIES, INTERPANEL BARRIER PILLARS, PILLARS in ROOM and PILLAR MINES, SHAFTS, and TUNNELS**


SUMMARY

This manual describes the steps necessary to implement three-dimensional finite element analyses of problems that are important to underground mine ground control including:

(1) main entry, crosscut and pillar geometry for safety,
(2) barrier pillar widths for safety of main entries,
(3) bleeder entry safety during longwall panel mining,
(4) interpanel barrier pillar safety,
(5) pillar and room safety in room and pillar mines,
(6) shafts (including winzes and raises)
(7) tunnels (including adits, drifts and crosscuts).

These problems are common to all mining in strata-bound deposits. Thus, "coal" is also a proxy for softrock mining of salt, potash and trona and for hardrock mining for lead, zinc and copper and other minerals in strata-form deposits such as limestone. Shafts and "tunnels" are life-lines to the underground and are applicable to softrock and hardrock mines alike.

The approach is for beginners in numerical modeling, allthough experienced numerical modelers may also find the software to be helpful in evaluting the listed seven design problems.

A validated, executable finite element program that takes into account stratigraphy and strata properties is used to compute resultant stress, strain and displacement fields associated with the mining geometry and premining stress field. Input data files are generated automatically with the aid of a mesh generator that produces numerically integrated "brick" elements. Up to one million nodes and elements in a mesh are allowed. The finite element program is **UT3PC**.

The mesh generator requires a **material property file**. This file includes strata type, elastic moduli, strengths, thicknesses and depths. This file is the only input file required of a user. Mining geometry of the five problems addressed is variable and defined interactively during mesh generation. Number of entries, widths of entries and crosscuts, widths and lengths of pillars, barrier pillar width and panel width according to the problem selected are required during mesh generation. Mining is always assumed to be full seam height. Consequently pillars are full seam height. However, provision is made for leaving top coal/ore and bottom coal/ore when pillars are not full seam height. Effects of caved ground or "gob" may be included. A discussion of gob models is given in APPENDIX III. Details of the mechanics of jointed rock and the procedure for generating equivalent properties of jointed rock are given in APPENDIX VII. Examples of effects of **joints** on each of the seven problem types are given in APPENDIX VIII and APPENDIX IX. An example problem from start to finish is given in APPENDIX X.

The distribution of element safety factors is also computed in conjunction with an elastic-plastic material model using associated rules of flow and a nonlinear, anisotropic failure criterion appropriate for each stratum in the geologic column. Observation of extent of yielding ground informs judgment concerning the overall suitability of a proposed layout and summarizes much of the practical design guidance obtained in an analysis. Run times vary with problem size and equation solver, but are expected to be several hours and perhaps overnight depending on problem type and size. In this regard, a one million element limit is implied, but there is some tolerance as an example problem shows.

Brief reviews of fundamentals and the finite element approach to solving equations in solid mechanics are presented. Mesh generation and related variables are described in detail. All necessary files for a finite element analysis are available following mesh generation. A short runstream file is then all that is needed to launch a finite element analysis. Although largely self-explanatory, each line of a typical runstream file is described in detail. Examples illustrate application to the seven types of problems addressed.

There are just three steps to doing an analysis using UT3PC:
**(1)** preparation of files describing strata properties at the considered mine site,
**(2)** generation (interactively) of a finite element mesh for the site and problem at hand,
**(3)** launching the finite element program UT3PC.
However, if joint effects are included, then an additional *Step 1j* is required to generate equivalent elastic moduli and strengths ( APPENDIX VII and APPENDIX VIII).

Mesh generation programs and UT3PC are in executable (binary) form intended for 64-bit operating systems. Post-processing output is another matter. Those familiar with numerical modeling may wish to go directly to the first step (site stratigraphy) in using UT3PC.

## BACKGROUND REVIEW

The fundamental equations of interest to strata mechanics are stress equations of equilibrium, strain displacement equations, and stress - strain equations. These equations arise from considerations of physical laws, kinematics and material laws. The finite element equations as such are derived from an application of the principle of virtual work after establishing an interpolation scheme for a single, representative finite element.

**Stress**. The stress equations of equilibrium are

$$\begin{aligned} \frac{\partial \sigma_{xx}}{\partial x} + \frac{\partial \tau_{yx}}{\partial y} + \frac{\partial \tau_{zx}}{\partial z} + \gamma_x = 0 \\ \frac{\partial \tau_{xy}}{\partial x} + \frac{\partial \sigma_{yy}}{\partial y} + \frac{\partial \tau_{zy}}{\partial z} + \gamma_y = 0 \\ \frac{\partial \tau_{xz}}{\partial x} + \frac{\partial \tau_{yz}}{\partial y} + \frac{\partial \sigma_{zz}}{\partial z} + \gamma_z = 0 \end{aligned} \qquad (1)$$

where $\sigma$, $\tau$ and $\gamma$ are normal stress, shear stress, and specific weight, respectively. The order of subscripts on the shear stresses is not important, that is, $\tau_{xy} = \tau_{yx}$ and so on. If inertia forces are important then acceleration terms appear on the right hand side of (1), which is to say, the finite element method is not restricted to static problems. Wave propagation dynamics are certainly within the realm of finite element analysis. However, UT3PC is a static code.

**Strain-Displacement**. The strain-displacement equations for "small" strains are

$$\begin{aligned} &\varepsilon_{xx} = \partial u / \partial x, \ \varepsilon_{yy} = \partial v / \partial y, \ \varepsilon_{zz} = \partial w / \partial z \\ &\gamma_{xy} = \partial u / \partial y + \partial v / \partial x, \ \gamma_{yz} = \partial v / \partial z + \partial w / \partial y, \ \gamma_{zx} = \partial w / \partial x + \partial u / \partial z \end{aligned} \tag{2}$$

where engineering shear strains are defined and the order of subscripts is not important, for example, $\gamma_{xy} = \gamma_{yx}$.

**Stress Strain Relations.** Most rocks and soils respond elastically to an initial application of load, but the range of a purely elastic response is limited by strength of material. Indeed, strength of a material may be defined as the state of stress at the elastic limit. Loadingl beyond the elastic limit induces yielding fracture or by flow or by a combination of both micro-mechanisms. The result in any case is plastic deformation. If flow or ductility is dominant, strain hardening may occur with an increase in the yield point (strength) with further strain as illustrated in Figure 1. If fracture dominates, then strain softening is likely with a decrease in the yield point (strength) with further strain. If neither strain hardening nor softening occurs, then the material response is ideally plastic. In a uniaxial compression test, the stress strain plot rises, remains flat or falls in case of work hardening, ideally plastic or in strain softening, respectively. In three dimensional analyses, an elastic zone generally contains yielding zones and thus constrains plastic components of strain to be of the same magnitude as the elastic part of strain. The total strain is still "small" or "infinitesimal". In this regard, many materials fail in uniaxial stress at 0.1% to 1.0% strain. Squares of these strains are $10^{-6}$ and $10^{-4}$, respectively. These failure strains could thus be considered "small". This observation is important because many finite element programs are based on the "small" strain assumption regarding material behavior and calculations containing squared terms can be neglected. "Large" or "finite" strain programs require much more elaborate solid mechanics. Fortunately, many important practical problems in strata mechanics including the five addressed here fall within the "small" strain domain of material behavior.

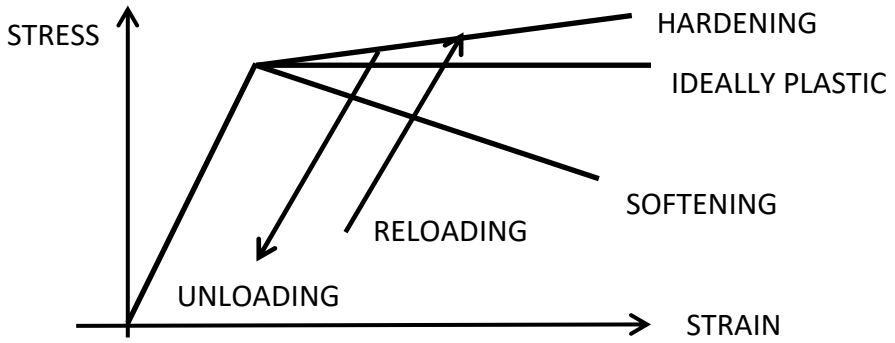


Figure 1 Idealized uniaxial stress-strain plots.

In the elastic range, the stress strain relations are a generalized Hooke's law, that is, the relations for an anisotropic material. In matrix form,

$$(3a)\qquad \begin{Bmatrix} \varepsilon_{xx} \\ \varepsilon_{yy} \\ \varepsilon_{zz} \\ \gamma_{yz} \\ \gamma_{zx} \\ \gamma_{xy} \end{Bmatrix} = \begin{bmatrix} a_{11} & a_{12} & a_{13} & a_{14} & a_{15} & a_{16} \\ & & .... & & & \\ a_{61} & a_{62} & a_{63} & a_{64} & a_{65} & a_{66} \end{bmatrix} \begin{Bmatrix} \sigma_{xx} \\ \sigma_{yy} \\ \sigma_{zz} \\ \tau_{yz} \\ \tau_{zx} \\ \tau_{xy} \end{Bmatrix}$$

In short form,

$$(3b)\qquad \{\varepsilon\} = [a]\{\sigma\} \text{ and } \{\sigma\} = [b]\{\varepsilon\}$$

where [*b*] is the inverse of [*a*]. The matrices [*a*] and [*b*] are symmetric, so there are at most 21 independent elastic constants in the most general case of anisotropy [9]. An *orthotropic* material has nine independent elastic constants. Rocks with flow structures are often orthotropic. A *transversely isotropic* material has five independent elastic constants. Rocks that have a distinct layering or foliation may be transversely isotropic. Rocks that lack directional features are *isotropic* and have just two independent elastic constants, for example, Young's modulus and Poisson's ratio or Young's modulus and a shear modulus. Other properties combinations are also possible in the isotropic case.

Hooke's law is only part of the stress strain relations needed to describe material behavior beyond the elastic limit. First, the elastic limit must be defined and then the computation of inelastic strains must be formulated. The elastic limit may be specified by a yield function or *failure criterion,* say, *F*, while the plastic part of strain may be computed using a *plastic potential Y*. Examples of failure criterion used in rock mechanics are the famous Mohr-Coulomb (MC) criterion, the popular Hoek-Brown (HB) criterion, and the well known Drucker-Prager (DP) criterion. Nonlinear forms of MC (n-type) and DP (N-type) are almost sure to be required for rock over an extended range of stress [10,11]. The subject of rock failure is a much discussed topic in the technical literature and is well beyond any detailed presentation here. However, some remarks are in order to complete the description of the stress strain relations beyond the elastic range.

If one neglects complications caused by time- and rate-dependencies, heterogeneity, temperature dependency and so on, then failure may be described by an implicit function *F*

$$(4a)\qquad F(\sigma_{xx},...,\tau_{xy},\varepsilon^{p}_{xx},...\gamma^{p}_{xy}) = 0 \text{ and if non-hardening or softening, then}$$

$$(4b)\qquad F(\sigma_{xx},...,\tau_{xy}) = 0 \text{ and if isotropic, then}$$

$$(4c)\qquad F(\sigma_1,\sigma_2,\sigma_3) = 0 \text{ in principal stress form,}$$

where superscript *p* indicates the plastic component of strain.
If isotropic and independent of the intermediate principal stress, then

(5) $F(\sigma_1, \sigma_3) = 0$ or $F(\sigma_m, \tau_m)$, that is, $\tau_m = f(\sigma_m)$
where $\sigma_m = (\sigma_1 + \sigma_3)/2$ and $\tau_m = (\sigma_1 - \sigma_3)/2$

In the linear case, one has MC, that is,

(6a) $\tau_m = \sigma_m \sin(\phi) + (c)\cos(\phi)$ or $\tau = \sigma \tan(\phi) + c$

where $\phi$ and $c$ are angle of internal friction and cohesion, respectively.

In the nonlinear case one has an n-type criterion

(6b) $(\tau_m)^n = \sigma_m \sin(\phi) + (c)\cos(\phi)$

where the exponent *n* defines the nonlinearity and is determined by experimental measurement.

When the intermediate principal stress effect is not negligible, then a nonlinear form of DP (N-type) may be used. In case of anisotropic strata, one has

(7) $J_2^{N/2} + I_1 - 1 = 0$

where
$J_2 = \{F(\sigma_{bb} - \sigma_{cc})^2 + G(\sigma_{cc} - \sigma_{aa})^2 + H(\sigma_{aa} - \sigma_{bb})^2 + L(\tau_{bc})^2 + M(\tau_{ca})^2 + N(\tau_{ab})^2\}$
and $I_1 = U\sigma_{aa} + V\sigma_{bb} + W\sigma_{cc}$

Here, the axis, *a,b,c* are the axes of anisotropy that may be skewed with respect to analysis coordinates *x,y,z*. The nine strength constants, *F, G,* etc., may be computed from unconfined compressive, tensile and shear strength test data, although adjustments to excavations scales may be necessary to account for geological features such as joints that are absent in laboratory test specimens.

Beyond the elastic limit, total strains are composed of an elastic and plastic part. Thus, in differential form

(8a) $\{d\varepsilon) = \{d\varepsilon^e\} + \{d\varepsilon^p\}$

The elastic part is given by Hooke's law; the plastic part is obtained from a plastic potential. Thus,

(8b) $\{d\varepsilon) = [a]\{d\sigma\} + \lambda\{\partial Y / \partial\sigma\}$

where the scalar function $\lambda$ is subsequently eliminated from consideration and where the assumption of perfect plasticity is made. Differentiation of the plastic potential $Y$ is with respect to each of the nine components of stress (neglecting symmetry of shear stress). The plastic part has a geometric interpretation. When the plastic potential is plotted in principal stress space, the plastic strain increment vector is parallel to the gradient of the plastic potential surface and is thus normal to this surface. After some algebra, the stress strain relations beyond the elastic limit are

(9) $$\{d\sigma\} = [E^e - E^p]\{d\varepsilon\}$$

where the $[E^e]$ is a matrix of elastic moduli and $[E^p]$ is a plastic "correction" that is nil below the elastic limit. In the case where the failure criterion and the plastic potential coincide, then the plasticity is "associated" and the plastic strain increments are obtained by "associated rules of flow" or "normality". The form (9), anisotropic or not, is the same in case of strain hardening [12] or softening and is needed for finite element calculations.

A local element factor concept defined as the ratio of strength to stress requires definitions of suitable measures of strengths and stress for analysis. Both arise in the context of stress – strain relations. Strength may be defined as stress at the elastic limit, so in case of the famous Mohr-Coulomb criterion (6a), one has

(9a) $$fs = \frac{\tau_m(strength)}{\tau_m(stress)}$$ which reduces to $fs = \frac{C_o}{\sigma_c}$ in unconfined compression and to $fs = \frac{T_o}{\sigma_t}$ in uniaxial tension where $C_o$ and $T_o$ are unconfined compressive and tensile strengths, respectively. In case of an N-type yield condition (7)

(9b) $$fs = \frac{J_2^{1/2}(strength)}{J_2^{1/2}(stress)}$$

that also reduces to the unconfined compression and tension cases.

## FINITE ELEMENT REVIEW IN BRIEF

The finite element method (FEM) is a numerical technique for solving differential equations. Development of the method occurred simultaneously with the development of digital computers beginning in the mid-1950's. Applications to ground control problems in mine engineering appeared in the mid-1960's. In this regard, origins of the finite element program UT3PC can be traced to the dissertations by Dahl [1] in application to mining and to Wilson [14] in civil engineering. FEM is an enormously popular numerical technique for solving differential equations described in many books, e.g., [2-8]. While the finite element method is a well understood numerical technique and has been in undergraduate engineering curricula for many years, a brief outline of the method is helpful in understanding FEM application to strata mechanics.

**Finite Element Concept** A finite element is simply a subdivision of the region of interest. Almost always an element is homogeneous. A triangle is a simple two-dimensional element that illustrates the concept. Consider the triangle in Figure 2. Vertices, corners or nodes, are numbered 1, 2, 3 and have the coordinates indicated.

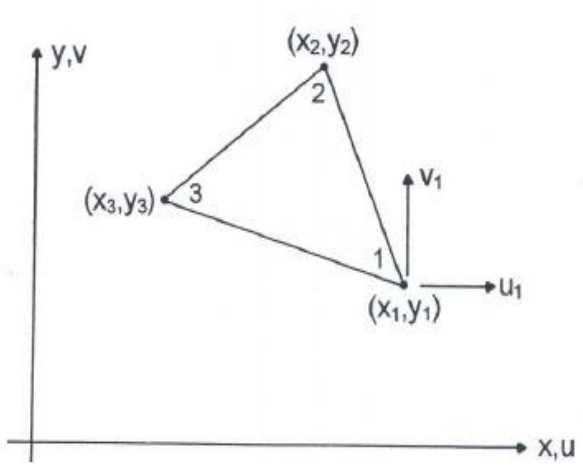


Figure 2 A plane triangular finite element.

Displacements in the x and y directions are u and v, respectively, and are considered known. Displacements in the interior are unknown but may be estimated by interpolation from the known displacements. A linear interpolation is the simplest. Thus,

(10) $u = a_o + a_1 x + a_2 y,\ v = b_o + b_1 x + b_2 y$

where *x* and *y* are coordinates of an interior point where the displacements are sought. The constants $a_o, a_1$, etc., must be known, of course. Also, the displacements given by (10) must agree with the known displacements at the nodes. Thus,

(11a)
$$u_1 = a_o + a_1 x_1 + a_2 y_1$$
$$u_2 = a_o + a_1 x_2 + a_2 y_2 \text{ or in matrix notation}$$
$$u_3 = a_o + a_1 x_3 + a_2 y_3$$

(11b)
$$\begin{Bmatrix} u_1 \\ u_2 \\ u_3 \end{Bmatrix} = \begin{bmatrix} 1 & x_1 & y_1 \\ 1 & x_2 & y_2 \\ 1 & x_3 & y_3 \end{bmatrix} \begin{Bmatrix} a_o \\ a_1 \\ a_2 \end{Bmatrix}$$

which can be solved for the desired constants and similarly for the *b's*. Inspection of (11) shows that the constants are given in terms of the node coordinates and displacements. When the solution for the constant terms is substituted back into (10), the result has the matrix form

(12) $$\begin{Bmatrix} u \\ v \end{Bmatrix} = [N]\{\delta\}$$

where $\{\delta\}$ is a column matrix (vector) of the known node displacements. The matrix $[N]$, a common notation, is thus an interpolation matrix for displacements. Elements of $[N]$ are linear functions $N(x, y)$ in this example.

Strains in the finite element method follow from the definition of strains in terms of displacement derivatives and the finite element approximation to displacements (12). The result has the form

$$(13) \qquad \begin{Bmatrix} \varepsilon_{xx} \\ \varepsilon_{yy} \\ \gamma_{xy} \end{Bmatrix} = \{\varepsilon\} = [B]\{\delta\}$$

where the elements of $[B]$ are derivatives of $[N]$ and the known displacements $\{\delta\}$are constant. The elements of $[B]$ are themselves constant, so *this triangle is a constant strain triangle*.

Stresses follow from strains via Hooke's law in the purely elastic case and via the elastic-plastic relationship (9) beyond the yield point. In compact incremental form

$$(14) \qquad \{\Delta\sigma\} = [E]\{\Delta\varepsilon\}$$

The increments in (14) are associated with increments of load from gravity and excavation in a problem of interest. These increments approximate the differentials in (9).

There are other types of triangles and other types of elements in two dimensions. If nodes are added to a triangle at midpoints along the sides of the triangle in Figure 2, then interpolation must be of degree two. Strains then vary linearly over the triangle. Quadrilateral elements are also possible with corner nodes and mid-side nodes. One very useful quadrilateral for analysis of plane (two dimensional) problems is one composed of four constant strain triangles. This element is a 4CST quadrilateral. In any event, one must consider an assemblage of many elements in a *mesh* for analyses of practical problems.

Three dimensional analogues of triangular and quadrilateral elements are tetrahedrons and rectangular parallelepipeds (brick shape). One could consider a tetrahedral analogue of the 4CST element by adding a center node to a tetrahedron and thus making it a composite of the internal tetrahedrons. However, the result is simply more tetrahedrons, unlike the 4CST result. One could also consider subdividing a brick shaped element into tetrahedrons as a quadrilateral is divided into four triangles to form the 4CST element. Interestingly, there are just two ways to divide a brick shaped element into five tetrahedrons; there are many ways of dividing a brick into more, say, six tetrahedrons.

Another interesting and important element type is an *isoparametric* element. This element involves a transformation from generic space to finite element space as illustrated in Figure 3.

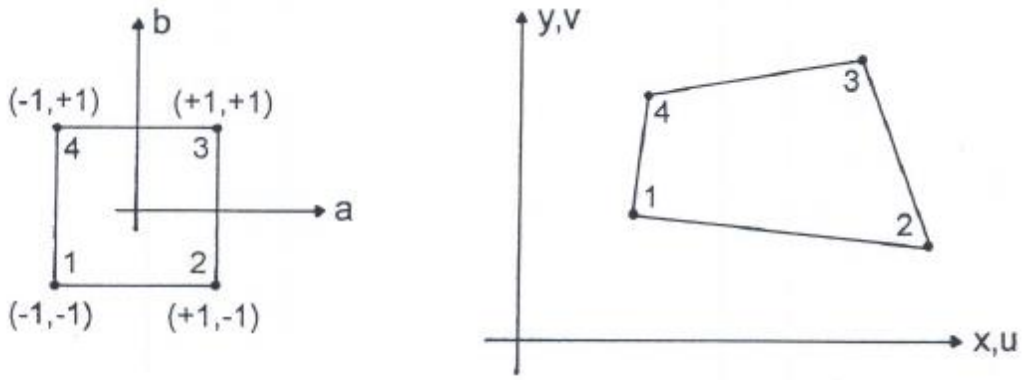


Figure 3 A square element in generic space (left) and a quadrilateral in analysis space (right)

Interpolation over the square element in generic space (*ab*) is done in a manner similar to interpolation of displacements over a triangular element. Thus,

(15a) $u = \alpha_o + \alpha_1 a + \alpha_2 b + \alpha_3 ab$

where *u* is the displacement component in the *a* direction and an *ab* term is added for the square (quadrilateral) element. After solving for the coefficients, the $\alpha$*'s*, displacements in the generic square element have the matrix form

(15b) $\begin{Bmatrix} u \\ v \end{Bmatrix} = [N(a,b)]\{\delta\}$

where $\{\delta\}$ is an 8x1 column matrix of displacements at the nodes of the square. A coordinate transformation between (*ab*) and (*xy*) is needed to connect the two elements in Figure 3. Symbolically, the transformation of coordinates is

(15c) $x = F(a,b),\ y = G(a,b),\ a = f(x,y),\ b = g(x,y).$

Coordinates in (*xy*) may be computed similarly to the way displacements are computed in (*ab*). Thus,

(15d) $x = S_1 x_1 + S_2 x_2 + S_3 x_3 + S_4 x_4,\ y = S_1 y_1 + S_2 y_2 + S_3 y_3 + S_4 y_4$

where $x_1$, $y_1$, etc., are coordinates of the element nodes in (*xy*). The functions $S_1, S_2, S_3, S_4$ are *shape* functions. When the interpolation and shape functions are the same, that is, when $N_1(a,b) = S_1(a,b)$, etc., , the element is an isoparametric element.

**Element Equilibrium** Element equilibrium is at the core of the finite element method. The most direct way of obtaining element equilibrium in finite element form is through the application of the principle of virtual work or more generally the divergence theorem. This theorem states that

the integral of the normal component of a vector over the surface of a body is equal to the integral of the divergence of the vector throughout the volume of the body. Thus,

(16a) $$\int_S (U \cdot n) dS = \int_V (\nabla \cdot U) dV$$

where $S$ and $V$ are surface and volume, respectively; $(U \cdot n)$ and $(\nabla \cdot U)$ are the inner product (dot product) of U on $S$ and divergence of $U$ in $V$. In two dimensions

(16b) $$U \cdot n = U_x n_x + U_y n_y \text{ and } \nabla \cdot U = \partial U / \partial x + \partial U / \partial y$$

In mechanical terms (16a) is

(16c) $$\int_S (T \cdot \delta) dS + \int_V (\gamma \cdot \delta) dV = \int_V (\varepsilon \cdot \sigma) dV, \text{ that is,}$$
$$\int_S (T_x u + T_y v) dS + \int_V (\gamma_x u + \gamma_y v) dV = \int_V (\varepsilon_{xx}\sigma_{xx} + \varepsilon_{yy}\sigma_{yy} + \gamma_{xy}\tau_{xy}) dV$$

In matrix form (16) is

(16d) $$\int_S \begin{Bmatrix} u \\ v \end{Bmatrix}^t \begin{Bmatrix} T_x \\ T_y \end{Bmatrix} dS + \int_V \begin{Bmatrix} u \\ v \end{Bmatrix}^t \begin{Bmatrix} \gamma_x \\ \gamma_y \end{Bmatrix} dV = \int_V \{\varepsilon\}^t \{\sigma\} dV$$

where the superscript $t$ means transpose. In finite element form one has

(17) $$\{\delta\}^t \int_S [N]^t \{T\} dS + \{\delta\}^t \int_V [N]^t \{\gamma\} dV = \{\delta\}^t \int_V [B]^t \{\sigma\} dV$$

where the constant node displacements are moved outside the integral signs. The result (17) implies

(18) $$\int_S [N]^t \{T\} dS + \int_V [N]^t \{\gamma\} dV = \int_V [B]^t \{\sigma\} dV = \int_V [B]^t [E][B] dV \{\delta\} \text{ or}$$

(19) $$\{f\} = [k]\{\delta\}$$

where $\{f\}$=left hand side of (18), a force vector and $[k]\{\delta\}$=right hand side of (18) a product of element stiffness $[k]$ and element node displacement vector $\{\delta\}$. Solution of (19) under prescribed forces allows for the determination of strains and then stresses in the element.

The element stiffness is an integral, that is,

(20) $$k = \int_V [B]^t [E][B] dV$$

which is readily integrated in the case of a linear displacement, constant strain element because all the terms under the integral sign are constants. Thus, $k = [B]^t[E][B]V$ and the integration can be explicit. Stiffness of higher order elements generally requires numerical integration as does stiffness of isoparametric elements.

**Global Equilibrium** Global equilibrium refers to an assemblage of elements, a finite element *mesh* as illustrated in Figure 4. The assemblage of elements in the figure covers a rectangular region in the *xy* plane. As an aside, data at any interior point on the rectangular grid could be determined by interpolation from known data at the nodes of the triangles. Indeed, the nodes were determined by the data point locations. The data could be temperatures, elevations, ore grade or some other quantity of interest such as water or gas pressure. However, interest here is in displacements that allow for determination of strains and stresses.

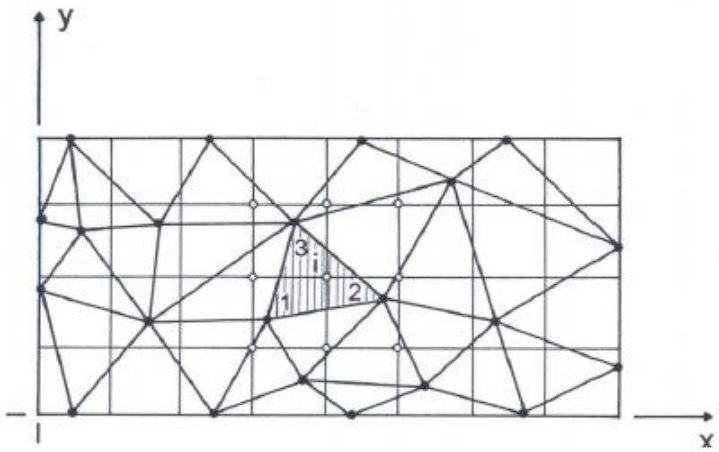


Figure 4 An assemblage of elements and interpolation of data to a regular grid.

Assembly of elements into a mesh requires a global numbering system in addition to the local numbering system of nodes. Figure 5 illustrates the concept. The figure also indicates a possibility of mixing element types, for example, quadrilaterals and triangles.

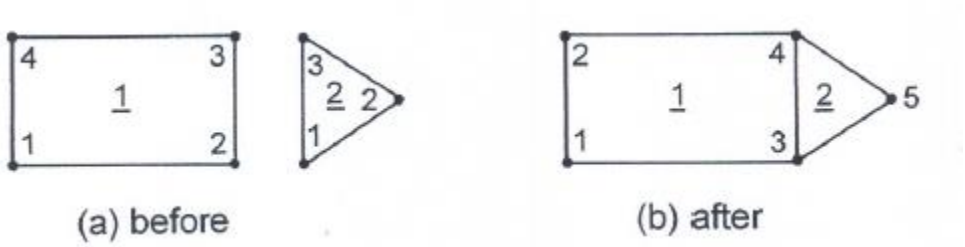


Figure 5 Local (a) and global (b) numbering of nodes.

The assembly process has a physical basis and that is the force at any node shared by adjacent elements is simply the sum of forces contributed by each element. Symbolically, the total force at a node in a mesh is

(21a) $$F_i = \sum_e f_i$$

where $F_i$ is the total force at node *i* that is shared by elements *e* with element node forces $f_i$ . In view of the element equilibrium equation

(21b) $$F_i = \sum_e \sum_{j=1}^{j=n} k_{ij}^e \delta_j$$

where the inner summation is over the *n* nodes of element *e* (4 for quadrilaterals, 3 for triangles). After arrangement of the nodes in the mesh in order from 1 to *N*, the result is global equilibrium. Thus,

(22) $$\{F\} = [K]\{\Delta\}$$

where $\{F\}$ and $\{\Delta\}$ are vectors of global node forces and displacements; $[K]$ is a *master stiffness matrix*. Solution of (22) gives the node displacements and thus allows for determination of element strains and subsequently element stresses throughout a mesh.

In two dimensions, there are two forces and two displacements at each node, so the force and displacement vectors have dimensions of 2Nx1. The master stiffness matrix is 2Nx2N. If there are 500,000 nodes in a mesh, then the master stiffness matrix dimension is $10^6$ x$10^6$. Computer storage of such a large array is obviously a serious challenge even in two dimensions and so is inversion of such a large matrix in any numerical analysis. Fortunately, the master stiffness matrix is sparsely populated meaning there are many zero entries. This feature gives rise to compact storage schemes that allow FEM to be implemented in a practical way that includes clever solution schemes. Very large problems are usually solved with iterative schemes rather than elimination schemes. Efficient and accurate solution strategies are much discussed in the literature concerning numerical methods and are often closely linked to computer architecture, topics beyond the scope of this manual. Suffice to say that the traditional Gauss-Seidel (GS) and conjugate gradient (CG) iterative schemes work quite well in solving FEM problems involving coal mine strata mechanics. The latter is particularly appealing because of the possibility of parallelization and thus speedup in solution time that is often 95 percent of a problem runtime.

**Boundary Conditions** Specification of displacements that prevent rigid body motion at mesh boundaries is essential. This specification is easily done by fixing two nodes. Forces (tractions) may be prescribed over a portion of a mesh boundary and displacements elsewhere on a boundary as well. Mixed forces and displacement conditions are possible, but the same components of force and displacement cannot be prescribed. If a force and displacement normal to a boundary are prescribed, an inconsistency occurs that may be resolved according to computer programming or the run may simply be aborted, again, according to programming. Of course, such an inconsistency should be avoided at the outset. In UTH3/PC, displacements prevail. Often displacements normal to an external boundary to a mesh are prescribed (fixed), while forces are prescribed at excavation (internal) boundaries. When displacements normal to an external boundary are set to zero, the boundary is “rollered” and indicated by a roller symbol in a diagram of the mesh for the problem at hand. Excavation forces are usually computed automatically as are gravity loads. When the preexcavation stresses (initial stresses) are known,

then forces associated with excavation can be automatically computed. However, the region to be excavated must be specified, usually as an input file of elements to be mined. Mined elements are effectively "cut" from the mesh and are "cut" elements. Only elements adjacent to an excavation wall need to be "cut". A file of cut elements is generated automatically during mesh generation.

**Practical Considerations** Several practical considerations arise in connection with finite element analysis. One is in element size; another is mesh size. Yet another is what to do with the voluminous output that is generated during a program run involving a mesh, say, of a million elements. An element file containing element stresses could easily be one million lines long and similarly for element strain and displacement output files. In a multi-step excavation sequence, output data may be truly enormous. Filtering output data for important design guidance is not at all a simple or trivial activity.

Several rules of thumb are helpful in deciding on element size and mesh size. *One rule* states that elements should have an aspect ratio no greater than four or five for numerical accuracy, that is, the ratio of greatest to least element edge length should be no greater than five. Although higher aspect ratios are permissible, solution time may be lengthened considerably at high aspect ratios. An aspect ratio of three or less is desirable. *Another rule* of thumb is that no less than five elements should be used across the least dimension of an excavation to obtain a reasonable approximation of stress distribution along the excavation walls. A *third rule* of thumb is that the external boundaries of mesh enclosing an excavation should be about five times "excavation size" away from an opening. In case of a circle, the excavation size is simply the circle diameter. In case of rectangular openings, excavation size is the long dimension of the opening. In case of three dimensional cavern-like or large brick shaped openings, excavation size is the intermediate edge length of the opening. In all cases, one may examine the change in stress in elements near the external boundaries of a mesh to see whether the changes in stress induced by excavation are small or negligible in which case the mesh is large enough. These rules of thumb are based on computational experience and the fact that stress concentration in the elastic domain, while greatest at excavation boundaries, decreases rapidly with distance from the excavation boundaries. Often a "1-D" (one dee) rule is invoked where D is the dimension used to quantify "excavation size" that in case of a circular excavation is the circle diameter, D.

## STEP 1 SITE STRATIGRAPHY

Specification of site stratigraphy in file form needed for mesh generation is illustrated in Figure 6. This file is also needed for a finite element program run. In essence, this file is a **material properties** file. File contents include elastic and strength properties and also strata depths and thicknesses. The italics in the figure are annotation and are not part of the file. The program UT3PC allows for anisotropy in elastic moduli and strengths up to a material having three planes of material symmetry (orthotropic model) such as gneiss (rift, grain and hard way in quarry terms).

Units of elastic moduli are pounds force per square inch (psi) and units of specific weight are pounds force per cubic foot (pcf). Units of strength are also pounds force per square inch (psi). Depth and thickness of strata are in feet (ft).

Strata are considered flat; no dip is allowed ($\delta$=0), although a small regional dip of a few degrees would not influence results to a noticeable degree.

```
NLYRS = 7                                        Number of layers in the stratigraphic column.
NSEAM = 5                                               Layer number of the seam of interest.
  (1) North Horn  N=2 (DP2) & WT.                            layer number and formation name.
  2.60e+06  2.60e+06  2.60e+06      0.26      0.26      0.26    E1   E2   E3   v12  v23  v31
  1.03e+06  1.03e+06  1.03e+06       0.0       0.0     158.0    G12  G23  G31  γ1   γ2   γ3
   11800.0   11800.0   11800.0     700.0     700.0     700.0    C1   C2   C3   T1   T2   T3
    1659.0    1659.0    1659.0                                 R1   R2   R3
       0.0       0.0       0.0     100.0                       α    δ    dpth thick
  (2) Price River
  3.20e+06  3.20e+06  3.20e+06      0.26      0.26      0.26
  1.27e+06  1.27e+06  1.27e+06       0.0       0.0     143.0
    9980.0    9980.0    9980.0     380.0     380.0     380.0
    1124.0    1124.0    1124.0
       0.0       0.0       100.0     191.0
  (3) Castle Gate sandstone
  3.00e+06  3.00e+06  3.00e+06      0.22      0.22      0.22
  1.23e+06  1.23e+06  1.23e+06       0.0       0.0     140.0
    9590.0    9590.0    9590.0     430.0     430.0     430.0
    1170.0    1170.0    1170.0
       0.0       0.0       291.0     190.0
  (4) Blackhawk formation
  4.00e+06  4.00e+06  4.00e+06      0.26      0.26      0.26
  1.59e+06  1.59e+06  1.59e+06       0.0       0.0     155.0
   15710.0   15710.0   15710.0     720.0     720.0     720.0
    1942.0    1942.0    1942.0
       0.0       0.0       481.0     591.0
 (5) Hiawatha coal
 0.430e+06 0.430e+06 0.430e+06      0.12      0.12      0.12
 0.192e+06 0.192e+06 0.192e+06       0.0       0.0      78.0
    4131.0    4131.0    4131.0     280.0     280.0     280.0
     621.0     621.0     621.0
       0.0       0.0       1072.0     10.0
  (6) Starpoint sandstone
  2.60e+06  2.60e+06  2.60e+06      0.22      0.22      0.22
  1.07e+06  1.07e+06  1.07e+06       0.0       0.0     135.0
    9630.0    9630.0    9630.0     360.0     360.0     360.0
    2140.0    2140.0    2140.0
       0.0       0.0       1082.0     200.0
  (7) Mancos Shale
  2.20e+06  2.20e+06  2.20e+06      0.35      0.35      0.35
 0.815e+06 0.815e+06 0.815e+06       0.0       0.0     145.0
   10300.0   10300.0   11920.0      60.0      60.0      60.0
     454.0     454.0     454.0
       0.0       0.0       1282.0     628.0
```

Figure 6 An example strata properties input file for mesh generation.

Reference axes (xyz) are assumed to coincide with the axes of anisotropy (abc) or (123); the x-axis is parallel to crosscuts, the y-axis is parallel to entries and the z-axis is vertical. Often x=+east, y=+north and z=+up with the bottom of the mined seam at z=0. Below the seam floor, z is negative. If the axis of anisotropy, (abc) or (123,) do not coincide with (xyz), then a rotation

about the z=c axes is necessary. This rotation is automatically accomplished during a finite element program run after specification of the applicable angle.

NLYRS is the number of formations or "layers" in the stratigraphic column that extends from ground surface to well below the coal seam of interest. As a guide, the column bottom should be as far below the seam of interest as the ground surface is above. There are seven (7) layers in this example. Layer numbering begins with the top layer as seen in the example.

NSEAM is the layer number where mining occurs. Layer five (5) is the seam of interest in this example.

*E1, E2, E3*=Young's moduli in the direction of the principal axes of anisotropy.
*v12, v23, v31*=Poisson's ratios.
*G12, G23, G31*= shear moduli.
*C1, C2, C3*=unconfined compressive strengths.
*T1, T2, T3*=tensile strengths.
*R1, R2, R3*=shear strengths.
$\alpha$=azimuth, $\delta$=dip, dpth=depth to top of stratum, thick=thickness of stratum

The next five lines characterize properties of the first stratum beginning at ground surface. The first line of this five line group

```
(1) North Horn  N=2 (DP2) & WT.
```

identifies the layer, say, by formation name, and is preceded by the layer number. Other information may be added to layer identification.

The next line below the layer name

```
 2.60e+06  2.60e+06  2.60e+06      0.26      0.26      0.26
```

contains Young's moduli (*E1, E2, E3)* and Poisson's ratios (*v12, v23, v31*). There are three Young's moduli, one for each material direction in case of an orthotropic material that has three material directions. In case of isotropy, the three Young's moduli are equal, as they are in this example. The three Poisson's ratios are also equal because of the assumed isotropy. In case of anisotropy, up to three distinct Poisson's ratios are allowed with numbering indicated in italics.

The second line below the layer name

```
  1.03e+06  1.03e+06  1.03e+06       0.0       0.0     158.0
```

contains shear moduli (*G12, G23, G31*). Three are allowed with labeling indicated in italics. The shear moduli are equal because of the assumption of isotropy and so are necessarily related to Young's modulus and Poisson's ratio by the standard formula $G = E / 2(1+v)$. On the same line, three components of unit weight (*GAMX, GAMY, GAMZ)* are allowed. In this example, the vertical axis is the z-axis, so there are no x- or y-components of unit weight (a force vector).

The third line below the layer name

```
11800.0   11800.0   11800.0     700.0     700.0     700.0
```

contains unconfined compressive and tensile strengths (*C1, C2, C3, T1, T2, T3*). In this example the unconfined compressive strengths are equal because of isotropy as are the tensile strengths.

The fourth line below the layer name

```
1659.0    1659.0    1659.0
```

contains shear moduli are related to the unconfined compressive and tensile strengths. The relationship depends on the failure criterion. In this example, a quadratic N-type criterion is assumed (N=2), so $R = \sqrt{CT/3}$. If N=1 with use of the DP yield criterion, then $R = \frac{2CT}{\sqrt{3}(C+T)}$ that differs somewhat from Mohr-Coulomb (MC) shear strength $R = \frac{CT}{(C+T)}$. However, MC is not an option in UT3PC and the use of N=2 is suggested.

The fifth line below the layer name

```
0.0       0.0       0.0       100.0
```

contains two angles and two distances. The $\alpha$ angle is an azimuth (clockwise) that allows for orientation of entries with respect to a mine north if desired. The angle $\delta$ is stratum dip and should be zero except in cases of shafts and tunnels. The first distance is depth to the top of the considered layer; the second distance is layer thickness. Because this is the first layer the top of the layer is at the ground surface and thus at zero depth.

A "free" file format is used, so spaces are required between numbers and some misalignment is allowed. However, alignment is recommended to reduce "typos". One could copy the example file and then simply edit it according to the site under consideration, provided one's word processor allows such activity.

As a reminder, in case of isotropy (as in the example listing) the three Young's moduli are equal as are the Poisson's ratios, shear moduli, and strengths. The shear moduli are related to Young's modulus and Poisson's ratio by the usual formula G=(E/2)/(1+v). The shear strengths in the isotropic case are related by the formula $R = \sqrt{CT/3}$ where C and T are unconfined compressive and tensile strengths and a nonlinear N-type failure criterion is implied (N=2). If N=1 with use of the DP yield criterion, then $R = \frac{2CT}{\sqrt{3}(C+T)}$ that differs somewhat from Mohr-Coulomb (MC) shear strength $R = \frac{CT}{(C+T)}$. However, MC is not an option in UT3PC for several reasons. One reason is the growing body of experimental evidence that indicates the

intermediate principal does affect yield and failure. Another is non-linearity with is more the rule than the exception. A third reason is in the three-dimensional complexity of MC failure.

In case of anisotropy (orthotropic model), the elastic stress strain relationship in matrix form is

$$(23)\qquad \begin{Bmatrix} \varepsilon_{xx} \\ \varepsilon_{yy} \\ \varepsilon_{zz} \\ \gamma_{yz} \\ \gamma_{zx} \\ \gamma_{xy} \end{Bmatrix} = \begin{bmatrix} 1/E_1 & -\nu_{21}/E_2 & -\nu_{31}/E_3 & 0 & 0 & 0 \\ -\nu_{12}/E_1 & +/E_2 & -\nu_{23}/E_2 & 0 & 0 & 0 \\ -\nu_{13}/E_1 & -\nu_{23}/E_2 & +/E_3 & 0 & 0 & 0 \\ 0 & 0 & 0 & G_{12} & 0 & 0 \\ 0 & 0 & 0 & 0 & G_{23} & 0 \\ 0 & 0 & 0 & 0 & 0 & G_{31} \end{bmatrix}$$

which is symmetric and engineering shear strains are used.

The properties input file is associated with a geologic column such as the one shown in Figure 7 taken from a coal mine in the Wasatch Plateau of central Utah. The colors represent the various formations present. The coal seam of interest is thin and barely seen in the close-up plot. The plots are from meshes developed for a different study. The stratigraphic column extends from ground surface to a considerable depth below the coal seam of interest (Hiawatha Coal). However, there is no need to develop a mesh for the entire column when addressing the problems of interest in this report. In fact, mesh dimensions are set automatically in consideration of numerical quality of results.

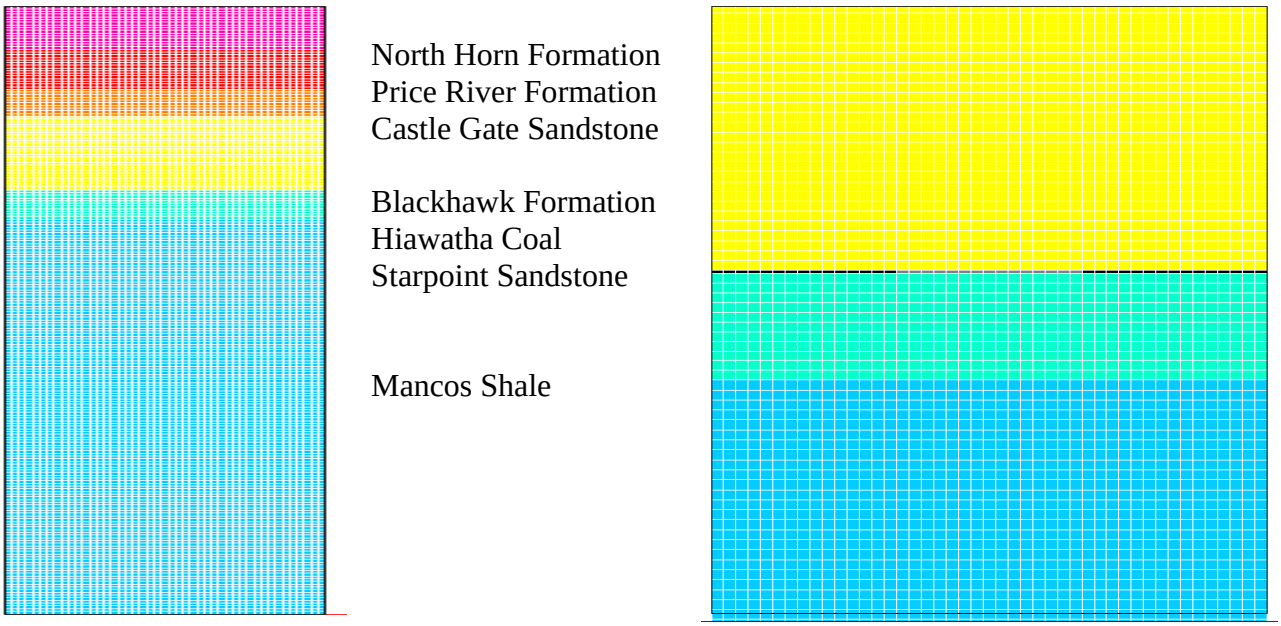


(a) (b)

Figure 7 Stratigraphic column: (a) overall, (b) close-up near the 10 ft (3. m) thick Hiawatha coal seam

If mining were not full seam height, but rather 1 ft of top coal and 2 ft of bottom coal were left, then the input data file figure 6) would require a partition of the coal seam and renumbering of the strata. The number of layers would be increased to 9 from 7 and the mined seam number would be 6. Thus, the modification is

```
NLYRS = 9
NSEAM = 6
  (4) Blackhawk formation
  4.00e+06  4.00e+06  4.00e+06      0.26      0.26      0.26
  1.59e+06  1.59e+06  1.59e+06       0.0       0.0     155.0
   15710.0   15710.0   15710.0     720.0     720.0     720.0
    1942.0    1942.0    1942.0
       0.0       0.0     481.0     591.0
  (5) Hiawatha coal
 0.430e+06 0.430e+06 0.430e+06      0.12      0.12      0.12
 0.192e+06 0.192e+06 0.192e+06       0.0       0.0      78.0
    4131.0    4131.0    4131.0     280.0     280.0     280.0
     621.0     621.0     621.0
       0.0       0.0    1072.0       1.0
  (6) Hiawatha coal
 0.430e+06 0.430e+06 0.430e+06      0.12      0.12      0.12
 0.192e+06 0.192e+06 0.192e+06       0.0       0.0      78.0
    4131.0    4131.0    4131.0     280.0     280.0     280.0
     621.0     621.0     621.0
       0.0       0.0    1073.0       6.0
  (7) Hiawatha coal
 0.430e+06 0.430e+06 0.430e+06      0.12      0.12      0.12
 0.192e+06 0.192e+06 0.192e+06       0.0       0.0      78.0
    4131.0    4131.0    4131.0     280.0     280.0     280.0
     621.0     621.0     621.0
       0.0       0.0    1079.0       3.0
 (8) Starpoint sandstone
  2.60e+06  2.60e+06  2.60e+06      0.22      0.22      0.22
  1.07e+06  1.07e+06  1.07e+06       0.0       0.0     135.0
    9630.0    9630.0    9630.0     360.0     360.0     360.0
    2140.0    2140.0    2140.0
       0.0       0.0    1082.0     200.0
```

A set of properties for caved ground or **gob** is generated automatically as are the properties of excavated or “air” elements. Air element properties are fixed. However, gob properties may be changed. In this regard, gob is nonlinear and experiences a stiffness increase with compaction. Discussion of gob behavior and model details is explained in APPENDIX III. In this regard, the gob model is an option in case of barrier pillar, bleeder entry and interpanel barrier pillar analyses. The gob option is exercised during mesh generation.

## STEP 2 MESH GENERATION

After preparation of the material properties file or stratigraphic column, mesh generation for the design problems under consideration, namely,

(1) main entry, crosscut and pillar geometry for safety,
(2) barrier pillar widths for safety of main entries, and
(3) bleeder entry safety during longwall panel mining,
(4) interpanel barrier pillar widths for safety of panel entries,
(5) pillar and room safety in room and pillar mining,
(6) shafts (including winzes and raises)
(7) tunnels (including adits, drifts and crosscuts).

begins with a proposed layout of entries, crosscuts and pillars. A single mesh generator serves all problem types. Figure 8 shows the nomenclature used to define entry, crosscut, and pillar geometry where the length of a pillar is defined parallel to the direction of entry drive.

Execution is done by simply "clicking" on the executable file name such **GMSAll7.exe.** Upon execution, problem selection is made by the user interactively. The mesh generator will ask if the selection is the correct choice, so there is an opportunity to restart. Widths of entries and crosscuts and widths and lengths of pillars should be at hand. If a barrier pillar problem is selected, then width of the barrier pillars should also be at hand and so on. Several other pauses for verification of input occur during mesh generation. More detail is given in discussions of examples of each of the five problem types.

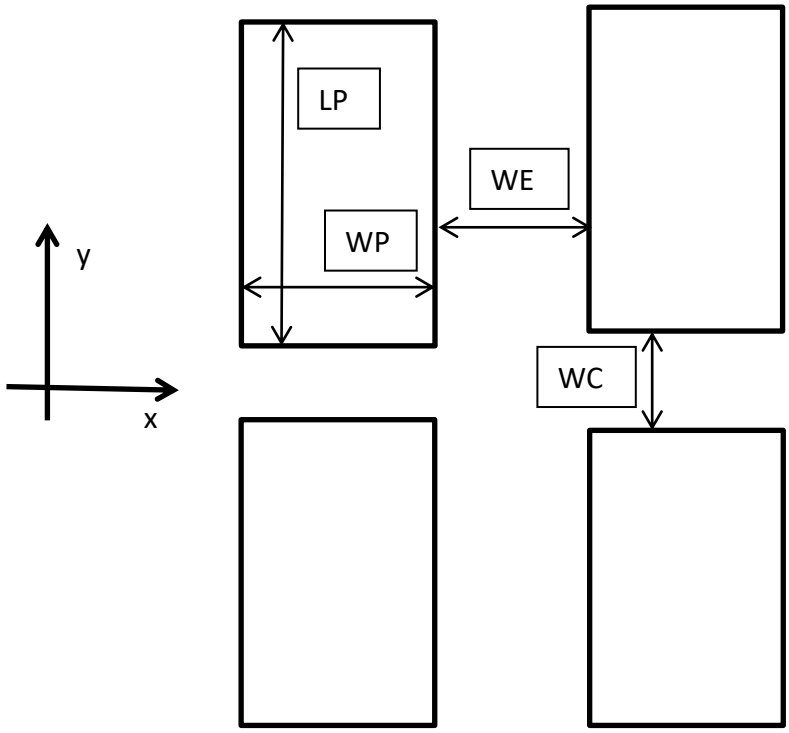


Figure 8 Definitions of entry width (WE), crosscut width (WC), pillar width (WP) and pillar length (LP).

**Mesh Generation Input.** During execution of the mesh generator, the mesh generating program requests various inputs and echoes these inputs from place to place with a question about correctness. For example, in Problem 1, "mains" the requests for data and example data are for:

| | |
|---|---|
| 1) the name of the material properties (stratigraphic column) file | *matTMnewG.txt* |
| 2) the number of main entries (NMS), | 8 |
| 3) entry and crosscut widths (WE, WC) | 20 20 (ft) |
| 4) pillar width and length (WP, LP) | 60 80 (ft) |
| 5) element width, length, height (EX, EY, EZ) | 4 4 2 (ft) |
| 6) add-in additional stresses Sxx, Syy, Szz, Tyz, Tzx, Txy? | N or n (no). |

Another example is Problem 4, interpanel barrier pillar analysis, illustrates the presentation of a gob model effects choice. Whatever the choice, if one were to make a comparison run, then regeneration of the mesh is necessary.

| | |
|---|---|
| 1) the name of the material properties (stratigraphic column) file | *matABDg.txt* |
| 2) the number of panel entries (NBS), | 3 |
| 3) entry and crosscut widths (WE, WC) | 20 20 (ft) |
| 4) pillar width and length (WP, LP) | 40 80 (ft) |
| 5) element width, length, height (EX, EY, EZ) | 4 4 4 (ft) |
| 6) do gob effect? | Y or y =yes or N or n=no |
| 7) add-in additional stresses Sxx, Syy, Szz, Tyz, Tzx, Txy? | Y or y =yes or N or n=no |

An example of Problem 7, tunnels, shows the InData output file that echoes the input requested during mesh generation.

```
Input Data
 DRIFT NPROB 7
 Tunnel Shape = Arched Rectangle
 Tunnel System = Twin Openings
 Tunnel Width =      18.0
 Width/Height Ratio =       1.0
 Pillar Width =      22.0
Section Depth (ft)   =     990.0
 Additional Sxx,Syy,Szz,Tyz,Tzx,Txy, tension +=
       0.0       0.0       0.0       0.0       0.0       0.0
 Tunnel Stress Sxx,Syy,Szz,Tyz,Tzx,Txy, tension +=
    -489.0   -1141.1    -489.0       0.0       0.0       0.0
```

The program will ask at several places whether the data are correct and thus present an opportunity to change. Dimensions are in feet. If top coal/ore or bottom coal/ore or both are left, then mining is not full seam height and the material properties files requires modification as explained later.

Element dimensions allow for some choice in mesh refinement and element size is adjusted to fit strata thicknesses. The thinnest stratum is almost always the coal seam. In this example, a 10-ft thick coal seam would have five 2-ft thick elements extending from seam

bottom to top. Elements would be 4 x 4 ft in plan view. The aspect ratio would be two. In fact, the program aspect ratio is set at two for the seam and is near one in strata above and below seam level. These restrictions are embedded in the program to ensure reliable numerical behavior. The number of elements in a mesh is restricted to less than one million. The data in this example generates over 0.5 million elements. If more elements in the seam were desired by setting EX=4, EY=4 and EZ=1, the program would redefine EX=2 and EY=2 (because of the aspect ratio restriction of two) and keep EZ=1. However, the number of elements would exceed the one million element limit (4+ million). If EZ=1.5, the number of elements is still over the one million limit (1.3+ million). There is an advantage to the one million element limit and that is in program run time. Multi-million element problems require much longer run times, often longer than a rather practical overnight runtime. However, the mesh generator runs fast and is done in seconds. This speed allows for some experimentation in meshing that is greatly facilitated by plotting as the preceding examples show, although plotting graphics are *not* part of the mesh generator programs.

Mesh generation computes a preexcavation stress field caused by gravity alone. If a different preexcavation stress field is desired, one can enter up to six stresses that are added to the gravity stresses in each element. This feature would be used in case of high horizontal stress.

The number of elements in the various problems varies between 0.5 and 1.0 million; the number of nodes is somewhat greater. Boundary conditions are generated automatically. Displacements perpendicular to the mesh sides and bottom are fixed at zero, while the top of the mesh is allowed to move freely in vertical planes that are the faces of the mesh front and back.

**Mesh Generation Output** Mesh generation output is a collection of files that contain all the data required for a runstream file needed for a FEM run. Figure 9a is an example of a runstream file from mesh generation of the "mains" problem. Similar output is obtained for the "barrier pillar" and "bleeder entries" problems. Italics are annotation and are not part of the file. The name of the runstream file is simply RunStrm

```
runstream title                 a label or title for the problem at hand
bmats                           material properties filename
belms                           element filename
bcrds                           coordinate filename
brcte                           excavated elements filename
bsigi                           initial stress filename
bnsps                           boundary specifications filename
bp1                             output file name prefix
nelem =  791466                 number of elements in the mesh
nnode =  860244                 number of nodes in the mesh
nspec =  134664                 number of boundary nodes
nmat  =       1                 number of material (strata) types
ncut  =      -1                 number specifying cut(-1), fill(+1,), external load (0)
ninc  =       5                 number of load increments
nsigo =       1                 flag 1=initial stress, 0=no initial stress
inter =     100                 number of iterations between writes of residuals
maxit =    1000                 maximum number of iterations per load increment
nyeld =       2                 flag indicating nonlinear yielding, =0 elastic run
nelcf =    2095                 number of cut elements
nsol  =       0                 flag to select equation solver, =0 GS, =2 CG
nprb =        1                 number of the problem type (1 to 7)
```

```
mgob.........0                  flag to indicate gob effect, 0=no effect, 1=with effect
 error=    1.0000               solver control, keep at 1
 orf  =    1.8600               over-relaxation factor, keep at 1.86 (near optimum)
 xfac =   12.0000               scale factor, converts x-mesh input units to inches
 yfac =   12.0000               scale factor, converts y-mesh input units to inches
 zfac =   12.0000               scale factor, converts z-mesh input units to inches
 efac =    1.0000               scale factor, multiplies elastic moduli
 cfac =    1.0000               scale factor, multiplies strength moduli
torl% =    0.0100               solver control
ENDRUN                          stops a run
```

Figure 9a A runstream file from mesh generation output for Main Entries Problem 1.

The **runstream title** aids in keeping track of an analysis when several are done.

The **filenames** are minimal and will require paths if not in the same directory as the finite element program.

The **output file prefix** is used to identify stress, displacement and element safety factor output files (bp1sig.txt, bp1dis.txt, bp1fac.txt) and also a file generated during the run (bp1) that echoes input and records other run information. The suffix identifies these files as text files that are easily recognized and read by programs such as Word and related or similar programs.

The numbers **inter**, **maxit** and **error** aid in control of the iterative equations solvers used.

The number **nyeld** is best kept at 2.

The number **nsol** selects the equation solver, nsol=0 selects Gauss-Seidel (GS), nsol=2 selects a conjugate gradient (CG) solver that is quite popular in solving large finite element problems. The choice is largely a matter of personal preference, although the CG solver is often faster. Experimentation is encouraged. If nsol=1, a Gauss elimination scheme is selected, but is unlikely to work because of excessive bandwidth.

Scaling of a mesh is possible with the numbers **xfac, yfac, zfac** which convert input units to inches. For example, if input coordinates (brds file) are in feet, then these factors should be 12. If input coordinates are meters, then these factors would be 39.37.

Scaling of elastic moduli and strengths is also possible using **efac** and **cfac**. For example, to ensure no element failures occur, one may set cfac=100. Or if one wished to soften the mesh from laboratory values of elastic moduli, one may set efac to 0.1, for example. This convenience saves redoing the entire material properties file.

The number **tolr** is also an equation solver control and is a percentage. When the residuals are reduced to less than this percentage, the solution is reached and the equation solver returns control to the mainline of the program. Residuals are essentially unbalanced forces, so when the forces not yet balanced by displacement are less than 0.01 percent of the applied forces,

the problem is considered solved in this example. Tolr is a user choice. The character string **ENDRUN** (or **endrun)** signals a normal stop at the end of the run.

A second output file from mesh generation is a log file of input data with the name InData. An example is shown in Figure 9b. The first line is the file name. The second line indicates the problem type. The remaining lines are self-explanatory.

Mesh generation apportions mesh size such that the outer boundaries are sufficiently remote from the region of interest, the entries, crosscuts, and pillars, to have negligible effect on the stress distribution in this region. To keep element numbers manageable (less than one million preferred, but an allowance for more is built-in), the overburden above the seam and the underburden below may be limited. Consequently, thicknesses of top and bottom strata may be reduced even to zero. This truncation of the stratigraphic column may be seen, for example, in the stress output file where material type numbers are present in the discussion of output files in the section on program execution.

```
Input Data
 INTERPANEL
   Number of panel entries, NES =   3
   Width of entries, WE (ft)   =      20.0
   Width of crosscuts, WC (ft) =      30.0
   Width of pillars, WP (ft)   =      40.0
   Length of pillars, LP (ft)  =      50.0
 Longwall panel width, LPW (ft)=     750.0
 Interpanel Barrier pillar width WBR (ft) =     300.0
 EX, EY, EZ, (ft)=       4.0       3.0       2.0
 Additional Sxx,Syy,Szz,Tyz,Tzx,Txy, tension +=
       0.0       0.0       0.0       0.0       0.0       0.0
 No gob effect
```

Figure 9b An example of a log file of input data from mesh generation in case of interpanel barrier pillar analysis.

A third mesh generation output file is PlotMesh that serves as an input file to mesh plotting explained in APPENDIX VI MESH PLOTTING. PlotSfac is a fourth mesh generation output file that aids in plotting element safety factors, although an easier approach is to change PlotMesh.

## STEP 3 PROGRAM EXECUTION

Two sets of axes may be used. The first set (abc) or (123) mentioned in the description of mesh generation aligns the a- or 1-axis parallel to crosscuts as shown in Figure 10 and the b- or 2-axis parallel to entries. The c- or 3- axis is up (normal to the page).

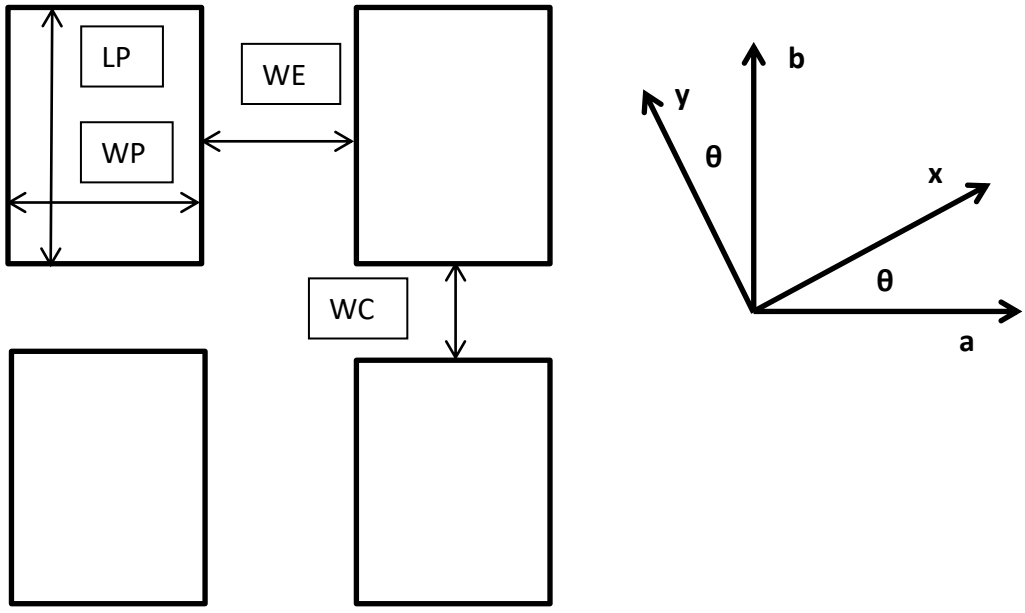


Figure 10 Definitions of entry width (WE), crosscut width (WC), pillar width (WP) and pillar length (LP) and orientation of axes. Angle θ is clockwise from **y**=north or ccc from **a** to **x**.

Initially, the (xyz) axes are aligned with (abc) during mesh generation. However, there is an advantage to aligning entry directions with mine maps, so if the y-axis is aligned with mine-north, then a rotation of axes is necessary. The rotation is about the vertical axis and specified by the angle θ shown in the figure. Entry axis **b** is at θ degrees clockwise from mine-north **y** as shown in the figure. Of course, mine-north may also be true north, but there are many instances where this is not the case. The parameter θ allows choice in orientation of entries with respect to material axes in any case.

**Input File Edit.** Program execution requires preparation of a finite element input file. An example input file for a finite element run is given in Figure 11. The differences between the mesh generator output file and the finite element input file arise from the application platform being used. In particular, full path names are required for filenames in this input file because the two applications (mesh generation and finite element analysis) are in different directories. If mesh generation and finite element analysis programs are in the same directory, then paths are not required. Usually, some editing of the mesh generation output file is desired. For example, the number of load steps **ninc** may be increased to 10 from 5 or decreased to 1 for a first trial run. Another possibility is a change in **nsol** from 0 to 2, that is, from Gauss-Seidel equation solving to conjugate gradient solving as a numerical experiment for comparison of results and run times obtained from the two solvers.

```
TRY 8/11/2016 MAINS 8 wgp                                          1
F:\Visual Studio 2010\Projects\SPK\GMB3\matTMnew.txt               2
F:\Visual Studio 2010\Projects\SPK\GMB3\belms                      3
F:\Visual Studio 2010\Projects\SPK\GMB3\bcrds                      4
F:\Visual Studio 2010\Projects\SPK\GMB3\brcte                      5
F:\Visual Studio 2010\Projects\SPK\GMB3\bsigi                      6
F:\Visual Studio 2010\Projects\SPK\GMB3\bnsps                      7
DEM1                                                               8
nelem =  556114                                                    9
nnode =  605052                                                   10
nspec =   95232                                                   11
nmat  =       7                                                   12
ncut  =      -1                                                   13
ninc  =       5                                                   14
nsigo =       1                                                   15
inter =     100                                                   16
maxit =    2000                                                   17
nyeld =       2                                                   18
nelcf =    2095                                                   19
nsol  =       2                                                   20
nprb  =       1                                                  20a
mgob..=       0                                                  20b
error =     0.000                                                21
 orf  =     1.860                                                22
 xfac =     12.00                                                23
 yfac =     12.00                                                24
 zfac =     12.00                                                25
 efac =      1.00                                                26
 cfac =      1.00                                                27
tolr% =      0.01                                                28
ENDRUN                                                           29
```

Figure 11 Example input file for UT3PC. Numbers on the right are *not* part of the file.

**1**. As before, the first line in the runstream file is a run title line that is useful for tracking runs.

**2**. The second line identifies the material properties file (stratigraphic column) which is the same as the file used in mesh generation.

**3**. The third line is the label of the element file **belms** that is computed during mesh generation. This file characterizes elements by nine numbers. Each line after the first line has the structure: **nel n1 n2 n3 n4 n5 n6 n7 n8 n9**. The number in the **nel** column is simply the element number that ranges from *1* to *nelem*. The next eight numbers are the corner numbers of the considered element. The numbering is counter-clockwise beginning with a first face of an element and running through the first four numbers. The second face runs counter-clockwise through the opposing element face. The last number **n9** is a material type number. This number corresponds

to the order of strata properties listed in the material properties (stratigraphic column) file. Figure 12 illustrates a typical element, a cuboid or "brick".

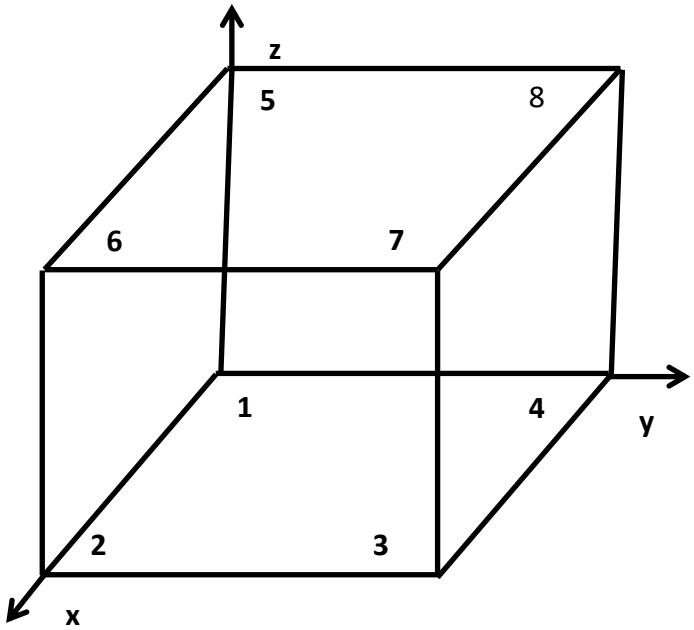


Figure 12 A generic element showing the order of local corner numbers with respect to xyz.

An example line from the middle of an element file is:

```
400000   418148   418199   418200   418149   420239   420290   420291   420240        5
```

Here, the element number is 40000 and nodes (corners) 1 to 4 have numbers 418148, 418199, 418200, 418149, respectively. Nodes 5 to 8 are 420239, 420290, 420921, 420240, respectively. The material type is 5.

The first line in this element file is

```
nelem=      800000
```

that states there are 800,000 elements in the file.

**4**. The foutth line in the runstream file identifies a file **bcrds** containing coordinates of all the nodes in a mesh. This file is computed during mesh generation. The first line in this file specifies the number of nodes in the file. Succeeding lines identify two nodes and lists coordinates. For example,

```
   nnode=      838491
        1       0.0       0.0    -190.0        2       0.0       1.0    -190.0
```

Here the number of nodes in the file is 838,491. Coordinates (xyz) of the first node **1** are **(0.0, 0.0, -190.0**). The second node **2** has coordinates **(0.0, 1.0, -190.0**). The y-coordinate of the second node has increased while the x- and z-coordinates have remained constant. This ordering is indicative of mesh node numbering. The y-coordinate increases first because the y-dimension of a mesh is the smallest dimension in the three problems considered. The x- and then the z-dimensions increase in that order. Generally, the practice of numbering meshes across the least dimension is favorable to compact storage schemes and is particularly important when elimination based equation solvers are used (bandwidth minimization).

**5**. The fifth line identifies a file containing a list of elements to be excavated. This is a "cut element" file. Cut elements are excavated physically but remain in the mesh. Excavation occurs digitally by reassignment of element properties from original strata properties to properties of "air". Air properties are extremely compliant, highly compressible, but also quite strong. The high strength prevents failure. Reassignment of element properties generates out of equilibrium forces, at the boundaries between air and solid. These excavation forces induce displacements, associated strains and stress changes relative to the preexcavation state. Two example lines from a cut element file **brcte** are:

```
    -1 nelct=     8000
  380001   380002   380003   380004   380005   380006   380007   380008   380009
380010
```

Here, the -1 indicates a cut. A +1 would indicate a fill. There are 8,000 cut elements in the file.
Ten elements per file row are given. Here the first cut element in the file is 380001. The last cut element on this line of 10 is 380010. Elements do not need to be in numerical order.

**6**. Line 6 of the runstream file identifies a file containing the preexcavation stresses, **bsigi**. The first two lines are:

```
  Elem Mat       Sxx      Syy      Szz      Tyz      Tzx      Txy
      1    6    -701.4    -701.4   -1302.6       0.0       0.0       0.0
```

Thus, the first element **1** is assigned three normal stresses Sxx=-701.4, Syy=-701.4 and Szz=-1302.4 psi at the outset. The horizontal stresses Sxx and Syy are equal because of the preexcavation stress state is assumed to be caused by gravity alone. This is also the reason why the shear stresses are nil. Compression is negative; tension is positive.

However, provision is made in the mesh generation step to add in stresses by the user (Sxx, Syy, Szz, Tyz, Tzx, Txy) to obtain a different preexcavation stress field. The add-in feature was not used in this example. Care must be exercised to add-in physically meaningful stresses, of course. The six add-in stresses are added to the gravity stress in every element. Most likely, this feature would be used to generate high horizontal stresses (Sxx, Syy).

**7**. Line 7 identifies a file **bnsps** that contains specification of boundary nodes and boundary conditions. The first three lines of this file are:

```
  nspec =       74091
```

```
1       1   7     0.000     0.000     0.000     0.000     0.000     0.000
2       2   6     0.000     0.000     0.000     0.000     0.000     0.000
```

The first line simply states the number of boundary nodes “nspec” to be 74091.

Subsequent lines are:

**List order, global node number, specification code, x-.,y-, z-displacements, x-, y-, z-forces.**

The first number in the second line of the file is **1** and so on to the last in the list **74091**. The next number **1** is the actual global node number in the mesh.

The third number in the second line **7** is a code that indicates the displacement components that are fixed.

**The code is: 1=x-displacement fixed, 2=y-displacement fixed, 3=z-displacement fixed, 4=x- and y-displacements fixed, 5=y- and z-displacements fixed, 6= z- and z-displacements fixed, 7=x-, y- and z-displacements fixed**

.

Force components are allowed provided corresponding displacement components are not specified. An 8 is used to code a node specification of force components only.

The first three zeroes in the second line indicate the x-, y- and z-displacements are fixed at zero.

The last three zeroes in the second line indicate the x-, y- and z-forces are zero. In fact, these force zeroes are cosmetic fill-ins because displacements take precedent over forces.

Another example line from the “node spec” file is

```
18700  194512   1     0.000     0.000     0.000     0.000     0.000     0.000
```

This line is the 18,700$^{th}$ line in the file, the considered node is number 194,512. This node has the x-displacement fixed at zero. The y- and z-displacements and all forces are not specified but rather are computed during program execution.

**8**. Line 8 identifies an output file prefix. In this example, **bp1**. Output files are then **bp1** that echoes some of the input and provides a record of the run, **bp1sig.txt, bp1dis.txt**, and **bp1fac.txt.** that contain element stresses, node displacements and element safety factors, respectively. The files are “text” files as indicated by the file extensions **.txt**.

**9**. **nelem**=the number of elements in the mesh.

**10**. **nnode**=the number of nodes in the mesh.

**11**. **nspec**=the number of nodes with specified boundary conditions.

**12**. **nmat**=the number of materials in the material properties files. The number of materials in the mesh may be less, but not more.

**13**. **ncut** is a flag that signifies a cut (-1), a fill (+1), neither (0) If ncut=+1, then the cut element file is actually a fill element file. If neither a cut nor fill is specified, then external forces are needed to load the mesh. These external forces must be specified in the **nsps** file.
**Only the ncut=-1 option is needed to run any of the three problems under consideration**.

**14**. **ninc**=the number of load increments to reach full load during program execution. Five to 10 steps are suggested. Incremental loading is needed to allow for nonlinearity of element response that occurs when elements yield. An increase in increment number increases run time depending on the number of element failures that occur during an increment. More failures results in additional run time.

**15**. **nsigo** = 1 is a flag indicating initial stress is present, nsigo=0 indicates no initial stress is present. An initial stress file is read only if nsigo=1 even if listed on line 6 of the runstream file.

**16**. **inter** is a number that indicates how many iterations occur in the equation solver before the status of the solution is written to the screen and to the output file echo. This number is linked informally to **maxit**, that maximum number of iterations allowed in a load increment. A reasonable value of **inter** is $1/5^{th}$ to $1/10^{th}$ of **maxit**, although a larger or smaller number is certainly allowable. By timing the iterations over an interval **inter** one can estimate problem run time. For example, if **inter** is 100 and the duration time is one minute so the iteration rate is 100 iterations per minute, the time for necessary for a single load step is no more than maxit/100 minutes. If maxit is 2000, then the time is 20 minutes. If the number of load increments is 5, then no more than 100 minutes are required for execution after equation solving commences. Total run would be more, of course. Assembly of the master stiffness matrix is particularly time consuming, perhaps one-half an hour more or less depending on problem size.

**17**. **maxit** is the maximum number of iterations allowed per load step. This number is related to **tolr** that specifies the percentage of applied forces that must be reached before solution convergence is achieved. A value of **maxit** that is sufficient to achieve convergence during each load increment is desirable.

**18**. **nyeld** is an exponent used in the yield condition. An exponent N of **2** is suggested, so the yield condition is quadratic. An exponent N=1 implies Drucker-Prager yield.. Other values are possible, for example N=1.5. This exponent dictates the rate of increase of rock strength with confining pressure. A value of 1 usually increases strength with confining pressure too fast according to experience with the well-known Drucker-Prager yield criterion.

**19**. **nelcf** is simply the number of cut (or fill) elements in the mesh and in the "cut" element file.

**20**. **nsol** is a flag that indicates the type of equation solver to use. When **nsol**=0, the equation solver is a conventional Gauss-Siedel (GS) iterative solver.

When **nsol**=1**,** solving is by conventional Gauss elimination. This option is unlikely to work for the mesh sizes involved in the three problems considered. The reason is in bandwidth limits imposed by computer hardware. A message is issued when elimination is selected and the bandwidth is too large.

When, **nsol**=2 a conjugate gradient (CG) solver is used. GS and CG are a well-known iterative equation solving techniques. CG is perhaps the most popular iterative solver in finite element analysis and appears to be faster than GS in solving the three problems under consideration. CG also has a potential advantage over GS in amenability to parallelization via OpenMP with an attendant speed up in solution time, although not implemented at the time of this writing. Thus, the **nsol**=2 option is suggested, but experimentation is also recommended using both iterative solvers. Comparisons in speed and accuracy are always interesting. The availability of choice also allows for checking results. Equation solvers are discussed at length in the technical literature including the references cited at the end of this manual.

A feature common to both iterative equation solvers is the possibility of increasing residuals between intervals of **inter** and then decreasing, so convergence may be oscillatory. In case of GS, oscillatory convergence is indicative of a highly over-estimated relaxation factor. The consequence is simply longer solution time. In case of CG, if residuals increase more than 5% between intervals of **inter**, the load increment is ended, provided convergence is within 5%, and the next load increment is started. If residuals are near **tol%**, then convergence is achieved as a practical matter. At later load increments normal behavior may occur with satisfactory convergence at the end of a load increment.

If residuals are high at the end of a load increment using GS, then **maxit** should be increased until convergence is obtained when iterations reach this new limit in a load increment.

There are two remedies for low quality results caused by early exit in CG. One is to try the other equation solver, GS instead of CG. The other alternative is to use many more load increments. Use of iterative equation solving is art as well as mathematics and thus benefits from experimentation and experience.

**20a. mgob** is a flag indicating whether a gob effect is in the analysis: **mgob**=0 indicates no effect; **mgob**=1 indicates a gob effect is present. Details are explained in an appendix.

**21**. **error** is a secondary convergence criterion and can be safely set to 0.0. A high value is likely to lead to a solution that is not well converged. Keeping **error** at 0.0 is suggested.

**22**. **orf** is an over-relaxation factor used in the GS iterative solver. An optimum value that gives the fastest rate of convergence is on the interval [1,2]. A value greater than 1.5 is suggested, i.e., 1.86 to start.. An approximation to the optimum value is computed in GS during execution and thus may change the input value at the end of a load increment.

**23,24,25**. x**fac, yfac** and **zfac** are scale factors that convert input coordinates to inches. Because the mesh generator computes node coordinates in feet, these scale factors are set to 12.0. These scale factors can be used to distort the mesh. For example, if **zfac**=24, then layer depths and

thicknesses are double the mesh generation values. If seam height were 10 ft, the rescaled height would be 20 ft and so on. There is no evident need to use scale factors other than 12.0, although if a coordinate file were developed outside the mesh generator and measured in meters, then scale factors that convert meters to inches would be needed.

**26, 27**. e**fac** and **cfac** are scale factors that multiply the input elastic moduli and strengths during program execution. These scale factors offer the convenience of changing material properties values without the need to redo the entire file. These scale factors act independently, so one can scale elastic moduli (E and G) independently of strengths (C, T and R). The dimensionless Poisson's ratios are not rescaled.

**28**. **tolr%** is a tolerance percentage that indicates convergence. For example, if **tolr%**=0.01, then when the residuals in equation solving reach a value of 0.0001, that is, $10^{-4}$, convergence is achieved. Tolerance is a force norm in mathematical parlance and is a percentage of applied forces (forces of excavation) not yet equilibrated by deformation when convergence is declared.

**29**. **ENDRUN** (or **endrun**) is a character string that signals a normal **stop** to the program. The program will stop regardless, but with a message otherwise.

A second problem involving barrier pillars uses information supplied by the sponsor of this study from a mine in another state. A third problem illustrates bleeder entry safety analysis after advance of a longwall panel. The identity of the mines is not critical to the study. Fourth and fifth problems involve interpanel barrier pillars and pillars in room and pillar mines. An option for effects of gob is offered in case of barrier pillar, bleeder entry and interpanel barrier pillar problems. Gob behavior is described in detail in APPENDIX III. However, stratigraphy, topography, and strata properties are very different in the examples. Such differences underscore the versatility of the finite element method in accommodating site-specific mine data.

**Output Files.** There are three output files containing results of a finite element analysis: (1) UT3sig.txt, (2) UT3dis.txt, and (3) UT3fac.txt. These files contain element stresses, node displacements and element safety factors, respectively.

Output from UT3sig.txt has the form:

```
Elem  Mat    Sxx     Syy     Szz     Tyz     Tzx     Txy     sfac      xc       yc
zc
       1    9   -1588.4   -1611.0   -3014.4       0.0       0.0       0.0      5.68
1.95      1.50   -302.50
       2    9   -1588.4   -1611.0   -3014.4       0.0       0.0       0.0      5.68
1.95      4.50   -302.50
```

The headings are: Elem=element number, Mat=material type, Sxx,…Tzy=stresses, xc, yc, zc= coordinates of the element center. Recall a +zc is above the floor of the mining horizon and a negative is below.

Output from UT3dis.txt has the form:

```
     Node      Ux      Uy      Uz        xp          yp          zp
283215      0.0593      0.0000     -0.2933    254.0000     40.0000     22.9000
```

```
283216      0.0546      0.0000     -0.4062    258.0000      0.0000     22.9000
283217      0.0548     -0.0056     -0.4037    258.0000      3.0000     22.9000
283218      0.0552     -0.0110     -0.3964    258.0000      6.0000     22.9000
```

The headings are Node=node number, Ux, Uy, Uz=total displacements induced by mining, xp, yp, zp=coordinates of the node point with + zp up from the floor of the mining horizion and –zp down.

Output from UT3fac.txt has the form:

```
Elem      Xc      Yc      Zc    Sfac
  1      1.95     1.50   -302.50      5.68
  2      1.95     4.50   -302.50      5.68
  3      1.95     7.50   -302.50      5.68
  4      1.95    10.50   -302.50      5.68
  5      1.95    13.50   -302.50      5.68
```

The headings are: Elem=element number, xc, yc, zc= coordinates of the element center, and Sfac=element safety factor ("strength" / "stress"). Recall a +zc is above the floor of the mining horizon and a negative is below

## 1 MAIN ENTRIES, CROSSCUTS AND PILLARS

The major steps to doing an analysis are: (1) preparation of problem input, (2) mesh generation, and (3) finite element analysis. These are the three steps to application of FEM. Presentation of results follows the third step.

**Example 1** An example problem involving main entries, crosscuts and pillars illustrates the processes of mesh generation and finite element analysis. This example uses information from underground coal mining in the Wasatch Plateau in central Utah.

*Step 1 Preparation of a materials property file (stratigraphic column)* Problem input for this example is presented in the previous discussion. The important material properties file is given in Figure 6. The stratigraphic column is shown in Figure 7. Inspection of Figure 6 shows the mining depth to be 1072 ft (327 m), indicated by the parameter *dpth* in the properties for Hiawatha coal.

*Step 2 Mesh Generation* Mesh generation input is in parts:

| | |
|---|---|
| 1) the name of the material properties (stratigraphic column) file | *matTMnewG.txt* |
| 2) the number of main entries (NMS), | 8 |
| 3) entry and crosscut widths (WE, WC) | 20 20 (ft) |
| 4) pillar width and length (WP, LP) | 60 80 (ft) |
| 5) element width, length, height (EX, EY, EZ) | 4 4 2 (ft) |
| 6) add-in additional stresses Sxx, Syy, Szz, Tyz, Tzx, Txy? | N or n (no). |

Mesh generation is done with the confines of the red rectangles shown in Figures 13 and 14 depending on whether the number of main entries is even or odd as indicated in the captions. Planes of symmetry are used to avoid unnecessary element and node generation.

The generated mesh is illustrated in Figures 15 and 16. Output from the mesh generator is presented in Figure 9 where the number of elements is given as 791,466. The mesh generation output file resembles the finite element input file which is given in Figure 10.

The first problem is illustrated in Figures 9 and 10 in the case of an even and odd number of main entries, respectively.

Element dimensions are an important part of mesh generation input. These data, EX, EY and EZ are horizontal dimensions (EX and EY) and (EZ) vertical element dimensions. Regardless of value, the ratio of horizontal to vertical dimensions is restricted to two. The reason is to insure acceptable numerical behavior. Specifying EX=EY to be $1/5^{th}$ entry width is a reasonable starting choice, for example, WE=20 ft, EX=EY=4 ft and EZ=2 ft.

Figures 15, and 16 are plan and vertical section views of a mesh for Problem1 “mains”. The plots are obtained from output of the mesh generator. In this example problem eight main entries 20 ft (6.1 m) wide are specified. These entries are spaced on 80 ft (24.4 m) centers. Pillars are 60 ft (18.3 m) wide by 80 ft (24.4 m) long. Crosscuts 20 ft (6.1 m) wide are spaced on 100 ft (30.0 m) centers. Mining is full seam height 10 ft (3 m). No top or bottom coal is left. The mesh extends above and below the seam a distance equal to the rib to rib width of the main entry set of 580 ft (177 m). Width of the mesh is equal to the width of the main entry set 580 ft (177 m). Mesh extent is computed automatically. There are 791,466 elements and 860,244 nodes in the mesh and the number of elements meets the suggested limit of less than one million. Run time was four hours.

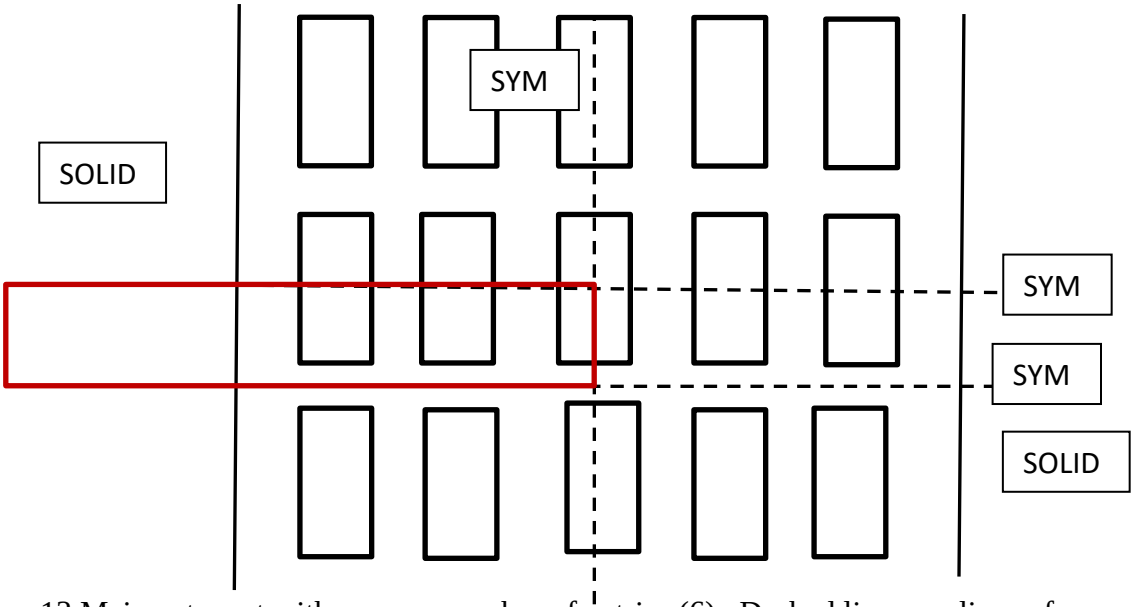


Figure 13 Main entry set with an even number of entries (6). Dashed lines are lines of symmetry (SYM). Mesh extent is outlined in red, but not to scale.

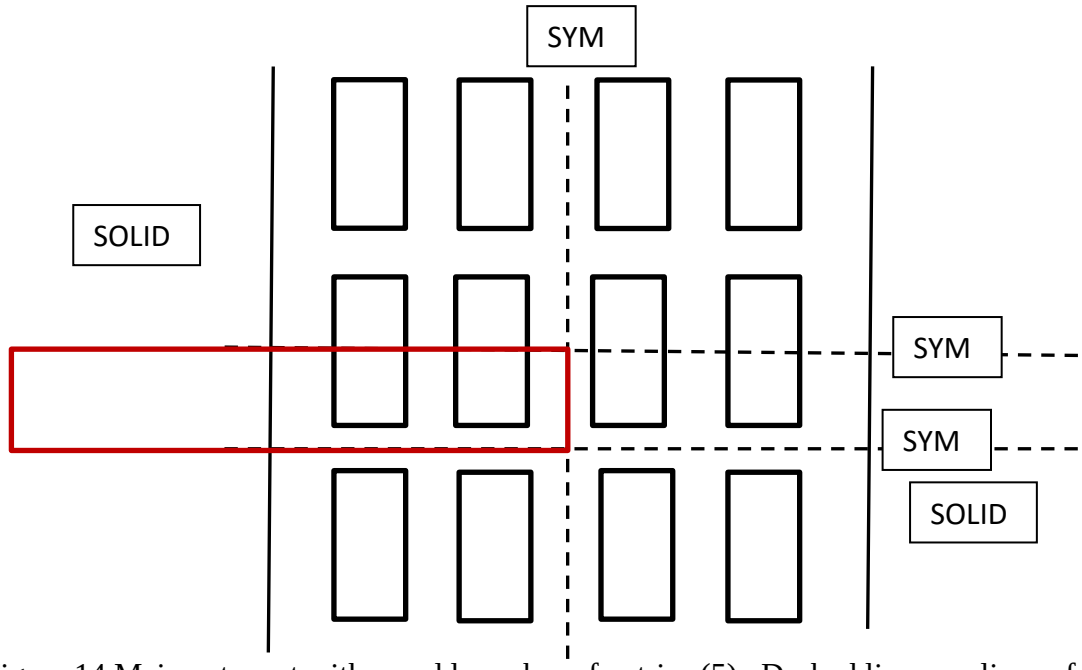


Figure 14 Main entry set with an odd number of entries (5). Dashed lines are lines of symmetry (SYM). Mesh extent is outlined in red, but not to scale.

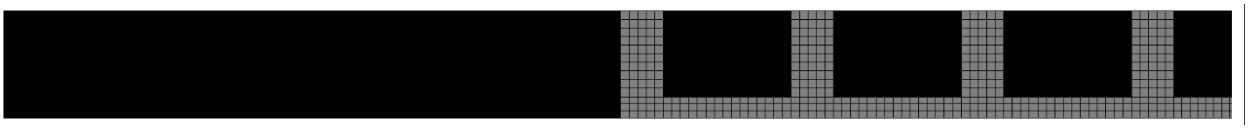

Figure 15 Plan view of seam level mesh of Problem 1. Grey elements are entries and crosscuts. Black is the coal seam. Entries and cross cuts are 20 ft (6.1 m) wide. Pillars are 60x80 ft (18.3x24.4 m). The mesh is symmetric about the right hand side. There are eight entries in the set of mains.

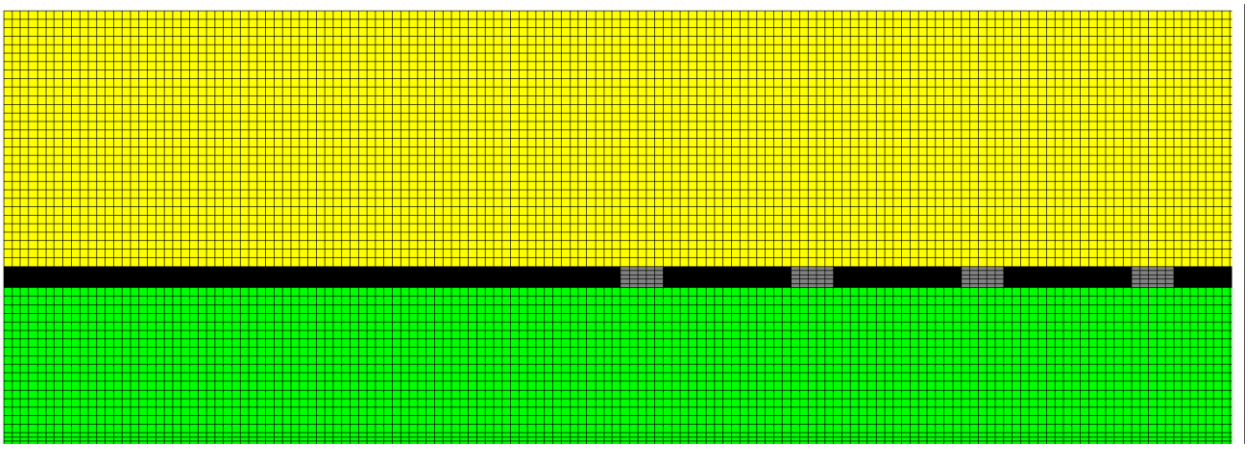

Figure 16 A window near seam level in vertical section. Seam thickness is 10 ft (3.0 m). The mesh is symmetric about the right hand side. There are eight entries in the set of mains. Colors represent different strata types.

*Step 3 FEM Execution and Results* Preparation of a runstream file precedes execution. Thus some editing of the file shown in Figure 9 is usually needed.

Practical results of the finite element analysis are given in safety factor distributions. Such distributions show where safety is threatened by the presence of yielding elements with a safety factor of one and also by elements with safety factors near one. Figure 17 shows element safety factor distributions in this example problem involving eight main entries. As a reminder, entries and crosscuts are 20 ft (7m) wide; mining height is 10 ft (3 m); pillars are 60 ft (18.3 m) wide and 80 ft (24.4 m) long. Because there is an even number of main entries a vertical plane of symmetry passes through a pillar center and only four entries are in the figure. Width of the "half mains" is 290 ft (88.4 m); width of the unmined coal to the left is also 290 ft (88.4 m). Total width is 580 ft (176.8 m). The mesh extends 580 ft (176.8 m) above and below the bottom of the coal seam of interest. However, the vertical extent shown in the figure is reduced for better detail at seam level. Seam height is 10 ft (3 m).

Element yielding is confined to seam floor elements below pillars as seen in Figures 17a,b. Safety factors increase rapidly with distance into the solid to *fs*=2.2 as seen in the orange color in the pillar cores and to *fs*=2.7 farther into the solid coal on the left hand side of the figure. Roof and floor safety factors are outside the main entries are safe where blue and green indicate *fs*=7 more or less. Safety factors above pillars are high, but the floor below pillars is yielding indicated by black elements and thus indicating a threat to safety. Overall, the results indicate a potentially unstable set of main entries where coal is mined full seam height at a depth of 1072 ft (326.7 m).

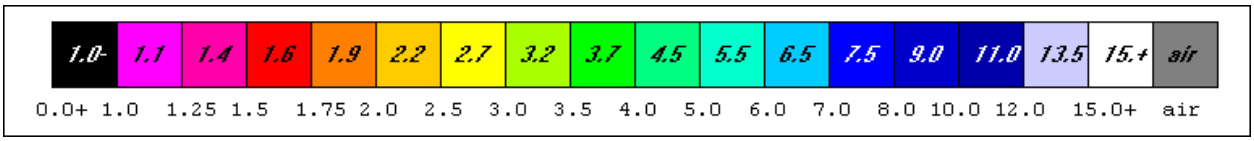


Element Safety Factor Color Scale

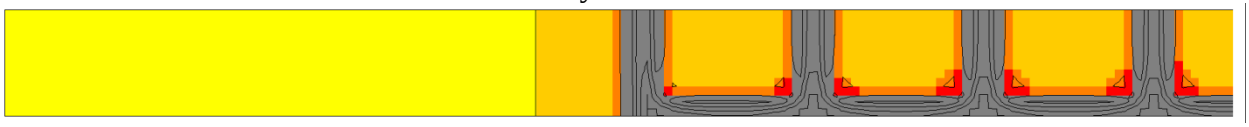

(a) Plan view of element safety factor distribution at pillar mid-height

(b) Plan view of element safety factor distribution at seam floor

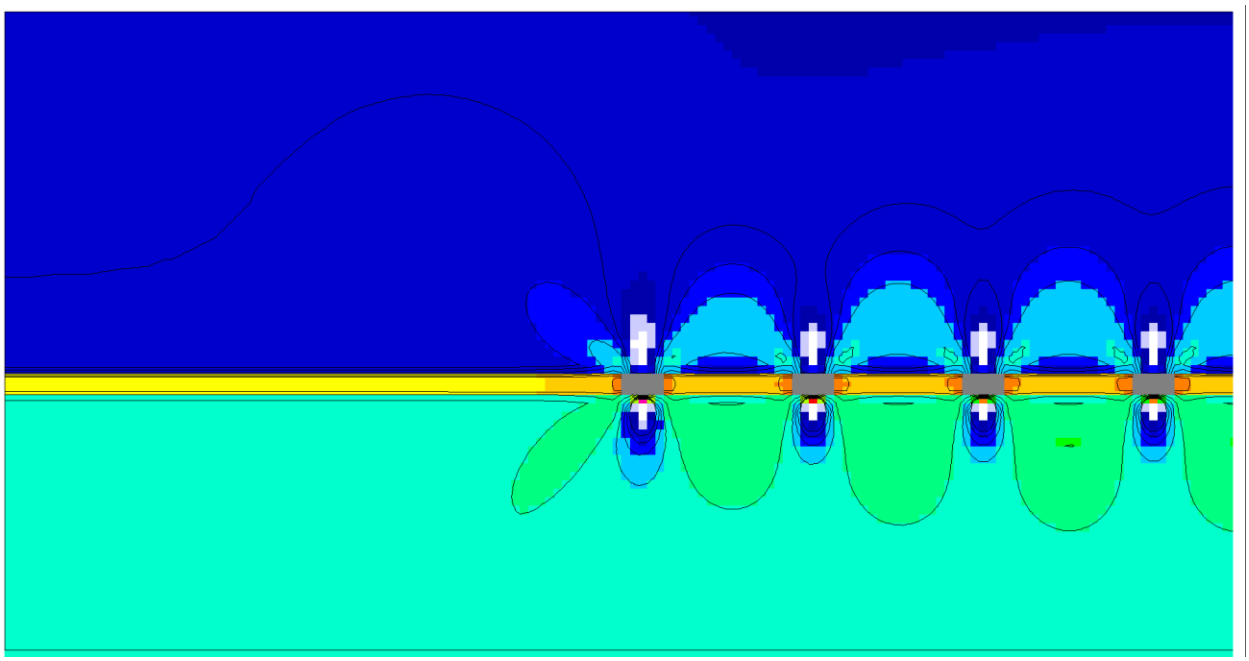

(c) Vertical section window through pillar centers showing element safety factor distribution.

Figure 17 Element safety factor distributions in the case of eight main entries.

**Example 2** A second example of analysis of main entry safety is given in APPENDIX IV.

## 2 BARRIER PILLARS

Barrier pillar safety relates to barrier pillar size for protection of main entries (and pillars) from effects of adjacent longwall mining. A new analysis that allows for gob effects is presented here for comparisons. The three step process is again followed in the new analysis for gob effects. An example of barrier pillar problem analysis that was done in previous work is also described using the three step process.

**Example 1** The three step process used in analysis of main entries is also followed in this example.

*Step 1 Preparation of a materials property file (stratigraphic column).* The material properties file for this problem is shown in Figure 18. The coal seam of interest is the 5th stratum of the seven in the column.

```
NLYRS = 7
NSEAM = 5
  (1) North Horn  N=2 (DP2) & wt, 2000-11000, 1/16/2022
  2.60e+06  2.60e+06  2.60e+06      0.26      0.26      0.26
  1.03e+06  1.03e+06  1.03e+06       0.0       0.0     158.0
   11800.0   11800.0   11800.0     700.0     700.0     700.0
    1659.0    1659.0    1659.0
       0.0       0.0       0.0    100.0
  (2) Price River
  3.20e+06  3.20e+06  3.20e+06      0.26      0.26      0.26
  1.27e+06  1.27e+06  1.27e+06       0.0       0.0     143.0
    9980.0    9980.0    9980.0     380.0     380.0     380.0
    1124.0    1124.0    1124.0
       0.0       0.0     100.0     191.0
  (3) Castle Gate sandstone
  3.00e+06  3.00e+06  3.00e+06      0.22      0.22      0.22
  1.23e+06  1.23e+06  1.23e+06       0.0       0.0     140.0
    9590.0    9590.0    9590.0     430.0     430.0     430.0
    1170.0    1170.0    1170.0
       0.0       0.0     291.0     190.0
  (4) Blackhawk formation
  4.00e+06  4.00e+06  4.00e+06      0.26      0.26      0.26
  1.59e+06  1.59e+06  1.59e+06       0.0       0.0     155.0
   15710.0   15710.0   15710.0     720.0     720.0     720.0
    1942.0    1942.0    1942.0
       0.0       0.0     481.0     591.0
 (5) Hiawatha coal
 0.430e+06 0.430e+06 0.430e+06      0.12      0.12      0.12
 0.192e+06 0.192e+06 0.192e+06       0.0       0.0      78.0
    4131.0    4131.0    4131.0     280.0     280.0     280.0
     621.0     621.0     621.0
       0.0       0.0    1072.0     10.0
  (6) Starpoint sandstone
  2.60e+06  2.60e+06  2.60e+06      0.22      0.22      0.22
  1.07e+06  1.07e+06  1.07e+06       0.0       0.0     135.0
    9630.0    9630.0    9630.0     360.0     360.0     360.0
    2140.0    2140.0    2140.0
       0.0       0.0    1082.0     200.0
  (7) Mancos Shale
  2.20e+06  2.20e+06  2.20e+06      0.35      0.35      0.35
 0.815e+06 0.815e+06 0.815e+06       0.0       0.0     145.0
   10300.0   10300.0   11920.0      60.0      60.0      60.0
     454.0     454.0     454.0
       0.0       0.0    1282.0     628.0
```

Figure 18 Stratigraphic column for barrier pillar analysis.

*Step 2 Mesh Generation*. Mesh generation example input is

| | |
|---|---|
| 1) the name of the material properties (stratigraphic column) file | *matTMg.txt* |
| 2) the number of main entries (NMS), | 5 |
| 3) entry and crosscut widths (WE, WC) | 20 20 (ft) |
| 4) pillar width and length (WP, LP) | 40 80 (ft) |
| 5) barrier pillar width (WB) | 150 (ft) |
| 6) element width, length, height (EX, EY, EZ) | 3 3 3 (ft) |
| 7) do gob effect? | Y or y =yes or N or n=no |
| 8) add-in additional stresses Sxx, Syy, Szz, Tyz, Tzx, Txy? | Y or y =yes or N or n=no |

Meshes for Problem 2 involving barrier pillars for protection of main entries are developed in much the same way as for Problem 1 involving main entries. In fact, mesh generation is done with the confines of the red rectangles shown in Figure 19. The planes of symmetry are used to avoid unnecessary element and node generation. The runstream file after some minor but necessary editing is given in Figure 20 which gives details such as the number of elements in the mesh and so forth.

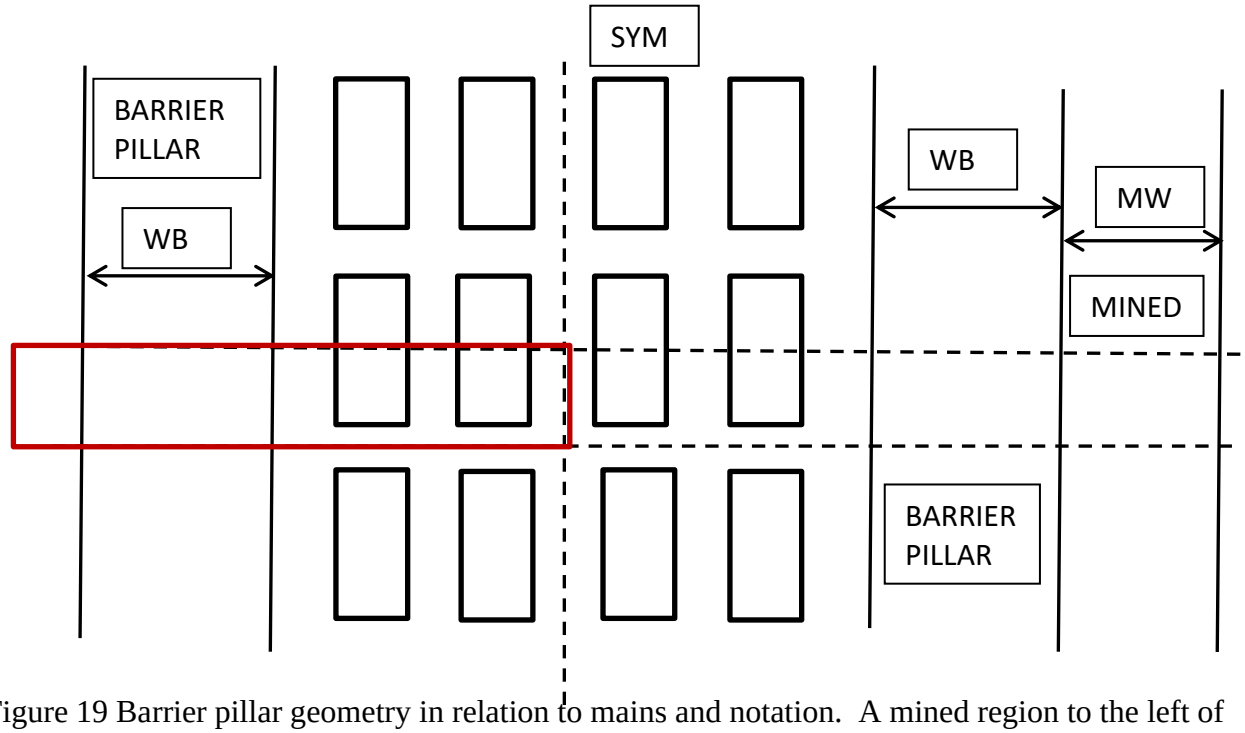


Figure 19 Barrier pillar geometry in relation to mains and notation. A mined region to the left of the left hand side barrier pillar is not shown but rather implied by the symmetry about the vertical centerline. Mesh extent is outlined in red, but not to scale. Although a 1 million element limit is highly recommended, there is some tolerance in this limit as the numbers in the runstream file suggest.

```
BARRIER PILLAR 1/16/2022 1/17/2022 no gob
F:\Visual Studio 2010\Projects\SPK\SPK\matTMg.txt
F:\Visual Studio 2010\Projects\SPK\GMB3\belms
F:\Visual Studio 2010\Projects\SPK\GMB3\bcrds
F:\Visual Studio 2010\Projects\SPK\GMB3\brcte
F:\Visual Studio 2010\Projects\SPK\GMB3\bsigi
F:\Visual Studio 2010\Projects\SPK\GMB3\bnsps
ABRn
nelem =  924336
nnode =  984409
nspec =  115879
nmat  =       7
ncut  =      -1
ninc  =       5
nsigo =       1
inter =     100
maxit =    1000
nyeld =       2
nelcf =    8944
nprb  =       2
nsol  =       2
mgob          0
 error=    1.0000
 orf  =    1.8600
 xfac =   12.0000
 yfac =   12.0000
 zfac =   12.0000
 efac =    1.0000
 cfac =    1.0000
torl% =    0.0100
ENDRUN
```

Figure 20 Runstream file for barrier pillar analysis first without gob and then with gob.

The finite element mesh is shown in Figure 21.

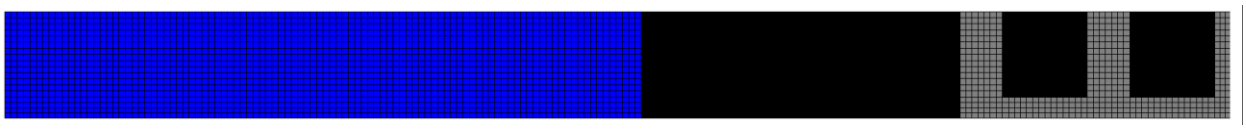

(a) plan view

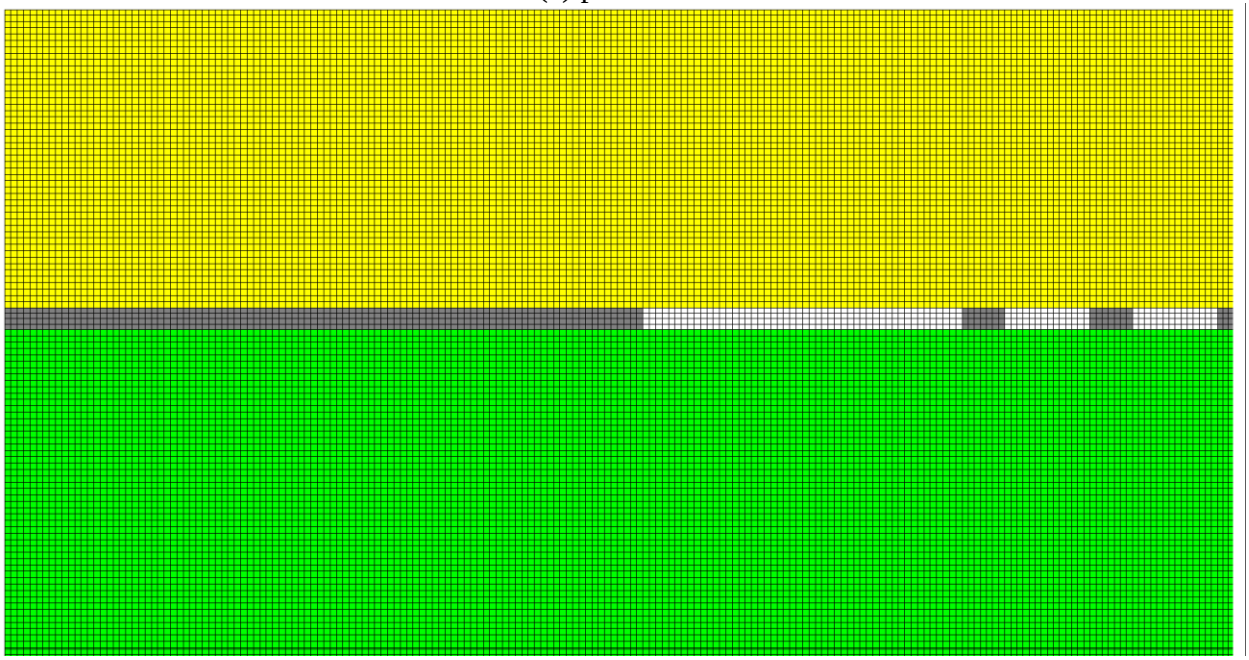

(b) vertical section close-up.

Figure 21 Plan and vertical section views of the mesh for a barrier pillar safety analysis. Only half of the five entry set is needed in the mesh. The blue elements to the left in plan view are excavated elements that may be air or gob. Grey elements define entry and crosscut regions. Black elements are coal in plan view, white in vertical section.

Results in the form of element safety factor distributions without and with gob present are given in Figure 22 in plan view at seam level and in Figure 23 in vertical section.

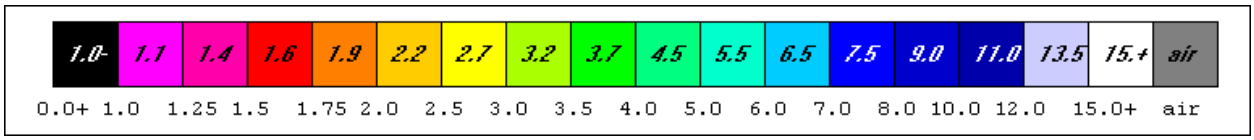


Element Safety Factor Color Scale

(a) without gob

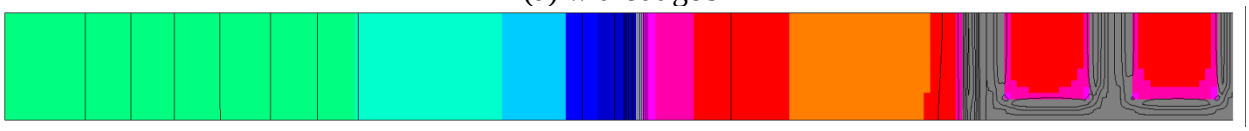

(b) with gob

Figure 22 Seam level element safety factors without gob (a) and with gob (b).

The results in the figures in comparison show no discernible effect of gob on main entry safety, although there is a small effect on the barrier pillar wall adjacent to the mined panel. The gob proper does not reach failure in this example.

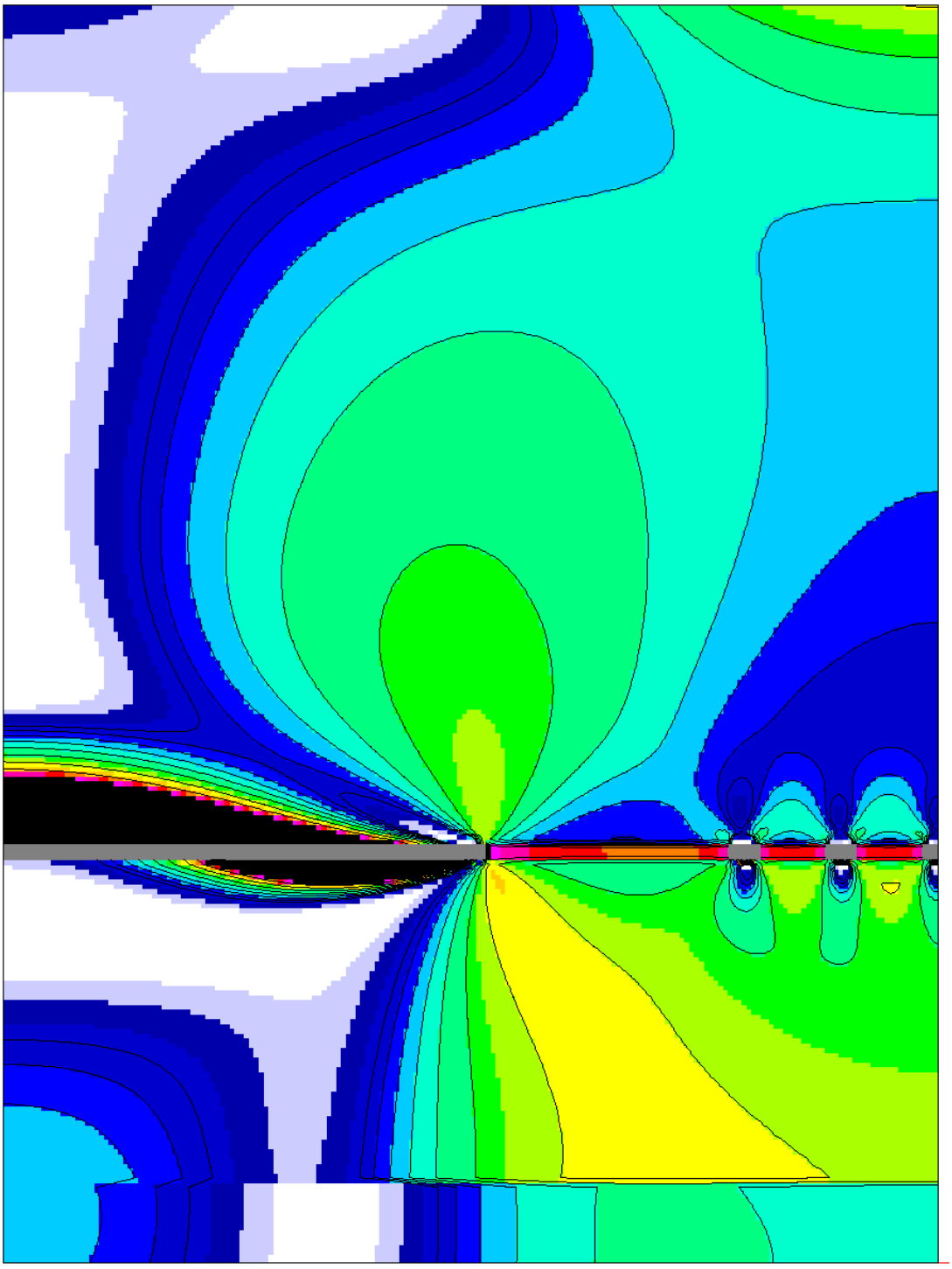

(a) without gob

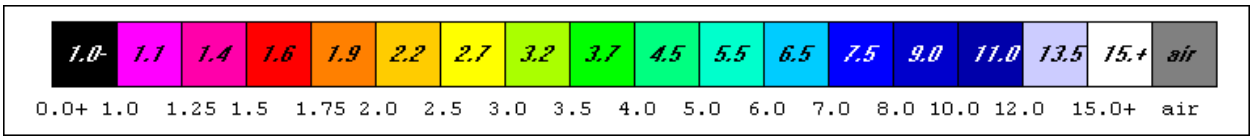


Element Safety Factor Color Scale

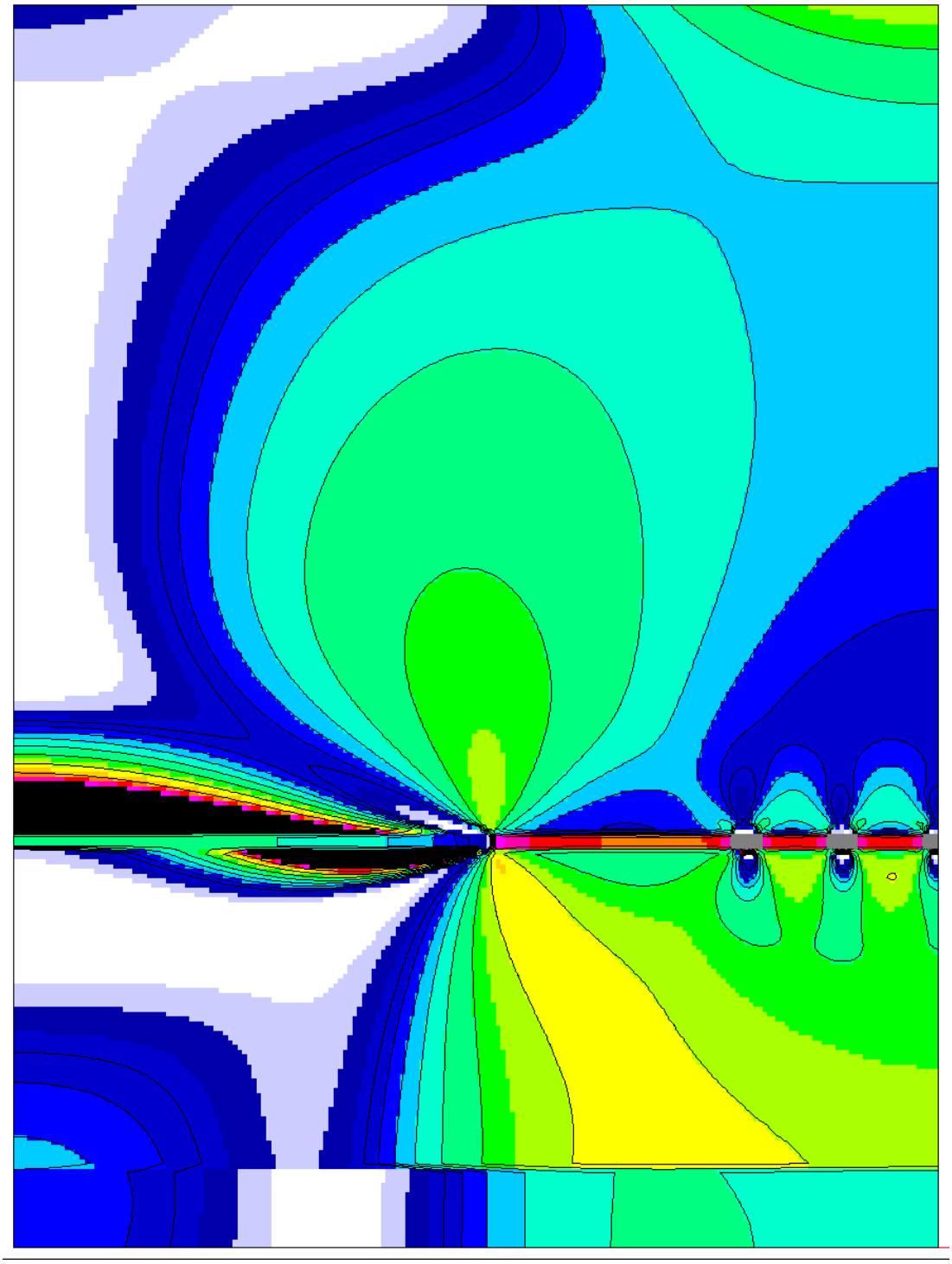

(b) with gob

Figure 23 Element safety factors in vertical section without gob (a) and with gob (b).

**Example 2** A second example of barrier pillar analysis relates to a deep, underground coal mine in the Western United States.

*Step 1 Preparation of a materials property file (stratigraphic column).* The material properties file is given in APPENDIX II and contains 32 layers. The thinnest layer is just 2 ft (0.6 m) thick. Many of the strata are quite weak with unconfined compressive strengths in the 1,000's of psi, an order of magnitude smaller than what one would expect of ordinary rock strata. These thin, weak strata yield readily and pose numerical challenges as the results show.

*Step 2 Mesh Generation*. Mesh generation example input is

| | | |
|---|---|---|
| ) the name of the material properties (stratigraphic column) file | *TES4new.txt* | |
| 2) the number of main entries (NMS), | 3 | |
| 3) entry and crosscut widths (WE, WC) | 20 20 | (ft) |
| 4) pillar width and length (WP, LP) | 170 180 | (ft) |
| 5) barrier pillar width (WB) | 300 | (ft) |
| 6) element width, length, height (EX, EY, EZ) | 4 4 2 | (ft) |
| 7) do gob effect? | Y or y =yes or N or n=no | |
| 8) add-in additional stresses Sxx, Syy, Szz, Tyz, Tzx, Txy? | Y or y =yes or N or n=no | |

The output file from the mesh generator for this problem is given in Figure 24. The element and node files exceed the file size limit but an exception was made to run the problem.

```
runstream title
TES4new.TXT
belms
bcrds
brcte
bsigi
bnsps
bp1
nelem = 2231736
nnode = 2333448
nspec =  195323
nmat  =      32
ncut  =      -1
ninc  =       5
nsigo =       1
inter =     100
maxit =    1000
nyeld =       2
nelcf =    25422
nsol  =       0
nprb  =       2
mgob..=       0
 error=    1.0000
 orf  =    1.8600
 xfac =   12.0000
 yfac =   12.0000
 zfac =   12.0000
 efac =    1.0000
 cfac =    1.0000
torl% =    0.0100
ENDRUN
```

Figure 24 Mesh generator output file for a barrier pillar analysis involving a 32 material layers. The mesh is shown in Figure 25. Symmetry allows viewing of only one-half the main entries and pillars.

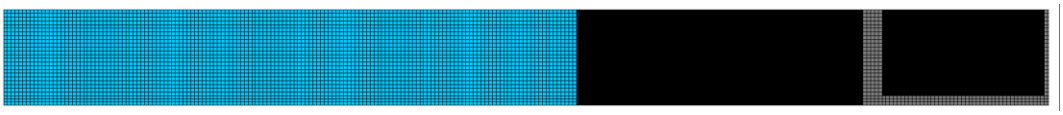

(a) plan view

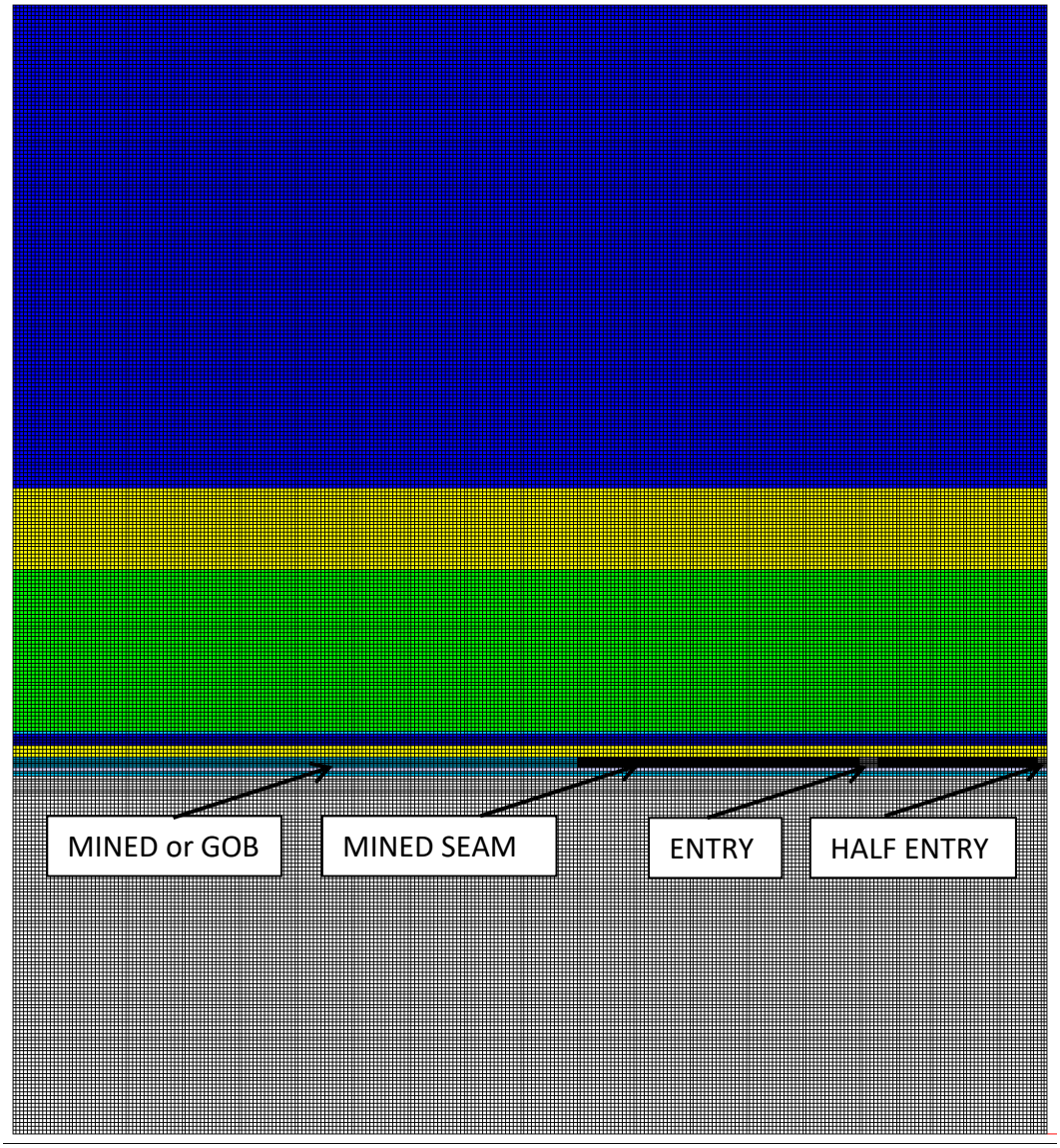


(b) vertical section

Figure 25 Plan and vertical section views of the mesh for a barrier pillar safety analysis. Only half of the three entry set is needed in the mesh. The blue elements to the left in plan view are excavated elements that may be air or gob. Grey elements define entry and crosscut regions. One half of the central entry (of three) does not show in these plots.

*Step 3 FEM Execution and Results* Figure 26 shows a plan view comparison of element safety factor distributions in this mine problem involving three main entries defended by a barrier pillar. Figure 27 shows element safety factor distribution in vertical section. Both indicate that the 300 ft (90 m) wide barrier pillar is inadequate for defending against high stress imposed by longwall panel mining outside the barrier pillar. This inference is made in noting that more than half the barrier pillar is yielding (black) and the remainder is close to failure with a safety factor 1.1 with the entry rib at failure. The entry pillar shows some failure near the entry crosscut intersection and shows low safety factors well into the pillar wall adjacent to the entry.

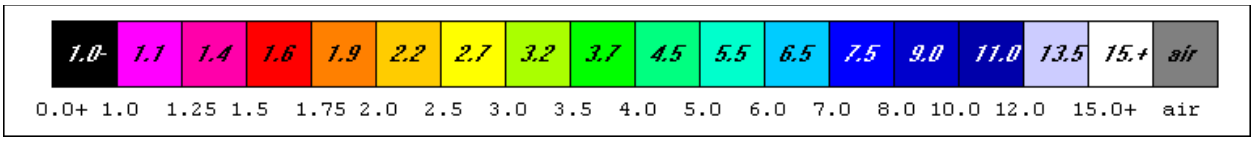


Element Safety Factor Color Scale

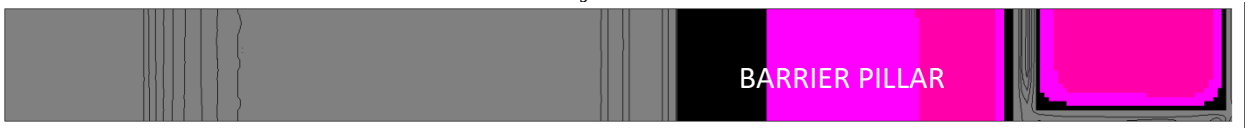


(a) plan view without gob

(b) plan view with gob

Figure 26 Plan view of element safety factor distribution for Problem 2 Mine B barrier pillar.

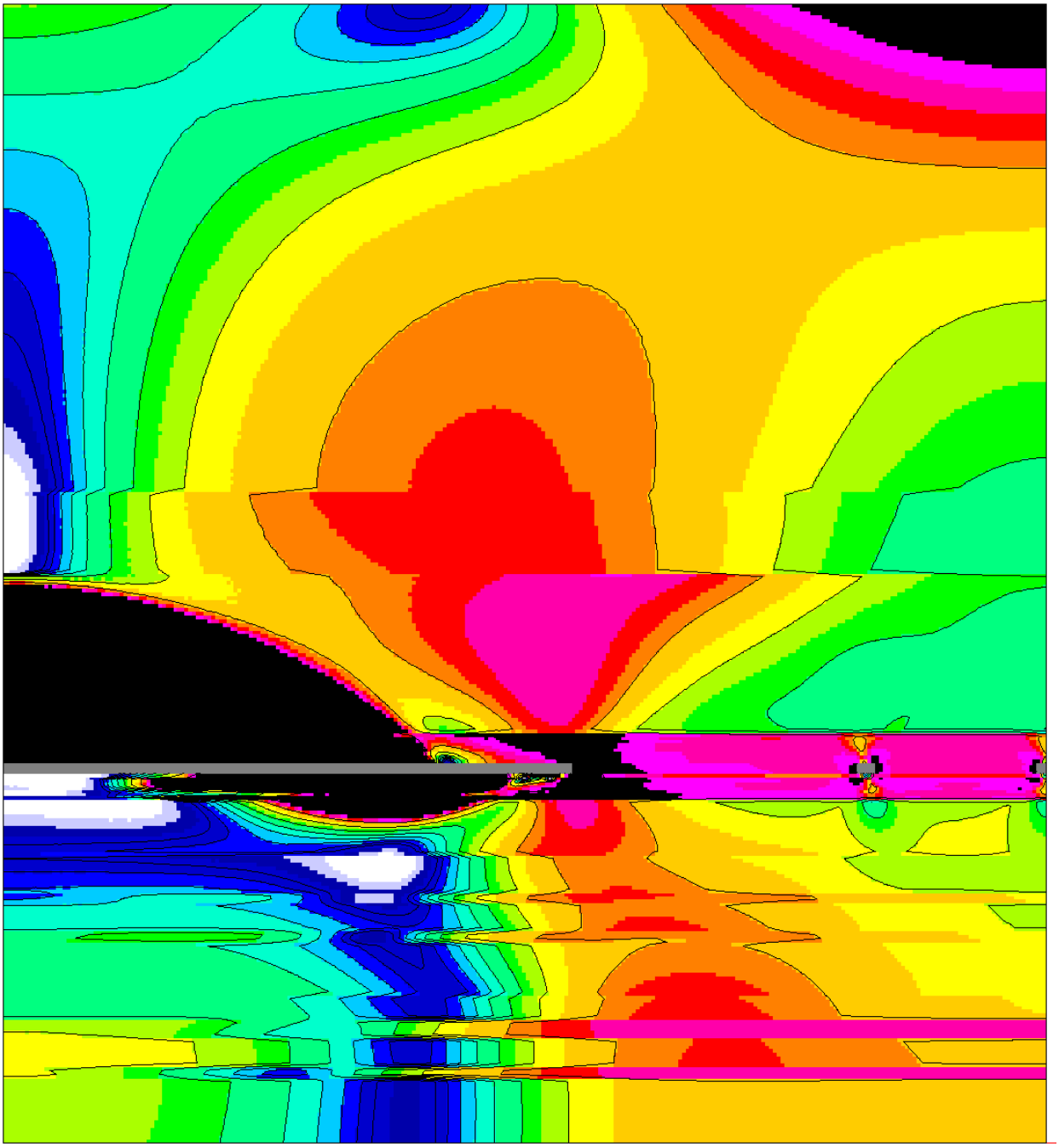

(a) vertical section with no gob

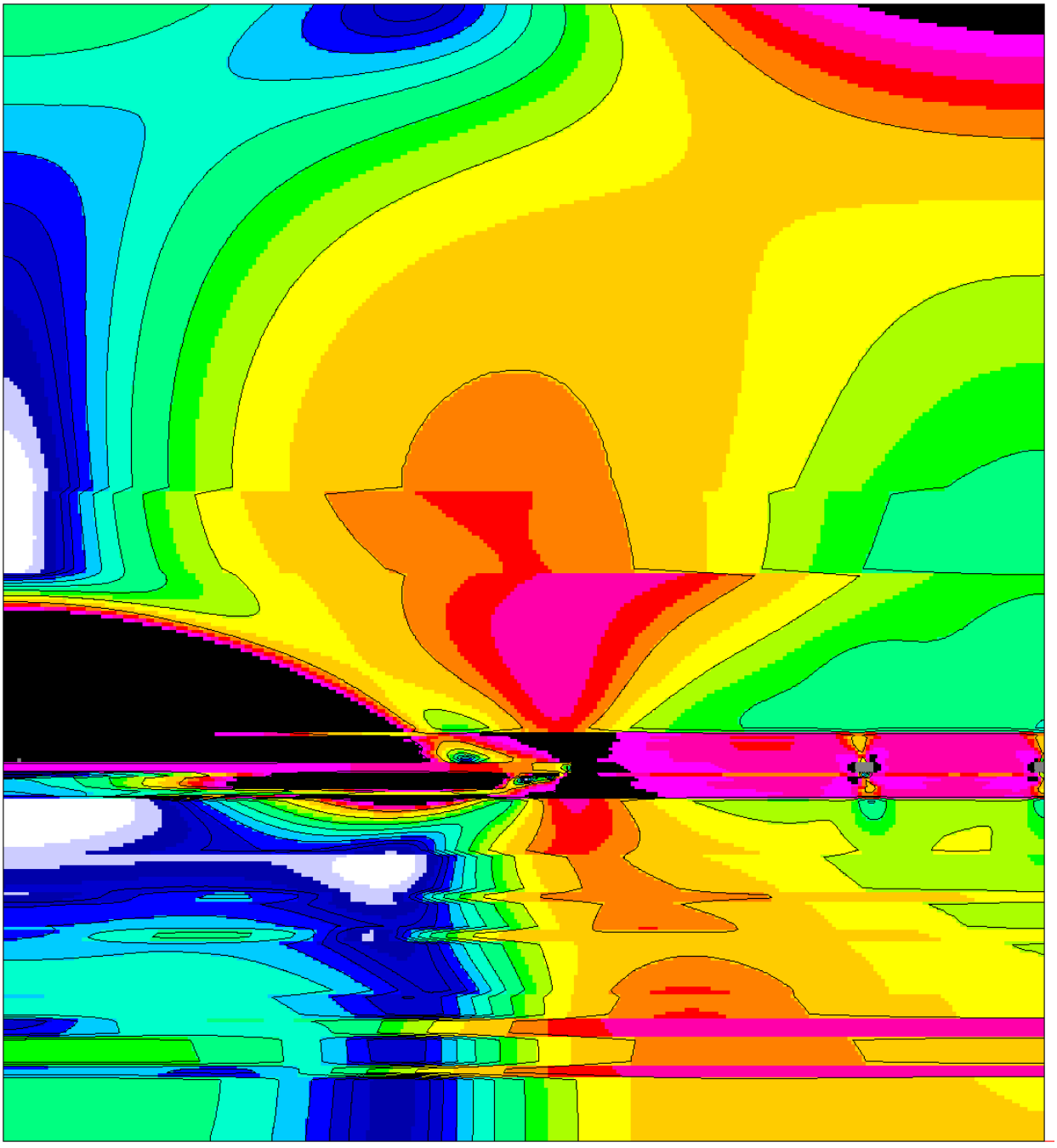

(b) vertical section with gob

Figure 27 Vertical section through pillar centers showing element safety factor distribution in Problem 2 Mine B barrier pillar analysis.

Figure 27 confirms inferences made from the seam level distribution of element safety factors. Extensive yielding is present above and below the longwall panel to the left of the barrier pillar. The floor contact of the barrier pillar is also a yielding zone. Interestingly, a large yield zone exists in the upper right hand side of the plot. This large black zone is associated with strata flexure and failure in horizontal tension.

Figure 28 provides close up views of element safety factors about the entry (grey) adjacent to the barrier pillar. Loading of the entry tends to be diagonal in the sense that a high compressive force acts across the entry (black to black), while unloading tends to occur at right angles (green to green). Overall, the presence of gob appears beneficial, but one concludes the barrier pillar fails (black) and is inadequate for entry protection.

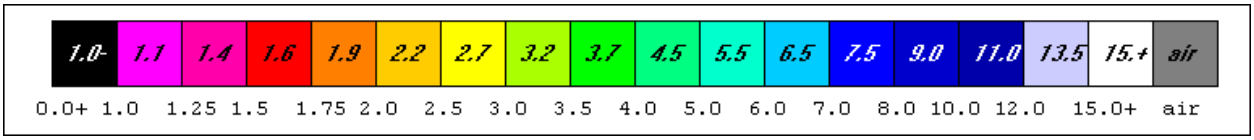


Element Safety Factor Color Scale

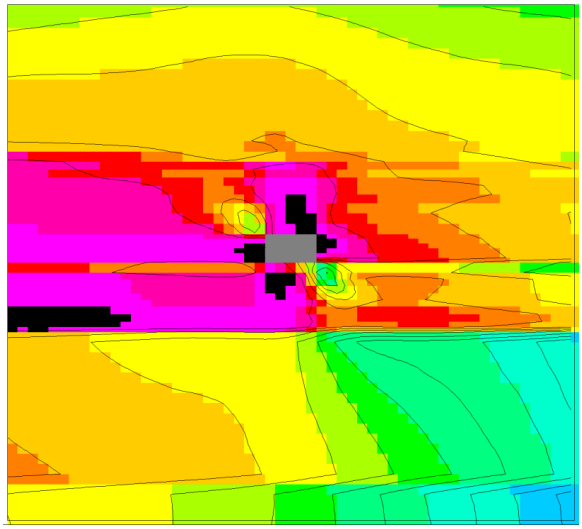

(a) no gob

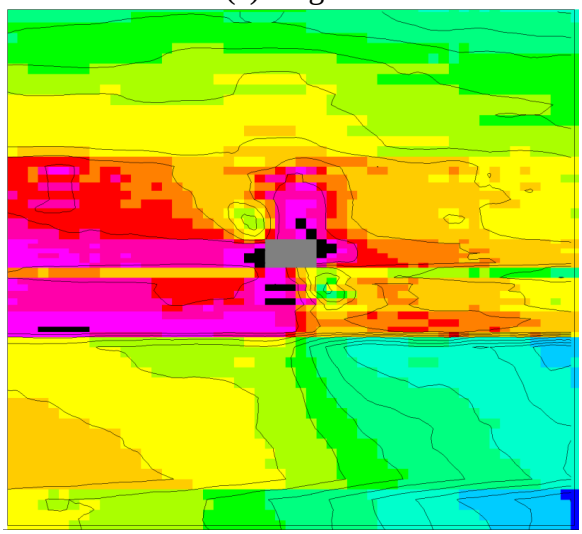

(b) with gob

Figure 28 Vertical section close-up of element safety factor distribution about an entry adjacent to a barrier pillar on the left hand side where a longwall panel is mined.

The erratic distribution of yielding elements in case of analysis with gob is caused by a lack of satisfactory convergence during equation solving. Although not evident in case of analysis without gob present, the same lack of satisfactory convergence occurred. The difficulty is in the nature of the problem involving thin and quite weak strata. Use of the alternative equation solver, Gauss-Seidel iteration (nsol-0) instead of the conjugate gradient solver (nsol=2) converges monotonically but the iterative improvement diminishes until the residuals decrease extremely slowly increasing run times to impractical lengths (days!). Combining thin strata, say strata less than three ft ( 1m) thick would perhaps aid in obtaining satisfactory convergence in a reasonable time (overnight turn-around time?). Whether the strata strengths are realistic is a question that should be revisited, too. In this regard, application of some other computer program such as FLAC3D, Elfin or Abaqus would be of interest and certainly worthy of study.

A test of the hypothesis that weak gob was the source of ill-conditioning of the system and consequently unsatisfactory convergence was done via a rerun of this second barrier pillar problem. This change is easily done increasing gob strength by a factor of 10. Results of the strong gob reanalysis are summarized in Figures 29, 30 and 31 showing element safety factors in plan view, vertical section and in close up (vertical section), respectively. These results indicate gob strength (weakness) was mainly responsible for lack of satisfactory convergence.

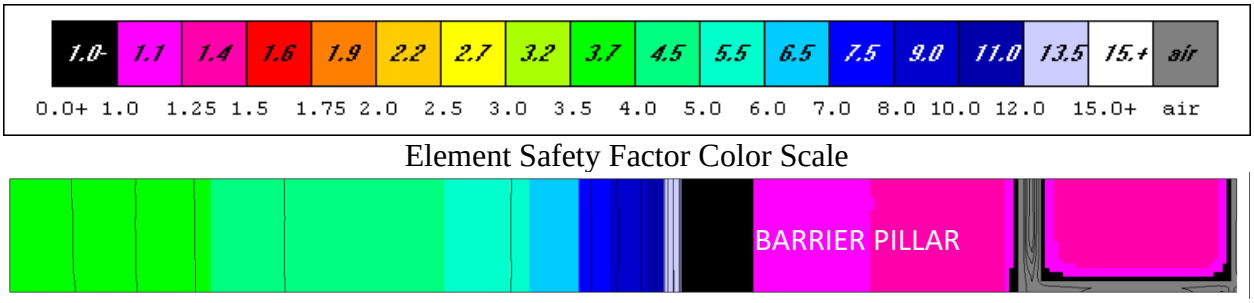

Figure 29 Element safety factor distribution in plan view at seam level with strong gob.

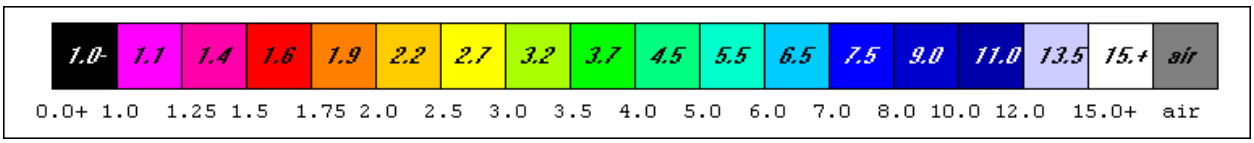


Element Safety Factor Color Scale

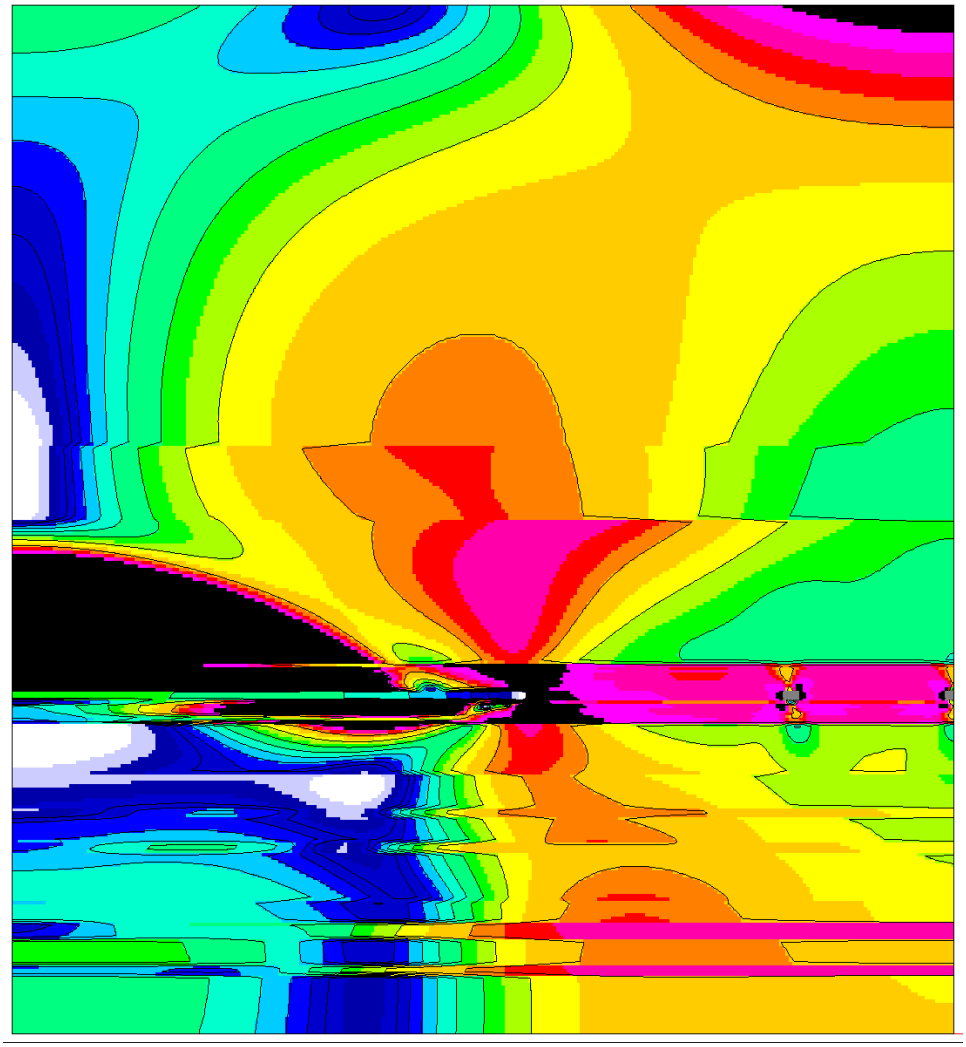

Figure 30 Element safety factor distribution in vertical section with strong gob.

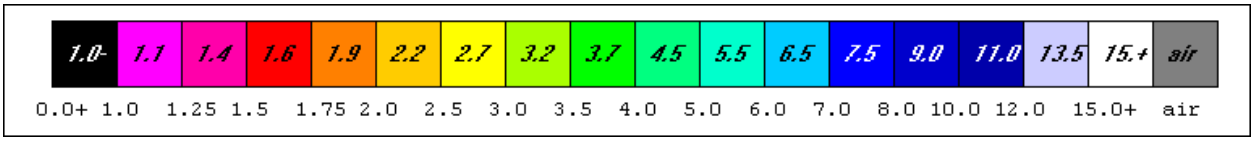


Element Safety Factor Color Scale

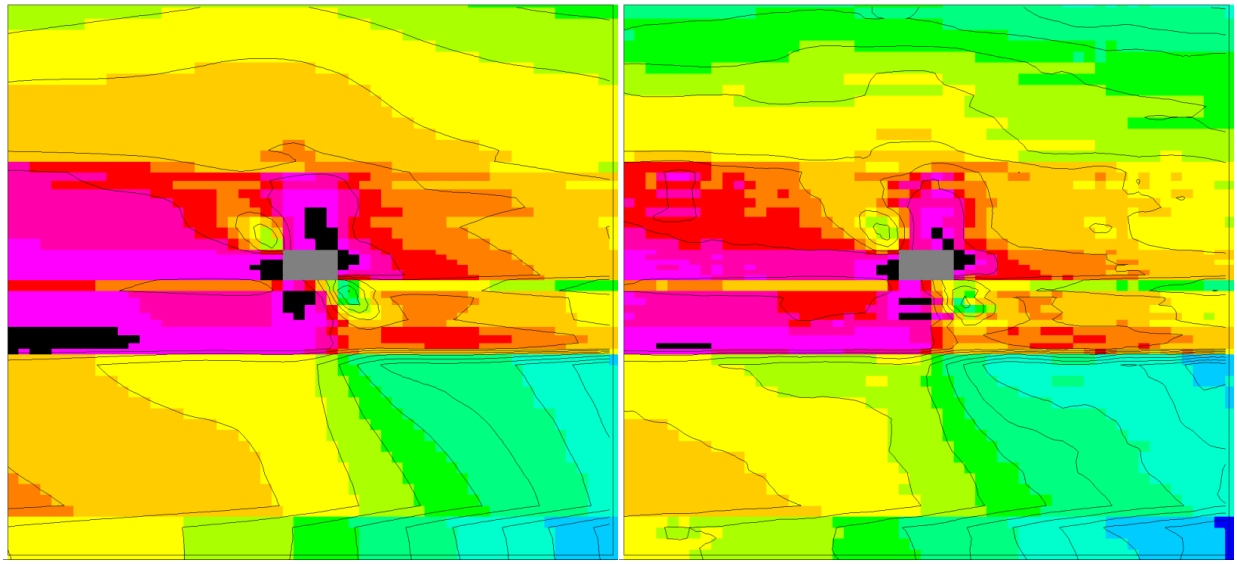

(a) no gob (b) weak gob

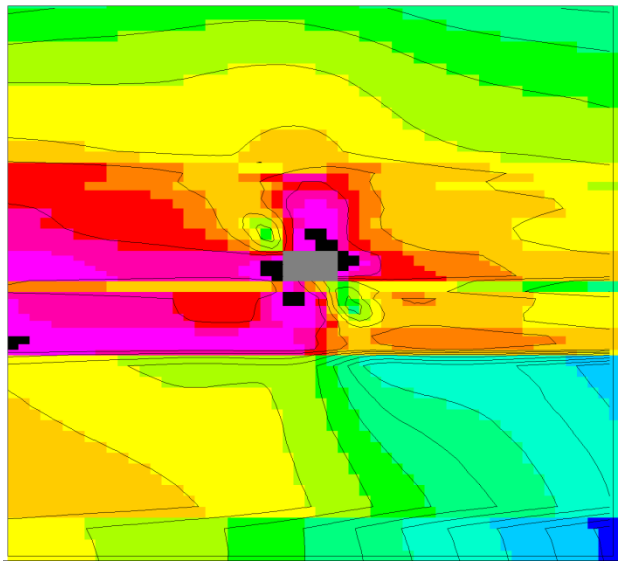

(c) strong gob

Figure 31 Element safety factor distributions about an entry protected by a barrier pillar.

## 3 BLEEDER ENTRIES

Effects of gob are included in a first example for comparison in this study. A second example from the original work is included. As usual, the process proceeds in three steps.

**Example 1** This example relates to an underground coal mine in the Wasatch Plateau coal field of central Utah.

*Step 1 Preparation of a materials property file (stratigraphic column).* The materials property file for this problem is given in Figure 32.

```
NLYRS = 7
NSEAM = 5
  (1) North Horn  N=2 (DP2) & wt, 2000-11000, 1/16/2017, 2/3/2022
  2.60e+06  2.60e+06  2.60e+06      0.26      0.26      0.26
  1.03e+06  1.03e+06  1.03e+06       0.0       0.0     158.0
   11800.0   11800.0   11800.0     700.0     700.0     700.0
    1659.0    1659.0    1659.0
       0.0       0.0     100.0
  (2) Price River
  3.20e+06  3.20e+06  3.20e+06      0.26      0.26      0.26
  1.27e+06  1.27e+06  1.27e+06       0.0       0.0     143.0
    9980.0    9980.0    9980.0     380.0     380.0     380.0
    1124.0    1124.0    1124.0
       0.0     100.0     191.0
  (3) Castle Gate sandstone
  3.00e+06  3.00e+06  3.00e+06      0.22      0.22      0.22
  1.23e+06  1.23e+06  1.23e+06       0.0       0.0     140.0
    9590.0    9590.0    9590.0     430.0     430.0     430.0
    1170.0    1170.0    1170.0
       0.0     291.0     190.0
  (4) Blackhawk formation
  4.00e+06  4.00e+06  4.00e+06      0.26      0.26      0.26
  1.59e+06  1.59e+06  1.59e+06       0.0       0.0     155.0
   15710.0   15710.0   15710.0     720.0     720.0     720.0
    1942.0    1942.0    1942.0
       0.0     481.0     591.0
 (5) Hiawatha coal
 0.430e+06 0.430e+06 0.430e+06      0.12      0.12      0.12
 0.192e+06 0.192e+06 0.192e+06       0.0       0.0      78.0
    4131.0    4131.0    4131.0     280.0     280.0     280.0
     621.0     621.0     621.0
       0.0    1072.0     10.0
  (6) Starpoint sandstone
  2.60e+06  2.60e+06  2.60e+06      0.22      0.22      0.22
  1.07e+06  1.07e+06  1.07e+06       0.0       0.0     135.0
    9630.0    9630.0    9630.0     360.0     360.0     360.0
    2140.0    2140.0    2140.0
       0.0    1082.0     200.0
  (7) Mancos Shale
  2.20e+06  2.20e+06  2.20e+06      0.35      0.35      0.35
 0.815e+06 0.815e+06 0.815e+06       0.0       0.0     145.0
   10300.0   10300.0   11920.0      60.0      60.0      60.0
     454.0     454.0     454.0
       0.0    1282.0     628.0
```

Figure 32 Materials property file for bleeder entry analysis.

*Step 2 Mesh Generation.* Mesh generation input is entered interactively and is

| | |
|---|---|
| 1) the name of the material properties (stratigraphic column) file | *matTMg.txt* |
| 2) the number of panel entries (NBS), | 3 |
| 3) entry and crosscut widths (WE, WC) | 20 20 (ft) |
| 4) pillar width and length (WP, LP) | 40 80 (ft) |
| 4) element width, length, height (EX, EY, EZ) | 3 3 3 (ft) |
| 6) do gob effect? | Y or y =yes or N or n=no |
| 7) add-in additional stresses Sxx, Syy, Szz, Tyz, Tzx, Txy? | Y or y =yes or N or n=no |

In case of Problem 3 "bleeder entries", a solid region exists parallel to the entries; a mined panel also exists adjacent to the bleeder entries as shown in Figure 33. The red rectangle indicates the extent of mesh generation in plan view. As before symmetry is used to reduce the digital size of the mesh.

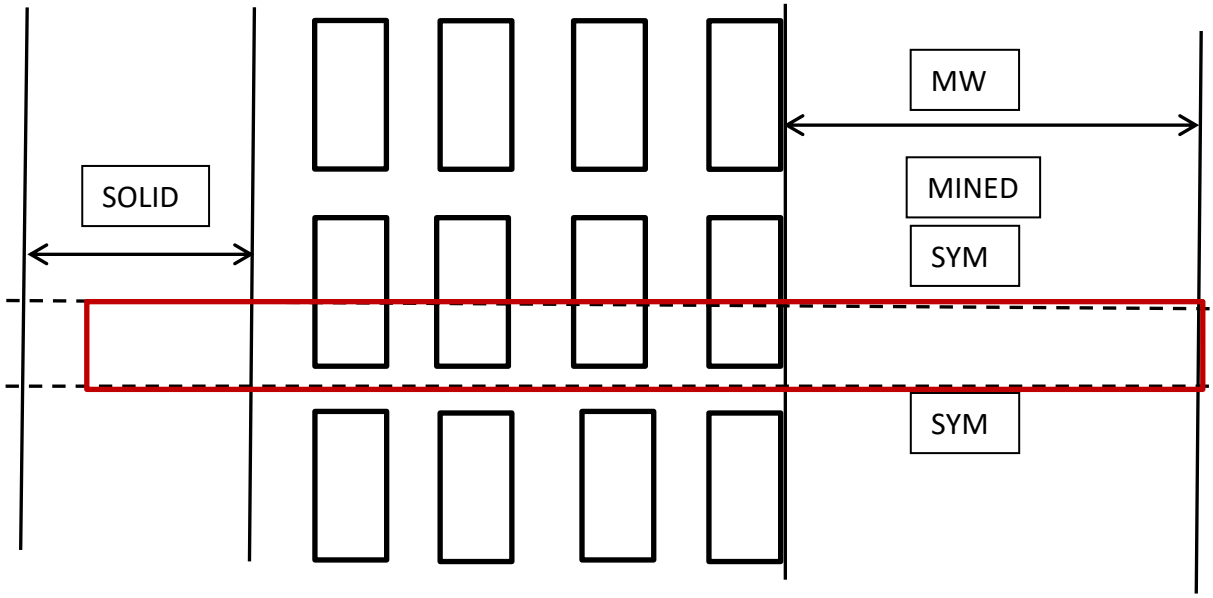


Figure 33 Bleeder entry geometry with unmined ground to the left side of the figure and a panel being mined to the right side of the figure. Mesh extent is indicated in red, but not to scale.

The runstream file for this analysis after some editing is shown in Figure 34. Results of mesh generation are illustrated in Figure 35. Thick formations exist above and below the coal seam of interest as seen in the material properties file and the vertical mesh section.

```
BLEEDER retest 3 3 3 8/12/2019 2/3/2022 psi no gob wgp
F:\Visual Studio 2010\Projects\SPK\GMB3\matTMg.txt
F:\Visual Studio 2010\Projects\SPK\GMB3\belms
F:\Visual Studio 2010\Projects\SPK\GMB3\bcrds
F:\Visual Studio 2010\Projects\SPK\GMB3\brcte
F:\Visual Studio 2010\Projects\SPK\GMB3\bsigi
F:\Visual Studio 2010\Projects\SPK\GMB3\bnsps
ABL
nelem =  955962
nnode = 1018020
nspec =  119944
nmat  =       7
ncut  =      -1
ninc  =       5
nsigo =       1
inter =     100
maxit =    2000
nyeld =       2
nelcf =    7000
nsol  =       2
nprb  =       3
mgob  =       0
 error=     0.000
 orf  =     1.860
 xfac =     12.00
 yfac =     12.00
 zfac =     12.00
 efac =      1.00
 cfac =      1.00
tolr% =      0.01
ENDRUN
```

Figure 34 Runstream file after editing output from the mesh generation process.

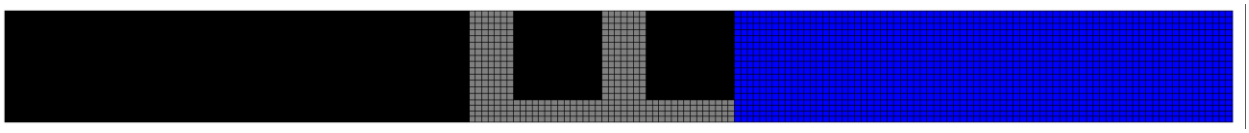

(a) plan view

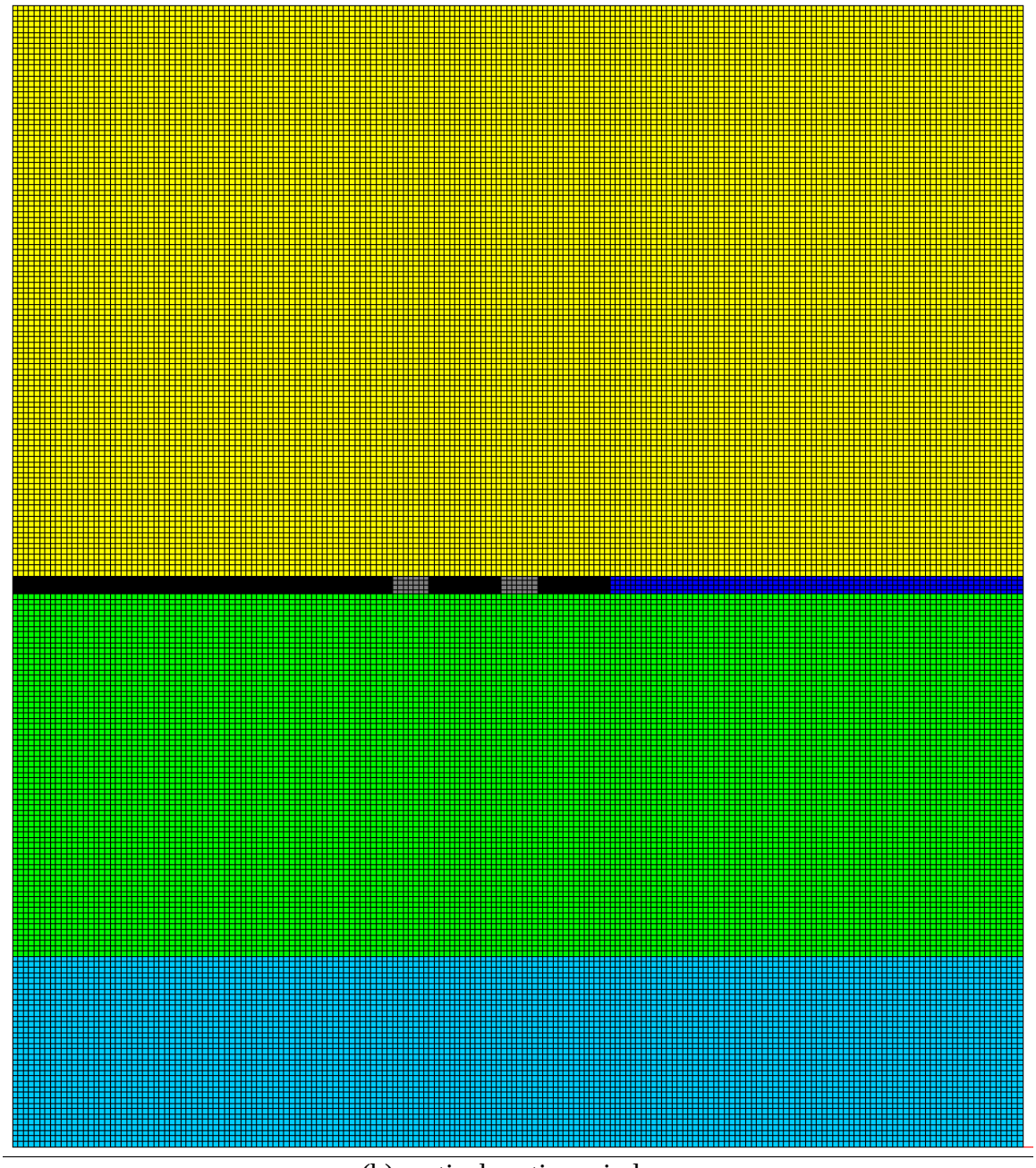

(b) vertical section window

Figure 35 Plan view and vertical sections of a three-dimensional mesh generated for bleeder entry safety analysis. Black=coal, grey=excavated elements, dark blue (seam level)=excavated elements or gob elements as the case may be.

*Step 3 FEM Execution and Results*. Figure 36 shows element safety factor distributions in plan view at seam level with no gob and with gob effects. Element boundaries are removed in the plots for ease of viewing. The contours have zig-zags induced by changes in material properties at strata boundaries.

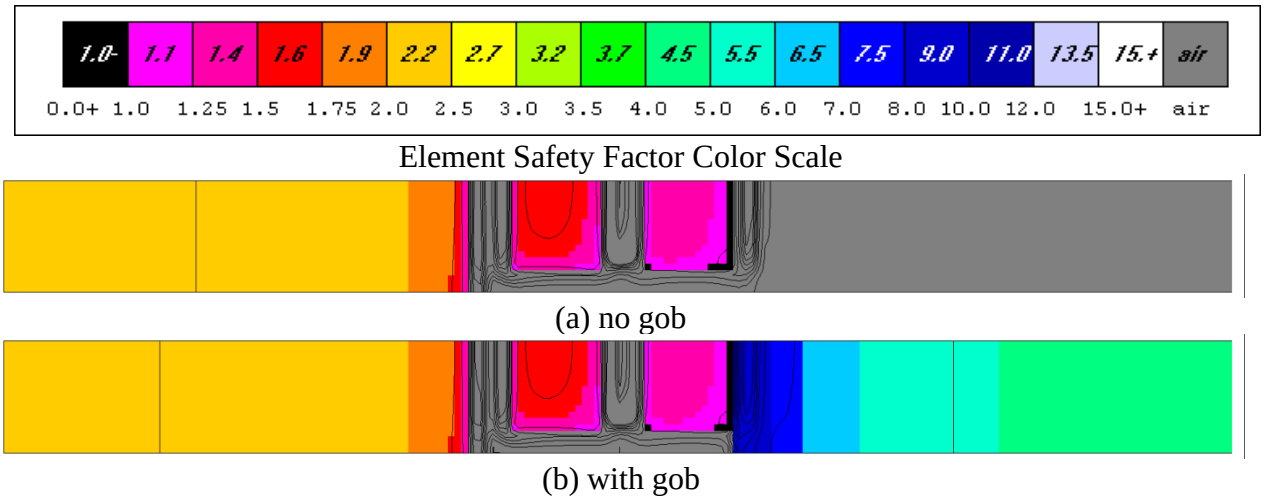


Figure 36 Element safety factor distributions in plan view at seam level in case a bleeder entry safety analyses: (a) no gob, (b) with gob. The coal seam is 10 ft (3 m) thick. Contours show gradation within color ranges.

Figure 37 provides for comparisons in vertical sections without and with gob relative to distributions of element safety factors near the bleeder entries. Again, the seam thickness (grey) is 10 ft (3 m). Elements are roughly 2.5 ft (0.75 m) cubes.

Figures 38 and 39 are close up views in vertical section of element safety factor distribution in case of no gob and with gob present, respectively. There are four element "layers" through the seam which gives a reasonable stress distribution from roof to floor. This size is evident in the roof and floor elements especially over and below the mined panel to the left (grey). The pillar nearest the mined panel shows low safety factors (pink, red, 1.2, 1.4) while the pillar near the solid on the right hand side shows higher safety factors with the core in orange (2.2). In fact, the pillar near the mined panel shows some yielding in the left hand side (black) near the pillar corner (also seen in plan view). The floor is a relatively strong stratum, a sandstone; no yielding is evident in the floor. However, there is considerable yielding in the roof over the mined region as seen in the large black area above the mined panel in the figures.

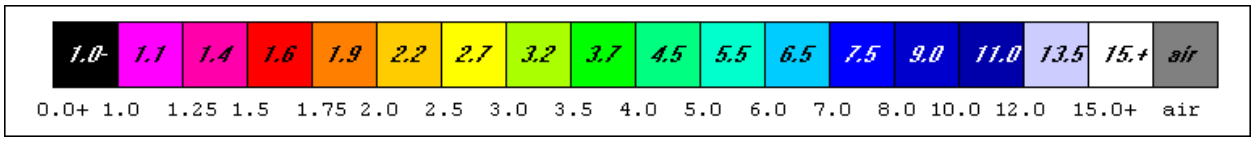


Element Safety Factor Color Scale

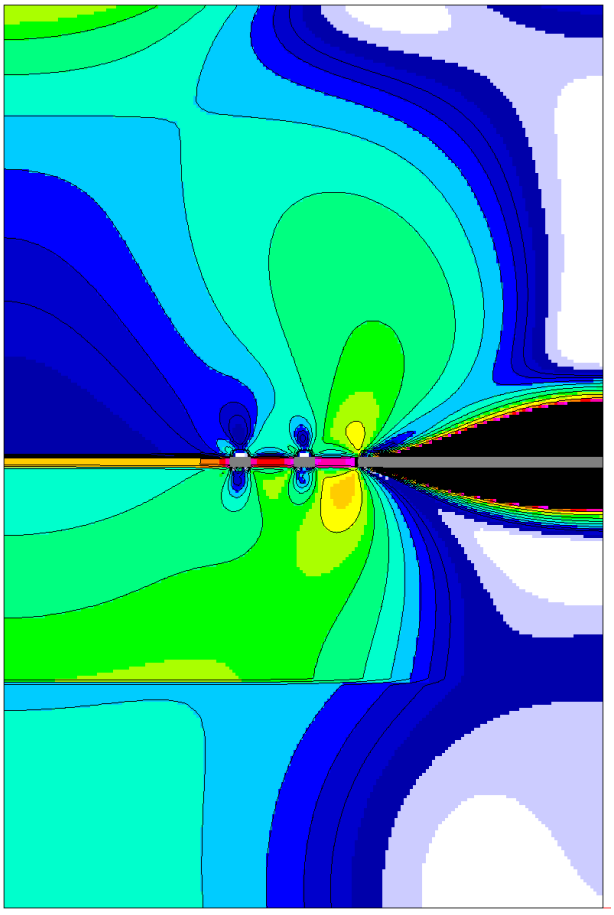

(a) no gob

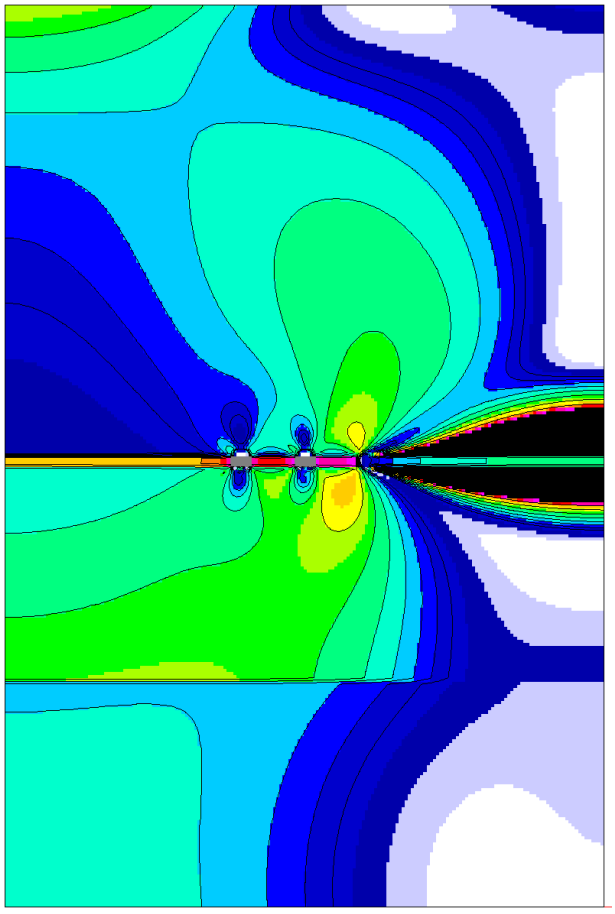

(b) with gob

Figure 37 Element safety factor distributions without gob (a) and with gob effects (b) in vertical sections in case of bleeder entry safety. The coal seam is 10 ft (3 m) thick. Gob is present to the right of the right side pillar.

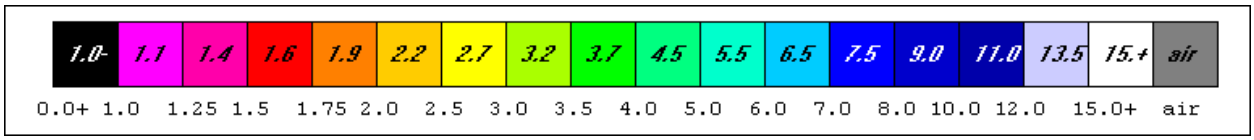


Element Safety Factor Color Scale

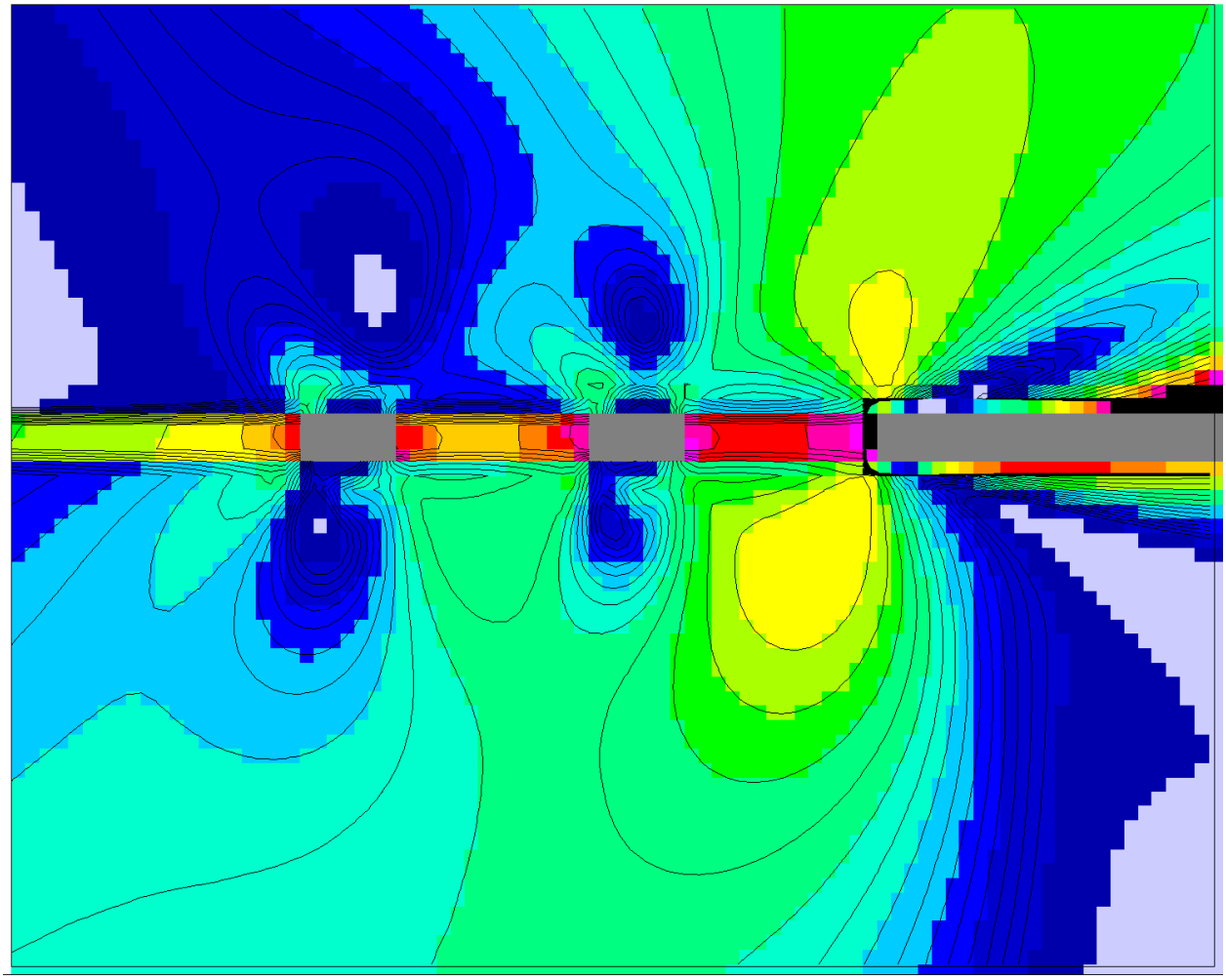

Figure 38 Close-up view of the element safety factor distribution in vertical section near the bleeder entries and pillars with no gob.

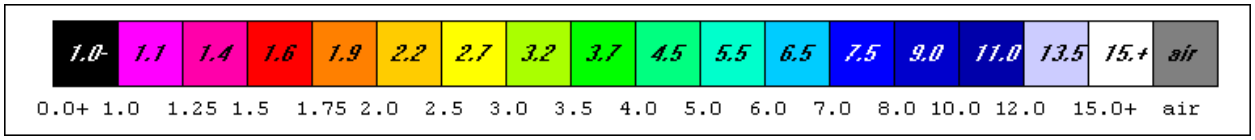


Element Safety Factor Color Scale

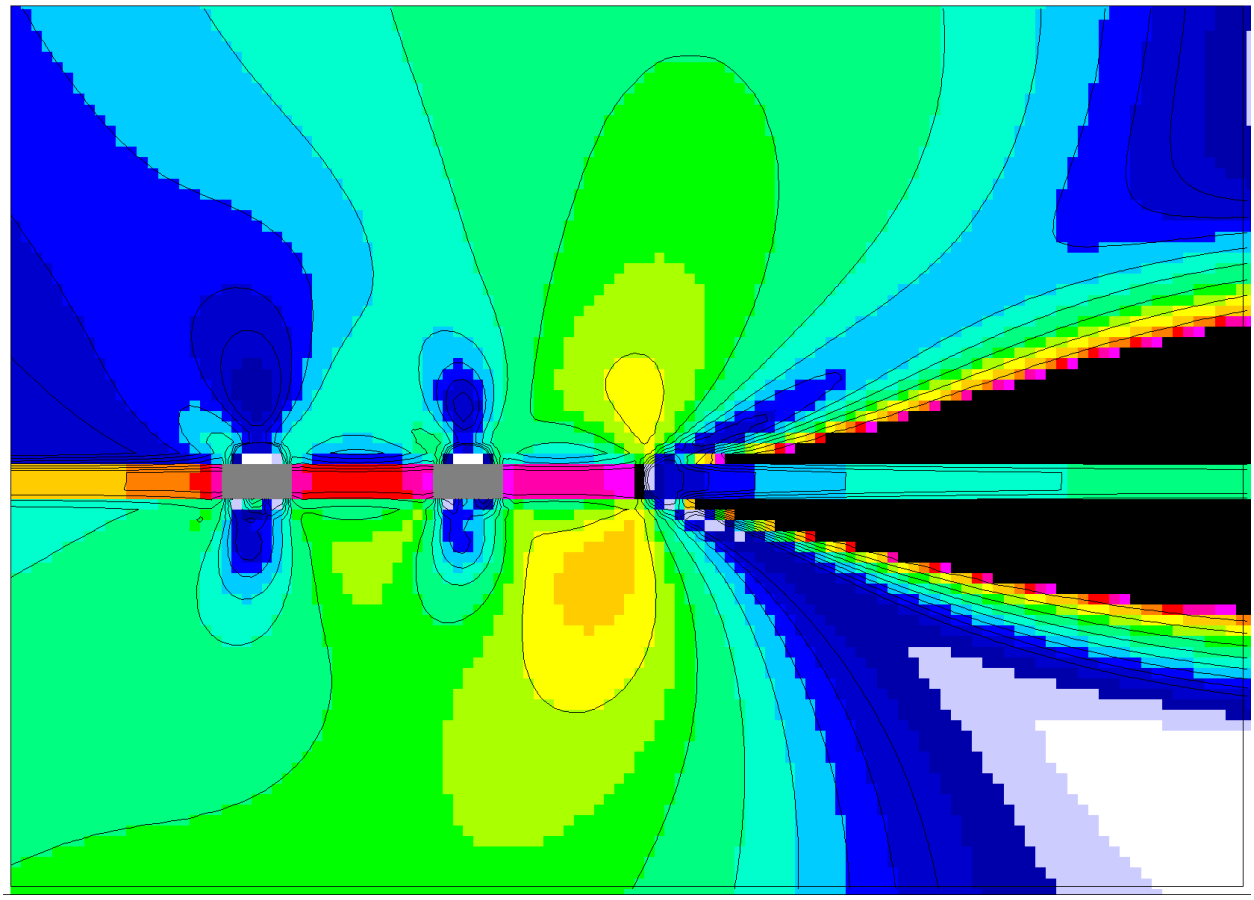

Figure 39 Close-up view of the element safety factor distribution in vertical section near the bleeder entries and pillars with gob present.

**Example 2** An example problem involving bleeder entry safety as a longwall panel advances away from the bleeder entries is Mine C. Mine C is an underground coal mine in the western United States but otherwise remains unidentified in this report. There are three main entries in this bleeder entry mine problem. As a reminder, bleeder entries are for ventilation and safety; they provide a secondary escape way from the mine. By law, bleeder entries must be maintained in a passable condition.

*Step 1 Preparation of a materials property file (stratigraphic column)* The problem input for "bleeder entries" mesh generation is given in Figure 1 in APPENDIX – II: BLEEDER ENTRIES. There are 26 layers in the geologic column; the 10$^{th}$ layer is the mined coal seam 11 ft (3.4 m) thick at a depth of 2,250 ft (686 m). The thinnest layer is 4 ft (1.2 m) thick. Order of strata is from the top down. As a reminder, the last line of each stratum properties set gives the

orientation, depth to the stratum top and stratum thickness. Depth to the top of the second stratum is simply the thickness of the first stratum as seen in the figure. Entries and crosscuts are 20 ft (6.1 m) wide. Pillars are 73x180 ft (22.3x54.9 m).

*Step 2 Mesh Generation* Mesh generation input is

| | |
|---|---|
| 1) the name of the material properties (stratigraphic column) file | TES3.*txt* |
| 2) the number of bleeder entries (NBS), | 3 |
| 3) entry and crosscut widths (WE, WC) | 20 20 (ft) |
| 4) pillar width and length (WP, LP) | 73 180 (ft) |
| 5) element width, length, height (EX, EY, EZ) | 8 8 4 (ft) |
| 6) do gob effect? | Y or y =yes or N or n=no |
| 7) add-in additional stresses Sxx, Syy, Szz, Tyz, Tzx, Txy? | Y or y=yes or N or n=no |

Figures 40 and 41 are plan and section views in case of a bleeder entry problem (but not Mine C). There are three bleeder entries in this example mesh. One entry is incorporated into the mined panel that extends to the right hand side of the figure (gray elements). Entries, crosscuts and pillars have the same dimensions as before. The color scheme is also the same as before.

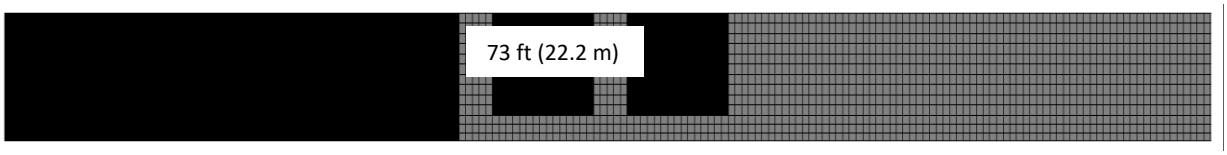


Figure 40 Seam level plan view of a three entry bleeder set after panel advance to the right (Problem 3). Pillars are 73 ft (22.2 m) wide.

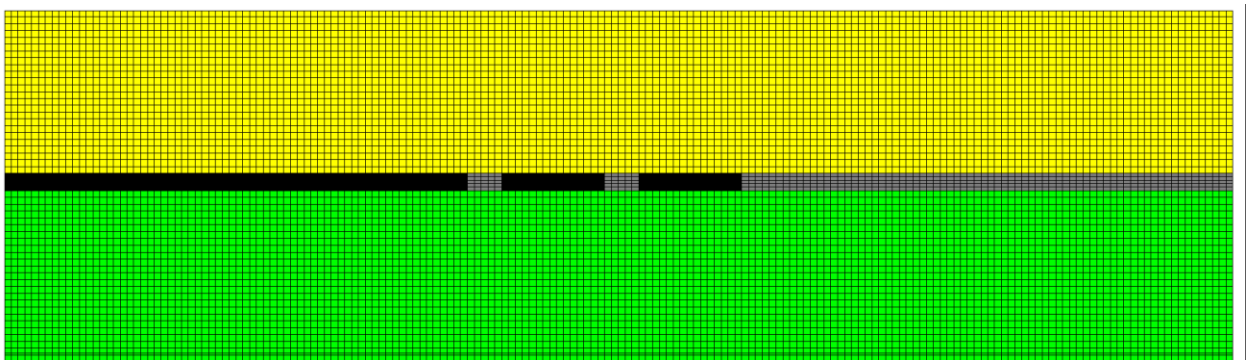

Figure 41 Vertical section close-up in case of Problem 3. Seam is 11 ft (3.3 m) thick and mined full height.

The output file from the mesh generator and input runstream file for finite element analysis of Mine C are given in Figures 42 and 43, respectively. The generated mesh is shown in Figure 44. There is a relatively small total number of elements in the mesh (188,748). Element aspect ratio is two. The mesh is 818 ft wide (249 m) and 100 ft (30 m) long. Mesh height is 1,236 ft (377 m).

```
runstream title
tes3.txt
belms
bcrds
brcte
bsigi
bnsps
bp1
nelem =  247170
nnode =  268920
nspec =   41550
nmat  =      26
ncut  =      -1
ninc  =       5
nsigo =       1
inter =     100
maxit =    1000
nyeld =       2
nelcf =    2136
nprb  =       3
nsol  =       0
mgob  =       0
 error=    1.0000
 orf  =    1.8600
 xfac =   12.0000
 yfac =   12.0000
 zfac =   12.0000
 efac =    1.0000
 cfac =    1.0000
tolr% =    0.0100
ENDRUN
```

Figure 42 Mesh generation output file.

```
TESARIK BLEEDERS 8/12/2019m 2/4/2022 wgp
F:\Visual Studio 2010\Projects\SPK\SPK\Tes3.txt
F:\Visual Studio 2010\Projects\SPK\GMB3\belms
F:\Visual Studio 2010\Projects\SPK\GMB3\bcrds
F:\Visual Studio 2010\Projects\SPK\GMB3\brcte
F:\Visual Studio 2010\Projects\SPK\GMB3\bsigi
F:\Visual Studio 2010\Projects\SPK\GMB3\bnsps
TES3
nelem =  247170
nnode =  268920
nspec =   41550
nmat  =      26
ncut  =      -1
ninc  =       5
nsigo =       1
inter =     100
maxit =    1000
nyeld =       2
nelcf =    2136
nprb  =       4
nsol  =       2
nprb  =       3
mgob  =       0
```

```
 error=    1.0000
 orf  =    1.8600
 xfac =   12.0000
 yfac =   12.0000
 zfac =   12.0000
 efac =    1.0000
 cfac =    1.0000
tolr% =    0.0100
ENDRUN
```

Figure 43 Finite element runstream file for the bleeder entry problem Mine C.

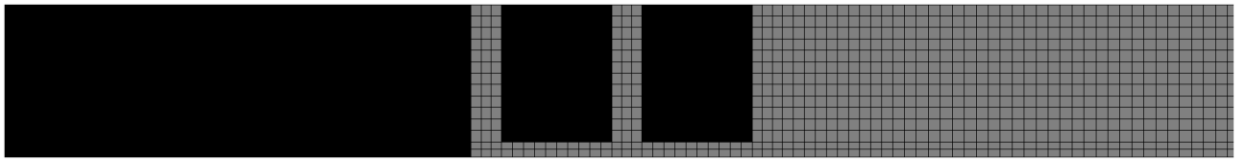

(a) Plan View

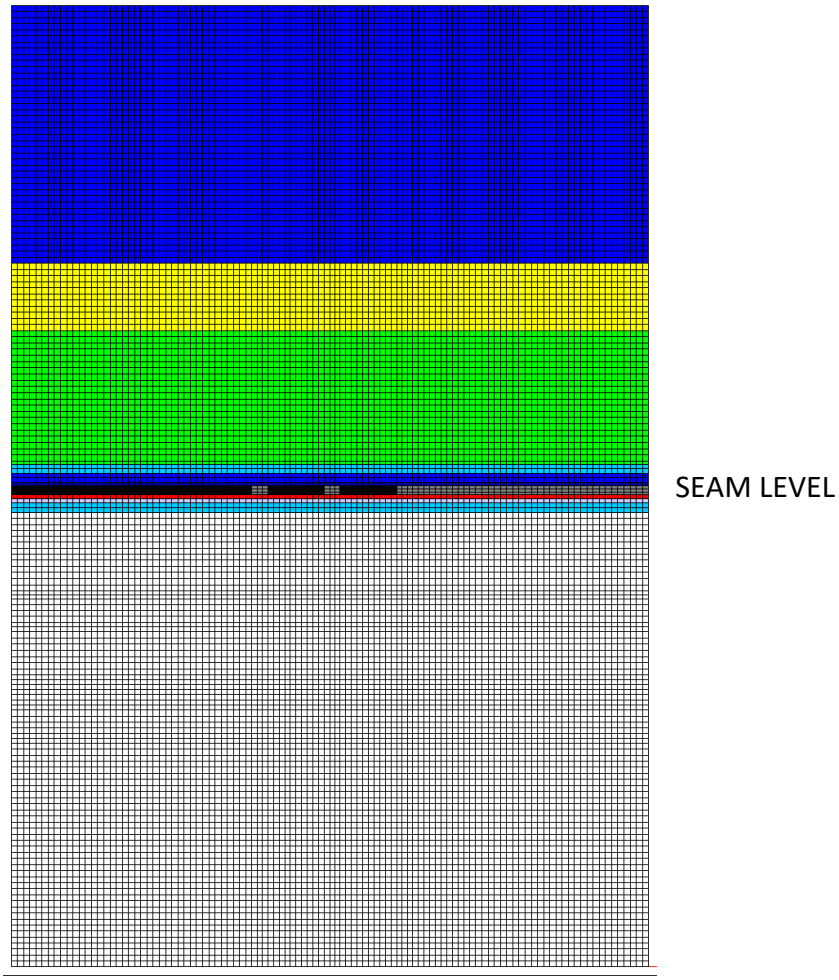


(b) Vertical Section

Figure 44 Finite element mesh in plan view (a) and vertical section (b) for analysis of bleeder entry safety. The mesh is 818 ft wide (249 m), 100 ft (30 m) long and 1,236 ft (377 m) high.

*Step 3 FEM Execution and Results* Run time for this mesh was 1-1/2 hrs. Plan and vertical section views of the distribution of element safety factors are shown in Figure 45. Element boundaries are shown. The plan view in the figure indicates yielding entry pillar ribs and pillar cores with low safety factors (*fs*<1.3). Indeed, the pillar adjacent to the longwall panel is yielding to the core. Entry ribs also show some yielding.

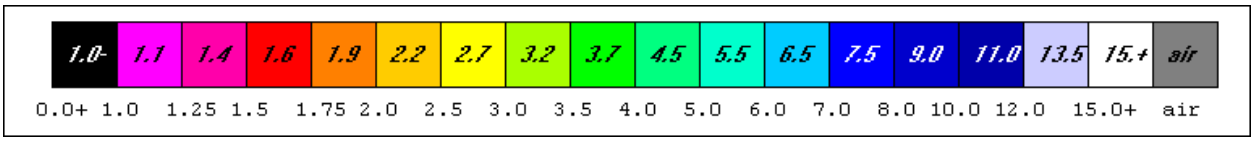


Element Safety Factor Color Scale

(a)

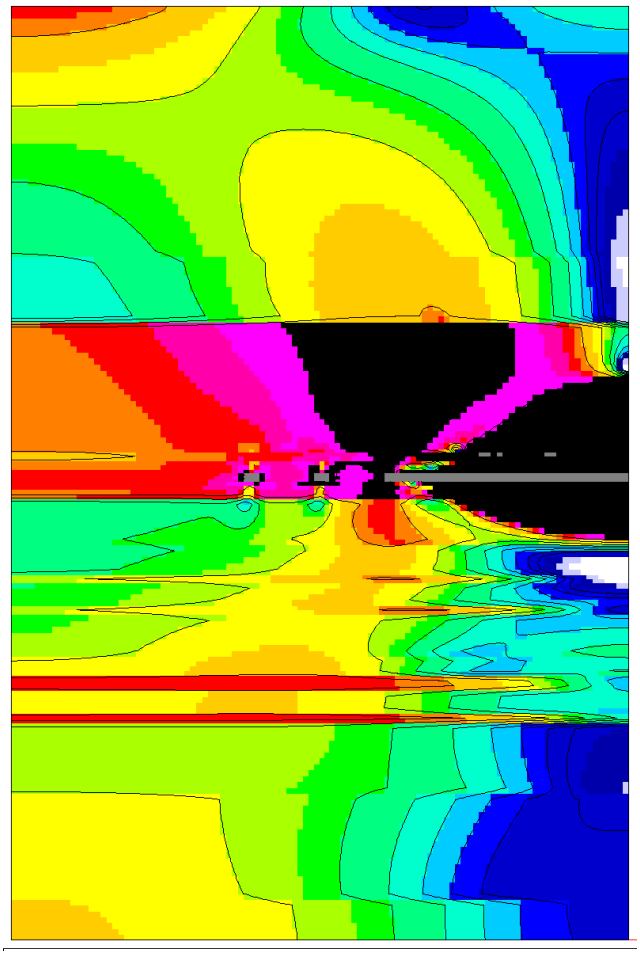

(b)

Figure 45 Element safety factor distributions in plan view (a) and vertical section (b) near bleeder entries with a long wall panel mined to the left (grey elements).

In vertical section, large zones of yielding extend above and below he longwall panel mined to the right. A large zone of yielding also extends above the left abutment of the panel and far into the roof where an abrupt termination of the yield zone occurs. Abrupt changes in contours are caused by abrupt change in strata properties that indirectly reveal stratigraphy. Floor yielding below the abutment corner is also indicated in vertical section. Low pillar safety factors are again indicated in vertical section where entry corners are yielding and threaten roof and floor safety.

A close-up vertical section in Figure 46 reveals more clearly the details of element safety factor distribution about the bleeder entries. Yielding is evident at entry ribs and corners where some yielding extends into the roof and floor. A suggestion of "diagonal" loading is present that is caused by mining the adjacent longwall panel. Pillars are under high stress as indicated by low safety factors in the pillar cores. The large yielding zone (black) that extends back over the abutment pillar threatens to extend retrograde over the bleeder entries in consideration of the large expanse of low safety factors over the entry adjacent to the abutment pillar.

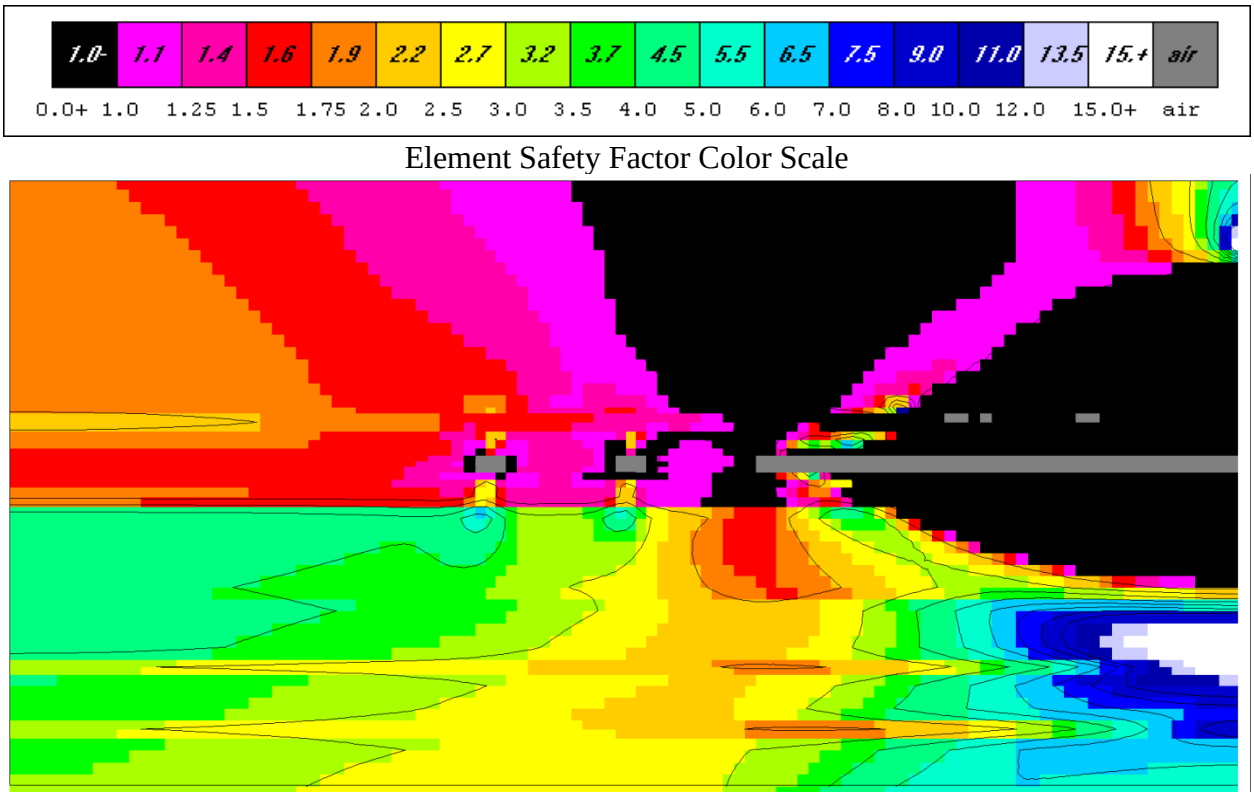

Element Safety Factor Color Scale

Figure 46 Close-up vertical section showing element safety factors about bleeder entries. Entries are 20 ft (6 m) wide and pillars are 73 ft (22 m) wide. Seam thickness is 11 ft (3.3 m).

Although the output from the finite element analysis is presented in two-dimensional views, the analysis is three-dimensional as seen in Figure 47 that shows the distribution of element safety factors overall. The grey area is excavated. Faces are planes of symmetry.

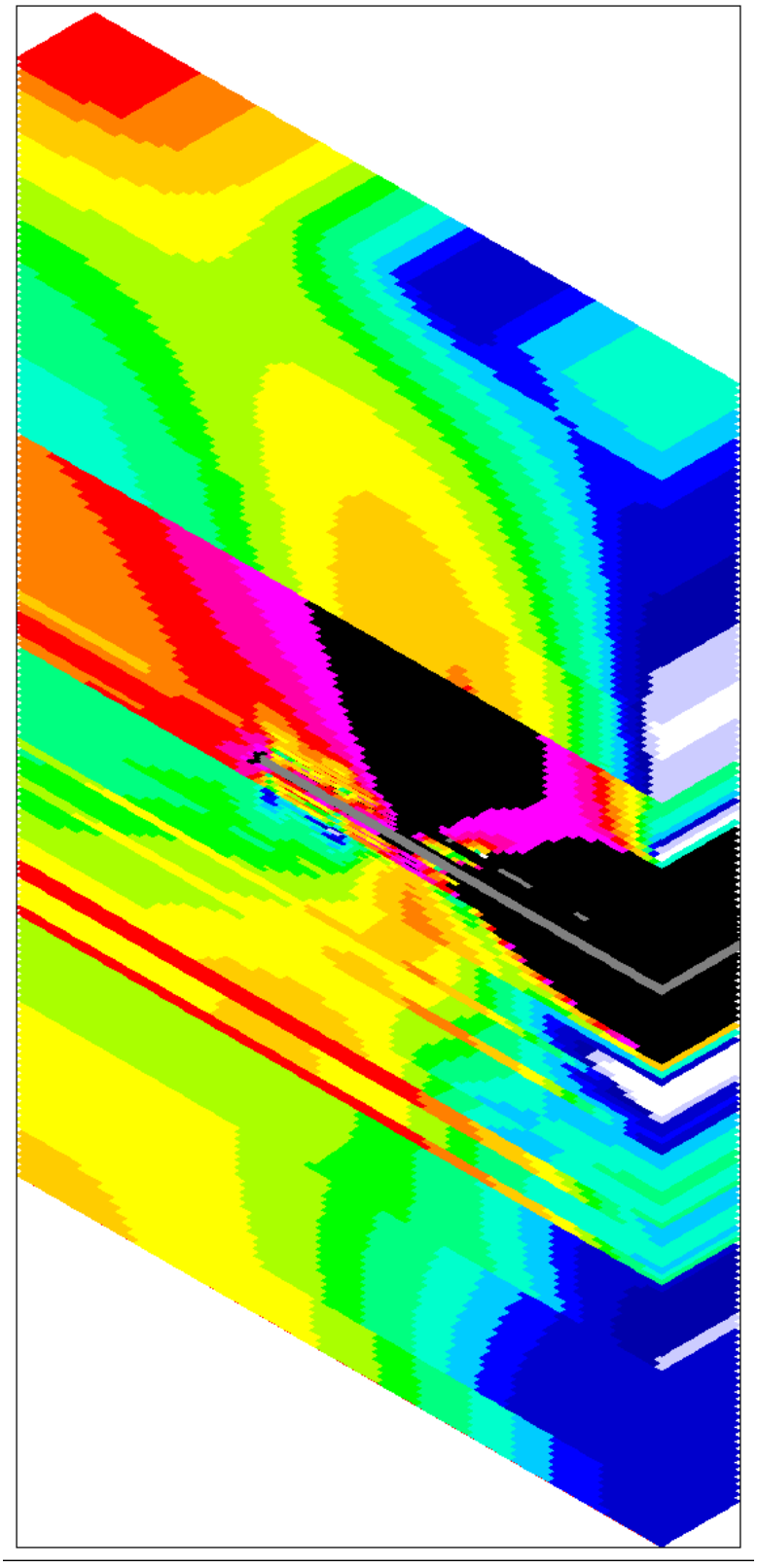

Figure 47 A three dimensional view of the distribution of element safety factors in the case of bleeder entries problem 3 Mine C.

The evidence from the finite element analysis in the form of safety factor distributions at seam level and in vertical section indicates the bleeder entries are marginally safe at best and likely to require considerable maintenance. Although the bleeder entry mesh is relatively coarse, the lesson learned from a coarse mesh – fine mesh comparison is that the conclusions would be similar if a finer mesh were used. Figure 48 is a vertical section showing element safety factors from a mesh containing over three million elements that required two days run time. Element density would obscure the view so element borders are removed in the figure. The similarity to Figure 45(b) is evident indicating the conclusion about bleeder entry safety would be the same.

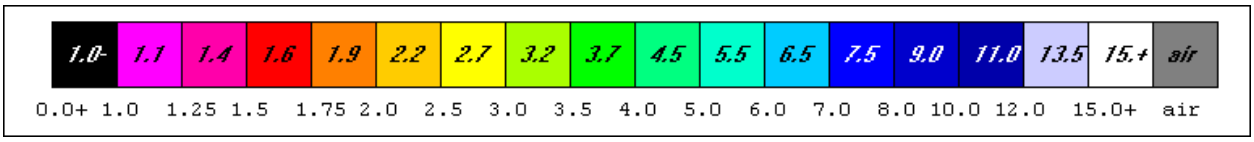

Element Safety Factor Color Scale

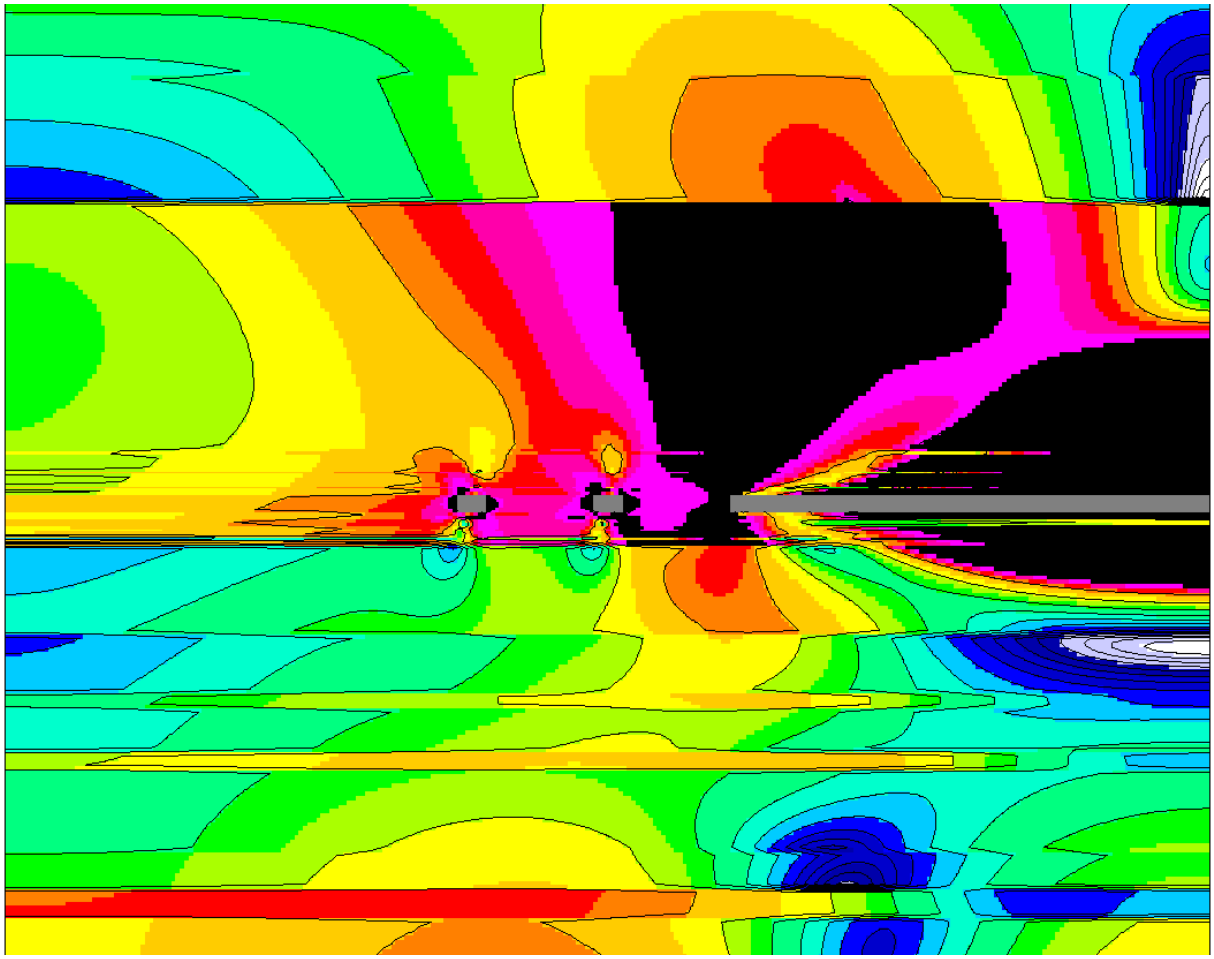

Figure 48 Element safety factor distribution from a three million element fine mesh for the bleeder entry problem. This figure has been cropped top and bottom for better viewing and element boundaries are removed for the same reason.

# 4 INTERPANEL BARRIER PILLARS

Example problems involving interpanel barrier pillars as a longwall panel advances parallel to the barrier pillar and panel entries illustrates the processes of mesh generation and finite element analysis for evaluation of barrier pillar protection of headgate and tailgate entries and chain pillars [17].

**Example 1** This example is from a mine in the Wasatch Plateau coal field of central Utah.

*Step 1 Preparation of a materials property file (stratigraphic column)* The problem input for interpanel barrier pillar mesh generation is given in Figure 49. There are 11 layers in the geologic column; the 8th layer is the mined coal seam 11 ft (3.4 m) thick at a depth of 2,707 ft (825 m) which is the thinnest layer in the column. Order of strata is from the top down. As a reminder, the last line of each stratum properties set gives the orientation (dip direction, dip), depth to the stratum top and stratum thickness.

```
NLYRS =11
NSEAM = 8
1 North Horn         N=2
2.60E+06      2.60E+06      2.60E+06      0.26   0.26   0.26
1.75E+06      1.75E+06      1.75E+06     0.0      0.0   155.0
11803  11803  11803  696    696    696
1655   1655   1655
0      0      0      951
2 PRICE RIVER FRM
3.20E+06      3.20E+06      3.20E+06      0.26   0.26   0.26
2.17E+06      2.17E+06      2.17E+06     0.0      0.0   143.0
9976   9976   9976   377    377    377
1120   1120   1120
0      0      951    548
3 CASTLEGATE SANDSTONE
3.00E+06      3.00E+06      3.00E+06      0.22   0.22   0.22
1.92E+06      1.92E+06      1.92E+06     0.0      0.0   140.0
9585   9585   9585   435    435    435
1179   1179   1179
0      0      1499   568
4 SAND+SILTSTONE
3.10E+06      3.10E+06      3.10E+06      0.24   0.24   0.24
2.04E+06      2.04E+06      2.04E+06       0.0    0.0   142.0
13500  13500  13500  1189   1189   1189
2313   2313   2313
0      0      2067   344
5 ROOF SILTSTONE
2.80E+06      2.80E+06      2.80E+06      0.23   0.23   0.23
1.82E+06      1.82E+06      1.82E+06     0.0      0.0   142.0
12180  12180  12180  1291   1291   1291
2289   2289   2289
0      0      2411   138
6 ROOF SANDSTONE
3.39E+06      3.39E+06      3.39E+06      0.26   0.26   0.26
2.29E+06      2.29E+06      2.29E+06     0.0      0.0   140.0
```

```
14500  14500  14500  1088   1088   1088
2293   2293   2293
0      0      2549   150
7 ROOF SANDSTONE
3.39E+06      3.39E+06      3.39E+06      0.26   0.26   0.26
2.29E+06      2.29E+06      2.29E+06     0.0      0.0   140.0
14500  14500  14500  1088   1088   1088
2293   2293   2293
0      0      2699    8
8 COAL
4.06E+05      4.06E+05      4.06E+05      0.12   0.12   0.12
2.31E+05      2.31E+05      2.31E+05     0.0      0.0   78.0
4133   4133   4133   276    276    276
616    616    616
0      0      2707   11
9 FLOoR SANDSTONE
3.39E+06      3.39E+06      3.39E+06      0.26   0.26   0.26
2.29E+06      2.29E+06      2.29E+06     0.0      0.0   140.0
11716  11716  11716  1175   1175   1175
2142   2142   2142
0      0      2718     9
10 FLOoR SANDSTONE
3.39E+06      3.39E+06      3.39E+06      0.26   0.26   0.26
2.29E+06      2.29E+06      2.29E+06     0.0      0.0   140.0
11716  11716  11716  1175   1175   1175
2142   2142   2142
0      0      2727   200
11 MANCOS SHALE
2.20E+06      2.20E+06      2.20E+06      0.35   0.35   0.35
1.70E+06      1.70E+06      1.70E+06     0.0      0.0   145.0
10295  10295  10295  158    158    158
736    736    736
0      0      2927    171
```

Figure 49 Input strata properties file for interpanel barrier pillar mesh generation and analysis.

*Step 2 Mesh Generation* Mesh generation input is

| | |
|---|---|
| 1) the name of the material properties (stratigraphic column) file | *matABDg.txt* |
| 2) the number of panel entries (NES), | 3 |
| 3) entry and crosscut widths (WE, WC) | 20 20 (ft) |
| 4) pillar width and length (WP, LP) | 40 80 (ft) |
| 5) barrier pillar width | 300 (ft) |
| 6)longwall panel width | 750 (ft) |
| 7) element width, length, height (EX, EY, EZ) | 4 4 4 (ft) |
| 8) do gob effect? | Y or y=yes or Nor n=no |
| 9) add-in additional stresses Sxx, Syy, Szz, Tyz, Tzx, Txy? | Y or y=yes or Nor n=no |

In case of Problem 4, interpanel barrier pillar safety, a barrier pillar exists parallel to the entries; a mined panel also exists adjacent to the panel entries as shown in Figure 50. The red rectangle indicates the extent of mesh generation in plan view. As before symmetry is used to reduce the digital size of the mesh.

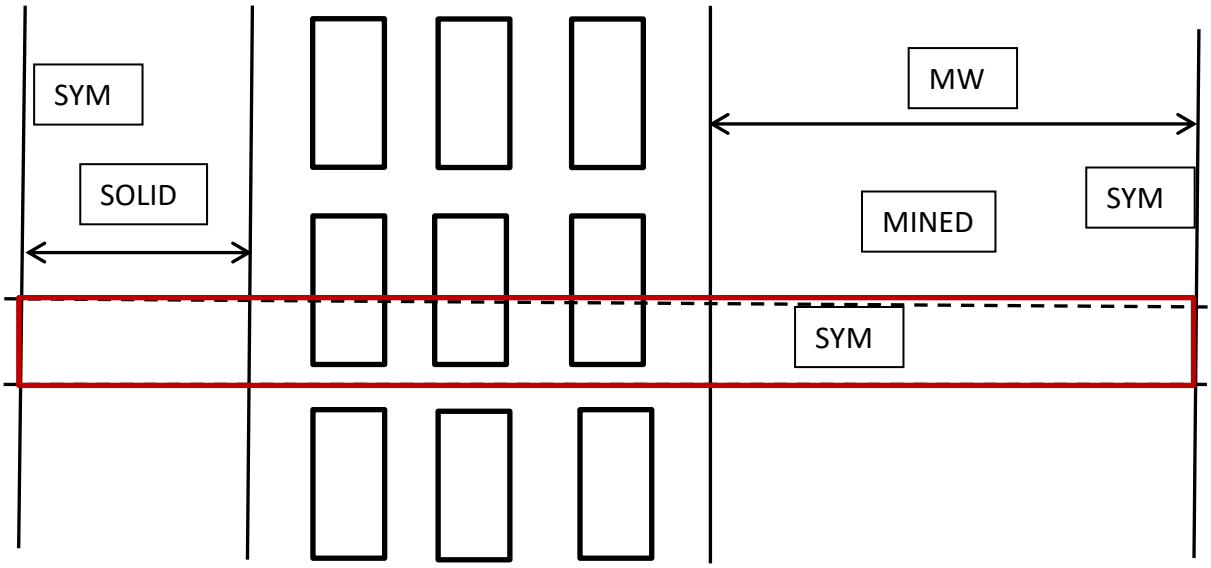


Figure 50 Interpanel barrier pillar geometry with unmined ground to the left side of the figure and a panel being mined to the right side of the figure. Mesh extent is indicated in red, but not to scale.

The runstream file after incorporating path names from the mesh generated output file is shown in Figure 51. Plan and vertical section mesh views are shown in Figures 52 and 53, respectively. Only part of the vertical section is shown so element size is discernible in the vertical section. In fact, elements are 4 ft (1.2 m) cubes.

```
2/4/2022 wgp interpanel barrier test
F:\Visual Studio 2010\Projects\SPK\GMB3\matABDg.txt
F:\Visual Studio 2010\Projects\SPK\GMB3\belms
F:\Visual Studio 2010\Projects\SPK\GMB3\bcrds
F:\Visual Studio 2010\Projects\SPK\GMB3\brcte
F:\Visual Studio 2010\Projects\SPK\GMB3\bsigi
F:\Visual Studio 2010\Projects\SPK\GMB3\bnsps
AIPa
nelem =  347360
nnode =  378672
nspec =   59952
nmat  =      11
ncut  =      -1
ninc  =       5
nsigo =       1
inter =     200
maxit =    2000
nyeld =       2
nelcf =    4431
nprb  =       4
nsol  =       2
mgob  =       0
 error=    1.0000
 orf  =    1.8600
```

```
 xfac =   12.0000
 yfac =   12.0000
 zfac =   12.0000
 efac =    1.0000
 cfac =    1.0000
tolr% =    0.0100
ENDRUN
```

Figure 51 Runstream file for interpanel barrier pillar Problem 4 analysis.

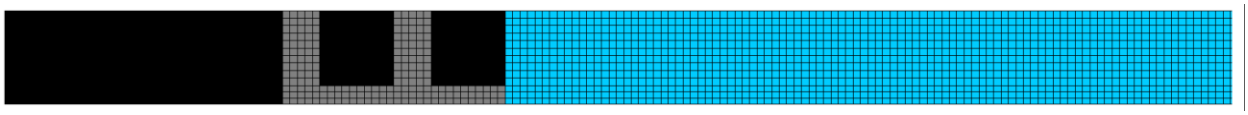

Figure 52 Plan view of interpanel barrier pillar mesh at seam level, black = coal, grey = entries and crosscuts, blue=longwall panel elements which may be air or gob as a matter of choice during program execution  Entries are 20 ft (6 m) wide.

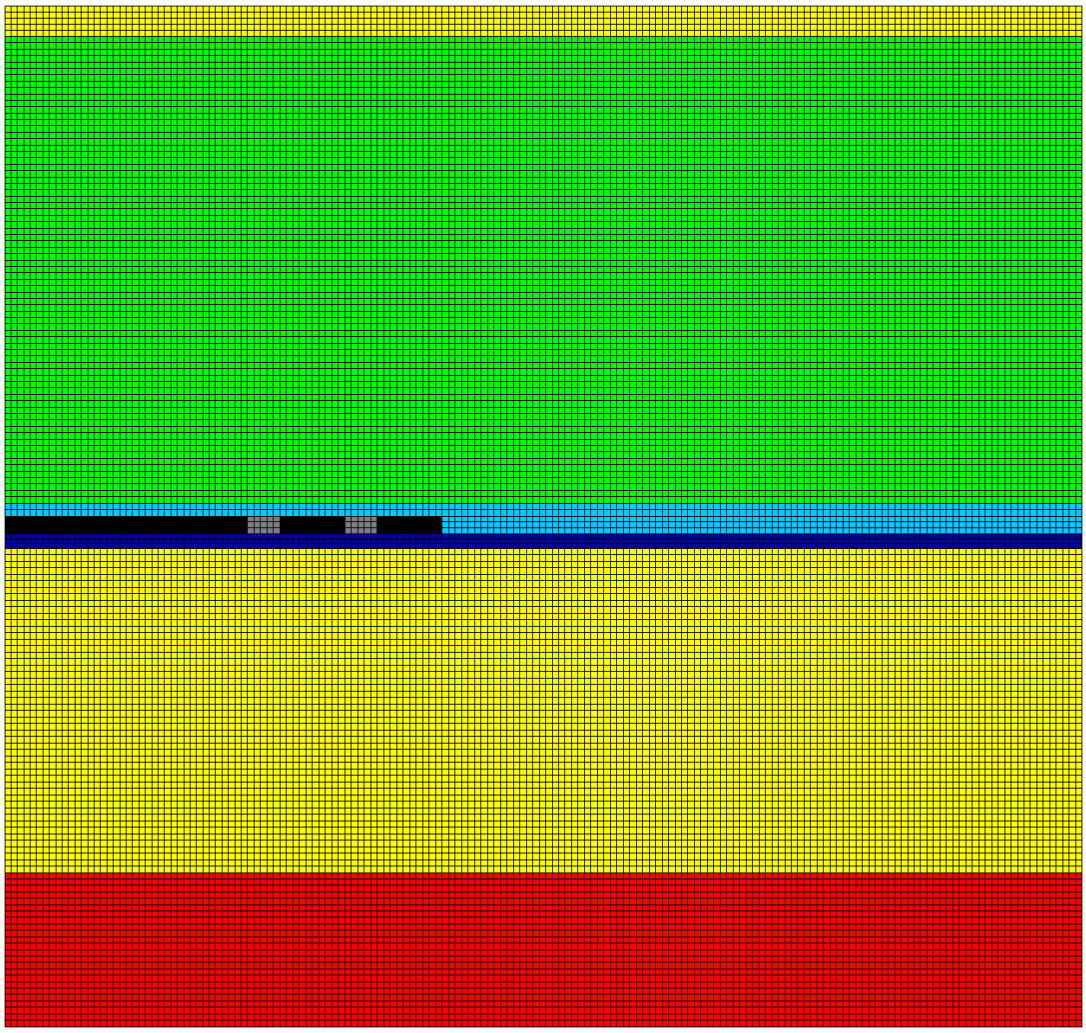

Figure 53 Vertical section of interpanel barrier pillar mesh.  Seam is 11 ft (3.3 m) thick.

*Step 3 FEM Execution and Results* Run time for this mesh was just under four hours. Vertical section views of the distribution of element safety factors are shown in Figure 54 in two cases: (a) without gob effect and (b) with gob effect. Element boundaries are not shown for clarity. The plan view in Figure 55 indicates yielding entry pillar ribs and pillar cores with low safety factors (*fs*<1.3). Indeed, the pillar adjacent to the longwall panel is yielding to the core. Entry ribs also show some yielding.

Comment: the gob appears to reduce stress at a distance as seen in the somewhat higher safety factors in the rib of the entry adjacent to the interpanel barrier pillar. Stress is also reduced in the vicinity of the other two entries, although not enough to avoid yielding of the chain pillars between.

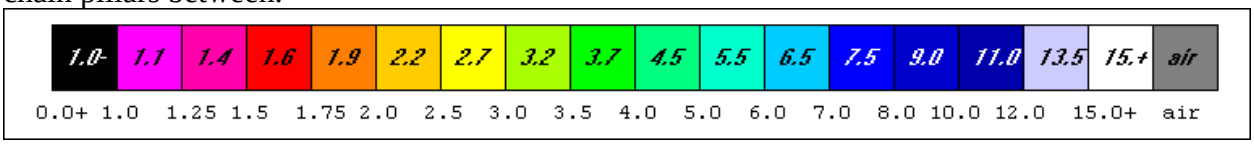


Safety Factor Color Scale

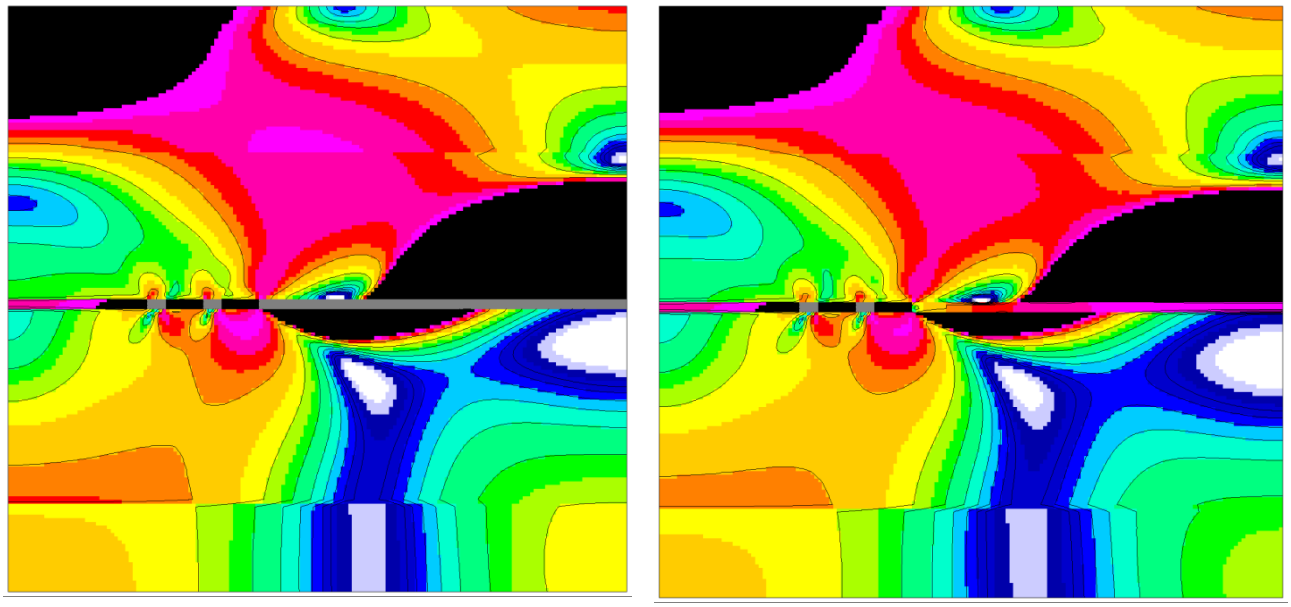

(a) no gob (b) with gob

Figure 54 Vertical section: interpanel barrier pillar (left hand side of plots), panel entries (3), longwall panel mined (right hand side of plots).

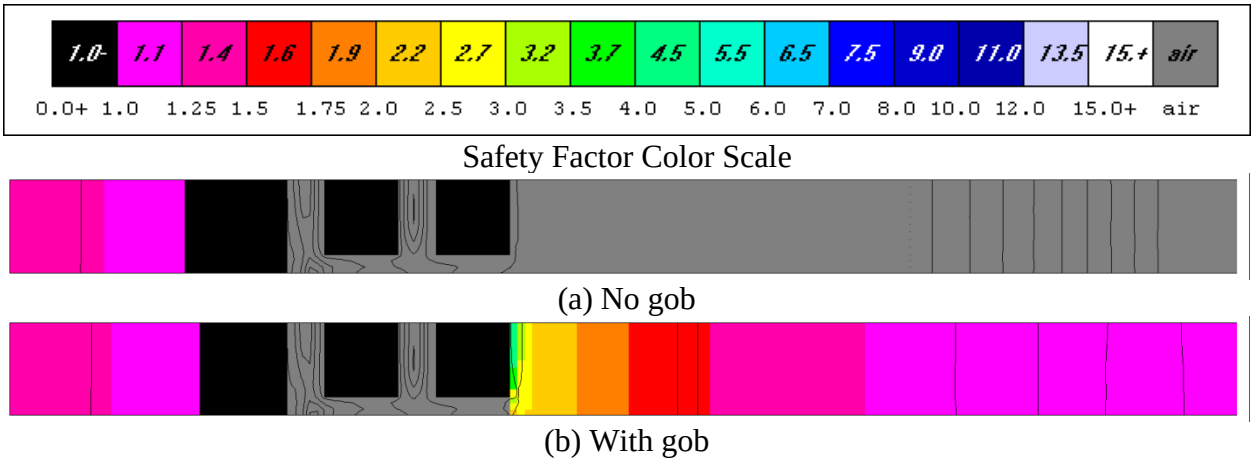


Safety Factor Color Scale

(a) No gob

(b) With gob

Figure 55 Plan view at seam level: interpanel barrier pillar (left), panel entries(3), longwall panel (right). (a) no gob, (b) with gob.

**Example 2** This example pertains to trona mining in southern Wyoming and is discussed in APPENDIX V.

## 5 PILLARS IN ROOM AND PILLAR MINING

Pillar safety in room and pillar mining is Problem 5 in the list of problems available for analysis upon execution of the mesh generator. Figure 44 is a plan view showing a typical pillar in an extensive array of similar pillars. Symmetry is used to reduce mesh size; only the area in the red rectangle is contained in the mesh in plan view. Vertical extent of the mesh above and below the floor of the mining level is 1.5ML where ML is a mining length that depends on width of crosscuts and entries and on pillar width and length.

Example problems involving room and pillar safety in wide area room and pillar mining illustrates processes of mesh generation and finite element analysis for pillar safety and safety of adjacent roof and floor spans.

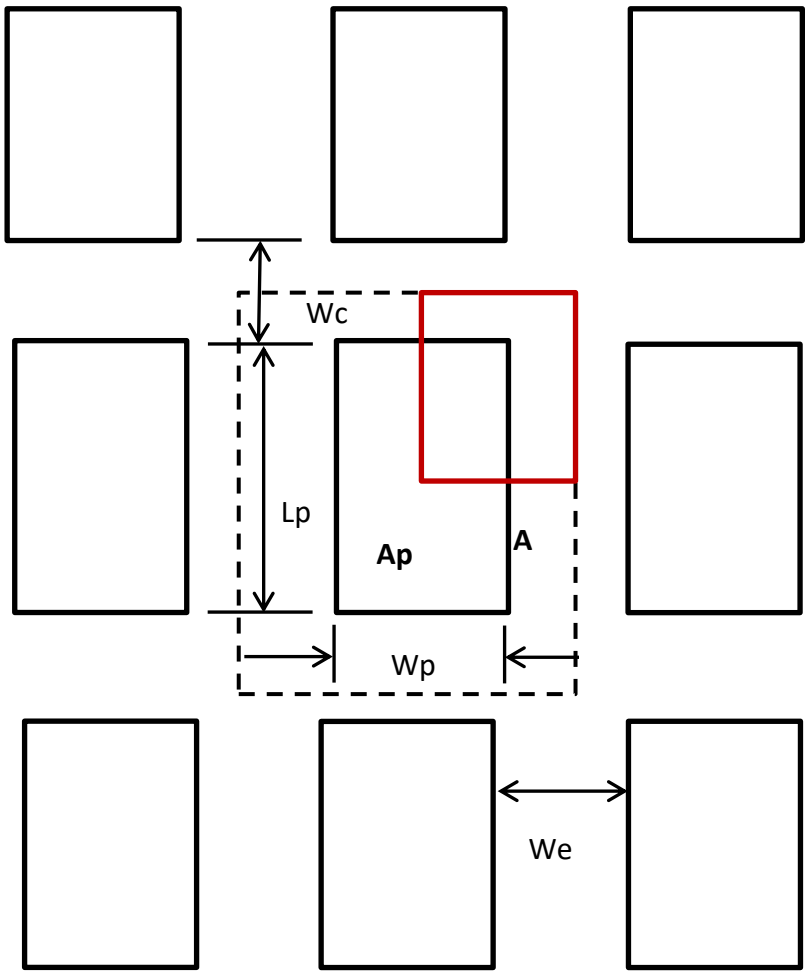


Figure 56 A typical pillar in a large array of pillars. Lp=pillar length, Wp=pillar width, We=entry width, Wc=cross cut width, **Ap**=area of pillar, **A=**total area (*tributary* area). Because of symmetry, only the region outlined by the red square in horizontal section is placed in the mesh. All four sides are planes of symmetry. The mesh extends above and below the bottom of the ore 1.5 times the mining width.

**Example 1** This example concerns an underground hardrock mine in southeast Missouri.

*Step 1 Preparation of a materials property file (stratigraphic column)* Figure 57 is a color schematic of the stratigraphic column from a mine in the New Lead Belt in southeast Missouri where room and pillar mining is used extensively [23]. Mining often occurs on several levels and on occasion just a single level and over a restricted zone in the ore-bearing Bonneterre dolomite.

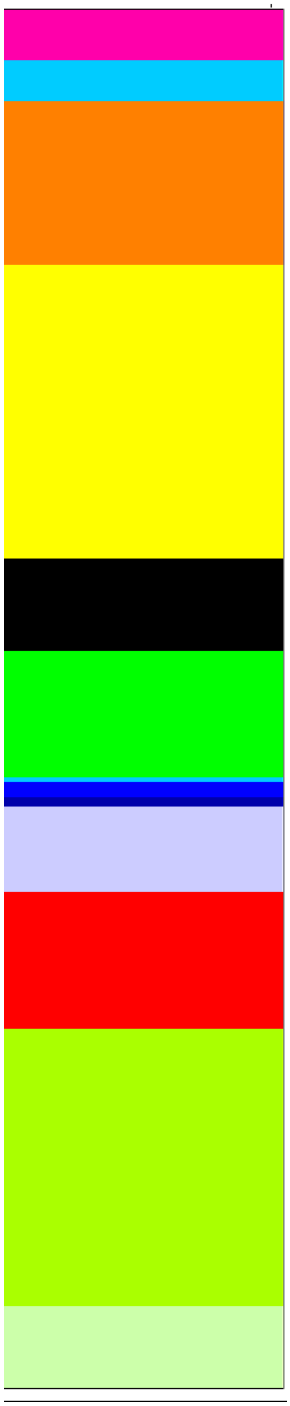


Figure 57 Stratigraphic column for example problems. Pillar is in Unit 10.

A material properties file is shown in Figure 58. Mining is not full seam height; top "ore" and bottom "ore" are not mined nor is "ore" in stratum (8) mined. Partitioning of an ore horizon or coal seam in this way allows for leaving "top coal/ore" and "bottom coal/ore" when desired.

```
NLYRS =15
NSEAM =11
  (1) OVERBURDEN
2.00E+03      2.00E+03      2.00E+03      0.3    0.3    0.3
1.43E+03      1.43E+03      1.43E+03      0      0      130
2000   2000   2000   100    100    100
120    120    120
0      0      0      60
  (2) GASCONADE DOLOMITE
6.92E+06      6.92E+06      6.92E+06      0.34   0.34   0.34
5.24E+06      5.24E+06      5.24E+06      0      0      163
11910  11910  11910  1174   1174   1174
1504   1504   1504
0      0      60     50
  (3) EMINENCE DOLOMITE
1.07E+07      1.07E+07      1.07E+07      0.31   0.31   0.31
7.72E+06      7.72E+06      7.72E+06      0      0      167
16120  16120  16120  734    734    734
888    888    888
0      0      110    195
  (4) POTOSI DOLOMITE
1.21E+07      1.21E+07      1.21E+07      0.26   0.26   0.26
8.17E+06      8.17E+06      8.17E+06      0      0      171
26870  26870  26870  1228   1228   1228
1486   1486   1486
0      0      305    350
  (5) DERBY-DOERUN DOLOMITE
7.58E+06      7.58E+06      7.58E+06      0.32   0.32   0.32
5.57E+06      5.57E+06      5.57E+06      0      0      162
23760  23760  23760  1285   1285   1285
1569   1569   1569
0      0      655    110
  (6) DAVIS SHALE
5.35E+06      5.35E+06      5.35E+06      0.21   0.21   0.21
3.39E+06      3.39E+06      3.39E+06      0      0      161
19610  19610  19610  1205   1205   1205
1483   1483   1483
0      0      765    150
  (7) BONNETERRE DOLOMIE
6.75E+06      6.75E+06      6.75E+06      0.31   0.31   0.31
4.89E+06      4.89E+06      4.89E+06      0      0      166
29260  29260  29260  935    935    935
1115   1115   1115
0      0      915    6
(8) ORE
8.75E+06      8.75E+06      8.75E+06      0.3    0.3    0.3
6.25E+06      6.25E+06      6.25E+06      0      0      219
18270  18270  18270  1007   1007   1007
1231   1231   1231
0      0      921    18
(9) FALSE DAVIS SHALE
3.79E+06      3.79E+06      3.79E+06      0.22   0.22   0.22
2.43E+06      2.43E+06      2.43E+06      0      0      152
5210   5210   5210   730    730    730
980    980    980
```

```
0      0      939    11
(10) TOP ORE
8.75E+06      8.75E+06      8.75E+06      0.3    0.3    0.3
6.25E+06      6.25E+06      6.25E+06      0      0      219
18270  18270  18270  1007   1007   1007
1231   1231   1231
0      0      950     10
(11) ORE
8.75E+06      8.75E+06      8.75E+06      0.3    0.3    0.3
6.25E+06      6.25E+06      6.25E+06      0      0      219
18270  18270  18270  1007   1007   1007
1231   1231   1231
0      0      960     30
(12) BOTTOM ORE
8.75E+06      8.75E+06      8.75E+06      0.3    0.3    0.3
6.25E+06      6.25E+06      6.25E+06      0      0      219
18270  18270  18270  1007   1007   1007
1231   1231   1231
0      0      990     10
(13) BONNETERRE DOLOMITE
6.75E+06      6.75E+06      6.75E+06      0.31   0.31   0.31
4.89E+06      4.89E+06      4.89E+06      0      0      166
29260  29260  29260  935    935    935
1115   1115   1115
0      0      1000   163
(14) LAMOTTE SANDSTONE
3.94E+06      3.94E+06      3.94E+06      0.41   0.41   0.41
3.34E+06      3.34E+06      3.34E+06      0      0      146
11240  11240  11240  790    790    790
981    981    981
0      0      1163   330
(15) PRECAMBIRAN FELSITES
1.07E+07      1.07E+07      1.07E+07      0.31   0.31   0.31
7.72E+06      7.72E+06      7.72E+06      0      0      167
16120  16120  16120  734    734    734
888    888    888
0      0      1493   100
```

Figure 58 Material properties file for a pillar analysis in room and pillar mining.

*Step 2 Mesh Generation.* Mesh generation input is entered interactively and is

| | |
|---|---|
| 1) the name of the material properties (stratigraphic column) file | *matMAG1.txt* |
| 2) entry and crosscut widths (WE, WC) | 30 25 (ft) |
| 3) pillar width and length (WP, LP) | 25 30 (ft) |
| 4) element width, length, height (EX, EY, EZ) | 2 2 2 (ft) |
| 5) add-in additional stresses Sxx, Syy, Szz, Tyz, Tzx, Txy? | N or n (no). |

The output file from the mesh generator is the runstream or input file for finite element analysis. After some minor but important editing, the runstream file is given in Figure 59.

```
MAGMONT MINE R & P 8/12/2019, 2/6/2022
F:\Visual Studio 2010\Projects\SPK\GMB3\matMAG1.txt
F:\Visual Studio 2010\Projects\SPK\GMB3\belms
F:\Visual Studio 2010\Projects\SPK\GMB3\bcrds
F:\Visual Studio 2010\Projects\SPK\GMB3\brcte
F:\Visual Studio 2010\Projects\SPK\GMB3\bsigi
F:\Visual Studio 2010\Projects\SPK\GMB3\bnsps
aMAGa
nelem =  152325
nnode =  173568
nspec =   40876
nmat  =      15
ncut  =      -1
ninc  =       5
nsigo =       1
inter =     200
maxit =    2000
nyeld =       1
nelcf =    2535
nsol  =       2
nprb =        5
mgob  =       0
 error=     0.000
 orf  =     1.860
 xfac =     12.00
 yfac =     12.00
 zfac =     12.00
 efac =      1.00
 cfac =      1.00
tolr% =      0.01
ENDRUN
```

Figure59 Finite element runstream file for pillar analysis in room and pillar mining.

The mesh for pillar analysis is shown in Figure 60 in close-up views. Elements in the mesh are 2 ft (0.6 m) cubes. As the runstream file indicates, there are 152,325 elements in the mesh. The number of layers is equal to the number of material types which is 15 as also seen in the runstream file. Entry width is 30 ft (9 m); crosscut width is 25 ft (7.5 m). Pillar width is also 25 ft (7.5 m); pillar length is 30 ft (9 m). The vertical section in the figure is not full height which is at least 30 times pillar height. In this example, 30 times pillar height is 900 ft (270 m).

*Step 3 FEM Execution and Results*. Practical results for this problem are illustrated in Figure 61 which shows element safety factor distributions in vertical section and plan view at pillar mid-height. High stress concentration associated with relatively low safety factors (red, 1.40) at the room corners where roof and floor meet the pillar are evident. The pillar corner seen in plan view is also threatened in consideration of the low safety factor at the corner (pink, 1.1). Edges of the pillar extending from the corner are also in red ($fs$=1.4) and pose a concern for spalling. Overall, the pillar is safe at an area extraction ratio of approximately 75 percent. In this, regard the green in the pillar core indicates $fs \approx 4$ as does the tributary area formula for average $fs$.

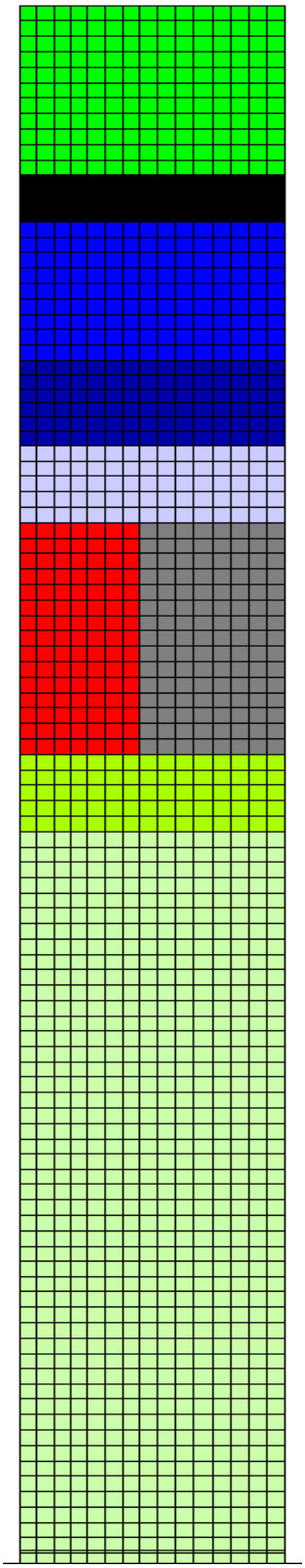

(A) vertical section

(B) plan view

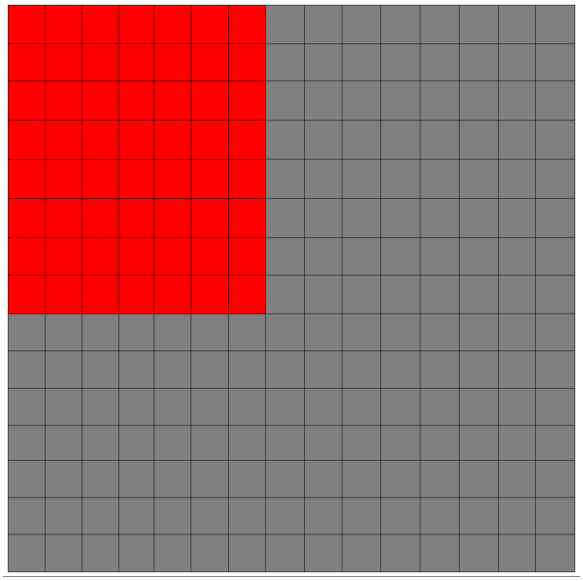

Figure 60 Vertical section (A) and plan view (B) of the finite element mesh for pillar analysis.

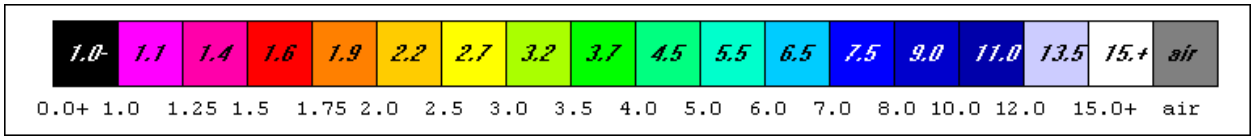


Element Safety Factor Color Scale

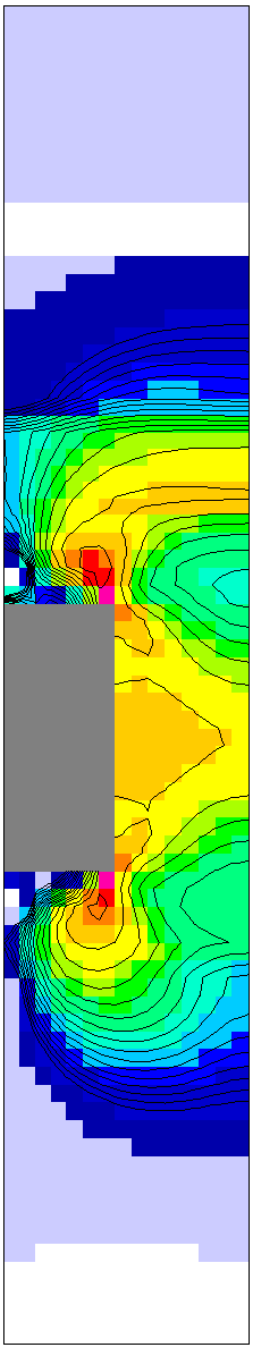

(A) vertical section

(B) plan view

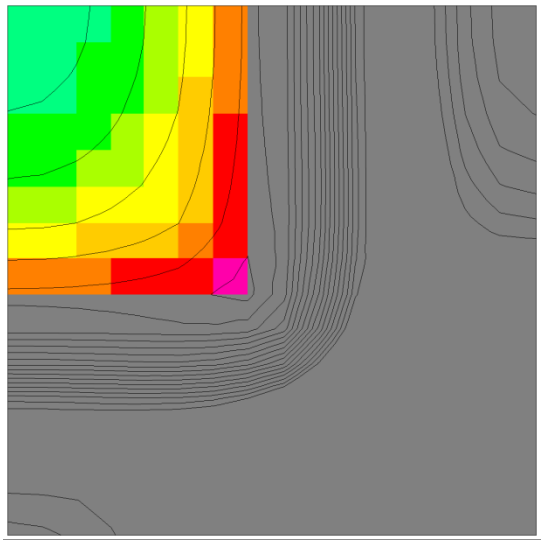

Figure 61 Element safety factor distributions in vertical section (A) and plan view (B) at pillar mid-height.

**Example 2** Another example of room and pillar safety analysis relates to trona mining in southern Wyoming.

Solution mining of pillars in sections of mines where first mining has occurred has potential for wide area collapse when the remaining pillars are long and slender. Square pillars by comparison are less threatening. Consider pillars in extensive arrays of similar pillars as shown in Figure 55. The pillar supports the overburden block with vertical sides one half the distances to adjacent pillars. In plan view, the overburden block has area *A*; the pillar has area $A_p$. Force equilibrium requires $S_p A_p = S_v A$ where $S_p$ and $S_v$ are average pillar stress and overburden stress, respectively. By definition, the area extraction ratio $R = A_m / A = 1 - A_p / A$ where $A = A_m + A_p$ and $A_m$ is the area mined. Thus, $S_p = S_v / (1 - R)$ which is the tributary area (extraction ratio) formula for average pillar stress. The actual distribution of pillar stress is U-shaped with high stress at the pillar walls and low stress near the pillar center as illustrated in Figure 56. The relatively high stress concentrated at the pillar sides often leads to spalling and an hour-glass pillar shape.

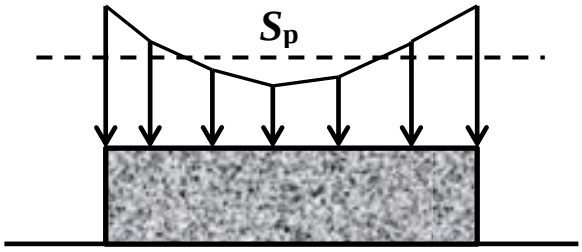


Figure 62 Schematic illustration of vertical stress distribution across a pillar.

A pillar safety factor $FS_p$ may be defined in terms of pillar stress $S_p$ and pillar compressive strength $C_p$. Thus, $FS_p = C_p / S_p$. A "size" effect on pillar strength may be considered. One well-known formula [24] is $C_p = C_1(0.78 + 0.22 W_p / H_p)$ where $H_p$ and $W_p$ are pillar height and width[1] respectively, and $C_1$ is unconfined compressive strength of a pillar with a width to height ratio of one. This "size" effect formula is more accurately an "end" effects formula in consideration of the formula source in laboratory testing where end friction confines test cylinders and increases strength through the effect of confinement. In the famous Mohr-Coulomb (MC) criterion for strength $\tau = \sigma \tan(\phi) + c$ where $\phi$ and $c$ are angle of internal friction and cohesion, respectively, the role of confining pressure can be made clear by rewriting MC as $C_p = C_o + (C_o / T_o) p$ where $C_o$, $T_o$ and $p$ are unconfined compressive strength, tensile strength and confining pressure, respectively. The ratio $C_o / T_o$ is often greater than 10 in rock mechanics,

[1] Pillar width is the smaller of the horizontal dimensions. Pillar length *Lp* is the longer horizontal dimension.

so a small confining pressure may induce a large increase in compressive strength. In case of pillars that are wide relative to height the confinement in the pillar core which may easily reach premining horizontal stress causes the core to be quite strong. However, the confinement in pillars that are high relative to width is generally low and consequently so is the pillar core strength. For this reason, tall, that is, slender pillars are susceptible to sudden collapse.

Solution mining of pillars is likely to dissolve all sides of a pillar at an equal rate. Square pillars would remain square under this assumption. Pillars that are long relative to width would become slender as the sides are dissolved. Consider a square pillar initially 46.7 x 46.7 ft and a long pillar initially 30 x 90 ft. If entries and crosscuts are 20 ft wide, then the extraction ratio is 51 percent after first mining in both cases. If seam depth is 1500 ft and unconfined compressive strength is 6000 psi, then the extraction ratio *R* of 51 percent and the tributary area formula give pillar safety factors of 2 for both pillars. As solution mining progresses and pillar widths and lengths are reduced equally by 24 ft, the square pillar is now 22 x 22 ft and the long pillar is now 6 x 66 ft. The square pillar extraction ratio and safety factor are 72 percent and 1.3, respectively. The long pillar extraction ratio and safety factor are 88 percent and 0.54. In a softrock mine where mining height is 10 ft, the long pillar is also a slender pillar in consideration of pillar height (10 ft) exceeding pillar width (6 ft). Consequently failure would be expected to occur suddenly. Of course, pillar yielding and failure would likely occur before reaching the 0.54 $FS_p$. The square pillar width to height ratio (22.7/10) indicates this pillar is not slender or tall and would likely have a relatively strong core. This example calculation shows that tributary area pillar design may mask a potential for a sudden, wide-area collapse when pillars are extracted by solution mining, despite an initially high pillar safety factor.

Finite element analysis allows for computation of actual stress distribution about roof, pillar, and floor and displacements induced by mining and as influenced by strata properties and depth of mining. Input data for an analysis includes strata properties (elastic moduli and strengths), premining stress and mining sequence. The geologic column in this example is given in Figure 63. Strata properties are given in Table 1. The premining stress is assumed to be caused by gravity alone, a reasonable assumption in consideration of the geological setting. A typical pillar in a large array of similar pillars is mined instantaneously to the given pillar dimensions including mining height (full seam height).

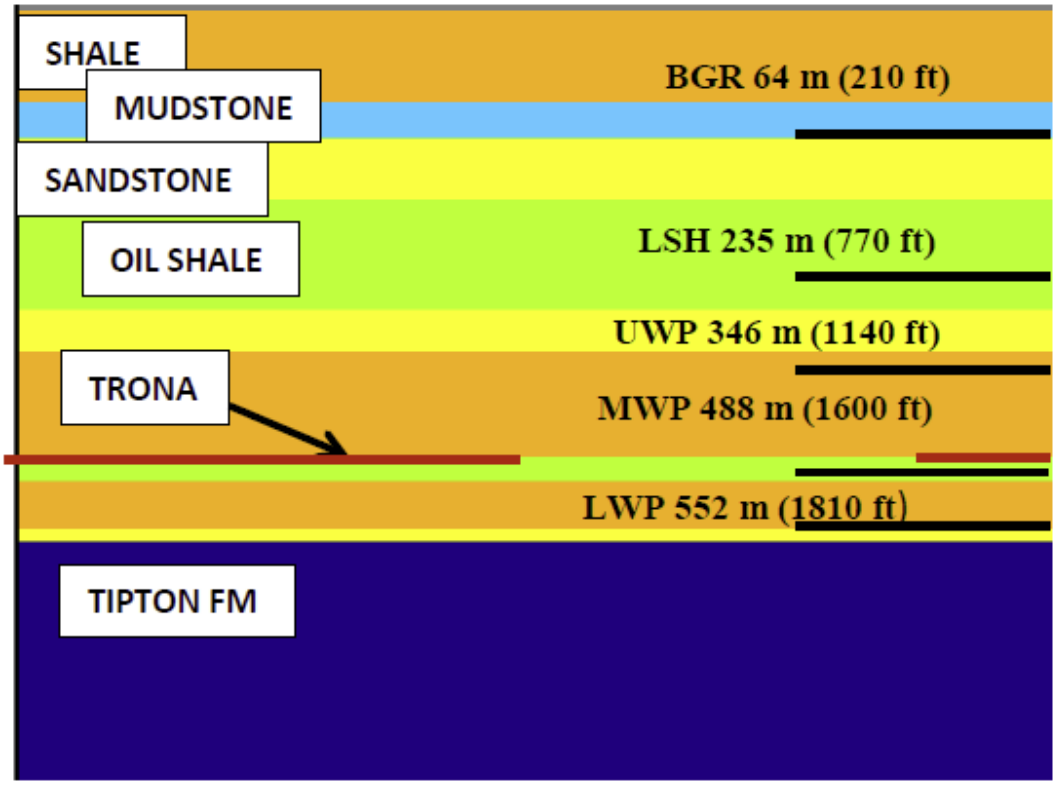


Figure 63 Simplified stratigraphic column. BGR=Bridger formation, LSH=Laney shale, UWP=Upper Wilson Peak formation, MWP=Middle Wilson Peak, LWP=Lower Wilson Peak, TRONA=Bed 17.

Table 1. Average strata properties (engineering units).

| | PROPERTY<br>ROCK | ν<br>- | E<br>(10^6 psi) | G<br>(10^6 psi) | SpWt<br>- | γ<br>(lbf/ft^3) | To<br>(psi) | Co<br>(psi) | Ratio<br>- |
|---|---|---|---|---|---|---|---|---|---|
| 1 | **mudstone** | 0.20 | 1.25 | 0.52 | 2.15 | 134 | 497 | 3580 | 7.20 |
| 2 | **Shale** | 0.22 | 0.87 | 0.36 | 2.31 | 144 | 520 | 4922 | 9.46 |
| 3 | **sandstone** | 0.23 | 2.03 | 0.82 | 2.24 | 140 | 480 | 6317 | 13.16 |
| 4 | **oil shale** | 0.33 | 0.82 | 0.31 | 2.28 | 142 | 460 | 5292 | 11.50 |
| 5 | **trona17** | 0.25 | 4.08 | 1.63 | 2.14 | 134 | 410 | 6804 | 16.59 |

v=Poisson's ratio, E=Young's modulus, G=shear modulus, SpWt=Specific Weight, γ=unit weight, To=tensile strength, Co=unconfined compressive strength (UCS), ratio=Co/To.

Figures 64 and 65 show element safety factor distributions in plan and vertical sections when the square and long pillars are mined to an extraction ratio of 51 percent. Very little yielding occurs in both cases. Not too surprisingly, the corners of the pillar show yielding and the floor center indicates some yielding in both case. Pillar cores show high safety factors

(green=3.5) while pillar ribs show lower safety (red=1.5) as one would expect. By comparison, the tributary area safety factor is 2.22.

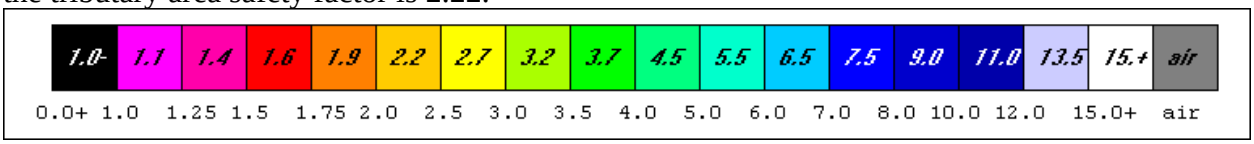


Safety Factor Color Scale

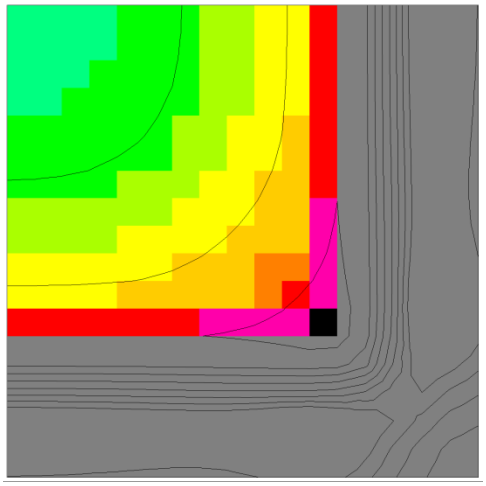

(a) Plan View

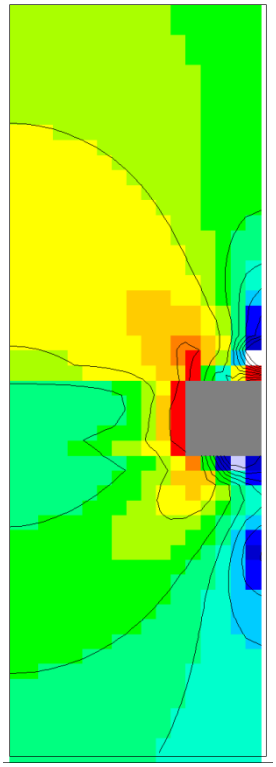

(b) vertical section

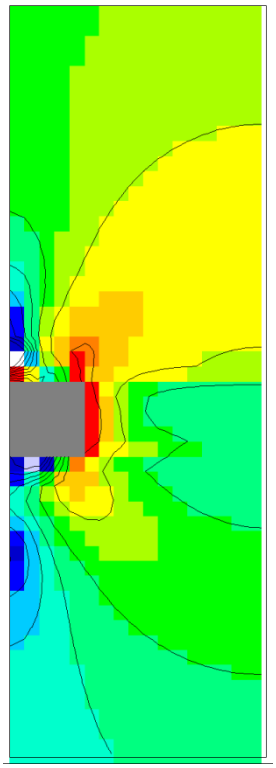

(c) vertical section

Figure 64 Plan and vertical sections showing element safety factor distributions in case of a square pillar with and extraction ratio of 51 percent. Gray=excavated entry and crosscut. Mining height is 10 ft. Entries and crosscuts are 20 ft wide. Pillar is 46.7x46.7 ft.

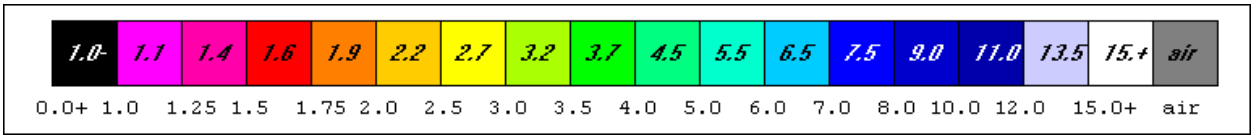


Safety Factor Color Scale

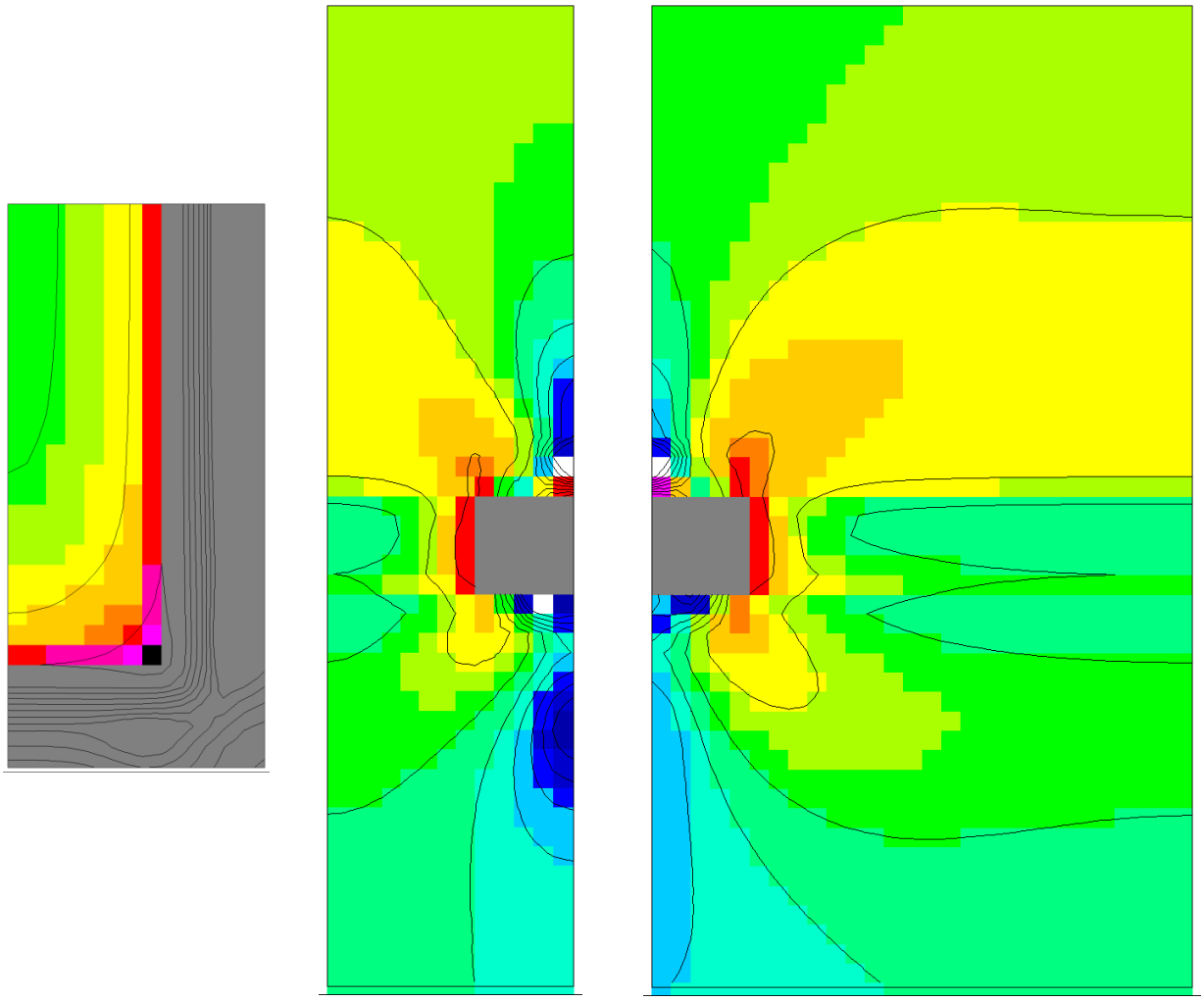

(a) Plan View (b) Vertical Narrow Section (c) Vertical Long Section

Figure 65 Plan and vertical sections showing element safety factor distributions in case of a long pillar with and extraction ratio of 51 percent. Gray=excavated entry and crosscut. Mining height is 10 ft. Entries and crosscuts are 20 ft wide. Pillar is 30x90 ft.

Figures 66 and 67 show element safety factor distributions in plan and vertical sections when solution mining has dissolved 6 ft of all pillar ribs; 12 ft in total. Extraction ratios for the square and long pillar cases are now 72 percent and 88 percent, respectively. Tributary area

safety factors are now1.27 and 0.55, respectively. The indication is a marginally safe square pillar, but a failed long pillar. Indeed, the long now slender pillar shows extensive yielding (black) at the pillar ends,. As the ends yield, additional load would be transferred to the pillar remaining causing more yielding. Collapse would surely have occurred before reaching the condition shown in Figure 67. Roof and floor yielding at centers of crosscuts and entries is also indicated. Details of computer output show this yielding is in biaxial tension, not too surprisingly.

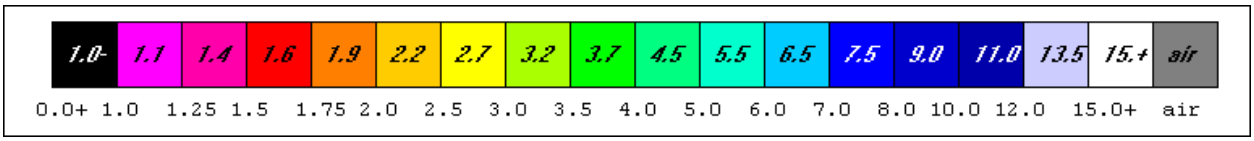


Safety Factor Color Scale

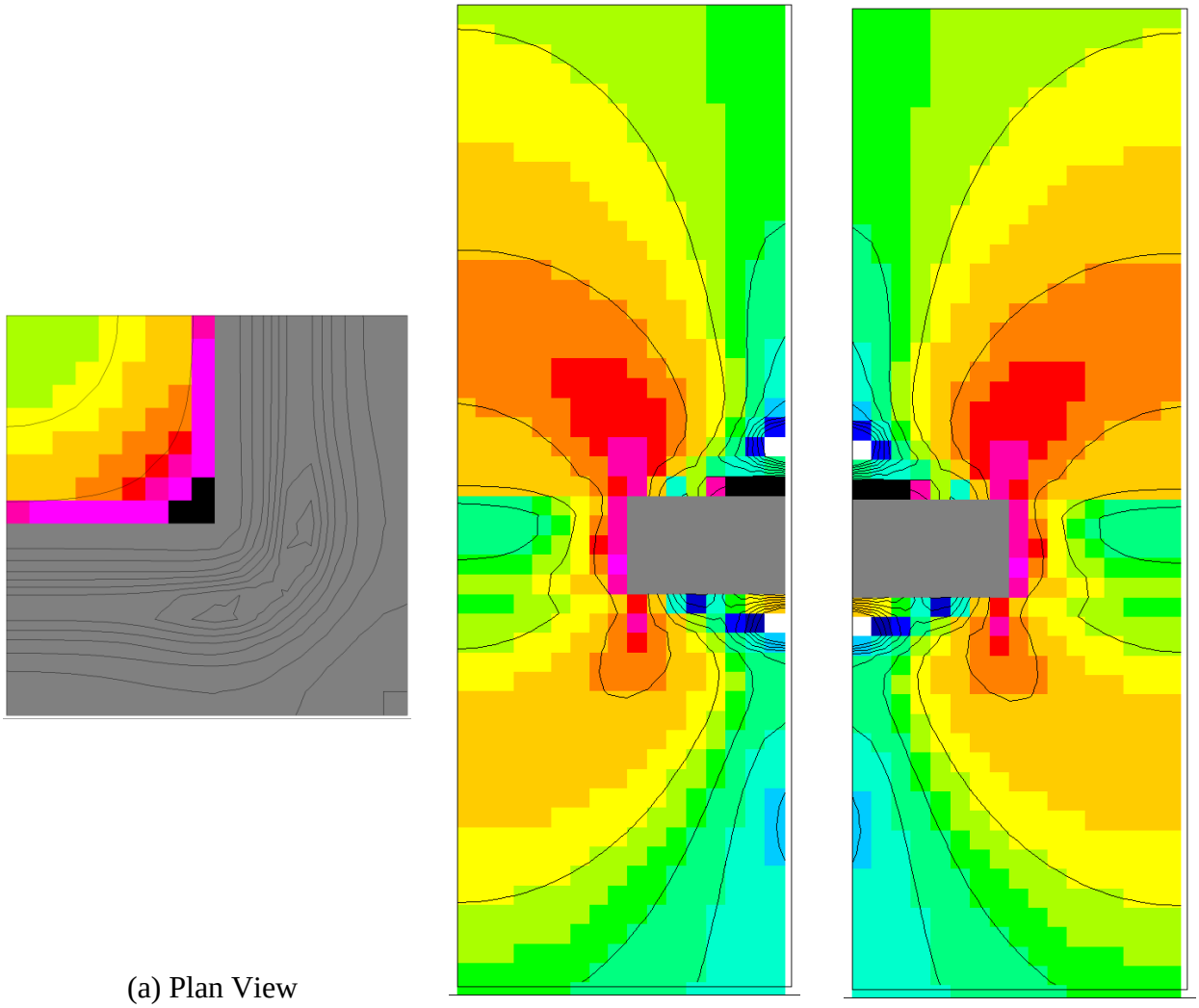

(a) Plan View
(b) Vertical Narrow Section (c) Vertical Long Section

Figure 66 Plan and vertical sections showing element safety factor distributions in case of a square pillar with an extraction ratio of 72 percent. Gray=excavated entry and crosscut. Mining height is 10 ft. Pillar is square; width is now34.7 ft. Crosscut and entry widths are now 32.0 ft.

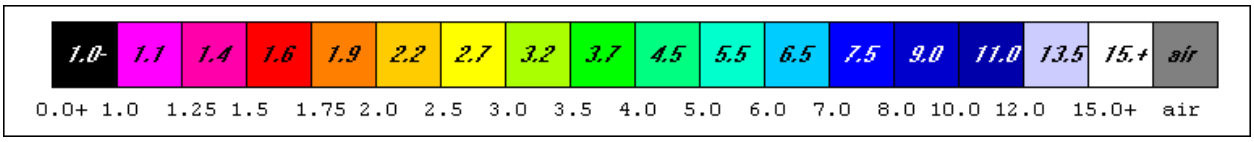


Safety Factor Color Scale

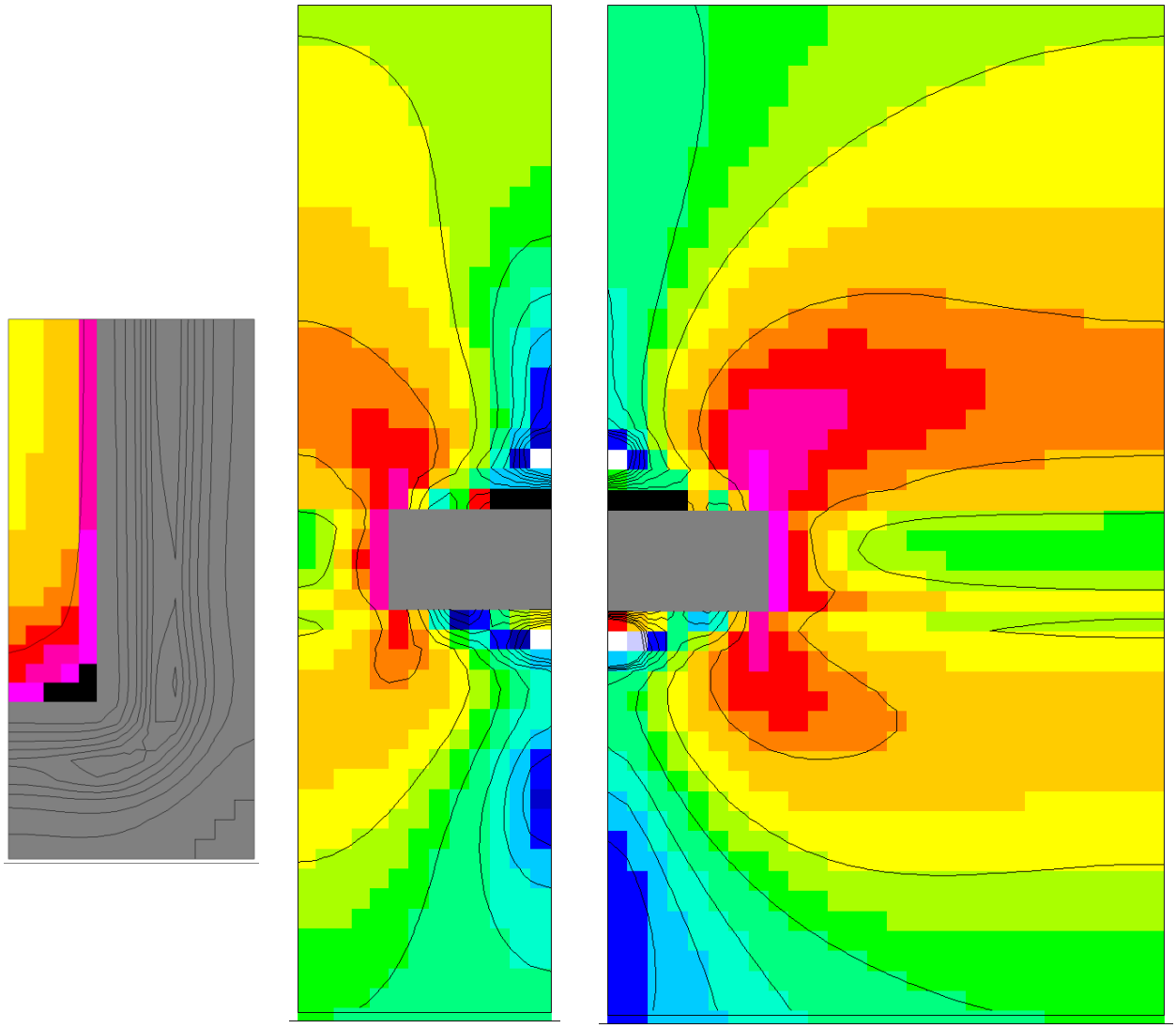

(a) Plan View (b) Vertical Narrow Section (c) Vertical Long Section

Figure 67 Plan and vertical sections showing element safety factor distributions in case of a long pillar with an extraction ratio of 88 percent. Gray=excavated entry and crosscut. Mining height is 10 ft.

Because these results apply to a pillar in a large array of similar pillars, wide area collapse is indicated. Of course, much depends on details of mine operations such as circulation

of water, deposition of tailings if present in the slurry, degree of saturation of return water if a circulation loop is used and so.

When collapse is sudden, no warning is available from monitoring surface subsidence. However, if collapse were to progress in discrete events, some warning may be available depending on the frequency of surface subsidence measurement. Some warning may also be available in the form of seismic events related to mine operations. In this regard, seismic monitoring is usually continuous. However, mine induced seismic events are usually small and may escape detection by a wide area network of seismometers. Although the results here pertain to trona mining south of Interstate Highway 80 (I-80), recent seismic events (February, 2019) in the trona patch north of I-80 are of some interest and certainly worth further study in the context of mine safety, ground control and rock mechanics.

# 6 SHAFTS

New shafts are most often circular; older shafts are often rectangular. Occasionally a shaft with an elliptical cross-section is excavated. Bolting shaft walls with mesh is commonly done during sinking. When water is encountered, a grout wall is generally required to contain seepage. A one foot (0.3 m) thick concrete liner is frequently cast after sinking when pouring from the bottom up is possible. However, deep shafts are often lined concurrently with sinking.

In almost all cases, stability of the shaft depends on the strength of the wall rock in relation to stress concentration at the shaft walls. For this reason, concern here is with the redistribution of stress induced by shaft excavation and the consequent distribution of shaft wall safety factor. Safety of winzes and raises is included, the distinction being mainly in the direction of excavation and the position of the collar and not so much in the analysis of stress, strain and displacement associated with excavation.

Side by side or twin shafts are of interest. Indeed, multiple shafts may be used in large underground mines to ensure adequate hoisting capacity. Separation of shafts in a row by pillars is an important consideration in case of multiple shafts of the same cross-section.

Shaft mesh generation allows for single shafts, twin shafts and a row of shafts. Circular, rectangular and elliptical cross-sections are allowed in every case. Mesh generation is interactive; choices available are made during execution of the mesh generation program. Examples of mesh for a single elliptical shaft, twin circular shafts and a row of rectangular shafts are shown in Figure 68. As a reminder, mesh generation must be preceded by preparation of a material properties file that includes elastic moduli, strengths, depths and thicknesses of strata, and importantly, the identification of the stratum or rock formation of interest where the shaft cross-section is located. In case of anisotropic strata, the dip direction and dip of the *a*-axis of anisotropy are required. This feature allows rectangular and elliptical shafts which are aligned with finite element coordinates (*xyz*) to be at an angle to the material axes (*abc*). The depth of the formation of interest can be varied, of course, but it is this depth where the mesh section is located and the analysis is done. Dipping formations are allowed. The dip and dip direction of the formation at the shaft section depth identified in the material properties file apply.

Preshaft stress may be caused by gravity alone. The vertical stress is computed using a formation thickness weighted specific weight that is multiplied by the depth to the center of the section in the formation of interest. However, an option allows for additional stress to be added to gravity stress during mesh generation. Another option is to zero gravity stress and then to simply specify the state of stress at the section depth of interest. Examples illustrate these options.

Examples of shafts from the mining industry in various geological settings illustrate analysis procedures and practical applications.

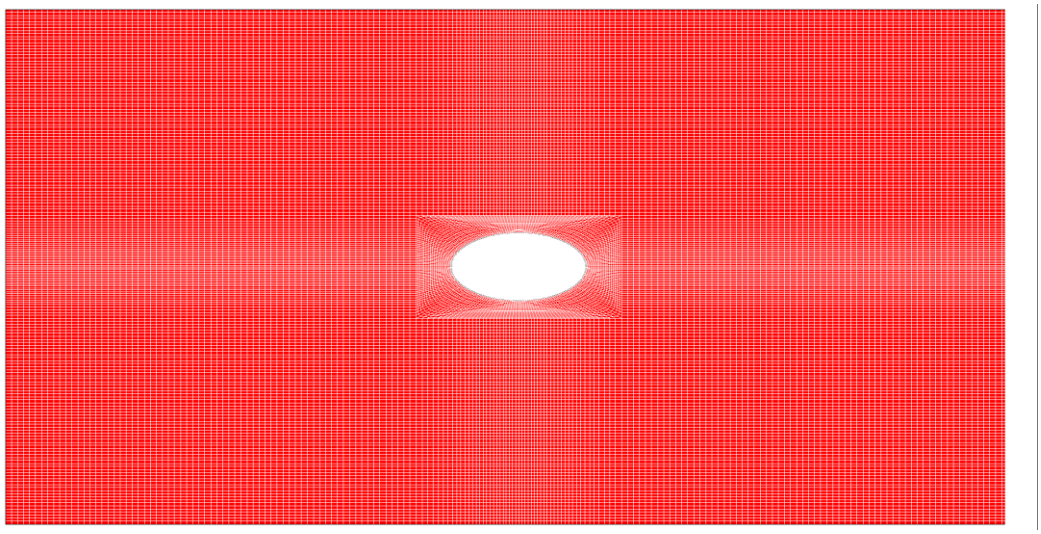

(A)

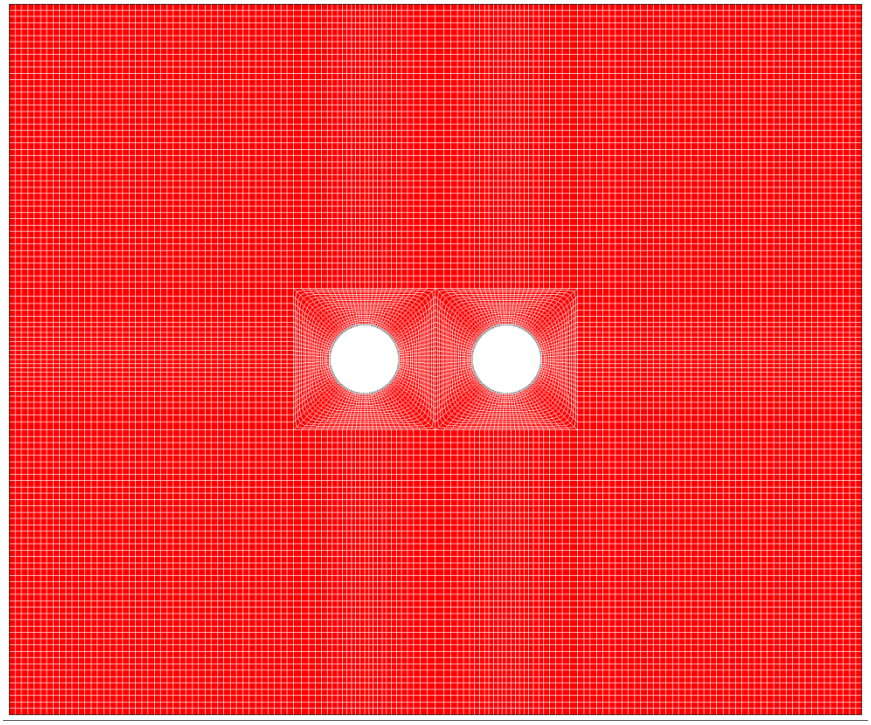

(B)

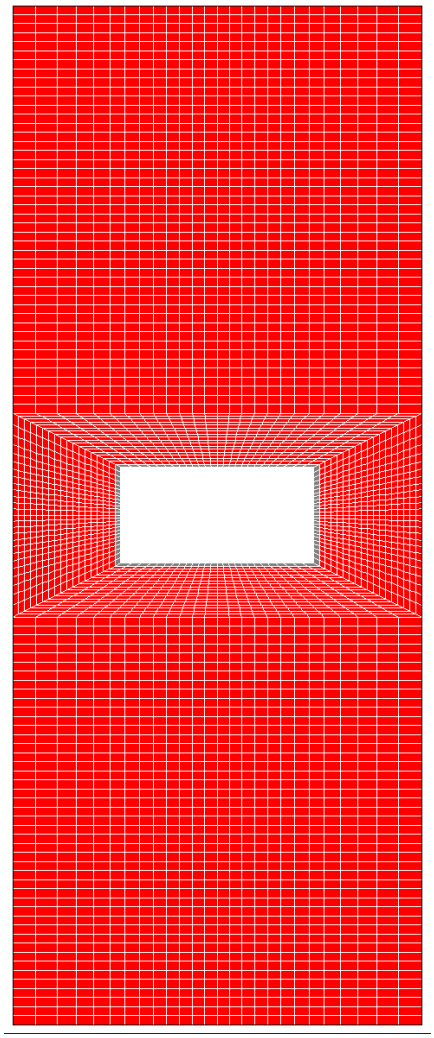

(C)

Figure 68 shaft mesh examples: (A) elliptical with a semi-axes ratio of two, (B) twin circular shafts separated by a pillar of the same width as shaft diameters, and (C) a row of rectangular shafts with a width to length ratio of two separated by pillars of width equal to the long dimension of the shaft. The shaft row mesh takes advantage of pillar symmetry while including the entire section which allows for dipping strata. Grey elements at the shaft wall are "cut" elements that allow for shaft excavation during an analysis.

Numbers of elements and nodes vary from mesh to mesh. Mesh dimensions also vary while allowing for external boundaries to be sufficiently distant from shaft walls to have negligible effect on stress concentration near the shaft walls. A central portion of these meshes is highly refined to allow for close approximation to the actual distributions of stress, strain, displacement and element safety factors. To be sure, these meshes are three-dimensional slabs

with thickness extending into the page. This thickness is adjusted to maintain an element aspect ratio of approximately three which ensures satisfactory numerical performance.

Mesh plotting is easy using the available plot program file **GMBP.exe** (in executable form). A double click on the file begins with presentation of a disclaimer. Acknowledgement of the disclaimer from the keyboard is followed with a request for the plot input file. This file is available following mesh generation and has the name PlotMesh and has the form that is largely self-explanatory. However, if mesh generation and plot routines are in different directories, then path names must precede file names (belms, bcrds, brcte). The last line AMSH is the output mesh plot file name. Editing the input plot file is readily done through a program such as Notepad.

```
PlotShaft
NPROB =       6
NLYRS =       1
NSEAM =       1
Nelem =    3240
belms
Nnode =    6800
bcrds
none
Nelcf=      72
brcte
AMSH
```

After plotting, the output may be re-plotted using a program such as Paint and saved as a png file which can be copied and pasted into a Word document, for example.

Plotting finite element output in the form of element safety factor distributions follows a similar path with a small but essential change to the input plot file. An example is

```
SHAFT TWINS 11 x 22 ft w/h=0.5 CALADAY Wp=22 ft 01/31/2021
NPROB =       6
NLYRS =       1
NSEAM =       1
Nelem =    3240
F:\Visual Studio 2010\Projects\SPK\GMB3\belms
Nnode =    6800
F:\Visual Studio 2010\Projects\SPK\GMB3\bcrds
F:\Visual Studio 2010\Projects\SPK\SPKFEM\ACMrfac.UT3
Nelcf =      72
F:\Visual Studio 2010\Projects\SPK\GMB3\brcte
ACMrwindow1Feb21fs
```

where path names are evident. The change required is in the “none” line following the “bcrds” line. The replacement line specifies the location and name of the finite element output file containing element safety factors. In this example, the file name is “ACMrfac.UT3 that is preceded by the digital path to the file. “SPKFEM” is the finite element program directory that contains the factor of safety output file.

The plot program automatically distinguishes between mesh and safety factor plots. Editing one line the PlotMesh file is all that is required for a safety factor plot. This plot may

also be redone in a program such as Paint. Of course, the plot output file names should be different to avoid overwriting, say, a mesh plot with a safety factor plot. Plotting runtimes are in seconds.

**Example 1** An example of a single, rectangular shaft is the Ross Shaft at the former Homestake Mine in the Northern Black Hills of South Dakota. Rock mechanics investigation of safety and stability of the Ross Shaft have been done in detail [15]. The geology of the mine is characterized by three major formations, the Poorman, Homestake and Ellison, consisting of Precambrian meta-sediments (phyllite, schist and gneiss)

*Step 1 Preparation of a materials property file (stratigraphic column)* Rock properties for this example are given in Table 2. These laboratory rock properties values were scaled as a consequence of calibrating finite element models to match extensometer readings of displacement in the mine. The scale factors for elastic moduli and strengths were 0.25 and 0.5, respectively. These two factors are related by guidance from a simple energy relationship [15].

Table 1 Laboratory Rock Properties for Example 1*

| FORMATION<br>PROPERTY | Poorman<br>- | Homestake | Ellison |
|---|---|---|---|
| Young's Moduli (GPa) | | | |
| Ea | 93.1 | 88.3 | 89.6 |
| Eb | 94.5 | 62.1 | 75.8 |
| Ec | 49.6 | 64.2 | 63.4 |
| Shear Moduli (GPa) | | | |
| Ga | 26.9 | 26.9 | 29.0 |
| Gb | 38.6 | 29.7 | 35.1 |
| Gc | 26.2 | 33.1 | 35.7 |
| Poisson's Ratios | | | |
| Vab | 0.23 | 0.14 | 0.20 |
| Vbc | 0.22 | 0.19 | 0.15 |
| Vca | 0.15 | 0.18 | 0.17 |
| Compressive Strength (MPa) | | | |
| Ca | 94.0 | 138.9 | 78.2 |
| Cb | 84.6 | 91.5 | 56.2. |
| Cc | 69.0 | 79.6 | 78.7 |
| Tensile Strength (MPa) | | | |
| Ta | 20.6 | 9.5 | 16.2 |
| Tb | 13.2 | 13.2 | 11.4 |
| Tc | 5.7 | 7.9 | 4.1 |
| Shear Strength (MPa) | | | |
| Ra | 10.3 | 14.1 | 7.9 |
| Rb | 8.8 | 14.5 | 8.6 |
| Rc | 19.3 | 17.0 | 14.6 |

a=down dip, b=parallel to foliation strike, c=normal to foliation
*From Table 3 of [15] (Part 1 corrected).

The material properties file is given in Figure 69. The repetition of the Poorman Formation is a consequence of overturned folds. An unconformity exists above the Ellison Formation, but this feature is of no consequence for the example at hand. Indeed, there is more interesting geology at the mine including rhyolite dikes, but again, of no consequence in this example. The data in Table 2 and Figure 69 reflect an orthotropic anisotropy with axes down dip, on strike and normal to the foliation. The dip direction is at 55 deg to the y-axis of the finite element mesh (a pseudo-north in this example). Mine north is at 35 deg counter-clockwise to the y-axis of the finite element mesh. The finite element axes are coincident with the shaft axes with the small dimension in the *x*-direction and the long dimension in the *y*-direction. The vertical direction coincides with the *z*-axis. Rotation of material properties from the given material axes (*abc*) is accomplished automatically in accordance with the angles given in the material properties file. In this regard, the first number in the last line of each material is the dip direction (0-360 deg); the second number is the dip (0-90 deg)

```
NLYRS = 3
NSEAM = 2
  (1) Poorman
  13.5e+06  13.7e+06  7.20e+06      0.23      0.22      0.15
   3.8e+06   5.6e+06  3.94e+06       0.0       0.0       0.0
   13630.0   12270.0   10000.0    2990.0    1910.0     820.0
    1500.0    1520.0    2800.0
      55.0      60.0    2900.0     560.0
  (2) Homestake
  12.8e+06   9.0e+06   9.3e+06      0.14      0.19      0.18
   4.8e+06   4.3e+06   3.9e+06       0.0       0.0       0.0
   20150.0   13270.0   11547.0    1378.0    1920.0    1139.0
    2025.0    2100.0    2470.0
      55.0      60.0    3460.0      80.0
 (3) Poorman
  13.5e+06  13.7e+06  7.20e+06      0.23      0.22      0.15
   3.8e+06   5.6e+06  3.94e+06       0.0       0.0       0.0
   13630.0   12270.0   10000.0    2990.0    1910.0     820.0
    1500.0    1520.0    2800.0
      55.0      60.0    3540.0     560.0
```

Figure 69 Material properties file for Example 1

*Step 2 Mesh Generation* Mesh generation input is given in the InData file that is developed during mesh generation: Thus,

```
Input Data
 SHAFT NPROB 6
 Shaft Shape = Rectangle
 Shaft System = Single Opening
 Shaft Width =      15.0
 Width/Height Ratio =       0.7
 Opening Height=      21.0
 Section Depth Seam Center (ft)   =    3500.0
 Additional Sxx,Syy,Szz,Tyz,Tzx,Txy, tension +=
   -3349.0   -2704.0   -4167.0       0.0       0.0    -886.0
 Shaft Stress Sxx,Syy,Szz,Tyz,Tzx,Txy, tension +=
   -3349.0   -2704.0   -4167.0       0.0       0.0    -886.0
```

The premining stresses were obtained from formulas developed for the Homestake Mine [15] that are with respect to mine coordinates. Rotation to finite element coordinates results in the stresses shown in the InData file above. This rotation of stress must be done offline before mesh generation. The given values take into account stress caused by gravity, so no specific weights are present in the material properties file, Figure 69.

A mesh plot is shown in Figure 70 in plan view. The mesh is actually a slab and has a thickness into the page. There are 73,728 nodes and 36,384 three-dimensional elements in the slab.

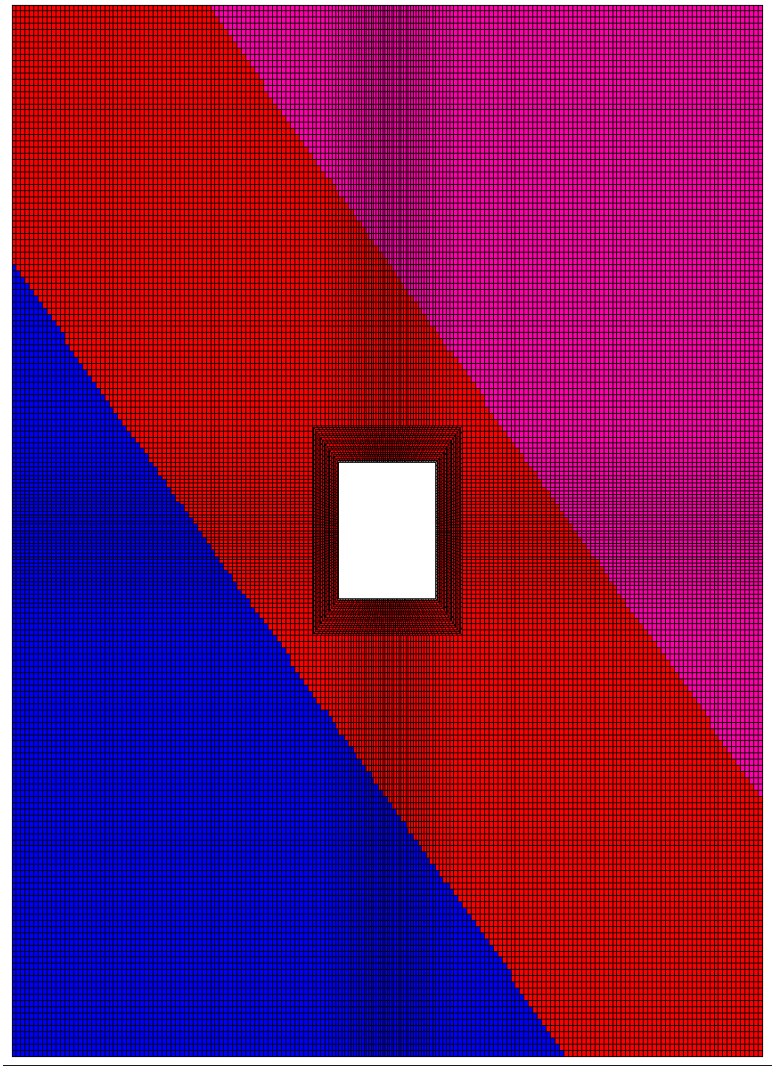

Figure 70 A mesh plot for an Example 1 of a deep, rectangular mine shaft. Light Red=Poorman Formation. Dark Red=Homestake Formation. Blue=Poorman Formation (again). The short dimensions of the shaft is 15 ft (4.5 m); the long dimension of the shaft is 21 ft (3.3 m) and bears 35 degrees clockwise from mine north. The mesh is approximately 112 x 158 ft (34 x 48 m).

*Step 3 FEM Execution and Results* Figure 71 shows results in the form of the consequent distribution of element safety factors. The skewed distribution is a consequence of the premining stress state. Not too surprisingly, the opposite corners at the shaft wall have the highest and lowest local safety factors, a result that is consistent with detailed studies [16]. Run time for the analysis is approximately 11.5 minutes.

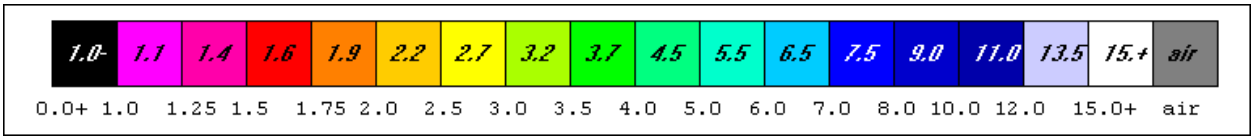


Factor of Safety Color Code

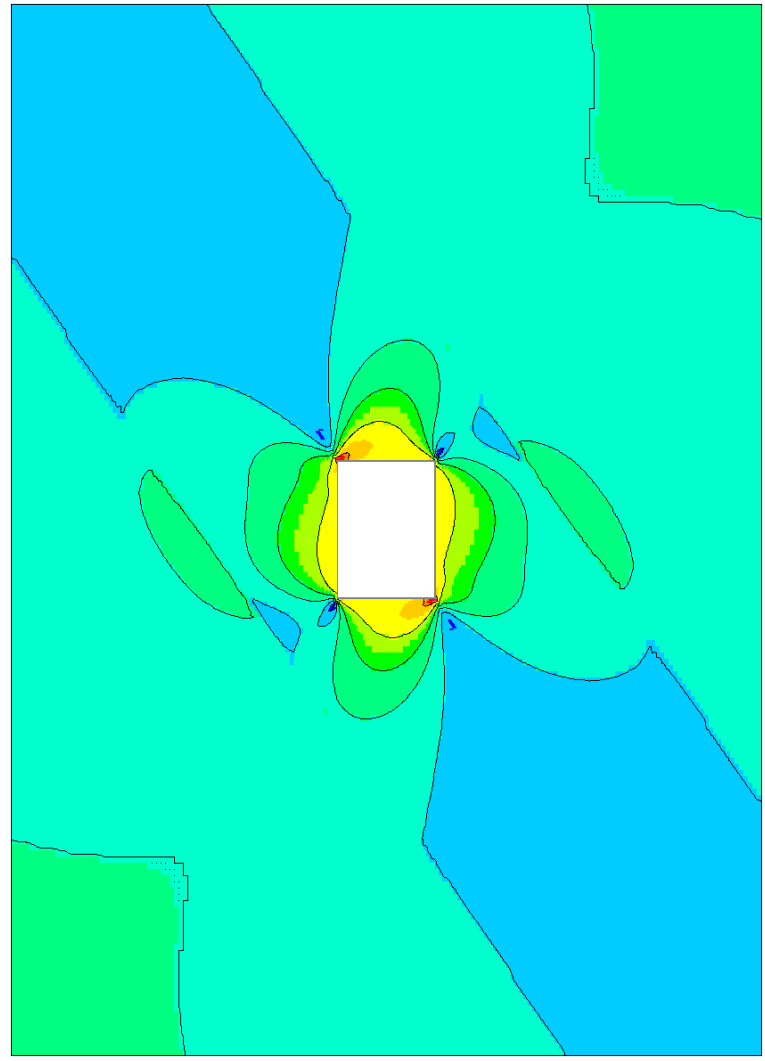

Figure 71 Element safety factors (laboratory rock properties and a thin Homestake Formation). Most of the shaft wall is yellow and has a safety factor of 2.7.

A more realistic analysis considers rock properties scaled to match mine measurements. The element safety factor distribution at shaft level is shown in Figures 72. No element failures occurred, although the highly stressed corner elements have safety factors of 1.4 as seen in the color scale.

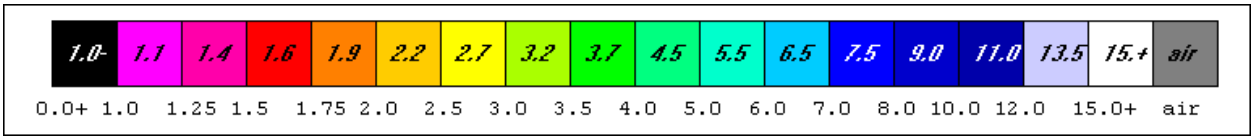


Factor of Safety Color Code

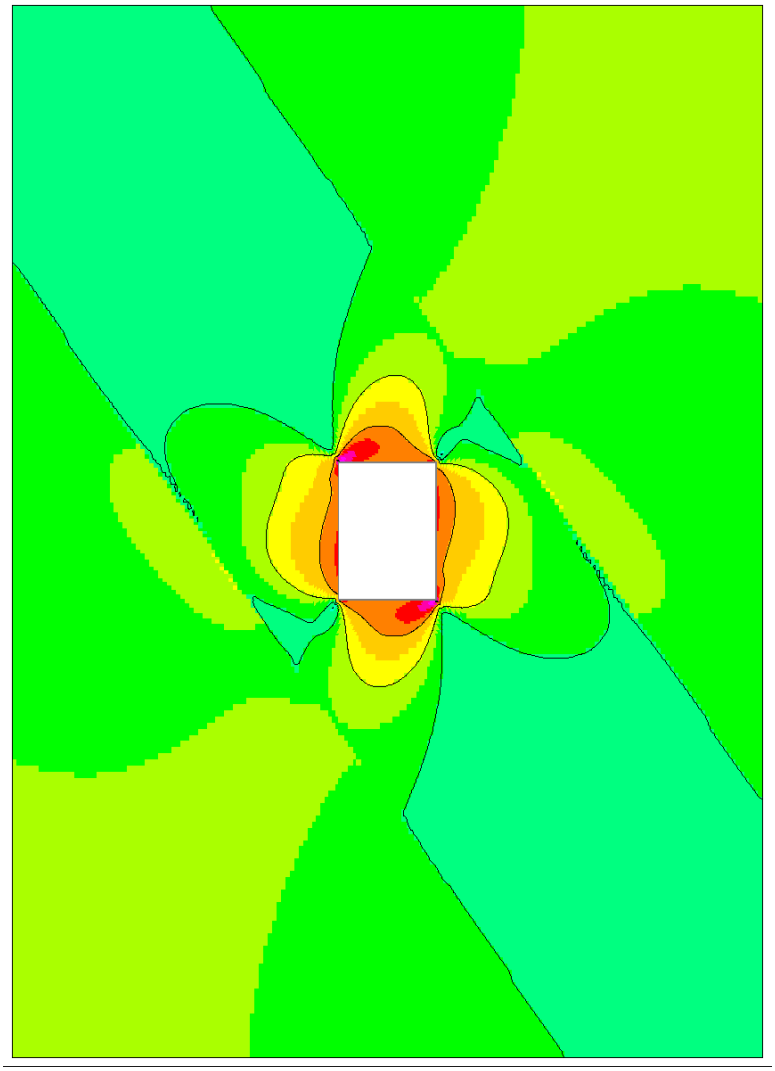

Figure 72 Element safety factors (scaled elastic moduli and strengths at 0.25 and 0.50, respectively). Most of the shaft wall is orange and has a safety factor of 1.9.

**Example 2** An example of a circular shaft is one motivated by a cooperative study at the Magmont Mine in the famous Viburnum Trend in Southeast Missouri.

*Step 1 Preparation of a materials property file (stratigraphic column)* The material properties file is given in Figure 73 where the stratum of interest is the False Davis Shale which is of lower strength relative to the limestones and dolomites in the stratigraphic column. In this regard, only the stratum of interest is required in the materials properties file. However, if strata above the stratum of interest have different specific weights and gravity stress is important, then the strata above the stratum of interest should be in the materials properties file. Depth to the section of interest is at the center of the stratum selected for analysis. Laboratory scale rock properties in the figure are tabulated in [18] and represent an amalgamation of properties from a variety of sources. These properties are isotropic as is evident in the figure.

```
NLYRS = 9
NSEAM = 9
  (1) OVERBURDEN
2.00E+03      2.00E+03      2.00E+03      0.3    0.3    0.3
1.43E+03      1.43E+03      1.43E+03      0      0      130
2000   2000   2000   100    100    100
120    120    120
0   0  0      60
  (2) GASCONADE DOLOMITE
6.92E+06      6.92E+06      6.92E+06      0.34   0.34   0.34
5.24E+06      5.24E+06      5.24E+06      0      0      163
11910  11910  11910  1174   1174   1174
1504   1504   1504
0   0  60     50
  (3) EMINENCE DOLOMITE
1.07E+07      1.07E+07      1.07E+07      0.31   0.31   0.31
7.72E+06      7.72E+06      7.72E+06      0      0      167
16120  16120  16120  734    734    734
888    888    888
0   0  110    195
  (4) POTOSI DOLOMITE
1.21E+07      1.21E+07      1.21E+07      0.26   0.26   0.26
8.17E+06      8.17E+06      8.17E+06      0      0      171
26870  26870  26870  1228   1228   1228
1486   1486   1486
0   0  305    350
  (5) DERBY-DOERUN DOLOMITE
7.58E+06      7.58E+06      7.58E+06      0.32   0.32   0.32
5.57E+06      5.57E+06      5.57E+06      0      0      162
23760  23760  23760  1285   1285   1285
1569   1569   1569
0   0  655    110
  (6) DAVIS SHALE
5.35E+06      5.35E+06      5.35E+06      0.21   0.21   0.21
3.39E+06      3.39E+06      3.39E+06      0      0      161
19610  19610  19610  1205   1205   1205
1483   1483   1483
0   0  765    150
  (7) BONNETERRE DOLOMIE
6.75E+06      6.75E+06      6.75E+06      0.31   0.31   0.31
4.89E+06      4.89E+06      4.89E+06      0      0      166
29260  29260  29260  935    935    935
1115   1115   1115
0   0  915    6
(8) ORE
```

```
8.75E+06      8.75E+06      8.75E+06      0.3    0.3    0.3
6.25E+06      6.25E+06      6.25E+06      0      0      219
18270  18270  18270  1007   1007   1007
1231   1231   1231
0   0  921    18
(9) FALSE DAVIS SHALE
3.79E+06      3.79E+06      3.79E+06      0.22   0.22   0.22
2.43E+06      2.43E+06      2.43E+06      0      0      152
5210   5210   5210   730    730    730
980    980    980
0   0  939    11
```

Figure 73 Material properties file for shaft Example 2.

*Step 2 Mesh Generation.* Mesh generation input is given in the InData file that is developed during mesh generation: Thus, (A circular shaft is an ellipse with a width to height ratio of one.)

```
Input Data
 SHAFT NPROB 6
 Shaft Shape = Ellipse (including circle)
 Shaft System = Single Opening
 Shaft Width =      19.0
 Width/Height Ratio =       1.0
 Opening Height=      19.0
 Section Depth Seam Center (ft)   =     944.5
 Additional Sxx,Syy,Szz,Tyz,Tzx,Txy, tension +=
       0.0       0.0       0.0       0.0       0.0       0.0
 Shaft Stress Sxx,Syy,Szz,Tyz,Tzx,Txy, tension +=
    -305.8    -305.8   -1084.1       0.0       0.0       0.0
```

If one were interested in safety of the shaft near the surface, then selection of the stratum of interest (NSEAM) would be the (1) stratum in the material properties file. Depth of the mesh center would be 30 ft (9 m). The mesh for the problem at hand is shown in Figure 74.

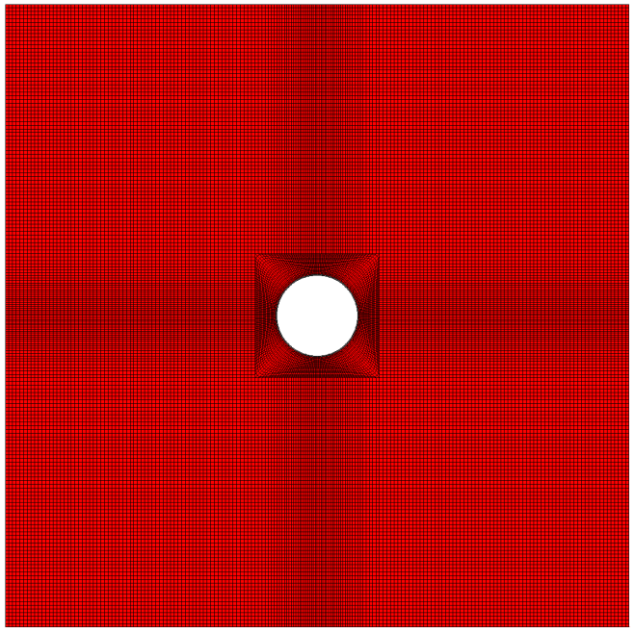

Figure 74 Mesh for Example 2 of a circular shaft. Shaft diameter is 19 ft (5.8 m).

*Step 3 FEM Execution and Results* The distribution of element safety factors is shown in Figure 75. The green colors are in the range 3.5 to5.0 and indicate a safe shaft despite the relatively weak False Davis Shale.

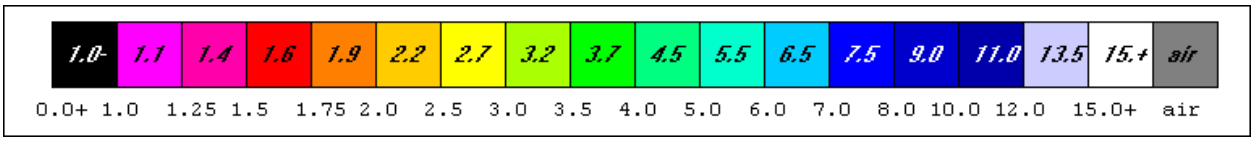


Factor of Safety Color Code

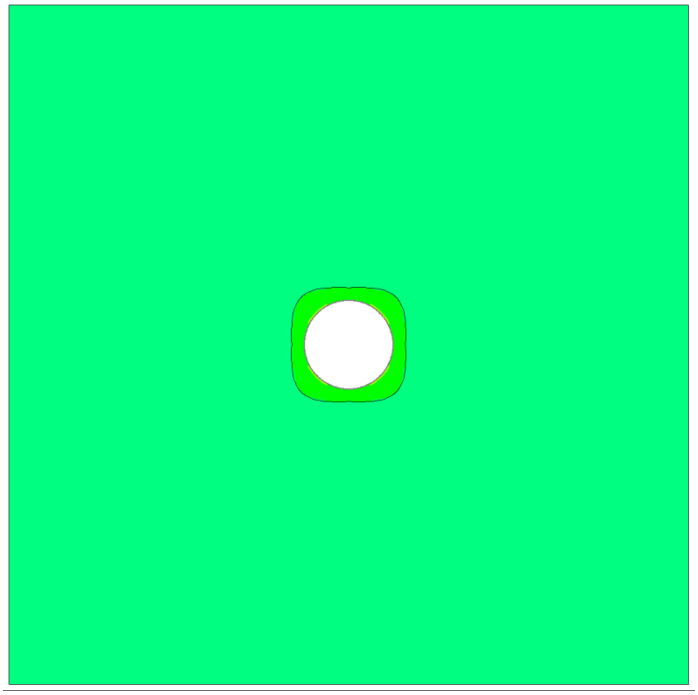

Figure 75 Element safety factor distribution: 19 ft (5.8 m) diameter circular shaft Example 2.

**Example 3** This example is motivated by mine shafts in the famous Coeur d'Alene Mining District of Northern Idaho where shafts were rectangular at the beginning of district development. At the Lucky Friday Mine the shape of the Silver Shaft was changed to circular and then to elliptical as ore was pursued to depth.

*Step 1 Preparation of a materials property file (stratigraphic column)* Material properties for this example are estimated from several sources as indicated in Table 2. Data in the table reflect transversely isotropic rock. The geological setting is one of Precambrian meta-sediments: sericitic quartzites, argillitic quartzites and vitreous quartzites.

Table 2 Estimated Rock Properties for Example 3*

| FORMATION<br>PROPERTY | Vitreous Quartzite | Sericitic Quartzite | Argillitic Quartzite |
|---|---|---|---|
| Young's Moduli (GPa/Mpsi) | | | |
| Ea | 42.1/6.1 | 37.9/5.5 | 29.0/4.2 |
| Eb | 42.1/6.1 | 37.9/5.5 | 29.0/4.2 |
| Ec | 42.1/6.1 | 27.6/4.0 | 12.4/1.8. |
| Shear Moduli (GPaMpsi) | | | |
| Ga | 16.5/2.4 | 13.1/1.9 | 7.61/1.1 |
| Gb | 16.5/2.4 | 13.1/1.9 | 7.61/1.1/ |
| Gc | 16.5/2.4 | 15.9/2.3 | 12.4/1.8 |
| Poisson's Ratios | | | |
| Vab | 0.26 | 0.21 | 0.18 |
| Vbc | 0.26 | 0.20 | 0.11 |
| Vca | 0.26 | 0.20 | 0.11 |
| Compressive Strength (MPa/psi) | | | |
| Ca | 169/24,500 | 120/17,470 | 59/8,500 |
| Cb | 169/24,500 | 120/17,470 | 59/8,500 |
| Cc | 169/24,500 | 180/26,040 | 84/12,230 |
| Tensile Strength (MPa/psi) | | | |
| Ta | 19.3/2,800 | 16.1/2,330 | 19.2/2,790 |
| Tb | 19.3/2,800 | 16.1/2,330 | 19.2/2,790 |
| Tc | 15.2/2,200 | 10.6/1,530 | 7.4/1,080 |
| Shear Strength (MPa/psi) | | | |
| Ra | 29.2/4,240 | 25.4/3,680 | 19.4/2,820 |
| Rb | 29.2/4,240 | 25.4/3,680 | 19.4/2,820 |
| Rc | 33.0/4,780 | 25.1/3,640 | 14.4/2,100 |

a=down dip (parallel to bedding), b=parallel to bedding on strike, c=normal to bedding
*With guidance from [19], [20] [21] and [22]

*Step 2 Mesh Generation.* Mesh generation input was developed for three shaft shapes, circular, elliptical-1 (20x23 ft), and elliptical-2 (20x26 ft). Orientation of foliation (dip direction) is 195 deg for the circular section, measured from the *y*-axis of the finite element model. Dip is 80 deg. Orientation of foliation is 180 deg for the elliptical sections. These angles are shown in the material properties files for circular and elliptical sections. Thus, for a circular section

```
NLYRS = 1
NSEAM = 1
  (1) Argillitic Quartzite
   4.2e+06   4.2e+06   1.8e+06      0.18      0.11      0.11
   1.1e+06   1.1e+06   1.8e+06       0.0       0.0       0.0
    8500.0    8500.0   12230.0    2790.0    2790.0    1080.0
    2820.0    2820.0    2100.0
     195.0      80.0    8500.0     400.0
```

and for elliptical sections

```
NLYRS = 1
NSEAM = 1
  (1) Argillitic Quartzite
   4.2e+06   4.2e+06   1.8e+06      0.18      0.11      0.11
   1.1e+06   1.1e+06   1.8e+06       0.0       0.0       0.0
    8500.0    8500.0   12230.0    2790.0    2790.0    1080.0
    2820.0    2820.0    2100.0
     180.0      80.0    8500.0     400.0
```

The elastic moduli and strengths were reduced from the values in Table 2 by scale factors or 0.25 and 0.50, respectively. Moduli in the finite element analyses were one-fourth of those in the table; strengths were one half of the table values. These were the same scale factors used in the Homestake Mine shaft example to account for "joints" at the mine scale.

An InData file example for and elliptical section 20 x 23 ft is

```
Input Data
 SHAFT NPROB 6
 Shaft Shape = Ellipse (including circle)
 Shaft System = Single Opening
 Shaft Width =                  20.0
 Width/Height Ratio =            0.9
 Opening Height=                23.0
 Section Depth Seam Center (ft)   =    8700.0
 Additional Sxx,Syy,Szz,Tyz,Tzx,Txy, tension +=
  -11407.0  -10549.0   -9640.0       0.0       0.0    1220.0
 Shaft Stress Sxx,Syy,Szz,Tyz,Tzx,Txy, tension +=
  -11407.0  -10549.0   -9640.0       0.0       0.0    1220.0
```

The stress input data are derived from formulas given in [19] using a depth of 8,700 ft. Rotation of these data to finite element coordinates was necessarily done prior to mesh generation. The first ellipse (20x23 ft) mesh is shown in Figure 76.

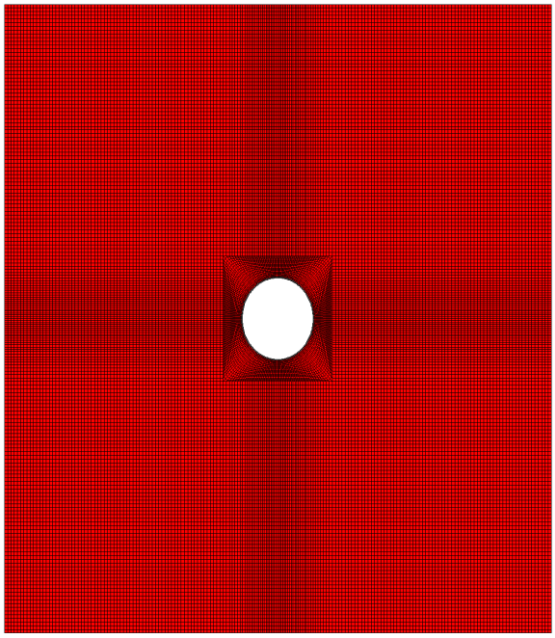

Figure 76 Elliptical shaft section (20x23 ft).

*Step 3 FEM Execution and Results* Distribution of element safety factors in case of the circular and first elliptical sections are sown in Figure 77.

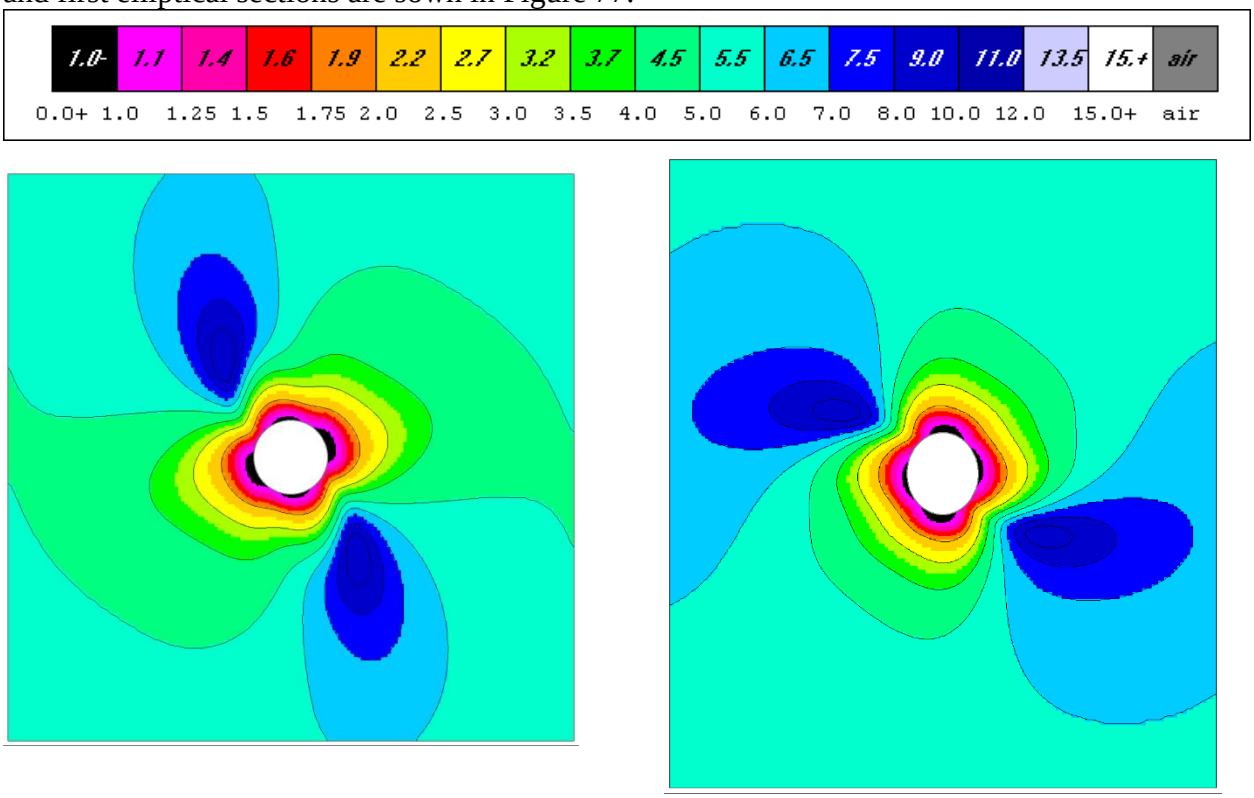


(A) (B)

Figure 77 Element safety factor distributions about (A) circular and (B) elliptical shaft sections.

The yielding elements in both sections of Figure 77 are mainly perpendicular to the foliation, although the orientation is different in the two parts of the figure. The number of yielding elements is slightly smaller in the ellipse and somewhat less in a second ellipse (20x26 ft), but the differences are small. In this regard, the rule for minimizing stress concentration that guides elliptical sections ("long axis parallel to the major principal stress") for isotropic rock is not applicable in this situation. Additionally, there are orientation differences between principal stress in the plane of the section and the foliation.

In this example, foliation appears to rule as Figure 78 shows. In this figure, the major principal stress is perpendicular to the long axis of the ellipse contrary to the isotropic rule, but the major principal stress is also parallel to the foliation and highest compressive strength direction.

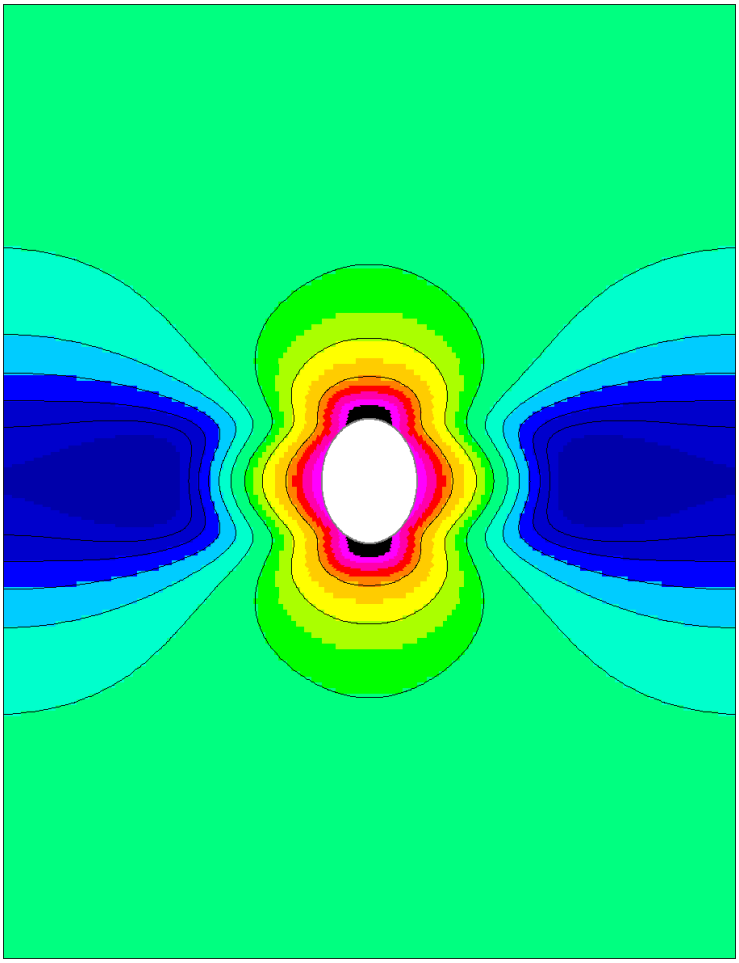

Figure 78 Element safety factor distribution about an ellipse 20 x 26 ft with the major principal stress and foliation aligned with the minor axis of the ellipse.

The actual shape appears more in keeping with breakouts than a true ellipse [22]. A more detailed study would certainly be of interest, but such is beyond the scope of this demonstration. However, these results do indicate fast, easy to use software capability for analysis of shaft safety.

**Example 4** Twin shafts and multiple shafts are found in high capacity underground mines such as block caving and sublevel caving mines. San Manuel Mine, a former underground copper mine is an example. The Kiruna underground iron ore mine in Sweden is another example. Twin shafts may be used when one is for air intake, access and hoisting, the other for exhaust. The example here of twin shafts is one motivated by a relatively recent rectangular shaft in the Coeur d'Alene Mining District of Northern Idaho, the Caladay Shaft. The Caladay Shaft was studied in considerable detail by Whyatt [20]. Although not a twin shaft set, the information available allows for a realistic example of twin shafts. In fact the shaft was collared at the end of an adit and is technically a winze.

*Step 1 Preparation of a materials property file (stratigraphic column)* The material property file is the same used for the Silver Shaft example. The material is transversely isotropic.

```
NLYRS = 1
NSEAM = 1
  (1) Argillitic Quartzite
   4.2e+06   4.2e+06   1.8e+06      0.18      0.11      0.11
   1.1e+06   1.1e+06   1.8e+06       0.0       0.0       0.0
    8500.0    8500.0   12230.0    2790.0    2790.0    1080.0
    2820.0    2820.0    2100.0
     180.0      70.0    5800.0     400.0
```

Accordingly, section depth is 6,000 ft.

*Step 2 Mesh Generation.* Mesh generation input is summarized in the InData file:

```
Input Data
 SHAFT NPROB 6
 Shaft Shape = Rectangle
 Shaft System = Twin Openings
 Shaft Width =             11.0
 Width/Height Ratio =       0.5
 Pillar Width =            22.0
 Section Depth Seam Center (ft)   =    6000.0
 Additional Sxx,Syy,Szz,Tyz,Tzx,Txy, tension +=
   -7571.0   -8441.0   -6688.0       0.0       0.0     927.0
 Shaft Stress Sxx,Syy,Szz,Tyz,Tzx,Txy, tension +=
   -7571.0   -8441.0   -6688.0       0.0       0.0     927.0
```

The mesh is shown in Figure 79. The short dimension is parallel to foliation by design.

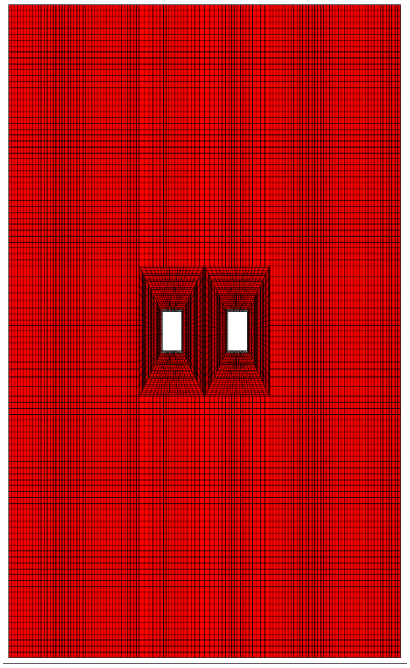

Figure 79 Finite element mesh for twin rectangular shafts 11 x 22 ft separated by a 22 ft pillar.

*Step 3 FEM Execution and Results*. Figure 80 summarizes the results in the form of the element safety factor distribution. Very few elements yield (black) and then only at the corners. However, the shaft is engulfed in a "hot zone" of elements with safety factors of 1.1 to 1.4 or so as indicated by the pink and red colors. The pillar between shafts is also "hot", so to speak. These results indicate concern for shaft wall safety at the considered depth of 6,000 ft under the conditions of the analysis.

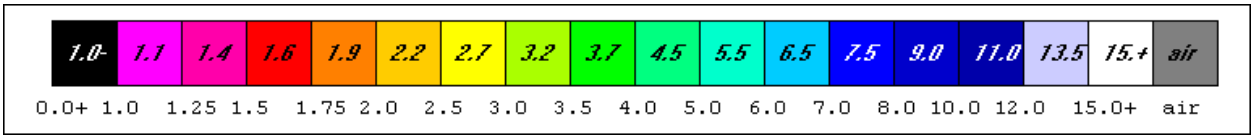


Safety Factor Color Code

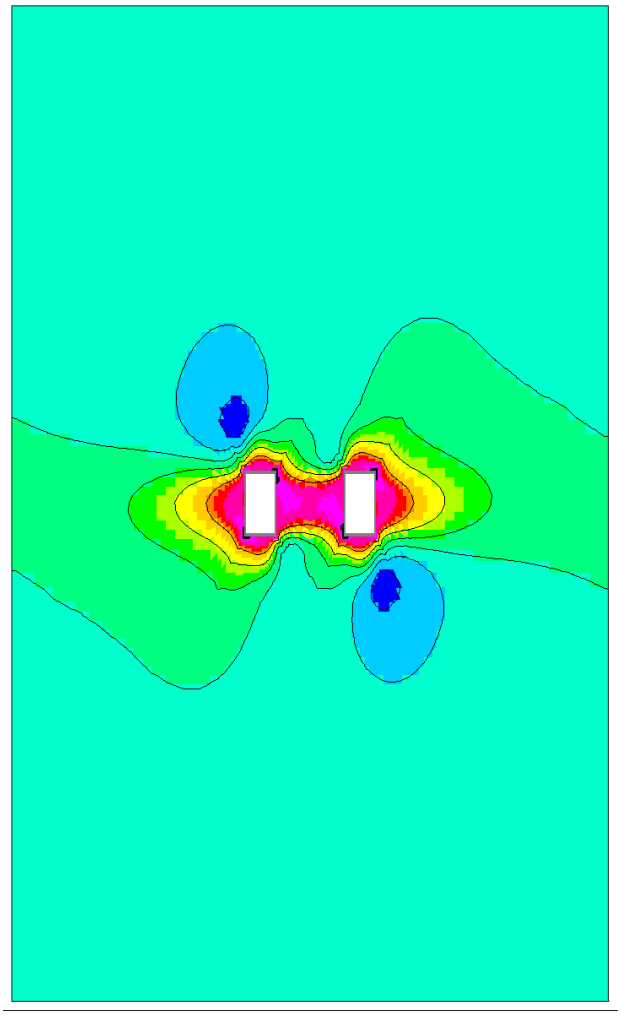

Figure 80 Element safety factor distribution for twin rectangular shafts.

**Example 5** This example continues the analysis of twin rectangular shafts and demonstrates the results of aligning shafts in a long row of similar shafts. In this case, the shaft and pillar center planes are planes of symmetry.

*Step 1 Preparation of a materials property file (stratigraphic column)* The material property file is the same used in the previous example. The material is transversely isotropic.

*Step 2 Mesh Generation.* Mesh generation leads to the mesh in Figure 81

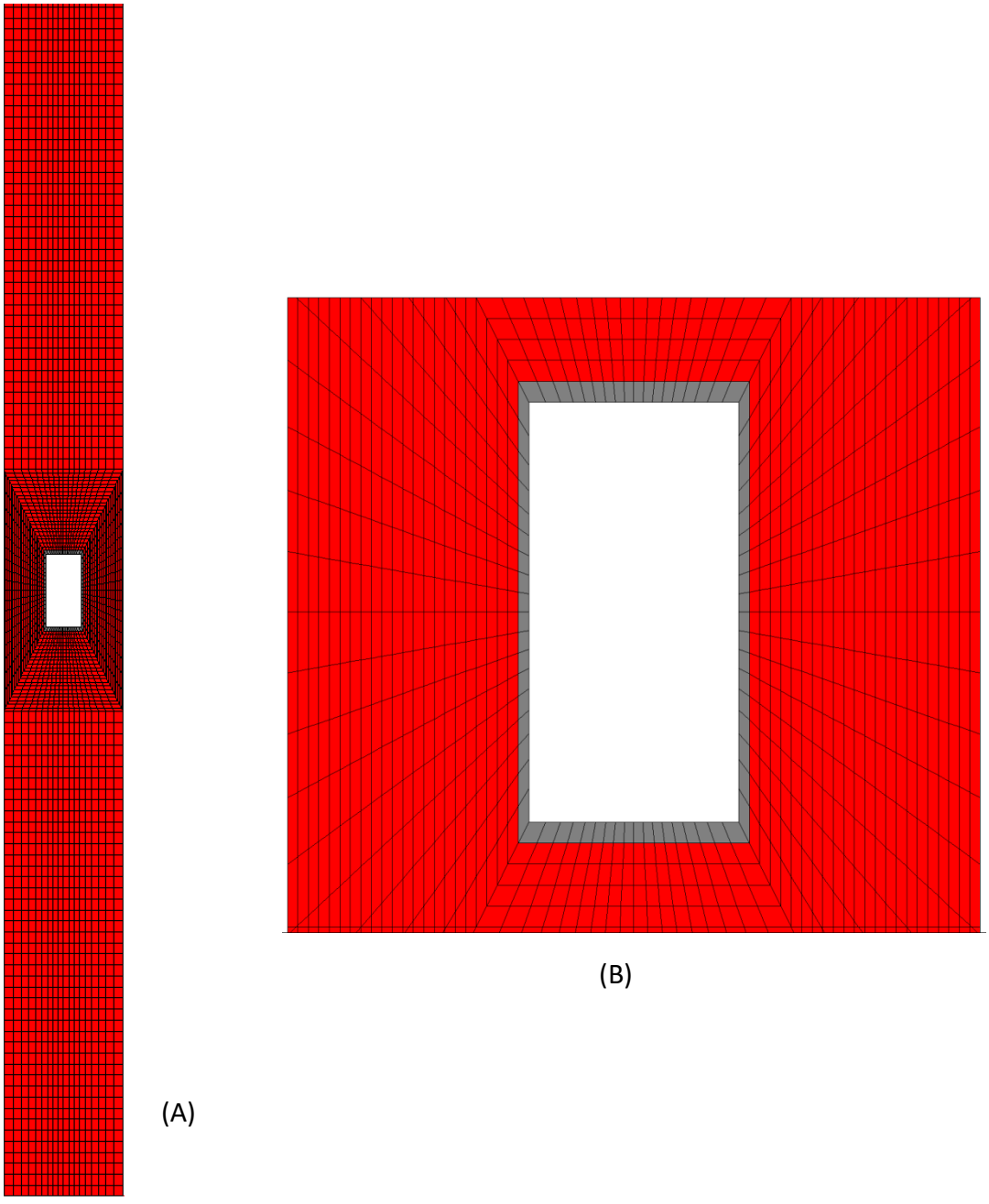


Figure 81 Mesh for a row of rectangular shafts 11 x 22 ft in section with a 22 ft pillar width (A) full mesh, (B) close-up. Grey elements are excavated.

*Step 3 FEM Execution and Results*. Results are summarized in Figure 82. There is little difference from the twin shaft results.

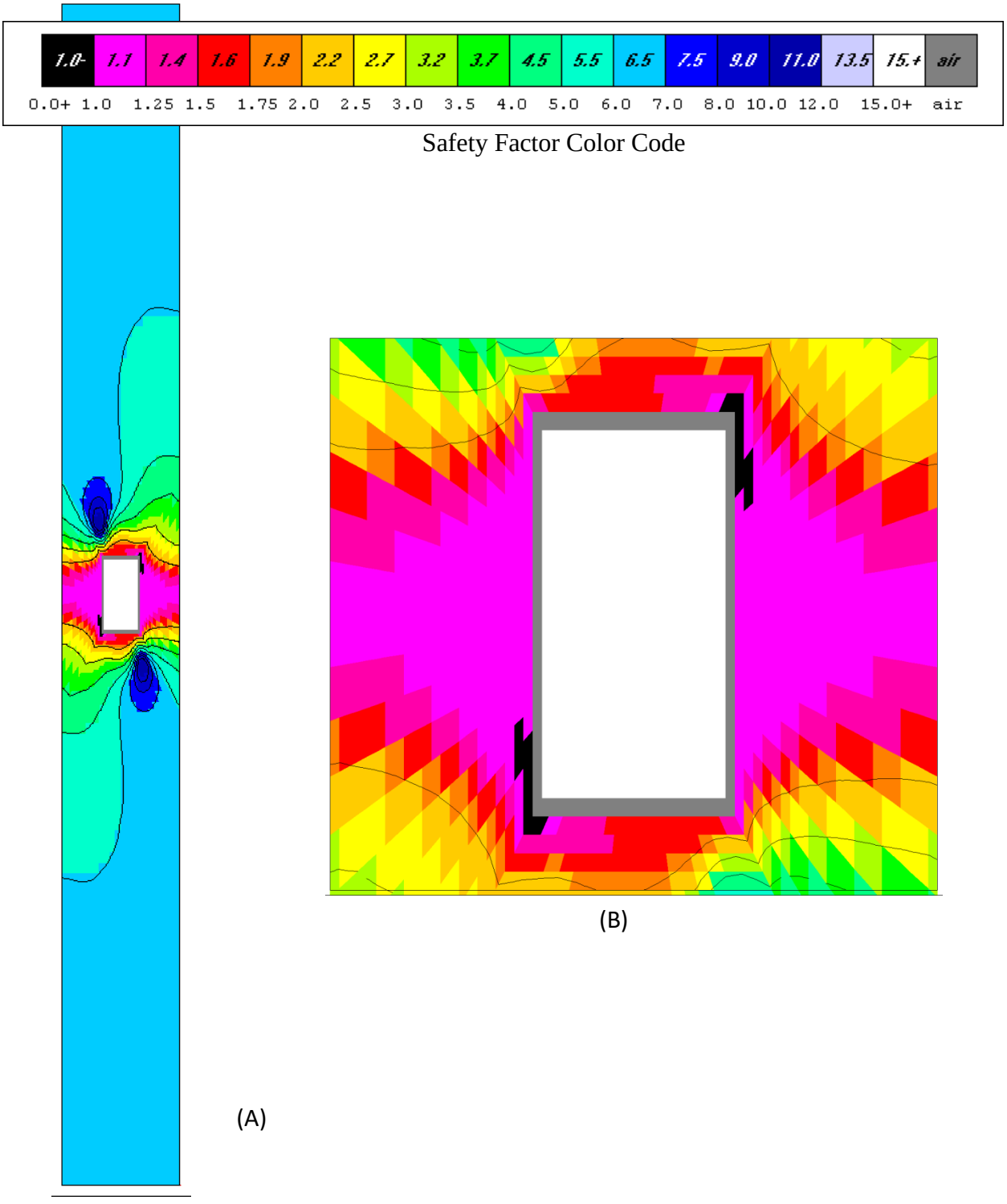


Figure 82 Safety factor distribution for a row rectangular shafts 11 x 22 ft in section with a 22 ft pillar width (A) full mesh, (B) close-up.

**Example 6** This example repeats the analysis of twin rectangular shafts and demonstrates accommodation of relatively thin, dipping rock bands that are not parallel to the long axis of the shafts. The dip direction is at 40 deg clockwise angle to the long axis of the shafts rather than at 180 deg (parallel to the long direction).

*Step 1 Preparation of a materials property file (stratigraphic column)* The material property file shows three transversely isotropic rock bands. Thus

```
NLYRS = 3
NSEAM = 2
   (1) Vitreous Quartzite
   6.1e+06   6.1e+06   6.1e+06      0.26      0.26      0.26
   2.4e+06   2.4e+06   2.4e+06       0.0       0.0       0.0
   24500.0   24500.0   24500.0    2800.0    2800.0    2800.0
    2400.0    2400.0    2400.0
      40.0      70.0    5800.0     180.0
   (2) Argillitic Quartzite
   4.2e+06   4.2e+06   1.8e+06      0.18      0.11      0.11
   1.1e+06   1.1e+06   1.8e+06       0.0       0.0       0.0
    8500.0    8500.0   12230.0    2790.0    2790.0    1080.0
    2820.0    2820.0    2100.0
      40.0      70.0    5980.0      40.0
   (3)  Sericitic Quartzite
   5.5e+06   5.5e+06   4.0e+06      0.21      0.20      0.20
   1.9e+06   1.9e+06   2.3e+06       0.0       0.0       0.0
   17470.0   17470.0   26040.0    2330.0    2330.0    1530.0
    3680.0    3680.0    3640.0
      40.0      70.0    6020.0     180.0
```

The InData file is the same as in the previous Caladay Shaft examples.

```
Input Data
 SHAFT NPROB 6
 Shaft Shape = Rectangle
 Shaft System = Twin Openings
 Shaft Width =             11.0
 Width/Height Ratio =       0.5
 Pillar Width =            22.0
 Section Depth Seam Center (ft)   =    6000.0
 Additional Sxx,Syy,Szz,Tyz,Tzx,Txy, tension +=
   -7571.0   -8441.0   -6688.0       0.0       0.0     927.0
 Shaft Stress Sxx,Syy,Szz,Tyz,Tzx,Txy, tension +=
   -7571.0   -8441.0   -6688.0       0.0       0.0     927.0
```

*Step 2 Mesh Generation.* Mesh generation leads to the mesh in Figure 83 that clearly reveals the presence of the three rock bands. Vitreous quartzite (red) is uppermost; argillitic quartzite (green) is in the middle, and sericitic quartzite (blue) is at the bottom

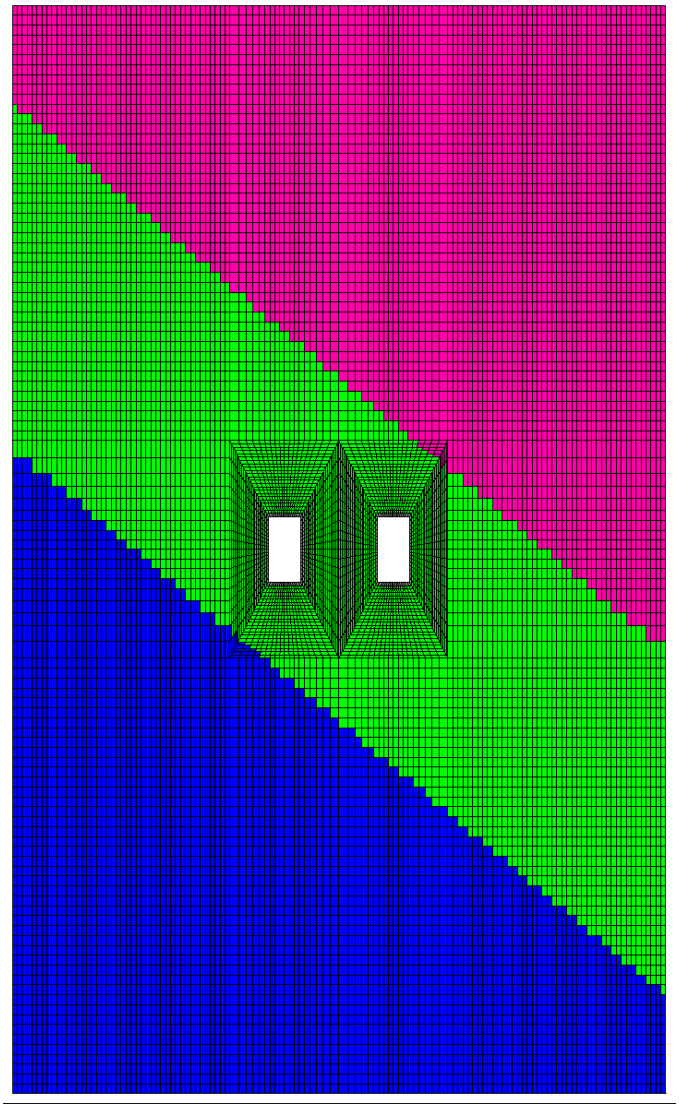

Figure 83 Twin shaft mesh with three rock types oriented at an angle to the long axis of the twin shafts. Shafts are 11 x 22 ft and are separated by a 22 ft wide pillar.

*Step 3 FEM Execution and Results*. Results are summarized in Figure 84. There is little difference from the twin shaft results. The number of yielding elements is only slightly larger. The twisted pattern in the figure is a consequence of rock band orientation, foliation orientation and orientation of principal stress. The finite element analysis takes all the orientation effects into account automatically.

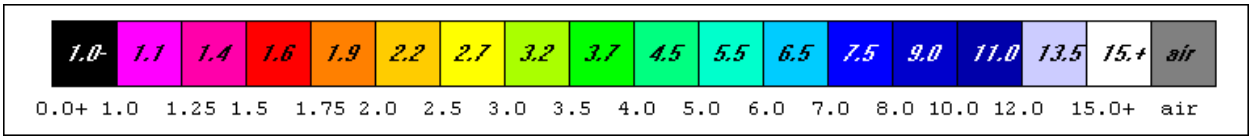


Safety Factor Color Code

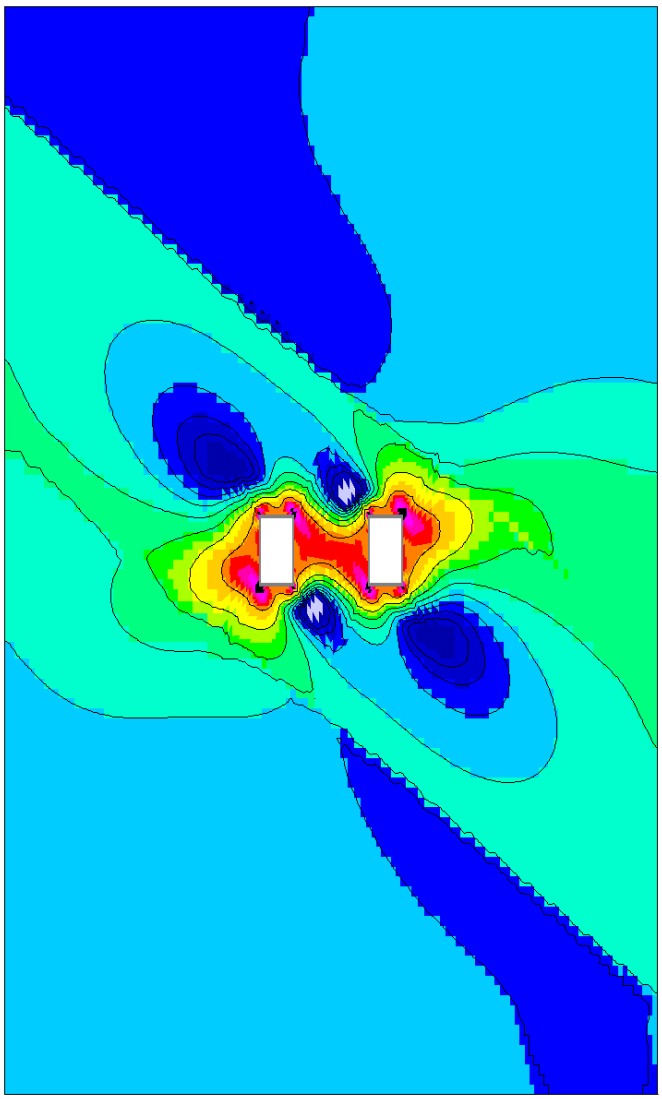

Figure 84 Element safety factor distribution about twin shafts with three rock types oriented at an angle to the long axis of the twin shafts. Shafts are 11 x 22 ft and are separated by a 22 ft wide pillar.

# 7 TUNNELS

Tunnels here include adits, crosscuts and drifts (in mine-speak) as well as tunnels in the usual meaning of the word. As in analyses of shafts, concern here is with the redistribution of stress induced by excavation and the consequent distribution of tunnel wall safety factors. Safety of tunnel excavations is of most importance, less so than numerical values of stress and strain associated with excavation. Displacements of unlined mine tunnels immediately after excavation are also of less concern, especially when assurance of an elastic response to excavation is obtained. As a reminder, an elastic ideally plastic stress-strain law is used in the three-dimensional finite element analyses presented here. Neither work-hardening nor softening occur beyond the elastic limit; time dependent behavior is not allowed.

Side by side or twin tunnels are of interest. Indeed, multiple tunnels (entries, drifts, crosscuts) may be used in large underground mines to ensure adequate ventilation and haulage capacity. Separation of tunnels in a row by pillars is an important consideration in case of multiple tunnels of the same cross-section.

Tunnel mesh generation allows for single, twin and rows of tunnels side by side. Circular, rectangular and elliptical cross-sections are allowed in every case as in the analyses of shafts. Importantly, the frequently used arched back shape is also allowed.

Mesh generation is interactive; choices available are made during execution of the mesh generation program. Examples of meshes for single elliptical, twin circular and a row of rectangular tunnels are shown in Figure 68 in the discussion of shafts. Figure 83 shows several examples of arched back tunnels. Tunnel width is the same in each of the examples in the figure. Pillar width is also the same and equal to the tunnel width. In this regard, only a tunnel with a width-to-height ratio of one has a circular arched back. All others have elliptical arched backs as seen in the figure. Multiple, dipping rock formations are also evident in the figure. The white band is designated as the formation of interest and passes through the center of coordinates in each case.

As usual, mesh generation must be preceded by preparation of a material properties file that includes elastic moduli, strengths, depths and thicknesses of strata, and importantly, the identification of the stratum or rock formation of interest where the center of the tunnel cross-section is located. In case of anisotropic strata, the dip direction and dip of the *a*-axis of anisotropy are required. This feature allows tunnels that are aligned with finite element coordinates (*xyz*) to be at an angle to the material axes (*abc*). The *z*-axis is the tunnel axis. The depth of the formation of interest can be varied, of course, but it is at this depth where the mesh section is located and the analysis is done. Dipping formations are allowed. The dip and dip direction of the formation at the depth of the tunnel center apply.

Pretunnel stress may be caused by gravity alone. The vertical stress is computed using a formation thickness weighted specific weight that is multiplied by the depth to the center of the section in the formation of interest. However, an option allows for additional stress to be added to gravity stress during mesh generation. Another option is to omit gravity stress and then to

simply specify the state of stress at the section depth of interest. Examples illustrate these options.

Examples of “tunnels” from the mining industry in various geological settings also illustrate analysis procedures and practical applications.

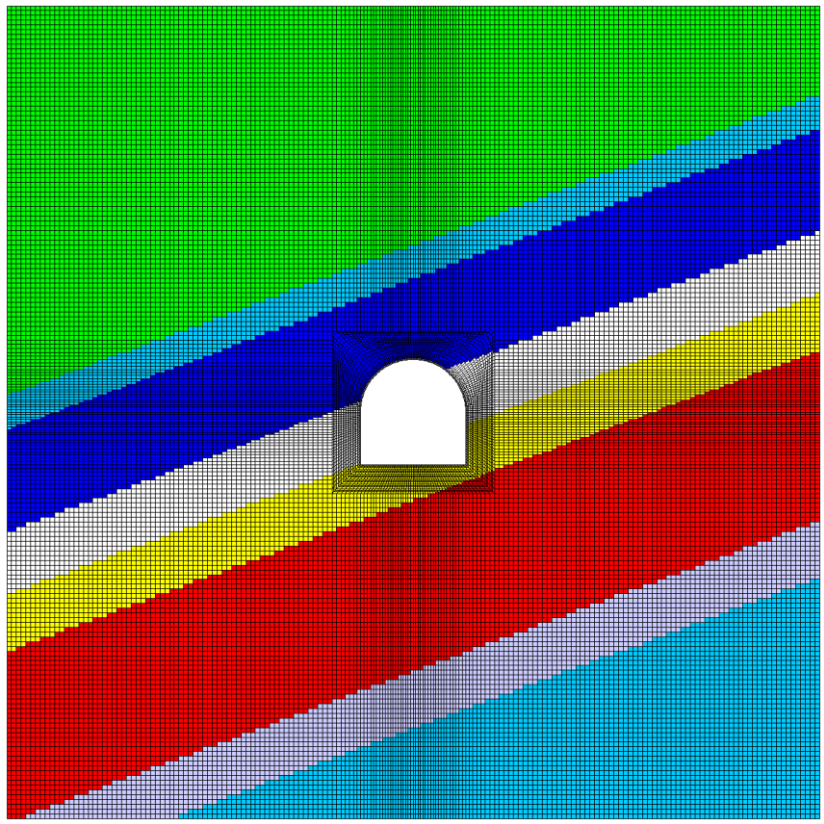

(A)

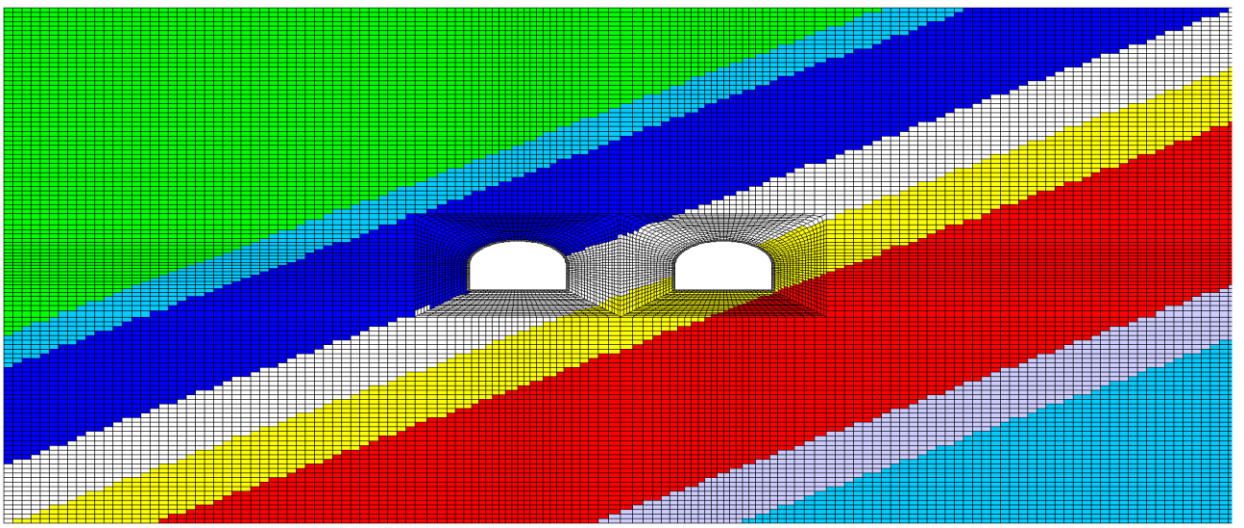

(B)

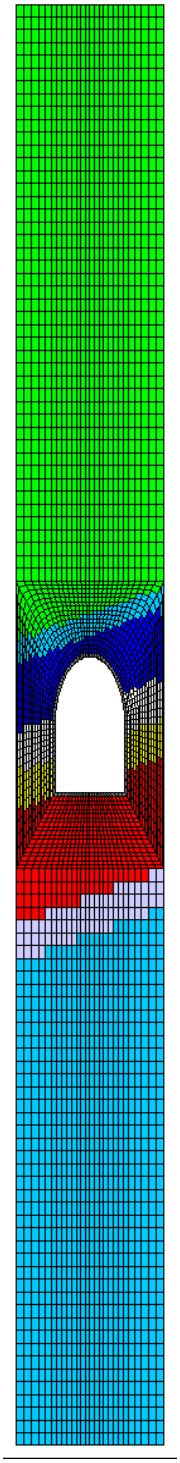

(C)

Figure 83 Arched back tunnel mesh examples: (A) single tunnel with a width to height ratio of one, (B) twin arched back tunnels with a width to height ratio of two separated by a pillar of the same width, and (C) a row of arched back tunnels with a width to height ratio of one-half separated by pillars of tunnel width. Grey elements are “cut” elements that allow for shaft excavation during an analysis.

Numbers of elements and nodes vary from mesh to mesh. Mesh dimensions also vary while allowing for external boundaries to be sufficiently distant from shaft walls to have negligible effect on stress concentration near the shaft walls. In case of rows of tunnels, symmetry about central pillar planes is exploited. A central portion of these meshes is highly refined to allow for close approximation to the actual distributions of stress, strain, displacement and element safety factors. To be sure, these meshes are three-dimensional slabs with thickness extending into the page. This thickness is adjusted to maintain an element aspect ratio of approximately three which ensures satisfactory numerical performance.

Mesh plotting is easy using the available plot program file **GMBP.exe** (in executable form). A double click on the file begins with presentation of a disclaimer. Acknowledgement of the disclaimer from the keyboard is followed with a request for the plot input file. This file is available following mesh generation and has the name PlotMesh in a form that is largely self-explanatory. However, if mesh generation and plot routines are in different directories, then path names must precede file names (belms, bcrds, brcte). The last line AMSH is the output mesh plot file name. Editing the input plot file is readily done through a program such as WordPad. For example,

```
PlotTunnel
NPROB =       7
NLYRS =       1
NSEAM =       1
Nelem =   15808
belms
Nnode =   32218
bcrds
none
Nelcf=     144
brcte
MSH
```

Plotting finite element output in the form of element safety factor distributions follows a path similar to mesh plotting with a small but essential change to the input plot file. An example safety factor plot file is

```
STILLWATER TWIN TBM W=15 w/h1 STM PROPS Wp=30 ft
NPROB =       7
NLYRS =       1
NSEAM =       1
Nelem =   15808
F:\Visual Studio 2010\Projects\SPK\GMB3\belms
Nnode =   32218
F:\Visual Studio 2010\Projects\SPK\GMB3\bcrds
F:\Visual Studio 2010\Projects\SPK\SPKFEM\ASTfac.UT3
Nelcf =    144
F:\Visual Studio 2010\Projects\SPK\GMB3\brcte
ASTfs
```

where path names are evident. The change required is in the "none" line following the "bcrds" line in the mesh plot file. The replacement line specifies the location and name of the finite element output file containing element safety factors. In this example, the file name is "ASTfac.UT3 that is preceded by the digital path to the file. SPKFEM is the finite element program directory that contains the factor of safety output file.

The plot program automatically distinguishes between mesh and safety factor plots. Plots may be redone in a program such as Paint and saved as a png file and later copied into a report written in, say, Word. Of course, the plot output file names should be different to avoid overwriting a mesh plot with a safety factor plot. Plotting runtimes are in seconds.

**Example 1** An example of circular tunnels is one motivated by long adits excavated by boring machines at the East Boulder project of the Stillwater Mine in south central Montana. Adit diameters of 13, 15 and 18 ft were excavated [25] Luxner, T., J. Deen and M. Koski (2012) Use of Tunnel Boring Machines at the Stillwater Mining Company's Underground PGM Mine, *Mining Engineering,* Vol 64, No 12, pp 50-57.

*Step 1 Preparation of a materials property file (stratigraphic column)* The material properties file for this example is

```
NLYRS = 1
NSEAM = 1
  (1) Gabbro Reef
  15.8e+06  15.8e+06  15.8e+06      0.25      0.25      0.25
  6.32e+06  6.32e+06  6.32e+06       0.0       0.0       0.0
   28000.0   28000.0   28000.0    1600.0    1600.0    1600.0
    3910.0    3910.0    3910.0
      90.0      90.0    2390.0     420.0
```

*Step 2 Mesh Generation* Mesh generation input is given in the InData file that is developed during mesh generation: Thus,

```
Input Data
 DRIFT NPROB 7
 Tunnel Shape = Ellipse (including circle)
 Tunnel System = Twin Openings
 Tunnel Width =      15.0
 Width/Height Ratio =       1.0
 Pillar Width =      30.0
 Section Depth Seam Center (ft)   =    2600.0
 Additional Sxx,Syy,Szz,Tyz,Tzx,Txy, tension +=
   -5616.0   -3120.0   -4680.0       0.0       0.0       0.0
 Tunnel Stress Sxx,Syy,Szz,Tyz,Tzx,Txy, tension +=
   -5616.0   -3120.0   -4680.0       0.0       0.0       0.0
```

The premining stresses were estimated from formulas and guidance presented in [26] Langston, R. and H. Kirsten (2002) *Ground Control Manual*, Stillwater Mining Company and [27]Johnson, J. C., T. Brady, M. MacLauglin, R. Langston and H. Kirstern (2003) In situ Stress Measurements at the Stillwater Mine, Nye, Montana. *Proc 12th Pan-American Conference on*

*Soil Mechanics and Geotechnical Engineering and the 39th U.S. Rock Mechanics Symposium, Massachusetts Institute of Technology*, Cambridge, Massachusetts, June, Vol. 1. Stresses are with respect to compass coordinates that are also mine coordinates in this example. Note: The vertical stress is Syy in tunnel analyses.

A mesh plot is shown in Figure 84 in cross-section. The mesh is actually a slab and has a thickness into the page. There are 15,088 elements and 32,218 nodes in the slab.

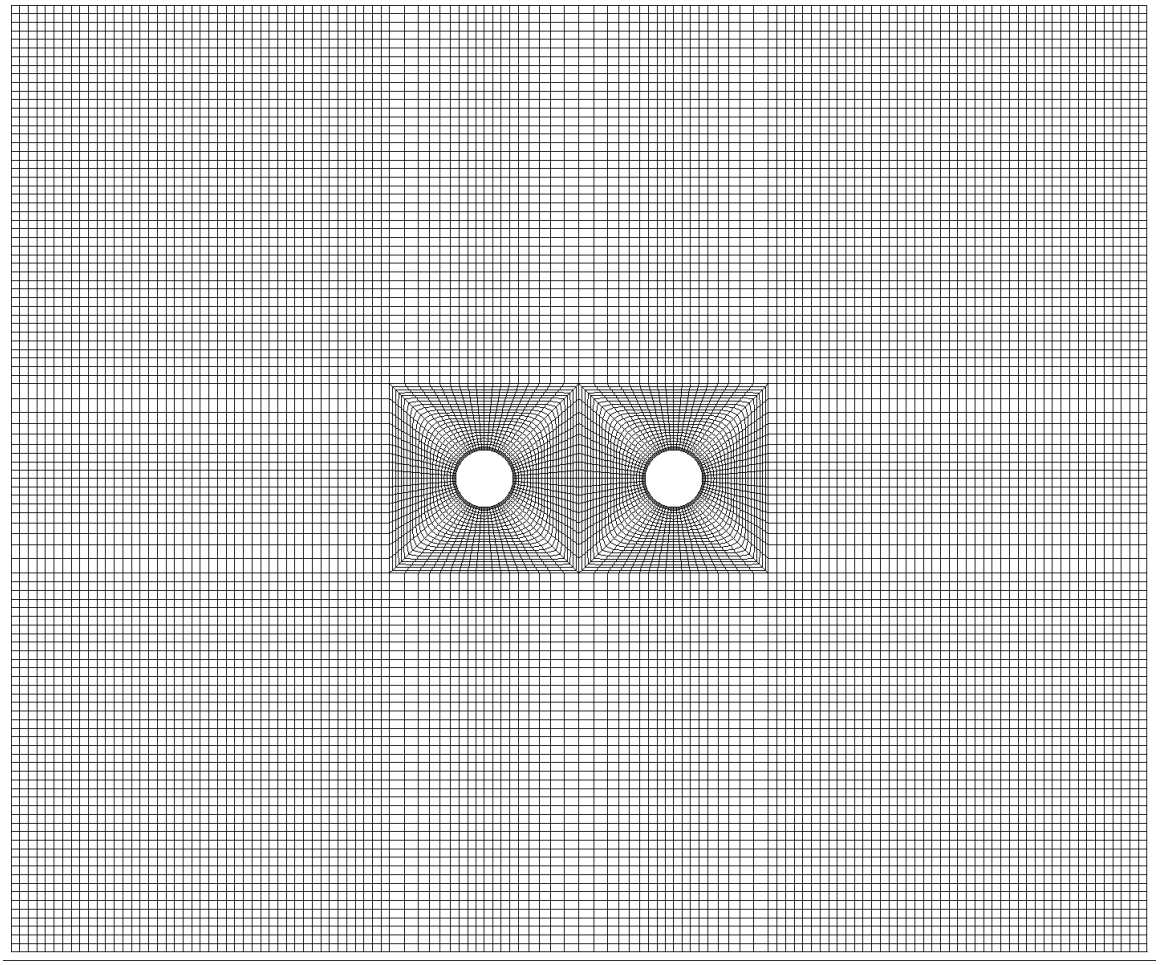

Figure 84 Finite element mesh for twin tunnels (adits) at the Stillwater Mine. Tunnel diameters are 15 ft; pillar width is 30 ft. Section depth is 2,600 ft.

*Step 3 FEM Execution and Results* Figure 85 shows results in the form of the distribution of element safety factors. As before, the elastic moduli and strengths at the laboratory scale were reduced using scale factors of 0.25 and 0.5, respectively. The pillar width is evidently adequate to prevent elevated stress arising from tunnel interaction.

As always in these examples, the intent is to demonstrate capability of user-friendly software for fast, reliable analysis of excavation safety using reasonable conditions in situ. A detailed, site-specific engineering design analysis is not the intention here.

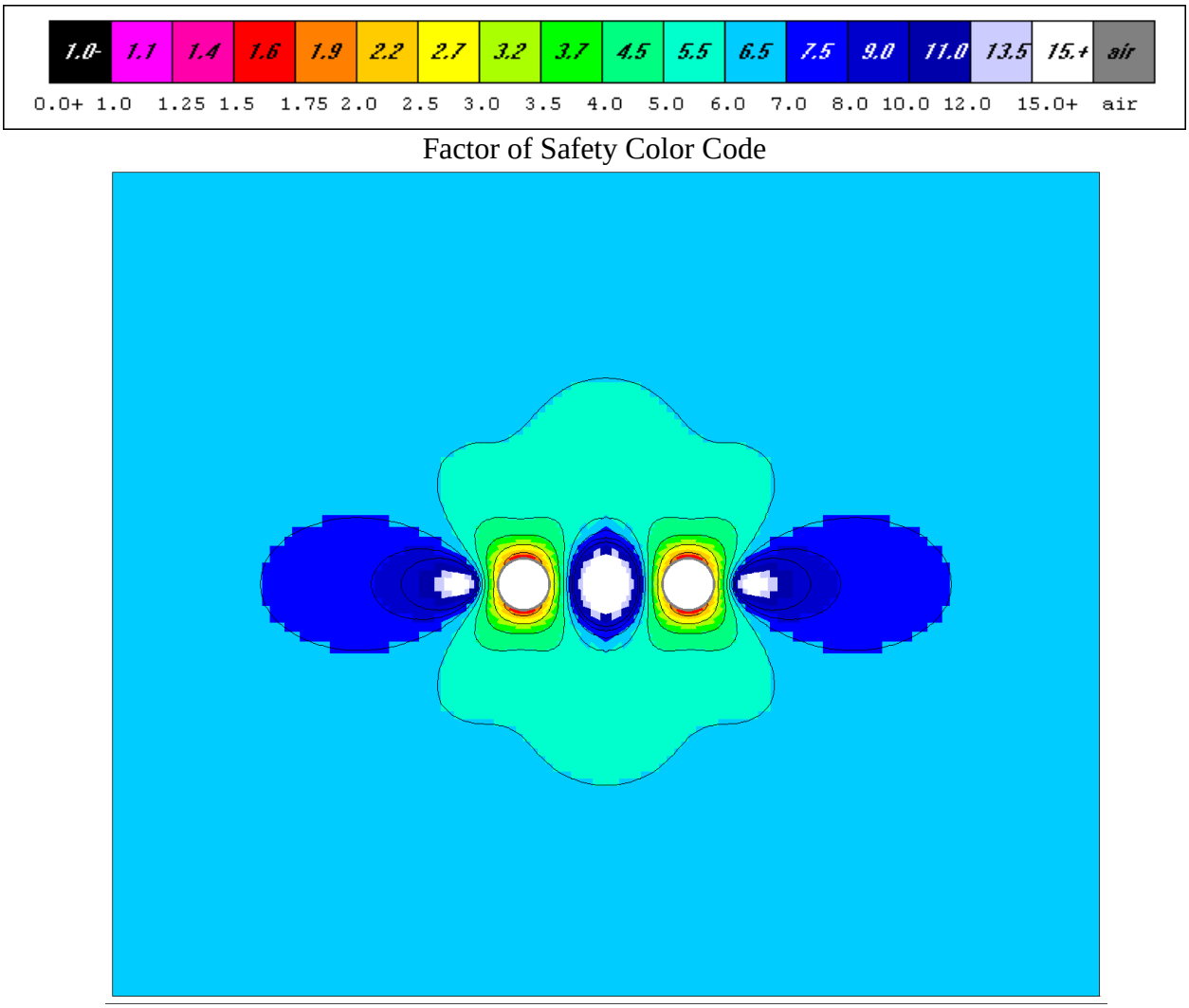


Factor of Safety Color Code

Figure 85 Element safety factors about twin tunnels excavated by a tunnel boring machine at the Stillwater Mine (East Boulder). Safety factors range from 1.6 (orange) to over 15 (white).

**Example 1a** A more realistic analysis considers *rock and joint* properties combined in a technically sound procedure that produces *equivalent* rock properties. Equivalent properties lead to the same stresses and strains in an element that would result from averaging stresses and strains in a jointed rock element. Taking joints into account as well as intact rock between joints using equivalent properties is a more realistic representation of rock formations in situ than simply scaling laboratory rock properties. Equivalent properties avoid the circular logic of "calibrating" numerical models by developing scale factors to match displacement measurements in situ, then adjusting input rock properties to produce matching displacements. The technology has been in service for many years [28] Pariseau, W. G. and H. Moon, (1988) "Elastic Moduli of Well-jointed Rock Masses", *Numerical Methods in Geomechanics* (Innsbruck), Balkema, pp, 815-822, [29] Pariseau, W. G. (1999) "An Equivalent Plasticity Theory for Jointed Rock Masses". *Int'l J. Rock Mech. Mng. Sci.*, Vol. 36, No.7, pp. 907-918, but is not yet available to the technical community at large.

*Step 1 Preparation of a materials property file (stratigraphic column)* The material properties file for this example is

```
NLYRS = 1
NSEAM = 1
  (1) Gabbro Reef with 2 jt sets
  3.97E+06  3.85E+06  6.45E+06      0.23      0.19      0.26
  2.06E+06    1.88E+06  1.41E+06       0.0       0.0       0.0
    7180.0    6980.0   11700.0     402.0     390.0     653.0
     980.0     952.0    1593.0
      90.0      90.0    2390.0     420.0
```

The input file to the procedure for computing equivalent properties is

```
1  --(1) joint N 155 E  02/08/021 Stillwater wgp 0.1 thik N=2
 15.80e+04 15.80e+04 15.80e+04      0.25      0.25      0.25
  6.32e+04  6.32e+04  6.32e+04       0.0       0.0       0.0
     286.0     286.0     286.0      16.0      16.0      16.0
     39.10     39.10     39.10.
    245.00      72.0       3.1      0.10
  2  --(2) joint N 81 E N=2
 15.80e+04 15.80e+04 15.80e+04      0.25      0.25      0.25
  6.32e+04  6.32e+04  6.32e+04       0.0       0.0       0.0
     286.0     286.0     286.0      16.0      16.0      16.0
     39.10     39.10     39.10.
     171.0      67.0       4.4      0.10
 (1) GABBRO  N=2 (DP2) 12/11/2017
 15.80e+06 15.80e+06 15.80e+06      0.25      0.25      0.25
  6.32e+06  6.32e+06  6.32e+06       0.0       0.0       0.0
   28600.0   28600.0   28600.0    1600.0    1600.0    1600.0
    3910.0    3910.0    3910.0
       0.0       0.0       0.0     150.0
```

The four numbers in the last line of the joint data are joint dip, dip direction, spacing and thickness. Joint Set 1 and 2 spacing is 3.1 and 4.4 ft, respectively.

*Step 2 Mesh Generation* Mesh generation input is given in the InData file that is developed during mesh generation: Thus,

```
Input Data
 DRIFT NPROB 7
 Tunnel Shape = Ellipse (including circle)
 Tunnel System = Twin Openings
 Tunnel Width =      15.0
 Width/Height Ratio =       1.0
 Pillar Width =      30.0
 Section Depth Seam Center (ft)   =    2600.0
 Additional Sxx,Syy,Szz,Tyz,Tzx,Txy, tension +=
   -5616.0   -3120.0   -4680.0       0.0       0.0       0.0
 Tunnel Stress Sxx,Syy,Szz,Tyz,Tzx,Txy, tension +=
   -5616.0   -3120.0   -4680.0       0.0       0.0       0.0
```

There is a qualification to the use of equivalent properties that should be mentioned and that is the element size must be representative of a well-jointed rock volume, that is, the element

size must be a representative volume element (RVE) or a representative elementary volume (REV). In this regard, regularly spaced joints in a joint set induce an RVE edge length equal to joint spacing. In case of multiple joint sets, the largest spacing rules. Unfortunately, an RVE may be larger than small elements near excavation walls and a non-representative jointed rock finite element model is then required.

*Step 3 FEM Execution and Results* Figure 86 shows results using equivalent properties in the form of the distribution of element safety factors. Adit geometry and preadit stress are the same as in Example1. The pillar width is evidently adequate to prevent elevated stress arising from tunnel interaction. Joints clearly matter as the lower tunnel wall safety factors indicate and the lower safety factors in the central region of the pillar.

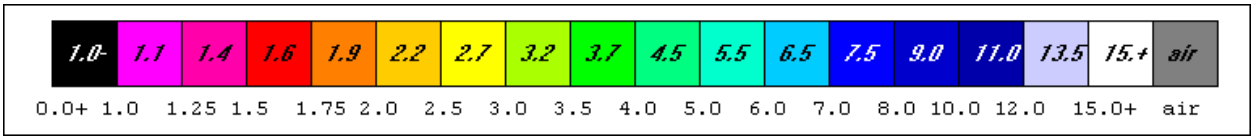


Factor of Safety Color Code

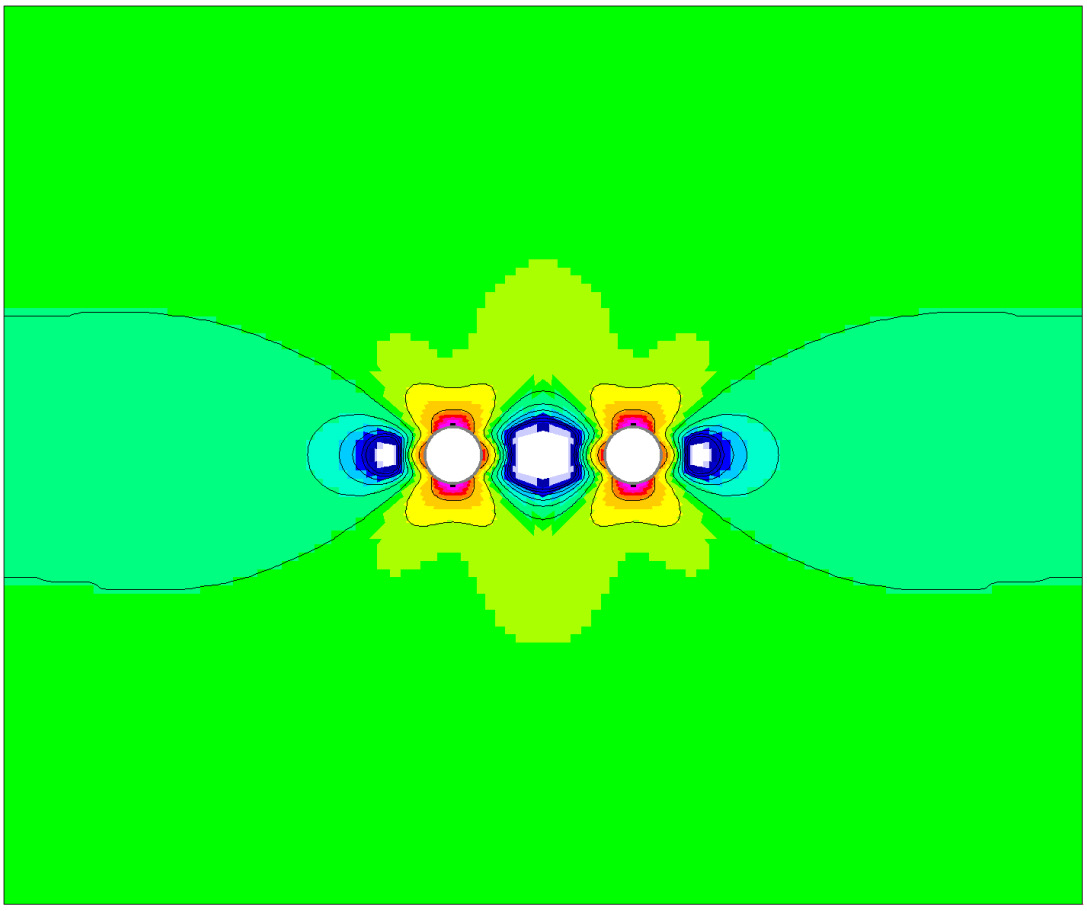

Figure 86 Element safety factors using equivalent properties to take joints into account. Most of the walls are red with a safety factor of 1.2, but there are several failures in the back and floor of the adits.

**Example 1b** A non-representative volume element (NRVE) approach to accommodate joint effects on tunnel safety is needed when the elements are too small to be representative, that is, to include many joints. This situation is almost always the case and is certainly the case in this example of twin adits. Elements at the adit walls are approximately 0.3 ft on edge; spacing of joints in Set 1 is 3 ft and in Set 2 spacing is 4.4 ft. Thus, maximum joint spacing is 4.4 ft. A schematic view of the two joint sets is shown in Figure 87. Intersection of joints creates many joint segments that are recognized as distinct joints even within a single finite element.

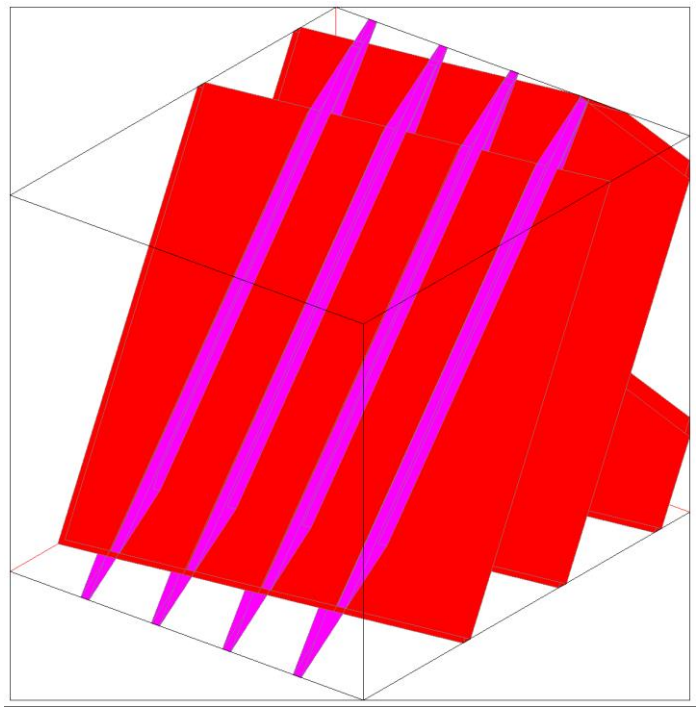

Figure 87 Schematic of two joint sets in Example 1b. Pink=Set 1, Red=Set2.

The result of a NRVE analysis is the element safety factor distribution shown in Figure 88. Safety factors in the figure are for intact rock present in each element.

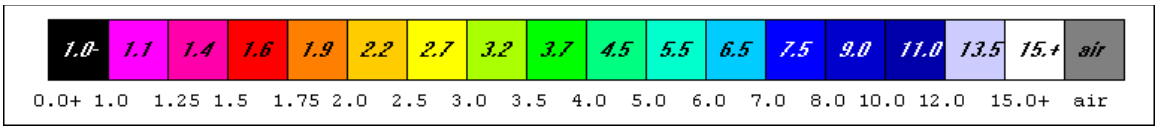


Factor of Safety Color Code

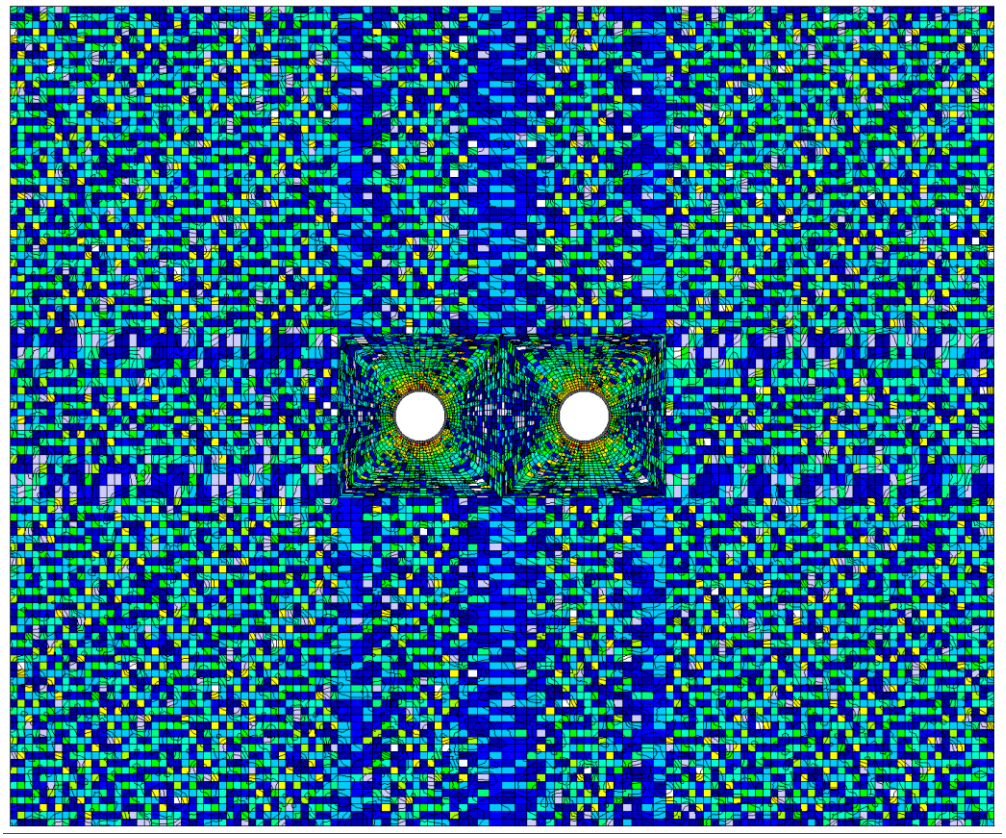

(A) Whole Mesh

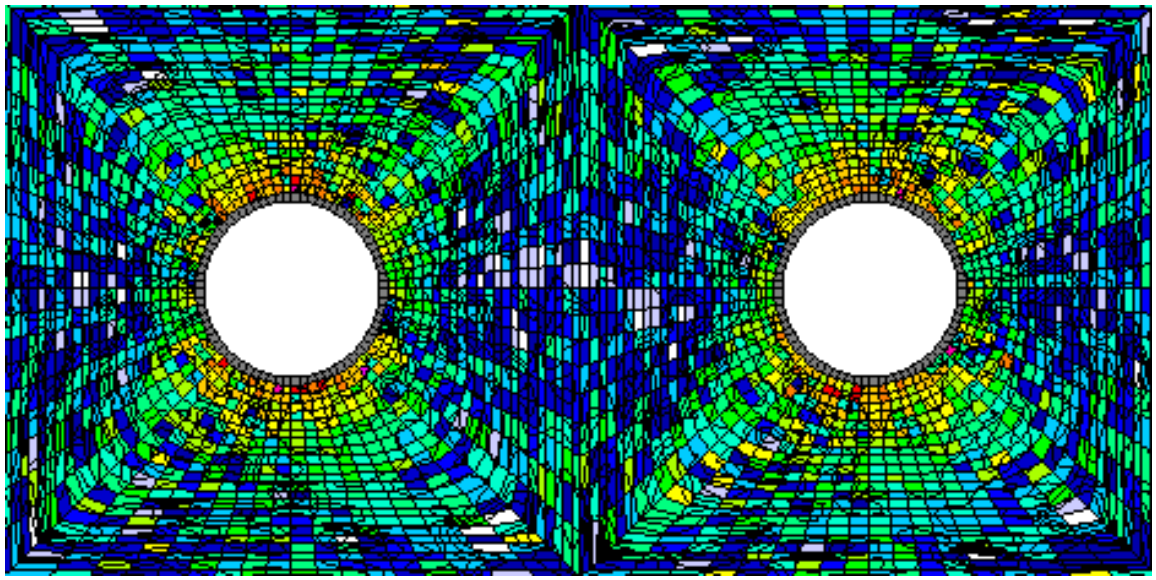

(B) Close Up

Figure 88 Element safety factor distribution relative to intact rock in a twin bore tunnel NRVE analysis of jointed rock.

Details of mesh and rock properties are the same as in the previous example. There are 15,808 elements and 20,748 joint segments in the mesh. No element failures occur, but 16,043 joint segments fail. Element safety factors in the figure are based on intact rock strength and average stress in an element. However, the close up view indicates a number of elements at the tunnel walls with intact rock safety factors less than two. Conventional wall support and reinforcement would certainly be required.

Joint failures are shown in Figure 89. They are widespread as seen in the figure with more joints in Set 2 (yellow) failing than in Set 1 (red).

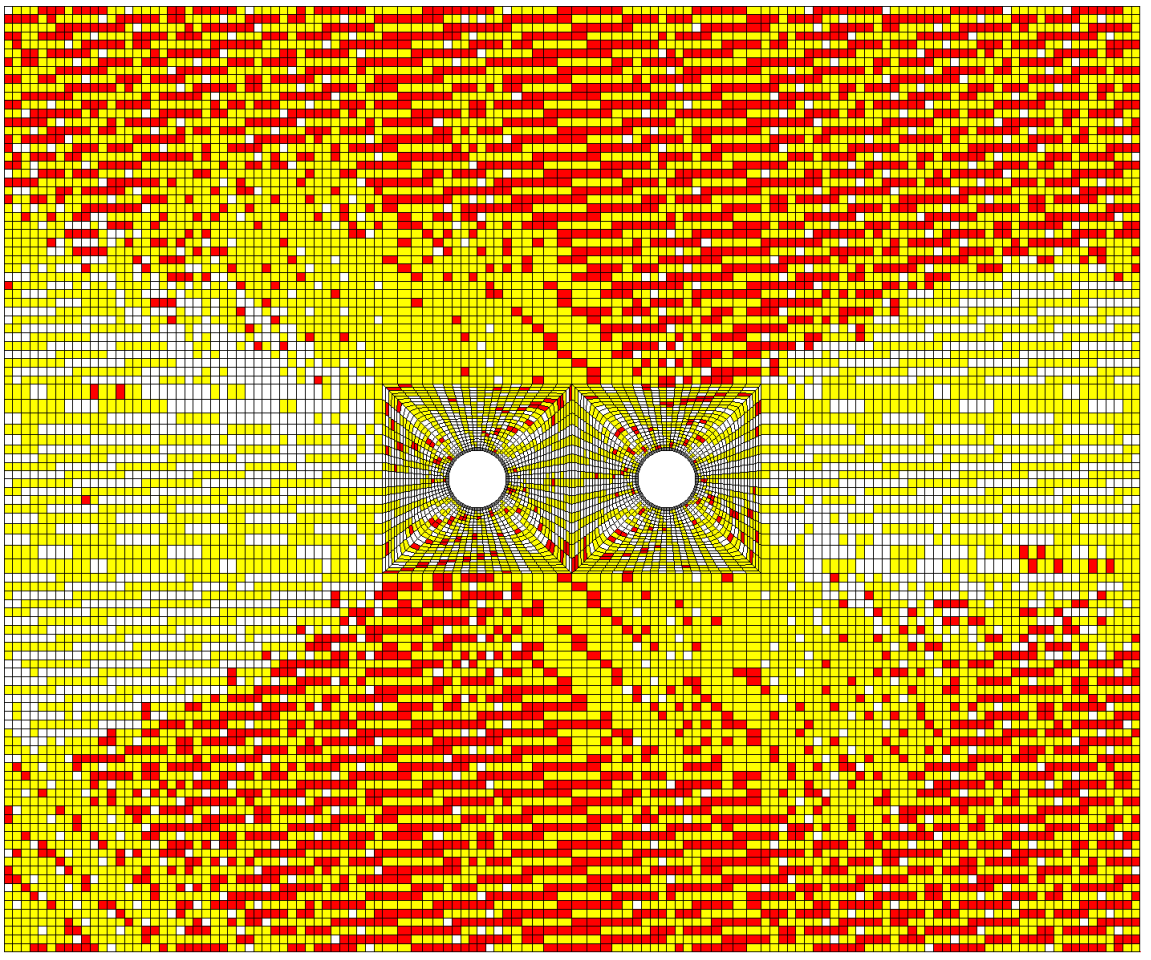

(A) Whole Mesh

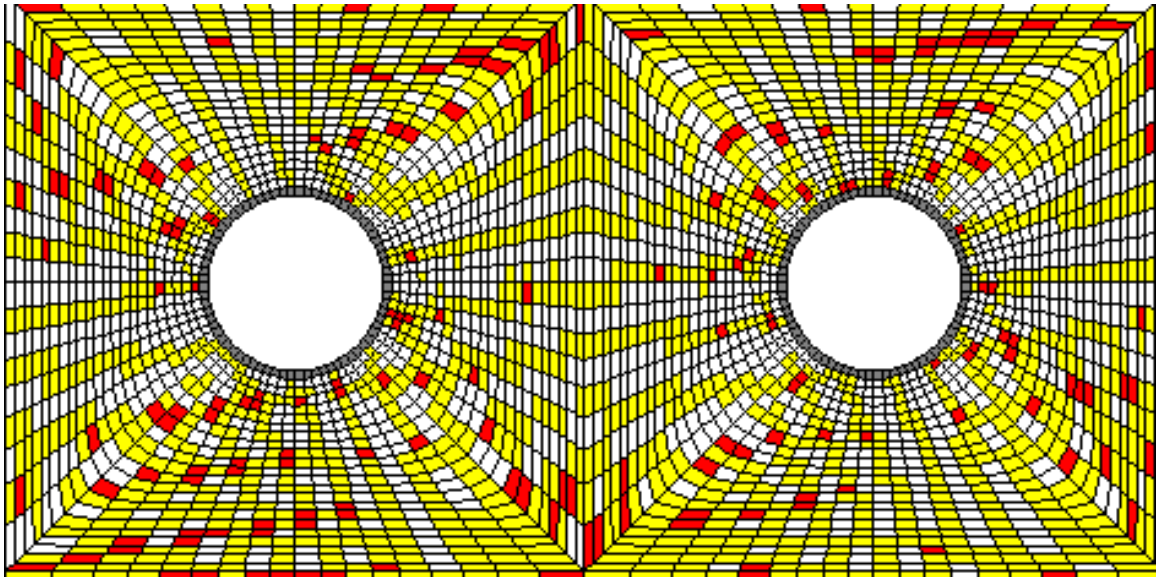

(B) Close Up

Figure 89 Joint failures: RED=joints in joint set 1 failures. YELLOW=joints in joint set 2 failures, WHITE=no joint failures. Tunnels are 15 ft in diameter and are separated by a 30 ft pillar.

Although the safety factor distribution relative to intact rock in Figure 88 indicates safety, whether the joint failures shown in Figure 89 indicate a threat to safety is an open question. Does joint failure in an element indicate whole element failure? If so, then almost all elements in the mesh fail, an unlikely physical result, especially in elements far from the tunnels. In this regard, software from one well-known consultancy does consider an element or cell to fail if any joint in the element fails. The question is certainly worthy of study because of the practical importance of the issue, but one that is beyond the scope of this work.

*To be sure, generation of jointing and embedment into the finite element mesh is not currently available in the FEM software made freely available on UT3PC.net at this juncture, but is an objective for future technology transfer.*

**Example 2a,b** Examples of a single, arched-back drift and an arched back crosscut at the former Homestake Mine in the Northern Black Hills of South Dakota are compared in this composite example. The geology of the mine is characterized by three major formations, the Poorman, Homestake and Ellison, consisting of Precambrian meta-sediments (phyllite, schist and gneiss)

*Step 1 Preparation of a materials property file (stratigraphic column)* Rock properties for this example are given in Table 1. These laboratory rock properties values were scaled as a consequence of calibrating finite element models to match extensometer readings of displacement in the mine. *The scale factors for elastic moduli and strengths were 0.25 and 0.5, respectively.* These two factors are related by guidance from a simple energy relationship [15].

Table 1 Laboratory Rock Properties for Example 2a*

| FORMATION<br>PROPERTY | Poorman<br>- | Homestake | Ellison |
|---|---|---|---|
| Young's Moduli (GPa) | | | |
| Ea | 93.1 | 88.3 | 89.6 |
| Eb | 94.5 | 62.1 | 75.8 |
| Ec | 49.6 | 64.2 | 63.4 |
| Shear Moduli (GPa) | | | |
| Ga | 26.9 | 26.9 | 29.0 |
| Gb | 38.6 | 29.7 | 35.1 |
| Gc | 26.2 | 33.1 | 35.7 |
| Poisson's Ratios | | | |
| Vab | 0.23 | 0.14 | 0.20 |
| Vbc | 0.22 | 0.19 | 0.15 |
| Vca | 0.15 | 0.18 | 0.17 |
| Compressive Strength (MPa) | | | |
| Ca | 94.0 | 138.9 | 78.2 |
| Cb | 84.6 | 91.5 | 56.2. |
| Cc | 69.0 | 79.6 | 78.7 |
| Tensile Strength (MPa) | | | |
| Ta | 20.6 | 9.5 | 16.2 |
| Tb | 13.2 | 13.2 | 11.4 |
| Tc | 5.7 | 7.9 | 4.1 |
| Shear Strength (MPa) | | | |
| Ra | 10.3 | 14.1 | 7.9 |
| Rb | 8.8 | 14.5 | 8.6 |
| Rc | 19.3 | 17.0 | 14.6 |

a=down dip, b=parallel to foliation strike, c=normal to foliation
*From Table 3 of [15] (Part 1 corrected).

The material properties file for the drift is given in Figure 90. The data in Table 1 and Figure 90 reflect an orthotropic anisotropy with axes down dip, on strike and normal to the foliation. The dip direction is at 90 deg to the y-axis of the finite element mesh (a pseudo-north in this example), that is, due east for the drift and parallel to north in the crosscut case.

```
NLYRS = 3
NSEAM = 3
  (1) Ellison
  13.0e+06  11.0e+06  9.19e+06      0.20      0.15      0.17
   4.2e+06  5.09e+06  5.18e+06       0.0       0.0       0.0
   11339.0    8149.0   11411.0    2349.0    1653.0     594.0
    1145.0    1247.0    2117.0
      90.0      70.0    3680.0     700.0
  (2) Homestake
  12.8e+06   9.0e+06   9.3e+06      0.14      0.19      0.18
   4.8e+06   4.3e+06   3.9e+06       0.0       0.0       0.0
   20150.0   13270.0   11547.0    1378.0    1920.0    1139.0
    2025.0    2100.0    2470.0
      90.0      70.0    4380.0     120.0
 (3) Poorman
  13.5e+06  13.7e+06  7.20e+06      0.23      0.22      0.15
   3.8e+06   5.6e+06  3.94e+06       0.0       0.0       0.0
   13630.0   12270.0   10000.0    2990.0    1910.0     820.0
    1500.0    1520.0    2800.0
      90.0      70.0    4500.0     700.0
```

Figure 90 Material properties file for Example 2a. In Example 2b, the dip direction is due north (0 deg).

*Step 2 Mesh Generation* Mesh generation input is given in the InData file that is developed during mesh generation for the drift: Thus,

```
Input Data
 DRIFT NPROB 7
 Tunnel Shape = Arched Rectangle
 Tunnel System = Single Opening
 Tunnel Width =       8.0
 Width/Height Ratio =       1.0
 Tunnel Height=       8.0
 Section Depth Seam Center (ft)   =    4850.0
 Additional Sxx,Syy,Szz,Tyz,Tzx,Txy, tension +=
   -4648.0   -2788.0   -6062.0       0.0       0.0       0.0
 Tunnel Stress Sxx,Syy,Szz,Tyz,Tzx,Txy, tension +=
  -4648.0   -6062.0   -2788.0       0.0       0.0       0.0
```

and for the crosscut

```
Input Data
 CROSSCUT NPROB 7
 Tunnel Shape = Arched Rectangle
 Tunnel System = Single Opening
 Tunnel Width =       8.0
 Width/Height Ratio =       1.0
 Tunnel Height=       8.0
 Section Depth Seam Center (ft)   =    4850.0
 Additional Sxx,Syy,Szz,Tyz,Tzx,Txy, tension +=
   -2788.0   -6062.0   -4648.0       0.0       0.0       0.0
 Tunnel Stress Sxx,Syy,Szz,Tyz,Tzx,Txy, tension +=
   -2788.0   -6062.0   -4648.0       0.0       0.0       0.0
```

Note the vertical stress is the same (Syy) but the horizontal stresses are reversed in keeping with the change in drift direction along strike to crosscut direction perpendicular to the strike direction.

The premining stresses were obtained from formulas developed for the Homestake Mine [15] that are with respect to mine coordinates. The given values take into account stress caused by gravity, so no specific weights are present in the material properties file, Figure 90.

A mesh plot is shown in Figure 91in vertical section. The mesh is actually a slab and has a thickness into the page. There are 73,728 nodes and 36,384 three-dimensional elements in the slab.

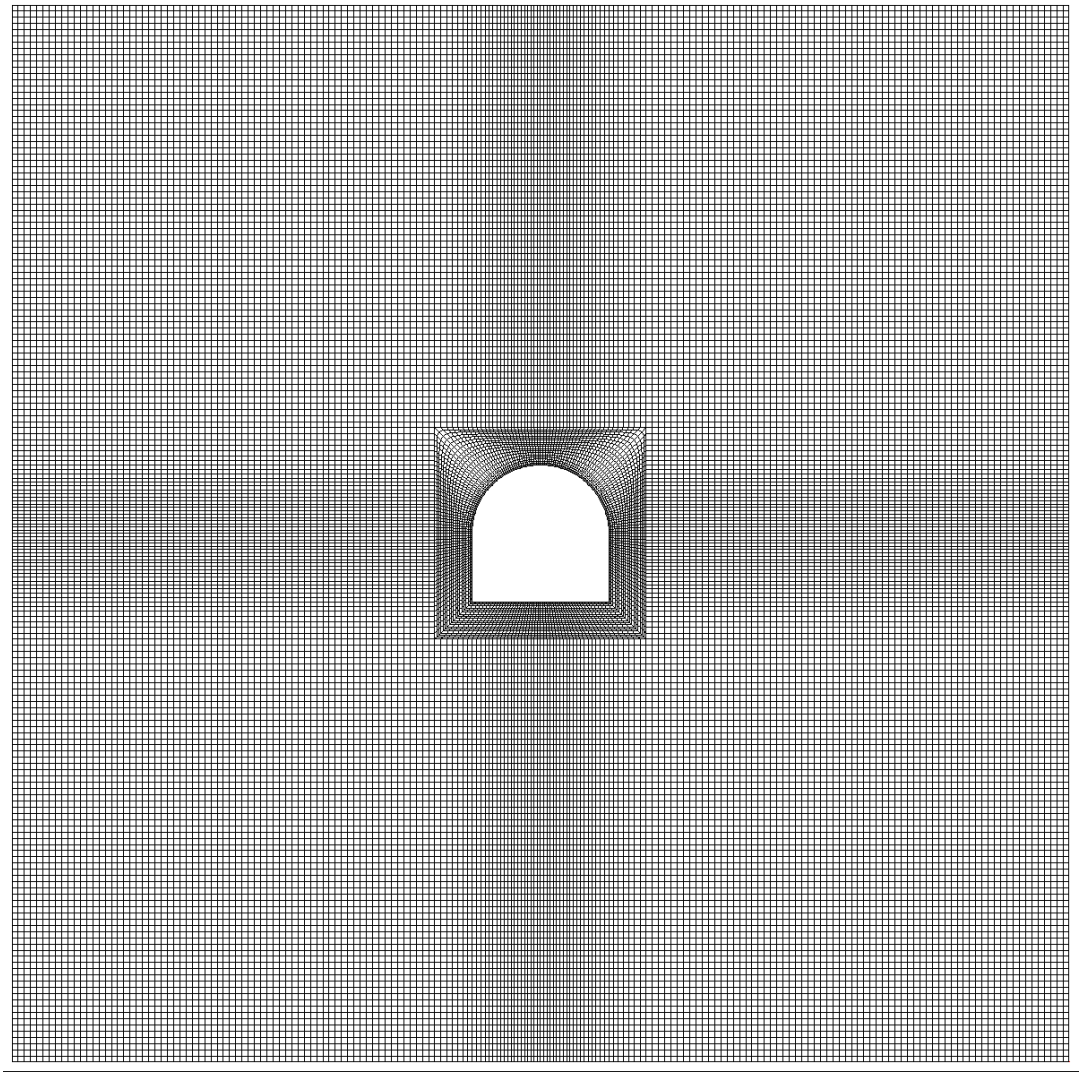

Figure 91 Example 2a,b mesh of an 8 x 8 arched back drift and crosscut.

*Step 3 FEM Execution and Results* Figure 92 shows results in the form of the consequent distribution of element safety factors. The drift plot shows red farther into the ribs of the drift than the crosscut. In fact, experience shows drifts along the "grain" are more likely to require support than crosscuts across the "grain".

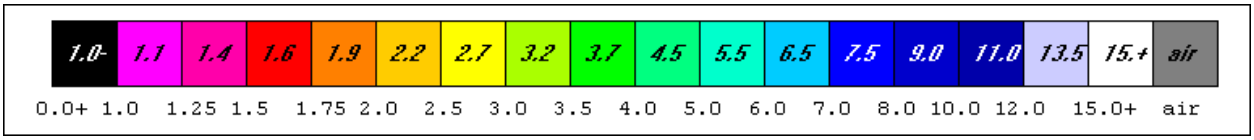


Factor of Safety Color Code

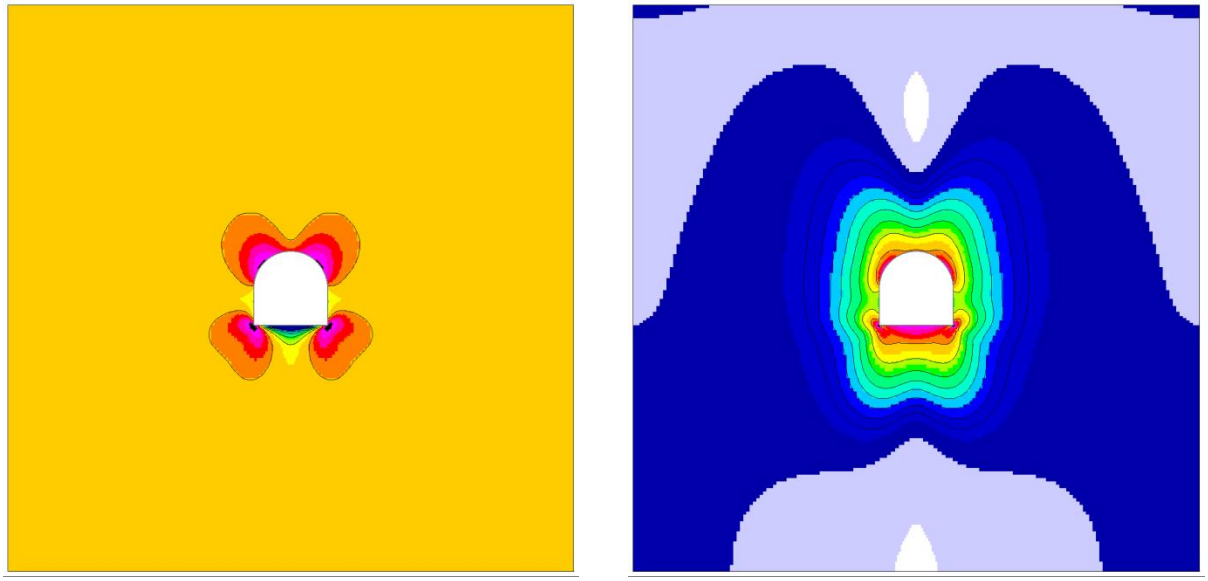

Figure 92 Element safety factors about an 8x8 ft arched back drift (a) and crosscut (b). Ribs are in red (1.5) in the drift where some floor failure is indicated (black). Crosscut back and floor are in red (1.5), but overall the crosscut appears less threatened than the drift.

**Example 3a** This example is inspired by a detailed study of a new mining method at the Carr Fork Mine (Pariseau et al 1984 [30], Pariseau 1985 [31]). The Carr Fork Mine was an underground copper mine in a contact metamorphic rock environment with an intended production of 10,000 short tons per day. Access was by vertical shaft in Pine Canyon near Tooele, Utah. Average depth in the vicinity of the new mining method study is 4,200 ft. Many measurements of stress and of Young's modulus in situ and other rock properties measured in the laboratory supported the study.

In situ stress was extrapolated from measurements such that $S_v = 1.1d$, $S_{ew} = 0.84S_v$, $S_{ns} = 0.54S_v$ where $S_v$, $S_{ew}$ and $S_{ns}$ are vertical, east-west and north-south normal stresses; *d* is depth below surface. Premining shear stress relative to compass coordinates (*x*=north-south, *y*=east-west, *z*=vertical) were negligible. The ore body is steeply dipping and trends east-west.

*Step 1 Preparation of a materials property file (stratigraphic column)* Rock properties for this example are given in Table 2. These laboratory rock properties values were scaled from laboratory values to the mine scale. The scale factors for elastic moduli and strengths were 0.25 and 0.5, respectively. The input material properties file follows from Table 2 and the geology in the test stope vicinity.

Table 2 Rock properties at the Carr Fork Mine (after Pariseau et al 1984)

| **Property Type** | **E** (GPa/Mpsi) | **v** | **G** (GPa/Mpsi) | **Co** (MPa/psi) | **To** (MPa/psi) | **Ro** (MPa/psi) |
|---|---|---|---|---|---|---|
| 1Garnetite/ Limestone | 24.6/ 3.56 | 0.20 | 10.2 /1.48 | 81.4 /11,800 | 6.14 /890 | 12.9/ 1,871 |
| 2Garnetite/ Quartzite | 8.14 /1.18 | 0.22 | 3.34 /0.484 | 24.8 /3,600 | 1.86 /270 | 3.92 /569 |
| 3Quartzite/ Hard Qtz. | 17.0 /2.46 | 0.25 | 6.79 /0.984 | 55.1 /8,000 | 4.97 /720 | 9.55 /1,385 |
| 4Hornfels | 19.4 /2.81 | 0.27 | 7.64 /1.11 | 63.4 /9,200 | 5.52 /800 | 10.8/ 1,566 |
| 5Quartz Monzonite | 15.0 /2.17 | 0.22 | 6.13 /0.889 | 48.3 /7,000 | 4.00 /580 | 8.03/ /1,163 |
| 6Quartz Latite | 8.97 /1.3 | 0.23 | 3.64 0.528/ | 27.6 /4,000 | 1.38 /200 | 3.56 /516 |
| 7 Garnetite Hornfels | 27.0 /3.91/ | 0.25 | 10.8 /1.56 | 93.1 /13,500 | 2.48 /360 | 8.77 1,273 |

E=Young's modulus, v=Poisson's ratio, G=shear modulus
Co=unconfined compressive strength, To=tensile strength, Ro=shear strength

```
NLYRS = 7
NSEAM = 2
  (4) Hornfels
  2.81e+06  2.81e+06  2.81e+06      0.27      0.27      0.27
  1.11e+06  1.11e+06  1.11e+06       0.0       0.0       0.0
    9200.0    9200.0    9200.0     800.0     800.0     800.0
    1566.0    1566.0    1566.0
       0.0      80.0    3800.0     350.0
  (5) Quartz Monzonite Porphyry
  2.17e+06  2.17e+06  2.17e+06      0.22      0.22      0.22
  0.89e+06  0.89e+06  0.89e+06       0.0       0.0       0.0
    7000.0    7000.0    7000.0     580.0     580.0     580.0
    1163.0    1163.0    1163.0
      55.0      60.0    4150.0     100.0
  (1) Garnetite Limestone
  3.56e+06  3/56e+06  3.56e+06      0.20      0.20      0.20
  1.48e+06  1.48e+06  1.48e+06       0.0       0.0       0.0
   11800.0   11800.0   11800.0     890.0     890.0     890.0
    1871.0    1871.0    1871.0
       0.0      80.0    4250.0     150.0
  (2) Garnetite Quartzite
  1.18e+06  1.18e+06  1.18e+06      0.22      0.22      0.22
  0.48e+06  0.48e+06  0.48e+06       0.0       0.0       0.0
    3600.0    3600.0    3600.0     270.0     270.0     270.0
```

```
    569.0     569.0     569.0
      0.0      80.0    4400.0      18.0
  (3) Hard Quartzite
  2.46e+06  2.46e+06  2.46e+06      0.25      0.25      0.25
  0.98e+06  0.98e+06  0.98e+06       0.0       0.0       0.0
    8000.0    8000.0    8000.0     720.0     720.0     720.0
    1385.0    1385.0    1385.0
      0.0      80.0    4418.0     122.0
  (6) Quartz Latite Porphyry
  1.30e+06  1.30e+06  1.30e+06      0.23      0.23      0.23
  0.53e+06  0.53e+06  0.53e+06       0.0       0.0       0.0
    4000.0    4000.0    4000.0     200.0     200.0     200.0
     516.0     516.0     516.0
      0.0      80.0    4540.0      20.0
  (4) Hornfels
  2.81e+06  2.81e+06  2.81e+06      0.27      0.27      0.27
  1.11e+06  1.11e+06  1.11e+06       0.0       0.0       0.0
    9200.0    9200.0    9200.0     800.0     800.0     800.0
    1566.0    1566.0    1566.0
      0.0      80.0    4560.0     160.0
```

Figure 93 Input material properties file for **Example 3**.

*Step 2 Mesh Generation* Mesh generation input is given in the InData file that is developed during mesh generation: Thus,

```
Input Data
 “TUNNEL” NPROB 7
 Tunnel Shape = Arched Rectangle
 Tunnel System = Single Opening
 Tunnel Width =      12.0
 Width/Height Ratio =       1.2
 Tunnel Height=      10.0
 Section Depth Seam Center (ft)   =    4200.0
 Additional Sxx,Syy,Szz,Tyz,Tzx,Txy, tension +=
   -3880.0   -4620.0   -2495.0       0.0       0.0       0.0
 Tunnel Stress Sxx,Syy,Szz,Tyz,Tzx,Txy, tension +=
   -3880.0   -4620.0   -2495.0       0.0       0.0       0.0
```

A single, arched back crosscut is specified to be 12 ft wide by 10 ft high in quartz monzonite porphyry at a depth of 4,200 ft. The premining stress state is computed from formulas developed from mine measurements. Figure 93 shows the mesh.

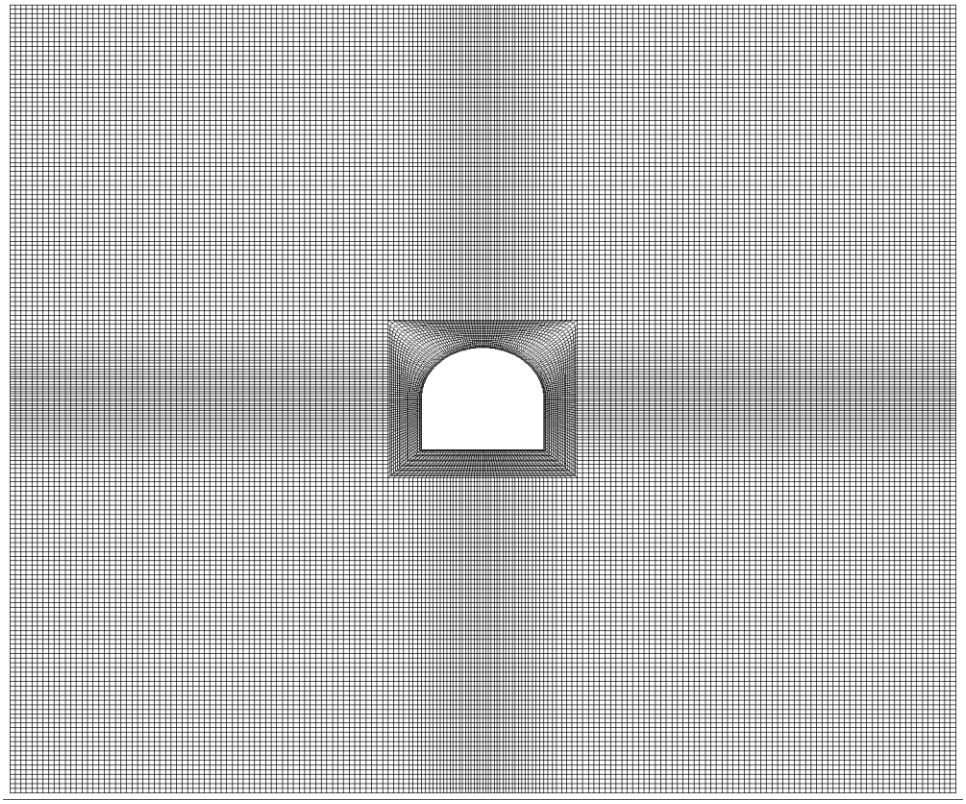

Figure 93 Mesh for **Example 3a**, a single 12 ft wide by 10 ft high arched back crosscut.

*Step 3 FEM Execution and Results* The runstream file for finite element analysis at the start of a crosscut in quartz monzonite porphyry to the ore is

```
Carr Fork Crosscut 12x10 ft  04/15/2021 wgp
F:\Visual Studio 2010\Projects\SPK\GMB3\matCAR.txt
F:\Visual Studio 2010\Projects\SPK\GMB3\belms
F:\Visual Studio 2010\Projects\SPK\GMB3\bcrds
F:\Visual Studio 2010\Projects\SPK\GMB3\brcte
F:\Visual Studio 2010\Projects\SPK\GMB3\bsigi
F:\Visual Studio 2010\Projects\SPK\GMB3\bnsps
CARc
nelem =   36384
nnode =   73728
nspec =   73728
nmat  =       7
ncut  =      -1
ninc  =       5
nsigo =       1
inter =     200
maxit =    4000
nyeld =       2
nelcf =     208
nsol  =       2
mgob  =       0
 error=    1.0000
```

```
 orf  =    1.8600
 xfac =   12.0000
 yfac =   12.0000
 zfac =   12.0000
 efac =    0.2500
 cfac =    0.5000
tolr% =    0.0100
ENDRUN
```

Figure 94 shows results in the form of the consequent distribution of element safety factors. Minor yielding occurs in the back and at the bottom corners as seen in black and the perimeter is highly stressed with noticeable zone having a 1.25 safety factor (pink, red).

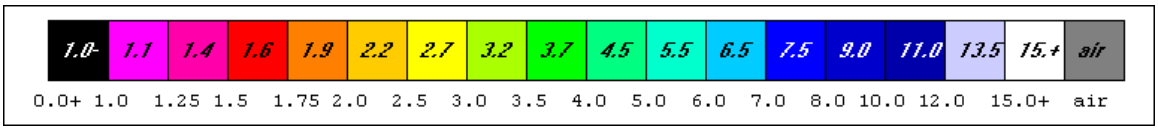


Safety Factor Color Code

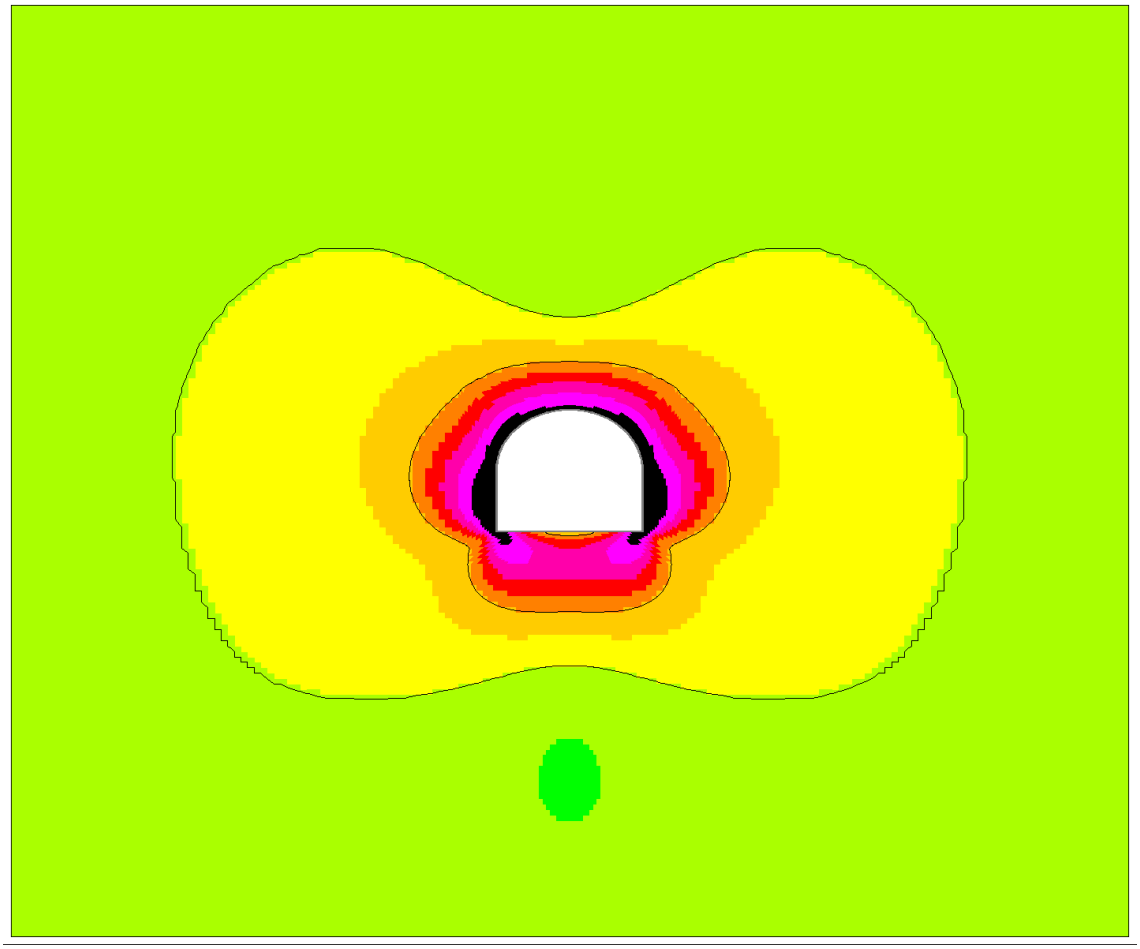

Figure 94 Element safety factor distribution in quartz monzonite porphyry, **Example 3a**. Failure (black) at the crosscut wall indicates a need for support of the 12 x 10 ft opening.

**Example 3b** This example continues the previous example but is modified to allow for the spacing of crosscuts along the main access drift in the hanging wall. Material properties are the same as is the premining stress state, so Step 1 is the same.

*Step 2 Mesh Generation* Mesh generation input is given in the InData file as before but with the added feature of a pillar 38 ft wide between crosscuts.

*Step 3 FEM Execution and Results* The runstream file for finite element analysis at the start of a crosscut in quartz monzonite porphyry to the ore is

```
Carr Fork Crosscut 12x10 ft  04/16/2021 wgp
F:\Visual Studio 2010\Projects\SPK\GMB3\matCAR.txt
F:\Visual Studio 2010\Projects\SPK\GMB3\belms
F:\Visual Studio 2010\Projects\SPK\GMB3\bcrds
F:\Visual Studio 2010\Projects\SPK\GMB3\brcte
F:\Visual Studio 2010\Projects\SPK\GMB3\bsigi
F:\Visual Studio 2010\Projects\SPK\GMB3\bnsps
CARrc
nelem =    4932
nnode =   10260
nspec =   10260
nmat  =       7
ncut  =      -1
ninc  =       5
nsigo =       1
inter =     200
maxit =    4000
nyeld =       2
nelcf =      72
nsol  =       2
mgob  =       0
 error=    1.0000
 orf  =    1.8600
 xfac =   12.0000
 yfac =   12.0000
 zfac =   12.0000
 efac =    0.2500
 cfac =    0.5000
tolr% =    0.0100
ENDRUN
```

Figure 95A shows the mesh and Figure 95B shows the element safety factor distribution. Evidently separation of crosscuts by the pillar between is sufficient to prevent interaction between crosscuts to the detriment of safety.

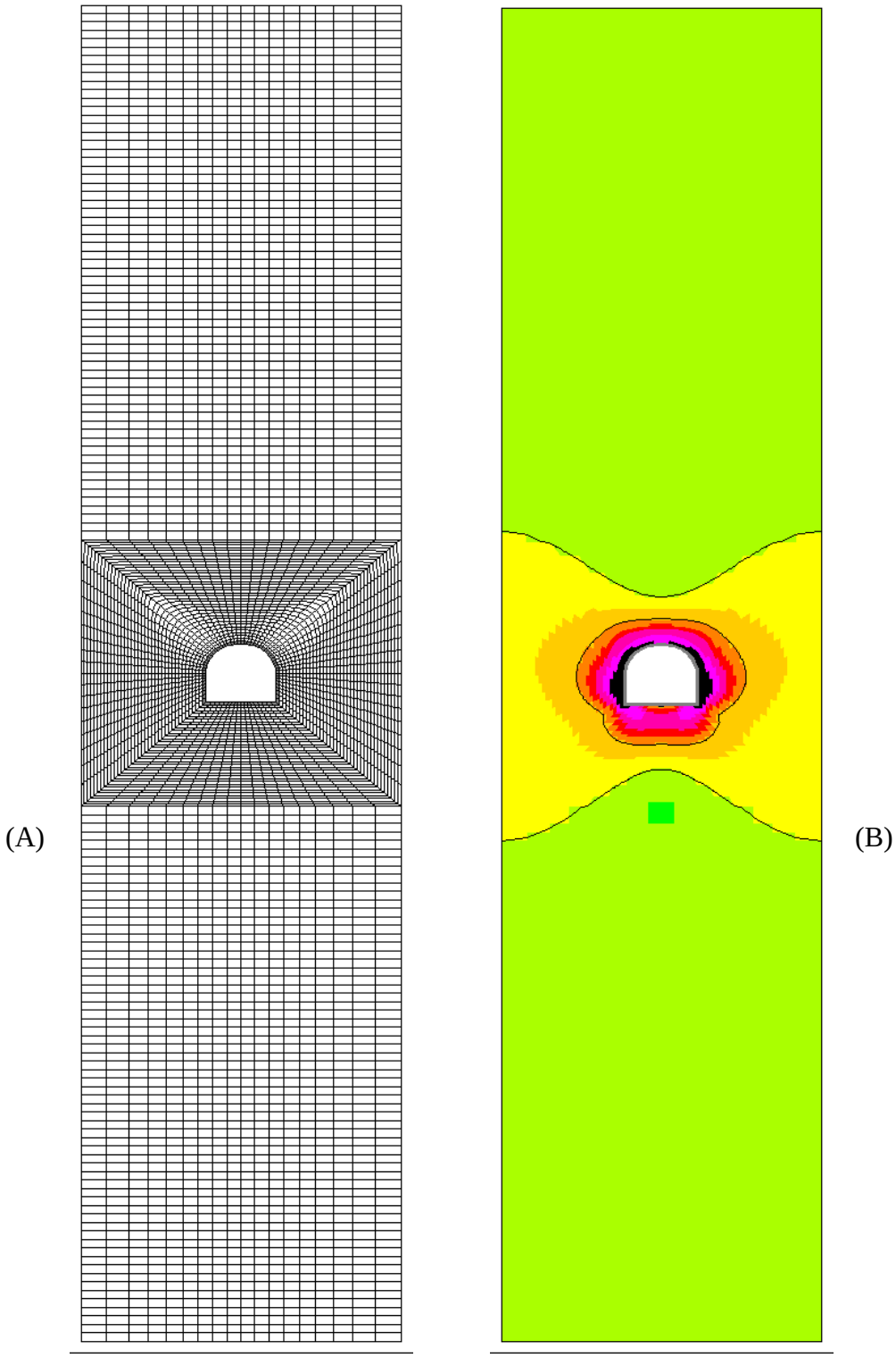


Figure 95 (A) Arched back crosscut in a row of crosscuts. Pillar width is 38 ft. Half pillars are on each side of the crosscut. (B) Element safety factor distribution. The pillar is certainly wide enough to avoid detrimental interaction between crosscuts.

**Example 3c** This example continues the previous example but is modified to allow for the crosscuts to pass through the different rock types encountered in driving from hanging wall to footwall for ore access. Material properties are the same as is the premining stress state, so Step 1 is the same with the exception of renumbering NSEAM to locate the crosscut section in another rock type. Figure 96 compares results when NSEAM=2, 3 and 4, respectively.

*Step 2 Mesh Generation* Mesh generation input is given in the InData file as before

*Step 3 FEM Execution and Results* The runstream file for finite element analysis at the start of a crosscut is also as before with the exception of NSEAM.

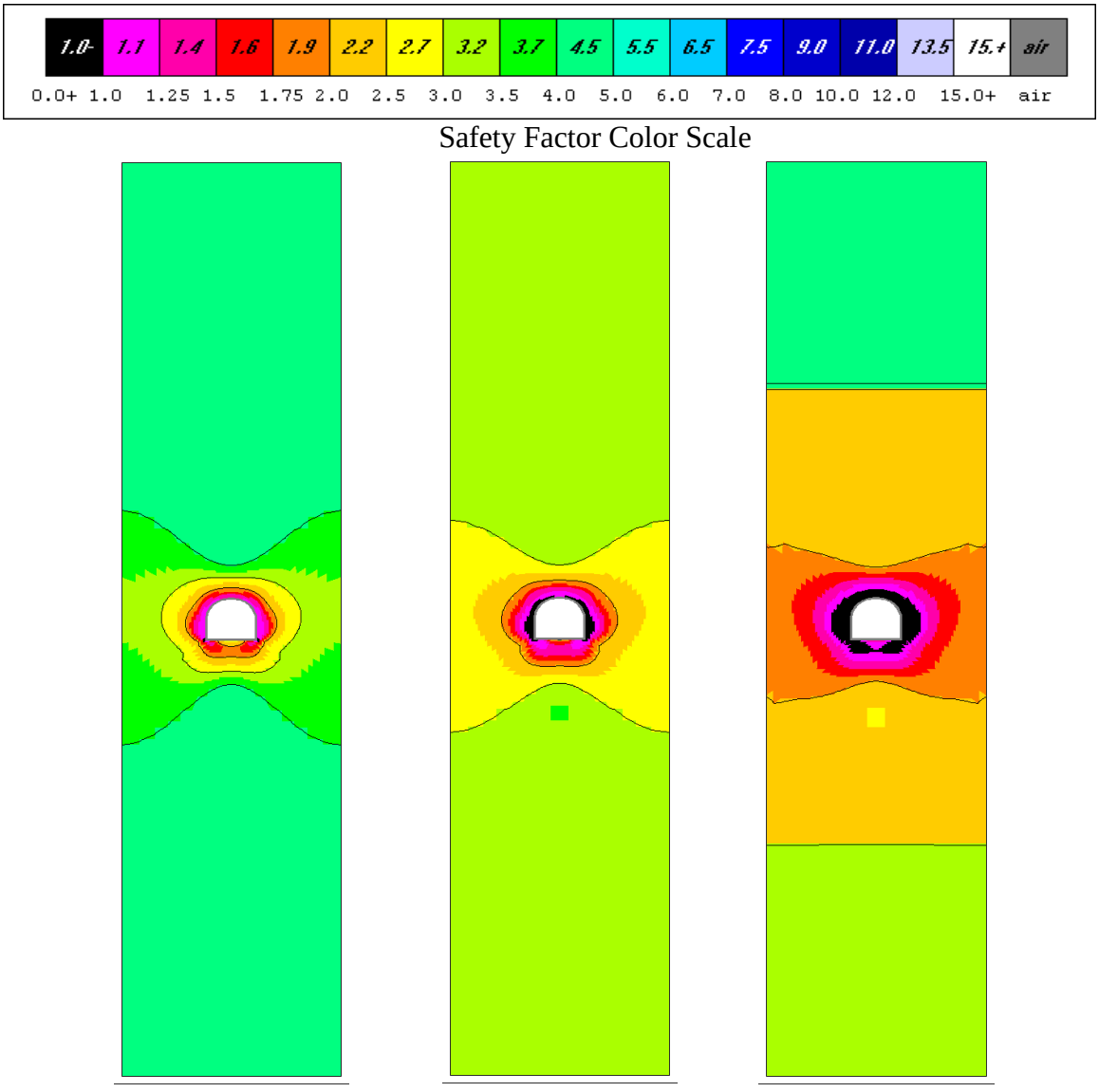

Figure 96 Comparison of strong (A), medium (B) and weak (C) rock crosscut safety.

The narrow and relatively weak case when NSEAM = 4 and the rock type is garnetite quartzite that occurs in a narrow, steeply dipping band indicates crosscut wall support is required. In fact, bolting is indicated in each case and perhaps screening in view of the red zone enclosing the crosscut. The pillar size is certainly adequate in view of the negligible interaction between crosscuts.

**Example 4a** This example considers twin crosscuts at the Caladay Mine and uses much the same data that was used in analysis of the Caladay Shaft. In fact, the Caladay Shaft was developed from an adit with an average depth of 1,200 ft according to Whyatt [20]. However, the intention here is to demonstrate analysis capability rather than to do a site-specific case study.

*Step 1 Preparation of a materials property file (stratigraphic column)* The material properties file used in this analysis is

```
NLYRS = 3
NSEAM = 2
   (1) Vitreous Quartzite
   6.1e+06   6.1e+06   6.1e+06      0.26      0.26      0.26
   2.4e+06   2.4e+06   2.4e+06       0.0       0.0       0.0
   24500.0   24500.0   24500.0    2800.0    2800.0    2800.0
    2400.0    2400.0    2400.0
     180.0      70.0    1200.0      18.0
   (2) Argillitic Quartzite
   4.2e+06   4.2e+06   1.8e+06      0.18      0.11      0.11
   1.1e+06   1.1e+06   1.8e+06       0.0       0.0       0.0
    8500.0    8500.0   12230.0    2790.0    2790.0    1080.0
    2820.0    2820.0    2100.0
     180.0      70.0    1218.0       8.0
   (3)  Sericitic Quartzite
   5.5e+06   5.5e+06   4.0e+06      0.21      0.20      0.20
   1.9e+06   1.9e+06   2.3e+06       0.0       0.0       0.0
   17470.0   17470.0   26040.0    2330.0    2330.0    1530.0
    3680.0    3680.0    3640.0
     180.0      70.0    1226.0     180.0
```

The dip direction of 180 deg indicates dip is to the mine south. The axis of the crosscut is parallel to mine north in keeping with the finite element axes convention *(x*=east, *y*=north, *z*=vertical). However, once the mesh is generated, the "tunnel" section is referred to *xy* coordinates (*x*=horizontal, *y*=vertical); the *z*-axis is then horizontal and out of the page in a plot. The formation of interest is argillitic quartzite (NSEAM=2) and is deliberately made thin at a thickness of just 8 ft.

*Step 2 Mesh Generation* Mesh generation input is given in the InData file. Thus,

```
Input Data
 "TUNNEL" NPROB 7
 Tunnel Shape = Arched Rectangle
 Tunnel System = Twin Openings
 Tunnel Width =       9.0
 Width/Height Ratio =       1.0
 Pillar Width =       9.0
 Section Depth Seam Center (ft)   =    1222.0
 Additional Sxx,Syy,Szz,Tyz,Tzx,Txy, tension +=
   -2351.0   -1736.0   -1790.0       0.0       0.0       0.0
 Tunnel Stress Sxx,Syy,Szz,Tyz,Tzx,Txy, tension +=
   -2351.0   -1736.0   -1790.0       0.0       0.0       0.0
```

Now *x* is in the width direction, *y* is vertical and *z* is parallel to the "tunnel", that is, adit axis. To be sure Syy is the vertical stress as input during mesh generation.

The mesh of twin arched back adits 9 x 9 ft separated by a 9 ft wide pillar is shown in Figure 97. Steeply dipping strata are evident in the figure because the adits are crosscuts.

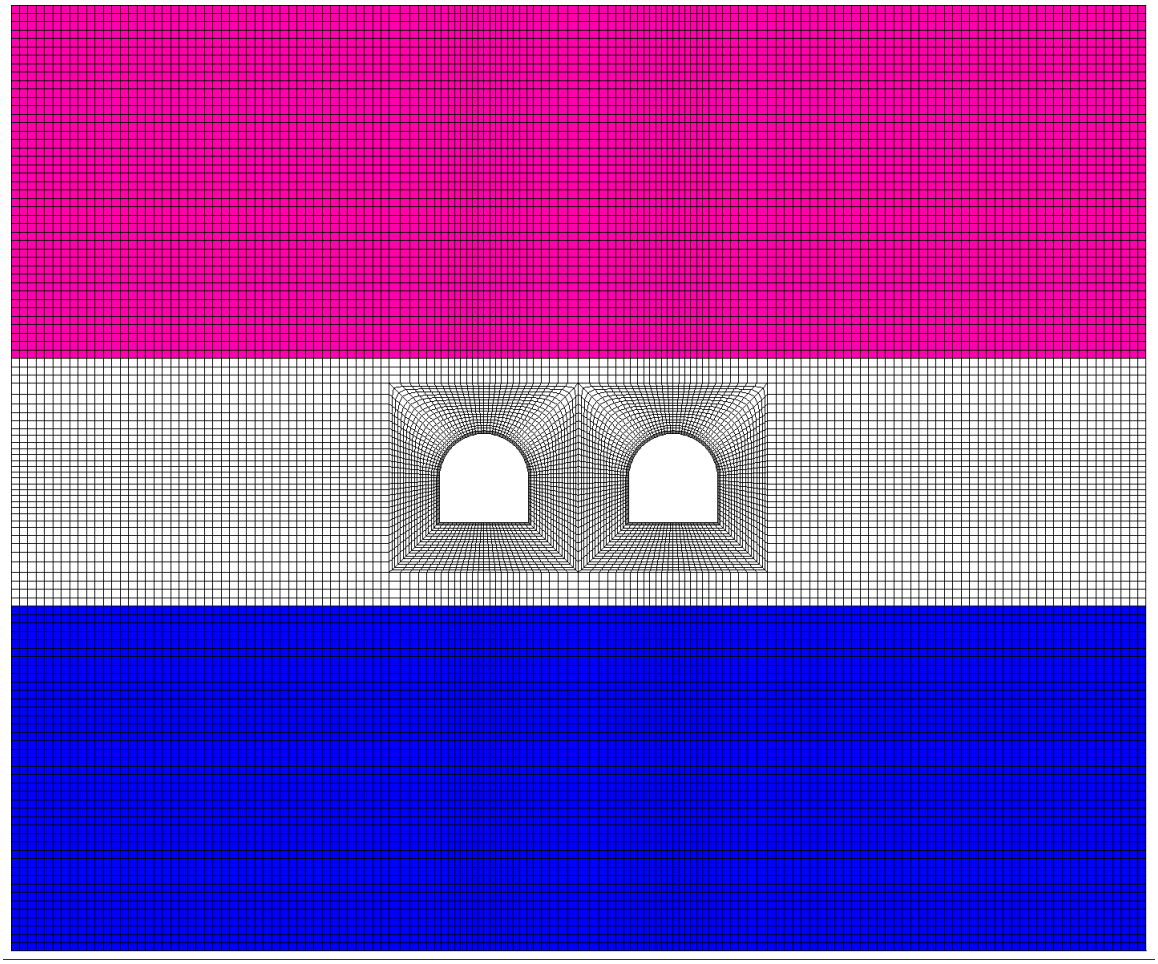

Figure 97 Twin arched back adits, 9x9ft each, separated by a 9 ft wide pillar.

*Step 3 FEM Execution and Results* The formation of interest in the finite element analysis is argillitic quartzite. The runstream file is

```
Calady Crosscut Twin 10x8 ft NS=2 04/16-17-19/2021 wgp
F:\Visual Studio 2010\Projects\SPK\GMB3\matCM3.txt
F:\Visual Studio 2010\Projects\SPK\GMB3\belms
F:\Visual Studio 2010\Projects\SPK\GMB3\bcrds
F:\Visual Studio 2010\Projects\SPK\GMB3\brcte
F:\Visual Studio 2010\Projects\SPK\GMB3\bsigi
F:\Visual Studio 2010\Projects\SPK\GMB3\bnsps
CM3c
nelem =   18864
nnode =   38450
nspec =   38450
nmat  =       3
ncut  =      -1
ninc  =       5
nsigo =       1
inter =     200
maxit =    4000
nyeld =       2
nelcf =     208
nsol  =       2
mgob  =       0
 error=    1.0000
 orf  =    1.8600
 xfac =   12.0000
 yfac =   12.0000
 zfac =   12.0000
 efac =    0.2500
 cfac =    0.5000
tolr% =    0.0100
ENDRUN
```

The scale factors for Young's moduli and strengths of 0.25 and 0.5, respectively, are used to adjust laboratory scale properties to the engineering scale in the mine. In a site-specific case study, scale factors would be developed from comparisons between mine measurements and model results. These scale factors would then be used to "calibrate" the model. A fundamental approach to engineering scale rock properties would use composite rock properties taking into account joint geometry, joint properties and intact rock properties.

*Step 3 FEM Execution and Results*. Figure 98 summarizes the results in the form of an element safety factor distribution. Wall safety factors are mostly yellow (2.7) with very little in orange (2.2) as one would expect because of the relatively shallow depth of 1,200 ft. The pillar also is safe in green (3.2) and indicates negligible interaction between openings as one would expect when pillar width is equal to opening width ("1-D" rule of thumb, that is, one "diameter" of separation is adequate).

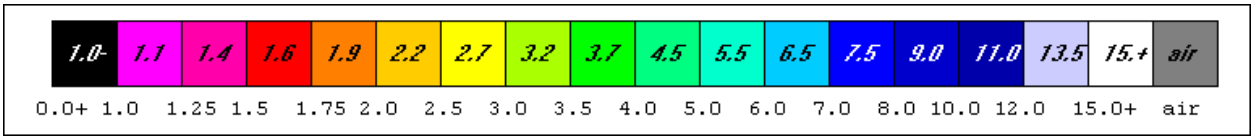


Safety Factor Color Code

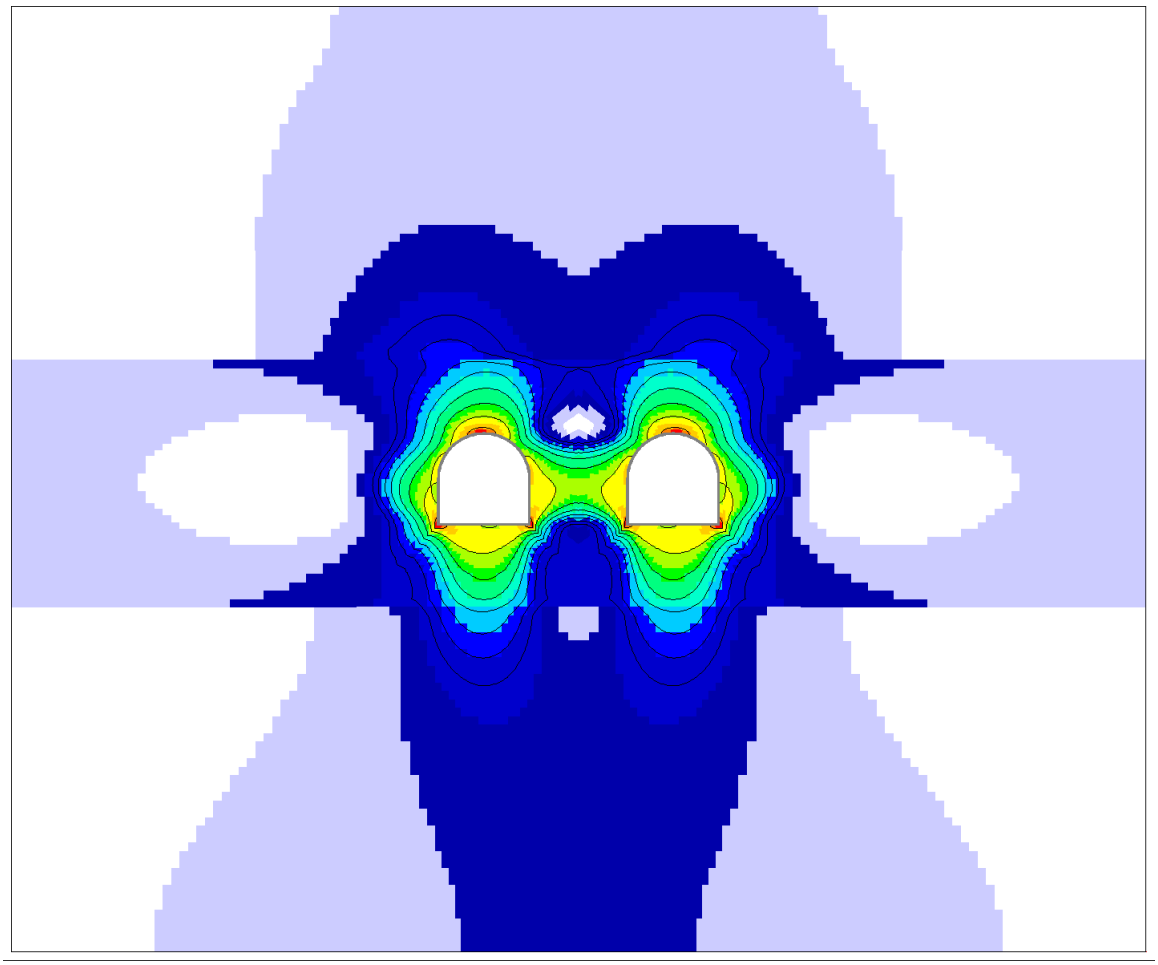

Figure 98 Element safety factor distribution for twin arched back adits (cross cuts).

**Example 4b** This example considers twin adits (crosscuts) at the Caladay Mine and is similar to Example 4a with a change in dip direction of strata and stress.

*Step 1 Preparation of a materials property file (stratigraphic column)* The material properties file used in this analysis is the same as in Example 4a.

The dip direction of 90 deg indicates dip is to the mine east. The axis of the drift is parallel to mine north in keeping with the finite element axes convention (*x*=east, *y*=north, *z*=vertical). The formation of interest is argillitic quartzite (NSEAM=2) and is deliberately made thin at a thickness of just 8 ft.

*Step 2 Mesh Generation* Mesh generation input is given in the InData file. Thus for this drift,

```
Input Data
 "TUNNEL" NPROB 7
 Tunnel Shape = Arched Rectangle
 Tunnel System = Single Opening
 Tunnel Width =       9.0
 Width/Height Ratio =       1.0
 Tunnel Height=       9.0
 Section Depth Seam Center (ft)   =    1222.0
 Additional Sxx,Syy,Szz,Tyz,Tzx,Txy, tension +=
   -1790.0   -1736.0   -2351.0       0.0       0.0       0.0
 Tunnel Stress Sxx,Syy,Szz,Tyz,Tzx,Txy, tension +=
   -1790.0   -1736.0   -2351.0       0.0       0.0       0.0
```

Again, *x* is in the width direction, *y* is vertical and *z* is parallel to the "tunnel", that is, adit axis.

The mesh of twin arched back adits 9 x 9 ft separated by a 9 ft wide pillar is shown in Figure 99. Steeply dipping strata are evident in the figure because the adits are drifts.

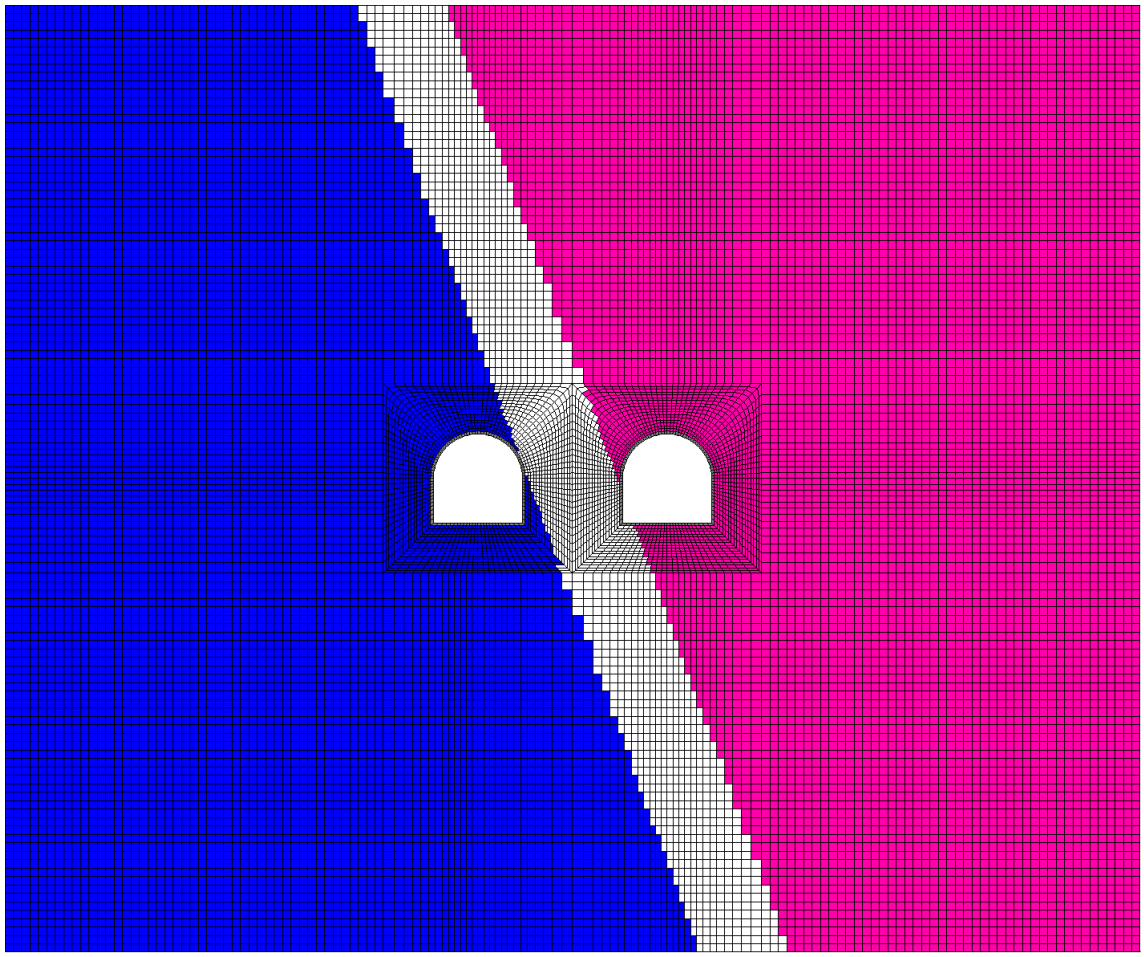

Figure 99 Twin arched back drifts, 9x9ft each, separated by a 9 ft wide pillar.

*Step 3 FEM Execution and Results* The formation of interest in the finite element analysis is argillitic quartzite. The runstream file is

```
Calady Drift Twin 10x8 ft NS=2 04/16-17-19/2021 wgp
F:\Visual Studio 2010\Projects\SPK\GMB3\matCM3.txt
F:\Visual Studio 2010\Projects\SPK\GMB3\belms
F:\Visual Studio 2010\Projects\SPK\GMB3\bcrds
F:\Visual Studio 2010\Projects\SPK\GMB3\brcte
F:\Visual Studio 2010\Projects\SPK\GMB3\bsigi
F:\Visual Studio 2010\Projects\SPK\GMB3\bnsps
CM3c
nelem =   18864
nnode =   38450
nspec =   38450
nmat  =       3
ncut  =      -1
ninc  =       5
nsigo =       1
inter =     200
maxit =    4000
nyeld =       2
nelcf =     208
nsol  =       2
mgob  =       0
 error=    1.0000
 orf  =    1.8600
 xfac =   12.0000
 yfac =   12.0000
 zfac =   12.0000
 efac =    0.2500
 cfac =    0.5000
tolr% =    0.0100
ENDRUN
```

The scale factors for Young's moduli and strengths of 0.25 and 0.5, respectively, are used to adjust laboratory scale properties to the engineering scale in the mine. In a site-specific case study, scale factors would be developed from comparisons between mine measurements and model results. These scale factors would then be used to "calibrate" the model, although a fundamental approach would negate the need for such empirical factors.

*Step 3 FEM Execution and Results*. Figure 100 summarizes the results in the form of an element safety factor distribution. The drift in the hanging wall formation shows lower safety factors about the drift wall (some orange, 2.2) than the footwall drift, mostly yellow (2.7), although neither appears unsafe, nor is the pillar threatened in view of the green, 3.7, safety factor through most of the pillar core.

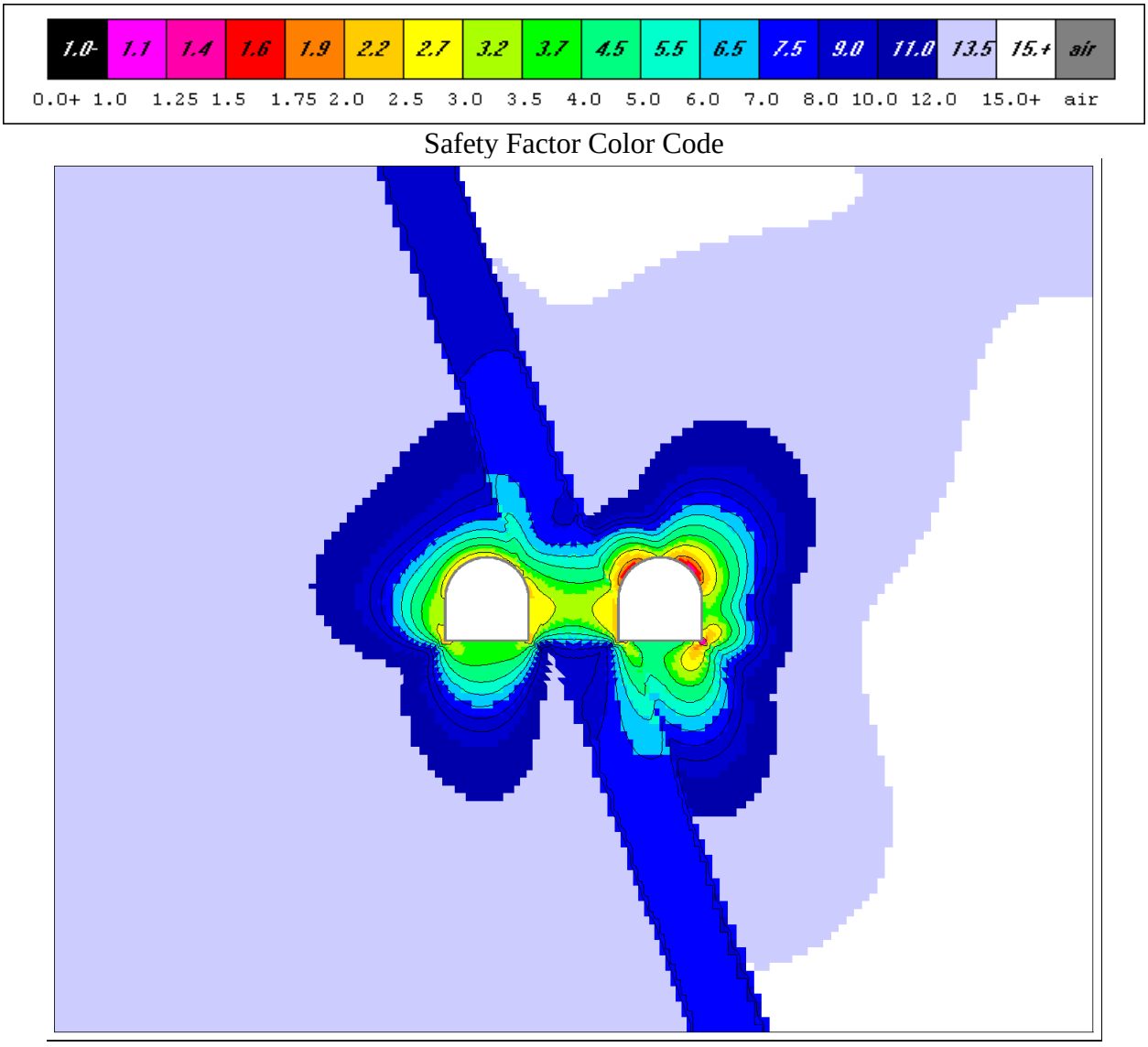


Safety Factor Color Code

Figure 100 Element safety factor distribution for twin arched back adits (drifts).

**Example 5a** This example concerns drifts and crosscuts at the Lucky Friday Mine in Coeur d'Alene mining district in northern Idaho. Rock properties were developed from joint mapping, joint properties and properties of intact rock on the 5100 Level of the mine by Pariseau and Moon 1988 [32].

*Step 1 Preparation of a materials property file (stratigraphic column)* The material properties file used in this example analysis follows where the dip direction of 90 deg indicates dip is to the mine east. The axis of the drift is parallel to mine north in keeping with the finite element axes convention (*x*=east, *y*=north, *z*=vertical). The formation of interest is quartzite that dips steeply (85 deg).

```
NLYRS = 1
NSEAM = 1
  (1) Quartzite
  5.92e+06  5.25e+06  7.15e+06      0.31      0.21      0.29
  2.07e+06  2.41e+06  2.02e+06       0.0       0.0       0.0
   11850.0   10500.0   14330.0     790.0     700.0     955.0
    1662.0    1565.0    2135.0
      90.0      85.0    5100.0     400.0
```

*Step 2 Mesh Generation* Mesh generation input is given in the InData file. Thus for this drift,

```
I Input Data
 "TUNNEL" NPROB 7
 Tunnel Shape = Arched Rectangle
 Tunnel System = Single Opening
 Tunnel Width =      10.0
 Width/Height Ratio =       1.0
 Tunnel Height=      10.0
 Section Depth Seam Center (ft)   =    5100.0
 Additional Sxx,Syy,Szz,Tyz,Tzx,Txy, tension +=
   -7695.0   -5753.0   -5880.0       0.0       0.0       0.0
 Tunnel Stress Sxx,Syy,Szz,Tyz,Tzx,Txy, tension +=
   -7695.0   -5753.0   -5880.0       0.0       0.0       0.0
```

Again, *x* is in the width direction, *y* is vertical and *z* is parallel to the "tunnel", that is,drift axis.

A close up view of the mesh for a 10x10 ft arched back drift is shown in Figure 101

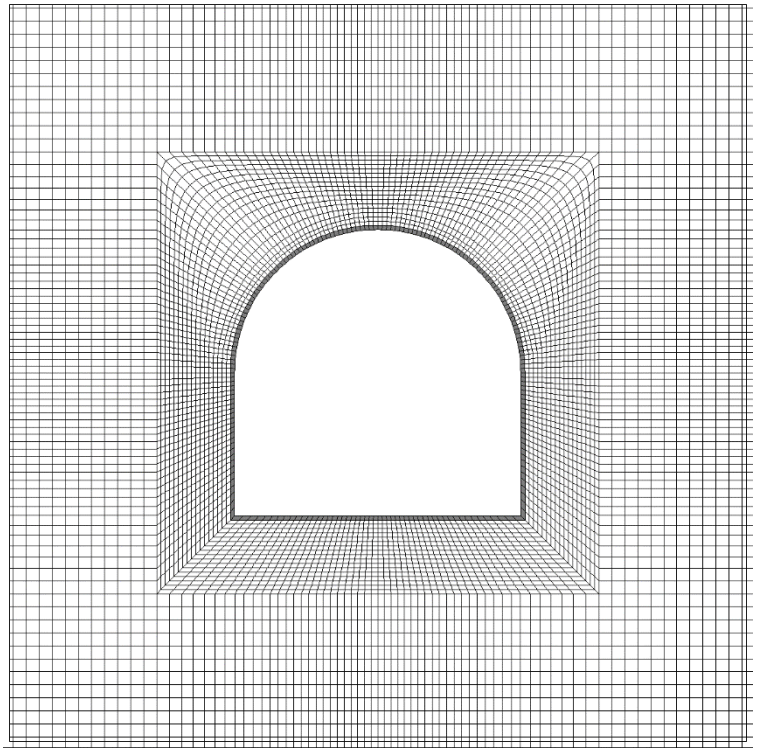

Figure 101 Close-up of the mesh for Example 5a, a 10x10 arched back drift.

*Step 3 FEM Execution and Results*. Figure 102 summarizes the finite element analysis results in the form of an element safety factor distribution. Inspection of the figure shows some failure at the sharp corners at the drift floor and some failures in the back. Although the strength of rock is high, the stress is also high leading to some failure. The wall of the drift is highly stressed as evident in the low safety factor enveloping the drift (pink, red,1.25). A robust support system would surely be required for overall safety.

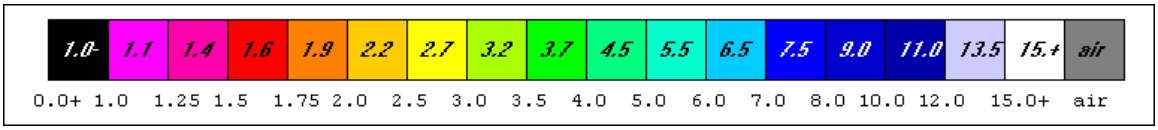


Safety Factor Color Code

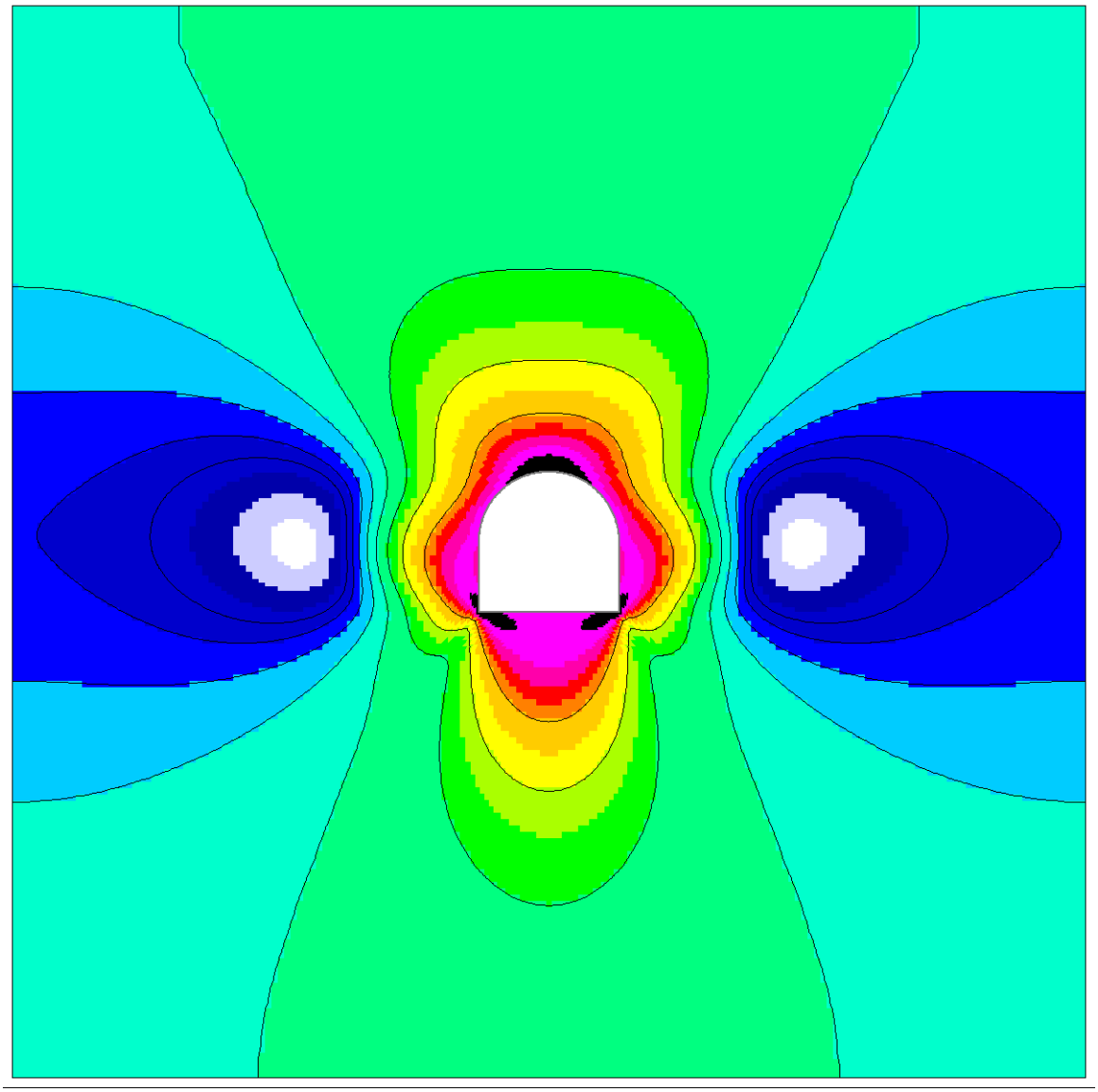

Figure 102 Element safety factor distribution about a 10x10 ft arched back drift, Example 5a.

**Example 5b** This example is a continuation of the previous example but the opening is a crosscut now instead of a drift.

*Step 1 Preparation of a materials property file (stratigraphic column)* The material properties file used in this example crosscut differs from Example 5a (drift) only in the dip direction (0 deg). Thus,

```
NLYRS = 1
NSEAM = 1
  (1) Quartzite
  5.92e+06  5.25e+06  7.15e+06      0.31      0.21      0.29
  2.07e+06  2.41e+06  2.02e+06       0.0       0.0       0.0
   11850.0   10500.0   14330.0     790.0     700.0     955.0
    1662.0    1565.0    2135.0
       0.0      85.0    5100.0     400.0
```

*Step 2 Mesh Generation* Mesh generation input is given in the InData file. Thus for this crosscut,

```
I Input Data
 "TUNNEL" NPROB 7
 Tunnel Shape = Arched Rectangle
 Tunnel System = Single Opening
 Tunnel Width =      10.0
 Width/Height Ratio =       1.0
 Tunnel Height=      10.0
 Section Depth Seam Center (ft)   =    5100.0
 Additional Sxx,Syy,Szz,Tyz,Tzx,Txy, tension +=
   -7695.0   -5753.0   -5880.0       0.0       0.0       0.0
 Tunnel Stress Sxx,Syy,Szz,Tyz,Tzx,Txy, tension +=
   -5880.0   -5753.0   -7695.0       0.0       0.0       0.0
```

Note: The stresses Sxx and Szz are interchanged from the previous drift analysis in Example 5a because of the 90 degree change in direction.

The mesh appears the same as in the previous example and is shown in Figure 101.

*Step 3 FEM Execution and Results*. Figure 103 summarizes the results in the form of an element safety factor distribution. Inspection of the figure shows some failure at the sharp corners at the crosscut floor and some failures in the back. Although the strength of rock is high, the stress is also high leading to some failure. The wall of the crosscut is also highly stressed as evident in the low safety factor enveloping the drift (pink, red,1.25). A robust support system would surely be required for overall safety.

Figure 104 is a side by side comparison of drift and crosscut safety factor distributions and shows the difference and indicates the crosscut is marginally more stable than the drift.

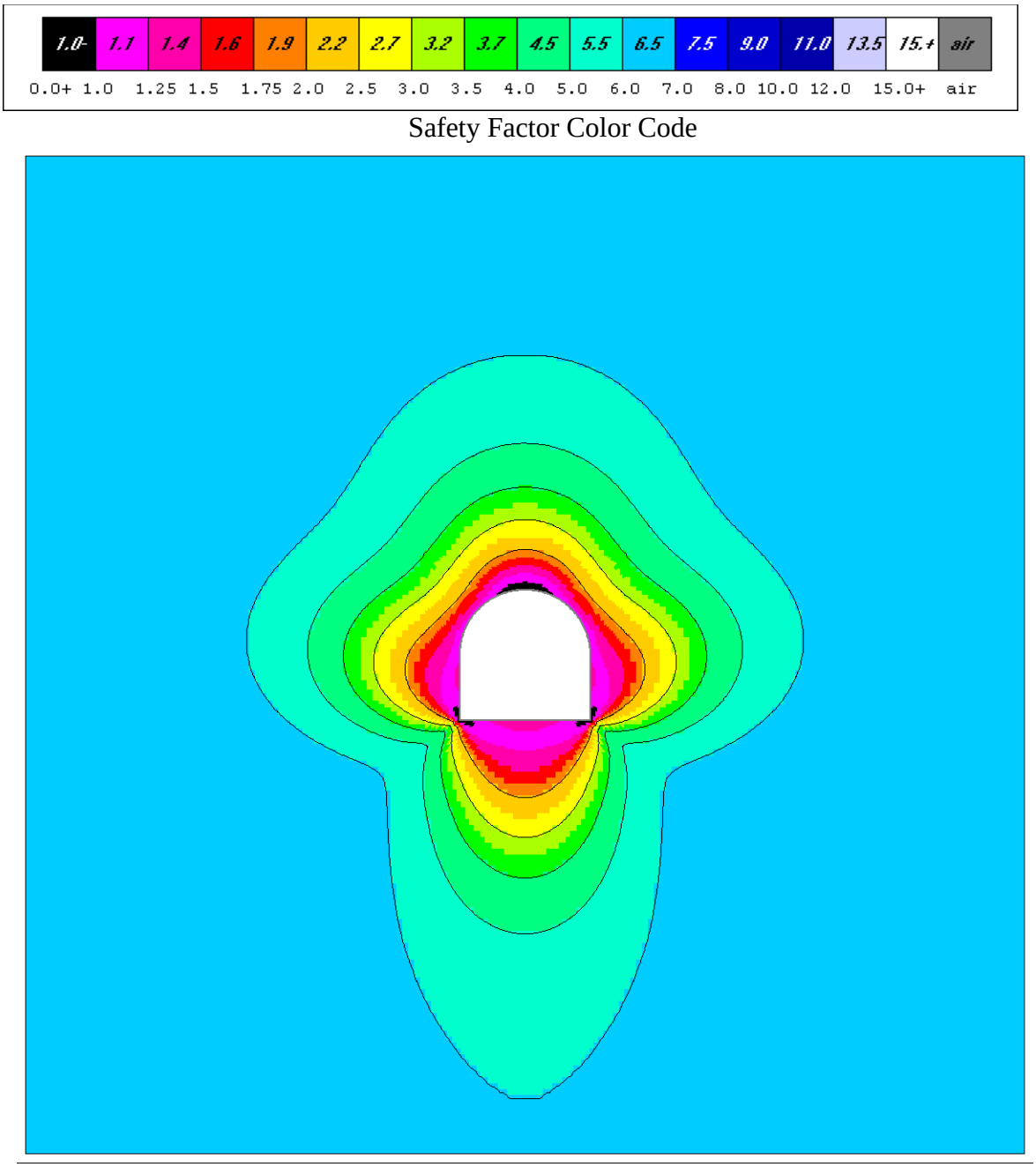


Safety Factor Color Code

Figure 103 Element safety factor distribution about a 10x10 ft arched back crosscut in Example 5b.

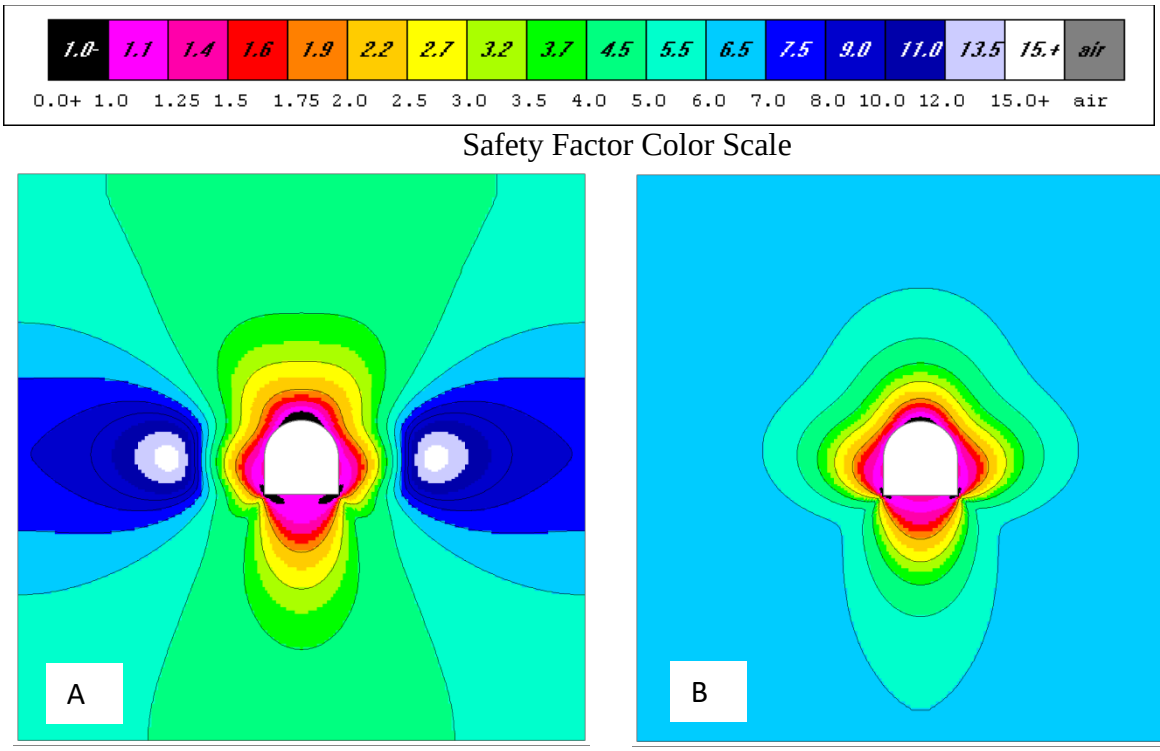


Figure 104 Side by side comparison of drift (A) with crosscut (B) safety factor distributions.

**Example 6** This example stems from a small mine, the Silver Strand Mine that was used as an experimental site by the former U.S. Bureau of Mines, Spokane Research Center, in northern Idaho. The property was developed by adits on three levels. The lowest adit provided access to the ore zone at an elevation just above a nearby stream. The property and adits were accessible by road [33] Sheik, A. K. (2000) "Coupled Finite element Modelling of Wet Mine Stope Stability." M.S. Thesis, University of Utah, pgs 97.

*Step 1 Preparation of a materials property file (stratigraphic column)* The material properties file used in this example is

```
NLYRS = 8
NSEAM = 6
  (4) Revett Qtz
   1.10e+06  1.10e+06  0.90e+06      0.24      0.24      0.24
   4.43e+05  4.43e+05  3.63e+05       0.0       0.0     162.0
    28100.0   28100.0   28100.0    1630.0    1630.0    1630.0
     3900.0    3900.0    3900.0
       90.0      75.0       0.0     435.0
  (1) Sheared Qtz
   1.2e+06   1.2e+06   1.1e+06      0.24      0.24      0.24
   4.8e+05   4.8e+05   4.4e+05       0.0       0.0     157.0
   23400.0   23400.0   23400.0    1370.0    1370.0    1370.0
    3300.0    3300.0    3300.0
      90.0      75.0     435.0      10.0
```

```
 (2) Porphry Dike
  1.5e+06   1.5e+06   1.4e+06      0.28      0.28      0.28
  5.9e+05   5.9e+05   5.4e+05       0.0       0.0     160.0
  16800.0   16800.0   16800.0    1230.0    1230.0    1230.0
   2620.0    2620.0    2620.0
     90.0      75.0     445.0      10.0
 (3) Diabase Dike
  4.9e+05   4.9e+05   4.9e+05      0.24      0.24      0.24
  2.0e+05   2.0e+05   2.0e+05       0.0       0.0     116.0
   1000.0    1000.0    1000.0      60.0      60.0      60.0
    140.0     140.0     140.0
     90.0      75.0     455.0      10.0
 (1) Sheared Qtz
  1.2e+06   1.2e+06   1.1e+06      0.24      0.24      0.24
  4.8e+05   4.8e+05   4.4e+05       0.0       0.0     157.0
  23400.0   23400.0   23400.0    1370.0    1370.0    1370.0
   3300.0    3300.0    3300.0
     90.0      75.0     465.0      10.0
 (4) Revett Qtz
 1.10e+06  1.10e+06  0.90e+06      0.24      0.24      0.24
 4.43e+05  4.43e+05  3.63e+05       0.0       0.0     162.0
  28100.0   28100.0   28100.0    1630.0    1630.0    1630.0
   3900.0    3900.0    3900.0
     90.0      75.0     475.0      50.0
(1) Sheared Qtz
  1.2e+06   1.2e+06   1.1e+06      0.24      0.24      0.24
  4.8e+05   4.8e+05   4.4e+05       0.0       0.0     157.0
  23400.0   23400.0   23400.0    1370.0    1370.0    1370.0
   3300.0    3300.0    3300.0
     90.0      75.0     525.0      10.0
(4) Revett Qtz
 1.10e+06  1.10e+06  0.90e+06      0.24      0.24      0.24
 4.43e+05  4.43e+05  3.63e+05       0.0       0.0     162.0
  28100.0   28100.0   28100.0    1630.0    1630.0    1630.0
   3900.0    3900.0    3900.0
     90.0      75.0     535.0       500.0
```

that reflects repeated dikes and rock types in cross-section.

*Step 2 Mesh Generation* Mesh generation input is given in the InData file. Thus, in case of an 8x8 ft arched back drift,

```
Input Data
 "TUNNEL" NPROB 7
 Tunnel Shape = Arched Rectangle
 Tunnel System = Single Opening
 Tunnel Width =       8.0
 Width/Height Ratio =       1.0
 Tunnel Height=       8.0
 Section Depth Seam Center (ft)   =     500.0
 Additional Sxx,Syy,Szz,Tyz,Tzx,Txy, tension +=
       0.0       0.0       0.0       0.0       0.0       0.0
 Tunnel Stress Sxx,Syy,Szz,Tyz,Tzx,Txy, tension +=
    -168.9    -534.8    -168.9       0.0       0.0       0.0
```

The low stresses are indicative of the shallow depth (500 ft) and loading by gravity only.

The mesh is shown in Figure 105.

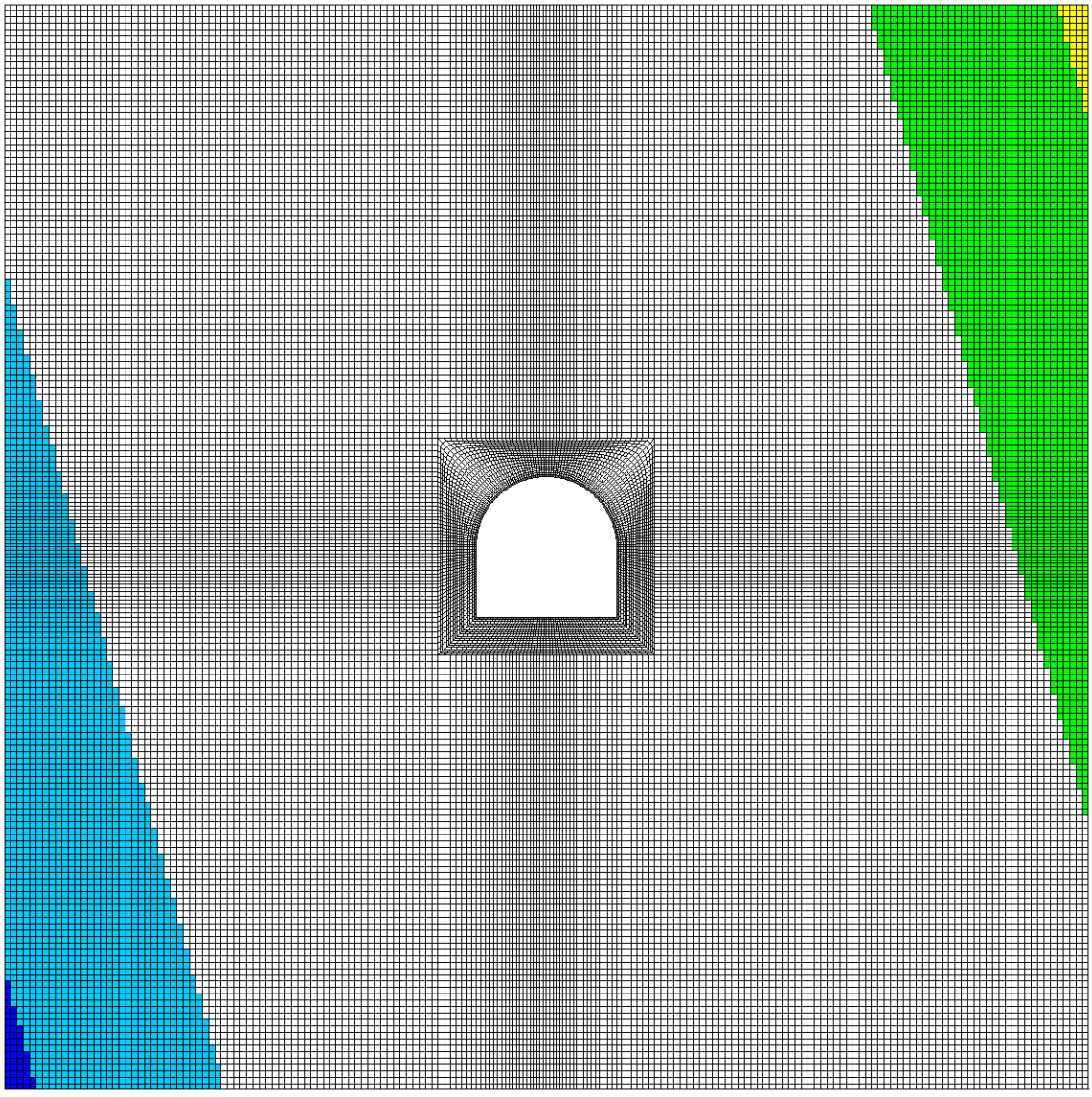

Figure 105 Mesh for Example 6 showing an 8x8 ft arched back drift in steeply dipping rock formations.

*Step 3 FEM Execution and Results*. Figure 106 summarizes the results in the form of an element safety factor distribution. Not too surprisingly, high strength and low stress combine to make the drift quite safe. Element safety factors at the corners are green (4.) and higher elsewhere.

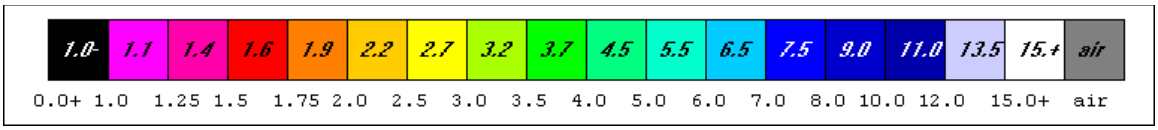


Safety Factor Color Scale

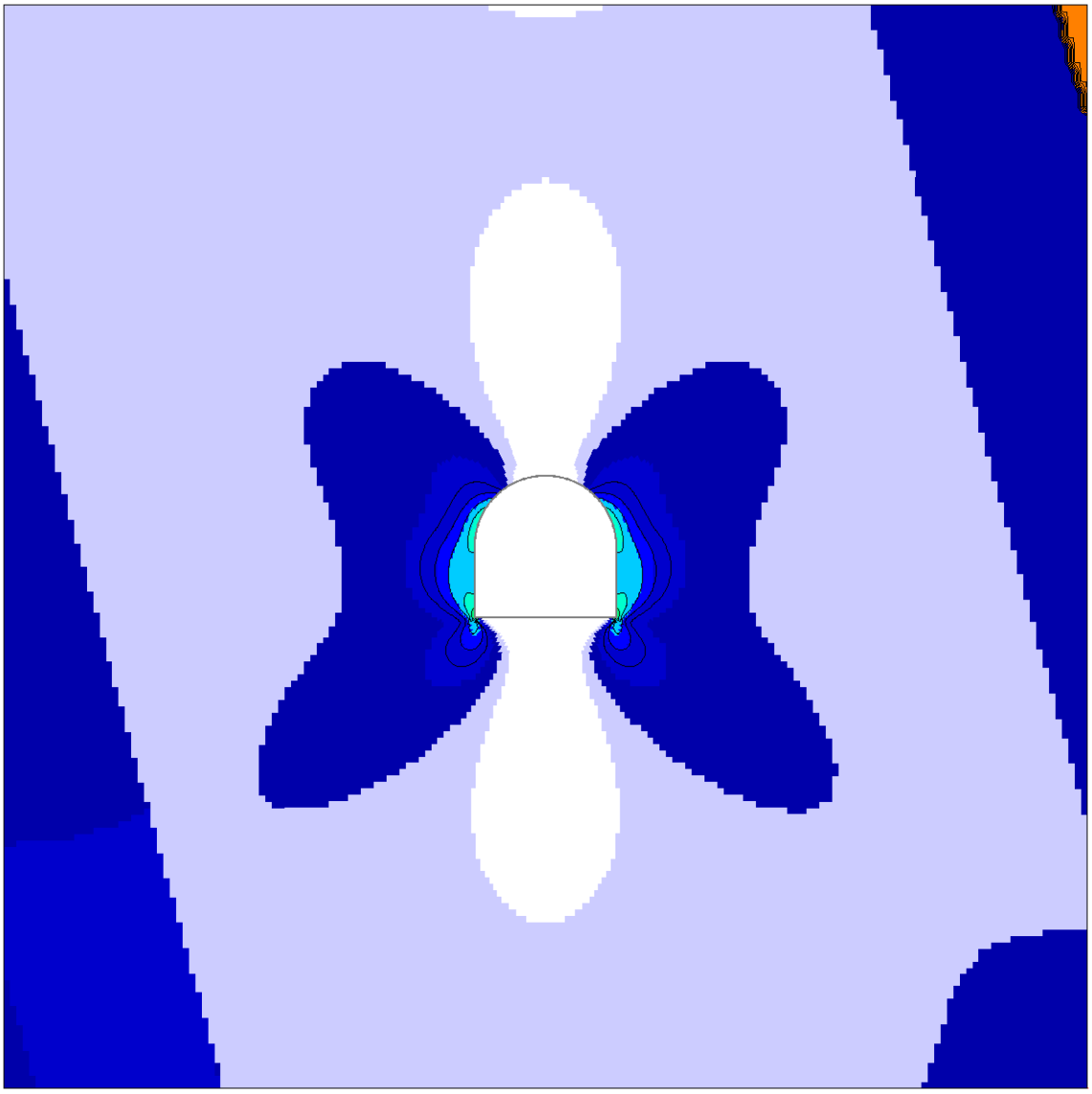

Figure 106 Safety factor distribution for Example 6 of a drift in near surface workings.

## REFERENCES

[1] Dahl, H. D. (1969) A Finite Element Model for Anisotropic Yielding in Gravity Loaded Rock. Ph.D. dissertation. The Pennsylvania State University, The College of Mineral Sciences Experiment Station, University Park, Pennsylvania.,pgs 155.

[2] Desai, C. S. and J.F. Abel (1972) *Introduction to the Finite Element Method, A Numerical Method for Engineering Analysis*. Van Nostrand Reinhold Company, New York.

[3] Oden, J. T. (1972) *Finite Elements of Nonlinear Continua*. McGraw-Hill, New York.

[4] Cook, R. D. (1974) *Concepts and Applications of Finite Element Analysis*. John Wiley & Sons, New York.

[5] Segerlind, L. J. (1976) *Applied Finite Element Analysis*. John Wiley & Sons, New York.

[6a] Zienkiewicz and Y. K. Cheung (1967) *The Finite element Method in Structural and Continuum Mechanics.* McGraw-Hill, London.

[6b] Zienkiewicz, O. C. (1977) *The Finite Element Method* (3rd edition). McGraw-Hill, London.

[7] Bathe, K-L. (1982) *Finite Element Procedures in Engineering Analysis*. Prentice-Hll, Englewood Cliffs, New Jersey.

[8] Logan, D. L. (1986) *A First Course in the Finite Element Method*. PWS-KENT Publishing Company, Boston.

[9] Lekhnitskii, S. G. (1963) *Theory of Elasticity of an Anisotropic Elastic Body* (Translated by P. Fern). Holden-Day, San Francisco.

[10] Pariseau, W.G. (1972) Plasticity Theory for Anisotropic Rocks and Soils. In: *Proc. 10th U.S. Symposium on Rock Mechanics* (ed: K. Gray). Society of Mining Engineers of the American Institute of Mining, Metallurgical and Petroleum Engineers, New York, pp 267-295.

[11] Pariseau. W. G. (2012) *Design Analysis in Rock Mechanics* (2nd edition). CRC Press, London.

[12] Fung, Y. C. (1965) *Foundations of Solid Mechanics*. Prentice-Hall, Englewood Cliffs, New Jersey.

[13] Muskhelishvili, N. I. (1953) *Some Basic Problems of the Mathematical Theory of Elasticity* (4th edition, Translated by J. R. M. Radok) P. Noordhoff Ltd, Groningen, The Netherlands.

[14] Wilson, E. L. (1963) Finite element Analysis of Two-Dimensional Structures. Ph.D. dissertation, University of California – Berkeley, University Microfilms, Ann Arbor, MI, pgs 72.

[15] Pariseaau, W. G., J. C. Johnson, M.M. McDonald and M. E. Poad (1995, 1996) *Rock Mechanics Study of of Shaft Stablity and Pillar Mining, Homestake Min, Lead, SD* U.S. Bureau of Mines Report of Investigations (In Three Parts) 1. Premining Geomechanical Modeling Using UTAH2, 2 Mine Measurements and of Premining Results, 3Geomechanical Monitoring Modeling Using UAH3.

[16] Brady, T.M., J.C. Johnson, M.A. Laurenti, W.G. Pariseau and M. Stahl (2001) *Mining the Remaining Portion of the Ross Shaft Pillar. In: Proc 38th U.S. Rock Mechanics Symp., Balkema, Vol. I, pp 395-399.*

[17] Pariseau, W. G., M. K. McCarter and J. McKenzie (2008) Interpanel Barrier Pillar Study in a Deep Utah Coal Mine. *Proc. 42th U.S., Rock Mechanics Symposium / 2nd U.S.-Canada Rock Mechanics Symposium,* American Rock Mechanics Association, Omnipress, CD, 2008.

[18] Banerjee, B. (1994) *Cable Bolt Modeling and Pillar Recovery at the Magmont Mine,* M.S. Thesis, University of Utah,.pgs 198.

[19] Board, M.P. and M.J. Beus (1989) *In Situ Measuements and Preliminary Design Analysis for Deep Mine Shafts in Highly Stressed Rock,* USBM RI 9231, pgs

[20] Whyatt, J.K. (1986) *Geomechanics of the Caladay Shaft*. M.S. Thesis, University of Idaho, pgs 195,

[21] Whyatt, J.K., B.G. White and J.C. Johnson (1996) *Strength and Deformation Properties of Belt Strata, Coeur d'Alene Mining District, ID*, USBM RI 9619, 65 pgs,

[22] Sturgis, G.A., D. Berberick, M.P. Board, W.H. Strickland and M.T. Swanson *Elliptical shaft Excavations and Furnishing in Response to Depth Induced Ground Pressure* (2017) Eighth International Conference on Deep and High Stress Mining ( J. Wesseloo, editor), Australian Center for Geomechanics, Perth., pp 883-898.

[23] Pariseau, W. G., S. R. Dismuke and J. M. Goris (1995) "Cable Bolting for Pillar Recovery at the Magmont Mine". *Mining Engineering*, Vol. 47, No. 4, 1995, pp 362-365.

[24] Obert, L. and W. I. Duvall. 1967. *Rock Mechanics and the Design of Structures in Rock.* John Wiley & soncs, Inc., New York, pp 154-156.

[25] Luxner, T., J. Deen and M. Koski (2012) Use of Tunnel Boring Machines at the Stillwater Mining Company's Underground PGM Mine, *Mining Engineering,* Vol 64, No 12, pp 50-57.

[26] Langston, R. and H. Kirsten (2002) *Ground Control Manual*, Stillwater Mining Company.

[27] Johnson, J. C., T. Brady, M. McLaughlin, R. Langston and H. Kirstern (2003) In situ Stress Measurements at the Stillwater Mine, Nye, Montana. *Proc 12th Pan-American Conference on Soil Mechanics and Geotechnical Engineering and the 39th U.S. Rock Mechanics Symposium, Massachusetts Institute of Technology*, Cambridge, Massachusetts, June, Vol. 1.

[28] Pariseau, W. G. and H. Moon, (1988) "Elastic Moduli of Well-jointed Rock Masses", *Numerical Methods in Geomechanics* (Innsbruck), Balkema, pp, 815-822.

[29] Pariseau, W. G. (1999) "An Equivalent Plasticity Theory for Jointed Rock Masses". *Int'l J. Rock Mech. Mng. Sci.*, Vol. 36, No.7, pp. 907-918.

[30] Pariseau, W. G., M. E. Fowler, J. C. Johnson, M. Poad and E. L. Corp (1984) "Geomechanics of the Carr Fork Mine Test Stope" *Geomechanics Applications in Underground hardrock Mining,* SME/AIME, New York, pp 3-38.

[31] Pariseau, W. G. (1985) "Research Study on Pillar Design for Vertical Crater Retreat." Final Report. U. S. Bureau of Mines Contract J0215043.

[32]Pariseau, W. G. and H. Moon (1989) "Influence of Joints on the Elastic Response of a LFUFL Stope to FEM Mining." *Proc. of the 30th U. S. Symposium on Rock Mechanics.* Balkema, Rotterdam, pp 931-941.

[33] Sheik, A. K. (2000) "Coupled Finite element Modelling of Wet Mine Stope Stability." M.S. Thesis, University of Utah, pgs 97.

## APPENDIX – I BARRIER PILLAR

This appendix contains strata properties files relating to Problem 2 Barrier Pillar.

```
NLYRS= 32
NCOAL= 11
1Wasatch_Formation
2350000       2350000       2350000       0.291  0.291  0.291
910147 910147 910147 0      0      162
9800   9800   9800   980    980    980
1789   1789   1789
0      0      0      364
2Ohio_Creek_Member
2350000       2350000       2350000       0.291  0.291  0.291
910147 910147 910147 0      0      162
9800   9800   9800   980    980    980
1789   1789   1789
0      0      364    400
3Barren_Member
2450000       2450000       2450000       0.277  0.277  0.277
959280 959280 959280 0      0      162
10200  10200  10200  1020   1020   1020
1862   1862   1862
0      0      764    1200
4InterBedded_Shale_and_Sandstone
1888372       1888372       1888372       0.325  0.325  0.325
712465 712465 712465 0      0      157
8000   8000   8000   800    800    800
1461   1461   1461
0      0      1964   86
5Paonia_SS_Sh_Siltst
4000000       4000000       4000000       0.25   0.25   0.25
1600000       1600000       1600000       0      0      162
8120   8120   8120   812    812    812
1483   1483   1483
0      0      2050   168
6Coal_1
400000 400000 400000 0.300  0.300  0.300
```

```
153846 153846 153846 0      0      80
1500   1500   1500   150    150    150
274    274    274
0      0      2218   4
7SS_1
2000000       2000000       2000000       0.250  0.250  0.250
800000 800000 800000 0      0      149
1655   1655   1655   166    166    166
303    303    303
0      0      2222   3
8MS_1
1600000       1600000       1600000       0.250  0.250  0.250
640000 640000 640000 0      0      142
1606   1606   1606   161    161    161
294    294    294
0      0      2225   3
9SS_2
2000000       2000000       2000000       0.250  0.250  0.250
800000 800000 800000 0      0      149
1655   1655   1655   166    166    166
303    303    303
0      0      2228   10
10MS_2
1600000       1600000       1600000       0.250  0.250  0.250
640000 640000 640000 0      0      142
1606   1606   1606   161    161    161
294    294    294
0      0      2238   12
11DU_seam
370000 370000 370000 0.300  0.300  0.300
142308 142308 142308 0      0      80
1500   1500   1500   150    150    150
274    274    274
0      0      2250   11
12MS_SS_3
1700000       1700000       1700000       0.238  0.238  0.238
686869 686869 686869 0      0      147
3235   3235   3235   323    323    323
590    590    590
0      0      2261   4
13MS_4
1600000       1600000       1600000       0.250  0.250  0.250
640000 640000 640000 0      0      142
1606   1606   1606   161    161    161
294    294    294
0      0      2265   5
14SS_4_MS_5
1900000       1900000       1900000       0.250  0.250  0.250
760000 760000 760000 0      0      147
1643   1643   1643   164    164    164
300    300    300
0      0      2270   3
15SS_5
2000000       2000000       2000000       0.250  0.250  0.250
800000 800000 800000 0      0      149
1655   1655   1655   166    166    166
303    303    303
0      0      2273   5
```

```
16Coal_2_Shale_1
666667 666667 666667 0.300  0.300  0.300
256410 256410 256410 0      0      101
1438   1438   1438   144    144    144
263    263    263
0      0      2278   3
17Coal_3
400000 400000 400000 0.300  0.300  0.300
153846 153846 153846 0      0      80
1500   1500   1500   150    150    150
274    274    274
0      0      2281   3
18Sh_2
1200000       1200000       1200000       0.300  0.300  0.300
461538 461538 461538 0      0      142
1314   1314   1314   131    131    131
240    240    240
0      0      2284   2
19SS_6
2000000       2000000       2000000       0.250  0.250  0.250
800000 800000 800000 0      0      149
1655   1655   1655   166    166    166
303    303    303
0      0      2286   2
20Paonia_Interbedded_Sandstone_Shale_and_Siltstone
2808095       2808095       2808095       0.296  0.296  0.296
1083609       1083609       1083609       0      0      158
7800   7800   7800   780    780    780
1424   1424   1424
0      0      2288   59
21Bowie_Upper_Sandstone
4000000       4000000       4000000       0.230  0.230  0.230
1626016       1626016       1626016       0      0      162
14000  14000  14000  1400   1400   1400
2556   2556   2556
0      0      2347   40
22Bowie_Siltstone
2000000       2000000       2000000       0.250  0.250  0.250
800000 800000 800000 0      0      162
8000   8000   8000   800    800    800
1461   1461   1461
0      0      2387   10
23Bowie_Middle_Sandstone
4000000       4000000       4000000       0.230  0.230  0.230
1626016       1626016       1626016       0      0      162
14000  14000  14000  1400   1400   1400
2556   2556   2556
0      0      2397   30
24Upper_Bowie_Shale
1316667       1316667       1316667       0.35   0.35   0.35
488861 488861 488861 0      0      149
4000   4000   4000   400    400    400
730    730    730
0      0      2427   12
25Bowie_Lower_Sandstone
3614286       3614286       3614286       0.241  0.241  0.241
1456535       1456535       1456535       0      0      154
14000  14000  14000  1400   1400   1400
```

```
2556   2556   2556
0      0      2439   56
26Bowie_Interbedded_Siltstone_Sandstone_and_Shale
2160000       2160000       2160000       0.269  0.269  0.269
851064 851064 851064 0      0      162
8900   8900   8900   890    890    890
1625   1625   1625
0      0      2495   25
27BU_Seam
400000 400000 400000 0.330  0.330  0.330
150376 150376 150376 0      0      85
1500   1500   1500   120    120    120
245    245    245
0      0      2520   20
28Lower_Bowie_Shale
1500000       1500000       1500000       0.350  0.350  0.350
555556 555556 555556 0      0      162
4000   4000   4000   400    400    400
730    730    730
0      0      2540   30
29BL_Seam
400000 400000 400000 0.330  0.330  0.330
150376 150376 150376 0      0      85
1500   1500   1500   120    120    120
245    245    245
0      0      2570   12
30Bowie_Interbedded_Shale_and_Sandstone
1788298       1788298       1788298       0.333  0.333  0.333
670844 670844 670844 0      0      159
7000   7000   7000   700    700    700
1278   1278   1278
0      0      2582   94
31Rollins_Sandstone
4000000       4000000       4000000       0.230  0.230  0.230
1626016       1626016       1626016       0      0      162
14000  14000  14000  1400   1400   1400
2556   2556   2556
0      0      2676   140
32Mancos_Shale
1500000       1500000       1500000       0.350  0.350  0.350
555556 555556 555556 0      0      162
4000   4000   4000   400    400    400
730    730    730
0      0      2816   2436
```

Figure 1 Input strata properties data for mesh generation for Mine B.

# APPENDIX – II BLEEDER ENTRIES

This appendix contains strata properties files relating to Problem 3 Bleeder Entries.

```
NLYRS= 26
NCOAL= 10
1Wasatch
2350000       2350000       2350000       0.291  0.291  0.291
910147 910147 910147 0      0      149
9800   9800   9800   980    980    980
1789   1789   1789
0      0      0      364
2Ohio_Creek
2350000       2350000       2350000       0.291  0.291  0.291
910147 910147 910147 0      0      162
9800   9800   9800   980    980    980
1789   1789   1789
0      0      364    400
3Ba
2450000       2450000       2450000       0.277  0.277  0.277
959280 959280 959280 0      0      162
10200  10200  10200  1020   1020   1020
1862   1862   1862
0      0      764    1200
4Intbd_Sh_SS
1888372       1888372       1888372       0.325  0.325  0.325
712465 712465 712465 0      0      157
8000   8000   8000   800    800    800
1461   1461   1461
0      0      1964   86
5SS1
2000000       2000000       2000000       0.250  0.250  0.250
800000 800000 800000 0      0      149
1655   1655   1655   166    166    166
303    303    303    0      0      0
0      0      2050   168
6MS_coal1
1000000       1000000       1000000       0.275  0.275  0.275
392157 392157 392157 0      0      111
1803   1803   1803   180    180    180
329    329    329
0      0      2218   4
7MS_3
1600000       400000 400000 0.300  0.300  0.300
640000 640000 640000 0      0      142
1606   1606   1606   161    161    161
294    294    294    0      0      0
0      0      2222   12
8MS_coal2
1381818       1381818       1381818       0.260  0.260  0.260
548341 548341 548341 0      0      131
1745   1745   1745   175    175    175
319    319    319
0      0      2234   11
9MS
1600000       1600000       1600000       0.250  0.250  0.250
640000 640000 640000 0      0      142
```

```
1606   1606   1606   161    161    161
294    294    294
0      0      2245   5
10Coal_1
370000 370000 370000 0.300  0.300  0.300
142308 142308 142308 0      0      80
1500   1500   1500   150    150    150
274    274    274
0      0      2250   11
11MS_5
1600000       1600000       1600000       0.250  0.250  0.250
640000 640000 640000 0      0      142
1606   1606   1606   161    161    161
294    294    294
0      0      2261   5
12Coal_4
400000 400000 400000 0.300  0.300  0.300
153846 153846 153846 0      0      80
1500   1500   1500   150    150    150
274    274    274
0      0      2266   5
13MS_SS6
1661538       1661538       1661538       0.246  0.246  0.246
666667 666667 666667 0      0      144
2111   2111   2111   211    211    211
385    385    385
0      0      2271   13
14Paonia_Interbedded_Sandstone_Shale_and
2808095       2808095       2808095       0.296  0.296  0.296
1083609       1083609       1083609       0      0      158
7800   7800   7800   780    780    780
1424   1424   1424
0      0      2284   61
15Bowie_Upper
4000000       4000000       4000000       0.230  0.230  0.230
1626016       1626016       1626016       0      0      162
14000  14000  14000  1400   1400   1400
2556   2556   2556
0      0      2345   40
16Bowie
2000000       2000000       2000000       0.250  0.250  0.250
800000 800000 800000 0      0      162
8000   8000   8000   800    800    800
1461   1461   1461
0      0      2385   10
17Bowie_Middle
4000000       4000000       4000000       0.230  0.230  0.230
1626016       1626016       1626016       0      0      162
14000  14000  14000  1400   1400   1400
2556   2556   2556
0      0      2395   30
18Upper_Bowie
1316667       1316667       1316667       0.347  0.347  0.347
488861 488861 488861 0      0      149
4000   4000   4000   400    400    400
730    730    730
0      0      2425   12
19Bowie_Lower
```

```
3614286       3614286       3614286       0.241  0.241  0.241
1456535       1456535       1456535       0      0      154
14000  14000  14000  1400   1400   1400
2556   2556   2556
0      0      2437   56
20Bowie_Interbedded_Siltstone_Sandstone_and
2160000       2160000       2160000       0.269  0.269  0.269
851064 851064 851064 0      0      162
8900   8900   8900   890    890    890
1625   1625   1625
0      0      2493   25
21BU
400000 400000 400000 0.330  0.330  0.330
150376 150376 150376 0      0      85
1500   1500   1500   120    120    120
245    245    245
0      0      2518   20
22Lower_Bowie
1500000       1500000       1500000       0.350  0.350  0.350
555556 555556 555556 0      0      162
4000   4000   4000   400    400    400
730    730    730
0      0      2538   30
23BL
400000 400000 400000 0.330  0.330  0.330
150376 150376 150376 0      0      85
1500   1500   1500   120    120    120
245    245    245
0      0      2568   12
24Bowie_Interbedded_Shale_and
1788298       1788298       1788298       0.333  0.333  0.333
670844 670844 670844 0      0      159
7000   7000   7000   700    700    700
1278   1278   1278
0      0      2580   94
25Rollins
4000000       4000000       4000000       0.230  0.230  0.230
1626016       1626016       1626016       0      0      162
14000  14000  14000  1400   1400   1400
2556   2556   2556
0      0      2674   140
26Mancos
1500000       1500000       1500000       0.350  0.350  0.350
555556 555556 555556 0      0      162
4000   4000   4000   400    400    400
730    730    730
0      0      2814   2436
```

Figure 1 Input strata properties data for mesh generation for Mine C.

APPENDIX – III: GOB MODELS, CAVING GROUND

*Gob* and *goaf* refer to caved rock behind face support of a longwall panel. A frequently cited image is presented in Figure 1. The figure illustrates initial caving in the immediate roof, the first stratum above the mined seam (A), subsequent caving into strata above (B), formation of a block-beam (C), separation for strata above and settlement of the gob below (D, E, F). A tacit assumption is that the rock forming the gob becomes a rubble pile as initially large blocks formed in consequence of joints and existing fractures are fragmented into smaller blocks that are in turn fragmented into even smaller blocks during the caving process.

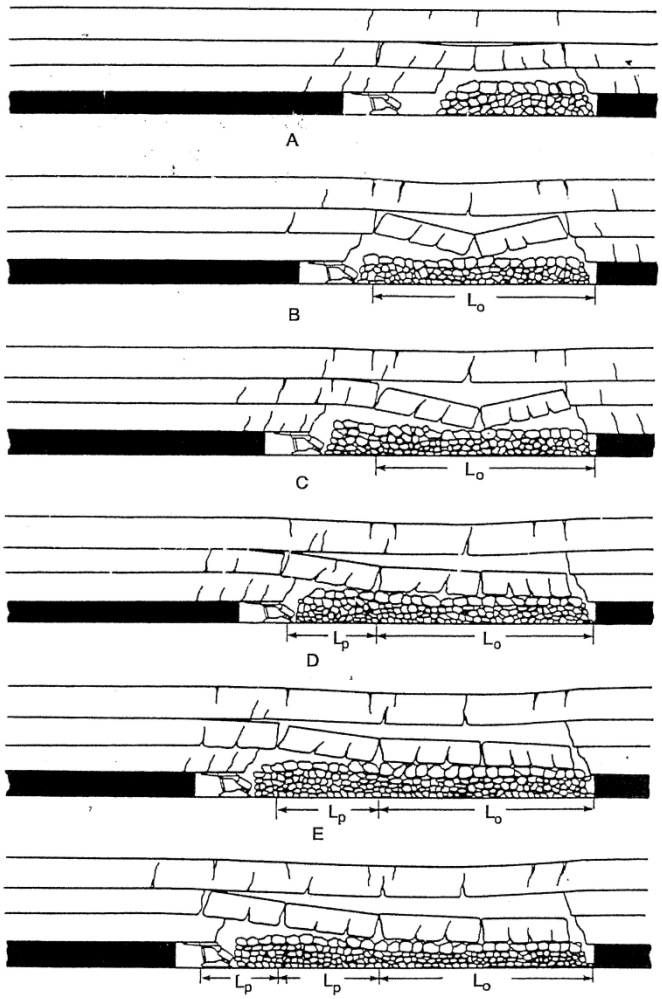


Figure 1 Conceptual model of a caving sequence in longwall mining of coal (after Peng, 2006)

Swell of the initially intact rock during gob formation is considerable and limits the gob height to just a few multiples of mining height. A simple mass balance illustrates this concept. With reference to Figure 2 that shows a schematic distribution of material before and after caving, the gob or cave height of rock rubble *H* is given by

$$H = (1/h)(1/n - 1)$$

(1) where: $h$=mining height, $H$ = cave height,

and $n$=porosity of the gob ($n$=Vv/V).

In essence, the void space created by mining is redistributed into the void space of the gob.

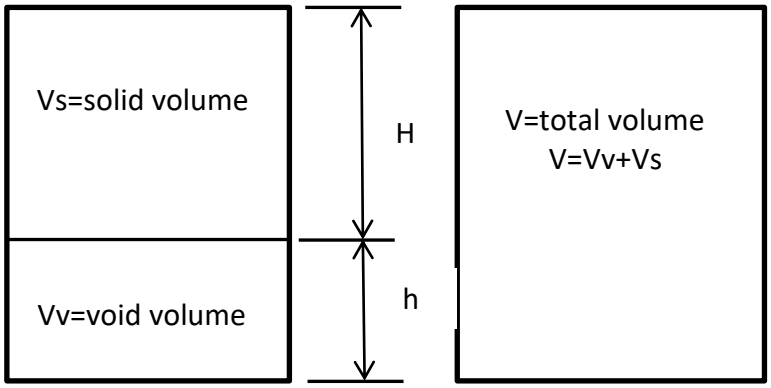


Figure 2 Schematic illustration of volumes before and after gob formation (caving).

For example, if gob porosity $n$=0.25, then gob cave height $H$=3$h$. Bulking or swell of the initial cave rock quickly fills the void space of the excavation even as overlying strata sag into contact with the gob. As overlying strata contact the gob, the gob becomes loaded and in turn supports the strata above. As the face advances, the process continues.

Particle size distribution of caved rock prohibits laboratory testing and mine measurements of gob forces are rare. However, physical modeling of gob at a laboratory scale shows a highly non-linear response (Pappas and Mark 1993). The main feature of the simulated longwall gob material is a scaling of size distribution. Figure 3 shows laboratory test data obtained from shale, weak sandstone and strong sandstone. The test data are essentially uniaxial strain data obtained from compression of the simulated gob in a steel cylinder, so the slope of the stress – strain curve is influenced by Poisson's ratio when considered within the context of non-linear elasticity. Differentiating Hooke's law to obtain a differential form of elasticity for isotropic material, one obtains

$$\frac{d\sigma}{d\varepsilon} = [\frac{E}{(1+\nu)(1-2\nu)}](1-\nu) \quad (2)$$

where $\sigma$ and $\varepsilon$ are axial stress and strain, respectively, and $E$ and $\nu$ are tangent Young's modulus and Poisson's ratio, respectively. If $\nu$=0.2, then the right-hand side of (2) is 1.11$E$ which is a small correction and perhaps negligible as a practical matter. An expression for a tangent modulus given by Pappas and Mark (1993) for simulated gob material is:

$$d\sigma / d\varepsilon = E = a\sigma^2 + b\sigma + c \quad (3)$$

where $a$, $b$, and $c$ are constants derived from test data.

Integration of (3) leads to a complicated stress – strain relationship:

(4) $$\varepsilon = \left(\frac{-2}{\sqrt{-(4ac-b^2)}}\right)\tanh^{-1}\left(\frac{2c\sigma+b}{\sqrt{-(4ac-b^2)}}\right)$$

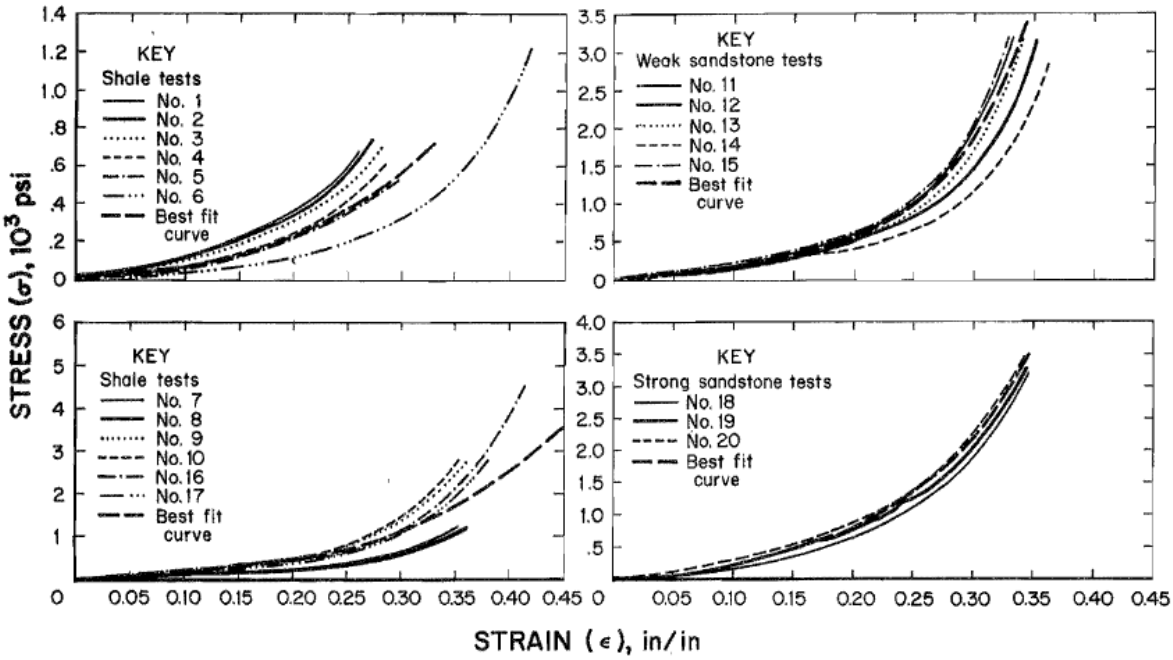


Figure 3 Stress – strain curves for simulated longwall gob material (after Pappas and Mark 1993).

The shapes of the plots in Figure 3 are suggestive of a parabola. Indeed, research on hydraulically placed sand back-fill after drainage shows the simple relationship

(5) $$\sigma = a\varepsilon + b\varepsilon^2$$

to give satisfactory results in finite element modeling of cut and fill stoping in narrow veins. Figure 3 shows several fill model stress-strain curves in comparison with mine measurements that were made over a two year period of mining and finite element modelling results.

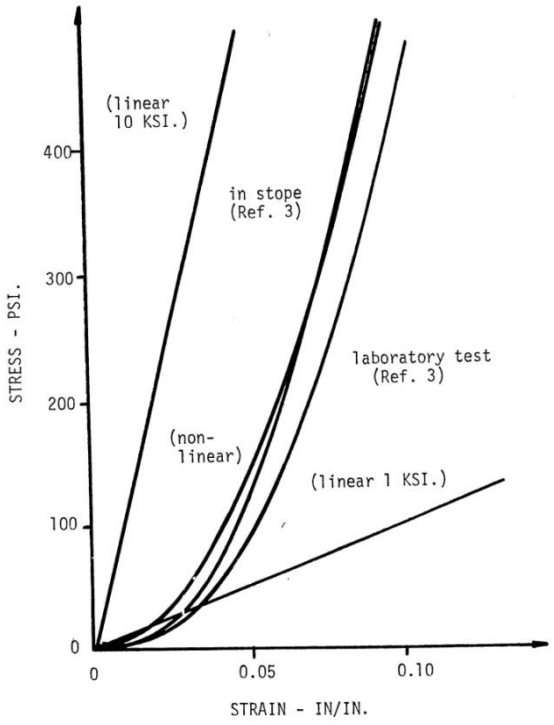


Figure 4 Uniaxial stress – strain plots for mine fill (after Pariseau, 1975). Ref 3=Corson, D. R. and W. R. Wayment. 1967. Load-Displacement Measurement in a Backfilled Stope of a Deep Vein Mine. U. S. Bureau of Mines Report of Investigation 7038.

The model (5) implies

(6) $$d\sigma / d\varepsilon = E = a + 2b\varepsilon = (a^2 + 4b\sigma)^{1/2} = (\text{tangent modulus})$$

where the constants *a* and *b* are determined from test measurement results. After some more algebra, the stress – strain rule (5) can be written as

(7) $$\sigma = (\frac{E + E_o}{2})\varepsilon$$

The terms in parenthesis in (7) constitute a secant modulus (mean value) where $E_o$ is the initial modulus ($E_o = a$). The tangent modulus relationship (6) is convenient in finite element analyses because the strains are obtained from solution for displacements. Stresses then follow from strains in increments of applied load. Of course, a full three-dimensional stress-strain relationship is used in finite element analysis, that is, (6) must be developed into a three-dimensional relationship. Figure 5 illustrates the non-linear gob model relationship (5). The initial modulus *a*=0.5 ksi; the high modulus $(a + 2b\varepsilon)$ =9.5 ksi with $\varepsilon$=0.09. These values would

be determined from test data that would span the range of vertical gob stress expected in practice.

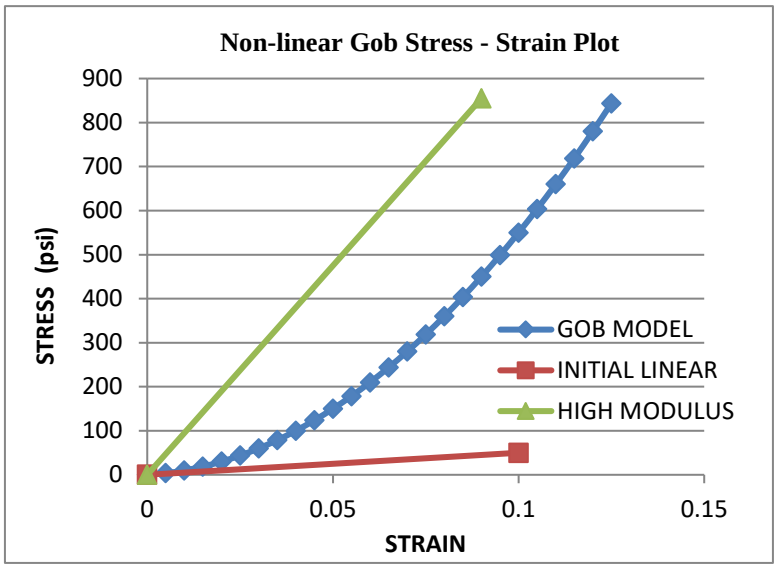


Figure 5 Computed gob uniaxial stress – strain plot following relationship (5).

Hooke's law for a linearly elastic isotropic material in differential form is

$$d\sigma_{zz} = E^*[(1-v)d\varepsilon_{zz} + v(d\varepsilon_{xx} + d\varepsilon_{yy})]$$
$$d\tau_{yz} = Gd\gamma_{yz} \quad (8)$$

and similarly for the normal and shear stresses associated with the *x* and *y* directions. In (7), $E^* = E/[(1+v)(1-2v)]$, *v*=Poisson's ratio, *G*=shear modulus, and $\gamma_{yz}$ =engineering shear strain. Again, *E*=tangent modulus given by (6). Poisson's ratio can be determined from the uniaxial strain test results in the laboratory. However, the effect is small, so any reasonable value such as 0.20, 0.25 or 0.33 suffices.

The conceptual model in Figure 1 illustrates only half of the situation, the top half so to speak. No indication of floor response is given. However, the distribution of stress tends to be symmetric with respect to the horizontal plane. Figure 6 illustrates a finite element result which shows distribution of element (local) safety factors (*fs*) in vertical cross section of a longwall panel. A local or element safety factor is by definition a ratio of "strength" to "stress; *fs*="strength"/"stress" where proper measures of strength and stress are used for multi-axial stress states encountered in three-dimensional stress analysis. Of course, exact symmetry is not expected because of the role of gravity and strata properties that surely differ from roof to floor. Indeed, the results in the figure show greater yielding in the roof than in the floor. The speckled pattern is a consequence of spatial variability of strata properties in the finite element model. The mined seam is a thin grey line that transects the elliptical shaped black region showing the extent of element yielding.

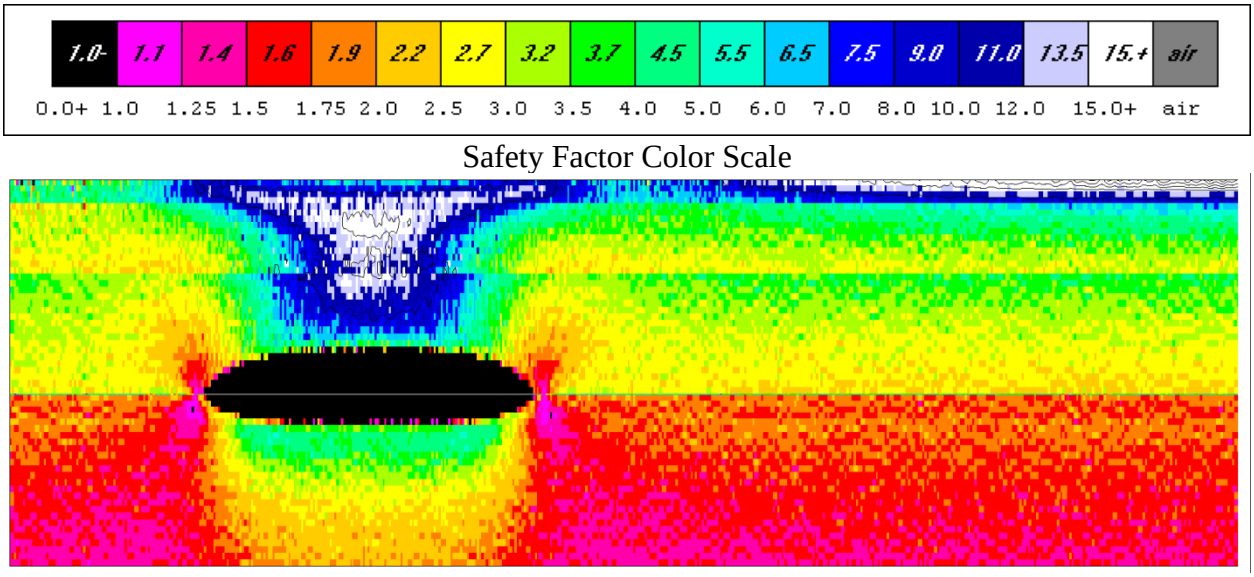


Safety Factor Color Scale

Figure 6 A vertical section showing element safety factors when the face has advanced 0.4 times panel length. Length of the section is approximately 2,400 m (8000 ft). Seam depth is approximately 418 m (1370 ft); mining height is 3 m (10 ft).

Figure 6 indicates several issues associated with gob modeling as envisioned in the conceptual model in Figure 1. One quite important issue whether the gob is modeled or not is the role of joints as they influence strata behavior. Generally, joints make strata more compliant and weaker compared with unjointed or intact rock between joints. An equivalent properties formulation is one approach that may be used to quantify the issue in a technically sound manner (Pariseau 1999).

A second and also quite important issue is how to generate gob, that is, how to simulate caving in finite element modelling. Caving certainly involves formation and fall of rock blocks, although a fall may be quite small when caved ground is in contact with overlying strata. The process suggests brittle behavior with loss of cohesion at the limit to elasticity, although frictional strength remains. How much depends on confinement and confining pressure provided by adjacent material. Figure 7 illustrates this simple concept in the context of the popular Mohr-Coulomb failure criterion. Use of other failure or yield criteria including non-linear and anisotropic criteria is certainly possible. The main feature in any case is loss of cohesive strength but retention of frictional strength.

A first step in finite element caving analysis would seem to be reassignment of material properties to elements that have reached the elastic limit for the first time. New elastic properties would be in accord with the gob model; new strength properties would be in accord with the cohesive loss, friction retention strength model. The stress and strain states in these elements would be reduced to zero. Out of equilibrium forces are created at the interface between these failing elements and adjacent elements that remain in the purely elastic domain. Application of these forces would drive the system further, perhaps causing additional failures. The process would then be repeated to accommodate these additional failures. Termination of the process would occur when no additional element failures occurred. As part of properties reassignment to

new element failures, these elements should be assigned weight which will contribute to the out of equilibrium forces thus allowing "settlement" under the self-weight of the newly caved ground (gob).

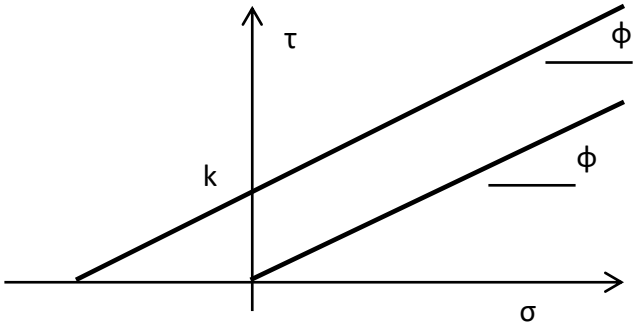


Figure 7 Mohr-Coulomb failure envelopes before and after caving. Cohesion=k, angle of internal friction =ϕ. Cohesion is lost but the angle of internal friction remains the same.

An important question is what to do about the floor? Because floor element failure is logically no different than roof element failure, the same reassignment of material properties should be done. Indeed, all new element failures should be treated the same.

Another question is what to do about "excavated" coal elements that are generated at the outset. Associated with this question is how to allow the failing roof elements to "drop" into a void space below, assuming there is a void space remaining. This question is not so easily addressed. One possibility is to reassign the mined elements ("air" elements) newly failed element properties. This action would seem to create material, but with due attention to mass conservation via a consistent computation of specific weight of newly failed material, the computational hazard would be avoided. Roof and floor swell would contribute to the void filling process and the necessary reduction in specific weight of the previously mined elements. In the event that no elements failed during an initial face advance, then the excavated elements would remain as such. Reassignment of excavated element properties to gob properties would remain linked to roof and floor element failures.

In finite element analysis, loads are applied incrementally in discrete steps to take into account non-linear behavior. However, caving and gob formation from newly failed elements is continued within a given load step until no new element failures occur. The next load step is then applied. A distinction between previously failed elements and newly failed elements is necessary. While newly failed elements experience gravity loading from self-weight, previously failed elements have already experienced gravity loads and no longer require loading by self-weight. Newly failed elements then settle under self-weight and compact previously failed elements below.

A general strata mechanics issue is bed separation. This phenomenon is well-known; analysis is simple analytically (e.g. Obert and Duvall 1967, Pariseau 2017), but not so easily modeled in finite element analysis. Use of special interface elements is one approach to the problem within the context of the finite element method. Another approach is the use of dual

nodes. Ordinarily elements at a stratum boundary share nodes. By assigning different node numbers to nodes of one of the elements at an interface, dual nodes are generated. Figure 8 illustrates dual node elements. Slip and separation of dual nodes is allowed, but overlap is prohibited. Interestingly, this technique has not been tested against the analytical solution.

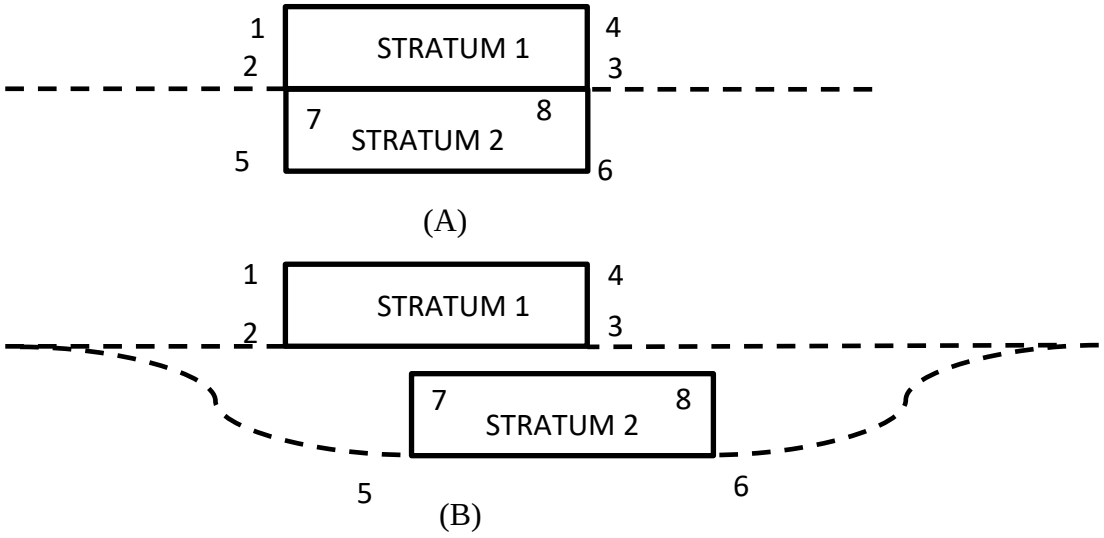


Figure 8 Schematic of dual node elements at an interface between strata. (A) before separation, (B) after separation.

Yet another gob model complication is the evolution of beam action in separated strata. First is formulation of an immediate roof beam supported at both ends with initial face advance from a start-up room. Next, following initial caving, is cantilever beam formation extending behind the face and back over face support. Cantilever beam failure with further face advance then leads to formation of another but shorter cantilever beam and so on. Although beam elements are well-understood within the context of the finite element method, they do increase computational complexity and cost.

However, if the main purpose of a gob model is to account for transfer of overburden load to caved ground at seam level and thus to modify the redistribution of stress in the vicinity of the face, headgate and tail gate entries, crosscuts and pillars, then a simple gob model may suffice. A simple model would avoid the many complications of a detailed caving model and the associated cost of development and verification. A simple gob model would replace excavated elements at seam level with gob elements. Replacement consists of reassignment of element properties to gob properties from excavated (air) elements. This simple gob model concept has been adopted by others using the well-known FLAC3D[2] computer code (Badr *et all* 2002).

[2] FLAC3D is a continuum code based on a finite difference method. Finite element codes are also continuum codes but based on the underlying finite element method.

Other simple gob models are cited by Pappas and Mark (1993). As shown in Figure 8, the authors cite a model by Salamon (1990) and one attributed to Terzaghi by Salamon (Pappas and Mark 1993). The Salamon model is based on much earlier work and has the form

(9) $$\sigma = E_o[\frac{\varepsilon}{(1-\varepsilon/b)}]$$

were $E_o$ = initial modulus and $b = \varepsilon_m$ = maximum possible strain. The Terzaghi model is given in Figure 8 and has the form

(10) $$\sigma = (E_o/b)(e^{b\varepsilon} - 1)$$

The "fill" model (4) can be recast into a form for comparison with (8) and (9)

(11) $$\sigma = E_o\varepsilon + b\varepsilon^2$$

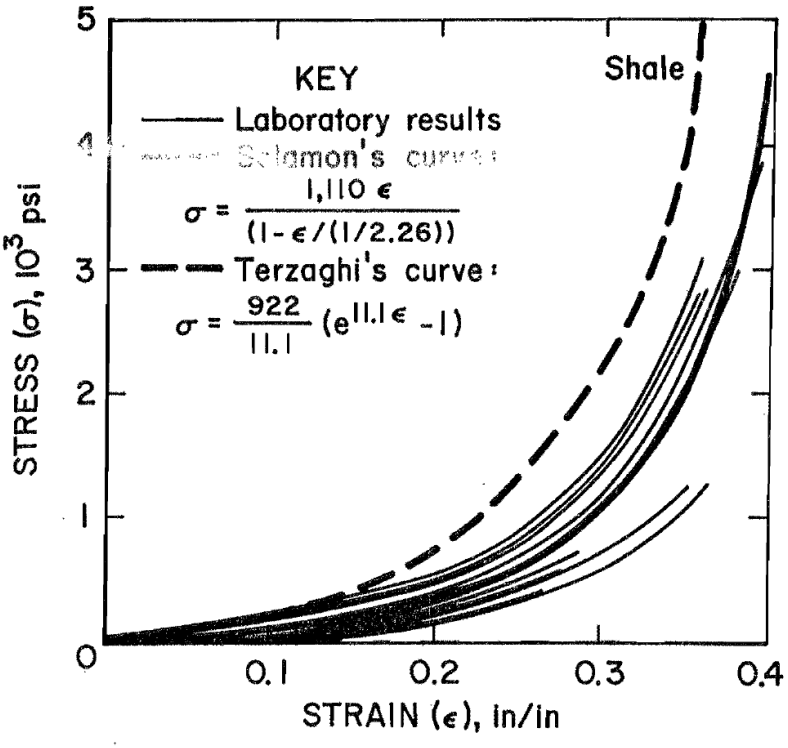


Figure 8 Gob stress – strain curves (after Pappas and Mark 1993).

Differentiating each model and evaluating at zero strain shows $E_o$ to be the initial modulus, that is, the modulus at zero strain. Inspection of (9), (10) and (11) shows the models are two parameter models. One of the parameters is obviously the initial modulus. The second parameter *b* allows for fitting to experimental test data. The three models using the same initial

modulus are compared in plots in Figure 9. The second fitting parameter was adjusted so each curve passed through the peak stress on the plot. Other fits to experimental data are certainly possible, for example, higher order polynomials as used by Pappas and Mark (1993). Model choice may be made on goodness of fit to test data but also on efficiency of use in numerical modeling. Generalization to three-dimensional stress – strain behavior may also be a consideration. Similarities between steeply dipping narrow vein cut and fill mining and nearly flat seam coal mining suggests use of the "fill" model.

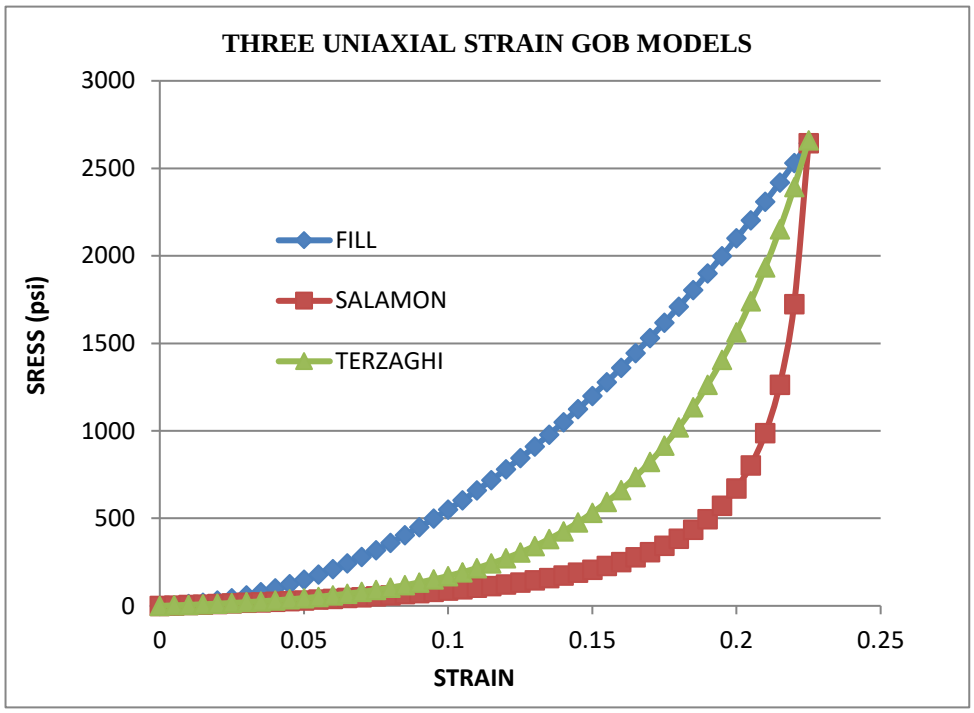


Figure 9 Three uniaxial strain gob models.

Figure 10 shows two other possible gob models in uniaxial strain. These models are EXP for "exponential" and ATANH for inverse hyperbolic tangent. Both use two parameters for fitting through a peak stress at a given strain. The EXP model is

(12) $\sigma = -b[\ln(1-\varepsilon/a)]$ or $\varepsilon = a(1-e^{-\sigma/b})$

The initial tangent modulus $E = b/a$. The ATANH model is

(13) $\sigma = a\tanh^{-1}(\varepsilon/b)$

The initial tangent modulus $E_o = 1/b$. In both models, *a* and *b* are different fitting parameters.

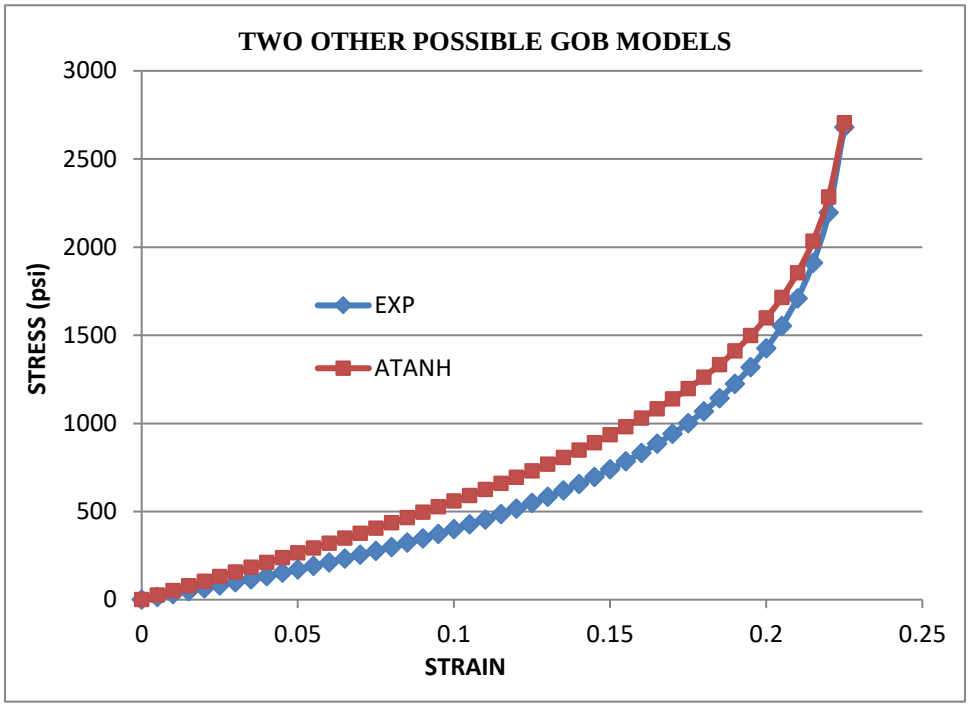


Figure 10 Two other possible gob models.

A simple finite element gob model involves replacing excavated air elements with gob elements, that is, reassigning excavated elements properties from air properties to gob properties. The gob model thus adds another material type to the list of strata types and material properties in a material properties input data file. In consideration of mining heights, gravity loading of gob would be small. For example, a 3m (10 ft) thick gob would experience an average gravity force of just 33 kPa (5 psi). For this reason gob weight may be neglected. Only contact forces with roof and floor then load the gob.

The switch to new gob elements occurs at the beginning of a run before the first load step is applied. The associated excavation forces do not differ noticeably from those associated with air elements because of the very low elastic modulus and hence element stiffness of gob in comparison with air element stiffness. As subsequent load increments are applied, compression of the gob is expected. In response, stiffness of the gob increases as do gob stress and strain in non-linear fashion according to the gob model.

An interesting alternative to taking effects of gob compaction into account during a finite element analysis is to use truss bar elements between roof and floor in the mined seam. Truss bar elements are one-dimensional and can be easily made non-linear so as to follow a one-dimensional plot. Such elements are installed at the beginning of an excavation step and subsequently updated with application of successive load steps. The effect on seam closure and adjacent entries, crosscuts and pillars, and the face would be much the same as with gob elements. However, this supposition remains to be demonstrated and is not pursued.

An important detail in any case is the need to distinguish between elements excavated behind the face and those excavated in headgate and tailgate entries and crosscuts. One approach to accomplishing this task is to do a separate panel development run before advancing the face. Ordinarily, a first run is done to initialize a prepanel mining stress state that is followed by a development run. Panel mining is done following the development run in a sequence of runs. Thus, the distinction between elements excavated before panel mining and during panel mining is almost automatic in the course of a panel mining study.

Another approach is to simply convert gob elements to excavated or air elements when gob effects are not desired. This model was inspired by successful finite element modeling of cut and fill hardrock mining (Pariseau, McDonald and Hill 1973). In coal mining "filling" is "stowing". This model approach is the one implemented in UT3PC. The material model is expressed by (5) and is implemented in incremental fashion thus taking non-linearity into account when gob effects are desired. The elastic range is limited by strength, of course[3]. The strength model is the same model used for all materials in an analysis. Another detail that is overlooked in all the gob models discussed is what to do if a tensile stress occurs. In the gob model used in UT3PC, the occurrence of a tensile stress in the axial direction (anti-parallel to vertical compression) induces assignment of the initial, no strain Young's modulus *a* in (5). Any tensile strain in a gob element is also limited by a very small but non-zero tensile strength.

Gob model parameters may be changed at the discretion of the user during a program run. The standard model specifies the parameters *a* and *b* in the model $\sigma = a\varepsilon + b\varepsilon^2$ as 1,000 psi and 10,000 psi, respectively. Figure 10 shows the model curve (vertical stress as a function of vertical strain) and also stiffer and more compliant model curves.

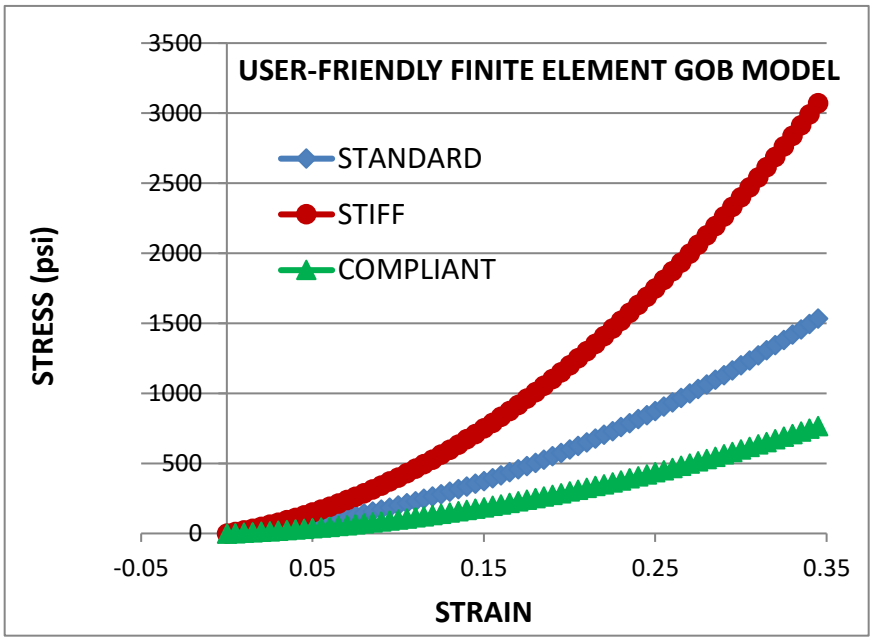


Figure 10 Gob model variations with *a*=1000, 2000 and 500 psi, b=10000, 20000 and 5000 psi.

[3] A very high strength is used. The gob then continues on a non-linear compaction path without entering the elastic-plastic domain. Computational experience indicates this procedure avoids potential ill-conditioing from a large number of gob element failures.

## References – Gob Models


Badr, S., A. Schissler, M. Salamon and U. Ozbay. 2002. Numerical Modeling of Yielding Chain Pillars in Longwall Mines. *Proc.5th North American Rock Mechanics Symp. and the Tunneling Association of Canada Conference.* University of Toronto, Toronto, Canada, pp 99-106.

Obert, L. and W. I. Duvall. 1967. *Rock Mechanics and the Design of Structures in Rock.* John Wiley & soncs, Inc., New York, pp 154-156.

Pappas, D. M. and C. Mark 1993. *Behavior of Simulated Longwall Gob Material*. U. S. Bureau of Mines Report of Investigations 9458.

Pariseau, W. G., M. M. McDonald and J. R. M. Hill. 1973. Support Performance Prediction for Hydraulic Fills. *Proc.Jubilee Symp. on Mine Filling.* Australasian Institute of Mining and Metallurgy. Victoria, pp 213-219.

Pariseau, W. G. 1975. Influence of Hydraulic Backfill on Closure and Pillar Stress in Narrow Cut and Fill Stopes. *Proc. 15th U.S. Symposium on Rock Mechanics.* AIME, New York, pp 23-33.

Pariseau, W. G. 1999. An Equivalent Plasticity Theory for Jointed Rock Masses. *Intl. J. Rock Mech. Mng. Sci.*, 36(7): 907-918.

Pariseau, W. G. 2017. *Design Analysis in Rock Mechanics 3rd Edition.* CRC Press, Taylor & Francis Group, London, pp 278-286.

Peng, S. S. 2006. *Longwall Mining* (2nd edition), Department of Mining Engineering, University of West Virginia. Morgantown, West Virginia.

Salamon, M. D. G. 1990. Mechanism of Caving in Longwall Coal Mining. *Proc.31st U.S. Symp. on Rock Mechanics.*

# APPENDIX –IV: MAIN ENTRIES

This appendix presents a second example of main entry analysis. Analysis procedure follows the same three step process as in the first example.

*Step 1 Preparation of a Materials Property File (Stratigraphic Column).* The material properties file for this problem is given in Figure 1. There are 12 formations in the stratigraphic column. The seventh formation is the ore horizon at a depth of 1499 ft.

```
NLYRS =12
NSEAM = 7
  (1) SHALE 1 N=2 (DP2) & spwts (pcf) dpth=m AVERAGES 5/30/2015, 2/2/22
  0.87e+06  0.87e+06  0.87e+06      0.22      0.22      0.22
  0.36e+06  0.36e+06  0.36e+06       0.0       0.0     144.0
    4922.0    4922.0   49220.0     520.0     520.0     520.0
     924.0     924.0     924.0
       0.0       0.0       0.0      62.0
  (2) MUDSTONE
  1.22e+06  1.22e+06  1.22e+06      0.20      0.20      0.20
  0.51e+06  0.51e+06  0.51e+06       0.0       0.0     134.0
    3580.0    3580.0    3580.0     497.0     497.0     497.0
     770.0     770.0     770.0
       0.0       0.0      62.0     148.0
  (3) SANDSTONE 1
  2.03e+06  2.03e+06  2.03e+06      0.23      0.23      0.23
  0.82e+06  0.82e+06  0.82e+06       0.0       0.0     140.0
    6317.0    6317.0    6317.0     480.0     480.0     480.0
    1005.0    1005.0    1005.0
       0.0       0.0     210.0     249.0
  (4) OIL SHALE 1
  0.82e+06  0.82e+06  0.82e+06      0.33      0.33      0.33
  0.31e+06  0.31e+06  0.31e+06       0.0       0.0     142.0
    5292.0    5292.0    5292.0     460.0     460.0     460.0
     908.0     908.0     908.0
       0.0       0.0     459.0     449.0
  (5) SANDSTONE 2
  1.22e+06  1.22e+06  1.22e+06      0.20      0.20      0.20
  0.51e+06  0.51e+06  0.51e+06       0.0       0.0     134.0
    6317.0    6317.0    6317.0     480.0     480.0     480.0
    1005.0    1005.0    1005.0
       0.0       0.0     988.0     171.0
  (6) SHALE 2
  0.87e+06  0.87e+06  0.87e+06      0.22      0.22      0.22
  0.36e+06  0.36e+06  0.36e+06       0.0       0.0     144.0
    5292.0    5292.0    5292.0     460.0     460.0     460.0
     908.0     908.0     908.0
       0.0       0.0    1079.0     420.0
  (7) TRONA 1
  4.08e+06  4.08e+06  4.08e+06      0.25      0.25      0.25
  1.63e+06  1.63e+06  1.63e+06       0.0       0.0     134.0
    6804.0    6804.0    6804.0     410.0     410.0     410.0
    1021.0       0.0    1021.0    1021.0
       0.0       0.0    1499.0      10.0
  (8) OIL SHALE 2
  0.82e+06  0.82e+06  0.82e+06      0.33      0.33      0.33
  0.31e+06  0.31e+06  0.31e+06       0.0       0.0     142.0
```

```
  5292.0    5292.0    5292.0     460.0     460.0     460.0
   908.0     908.0     908.0
     0.0       0.0    1509.0      89.0
(9) TRONA 2
4.08e+06  4.08e+06  4.08e+06      0.25      0.25      0.25
1.63e+06  1.63e+06  1.63e+06       0.0       0.0     134.0
  6804.0    6804.0    6804.0     410.0     410.0     410.0
  1021.0    1021.0    1021.0
     0.0       0.0    1598.0      10.0
(10) SHALE 3
0.87e+06  0.87e+06  0.87e+06      0.22      0.22      0.22
0.36e+06  0.36e+06  0.36e+06       0.0       0.0     144.0
  5292.0    5292.0    5292.0     460.0     460.0     460.0
   908.0     908.0     908.0
     0.0       0.0    1608.0    190.0
(11) SANDSTONE 3
2.03e+06  2.03e+06  2.03e+06      0.23      0.23      0.23
0.82e+06  0.82e+06  0.82e+06       0.0       0.0     140.0
  6317.0    6317.0    6317.0     480.0     480.0     480.0
  1005.0    1005.0    1005.0
     0.0       0.0    1798.0      49.0
(12) TIPTON FM
0.87e+06  0.87e+06  0.87e+06      0.22      0.22      0.22
0.36e+06  0.36e+06  0.36e+06       0.0       0.0     144.0
  5292.0    5292.0    5292.0     460.0     460.0     460.0
   908.0     908.0     908.0
     0.0       0.0    1807.0   3313.0
```

Figure 1 Material properties file for Example 2 involving main entries.

*Step 2 Mesh Generation.* Mesh generation input is:

| | |
|---|---|
| 1) the name of the material properties (stratigraphic column) file | *matsSLVft.txt* |
| 2) the number of main entries (NMS), | 7 |
| 3) entry and crosscut widths (WE, WC) | 15 15 (ft) |
| 4) pillar width and length (WP, LP) | 65 76 (ft) |
| 5) element width, length, height (EX, EY, EZ) | 3 3 2 (ft) |
| 6) add-in additional stresses Sxx, Syy, Szz, Tyz, Tzx, Txy? | N or n (no). |

There are seven main entries in this example, but symmetry allows for consideration of just one half of the main entry set. There are 1,370,736 elements and 1,467,984 nodes in the mesh. Elements are approximately 2.5 x 2.5 ft in lateral extent and about 3.0 ft in height. Figure 2 shows the mesh in plan view and vertical section where black=trona and grey=excavated elements (entries and crosscuts).

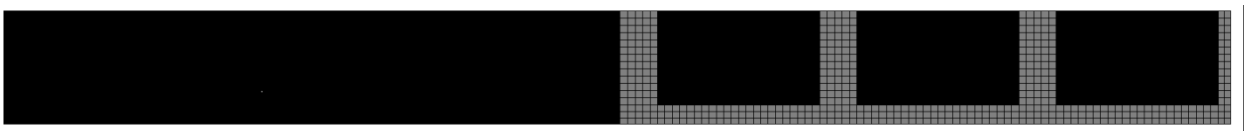

(a) Plan View

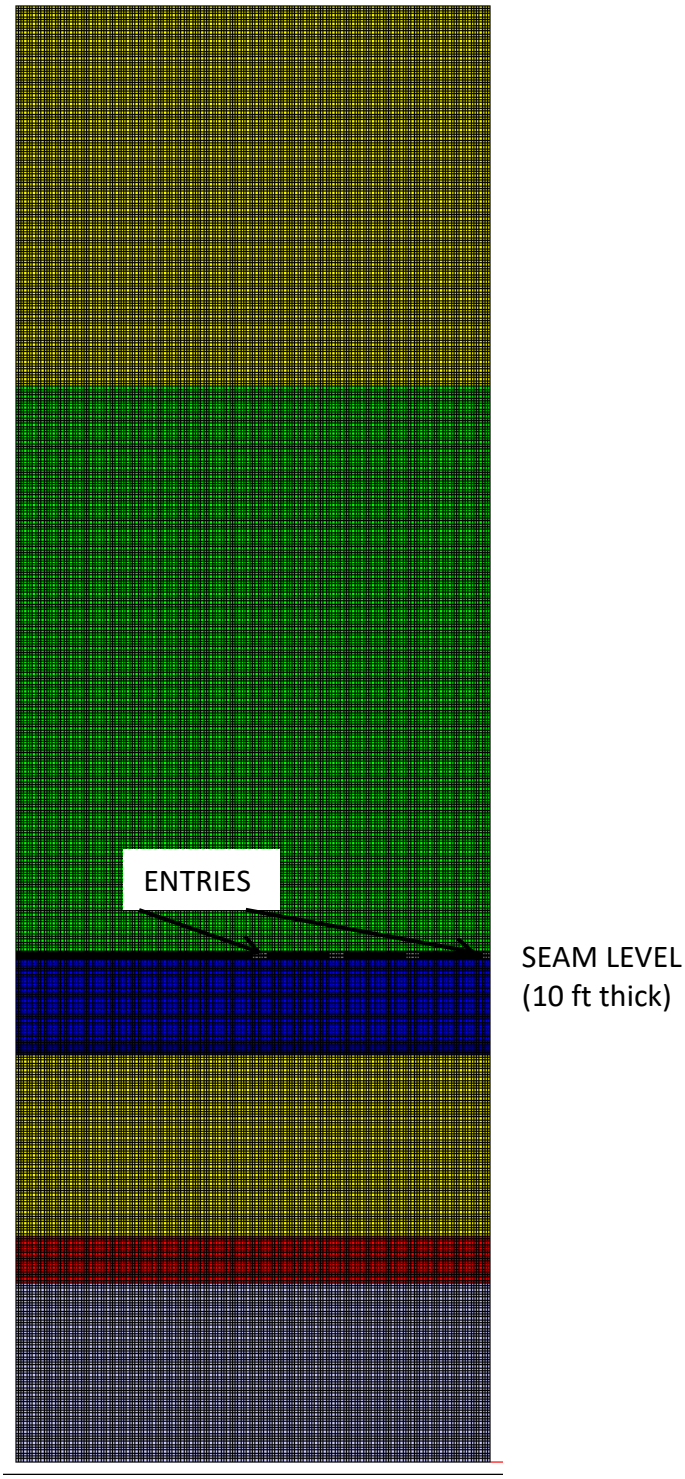


(b) Vertical Section

Figure 2 Mains mesh in plan view and vertical section.

*Step 3 FEM Execution and Results*. Results in the form of element safety factor distributions are shown in Figure 3. These results indicate a safe set of main entries, pillars and crosscuts.

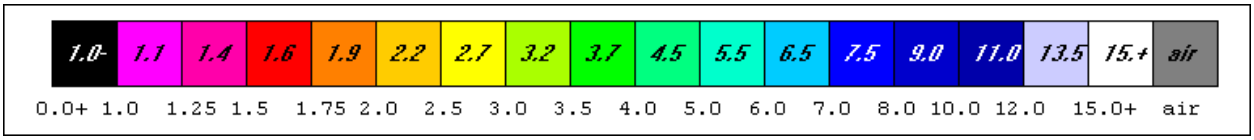


Safety Factor Color Scale

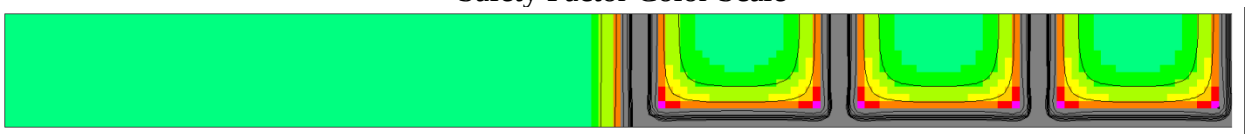

(a) Plan View

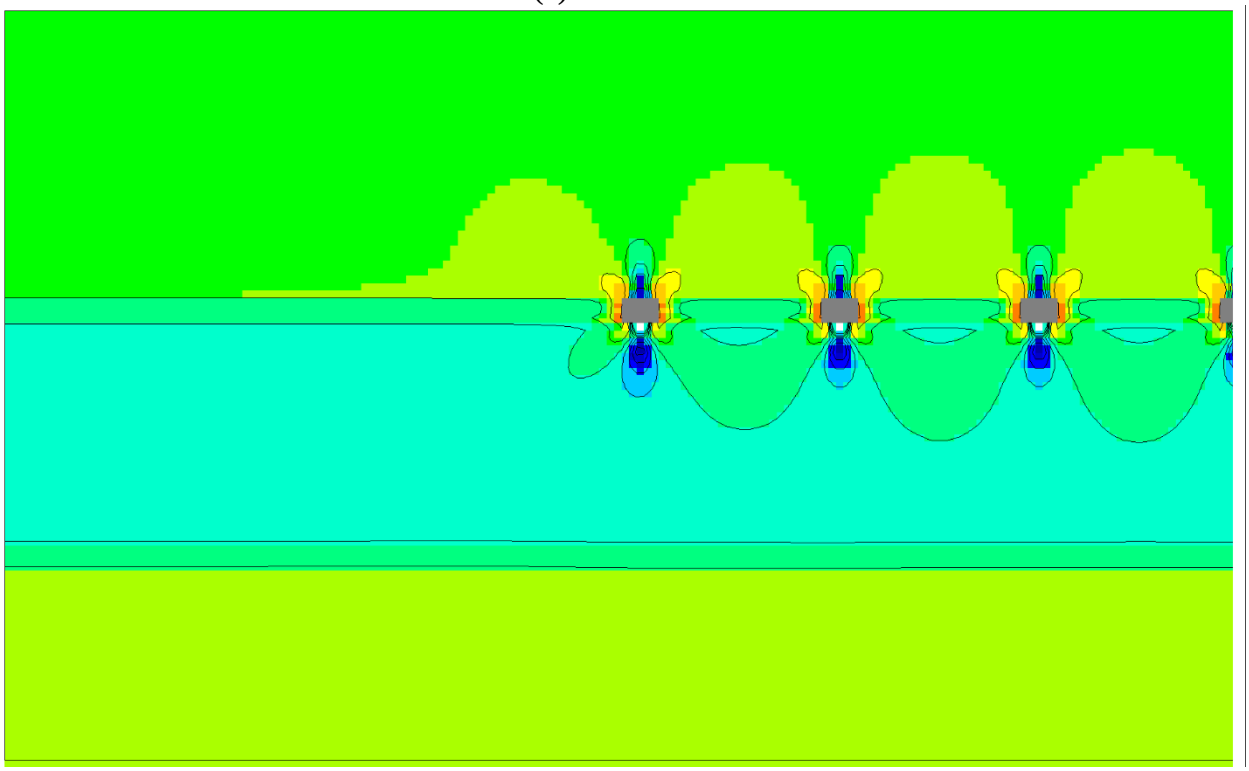

(b) Vertical Section Window

Figure 3 Element safety factor distributions in plan view (a) and vertical section close-up(b). Note: The black lines in (a) are closely spaced contour lines.

Results in Figure 3 indicates safe roof and floor of entries and crosscuts and safe pillars in between.

# APPENDIX V INTERPANEL BARRIER PILLARS

This appendix presents a second example of interpanel barrier pillar protection of panel entries and pillars. Analysis procedure follows the same three step process as in the first example.

**Example 2** This example is from a trona mine in southwest Wyoming.

*Step 1 Preparation of a Materials Property File (Stratigraphic Column).* The material properties file for this problem is given in Figure 1. There are 12 formations in the stratigraphic column. The seventh formation is the ore horizon at a depth of 1499 ft.

```
NLYRS =12
NSEAM = 7
  (1) SHALE 1 N=2 (DP2) & spwts (pcf) dpth=m AVERAGES 5/30/2015,SOLVAY
  0.87e+06  0.87e+06  0.87e+06      0.22      0.22      0.22
  0.36e+06  0.36e+06  0.36e+06       0.0       0.0     144.0
    4922.0    4922.0   49220.0     520.0     520.0     520.0
     924.0     924.0     924.0
       0.0       0.0       0.0      62.0
  (2) MUDSTONE
  1.22e+06  1.22e+06  1.22e+06      0.20      0.20      0.20
  0.51e+06  0.51e+06  0.51e+06       0.0       0.0     134.0
    3580.0    3580.0    3580.0     497.0     497.0     497.0
     770.0     770.0     770.0
       0.0        0.0      62.0     148.0
  (3) SANDSTONE 1
  2.03e+06  2.03e+06  2.03e+06      0.23      0.23      0.23
  0.82e+06  0.82e+06  0.82e+06       0.0       0.0     140.0
    6317.0    6317.0    6317.0     480.0     480.0     480.0
    1005.0    1005.0    1005.0
       0.0       0.0     210.0     249.0
  (4) OIL SHALE 1
  0.82e+06  0.82e+06  0.82e+06      0.33      0.33      0.33
  0.31e+06  0.31e+06  0.31e+06       0.0       0.0     142.0
    5292.0    5292.0    5292.0     460.0     460.0     460.0
     908.0     908.0     908.0
       0.0       0.0     459.0     449.0
  (5) SANDSTONE 2
  1.22e+06  1.22e+06  1.22e+06      0.20      0.20      0.20
  0.51e+06  0.51e+06  0.51e+06       0.0       0.0     134.0
    6317.0    6317.0    6317.0     480.0     480.0     480.0
    1005.0    1005.0    1005.0
       0.0       0.0     908.0     171.0
  (6) SHALE 2
  0.87e+06  0.87e+06  0.87e+06      0.22      0.22      0.22
  0.36e+06  0.36e+06  0.36e+06       0.0       0.0     144.0
    5292.0    5292.0    5292.0     460.0     460.0     460.0
     908.0     908.0     908.0
       0.0       0.0    1079.0     420.0
  (7) TRONA 1
  4.08e+06  4.08e+06  4.08e+06      0.25      0.25      0.25
  1.63e+06  1.63e+06  1.63e+06       0.0       0.0     134.0
    6804.0    6804.0    6804.0     410.0     410.0     410.0
    1021.0    1021.0    1021.0
```

```
     0.0       0.0    1499.0      10.0
(8) OIL SHALE 2
0.82e+06  0.82e+06  0.82e+06      0.33      0.33      0.33
0.31e+06  0.31e+06  0.31e+06       0.0       0.0     142.0
  5292.0    5292.0    5292.0     460.0     460.0     460.0
   908.0     908.0     908.0
     0.0       0.0     1509.0      89.0
(9) TRONA 2
4.08e+06  4.08e+06  4.08e+06      0.25      0.25      0.25
1.63e+06  1.63e+06  1.63e+06       0.0       0.0     134.0
  6804.0    6804.0    6804.0     410.0     410.0     410.0
  1021.0    1021.0    1021.0
     0.0       0.0    1598.0      10.0
(10) SHALE 3
0.87e+06  0.87e+06  0.87e+06      0.22      0.22      0.22
0.36e+06  0.36e+06  0.36e+06       0.0       0.0     144.0
  5292.0    5292.0    5292.0     460.0     460.0     460.0
   908.0     908.0     908.0
     0.0       0.0    1608.0    190.0
(11) SANDSTONE 3
2.03e+06  2.03e+06  2.03e+06      0.23      0.23      0.23
0.82e+06  0.82e+06  0.82e+06       0.0       0.0     140.0
  6317.0    6317.0    6317.0     480.0     480.0     480.0
  1005.0    1005.0    1005.0
     0.0       0.0    1798.0      49.0
(12) TIPTON FM
0.87e+06  0.87e+06  0.87e+06      0.22      0.22      0.22
0.36e+06  0.36e+06  0.36e+06       0.0       0.0     144.0
  5292.0    5292.0    5292.0     460.0     460.0     460.0
   908.0     908.0     908.0
     0.0       0.0    1807.0   3313.0
```

Figure 1 Material properties file for Example 2 involving main entries.

*Step 2 Mesh Generation* Mesh generation input is

| | |
|---|---|
| 1) name of the material properties (stratigraphic column) file | *matsSLVft.txt* |
| 2) number of panel entries (NES), | 3 |
| 3) entry and crosscut widths (WE, WC) | 20 20 (ft) |
| 4) pillar width and length (WP, LP) | 40 80 (ft) |
| 5) barrier pillar width | 300 (ft) |
| 6) longwall panel width | 750 (ft) |
| 7) element width, length, height (EX, EY, EZ) | 4 4 4 (ft) |
| 8) do gob effect? | Y or y=yes or Nor n=no |
| 9) add-in additional stresses Sxx, Syy, Szz, Tyz, Tzx, Txy? | Y or y=yes or Nor n=no |

Figure 2 shows a plan view of the mesh and Figure 3 shows a vertical cross section of the mesh used in this analysis. A three-entry system is used for panel development.

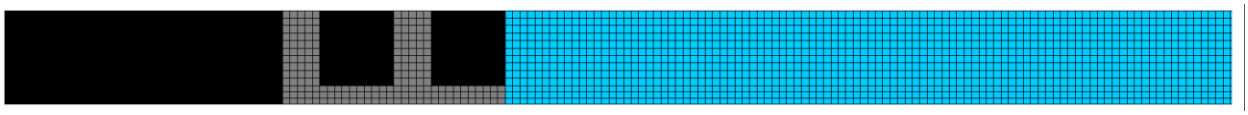

Figure 2 Plan view of interpanel barrier pillar mesh at seam level, black = trona, grey = entries and crosscuts, blue=longwall panel elements which may be air or gob as a matter of choice during program execution  Entries are 20 ft (6 m) wide.

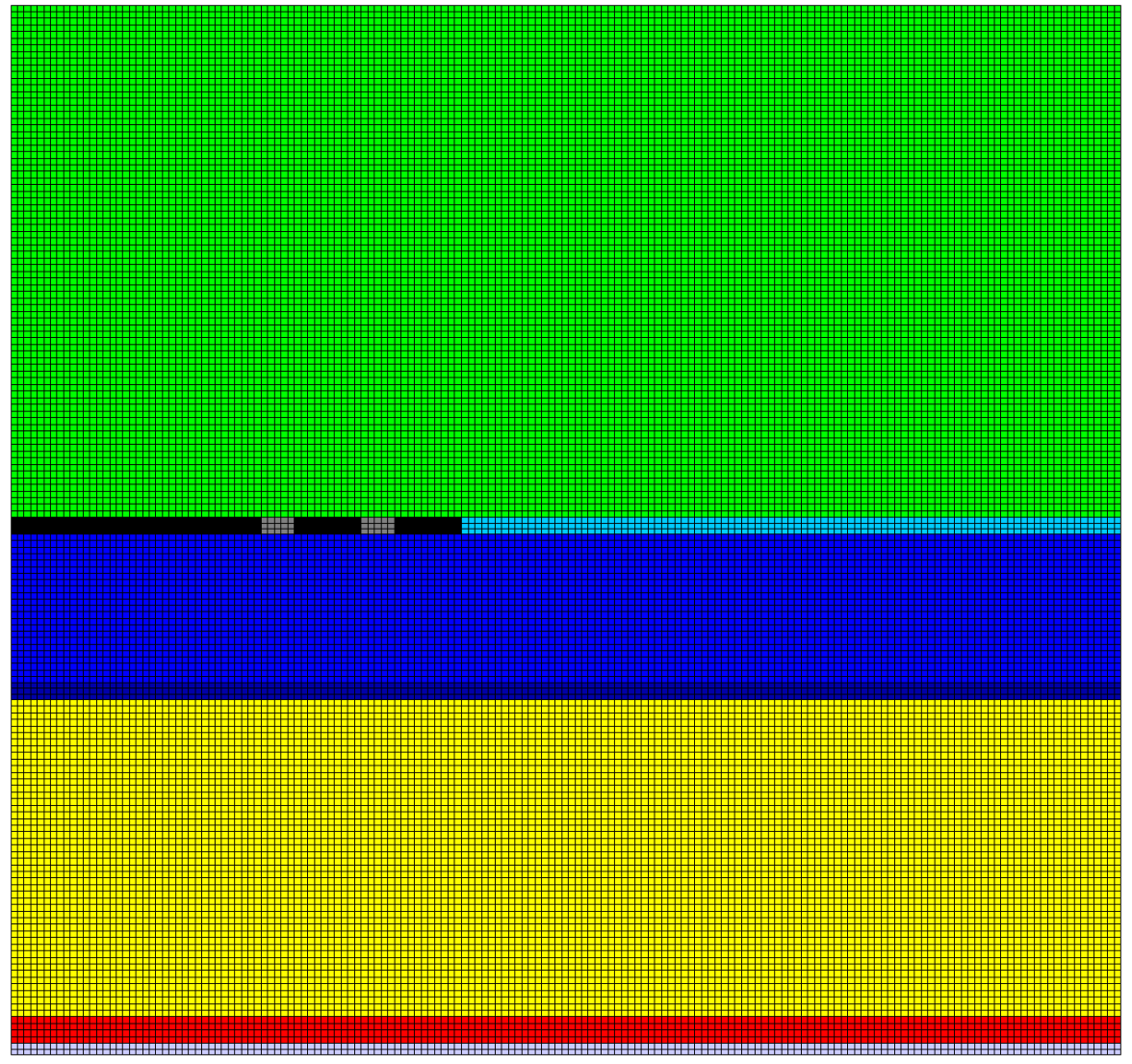

Figure 3 Vertical section of interpanel barrier pillar mesh.  Seam is 10 ft (3 m) thick.

*Step 3 FEM Execution and Results* Run time for this mesh was just under four hours.  Vertical section views of the distribution of element safety factors are shown in Figure 4 in two cases: (a) without gob effect and (b) with gob effect.  Element boundaries are not shown for clarity.

The plan view in Figure 5 indicates yielding entry pillar ribs and pillar cores with low safety factors (*fs*<1.3). Indeed, the pillar adjacent to the longwall panel is yielding to the core. Entry ribs also show some yielding. Note: standard gob, compliant go b and stiff gob are defined in APPENDIX III (see Figure 10).

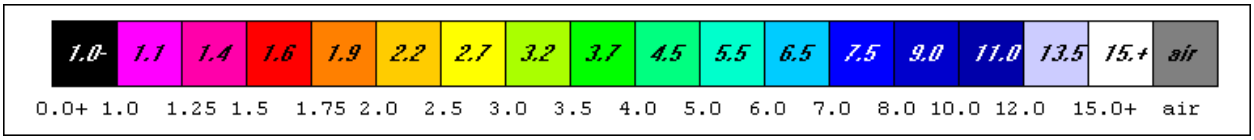


Safety Factor Color Scale

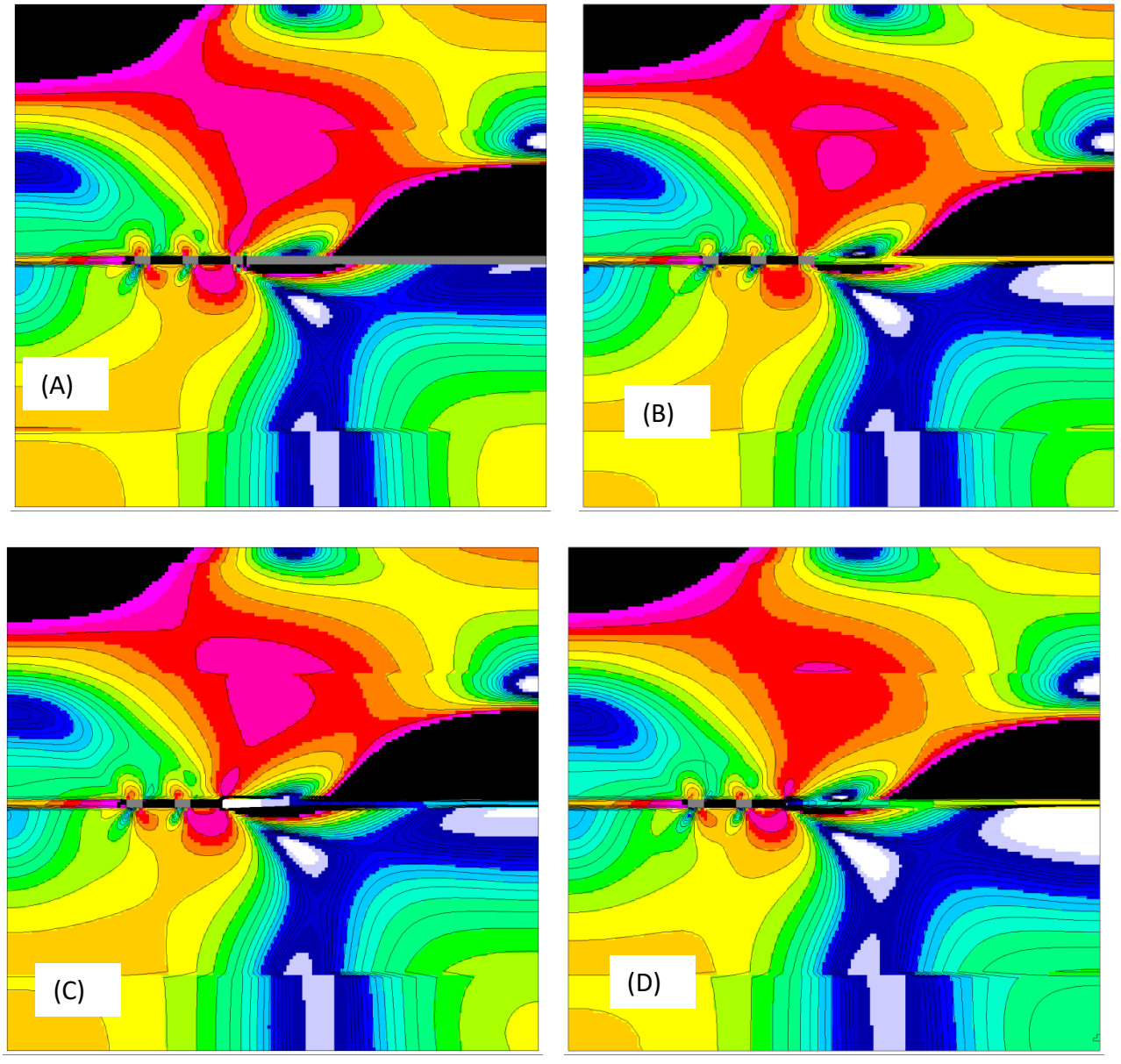


Figure 4 Vertical section: interpanel barrier pillar (left), panel entries (3), longwall panel (right) showing element safety factor distributions. (A) no gob, (B) standard gob, (C) compliant gob, (D) stiff gob. The red and pink area shows an effect.

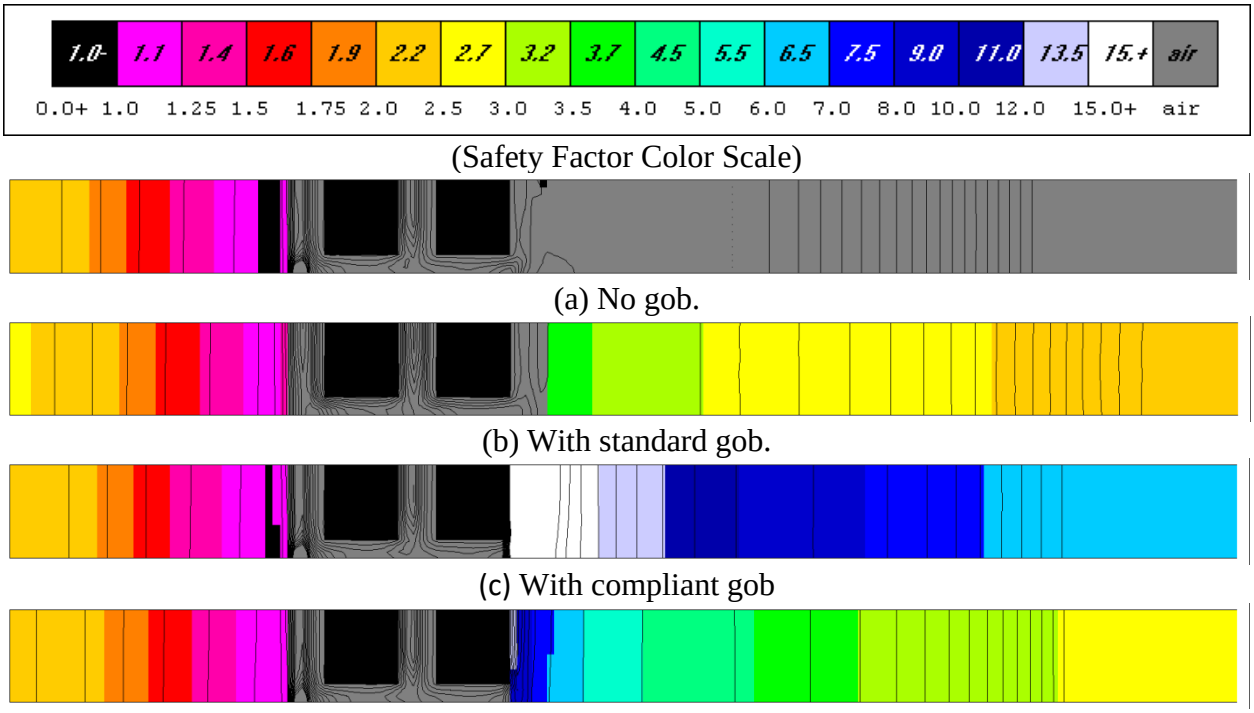


(Safety Factor Color Scale)

(a) No gob.

(b) With standard gob.

(c) With compliant gob

(d) With stiff gob

Figure 5 Plan views of element safety factor distributions at seam level in case of interpanel barrier pillar analysis. The compliant gob shows higher safety factors than the standard gob because greater seam closure is necessary to obtain similar stresses. Comment: gob reduces stress in ribs of the entries.

## APPENDIX VI MESH PLOTTING

Mesh plotting is enabled by a program GPL3. Input to this program is a file PlotMesh which is generated during mesh generation along with the files InData and RunStrm. Figure 1 is an example of a PlotMesh file. Information in italics to the right side is not part of the plot file but is merely explanatory. The output plot file (AMSH) can be viewed in programs such as Paint where a save as a png file will allow for copying and pasting into a report as desired.

```
PlotBleeders                    :file name indicating problem type
NLYRS =       5                 :number of layers in the mesh
NSEAM =       3                 :layer number of the mined stratum
Nelem = 1450440                 :number of elements in the mesh
Belms                           :name of file containing the elements
Nnode = 1546326                 :number of nodes in the mesh
Bcrds                           :name of file containing nodes
Nelcf =    1260                 :number of excavated or cut element
Brcte                           :name of file containing cut elements
AMSH                            :name of the file after plotting
```

Figure 1 An example PlotMesh file developed during mesh generation.

Execution of the plot program results in a screen request for a plot file "Enter the runstream file name PlotMesh". After entering PlotMesh, a list of plot choices will appear following screen printing of NLYRS and NSEAM (number of layers in the mesh, layer number of the mining stratum). Also printed are the number of elements and nodes (nelem, nnode). Coordinate minimums and maximums are printed, too. In this regard, x and y coordinates are horizontal. The z coordinate is vertical with z=0 at the bottom of the mined seam. Thus, mesh bottom is a negative number; mesh top is a positive number.

Following selection of the plot type, a new set of coordinate minimums and maximums will appear on the screen. The x and y minimums and maximums remain the same as in the first screen print. However, the origin of the z coordinate is now at the mesh bottom rather than the mining seam bottom.

During plotting there is an opportunity to zoom in on a portion of the plot. This opportunity is presented by a question "Do a window plot (Y/N)? Responding with Y (or y) brings up a request for window coordinate ranges for **x** and **y**. These coordinates are **screen coordinates** with origin in the lower left side of the screen; **x** is horizontal increasing to the right and **y** is vertical increasing towards the top of the screen. A screen plot is necessarily two-dimensional.

In cases of plot choices 4, 7, or 8, zmin, zmax, or z=0 (seam level view), respectively, the screen and mesh coordinates coincide. Thus, in these cases, setting a range to x (**x**) and allowing y (**y)** to be the value printed on the screen will zoom in on a segment of a plan view at the selection (4, 7 or 8)

Plot choices 2, 3, 5, 6 (xmin, ymin, xmax, ymax) are vertical sections, so **x**=x in cases of ymin and ymax (3 and 6) but **y=**z. Thus, the vertical screen coordinate **y** is now the vertical mesh coordinate z. In cases of xmin and xmax (2 and 5), **x**=y and again **y**=z.

In case of a three-dimensional choice of views (1 and 9) and a Y or y response, a set of screen coordinates will appear. This set of **x** and **y** coordinates gives guidance to a three-dimensional window.

As an example of mesh plotting, consider PlotMesh for a bleeder entry problem shown in Figure 1 and select 1 for a three-dimensional view. The result is shown in Figure 2 (1) where element boundaries are not shown to better view the strata where grey=excavated elements, black=coal, blue=gob. In Figure 2 (2) which is a xmin view, element boundaries are in white to reveal mesh refinement. This view is a cross-section relative to the longwall panel. Figure 2 (3) is a long section, a ymin view. Figure 2 (7) is a plan view at the floor of the mining stratum. Figure 2 (W) is a window plot of a ymax view using screen coordinates: **xmin**=700, **xmax**=1000, **ymin**=550, **ymax**=750. These dimensions were used only after two plots at values of **y** of (500,700) and (600, 800) with the same x values. The window plot allows one to visualize mesh refinement with ease. In this example, there are five elements through the seam which should give a reasonable distribution of stress at the pillar ribs. There are four elements across the entry which perhaps is somewhat coarse but still reasonable in consideration of the overall mesh size of more than one million elements and nodes.

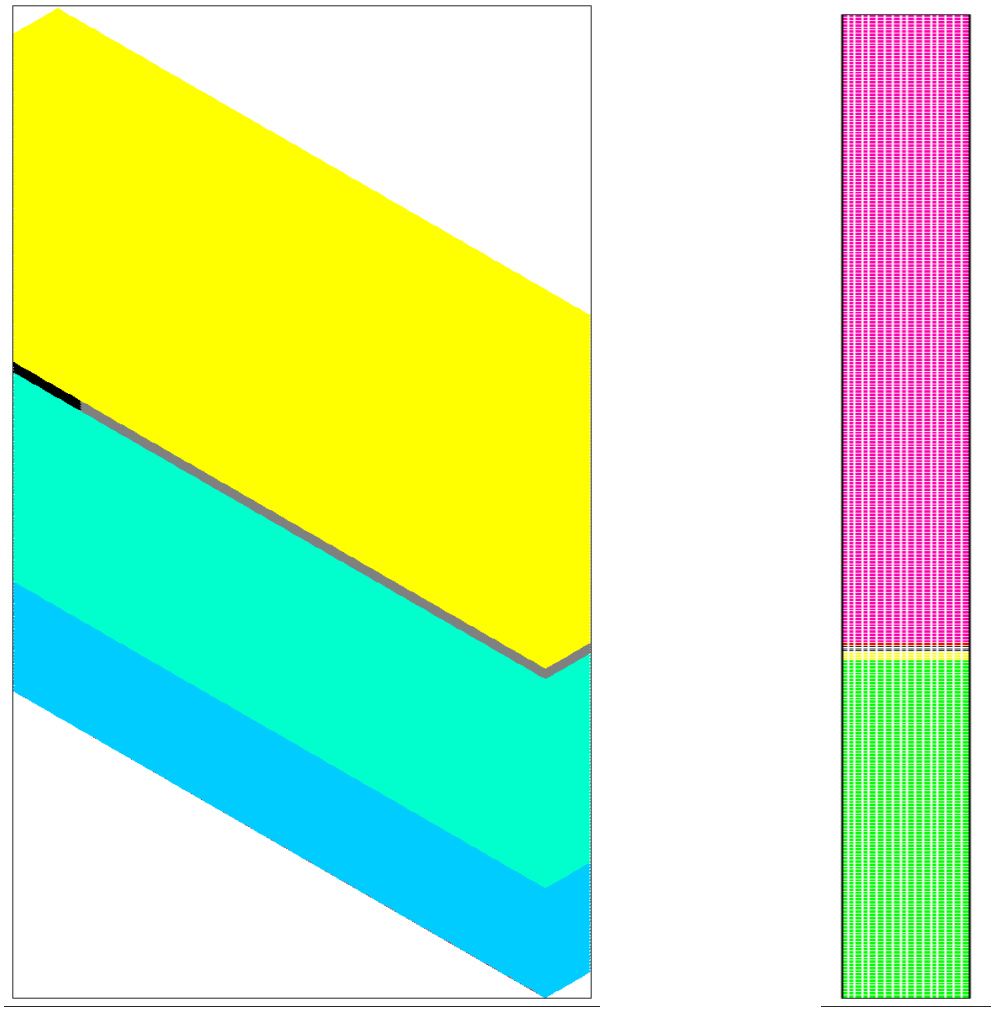

(1)…… ……..(2)

Figure 2 Plots of an interpanel barrier pillar mesh. (1) three-dimensional view. (2) ymin view plotted to a different scale than the three-dimensional view..

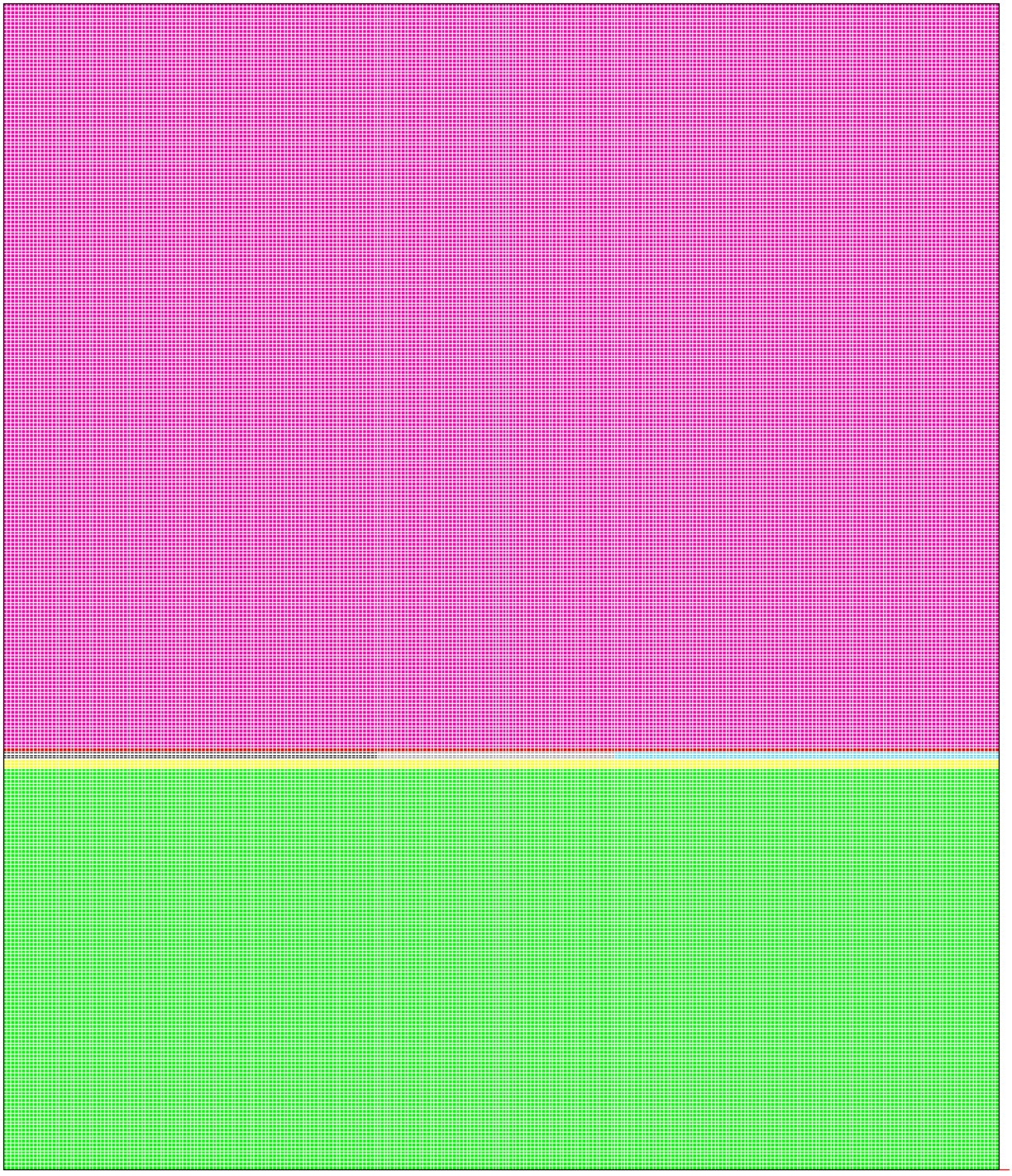

Figure 2 (3) A ymin view or long section

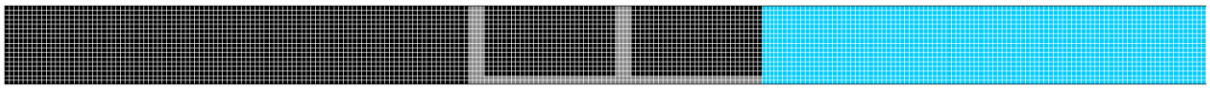

Figure 2 (7) A z=0 view at the floor of the mined stratum.

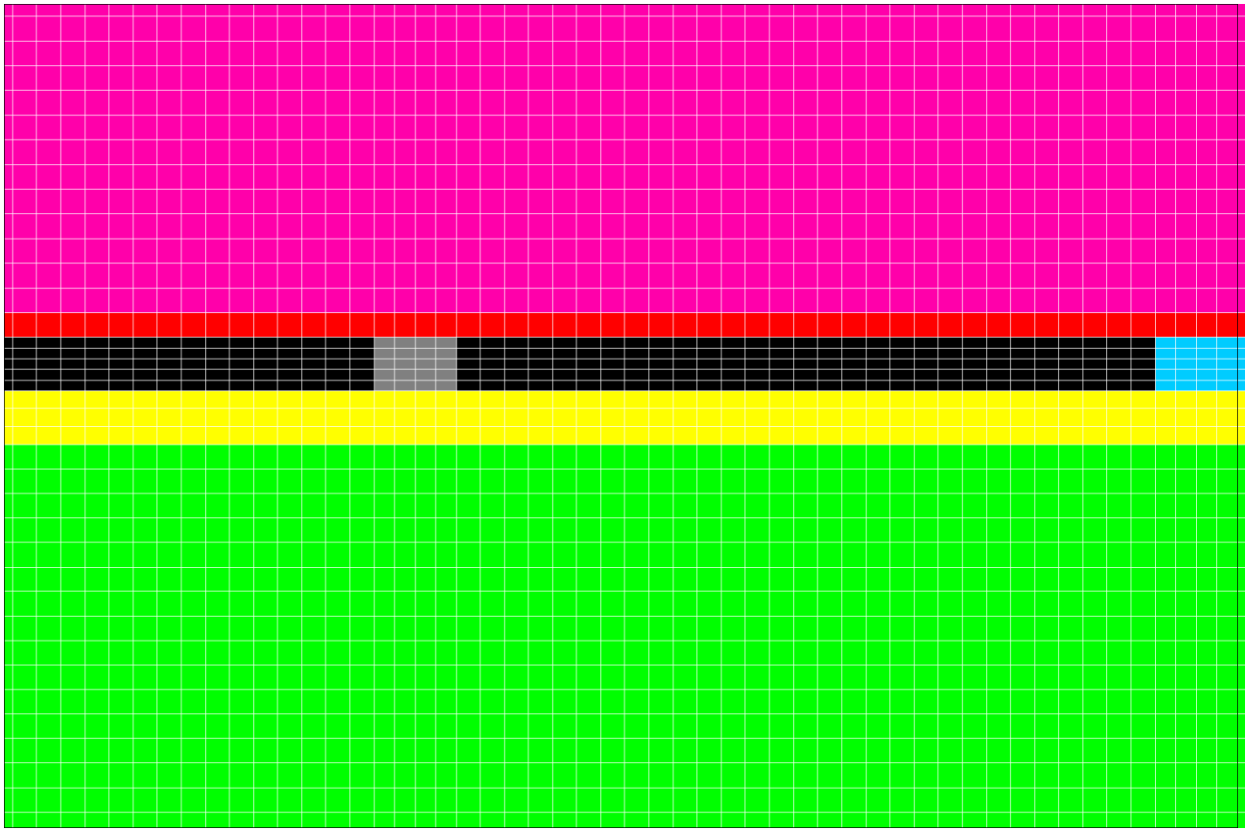

Figure 2 (W) A window plot near the bleeder entries in the ymax view.

As another example of mesh plotting, consider a room and pillar problem. The InData file from the mesh generator is shown in Figure 3 and the PlotMesh file is shown in Figure 4

```
Input Data
 PILLARS
 Width of entries, WE (ft)  =      30.0
 Width of crosscuts, WC (ft)=      25.0
 Width of pillars, WP (ft)  =      25.0
 Length of pillars, LP (ft) =      30.0
 Height of pillars, HP (ft) =      30.0
 EX, EY, EZ, (ft)=       2.0       2.0       2.0
 Additional Sxx,Syy,Szz,Tyz,Tzx,Txy, tension +=
       0.0       0.0       0.0       0.0       0.0       0.0
```

Figure 3 InData file for a room and pillar problem

```
PlotR&P
NLYRS =      15
NSEAM =      11
Nelem =  152325
belms
Nnode =  173568
bcrds
Nelcf =    2535
brcte
AMSH
```

Figure 4 PlotMesh file for a room and pillar problem.

Figure 3 (1) shows a three-dimensional view where again element boundaries are not shown to better view the strata and where grey=excavated elements, black=ore.

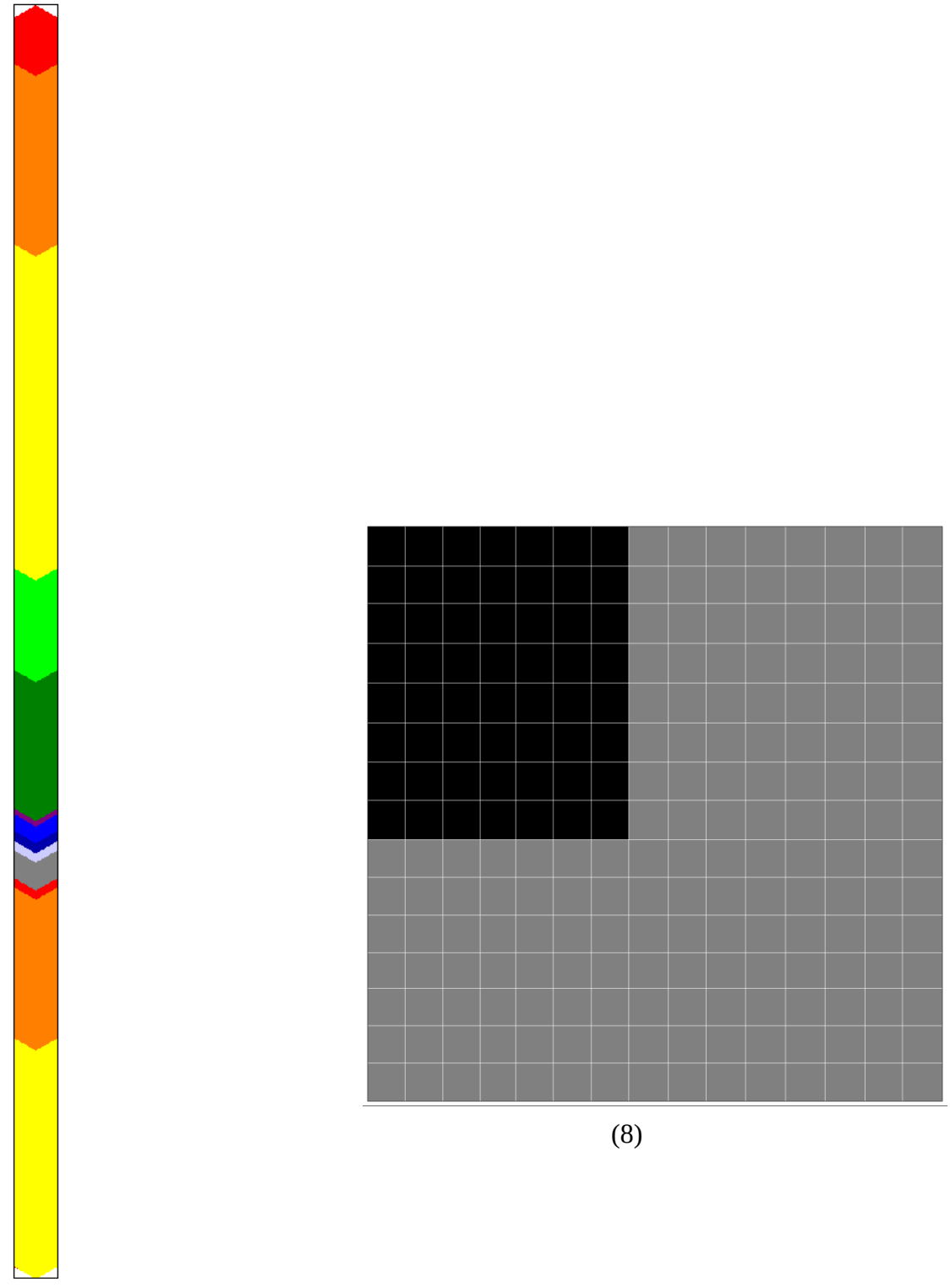

(8)

Figure 3 (1) Three-dimensional view of a room and pillar mesh plot. (8) Plan view at ore floor.

Figure 3 (6W) shows a window plot near the ore horizon and reveals details of the mesh near the rooms and pillars. The horizontal dimensions of mesh and screen are the same and span the interval (0,27.5). The vertical (z) mesh range at the plot run beginning is (-656, +1213). The screen plot dimensions for the window plot are **x (0, 27.5), y(550, 750)** for minimums and maximums. Again, black=ore, grey=excavated..

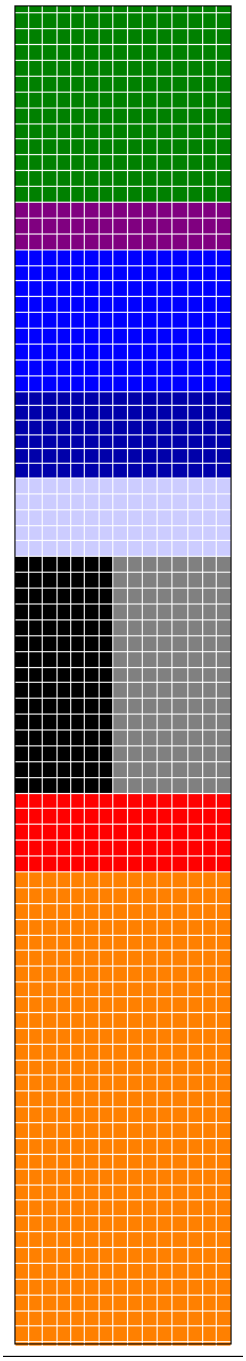

Figure 3 (6W) A window plot near the ore horizon and reveals details of the mesh near the rooms and pillars. The pillar is 30 ft high (black).

Figure 3 (9W) is a window plot of excavated elements and strata near the ore horizon in this room and pillar example using **x** (0, 47.6) and **y** (350, 520).

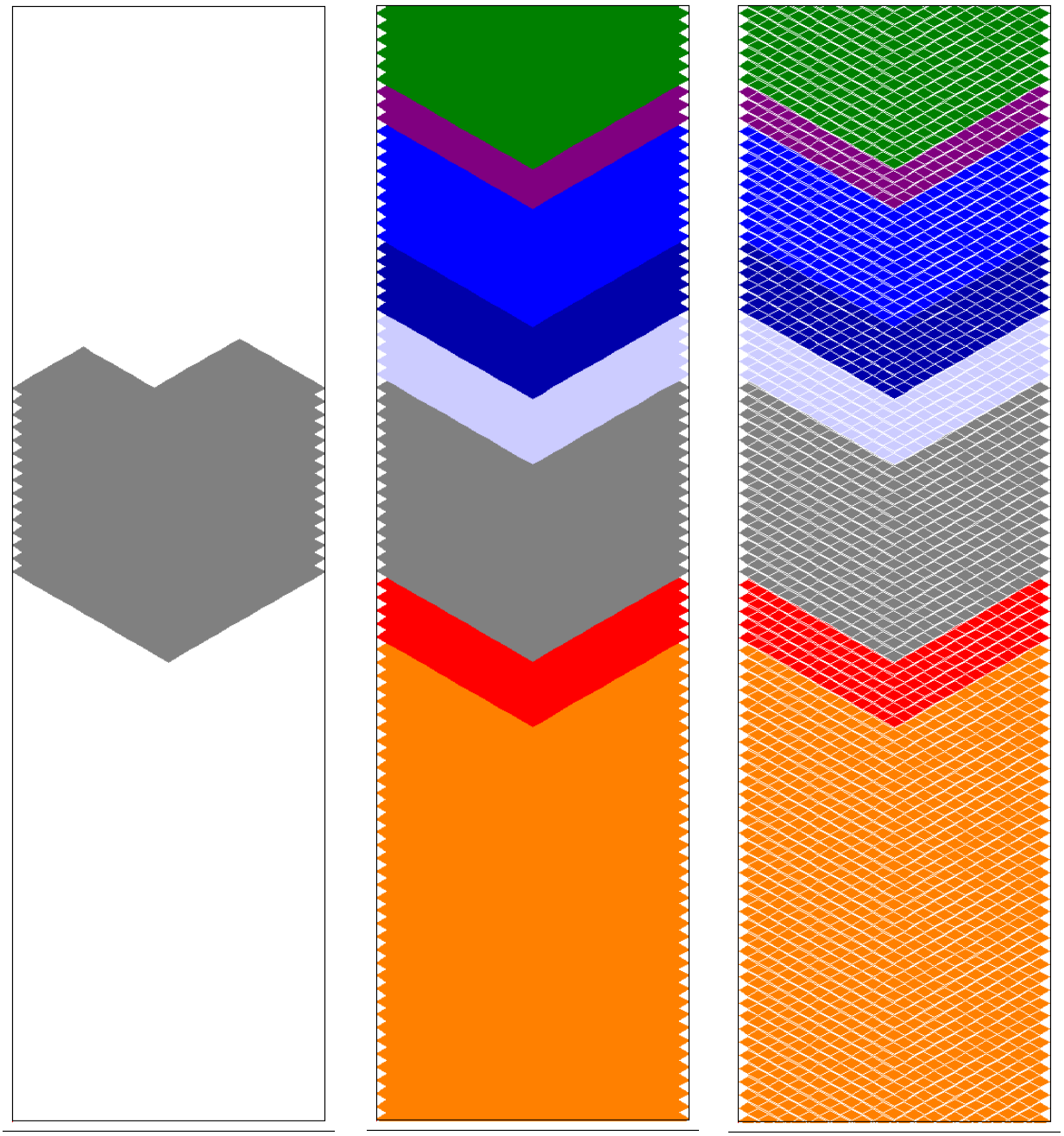

(a) (b) (c)

Figure 3 (9W) A three-dimensional perspective in a window plot: (a) excavated elements, (b) strata near ore, (c) strata near ore with element top and bottom faces in white in a room and pillar example problem.

## APPENDIX VII - MECHANICS OF JOINTED ROCK

This appendix describes theory and implementation of jointed rock elements in finite element analyses using UT3PC where joints are treated as ordinary but thin finite elements; these elements have a thickness specified on input. Dip direction, dip and spacing are also specified in an input file that in addition contains the usual properties, elastic moduli and strengths. Multiple joint sets with different properties are possible in each formation present in the geological column (Pariseau 2017). Examples illustrating the role of joints in each of seven problem types are given in APPENDIX VIII and in APPENDIX IX.

**Theory** Rock masses at the engineering scale are composite materials composed of joints and intact rock between joints. Properties of both may be determined by laboratory tests for intact rock elastic moduli and strengths and for joint stiffnesses and strengths, although the later are not done nearly as often as the former. However, even with the properties of intact rock and joints at hand, there remains the task of determining properties of the rock mass which depend on joint geometry as well. Of course, joint geometry may be determined by mapping to obtain joint spacing, dip and dip direction. The problem then is to determine the composite rock mass properties from the testing and mapping data. These properties are *equivalent* elastic moduli and strengths (Pariseau and Moon 1988, Pariseau 1995). In this regard, strengths limit the range of a purely elastic deformation; deformation beyond the elastic limit is elastic-plastic deformation (Pariseau 1999). Equivalent strengths must also be computed for the composite of rock and joints.

Equivalent properties are defined as properties that relate average stress to strain in a jointed and thus a heterogeneous finite element. Figure 1 is a schematic illustration of equivalent properties of a jointed rock element. There are two averages to consider; (1) averaging over an entire element which is a *global* average, and (2) averaging over a joint segment which is a *local* average. Influence functions relate global to local averages. For example, stress influence functions $[B_j]$ and $[B_r]$ for *joint* and *rock* portions of a jointed element are

$$\{\bar{\sigma}_j\} = [B_j] < \{\sigma\} > \text{ and } \{\bar{\sigma}_r\} = [B_r] < \{\sigma_r\} > \tag{1}$$

where $\{\bar{\sigma}_j\}$ and $< \{\sigma\} >$ are local and global avearages, respectively. Note: a matrix of averages is also an average of the matrix. Thus, $\{\bar{\sigma}\} = \overline{\{\sigma\}}$ and $< \{\sigma\} > = \{< \sigma >\}$. Preliminary definitions and relatioships are next, followed by details and examples.

Fundamentals that form the basis of the computation are the famous Hadamard[4] stability criteria required at an interface between different elastic materials. These criteria are essentially requirements for continuity of tractions and displacements as explained by Hudson (1980). If *z* is normal to the *xy* plane which is a tangent segment of an interface between two elastic materials, then the tractions, that is, stresses $\sigma_{zz}$, $\tau_{zy}, \tau_{zx}$ must be continuous at the interface.

[4] See e.g. Hadamard, J (1949) Lecons sur la Propagation des Ondes et les Equations de l'Hydrodynamique. Chelsea Publishing Company, New York. The original book was published in Paris in 1903.

Displacement normal to the interface must also be continuous to avoid separation or a physically impossible overlap of material. In conjunction with Hooke's law for elastic materials, the strains $\varepsilon_{xx}$, $\varepsilon_{yy}$, $\varepsilon_{xy}$ are required to be continuous at the interface. Additionally, an energy equivalence of equivalent properties is reasonable (Pariseau and Moon 1988). The same fundamentals apply to saturated fluid flow in jointed rock (Pariseau 1993). Further details of theory and application are given by Pariseau (1995) in the case where a finite element is of arbitrary size.

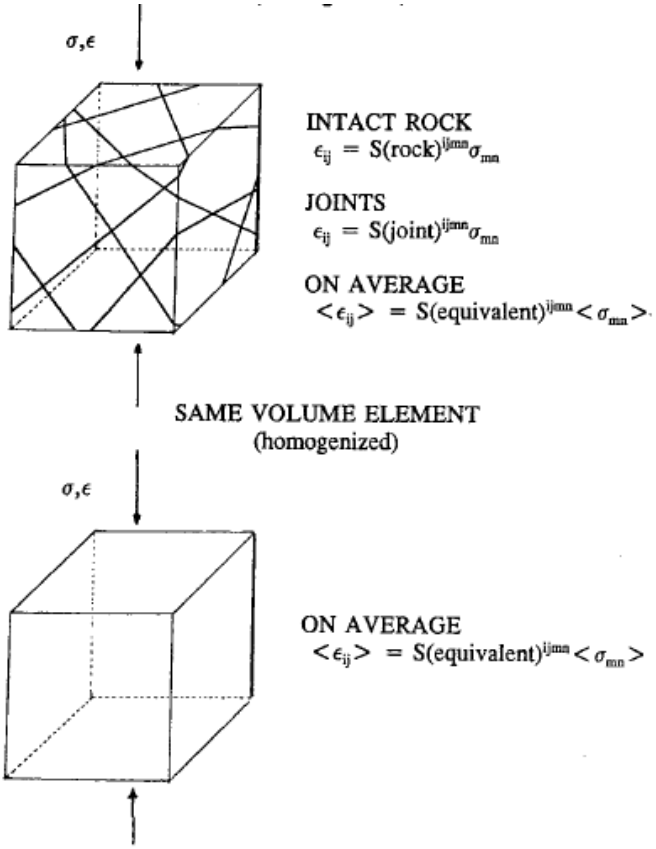


Figure 1 A schematic representation of generating equivalent rock properties in a sample cube. The angle brackets represent averaging (Pariseau 1999).

*Preliminaries* The composite rock mass properties include elastic properties and strength properties. Elastic properties relate average stress and strain in an element; strength properties define the limit to elasticity also based on average stress. Average is defined as a volume average. There are two volume averages to consider. One is over the composite volume and is indicated by angle brackets. Thus, symbolically

$$<\sigma>=(1/V)\int_V \sigma dV \text{ and } <\varepsilon>=(1/V)\int_V \varepsilon dV \qquad (2)$$

where $V$ is the composite element volume. The second is over a single material volume, rock or joint, in a composite volume and is indicated by an overbar. Examples are

$$\{\bar{\sigma}_r\} = (1/V_r)\int_{Vr}\{\sigma\}dV \text{ and } \{\bar{\varepsilon}_j\} = (1/V_j)\int_{Vj}\{\varepsilon\}dV \tag{3}$$

where the subscript *j* indicates joint and *r* indicates rock.

Stress and strain may be expressed as an average plus a deviation from an average. Thus

$$\begin{aligned}\{\sigma\} &= <\{\sigma\}> + \Delta\{\sigma\} \text{ and } \{\sigma\} = \{\bar{\sigma}\} > + \delta\{\sigma\} \\ \{\varepsilon\} &= <\{\varepsilon\}> + \Delta\{\varepsilon\} \text{ and } \{\varepsilon\} = \{\bar{\varepsilon}\} + \delta\{\varepsilon\}\end{aligned} \tag{4a,b}$$

where $\Delta$ and $\delta$ indicate deviations from global and local averages, respectively. Note:

$$\Delta\{\sigma\} = \{\Delta\sigma\} \text{ and } \delta\{\sigma\} = \{\delta\sigma\} \tag{5a}$$

Similar relationships hold for strains. Also note that from (4a)

$$<\{\sigma\}> = <\{\sigma\}> + <\{\Delta\sigma\}> \text{ and } \{\bar{\sigma}\} = \{\bar{\sigma}\} > + \overline{\{\delta\sigma\}} \tag{5b}$$

Hence, averages of deviations must satisfy

$$<\{\Delta\sigma\}> = 0 \text{ and } \overline{\{\delta\sigma\}} = 0 \tag{5c}$$

Similar relations hold for strains. Local averaging of (4a,b) leads to

$$\begin{aligned}\{\bar{\sigma}\} &= <\{\sigma\}> + \overline{\{\Delta\sigma\}}, \quad \{\bar{\varepsilon}\} = <\{\varepsilon\}> + \overline{\{\Delta\varepsilon\}} \\ \{\Delta\sigma\} &= \overline{\{\Delta\sigma\}} + \{\delta\sigma\}, \quad \{\Delta\varepsilon\} = \overline{\{\Delta\varepsilon\}} + \{\delta\varepsilon\}\end{aligned} \tag{6}$$

where averages are constants and remain unchanged with further averaging.

Hooke's law for the composite is by definition

$$\{<\sigma>\} = [S^*]\{<\varepsilon>\}, \quad \{<\varepsilon>\} = [C^*]\{<\sigma>\} \tag{7}$$

where the star * indicates equivalent properties; the curly brackets {} are 6x1 column matrices and the square brackets [ ] are 6x6 matrices. The problem at hand is to compute the compliance and stiffness matrices $[S^*]$ and $[C^*]$ and associated strengths.

The approach to the problem considers a jointed rock mass as a composite material. First consider a sample cube containing just one joint as shown schematically in Figure 2. The joint is a thin layer of material that is in secure contact with adjacent rock; slip and separation are not allowed under load. The sample cube is clearly a two-material composite.

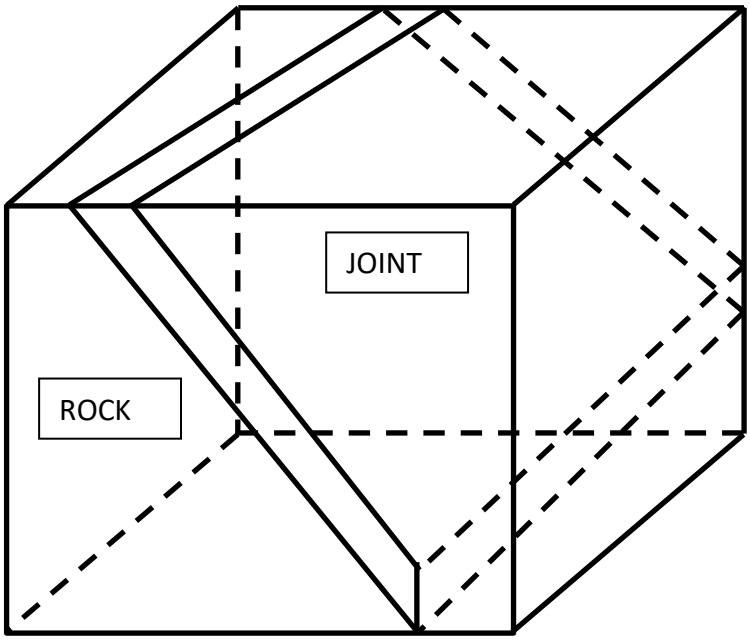


Figure 2 A sample cube containing a joint making a two-material composite.

Both materials are linearly elastic and thus have stresses and strains related through generalized Hooke's law. Hence,

$$\{\sigma\}=[C]\{\varepsilon\},\ \{\varepsilon\}=[S]\{\sigma\} \tag{8}$$

where $\{\sigma\},\{\varepsilon\},[C],$ and $[S]$ are 6x1 colum matrix of stress and strain, and 6x6 matrices of elastic moduli and compliances, respectively. The elastic moduli and compliances are mutual inverses: $[C]^{-1}=[S],[S]^{-1}=[C],$ and $[C][S]^{-1}=[C]^{-1}[S]=[I]$ where the superscript -1 implies inverse and $[I]$ is a 6x6 indentity matrix. Averaging of (8) gives

$$\begin{aligned}&<\{\sigma\}>=<[C]\{\varepsilon\}>\\&\quad=(1/V)\int_V[C]\{\varepsilon\}dV\\&<\{\sigma\}>=<[C]\{\varepsilon\}>\end{aligned} \tag{9}$$

But note $<[C]\{\varepsilon\}>\neq[C^*]<\{\varepsilon\}>$. Simple volume averaging does not lead to equivalent elastic moduli $[C^*]$ or compliances $[S^*]$ for that matter.

Influence functions allow for a way forward. These functions relate local to global averages of stress and strain in two-material composites (Hill 1963). Again, a local average is

over a volume of a single material, joint or rock, and a global average is over a composite volume of joint and rock.

Local averages of strain are

$$\{\bar{\varepsilon}_j\} = (1/V_j)\int_{V_j} \{\varepsilon\} dV \text{ and } \{\bar{\varepsilon}_r\} = (1/V_r)\int_{V_r} \{\varepsilon\} dV \tag{10}$$

where the subscripts *j* and *r* imply joint and rock, respectively, and similarly for stress. A global volume average of strain is

$$<\{\varepsilon_j\}> = (f_j)\{\bar{\varepsilon}_j\} + (f_r)\{\bar{\varepsilon}_r\} \tag{11}$$

where the *f*'s are volume fractions: $f_j = V_j/V$, $f_r = V_r/V$ and $V = V_r + V_j$.

Strain influence functions $[A_j]$ and $[A_r]$ then operate such that

$$\{\bar{\varepsilon}_j\} = [A_j] < \{\varepsilon\} > \text{ and } \{\bar{\varepsilon}_r\} = [A_r] < \{\varepsilon_r\} > \tag{12}$$

Returning to (8)

$$\begin{aligned}
<\{\sigma\}> &= <[C]\{\varepsilon\}> \\
&= (1/V)\int_V [C]\{\varepsilon\} dV \\
&= (1/V)\left(\int_{Vr} [C_r]\{\varepsilon\} dV + \int_{Vj} [C_j]\{\varepsilon\} dV\right) \\
&= (V_r/V)[C_r]\{\bar{\varepsilon}_r\} + (V_j/V)[C_j]\{\bar{\varepsilon}_j\} \qquad (13) \\
&= (f_r)[C_r][A_r] < \{\varepsilon\} > + (f_j)[C_j][A_j] < \{\varepsilon\} > \\
&= \left( (f_r)[C_r][A_r] + (f_j)[C_j][A_j] \right) < \{\varepsilon\} > \\
<\{\sigma\}> &= [C^*] < \{\varepsilon\} >
\end{aligned}$$

Hence,

$$[C^*] = (f_r)[C_r][A_r] + (f_j)[C_j][A_j] \tag{14a}$$

Similarly using stress influence functions

$$[S^*] = (f_r)[S_r][B_r] + (f_j)[S_j][B_j] \tag{14b}$$

Influence functions of strain and stress $[A_r],[A_j],[B_r],[B_j]$ thus allow for the compuation of equivalent elastic moduli and stiffnesses. Note: $(f_j)[A_j]+(f_r)[A_r]=[I]$ from (11) and (12). One can then show that $[A_r]=(1/f_r)([C_r]-[C_j])([C^*]-[C_j])$ and similarly for $[A_j]$ thus demonstrating the relationship between influence functions and equivalent properties. Knowledge of one implies knowledge of the other. However, the problem of computing influence functions and thus equivalent properties remains.

**Computation Details** Consider the "energy" equivalence

$$\begin{aligned}\int_V \{u\}^t\{T\}dV &= \int_V \{\varepsilon\}^t\{\sigma\}dV \\ &= \int_V \{<\varepsilon>+\Delta\varepsilon\}^t\{<\sigma>+\Delta\sigma\}dV \\ \int_V \{u\}^t\{T\}dV &= V\{<\varepsilon>\}^t\{<\sigma>\}+\int_V \{\Delta\varepsilon\}^t\{\Delta\sigma\}dV\end{aligned} \tag{15}$$

where stress and strain are composed of an average and a deviation from the average. Note: The integrals

$$\int_V \{<\varepsilon>\}^t\{\Delta\sigma\}dV,\ \int_V \{\Delta\varepsilon\}^t\{<\sigma>\}dV \tag{16}$$

vanish because the average terms are constants and the deviation terms integrate to zero over the considered volume. Only if the integral of deviation terms on the right hand side of (15) vanish are the equivalent properties energy equivalent in the sense that

$$\{<\varepsilon>\}^t\{<\sigma>\}=\{<\sigma>\}^t[S^*]\{<\sigma>\}=\{<\varepsilon>\}^t[C^*]\{<\varepsilon>\} \tag{17}$$

where symmetry of the elastic compliances and moduli matrices is implied. There are seven combinations of $\{\Delta\sigma\}$ and $\{\Delta\varepsilon\}$ that lead to $\{\Delta\varepsilon\}^t\{\Delta\sigma\}=0$. These are the complimentary conditions

$$\{\Delta\sigma\}=0 \text{ when } \{\Delta\varepsilon\}\neq 0,\ \{\Delta\varepsilon\}=0 \text{ when } \{\Delta\sigma\}\neq 0 \tag{18}$$

For example, a 4-2 combination is

$$\begin{Bmatrix}\Delta\varepsilon_{xx}\\ \Delta\varepsilon_{yy}\\ \Delta\varepsilon_{zz}\\ \Delta\gamma_{yz}\\ 0\\ 0\end{Bmatrix}^t \begin{Bmatrix}0\\ 0\\ 0\\ 0\\ \Delta\tau_{zx}\\ \Delta\tau_{xy}\end{Bmatrix}=0 \tag{19}$$

The 0 strain deviation, 6 stress deviation combination implies uniform strain and is associated with the Voight upper bound to the elastic moduli of the composite. The 6 strain deviation, 0 stress deviation corresponds to the Reuss lower bound to the composite elastic moduli. These bounds are volume weighted averages. However, the assumption of uniform strain violates equilibrium, while the assuption of uniform stress violates compatability. An approach to a 3-3 combination of deviations from the 0-6 combination increases equilibrium, while the approach from the 6-0 combination increases compatibility.

The 3-3 combination of deviations is optimal and satisfies traction and displacement continuity requirements for elastic stability at a material discontinuity (joint-rock interface). If *z* is the direction of a joint normal so *x* and *y* are parallel to a joint, then stress and strain may be reorganized into compatible and equilibrium parts. Thus,

$$\{\sigma\}=\begin{Bmatrix}\sigma_c\\ \sigma_e\end{Bmatrix}=\begin{Bmatrix}\sigma_{xx}\\ \sigma_{yy}\\ \tau_{xy}\\ \sigma_{zz}\\ \tau_{yz}\\ \tau_{zx}\end{Bmatrix},\qquad \{\varepsilon\}=\begin{Bmatrix}\varepsilon_c\\ \varepsilon_e\end{Bmatrix}=\begin{Bmatrix}\varepsilon_{xx}\\ \varepsilon_{yy}\\ \gamma_{xy}\\ \varepsilon_{zz}\\ \gamma_{yz}\\ \gamma_{zx}\end{Bmatrix} \tag{20}$$

Rewriting the first of (8) using the notation in (20) gives the system

$$\begin{Bmatrix}\{<\sigma_c>\}+\overline{\{\Delta\sigma_c\}}\\ \{<\sigma_e>\}+\overline{\{\Delta\sigma_e\}}\end{Bmatrix}=\begin{bmatrix}[C_{cc}]&[C_{ce}]\\ [C_{ec}]&[C_{ee}]\end{bmatrix}\begin{Bmatrix}\{<\varepsilon_c>\}+\overline{\{\Delta\varepsilon_c\}}\\ \{<\varepsilon_e>\}+\overline{\{\Delta\varepsilon_e\}}\end{Bmatrix} \tag{21}$$

Use of (19) reduces (21) to a system of just six equations in six unknown deviation terms. Thus from the second line in (21)

$$\overline{\{\Delta\varepsilon_e\}}=[C_{ee}]^{-1}(\{<\sigma_e>\}-[C_{ec}]<\{\varepsilon_c\}>)-\{<\varepsilon_e>\} \tag{22}$$

and from the first line in (21)

$$\overline{\{\Delta\sigma_c\}}=-\{<\sigma_c>\}+[C_{cc}]\{<\varepsilon_c>\}+[C_{ce}](<\{\varepsilon_e\}>+\overline{\{\Delta\varepsilon_e\}}) \tag{23}$$

Averaging (21) and (22) after some algebra leads to the equivalent properties matrices

$$\begin{aligned}
&[C^*_{ee}]=(<[C_{ee}]^{-1}>)^{-1}\\
&[C^*_{ec}]=[C^*_{ee}]<[C^{-1}_{ee}][C_{ec}]>\\
&[C^*_{ce}]=<[C_{ce}][C^{-1}_{ee}]>[C^*_{ee}]\\
&[C^*_{cc}]=<[C_{cc}]-[C_{ce}][C^{-1}_{ee}][C_{ec}]>+<[C_{ce}][C^{-1}_{ee}]>[C^*_{ce}]
\end{aligned} \tag{24}$$

where the global average of global deviations is zero and the definition of equivalent properties is used.

**Progaming Steps for a Single Joint** A brief outline of programming steps begins with the determination of joint element geometry relative to a given element, usually a sample cube with an edge length at least as large as the spacing of the joints in the given joint set. The joint dip direction, dip, spacing and thickness are specified in the last line of an input file of joint properties. Because volume weighted averages are needed, joint and rock volume fractions are especially important. Recall joints are treated as ordinary finite elements, a feature that circumvents many of the numerical difficulties associated with specialized joint elements. However, joint elements are virtual elements in the sense that they do not require explicit representation in ordinary file formats for elements and coordinates. This feature offers considerable savings in storage requirements. In fact, recomputation was favored over retreival from storage from the outset, a choice that has proved favorable during many years of program development.

The element cube in Figure 2 is partioned into two parts by the first of the two planes defining the joint. Each part is a convex polyhdedron because the original cube is a convex polyhedron. Geometry of the polyhedrons is characterized by numbers of corners, edges and facets. Each could be considered as a finite element but with a variable numbers of corners or nodes rather than fixed. The second of the two joint planes at a normal distance equal to joint thickness is used to partition one of the two polyhedrons produced in the first partition. Corners, edges and facets for each new polyhedron are added to related lists of such. Subroutines for doing the required calculations are called as required. Some checks are built into the partitioning process. For example, a facet must have at least three corners (vertices). An edge may have only two corners. A volume must have at least three facets and four corners. Points that are nearly coincident are merged into a single point according to a preset tolerance and so on. In fact, the Euler-Descart rule applies: C-E+F=2 where C is the number of corners, E is the number of edges and F is the number of facets in a given polyhedron. In case of a tetrahedron the formula is 4-6+4=2. The current program limit to F is 30 and to C the current limit is 29. Thus a polyhedron may have 30 facets each with up to 29 corners. These parameters are easy to change in the appropriate subroutines as problems dictate.

Programing for finite elements cosisting of polyhedrons with a variable number of nodes (corners, vertices) is possible and indeed has been done. In case of a single jointed test cube, a direct comparison with jointed rock properties is possible.

There are numerous exceptions to the joint and cube geometry shown in Figure 2. For example, the joint may intersect a corner of the sample cube and thus not be entirely in the given sample cube. Another example is a joint plane that coincides with an element face. Programming must recognize and accommodate such exceptions. Although easy to visualize, programming is not so easy and required many hours of testing and correcting.

Once joint geometry is determined, rotation of joint and rock properties to align with the joint normal ($z$) and tangential ($xy$) directions is done followed by partitioning of rock and joint material properties matrices into compatible and equilibirium parts as shown in (21). Volume weighted inverses and so on follow with eventual composition of submatrices into equivalent properties matrices shown in (24). A number of specialized matrix handling subroutines as well as routine rotation, addition and multiplication subroutines aid in the computation. Finally, rearrangment of the partitioned equivalent properties matrices into the usual arrangement of normal and shear compliances is done.

**Multiple Joint Programming Steps** Next, consider a sample cube with a linear dimension at least as large of the largest spacing of joints in all the joint sets present. This sample cube is a representative volume element (RVE) of the jointed rock mass and thus is the required size. Then embed joints from each joint set one by one into the sample cube. After the last joint is embedded, compute the composite properties of the sample cube. Figure 3 illustrates the process in case of multiple joints. The process is essentially one of homogenization where a heterogeneous material volume is reconfigured as a homogeneous volume. The latter responds on average as the former. Average stresses and strains are the same in both volumes.

Addition of a second joint to the cube containing a single joint in Figure 2 shows the result in Figure 3. The result is the generation of four joint elements (dashed lines) and a fifth long, narrow element of intersection (dotted lines). New joint elements (two) from the first joint element are assigned the same properties and the two new joint elements from the second joint are assigned second joint properties. Assignment of properties to the fifth "intersection" joint is problematic. No new properties are justified, so the properties should be either joint 1 or joint 2 properties. The choice made in programming is to assign the newest additional joint (joint 2) properties to the intersecting joint. Addition of a third joint from a third joint set (or an existing joint set) will complicate the geometry and will likely produce a small cuboid element at intersection with a long, narrow intersection element. However, assignment of material properties follows the same choice and is made throughout joint additions.

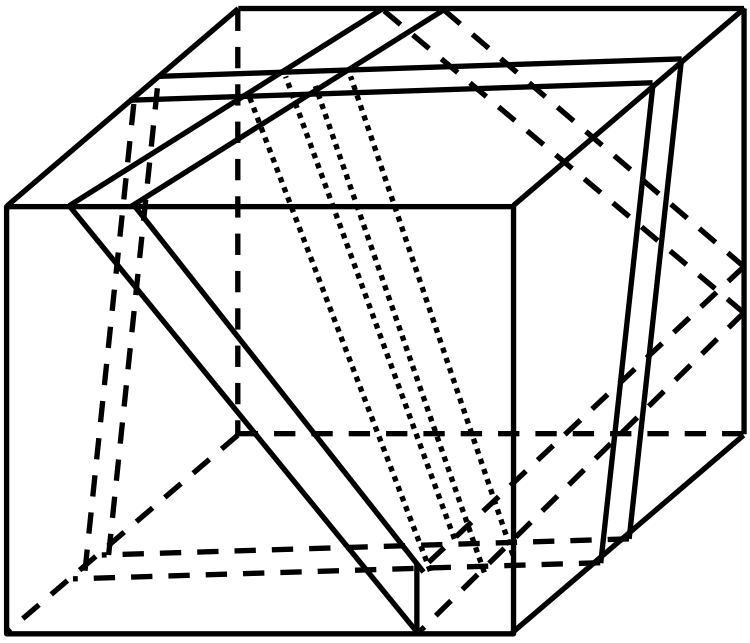

Figure 3 A sample cube containing two intersecting joints from different joint sets.

Equivalent properties calculations are sequential with each joint addition. After addition of a first joint, equivalent properties are calculated. These equivalent properties are now rock properties. Addition of a second joint leads to a second set of equivalent properties and so on until all joints have been added to the sample cube. Different joint sets in different formations in the geological column are treated in the same manner. The computer program obliging keeps tract of the data necessary for subsequent finite element analysis.

The geometry of joint creation is essential to calculating volume fractions of each joint segment and the calculation of volume weighted averages. Figure 4 shows the geometry of a sample cube containing four joints each 0.1 ft thick with a maximum spacing of 4.4 ft. The sample cube is 5 ft on edge.

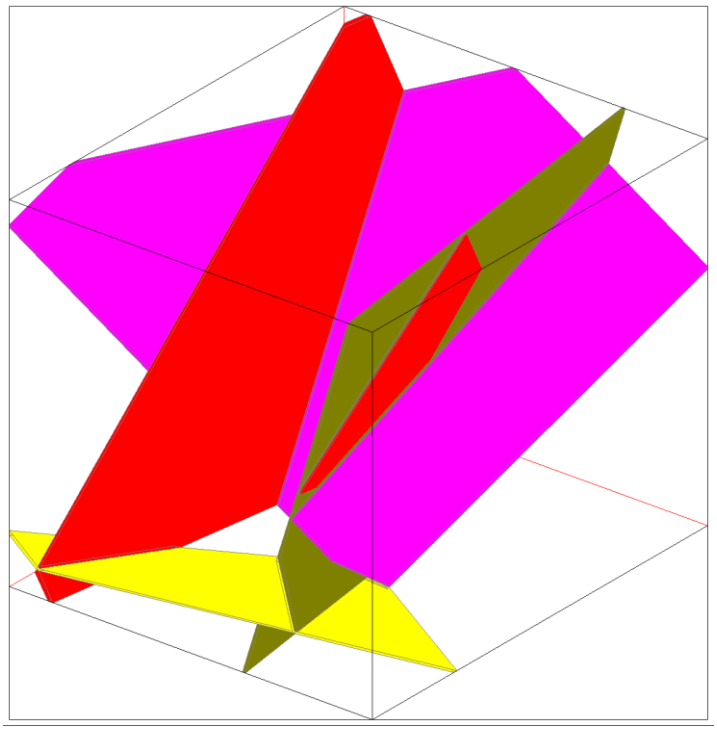

Figure 4 A 5 ft sample cube containing four joints with a maximum spacing of 4.4 ft. Joints are 0.1 ft thick.

If joints are embedded element by element in a finite element mesh, then small elements may not contain any joints while large elements may contain many joints. For example, if an element is 20 ft on edge rather than 5 ft illustrated in Figure 4, the element contains not four but rather 47 joint elements (10 of joint 1, 20 of joint 2, 11 of joint 3 and 6 of joint 4). Each element in the mesh then has unique equivalent properties! During an analysis, strains and stresses in

each of the 47 joint elements and in the rock portion of the finite element would need to be computed. Any joint or rock element stress exceeding the elastic limit would require elastic plastic computation. The process would be repeated for all elements in the mesh at the end of each load step.

There is a subtlety that occurs in the process of computing and using equivalent properties and that is the computation of influence functions, especially strain influence functions. A finite element analysis based on equivalent properties produces global (element) strains. Strains in the contained joint and rock sub-elements of each finite element are necessary for computation of stress which is necessary to determine whether the elastic limit is reached. The sub-element strains are computed from the element (global) strain using influence functions and volume fractions. The latter follow from a backward recursive relationship that is programmed in the equivalent properties computation. Thus, $\{\bar{\varepsilon}_j\} = [A_j] < \{\varepsilon\} >$ and $\{\bar{\sigma}_j\} = [E_j]\{\bar{\varepsilon}_j\}$ for each joint sub-element and for the rock portion $\{\bar{\varepsilon}_r\} = [A_r] < \{\varepsilon_r\} >$ and $\{\bar{\sigma}_r\} = [E_r]\{\bar{\varepsilon}_r\}$ in an element. Stresses in joint and rock sub-elements are then processed to determined whether the elastic limit is reached and if so an elastic-plastic properties matrix is computed. The entire process is incremental and repeated element by element after each load step when updating, if necessary, is done.

**Examples of Jointed Rock Analyses** Jointed rock analysis requires an additional step between the usual *Step 1* (specification of a material properties file), and *Step 2* (mesh generation). This step is *Step 1j* for generation of equivalent properties of jointed rock formations. The usual three steps with examples are given in considerable detail in a USER MANUAL (Pariseau 2022). *Step 1j* produces equivalent properties of a jointed rock mass. These properties apply to all elements in the mesh, large and small. While equivalent properties for each and every element in a mesh are possible, the practice greatly reduces the mesh size because of hardware limitations. Currently, a suggested limit is one million elements. An order of magnitude reduction would likely occur if equivalent properties were assigned element by element. For this reason, the same equivalent properties are assigned to all elements in a given formation. This practice is on the conservative side in the sense that a small element near an excavation wall may not be intersected by any joints and thus have laboratory scale moduli and strengths. Assignment of equivalent properties would make a small element more deformable and weaker. To be sure, a small element with a joint would likely be quite deformable and weak, almost joint-like in response to load, so the "conservatism" is qualified.

*Step 1j* begins with specification of the size of a *representative elementary volume* (REV) in the file of coordinates that define a single element under consideration. Figure 5 illustrates a REV with five joint sets. Four sets have vertical joints; the fifth joint set has horizontal joints, that is, bedding plane joints. There are 364 jointed elements in the REV. In a mesh of one million conventional elements containing joints, there would be 364 million total elements were joints to be considered individually!

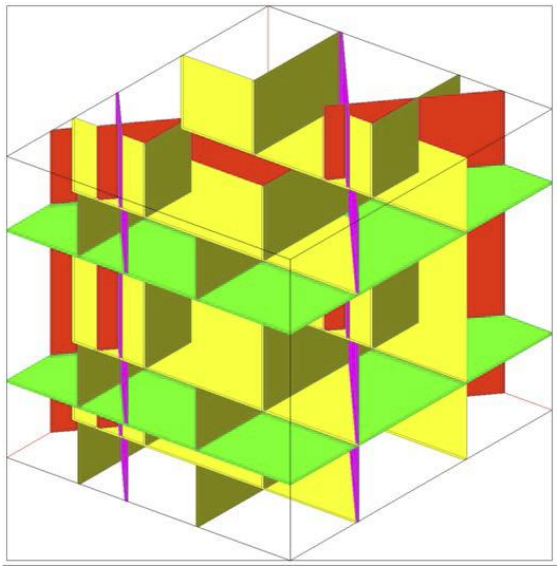

Figure 5 A REV used for computing equivalent properties when five joint sets are present (Pariseau, 2017).

Figure 6 shows the change in elastic moduli with change in size of the REV and shows quite clearly that the REV size is conditioned by the maximum joint spacing. The reason why maximum joint spacing serves as the linear dimension of a REV is the periodic structure defined by the joint sets. A cell in a periodic structure is a REV just as bricks in a brick wall define a periodic structure (and a REV).

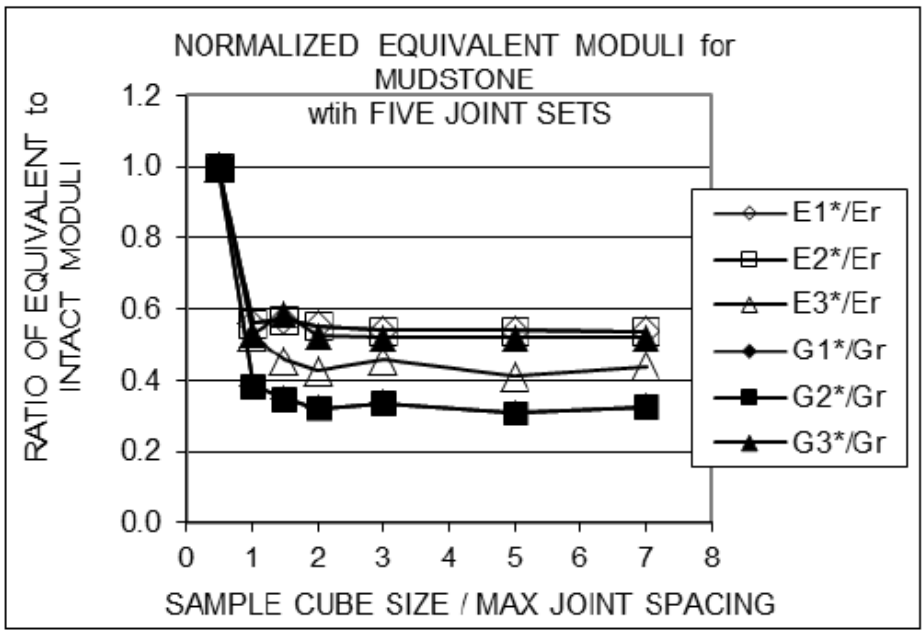


Figure 6 Equivalent moduli as functions of relative REV size (Pariseau 2017).

The implicit assumption of a continuum of equivalent elastic properties of rock also implies equivalent rock strengths which limit the range of a purely elastic response to load. One method of computing equivalent rock strengths is to assume the same strain to failure in case of equivalent moduli as in intact properties of rock. Under uniaxial compressive stress the strain to failure $\varepsilon_f = C_o / E$ where $C_o$ and $E$ are unconfined compressive strength and Young's modulus, respectively. Thus, $\varepsilon_f = (C_o / E)_{lab} = (C_o / E)_{equ}$ where "lab" and "equ" signify laboratory and equivalent values, respectively. Consequently, $(C_o)_{equ} = (C_o)_{lab}(E_{equ} / E_{lab})$.

Equivalent tensile strength may be estimated by keeping the ratio of compressive to tensile strength the same for equivalent strengths as for laboratory strengths, that is, $(C_o / T_o)_{lab} = (C_o / T_o)_{equ}$. Hence, $(T_o)_{equ} = (T_o / C_o)_{lab}(C_0)_{equ}$.

The shear strengths are computed as in the laboratory case. For example $R_a = \sqrt{C_o T_o / 3}$ which implies a quadratic failure criterion (*n*=2). If a different exponent (*n*) is used in the laboratory case, this same *n* should be used in the equivalent properties calculation. All the same processes are carried out for the *b* and *c* directions. In this regard, orthotropic elasticity and strength are implied: *a*=down dip, *b*=on strike, *c*=normal to *ab*.

In case of a simple energy to failure criterion such that $U_f = (\sigma\varepsilon / 2)_{lab} = (\sigma\varepsilon / 2)_{eqi}$ one has $(E_{equ} / E_{lab}) = (C_{equ} / C_{lab})^2$. Hence, $(C_{equ}) = C_{lab})\sqrt{(E_{equ} / E_{lab})}$. For example, if the modulus ratio $(E_{equ} / E_{lab})$ is ¼, then the equivalent unconfined compressive strength $C_{equ}$ is just ½ of the laboratory value of unconfined compressive strength $C_{lab}$. Tensile and shear strengths follow as in the case of a strain to failure criterion.

**Example 1** Equivalent properties should be calculated for each formation in the material properties file. This requirement allows for different jointing in different formations but also requires the joint set data of dip direction, dip, spacing and thickness. Because joints are treated as regular elements in the embedment process, joint moduli and strengths are also required as well as the elastic moduli and strengths of intact rock. Figure 7 is an example of a material property file related to the former Homestake Mine in Lead, SD. The first line is label of sorts; the second line specifies three Young's moduli and three Poisson's ratios, and the third line specifies shear moduli and specific weights (zero in this example). The fourth line specifies unconfined compressive and tensile strengths; the fifth line specifies shear strengths. To be sure, the file allows for anisotropy up to orthotropy. The sixth and last line specifies dip direction, dip, joint spacing and joint thickness. Joint thickness is negative to alert the program UT3PC that a joint is under consideration. Rock thickness is positive as usual. In case of rock, the last line specifies dip direction, dip, formation depth and thickness as seen in the figure. Free formatting is used, so spacings are not critical.

```
(1) joint N 120 E  02/12/2022 Homestake wgp 0.1 thik N=2
 15.80e+04 15.80e+04 15.80e+04      0.25      0.25      0.25
```

```
 6.32e+04  6.32e+04  6.32e+04       0.0       0.0       0.0
    286.0     286.0     286.0      16.0      16.0      16.0
    39.10     39.10     39.10
   120.00      36.0       3.1     -0.10
 (2) joint N 216 E N=2
 15.80e+04 15.80e+04 15.80e+04      0.25      0.25      0.25
  6.32e+04  6.32e+04  6.32e+04       0.0       0.0       0.0
    286.0     286.0     286.0      16.0      16.0      16.0
    39.10     39.10     39.10
    216.0      52.0       1.6     -0.10
(3) joint N 261 E  02/11/2022  wgp 0.1 thik N=2
 15.80e+04 15.80e+04 15.80e+04      0.25      0.25      0.25
  6.32e+04  6.32e+04  6.32e+04       0.0       0.0       0.0
    286.0     286.0     286.0      16.0      16.0      16.0
    39.10     39.10     39.10
   261.00      74.0       2.4     -0.10
 (4) joint N 358 E N=2
 15.80e+04 15.80e+04 15.80e+04      0.25      0.25      0.25
  6.32e+04  6.32e+04  6.32e+04       0.0       0.0       0.0
    286.0     286.0     286.0      16.0      16.0      16.0
    39.10     39.10     39.10
    358.0      58.0       4.4     -0.10
 (1) Poorman
 13.5e+06  13.7e+06  7.20e+06      0.23      0.22      0.15
  3.8e+06   5.6e+06  3.94e+06       0.0       0.0       0.0
  13630.0   12270.0   10000.0    2990.0    1910.0     820.0
   1500.0    1520.0    2800.0
    184.0      49.0    4650.0      250.0
```

Figure 7 An example of a material property file with four joint sets and intact rock. The Poorman formation is a Precambrian meta-sediment and is highly directional (anisotropic).

Figure 8a illustrates the four “joints” described in Figure 7; Figure 8b shows equivalent moduli as functions of sample cube size in the case of four joints.

The runstream file for computing equivalent properties associated with the property file in Figure 7 (HMEprop.txt) is shown in Figure 9. The file is similar in structure to files used for finite element analysis of large structures such as main entries in underground coal mines and so on. However, the calculation of displacement, strain and stress is trivial. Run time is in seconds.

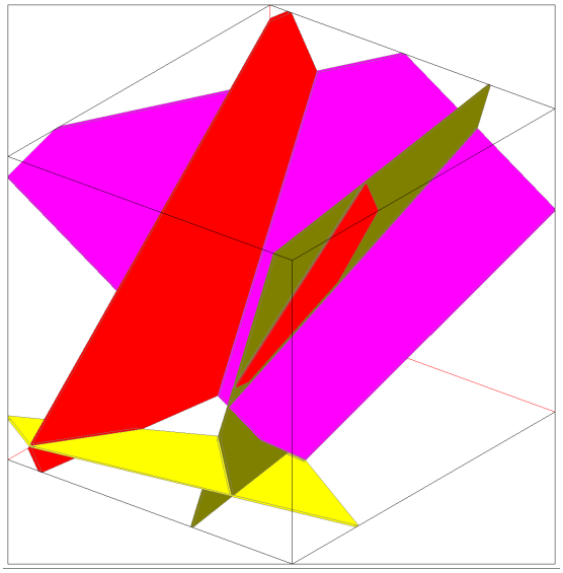

(b)

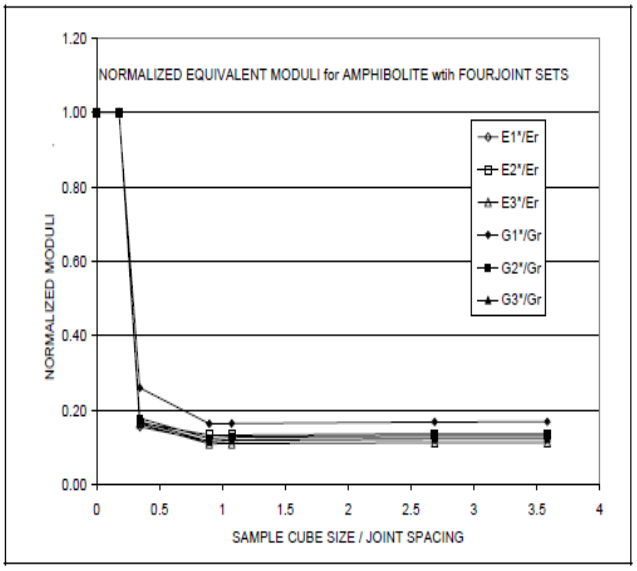


(a)

Figure 8 (a) plot of four joints with properties given in Figure 7, (b) moduli as a function of sample cube (REV) size (Pariseau et al 2012).

Homestake Drift with Joints 2/11-25/2022 wgp
HMEprop.txt
celms.txt
ccrds.txt
none
none
RNDCT
cnsps.txt
aH1
nelem = 1
nnode = 8
nspec = 8
nmat = 5
ncut = 1
ninc = 1
nsigo = 0
inter = 100
maxit = 1000
nyeld = 2
nelcf = 0
ncave = 0
nfile = 1
npsi = 1
nrstrt= 0
error= 1.0000
orf = 1.8600
xfac = 12.0000

```
 yfac =   12.0000
 zfac =   12.0000
 efac =    1.0000
 cfac =     100.0
RUN END
```

Figure 9 An example runstream file for computing equivalent properties.

The outputs from an equivalent properties computation are 6x6 matrices of elastic compliances and stiffnesses (moduli). Compliance $[S]$ relates stress $\{\sigma\}$ to strain $\{\varepsilon\}$. Thus, $\{\varepsilon\}=[S]\{\sigma\}$. Stiffness $[C]$ relates strain $\{\varepsilon\}$ to stress $\{\sigma\}$. Thus, $\{\sigma\}=[C]\{\varepsilon\}$. In conventional finite element notation the stiffness matrix is often expressed as $[E]$ and sometimes as $[D]$. The compliance and stiffness matrices are symmetric, mutual inverses. Thus, $[C][S]=[S][C]=[I]$ where the last is a six by six identity matrix. A fully populated compliance matrix couples normal stress to shear strains and shear stress to normal strains.

Figure 10 shows a stiffness matrix in the case of an orthotropic rock with three planes of elastic symmetry and three axes of anisotropy. The orthotropic model is used in UT3PC. Symmetry dictates $\nu_{12}/E_1=\nu_{21}/E_2$ and so on.

$$\begin{Bmatrix}\varepsilon_{xx}\\ \varepsilon_{yy}\\ \varepsilon_{zz}\\ \gamma_{yz}\\ \gamma_{zx}\\ \gamma_{yz}\end{Bmatrix}=\begin{bmatrix} 1/E_1 & -\nu_{21}/E_2 & -\nu_{31}/E_3 & 0 & 0 & 0\\ -\nu_{12}/E_1 & 1/E_2 & -\nu_{32}/E_3 & 0 & 0 & 0\\ -\nu_{13}/E_1 & -\nu_{23}/E_2 & 1/E_3 & 0 & 0 & 0\\ 0 & 0 & 0 & 1/G_{23} & 0 & 0\\ 0 & 0 & 0 & 0 & 1/G_{31} & 0\\ 0 & 0 & 0 & 0 & 0 & 1/G_{12}\end{bmatrix}\begin{Bmatrix}\sigma_{xx}\\ \sigma_{yy}\\ \sigma_{zz}\\ \tau_{yz}\\ \tau_{zx}\\ \tau_{xy}\end{Bmatrix}$$

Figure 10 An analytical expression for an orthotropic rock. E=Young's moduli, G=shear moduli, $\nu$=Poisson's ratio, $\varepsilon$, $\gamma$, $\sigma$, $\tau$ are normal strain, shear strain, normal stress and shear stress, respectively. (Lekhnitiskii 1963).

Figure 11a shows the results in the form of compliances for the Homestake example using data in Figure 7 and the runstream in Figure 9. The matrix of compliances in Figure 11a is symmetric and provides a check on the calculation. In this respect, symmetry is not imposed but rather is a result. Figure 11b shows the compliance matrix associated with Figure 11a but with neglect of the coupling terms in Figure 11a. Inspection of the coupling terms show some to be an order of magnitude smaller than the Poisson ratio terms, so there is justification for neglecting these relatively small terms and the assumption of an orthotropic equivalent elastic model. However, in finite element analysis, there is no need for such an approximation. The full 6x6 matrix of elastic properties may be used in the course of computation.

| | | | | | |
|---|---|---|---|---|---|
| 5.75E-07 | -9.12E-08 | -1.54E-07 | 1.66E-07 | -2.95E-08 | 1.03E-07 |
| -9.12E-08 | 5.34E-07 | -1.75E-07 | -2.75E-07 | 1.21E-07 | 1.37E-07 |
| -1.54E-07 | -1.75E-07 | 6.99E-07 | -1.09E-07 | -2.24E-07 | -7.20E-08 |
| 1.66E-07 | -2.75E-07 | -1.09E-07 | 1.06E-06 | 1.17E-07 | 3.44E-08 |
| -2.95E-08 | 1.21E-07 | -2.24E-07 | 1.17E-07 | 1.43E-06 | -4.11E-09 |
| 1.03E-07 | 1.37E-07 | -7.20E-08 | 3.44E-08 | -4.11E-09 | 1.55E-06 |

(a)

| | | | | | |
|---|---|---|---|---|---|
| 5.75E-07 | -9.12E-08 | -1.54E-07 | | | |
| -9.12E-08 | 5.34E-07 | -1.75E-07 | | | |
| -1.54E-07 | -1.75E-07 | 6.99E-07 | | | |
| | | | 1.06E-06 | | |
| | | | | 1.43E-06 | |
| | | | | | 1.55E-06 |

(b)

Figure 11 (a) Compliances for the Homestake example. (b) orthotropic approximation to the Homestake example compliances.

**Example 2** Figure 12a is an example of a compliance matrix of equivalent properties in case of trona with five joint sets as shown in Figure 5. The matrix is symmetric as required by theory and again provides a check on the numerical calculation. These results indicate a negligible coupling between normal strain and shear stress is present and between shear strain and normal stress where the coupling terms are orders of magnitude smaller than other terms in the matrix. Figure 12b shows an orthotropic approximation with neglect of the coupling terms in Figure 12a.

| | | | | | |
|---|---|---|---|---|---|
| 9.64E-07 | -2.96E-07 | -5.95E-08 | 1.21E-12 | 2.45E-13 | 2.65E-10 |
| -2.96E-07 | 9.64E-07 | -6.20E-08 | -4.73E-13 | 2.83E-15 | 2.63E-10 |
| -5.95E-08 | -6.20E-08 | 2.48E-07 | -2.93E-12 | -9.84E-13 | 7.08E-14 |
| 1.21E-12 | -4.73E-13 | -2.93E-12 | 1.91E-06 | 7.07E-10 | -9.73E-13 |
| 2.45E-13 | 2.83E-15 | -9.84E-13 | 7.07E-10 | 1.91E-06 | -4.88E-13 |
| 2.65E-10 | 2.63E-10 | 6.60E-14 | -9.73E-13 | -4.88E-13 | 2.25E-06 |

(a)

| | | | | | |
|---|---|---|---|---|---|
| 9.64E-07 | -2.96E-07 | -5.95E-08 | | | |
| -2.96E-07 | 9.64E-07 | -6.20E-08 | | | |
| -5.95E-08 | -6.20E-08 | 2.48E-07 | | | |
| | | | 1.91E-06 | | |
| | | | | 1.91E-06 | |
| | | | | | 2.25E-06 |

(b)

Figure 12 An example of equivalent compliances in case of five joint sets. (a) compliances, (b) with neglect of coupling terms to an orthotropic model.

Inspection of Figure 12a suggests a transversely isotropic model.
The transversely isotropic jointed rock model in case of trona is not too surprising because of the vertical and horizontal orientation of the joints. Further details are given in Pariseau (2017).

**Example 3** When several formations are in the geological column specified in the material properties file for a finite element analysis, a *Step1j* must be taken to obtain equivalent properties for each formation that is considered jointed. Surface outcrops are accessible for joint mapping and so are seam-level strata. Exploration borehole mapping of joints is also possible and provides a means of obtaining joint data between surface and the mining horizon. If joint data are lacking, then improvisation is necessary before taking *Step 1j* and computing equivalent properties. For example, surface jointing may be assumed to extend to the mining horizon and below. *Step 1j* for equivalent properties is still necessary for each formation because the rock type enters the calculation (Pariseau 2017).

Equivalent properties of each formation may be generated sequentially by stacking each set of jointed rock properties one following the other and only using the RUN END statement in the last properties set. An example stacking of jointed properties is shown in Figure 13. The runstream is shown in Figure 14 where the one element, one load increment assures a runtime of just seconds. The equivalent material property file for each formation is saved for the actual finite element analysis of the problem at hand. This analysis follows immediately after the computation of equivalent properties as indicated in the last input file beginning with SkyMine 3/12/2022 in the runstream of Figure 14. Figures 13 and 14 are for illustrative purposes only.

```
SKY1prop.txt
  1  --(1) joint  N 5 E/Jan/2018 wgp 0.1 thik N=2
 1.25E+04  1.25E+04  1.25E+04      0.20      0.20      0.20
 0.52E+04  0.52E+04  0.52E+04       .00       .00      2.88
    35.80     35.80     35.80      4.97      4.97      4.97
     7.70      7.70      7.70
    95.00      90.0       3.0     -0.10
  2  --(2) joint N 65 W N=2
 1.25E+04  1.25E+04  1.25E+04      0.20      0.20      0.20
 0.52E+04  0.52E+04  0.52E+04       .00       .00      2.88
    35.80     35.80     35.80      4.97      4.97      4.97
     7.70      7.70      7.70
     25.0      90.0       3.0     -0.10
  3  --(3) joint BEDDING PLANES N=2
 1.25E+04  1.25E+04  1.25E+04      0.20      0.20      0.20
 0.52E+04  0.52E+04  0.52E+04       .00       .00      2.88
    35.80     35.80     35.80      4.97      4.97      4.97
     7.70      7.70      7.70
      0.0       0.0       3.0     -0.10
 (1) North Horn  N=2 (DP2) & sp wts (pcf) z=vert 12/11/2017
 2.60e+06  2.60e+06  2.60e+06      0.26      0.26      0.26
 1.03e+06  1.03e+06  1.03e+06       0.0       0.0       0.0
  11800.0   11800.0   11800.0     700.0     700.0     700.0
   1659.0    1659.0    1659.0
      0.0       0.0       0.0     150.0
```

SKY2prop.txt

```
  1  --(1) joint  N 5 E/Jan/2018 wgp 0.1 thik N=2
 1.25E+04  1.25E+04  1.25E+04      0.20      0.20      0.20
 0.52E+04  0.52E+04  0.52E+04       .00       .00      2.88
    35.80     35.80     35.80      4.97      4.97      4.97
     7.70      7.70      7.70
    95.00      90.0       3.0     -0.10
  2  --(2) joint N 65 W N=2
 1.25E+04  1.25E+04  1.25E+04      0.20      0.20      0.20
 0.52E+04  0.52E+04  0.52E+04       .00       .00      2.88
    35.80     35.80     35.80      4.97      4.97      4.97
     7.70      7.70      7.70
     25.0      90.0       3.0     -0.10
  3  --(3) joint BEDDING PLANES N=2
 1.25E+04  1.25E+04  1.25E+04      0.20      0.20      0.20
 0.52E+04  0.52E+04  0.52E+04       .00       .00      2.88
    35.80     35.80     35.80      4.97      4.97      4.97
     7.70      7.70      7.70
      0.0       0.0       3.0      -.10
 (2) Price River
 3.20e+06  3.20e+06  3.20e+06      0.26      0.26      0.26
 1.27e+06  1.27e+06  1.27e+06       0.0       0.0       0.0
   9980.0    9980.0    9980.0     380.0     380.0     380.0
   1124.0    1124.0    1124.0
      0.0       0.0     150.0     200.0
```

SKY3prop.txt

```
  1  --(1) joint  N 5 E/Jan/2018 wgp 0.1 thik N=2
 1.25E+04  1.25E+04  1.25E+04      0.20      0.20      0.20
 0.52E+04  0.52E+04  0.52E+04       .00       .00      2.88
    35.80     35.80     35.80      4.97      4.97      4.97
     7.70      7.70      7.70
    95.00      90.0       3.0      0.10
  2  --(2) joint N 65 W N=2
 1.25E+04  1.25E+04  1.25E+04      0.20      0.20      0.20
 0.52E+04  0.52E+04  0.52E+04       .00       .00      2.88
    35.80     35.80     35.80      4.97      4.97      4.97
     7.70      7.70      7.70
     25.0      90.0       3.0     -0.10
  3  --(3) joint BEDDING PLANES N=2
 1.25E+04  1.25E+04  1.25E+04      0.20      0.20      0.20
 0.52E+04  0.52E+04  0.52E+04       .00       .00      2.88
    35.80     35.80     35.80      4.97      4.97      4.97
     7.70      7.70      7.70
      0.0       0.0       3.0     -0.10
 (3) Castle Gate sandstone
 3.00e+06  3.00e+06  3.00e+06      0.22      0.22      0.22
 1.23e+06  1.23e+06  1.23e+06       0.0       0.0       0.0
   9590.0    9590.0    9590.0     430.0     430.0     430.0
   1170.0    1170.0    1170.0
      0.0       0.0     350.0     250.0
```

Figure 13 An example of a sequential input file for equivalent properties of several jointed rock formations (*Step 1j*) in the Wasatch coal field of central Utah.

SkyMine 3/12/2022 wgp
SKY1prop.txt
cubelem.txt
cubecrds.txt
none
none
ndct
cubensps.txt
A1
nelem =  1
nnode =  8
nspec =  8
nmat  =  4
ncut  = +1
ninc  =  1
nsigo =  0
inter = 200
maxit = 15000
nyeld =  2
nelct =  0
ncave =  0
nfile =  1
npsi  =  1
 error= 1.0000
 orf  = 1.8600
 xfac = 12.0000
 yfac = 12.0000
 zfac = 12.0000
 efac = 1.0000
 cfac = 100.0
SkyMine 3/12/2022 wgp
SKY2prop.txt
cubelem.txt
cubecrds.txt
none
none
ndct
cubensps.txt
A2
nelem =  1
nnode =  8
nspec =  8
nmat  =  4
ncut  = +1
ninc  =  1
nsigo =  0
inter = 200
maxit = 15000
nyeld =  2
nelct =  0
ncave =  0
nfile =  2
npsi  =  1
 error= 1.0000

orf = 1.8600
xfac = 12.0000
yfac = 12.0000
zfac = 12.0000
efac = 1.0000
cfac = 100.0
SkyMine 3/12/2022 wgp
SKY3prop.txt
cubelem.txt
cubecrds.txt
none
none
ndct
cubensps.txt
A3
nelem = 1
nnode = 8
nspec = 8
nmat = 4
ncut = +1
ninc = 1
nsigo = 0
inter = 200
maxit = 15000
nyeld = 2
nelct = 0
ncave = 0
nfile = 3
npsi = 1
error= 1.0000
orf = 1.8600
xfac = 12.0000
yfac = 12.0000
zfac = 12.0000
efac = 1.0000
cfac = 100.0
SkyMine 3/12/2022 wgp
SKYprop.txt
elem.txt
crds.txt
elct.txt
sigo.txt
ndct
nsps.txt
A4
nelem =1000000
nnode =2000000
nspec =2000000
nmat = 3
ncut = -1
ninc = 10
nsigo = 0
inter = 200
maxit = 5000
nyeld = 2
nelct = 500

```
ncave =      0
nfile =      4
npsi  =      1
 error=    1.0000
 orf  =    1.8600
 xfac =   12.0000
 yfac =   12.0000
 zfac =   12.0000
 efac =    1.0000
 cfac =     100.0
RUN END
```

Figure 14 An example runstream for equivalent properties of several jointed formations associated with the input material properties file in Figure 13.

The first five problems of the seven problem types described in the User Manual for using UT3PC involve multiple strata above and below the mining horizon and thus require multiple runs of *Step 1j*. Problems six and seven involving shafts and tunnels are analysis of sections ("slabs") and may be in a single rock type and thus require just one *Step 1j* calculation of equivalent properties. However, thin formations that are inclined may appear in a section and thus require several *Step 1j* analyses for equivalent properties of the jointed formations present.

**Computation of Equivalent Properties** Once the equivalent properties of all formations present are computed, the finite element analysis may proceed (*Step 3*). *Step 1* requiring preparation of a material properties file containing only rock properties is necessary before hand as usual. *Step 2* requires mesh generation and must also be done in advance of *Step 3*, finite element analysis. In this regard, *Step 2* mesh generation assigns material property type by *number* to each element in the stratigraphic column regardless of the actual properties in the material property file. Indeed, the properties in the material property file are not required for mesh generation; rather the *equivalent* properties computed in *Step 1j* may be used in *Step 2*.

The implicit assumption of a continuum of equivalent elastic properties of rock also implies equivalent rock strengths which limit the range of a purely elastic response to load. As remarked previously, one method of computing equivalent rock strengths is to assume the same strain to failure in case of equivalent moduli as in intact properties of rock. Under uniaxial compressive stress the strain to failure $\varepsilon_f = C_o / E$ where $C_o$ and $E$ are unconfined compressive strength and Young's modulus, respectively. Thus, $\varepsilon_f = (C_o / E)_{lab} = (C_o / E)_{equ}$ where "lab" and "equ" signify laboratory and equivalent values, respectively. Consequently, $(C_o)_{equ} = (C_o)_{lab}(E_{equ} / E_{lab})$. For example, in case of the Poorman formation in the down dip (*a*) direction

$$(C_o)_{equ} = (13,630)(1.74e+06 / 13.5e+06)$$
$$(C_o)_{equ} = 1,756 \text{ psi.}$$

and similarly for the strike direction and normal direction.

Equivalent tensile strength may be estimated by keeping the ratio of compressive to tensile strength the same for equivalent strengths as for laboratory strengths, that is, $(C_o / T_o)_{lab} = (C_o / T_o)_{equ}$. Hence, $(T_o)_{equ} = (T_o / C_o)_{lab}(C_0)_{equ}$ and in the case of the Poorman formation in the *a* direction

$$(T_o)_{equ} = (T_o / C_o)_{lab}(C_0)_{equ}$$
$$= (2,990 / 13,630)(1,756)$$
$$(T_o)_{equ} = 385 \text{ psi}$$

The shear strengths are computed as in the laboratory case. For example $R_a = \sqrt{C_o T_o / 3}$ which implies a quadratic failure criterion (*n*=2). If a different exponent (*n*) is used in the laboratory case, this same *n* should be used in the equivalent properties calculation. In the present example

$$(R_o)_{equ} = \sqrt{(C_o T_o / 3)_{equ}}$$
$$= \sqrt{(1756)(385) / 3}$$
$$(T_o)_{equ} = 475 \text{ psi}$$

All the same processes are carried out for the *b* and *c* directions.

The results of sequencing in *Step 1j* as in Figure 14 are files for each of the run streams that contain joint information and moduli and compliances data. Most importantly is the file of equivalent properties which is in the form of the usual material properties file developed in *Step 1*. For example, after sequencing Trona, Homestake (Poorman formation) and Stillwater (Gabbro) data with five, four and two joint sets each, the equivalent properties file is

```
6  --(6) TRONA N=2
  0.101E+07  0.101E+07  0.832E+06       0.29       0.07       0.05
  0.223E+06  0.223E+06  0.411E+06       0.00       0.00       0.00
     1691.5     1691.4     1388.2      101.9      101.9       83.7
      239.7      239.7      196.7
        0.0        0.0     1499.0       10.0
 (5) Poorman
  0.176E+07  0.190E+07  0.146E+07       0.16       0.33       0.22
  0.968E+06  0.711E+06  0.655E+06       0.00       0.00       0.00
     1778.1     1705.4     2024.7      390.1      265.5      166.0
      480.8      388.5      334.7
      184.0       49.0     4650.0      500.0
 (3) GABBRO  N=2 (DP2) & sp wts (pcf) z=vert 12/11/2017
  0.390E+07  0.379E+07  0.636E+07       0.23       0.19       0.26
  0.203E+07  0.185E+07  0.138E+07       0.00       0.00       0.00
     7052.8     6855.9    11510.2      394.6      383.5      643.9
      963.1      936.2     1571.8
        0.0        0.0        0.0      150.0
```

This file is simply to illustrate a result, of course, but it is clearly in the form required for mesh generation and a finite element analysis (*Step 2* and *Step* 3) when using UT3PC. In fact, with a mesh already generated, the finite element analysis can be executed with just some minor editing of the equivalent properties file produced in *Step 1j*.

A comparison of properties before and after introducing joints is given in Figure 15 in the case of 12 layers each with the five joint sets shown in Figure 5 that are related to trona mining in southwest Wyoming. The first group of properties in each formation consists of intact rock properties. The second group following the intact properties consists of equivalent jointed rock properties. The first are isotropic rock properties; the second are anisotropic (approximately transversely isotropic). A sequential file of 12 runstreams ending with the required RUN END as a last statement in the 12$^{th}$ runstream was used to obtain the equivalent properties. However, 12 separate runstreams could be used followed by "cut and paste" to obtain the equivalent properties file containing all 12 formations required for *Step 3*, execution. A second run for equivalent properties was done using a REV size of 70 versus 30 (maximum joint spacing of the five sets present) for the first run to insure satisfactory results. The differences between runs were small, just a few percent. Eight joints were present in the 30 size REV; 22 joints were present in the 70 size REV. Thus, maximum joint spacing does serve the purpose of defining REV size.

```
NLYRS =12
NSEAM = 7
NJNTS = 5

 (1) SHALE 1 N=2 (DP2) & spwts (pcf) dpth=m AVERAGES 5/30/2015 for SOLVAY
 0.87e+06  0.87e+06  0.87e+06      0.22      0.22      0.22
 0.36e+06  0.36e+06  0.36e+06       0.0       0.0     144.0
   4922.0    4922.0    4922.0     520.0     520.0     520.0
    924.0     924.0     924.0
      0.0       0.0       0.0     62.0
(1) SHALE 1 N=2 (DP2) & spwts (pcf) dpth=m AVERAGES 5/30/2015 for SOLVAY
  0.527E+06   0.527E+06   0.474E+06       0.25       0.14       0.12
  0.151E+06   0.151E+06   0.217E+06       0.00       0.00       0.00
     2980.7      2980.7      2683.1       314.9       314.9       283.5
      559.4       559.3       503.5
        0.0         0.0         0.0        62.0

 (2) MUDSTONE
 1.22e+06  1.22e+06  1.22e+06      0.20      0.20      0.20
 0.51e+06  0.51e+06  0.51e+06       0.0       0.0     134.0
   3580.0    3580.0    3580.0     497.0     497.0     497.0
    770.0     770.0     770.0
      0.0       0.0      62.0     148.0
 (2) MUDSTONE
  0.639E+06   0.639E+06   0.563E+06       0.25       0.11       0.10
  0.172E+06   0.172E+06   0.264E+06       0.00       0.00       0.00
     1874.5      1874.5      1650.8       260.2       260.2       229.2
      403.2       403.2       355.1
        0.0         0.0        62.0       148.0
```

(3) SANDSTONE 1
2.03e+06 2.03e+06 2.03e+06 0.23 0.23 0.23
0.82e+06 0.82e+06 0.82e+06 0.0 0.0 140.0
6317.0 6317.0 6317.0 480.0 480.0 480.0
1005.0 1005.0 1005.0
0.0 0.0 210.0 249.0
(3) SANDSTONE 1
0.809E+06 0.809E+06 0.690E+06 0.28 0.10 0.08
0.197E+06 0.197E+06 0.328E+06 0.00 0.00 0.00
2518.5 2518.4 2146.6 191.4 191.4 163.1
400.8 400.8 341.6
0.0 0.0 210.0 249.0

(4) OIL SHALE 1
0.82e+06 0.82e+06 0.82e+06 0.33 0.33 0.33
0.31e+06 0.31e+06 0.31e+06 0.0 0.0 142.0
5292.0 5292.0 5292.0 460.0 460.0 460.0
908.0 908.0 908.0
0.0 0.0 459.0 449.0
(4) OIL SHALE 1
0.508E+06 0.508E+06 0.459E+06 0.32 0.21 0.19
0.142E+06 0.142E+06 0.197E+06 0.00 0.00 0.00
3277.6 3277.6 2959.5 284.9 284.9 257.3
557.9 557.9 503.8
0.0 0.0 459.0 449.0

(5) SANDSTONE 2
1.22e+06 1.22e+06 1.22e+06 0.20 0.20 0.20
0.51e+06 0.51e+06 0.51e+06 0.0 0.0 134.0
6317.0 6317.0 6317.0 480.0 480.0 480.0
1005.0 1005.0 1005.0
0.0 0.0 908.0 171.0
(5) SANDSTONE 2
0.639E+06 0.639E+06 0.563E+06 0.25 0.11 0.10
0.172E+06 0.172E+06 0.264E+06 0.00 0.00 0.00
3307.6 3307.6 2912.9 251.3 251.3 221.3
526.4 526.4 463.6
0.0 0.0 908.0 171.0

(6) SHALE 2
0.87e+06 0.87e+06 0.87e+06 0.22 0.22 0.22
0.36e+06 0.36e+06 0.36e+06 0.0 0.0 144.0
5292.0 5292.0 5292.0 460.0 460.0 460.0
908.0 908.0 908.0
0.0 0.0 1079.0 420.0
(6) SHALE 2
0.527E+06 0.527E+06 0.474E+06 0.25 0.14 0.12
0.151E+06 0.151E+06 0.217E+06 0.00 0.00 0.00
3204.8 3204.7 2884.8 278.6 278.6 250.8
545.5 545.5 491.0
0.0 0.0 1079.0 420.0

(7) TRONA 1
4.08e+06 4.08e+06 4.08e+06 0.25 0.25 0.25
1.63e+06 1.63e+06 1.63e+06 0.0 0.0 134.0
6804.0 6804.0 6804.0 410.0 410.0 410.0
1021.0 1021.0 1021.0
0.0 0.0 1499.0 10.0
(7) TRONA 1
0.101E+07 0.101E+07 0.832E+06 0.29 0.07 0.05
0.223E+06 0.223E+06 0.411E+06 0.00 0.00 0.00
1691.5 1691.4 1388.2 101.9 101.9 83.7
239.7 239.7 196.7
0.0 0.0 1499.0 10.0

(8) OIL SHALE 2
0.82e+06 0.82e+06 0.82e+06 0.33 0.33 0.33
0.31e+06 0.31e+06 0.31e+06 0.0 0.0 142.0
5292.0 5292.0 5292.0 460.0 460.0 460.0
908.0 908.0 908.0
0.0 0.0 1509.0 89.0
(8) OIL SHALE 2
0.508E+06 0.508E+06 0.459E+06 0.32 0.21 0.19
0.142E+06 0.142E+06 0.197E+06 0.00 0.00 0.00
3277.6 3277.6 2959.5 284.9 284.9 257.3
557.9 557.9 503.8
0.0 0.0 1509.0 89.0

(9) TRONA 2
4.08e+06 4.08e+06 4.08e+06 0.25 0.25 0.25
1.63e+06 1.63e+06 1.63e+06 0.0 0.0 134.0
6804.0 6804.0 6804.0 410.0 410.0 410.0
1021.0 1021.0 1021.0
0.0 0.0 1598.0 10.0
(9) TRONA 2
0.101E+07 0.101E+07 0.832E+06 0.29 0.07 0.05
0.223E+06 0.223E+06 0.411E+06 0.00 0.00 0.00
1691.5 1691.4 1388.2 101.9 101.9 83.7
239.7 239.7 196.7
0.0 0.0 1598.0 10.0

(10) SHALE 3
0.87e+06 0.87e+06 0.87e+06 0.22 0.22 0.22
0.36e+06 0.36e+06 0.36e+06 0.0 0.0 144.0
5292.0 5292.0 5292.0 460.0 460.0 460.0
908.0 908.0 908.0
0.0 0.0 1608.0 190.0
(10) SHALE 3
0.527E+06 0.527E+06 0.474E+06 0.25 0.14 0.12
0.151E+06 0.151E+06 0.217E+06 0.00 0.00 0.00
3204.8 3204.7 2884.8 278.6 278.6 250.8
545.5 545.5 491.0
0.0 0.0 1608.0 190.0

```
(11) SANDSTONE 3
2.03e+06  2.03e+06  2.03e+06      0.23      0.23      0.23
0.82e+06  0.82e+06  0.82e+06       0.0       0.0     140.0
  6317.0    6317.0    6317.0     480.0     480.0     480.0
  1005.0    1005.0    1005.0
     0.0       0.0    1798.0      49.0
(11) SANDSTONE 3
 0.809E+06   0.809E+06   0.690E+06        0.28        0.10        0.08
 0.197E+06   0.197E+06   0.328E+06        0.00        0.00        0.00
    2518.5      2518.4      2146.6       191.4       191.4       163.1
     400.8       400.8       341.6
       0.0         0.0      1798.0        49.0

(12) TIPTON FM
0.87e+06  0.87e+06  0.87e+06      0.22      0.22      0.22
0.36e+06  0.36e+06  0.36e+06       0.0       0.0     144.0
  5292.0    5292.0    5292.0     460.0     460.0     460.0
   908.0     908.0     908.0
     0.0       0.0    1847.0    3313.0
(12) TIPTON FM
 0.527E+06   0.527E+06   0.474E+06        0.25        0.14        0.12
 0.151E+06   0.151E+06   0.217E+06        0.00        0.00        0.00
    3204.8      3204.7      2884.8       278.6       278.6       250.8
     545.5       545.5       491.0
       0.0         0.0      1847.0      3313.0
```

Figure 15 Comparison of intact and jointed rock in case of 12 formations each with the same five joint sets. All rock formations are flat.

Table 1 show the equivalent elastic properties of the major formations obtained at a much larger REV size than the 70 size REV used as a check on the 30 size REV. The differences are still small and only a few percent. Recall that Figure 6 shows the six moduli, three Young's moduli and three shear moduli, as functions of REV size. Little change occurs beyond the maximum joint spacing of 30 ft or a ratio of one on the x-axis. A similar result holds for equivalent strengths.

Table 1 Equivalent elastic properties (GPa/10^6 psi except for Poisson's ratios)*.

| Property/ Rock Type | E1 | E2 | E3 | PR12 | PR23 | PR31 | G12 | G23 | G31 |
|---|---|---|---|---|---|---|---|---|---|
| SHALE | 3.76/ 0.545 | 3.76/ 0.545 | 3.17/ 0.460 | 0.246 | 0.142 | 0.120 | 1.03/ 0.149 | 1.03/ 0.149 | 1.52/ 0.220 |
| MUDSTONE | 4.65/ 0.674 | 4.65/ 0.674 | 3.79/ 0.549 | 0.242 | 0.112 | 0.091 | 1.18/ 0.171 | 1.18/ 0.171 | 1.87/ 0.271 |
| SANDSTONE | 5.88/ 0.853 | /5.88 0.853 | 4.55/ 0.660 | 0.266 | 0.100 | 0.078 | 1.33/ 0.193 | /1.33 0.193 | 2.32/ 0.336 |
| OIL SHALE | 3.61/ 0.524 | 3.61/ 0.524 | 307/ 0.445 | 0.316 | 0.215 | 0.183 | 0.97/ 0.140 | 0.97/ 0.140 | 1.38/ 0.200 |
| TRONA | 7.45/ 1.08 | 7.45/ 1.08 | 5.45/ 0.790 | 0.282 | 0.070 | 0.049 | 1.51/ 0.219 | 1.51/ 0.219 | 2.91/ 0.422 |

* from Pariseau (2017)

A comparison of pillars without joints and with joints illustrates the importance of considering not only intact rock based on laboratory tests but also on joints as mapped in the mine. Figure 16 shows a side by side comparisons of element safety factor distributions in the neighborhood of a typical pillar in a large array of pillars in an underground trona mine. The room and pillar safety factor distributions are without joints based on laboratory rock properties of all formations present in the geological column. The safety factor distributions with joints are based on *equivalent properties* of the same formations. Figure 17 shows a comparison in plan views.

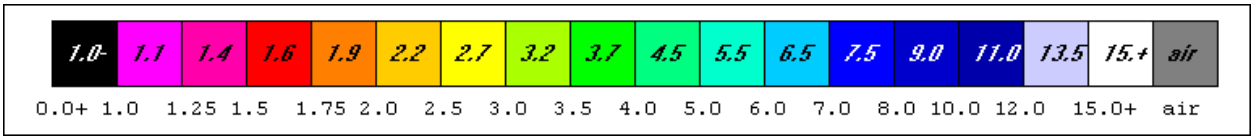


Factor of Safety Color Scale

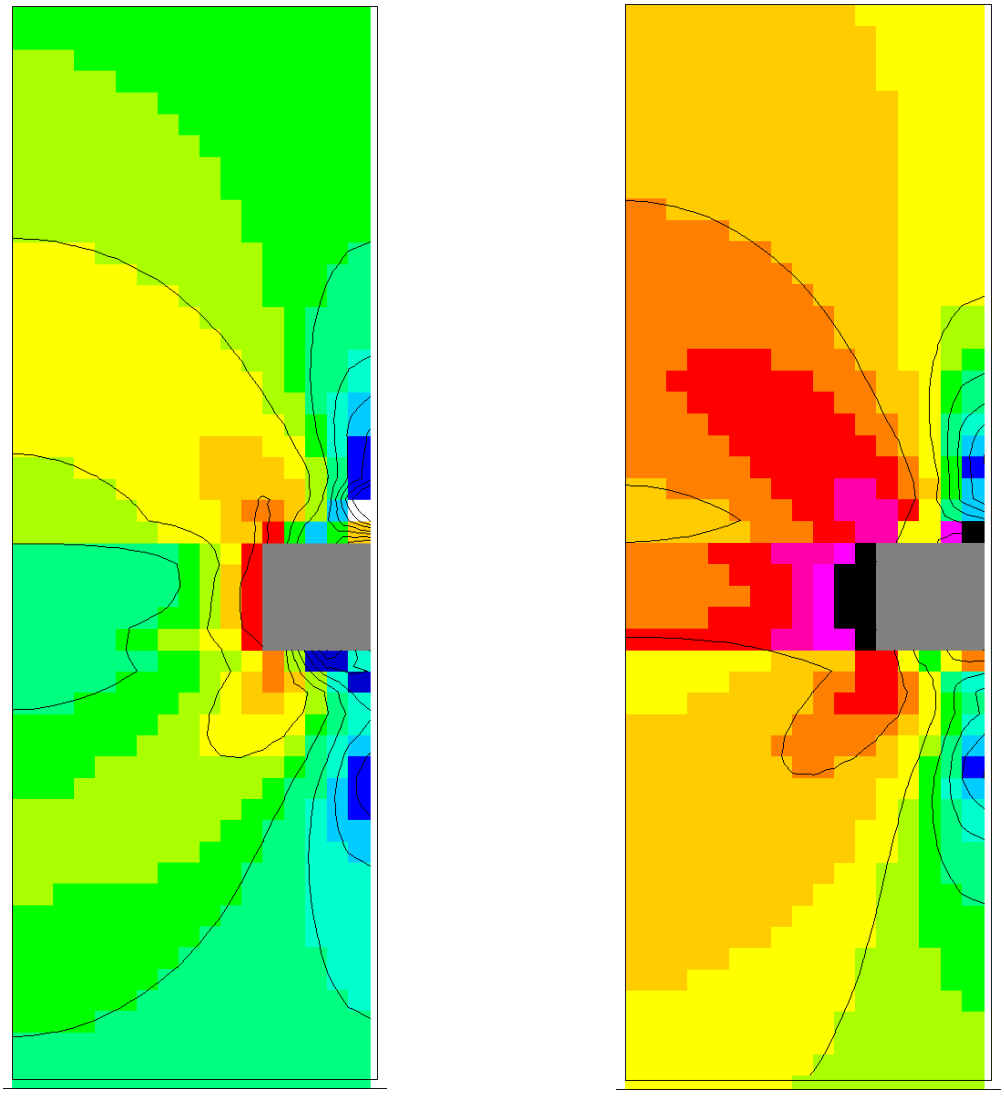

(a) (b)

Figure 16 Element safety factor distributions in a vertical section about a square pillar in an underground room and pillar trona mine: (a) no joints, (b) with joints. Area extraction ratio is 51%. Entries and crosscuts are 20 ft wide; the pillar is square 46.7x46.7 ft. Mining height is 10 ft. Use of symmetry allows for showing only one-half of the pillar in vertical section and only one-half of the entries and crosscuts.

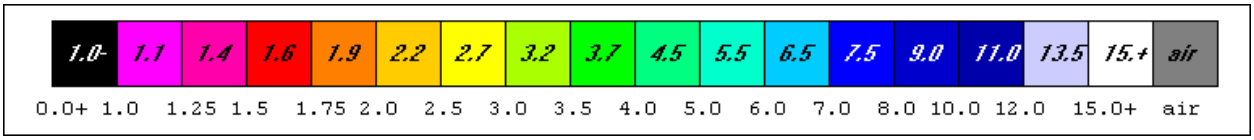


Factor of Safety Color Scale

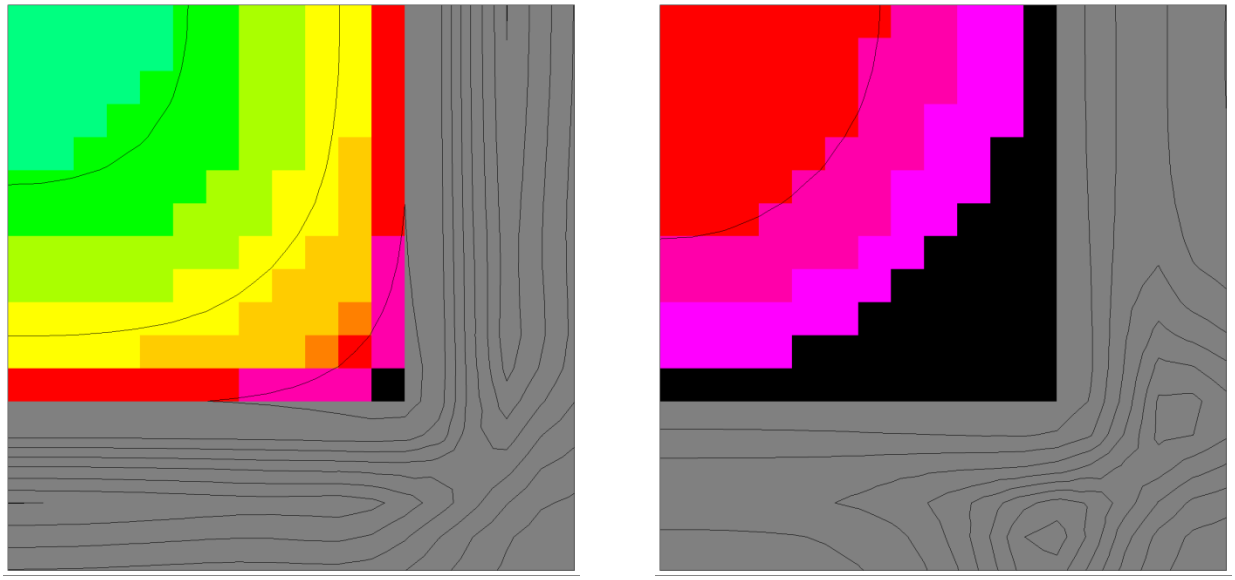

(a) (b)

Figure 17 Element safety factor distributions in plan views: (a) no joints, (b) with joints. Area extraction ratio is 51%. Entries and crosscuts are 20 ft wide; the pillar is square 46.7x46.7 ft. Mining height is 10 ft. Use of symmetry allows for showing only one-fourth of the pillar in plan view and only one-half of the entries and crosscuts.

Clearly joints matter. Additional analyses of pillars in underground trona mining in southern Wyoming are presented in the User Manual as Example 2 of Problem type 5, Pillar Safety(Room & Pillar Mining) beginning on page 80.

Another comparison of element safety factor distributions computed without joints and with *joint equivalent properties* is shown in Figures 18 and 19. These figures are associated with Problem 1 Main Entry Safety. Details of the Main Entry Problem without joints are presented in the User Manual and relate to the Trail Mountain Mine in the Wasatch coal field in central Utah.

There are eight main entries 20 ft in width in the problem. Pillars are 60 ft wide and 80 ft long. Mining height is full seam height at 10 ft.

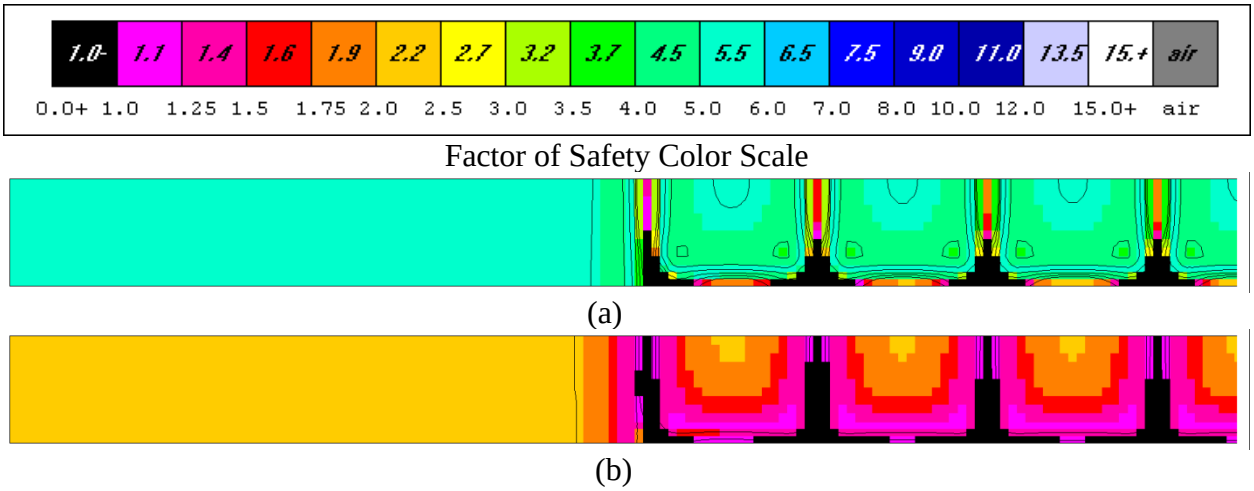


Factor of Safety Color Scale

(a)

(b)

Figure 18 Element safety factor distributions in plan view: (a) without joints at seam floor, (b) with joints

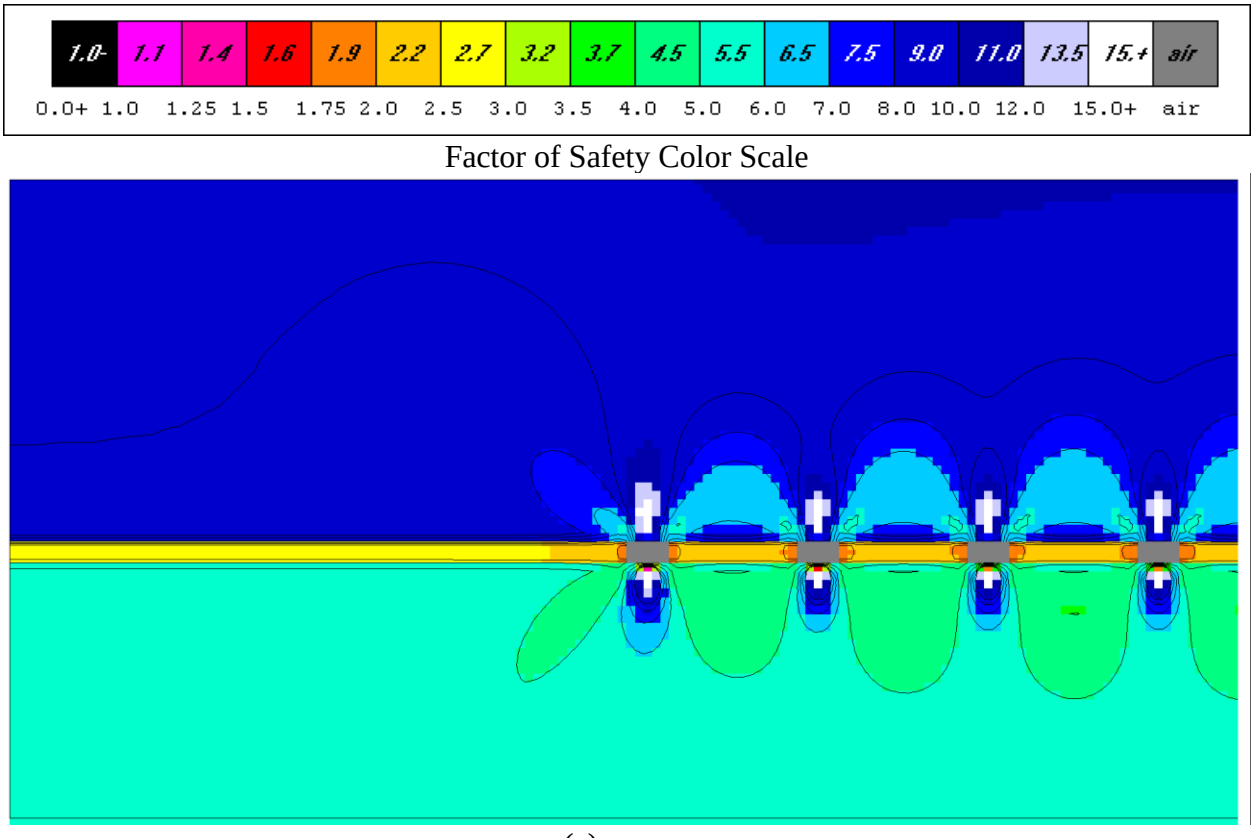


Factor of Safety Color Scale

(a)

(b)

Figure 19 Element safety factor distributions in vertical section close up: (a) no joints, (b) with joints. Seam height is 10 ft. Entries (gray) are 20 ft wide.

**Numerical Experiments** A third example of the influence of scaling moduli and strengths and equivalent joint properties is a drift at the former Homestake Mine. Figure 20 compares three cases: (a) intact rock, (b) scaling moduli by 0.25 and strengths by 0.5, and (c) equivalent jointed rock properties based on foliation and joint mapping to produce four discontinuities ("joints"). The issue of interest is whether direct scaling of moduli and strengths from mine measurements and observations compare favorably with equivalent properties moduli and strengths. In this regard, equivalent strengths may be based on a strain to failure criterion or on an energy at failure criterion. In a mine, displacement measurements are used to "calibrate" finite element models with respect to elastic moduli because moduli largely control displacements. Loss of multiple point extensometer anchors enable an estimate of extent of yielding and thus constrain strengths. In this way strength scale factors may be estimated from mine observations. However, the two scale factors are not independent. A simple energy at failure criterion was used to relate the two scale factors at the Homestake Mine. Comparisons of element safety factor distributions aid in evaluating the two criteria that relate moduli and strength scale factors.

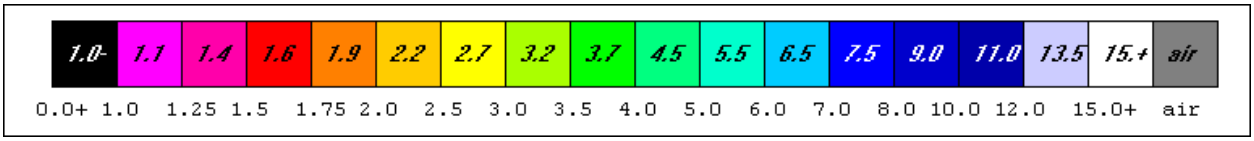


Factor of Safety Color Scale

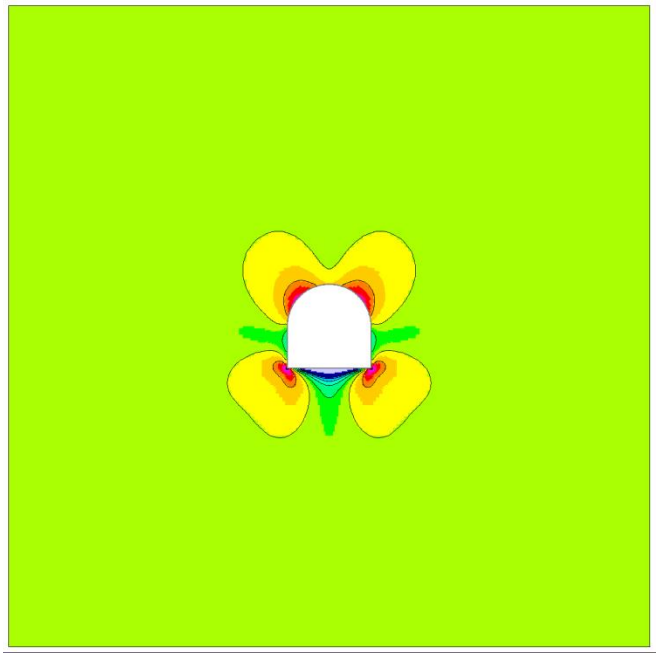

(a)

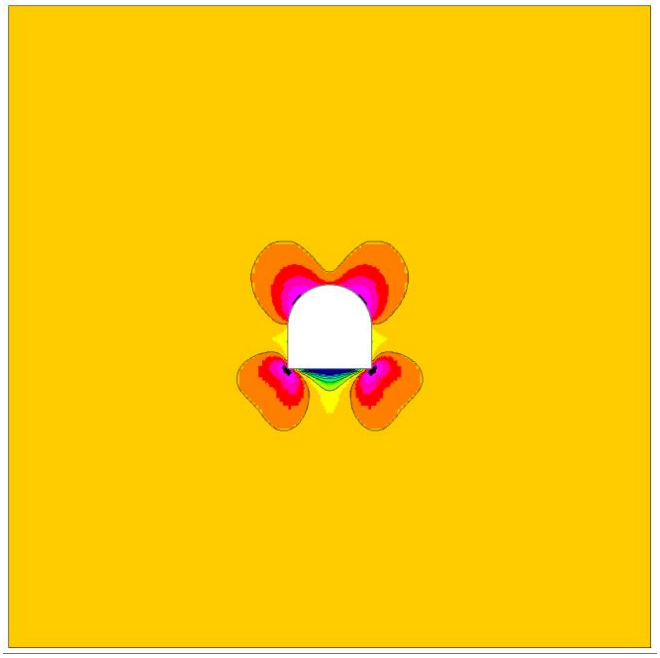

(b)

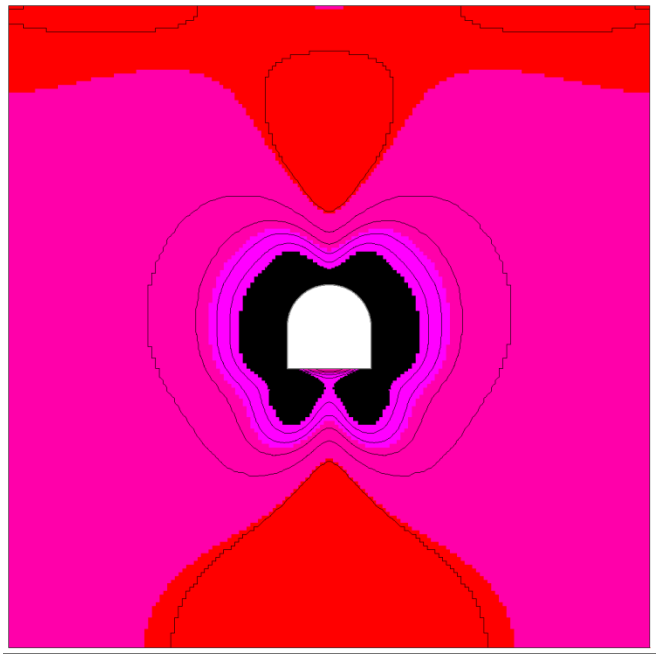

(c)

Figure 20 Element safety factor distributions about an 8x8 ft drift at the former Homestake Mine in the Poorman formation on the 4850 Level: (a) intact rock, (b) scaled rock moduli and strengths, (c) equivalent jointed rock mass properties.

The joints clearly have an enormous effect on the analysis of safety and stability of a drift in the Poorman formation as seen in Figure 20(c). Scaling, that is, reducing the elastic moduli and strengths also has a noticeable effect seen in Figure 20(b) relative to intact rock in Figure 20(a). The equivalent properties result in Figure 20(c) may be pessimistic because of the inclusion of foliation as two sets of discontinuities when only two actual joint sets were in the listing of "joints".

A reexamination of drift stability using only the two joint sets is indicated by the results in Figure 20. In fact, on-site visits show drifts in the Poorman formation on the 4850 Level to be stable, although bolting and screening are done. In Figure 21, the two foliation sets are eliminated and only the two joint sets are used to compute equivalent properties. Comparison of Figure 21 with Figure 20 (c) shows a significant difference. The two joint set equivalent properties used in computing the results in Figure 21 appear much more realistic in keeping with onsite observation.

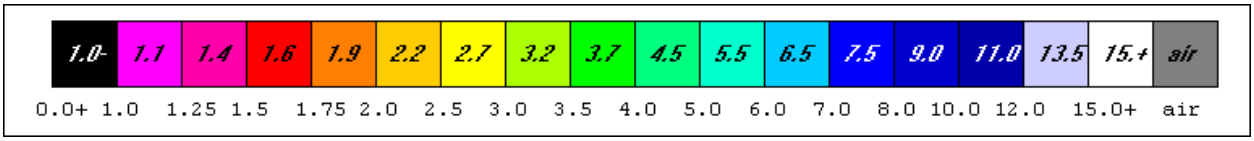


Factor of Safety Color Scale

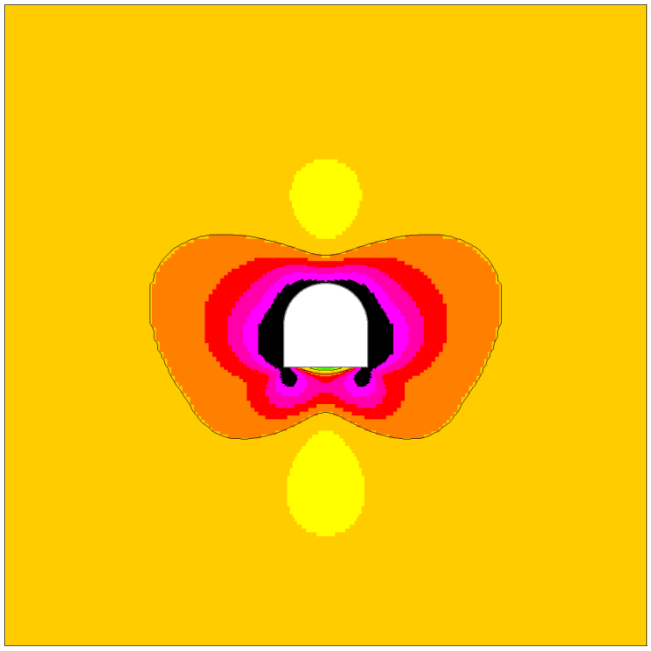

Figure 21 Element safety factor distribution about an 8x8 ft drift at the former Homestake Mine in the Poorman formation on the 4850 Level using equivalent jointed rock mass properties based on just two joint sets and strain to failure guidance. The two foliations as joint sets are omitted.

Figure 22 show a side by side comparison of element safety factor distribution using equivalent properties based on two joint sets and properties based on scale factors and mine observations of displacements and casual observations onsite. The background safety factor color away from the influence of the drift is the same (2.2 light orange). Near the drift there is more yielding in the case of equivalent properties (1.0 black). The red zone (1.5) is also more extensive in the case of equivalent properties. The elastic moduli are higher in the case of scaling, almost twice as high than in the case of equivalent properties. Interestingly, strengths are roughly the same in both cases

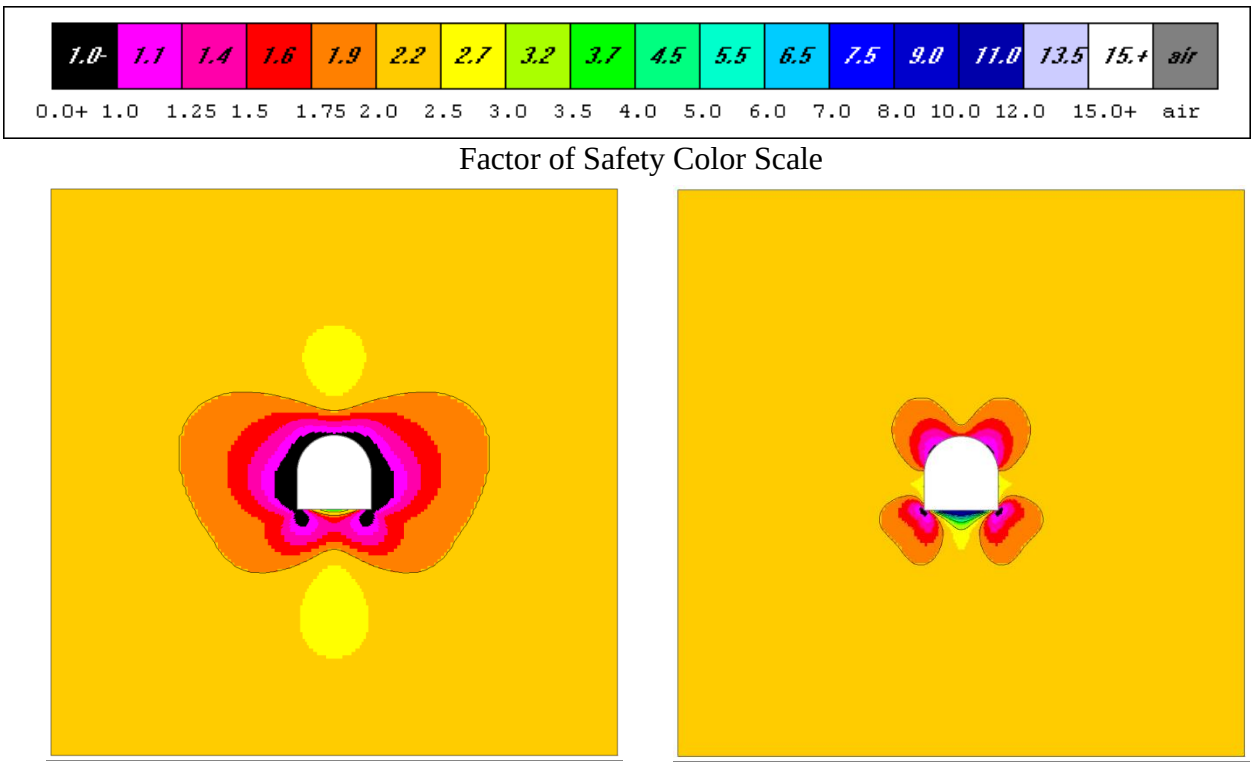


Figure 22 A side by side comparison of element safety factor distribution: (a) equivalent properties based on strain to failure and two joint sets, (b) using scale factors of 0.25 for moduli and 0.5 for strengths.

Figure 23 shows the distribution of element safety factors when two joint sets are embedded directly into the finite element mesh. The drift is 8 ft wide and 8 ft high. Joints are spaced 2.4 ft and 4.4 ft in joints sets 1 and 2, respectively. The pattern of jointing is evident in the figure. However, element safety factors in the immediate vicinity of the drift wall while low (red) in places, the drift is not threatened. The overall pattern of element safety factors near the drift is similar to the pattern in Figure 22(b) obtained using scale factors for moduli and strengths. This result supports the notion of conservatism in the use of equivalent properties for finite element analysis of excavation safety. In this regard, the option of scaling moduli and strengths is still available when using equivalent properties. If equivalent moduli or strengths are considered to be too low, one can use scale factors to increase moduli or strengths or both, for that matter.

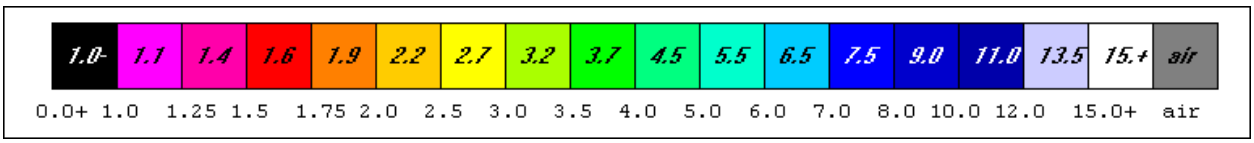


Factor of Safety Color Scale

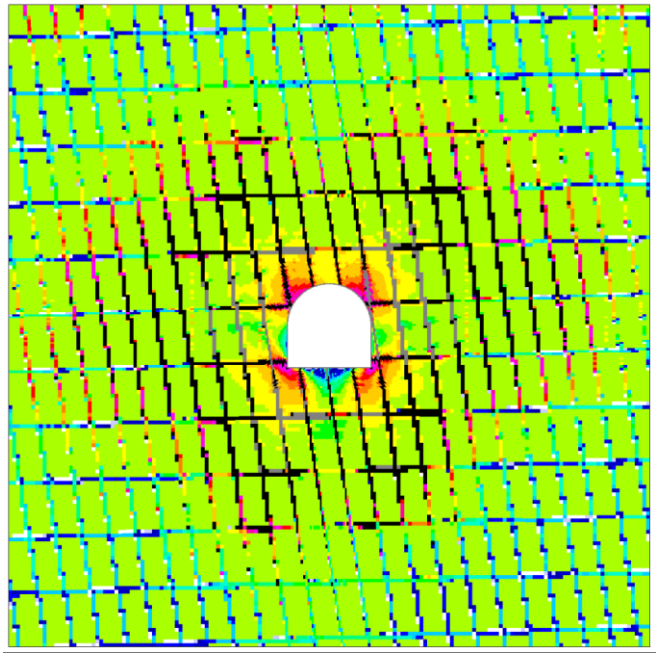

Figure 23 Element safety factor distribution when two joint sets are embedded in the finite element mesh.

Figure 24 shows the distribution of element safety factors when two joint sets are present and equivalent properties are used but with increased equivalent strengths by using scale factors of cfac=1.5 and cfac=2.0, respectively. Doubling the equivalent strengths brings the distribution much closer to that using scale factors alone.

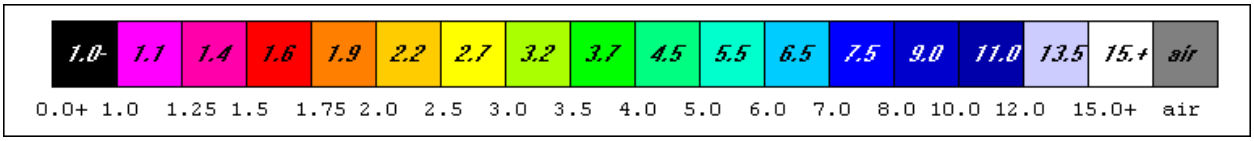


Safety Factor Color Scale

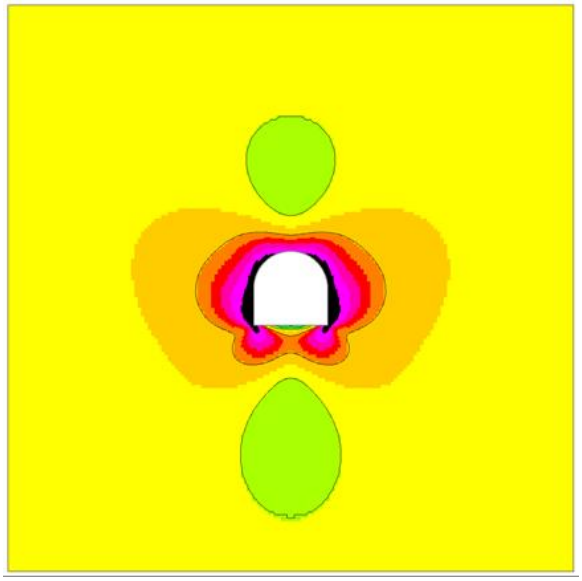

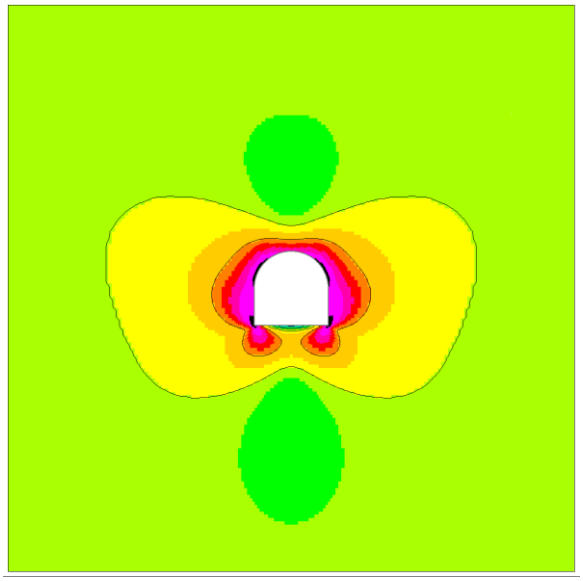

(a) (b)

Figure 24 Element safety factor distributions using equivalent properties and strength scale factors: (a) of 1.5 and (b) of 2.0.

**Results of Numerical Experiments** As a reminder, strengths in equivalent properties computations may be based on the assumption of the same strain to failure in the laboratory and in the field. An alternative computation of equivalent strengths may be based on a simple energy scaling scheme. This scheme was used in arriving at moduli and strength scale factors of 0.25 and 0.50, respectively. This computation implies that the ratio of strengths is the square root of the ratio of moduli. Thus, if the ratio of moduli is ¼, then the ratio of strengths is ½. Ratio refers to the ratio of laboratory to field scale values. Figure 25 compares element safety factor distributions using the energy scaling guide for computing equivalent strengths with direct scaling from mine observations.

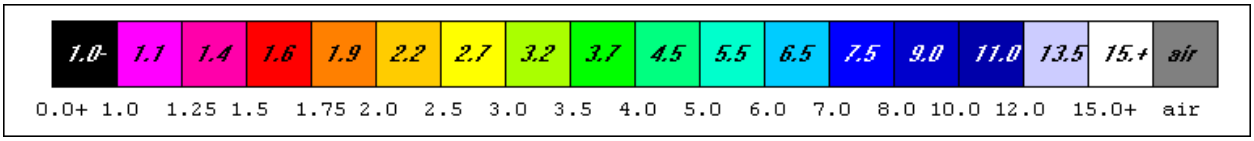


Factor of Safety Color Scale

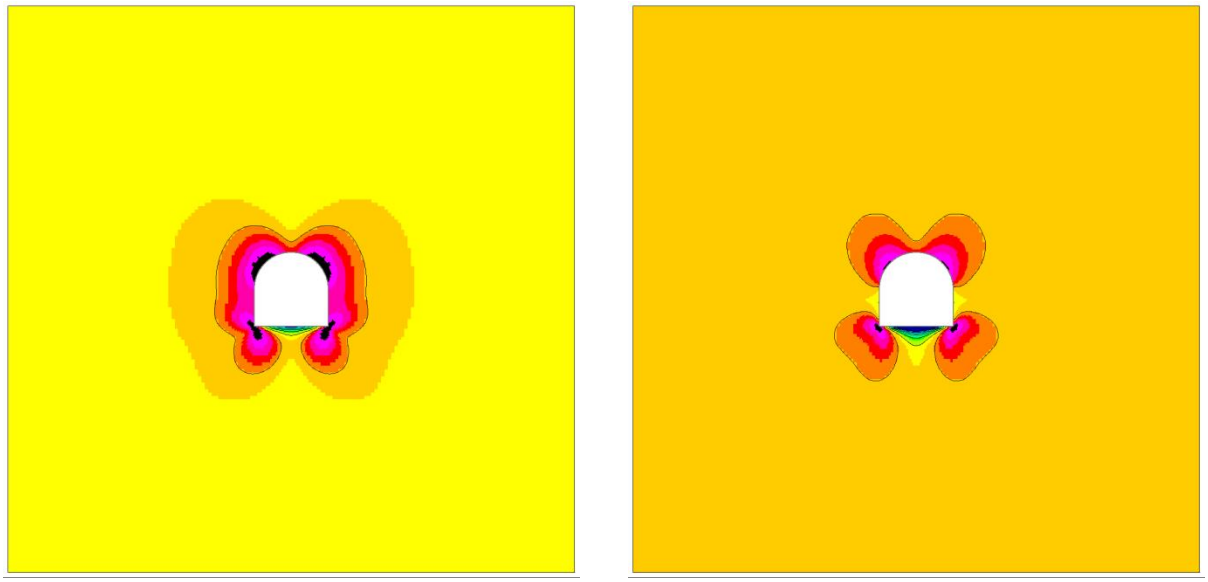

(a) (b)

Figure 25 Factor of safety distributions about an 8x8 drift in the Poorman Formation at the former Homestake Mine: (a) using equivalent properties based on an energy equivalent rule, (b) using scaling factors for moduli and strengths in conjunction with mine observations.

The differences between Figure 25(a) and (b) are small and of no practical consequence for engineering design it would seem.

Thus, the results in Figure 25 and Figure 22 indicate that the use of an energy guide for equivalent strengths is preferable to a strain to failure guide.

Figure 26 presents a side by side comparison of element safety factor distributions about a drift and crosscut in the Poorman formation at the former Homestake Mines. The drift and crosscut have the same 8x8 ft arched back cross-section. The comparison indicates the crosscut is less threatened than the drift in keeping with visual observation at the mine. Orientation with respect to foliation is important, but to be sure, orientation with respect to the preexcavation stress field is also important. Both factors enter comparisons of drift and crosscut.

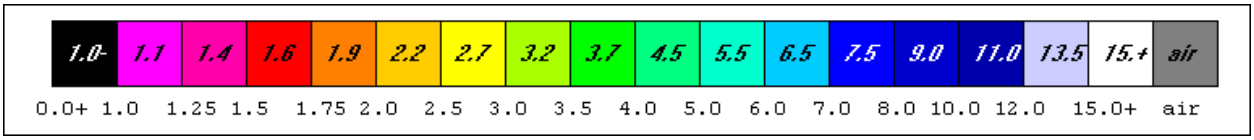


Factor of Safety Color Code

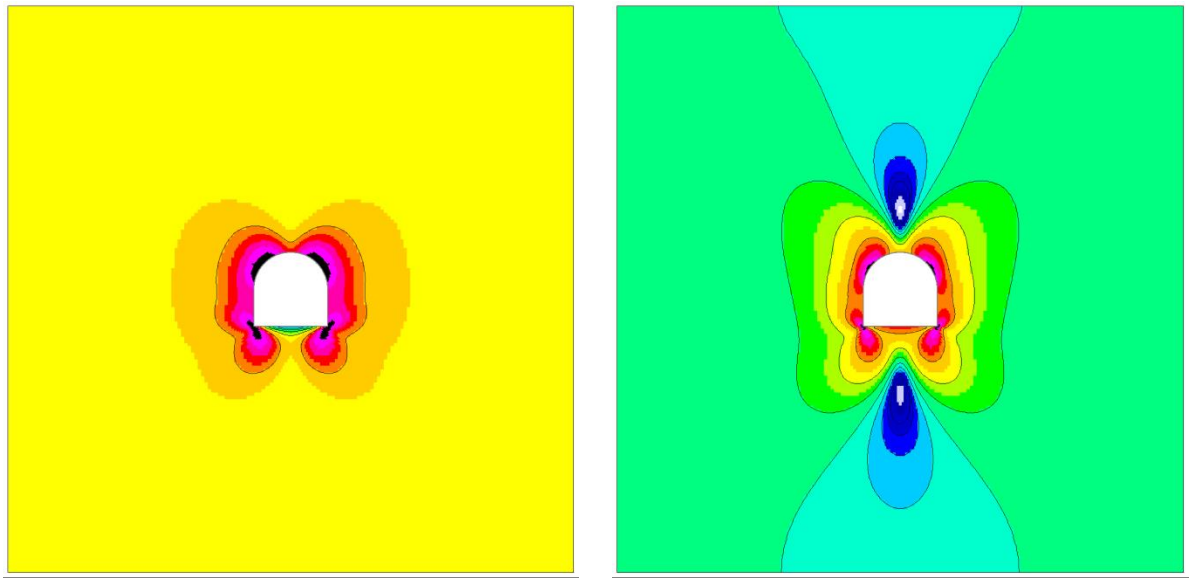

(a) (b)

Figure 26 Element safety factors about an 8x8 ft arched back drift (a) and crosscut (b) using equivalent properties with energy to failure for strengths rather than strain to failure. Ribs are in red (fs=1.5) in the drift where some floor failure and back failure are indicated (black). Crosscut back and floor are mostly in red (fs=1.5). Overall the crosscut appears less threatened than the drift.

Figure 27 is a side by side comparison of safety factor distributions about crosscuts, one based on scaling moduli and strengths directly using scale factors of 0.25 for moduli and 0.5 for strengths, the other based on equivalent properties using an energy guide to strength estimation. Direct scaling appears more optimistic than equivalent properties results in the figure. This result is plainly evident in the region away from the crosscut where direct scaling indicates blue (fs=8) and equivalent properties indicates green (fs=4.5). Near the crosscut wall, direct scaling shows only a few elements yielding (black); equivalent properties results show a few elements yielding in the floor and also in the back. Overall, the equivalent properties results are "conservative" relative to direct scaling. A similar conclusion was reached in the case of drifts in the Poorman formation.

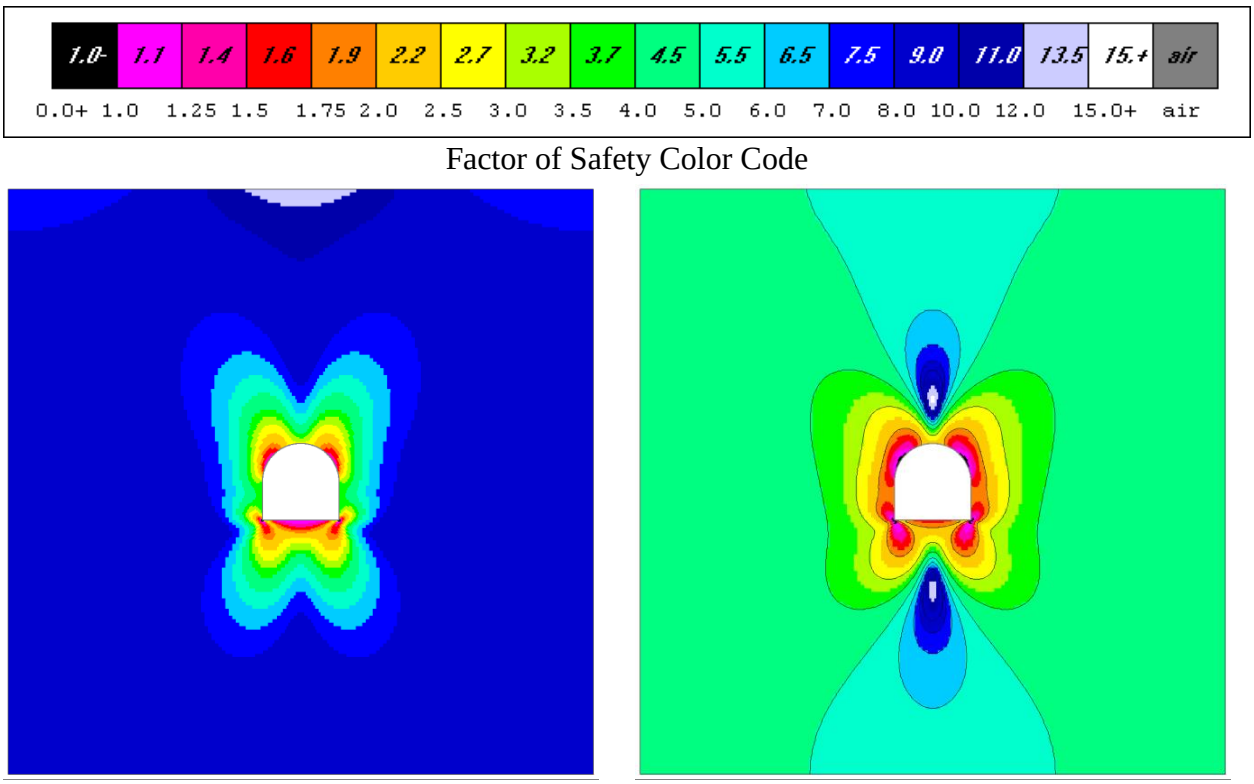


Figure 27 Element safety factors about an 8x8 ft arched back crosscut: (a) using direct scaling (b) using equivalent properties with energy to failure for strengths rather than strain to failure.

**Summary** Computation of equivalent properties of jointed rock using the finite element program UT3PCJ requires a *Step 1j* that follows the usual *Step 1* and precedes *Step 2* in the usual three steps to a finite element analysis. *Step 1j* requires preparation of a jointed rock properties file that contains joint set and intact rock properties. This file is the properties file for a finite element runstream that is similar to an ordinary finite element runstream, but only one element is involved. This one element is a cube with edge length at least as large as the maximum joint spacing in the joint sets listed in the properties file. The finite element program UT3PCJ is used for generating equivalent properties, elastic moduli and strengths (based on energy to failure guidance). Each rock formation present in the geological column is processed in similar fashion. Each formation equivalent properties file is then placed sequentially in an equivalent property file for finite element analysis using the program UT3PC. Mesh plotting before analysis is recommended. Plotting of element safety factors for design guidance after program execution can be done in the usual manner.

## References - Jointed Rock Models

Hill, R. (1963) Elastic Properties of Reinforced Solids: Some Theoretical Principles. *J Mech Phys Solids*.Vol 11, pp 357-372.

Hudson, J. A. (1980) *The Excitation and Propagation of Elastic Waves*. Cambridge University Press.

Lekhnitiskii (1963) *Theory of Elasticity of an Anisotropic Elastic Body*. Holden-Day, San Francisco, pgs 404.

Pariseau, W. G. and H. Moon (1988) "Elastic Moduli of Well-jointed Rock Masses." *Numerical Methods in Geomechanics (Innsbruck,* Balkema, Rotterdam, pp 815-822.

Pariseau, W. G. (1993) "Equivalent Properties of a Jointed Biot Material", *Int'l. J. Rock Mech. Min. Sci. & Geomech. Abstr.*, Vol. 30, No. 7, pp 1151-1157.

Pariseau, W. G. (1995)"Non-representative Volume Element Modeling of Equivalent Jointed Rock Mass Properties". *Proc. Mechanics of Jointed and Faulted Rock – 2.* Balkema, Rotterdam, pp 563-568.

Pariseau, W. G. (1999) "An Equivalent Plasticity Theory for Jointed Rock Masses". *Int'l J. Rock Mech. Mng. Sci.*, Vol. 36, No.7, pp. 907-918.

Pariseau, W. G., D. Tesarik and T. Trancynger, (2012) "Rock Mechanics of the Davis Detector Cavern", SME Annual Meeting, Seattle, Washington, February 19-22, 2012, Preprint CD 12-022 and SME Transactions, Vol. 332, pp 2-20.

Pariseau, W. G. (2017) "Comparison of Underground Coal and Trona Mine Seismicity". Preprint 17-027, SME Annual Meeting & Exhibit, February 19-22, 2017 Denver, Colorado.

Pariseau, W. G. (2022) "User Manual **for a T**hree-dimensional Finite Element Program UT3PC (2nd edition) A Fundamental Approach to Design of Coal Mine Entries, Barrier Pillars, Bleeder Entries, Interpanel Barrier Pillars, Pillars and Rooms in Room and Pillar Mines, Shafts and Tunnels." Website UT3PC.net.

END

## APPENDIX VIII EXAMPLES of JOINT EFFECTS

This appendix presents analyses outcomes using equivalent properties of jointed rock formations in case of all seven problem types addressed in this User Manual. Details of computations leading to equivalent properties, elastic moduli and strengths, are presented in APPENDIX VII. Comparisons are made here between intact and jointed rock formation cases to allow for assessment of joint effects on the distribution of element safety factors. In this regard, distributions of element safety factors in graphic form show whether yielding occurs and if so,

the extent of yielding, thus presenting useful design guidance at a glance for a proposed excavation layout.

As a reminder, the study results in the previous appendix indicated that energy to failure was preferable to strain to failure as a guide to equivalent strengths. An energy to failure guide to strength that is used in finite element analysis without joints is also used for equivalent strength in the jointed rock examples following.

In case of jointed rock, the computation of equivalent properties requires a change in the usual three step process where *Step 1* requires specification of material properties of intact rock; *Step 2* involves mesh generation, and *Step 3* is execution of a finite element analysis. The change is an additional *Step 1j* that follows the usual *Step 1* but precedes *Step 2*. This additional step involves computation of equivalent material properties in case of jointed rock formations and uses a finite element program UT3PCJ. With or without joints, *Step 3* is done using the finite element program UT3PC.

**Problem 1**This problem example concerns safety of main entries. The problem is presented in detail when joints are absent in the User Manual. When several formations are in the geological column that are specified in a material properties file for a finite element analysis, a *Step 1j* must be taken to obtain equivalent properties for each formation that is considered jointed. Surface outcrops are accessible for joint mapping and so are seam-level strata. Exploration borehole mapping of joints is also possible and provides a means of obtaining joint data between surface and the mining horizon. If joint data are lacking, then improvisation is necessary before taking *Step 1j* and computing equivalent properties. For example, surface jointing may be assumed to extend to the mining horizon and below. *Step 1j* for equivalent properties is still necessary for each formation because the rock type enters the calculation (Pariseau 2017). Thus, this file requires material properties of the formations present as well as joint properties for each formation. *Step 1j* is thus an addition of sorts to *Step1* leading to strata properties used in analysis (*Step 3*). Mesh generation, *Step 2*, may be done before or after generating equivalent properties.

An easy procedure is then to do *Step 1* preparing a material property file as if joints were not present. The file in this example consists of isotropic rock and is the same file used in Problem 1,Example 1, in the User Manual. Thus,

```
NLYRS = 7
NSEAM = 5
  (1) North Horn  N=2 (DP2) & wt, 2000-11000, 1/16/2022
  2.60e+06  2.60e+06  2.60e+06      0.26      0.26      0.26
  1.03e+06  1.03e+06  1.03e+06       0.0       0.0     158.0
   11800.0   11800.0   11800.0     700.0     700.0     700.0
    1659.0    1659.0    1659.0
       0.0       0.0       0.0    100.0
  (2) Price River
  3.20e+06  3.20e+06  3.20e+06      0.26      0.26      0.26
  1.27e+06  1.27e+06  1.27e+06       0.0       0.0     143.0
    9980.0    9980.0    9980.0     380.0     380.0     380.0
    1124.0    1124.0    1124.0
       0.0       0.0     100.0     191.0
```

```
 (3) Castle Gate sandstone
 3.00e+06  3.00e+06  3.00e+06      0.22      0.22      0.22
 1.23e+06  1.23e+06  1.23e+06       0.0       0.0     140.0
   9590.0    9590.0    9590.0     430.0     430.0     430.0
   1170.0    1170.0    1170.0
      0.0       0.0     291.0     190.0
 (4) Blackhawk formation
 4.00e+06  4.00e+06  4.00e+06      0.26      0.26      0.26
 1.59e+06  1.59e+06  1.59e+06       0.0       0.0     155.0
  15710.0   15710.0   15710.0     720.0     720.0     720.0
   1942.0    1942.0    1942.0
      0.0       0.0     481.0     591.0
(5) Hiawatha coal
0.430e+06 0.430e+06 0.430e+06      0.12      0.12      0.12
0.192e+06 0.192e+06 0.192e+06       0.0       0.0      78.0
   4131.0    4131.0    4131.0     280.0     280.0     280.0
    621.0     621.0     621.0
      0.0       0.0    1072.0     10.0
 (6) Starpoint sandstone
 2.60e+06  2.60e+06  2.60e+06      0.22      0.22      0.22
 1.07e+06  1.07e+06  1.07e+06       0.0       0.0     135.0
   9630.0    9630.0    9630.0     360.0     360.0     360.0
   2140.0    2140.0    2140.0
      0.0       0.0    1082.0     200.0
 (7) Mancos Shale
 2.20e+06  2.20e+06  2.20e+06      0.35      0.35      0.35
0.815e+06 0.815e+06 0.815e+06       0.0       0.0     145.0
  10300.0   10300.0   11920.0      60.0      60.0      60.0
    454.0     454.0     454.0
      0.0       0.0    1282.0     628.0
```

Mesh generation *Step 2* may be done next or after generation of the equivalent properties file, but before analysis, of course. Preparation of equivalent properties of jointed strata is done as *Step 1j* using joint and rock properties. Finite element analysis, that is, *Step 3* may be done once *Step 1j* and *Step 2* are complete; equivalent properties are available, and the mesh is generated. Figure 1 illustrates the joint pattern for the mine site.

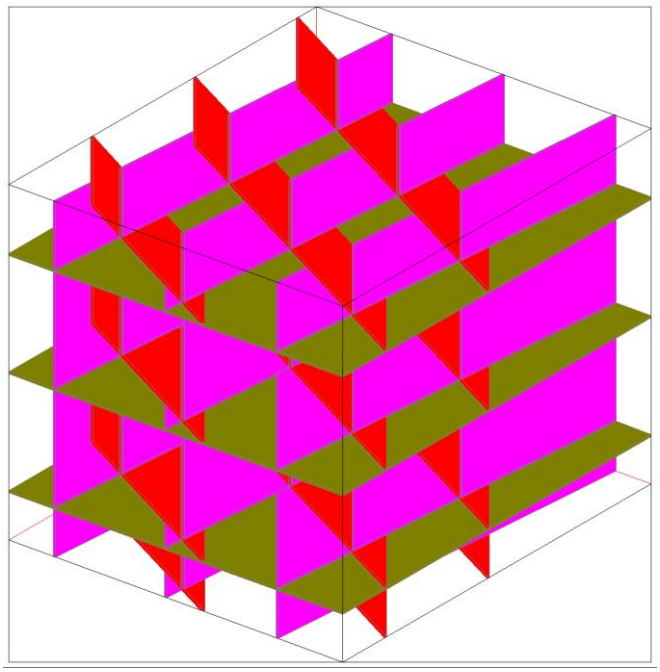

Figue 1 A schematic illustration of the the joint pattern at the mine. Horizontal joints are bedding planes.

Equivalent properties of each formation may be generated sequentially by stacking each set of jointed rock properties one following the other and only using the RUN END statement in the last properties set. An example stacking of jointed properties is shown in Figure 2 where seven rock formations are present. The runstream shown in Figure 2 shows just one element with a dimension equal to the maximum joint spacing of all the joint sets. One load increment assures a runtime of just seconds.

```
Trail Mount w/ Joints 3/22/2022 wgp
TM1.txt
celms.txt
ccrds.txt
none
none
cnsps.txt
aTM1
nelem =       1
nnode =       8
nspec =       8
nmat  =       4
ncut  =       1
ninc  =       1
nsigo =       0
inter =     100
maxit =    1000
nyeld =       2
nelcf =       0
ncave =       0
nfile =       1
npsi  =       1
nrstrt=       0
 error=    1.0000
 orf  =    1.8600
 xfac =   12.0000
 yfac =   12.0000
 zfac =   12.0000
 efac =    1.0000
 cfac =     100.0
 Trail Mount w/ Joints 3/22/2022 wgp
TM2.txt
celms.txt
ccrds.txt
none
none
cnsps.txt
aTM2
nelem =       1
nnode =       8
```

nspec =  8
nmat  =  4
ncut  =  1
ninc  =  1
nsigo =  0
inter =  100
maxit =  1000
nyeld =  2
nelcf =  0
ncave =  0
nfile =  2
npsi  =  1
nrstrt=  0
 error=  1.0000
 orf  =  1.8600
 xfac =  12.0000
 yfac =  12.0000
 zfac =  12.0000
 efac =  1.0000
 cfac =  100.0
 Trail Mount w/ Joints 3/22/2022 wgp
TM3.txt
celms.txt
ccrds.txt
none
none
cnsps.txt
aTM3
nelem =  1
nnode =  8
nspec =  8
nmat  =  4
ncut  =  1
ninc  =  1
nsigo =  0
inter =  100
maxit =  1000
nyeld =  2
nelcf =  0
ncave =  0
nfile =  3
npsi  =  1
nrstrt=  0
 error=  1.0000
 orf  =  1.8600
 xfac =  12.0000
 yfac =  12.0000
 zfac =  12.0000
 efac =  1.0000
 cfac =  100.0
Trail Mount w/ Joints 3/22/2022 wgp
TM4.txt
celms.txt
ccrds.txt
none
none

cnsps.txt
aTM4
nelem =  1
nnode =  8
nspec =  8
nmat  =  4
ncut  =  1
ninc  =  1
nsigo =  0
inter =  100
maxit =  1000
nyeld =  2
nelcf =  0
ncave =  0
nfile =  4
npsi  =  1
nrstrt=  0
 error=  1.0000
 orf  =  1.8600
 xfac =  12.0000
 yfac =  12.0000
 zfac =  12.0000
 efac =  1.0000
 cfac =  100.0
Trail Mount w/ Joints 3/22/2022 wgp
TM5.txt
celms.txt
ccrds.txt
none
none
cnsps.txt
aTM5
nelem =  1
nnode =  8
nspec =  8
nmat  =  4
ncut  =  1
ninc  =  1
nsigo =  0
inter =  100
maxit =  1000
nyeld =  2
nelcf =  0
ncave =  0
nfile =  5
npsi  =  1
nrstrt=  0
 error=  1.0000
 orf  =  1.8600
 xfac =  12.0000
 yfac =  12.0000
 zfac =  12.0000
 efac =  1.0000
 cfac =  100.0
 Trail Mount w/ Joints 3/22/2022 wgp
TM6.txt

celms.txt
ccrds.txt
none
none
cnsps.txt
aTM6
nelem =  1
nnode =  8
nspec =  8
nmat  =  4
ncut  =  1
ninc  =  1
nsigo =  0
inter =  100
maxit =  1000
nyeld =  2
nelcf =  0
ncave =  0
nfile =  6
npsi  =  1
nrstrt=  0
 error=  1.0000
 orf  =  1.8600
 xfac =  12.0000
 yfac =  12.0000
 zfac =  12.0000
 efac =  1.0000
 cfac =  100.0
 Trail Mount w/ Joints 3/22/2022 wgp
TM7.txt
celms.txt
ccrds.txt
none
none
cnsps.txt
aTM7
nelem =  1
nnode =  8
nspec =  8
nmat  =  4
ncut  =  1
ninc  =  1
nsigo =  0
inter =  100
maxit =  1000
nyeld =  2
nelcf =  0
ncave =  0
nfile =  7
npsi  =  1
nrstrt=  0
 error=  1.0000
 orf  =  1.8600
 xfac =  12.0000
 yfac =  12.0000
 zfac =  12.0000

```
 efac =    1.0000
 cfac =     100.0
RUN END
```

where TM1.txt is

```
    1  --(1) joint  N 95 EN=2
  1.25E+04  1.25E+04  1.25E+04      0.20      0.20      0.20
  0.52E+04  0.52E+04  0.52E+04       .00       .00       0.0
     35.80     35.80     35.80      4.97      4.97      4.97
      7.70      7.70      7.70
     95.00      90.0       3.0     -0.10
    2  --(2) joint N 65 W N=2
  1.25E+04  1.25E+04  1.25E+04      0.20      0.20      0.20
  0.52E+04  0.52E+04  0.52E+04       .00       .00       0.0
     35.80     35.80     35.80      4.97      4.97      4.97
      7.70      7.70      7.70
      25.0      90.0       3.0     -0.10
      3  --(3) joint BEDDING PLANES N=2
  1.25E+04  1.25E+04  1.25E+04      0.20      0.20      0.20
  0.52E+04  0.52E+04  0.52E+04       .00       .00       0.0
     35.80     35.80     35.80      4.97      4.97      4.97
      7.70      7.70      7.70
       0.0       0.0       3.0     -0.10
  (1) North Horn  N=2 (DP2) & wt, 2000-11000, 1/16/2017
  2.60e+06  2.60e+06  2.60e+06      0.26      0.26      0.26
  1.03e+06  1.03e+06  1.03e+06       0.0       0.0     158.0
   11800.0   11800.0   11800.0     700.0     700.0     700.0
    1659.0    1659.0    1659.0
       0.0       0.0       0.0     100.0
```

and so on to TM7.txt for Formation 7, the Mancos Shale.

Figure 2 An example of a sequential input file for equivalent properties of seven jointed rock formations (*Step 1j*) in the Wasatch coal field of central Utah.

The equivalent material property file for each formation is saved for the actual finite element analysis of the problem at hand. This file is labeled EQ.txt and is

```
(1) North Horn  N=2 (DP2) & wt, 2000-11000, 1/16/2017
  0.285E+06  0.309E+06  0.354E+06       0.2       0.0       0.0
  0.777E+05  0.734E+05  0.948E+05       0.0       0.0     158.0
     3904.3     4069.8     4351.6     231.6     241.4     258.1
      549.0      572.3      611.9
        0.0        0.0        0.0     100.0
 (2) Price River
  0.291E+06  0.317E+06  0.363E+06       0.2       0.0       0.0
  0.788E+05  0.743E+05  0.965E+05       0.0       0.0     143.0
     3008.1     3138.8     3362.2     114.5     119.5     128.0
      338.9      353.6      378.8
        0.0        0.0      100.0      191.0
 (3) Castle Gate sandstone
  0.289E+06  0.314E+06  0.360E+06       0.2       0.0       0.0
```

```
 0.787E+05  0.742E+05  0.963E+05      0.0      0.0      140.0
   2976.3     3104.7     3324.0     133.5     139.2     149.0
    363.9      379.6      406.4
      0.0        0.0      291.0     190.0
(4) Blackhawk formation
 0.296E+06  0.323E+06  0.372E+06      0.2      0.0        0.0
 0.798E+05  0.752E+05  0.980E+05      0.0      0.0      155.0
   4275.0     4464.8     4790.7     195.9     204.6     219.6
    528.4      551.9      592.1
      0.0        0.0      481.0     591.0
(5) Hiawatha coal
 0.182E+06  0.192E+06  0.207E+06      0.2      0.1        0.1
 0.589E+05  0.565E+05  0.678E+05      0.0      0.0       78.0
   2690.8     2758.4     2867.1     182.4     187.0     194.3
    404.5      414.6      431.0
      0.0        0.0     1072.0      10.0
(6) Starpoint sandstone
 0.285E+06  0.309E+06  0.354E+06      0.2      0.0        0.0
 0.780E+05  0.736E+05  0.952E+05      0.0      0.0      135.0
   3186.4     3321.5     3551.6     119.1     124.2     132.8
    355.7      370.8      396.5
      0.0        0.0     1082.0     200.0
(7) Mancos Shale
 0.279E+06  0.303E+06  0.345E+06      0.2      0.1        0.1
 0.763E+05  0.721E+05  0.926E+05      0.0      0.0      145.0
   3667.4     3819.4     4717.5      21.4      22.2      23.7
    161.6      168.3      193.2
      0.0        0.0     1282.0     628.0
```

where all formations are now anisotropic.

**Importantly**, generation of equivalent jointed rock mass properties is done using the finite element program UT3PCJ, not UT3PC.

An analysis may be done following mesh generation (*Step 2*) using the equivalent material property file. Input for mesh generation in this problem ("mains") is shown in Figure 3 where intact rock properties are used (*matTMnewG.txt*). The use of the material property file *matTMnewG.txt* is a convenience for mesh generation. The mesh is shown in Figures 4 and 5.

| | |
|---|---|
| 1) the name of the material properties (stratigraphic column) file | *matTMnewG.txt* |
| 2) the number of main entries (NMS), | 8 |
| 3) entry and crosscut widths (WE, WC) | 20 20 (ft) |
| 4) pillar width and length (WP, LP) | 60 80 (ft) |
| 5) element width, length, height (EX, EY, EZ) | 4 4 2 (ft) |
| 6) add-in additional stresses Sxx, Syy, Szz, Tyz, Tzx, Txy? | N or n (no). |

Figure 3 Mesh generation input in part using an original (unjointed) material properties file.

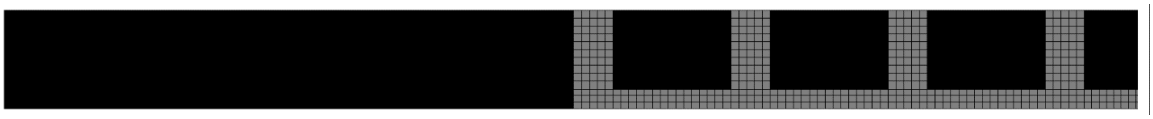

Figure 4 Plan view of seam level mesh of Problem 1. Grey elements are entries and crosscuts. Black is the coal seam. Entries and cross cuts are 20 ft (6.1 m) wide. Pillars are 60x80 ft (18.3x24.4 m). The mesh is symmetric about the right hand side. There are eight entries in the set of mains. There are 791,466 elements in the mesh.

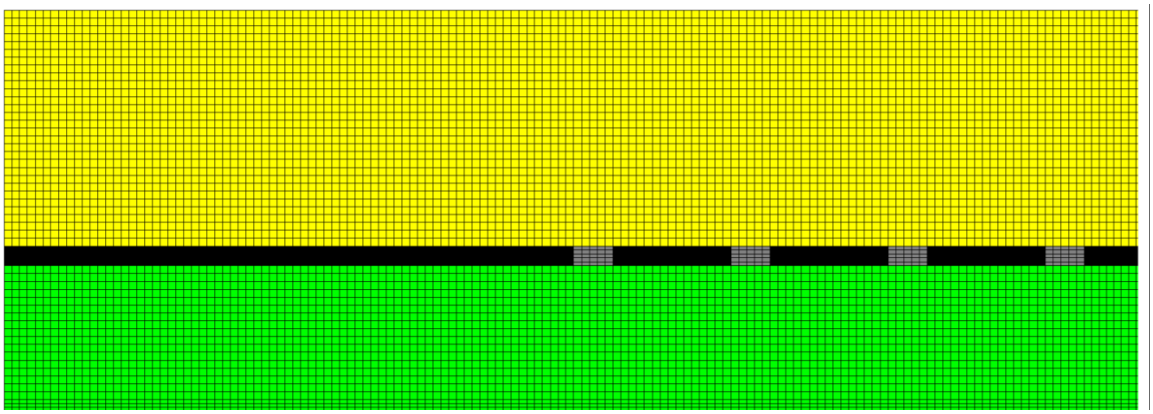

Figure 5 A window near seam level in vertical section. Seam thickness is 10 ft (3.0 m). The mesh is symmetric about the right hand side. There are eight entries in the set of mains. There are 860,244 nodes in the mesh. Colors represent different strata types.

Results of analysis without joints and with joints (equivalent properties) are shown as element safety factor distributions in Figure 6. **Both are done using UT3PC**. Runtime was four hours.

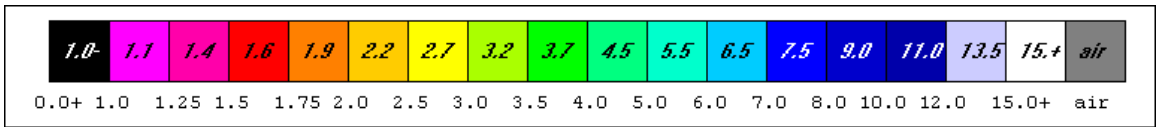


Element Safety Factor Color Scale

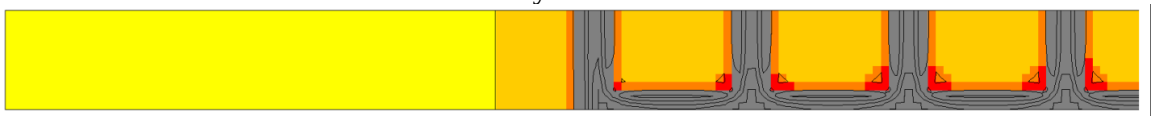

(a) Plan view of element safety factor distribution at pillar mid-height without joints

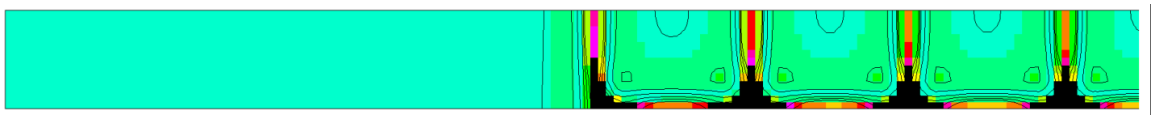

(b) Plan view of element safety factor distribution at seam floor without joints

(c) Plan view of element safety factor distribution at pillar mid-height using equivalent properties

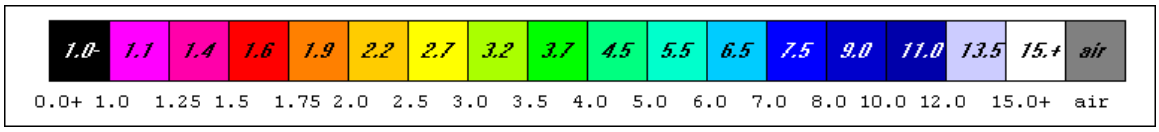


Element Safety Factor Color Scale

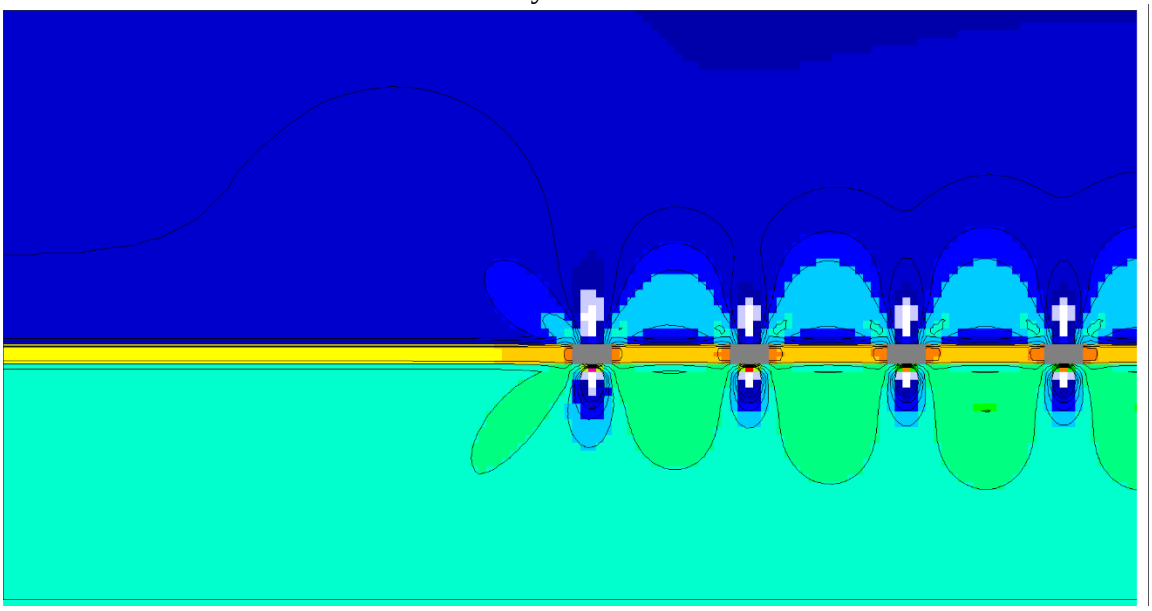

(d) Vertical section window through pillar centers showing element safety factor distribution without joints.

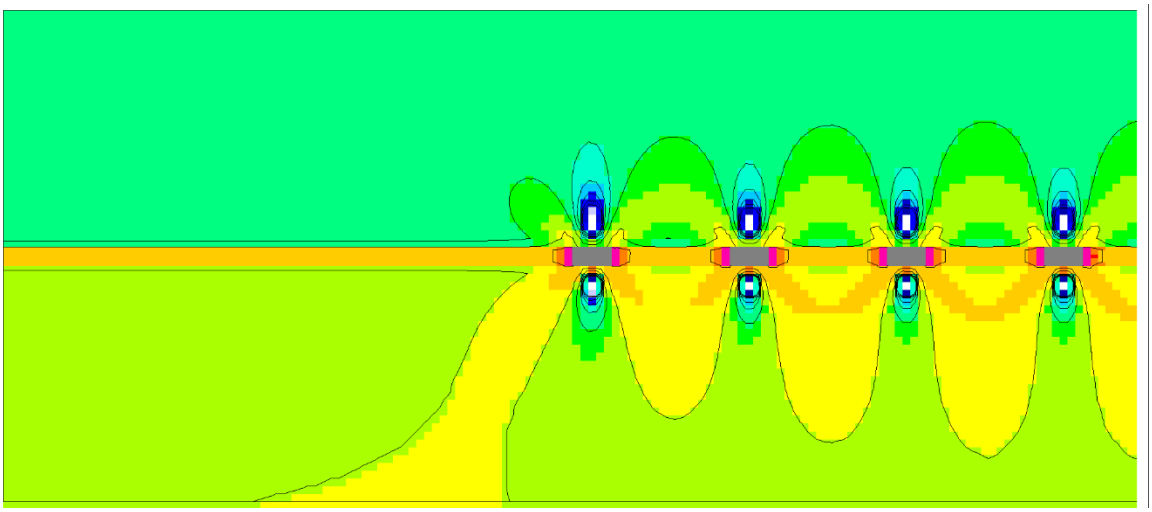

(e) Vertical section window through pillar centers showing element safety factor distribution using equivalent properties.

Figure 6 Element safety factor distributions in the case of eight main entries, Problem 1.

Inspection of Figure 6 indicates a general reduction in element safety factors, although there is no great increase in element failures. In fact, there are few element failures in both cases in this example problem involving main entries.

**Problem 2** This problem relates to barrier pillar size for protection of main entries, crosscuts, and pillars from effects of adjacent longwall mining. An analysis that allows for gob effects is presented here and in the User Manual in the case where joints are absent. The three step process is again followed in the new analysis for gob effects but is accompanied by *Step 1j* in case joints are present. Of course, there are no joints in gob, regardless. An example of barrier pillar problem analysis (Problem 2 "barriers") follows in combination with the usual three-step process and the *Step 1j* process.

*Step 1 Preparation of a materials property file (stratigraphic column).* The material property file for rock in this problem is the same as in **Problem 1**, "mains".

*Step 1j Preparation of an equivalent properties file.* Equivalent properties for this example problem are the same as in the previous example.

*Step 2 Mesh Generation*. Mesh generation input uses the same material properties for rock (and joints) as in the previous example.

*Step 3Execution* The new finite element runstream uses the same equivalent properties file used in the previous example and is

```
Trail Mtn Barriers with equiprops joints 08/17/2022 01/16/2022  wgp
F:\Visual Studio 2010\Projects\SPK\SPKJ\EQ.txt
F:\Visual Studio 2010\Projects\SPK\GMB3\belms
F:\Visual Studio 2010\Projects\SPK\GMB3\bcrds
F:\Visual Studio 2010\Projects\SPK\GMB3\brcte
F:\Visual Studio 2010\Projects\SPK\GMB3\bsigi
F:\Visual Studio 2010\Projects\SPK\GMB3\bnsps
aTBeq
nelem =  924336
nnode =  984409
nspec =  115879
nmat  =       7
ncut  =      -1
ninc  =       5
nsigo =       1
inter =     100
maxit =    2000
nyeld =       2
nelcf =    8944
nsol  =       2
nprb  =       1
mgob  =       0
 error=     0.000
 orf  =     1.860
```

```
 xfac =     12.00
 yfac =     12.00
 zfac =     12.00
 efac =      1.00
 cfac =      1.00
tolr% =      0.01
ENDRUN
```

The Indata file generated as output during mesh generation is similar to

| | | |
|---|---|---|
| 1) the name of the material properties (stratigraphic column) file | *matTMnewG.txt* | |
| 2) the number of main entries (NMS), | 5 | |
| 3) entry and crosscut widths (WE, WC) | 20 20 | (ft) |
| 4) pillar width and length (WP, LP) | 40 80 | (ft) |
| 5) barrier pillar width (WB) | 150 | (ft) |
| 6) element width, length, height (EX, EY, EZ) | 3 3 3 | (ft) |
| 7) do gob effect? | Y or y =yes or N or n=no | |
| 8) add-in additional stresses Sxx, Syy, Szz, Tyz, Tzx, Txy? | Y or y =yes or N or n=no | |

The finite element mesh is shown in Figure 7.

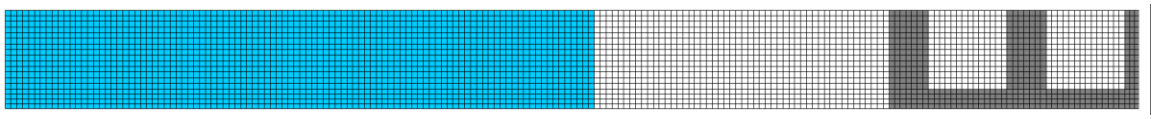

(a) plan view

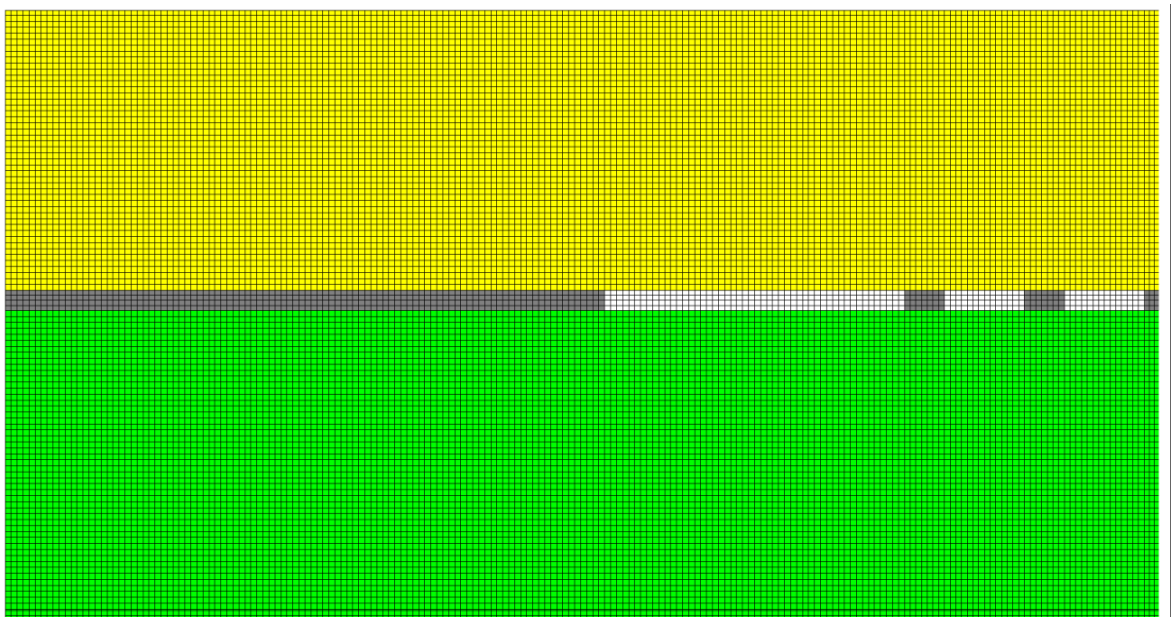

(b) vertical section close-up.

Figure 7 Plan and vertical section views of the mesh for a barrier pillar safety analysis. Only half of the five entry set is needed in the mesh. The blue elements to the left in plan view are

excavated elements that may be air or gob. Grey elements define entry and crosscut regions. White elements are coal in plan view, white in vertical section.

Results in the form of element safety factor distributions without and with gob present are given in Figure 8 in plan view at seam level and in Figure 9 in vertical section.

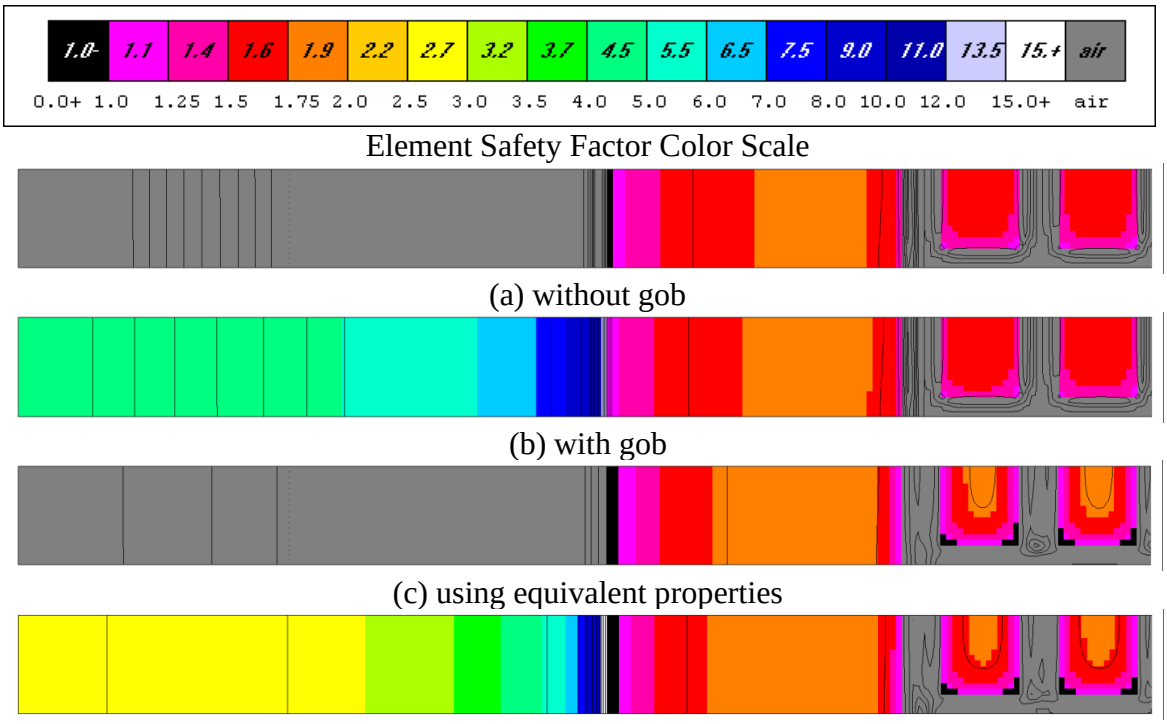


Figure 8 Seam level element safety factors without gob (a), with gob (b). (c) using equivalent properties ( no gob), (d) using equivalent propeties with gob.

The results in comparison show no discernible effect of gob on main entry safety, although there is a small effect on the barrier pillar wall adjacent to the mined panel. The gob proper does not reach failure in this example (no joints). However, joints have a noticeable effect as seen in element failures at the corners of pillars where crosscuts and entries meet in Figure 8 (c). Indeed, there is approximately 50% more element failure in case of joints. The gob effect is also negligible in case of equivalent properties as see in comparing Figures 8 (c) and (d).

Figure 9 also shows more element failures in case of joints, especially near the barrier pillar wall adjacent to the mined region. However, the strong gob appears to inhibit caving in the roof and failure in the floor in case of equivalent properties. However, safty of the entries, pillars and crosscuts appears unaffected. This example indicates joints are important to barrier pillar design for defense of main entries.

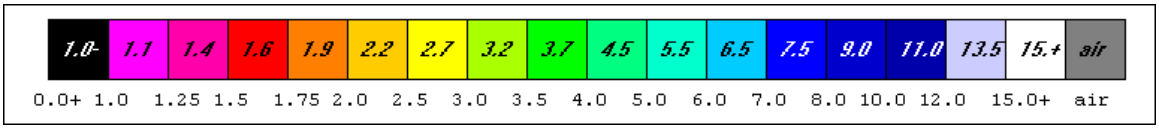


Element Safety Factor Color Scale

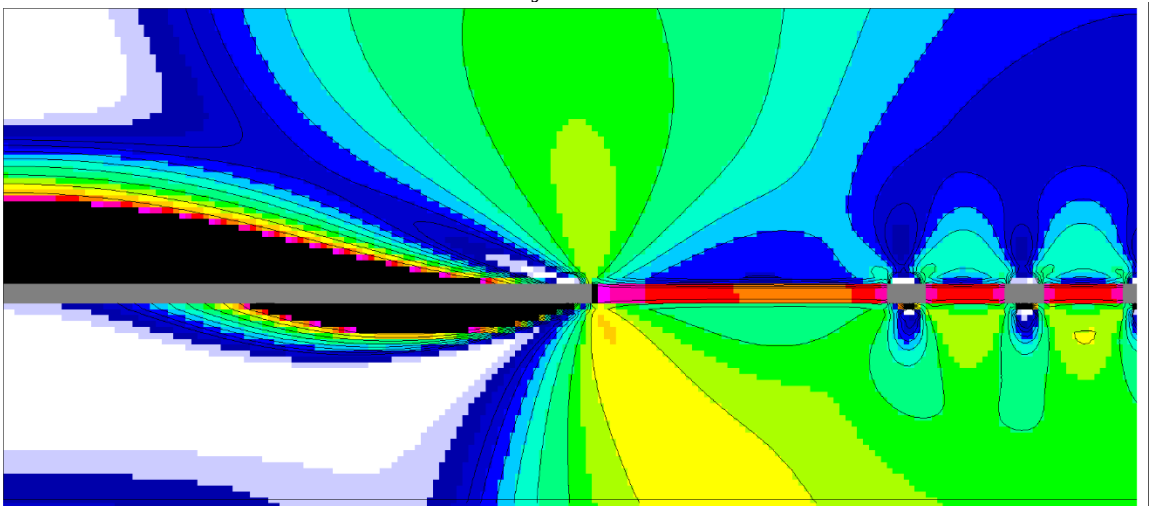

(a) no joints, no gob

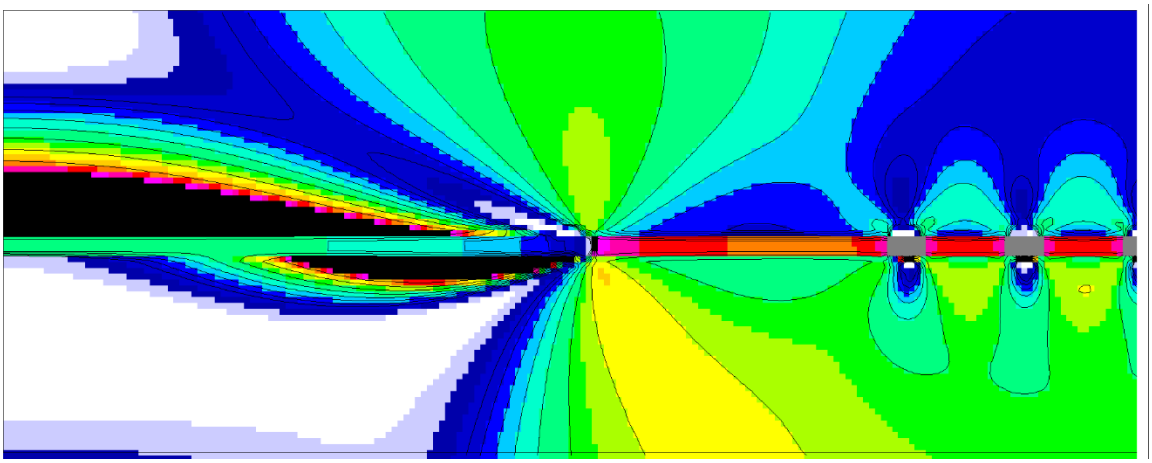

(b) no joints with gob

(c) using equivalent properties

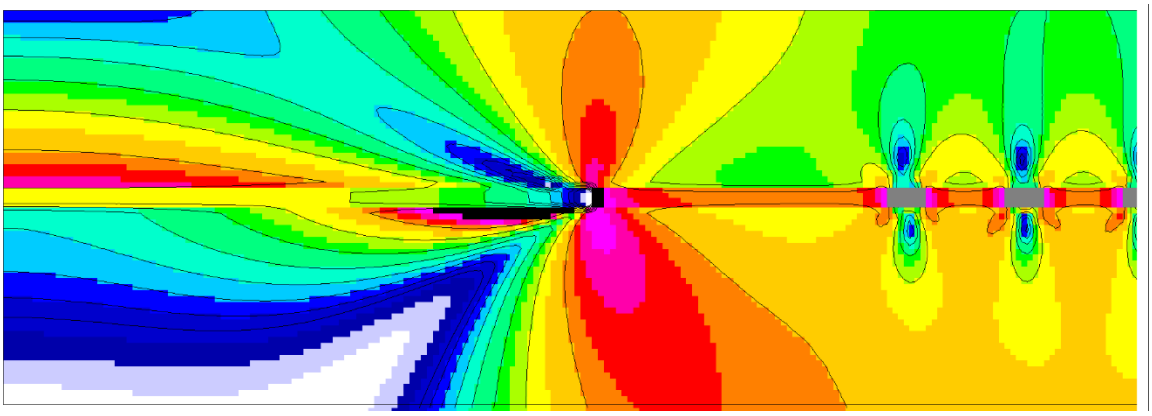

(d) using equivalent properties with gob

Figure 8 Element safety factors in vertical section without gob and joints (a) and (b) using equivalent properties.

**Problem 3** This problem concerns safety of bleeder entries and cross cuts used in longwall mining. Bleeder entries provide ventilation and a secondary escape route that must be maintained in a passable condition. Gob effects are analyzed without joints using intact rock properties and with joints using equivalent properties. Not too surprisingly, gob effects are minimal. As a reminder, thee are no joints in gob.

*Step 1 Preparation of a materials property file (stratigraphic column).* The material property file for rock in this problem is the same as in **Problem 1** "mains" and **Problem 2** "barriers". *Step 1j Computation of equivalent properties of jointed rock.* The equivalent jointed rock properties for this problem ("barriers") are the same used in the previous problem ("mains"). No additional computation is needed.

*Step 2 Mesh Generation*. Mesh generation input uses the same material properties for rock (and joints) as in the previous two examples. As always, mesh generation input is is

| | |
|---|---|
| 1) the name of the material properties (stratigraphic column) file | *matTMg.txt* |
| 2) the number of panel entries (NBS), | 3 |
| 3) entry and crosscut widths (WE, WC) | 20 20 (ft) |
| 4) pillar width and length (WP, LP) | 40 80 (ft) |
| 4) element width, length, height (EX, EY, EZ) | 3 3 3 (ft) |
| 6) do gob effect? | Y or y =yes or N or n=no |
| 7) add-in additional stresses Sxx, Syy, Szz, Tyz, Tzx, Txy? | Y or y =yes or N or n=no |

The runstream file for this analysis after some editing is shown in Figure 9 and the mesh is shown in Figure 10.

```
BLEEDER Trail MTN joints 08/17/2022 12/19/2018 2/3/2022 no gob psi wgp
F:\Visual Studio 2010\Projects\SPK\SPKJ\EQ.txt
F:\Visual Studio 2010\Projects\SPK\GMB3\belms
F:\Visual Studio 2010\Projects\SPK\GMB3\bcrds
F:\Visual Studio 2010\Projects\SPK\GMB3\brcte
F:\Visual Studio 2010\Projects\SPK\GMB3\bsigi
F:\Visual Studio 2010\Projects\SPK\GMB3\bnsps
aTBLeq
nelem =  955962
nnode = 1018020
nspec =  119944
nmat  =       7
ncut  =      -1
ninc  =      10
nsigo =       1
inter =     200
maxit =    4000
nyeld =       2
nelcf =    7000
nsol  =       2
nprb  =       3
mgob  =       0
 error=     0.000
 orf  =     1.860
 xfac =     12.00
 yfac =     12.00
 zfac =     12.00
 efac =      1.00
 cfac =      1.00
tolr% =      0.01
ENDRUN
```

Figure 9 Runstream for Problem 3 “bleeders”.

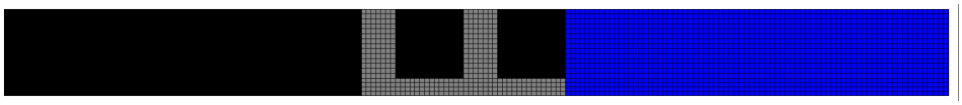

(a) plan view

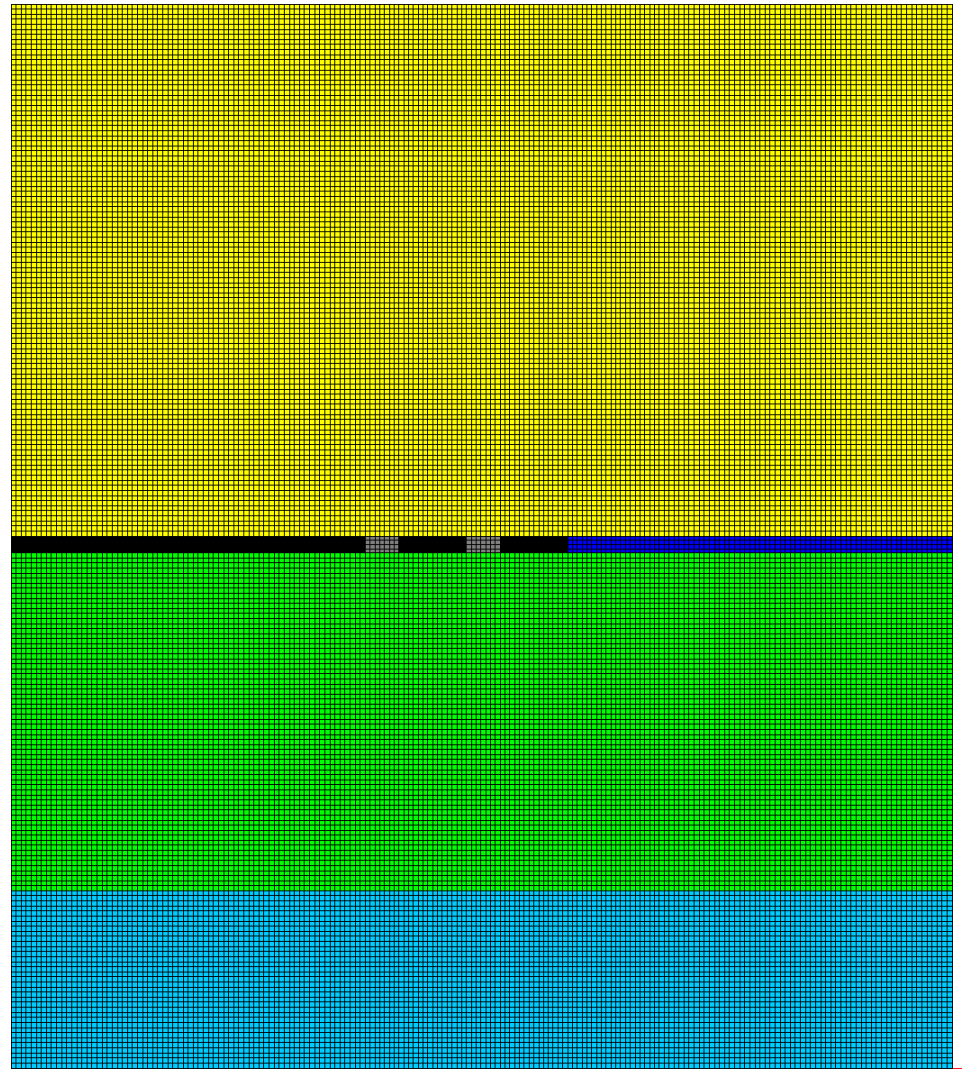

(b) vertical section window

Figure 10 Plan view and vertical sections of a three-dimensional mesh generated for bleeder entry safety analysis. Black=coal, grey=excavated elements, dark blue (seam level)=excavated elements or gob elements as the case may be.

*Step 3 FEM Execution and Results*. Figure 11 shows element safety factor distributions in plan view at seam level with no gob and with gob effects. Element boundaries are removed in the plots for ease of viewing.

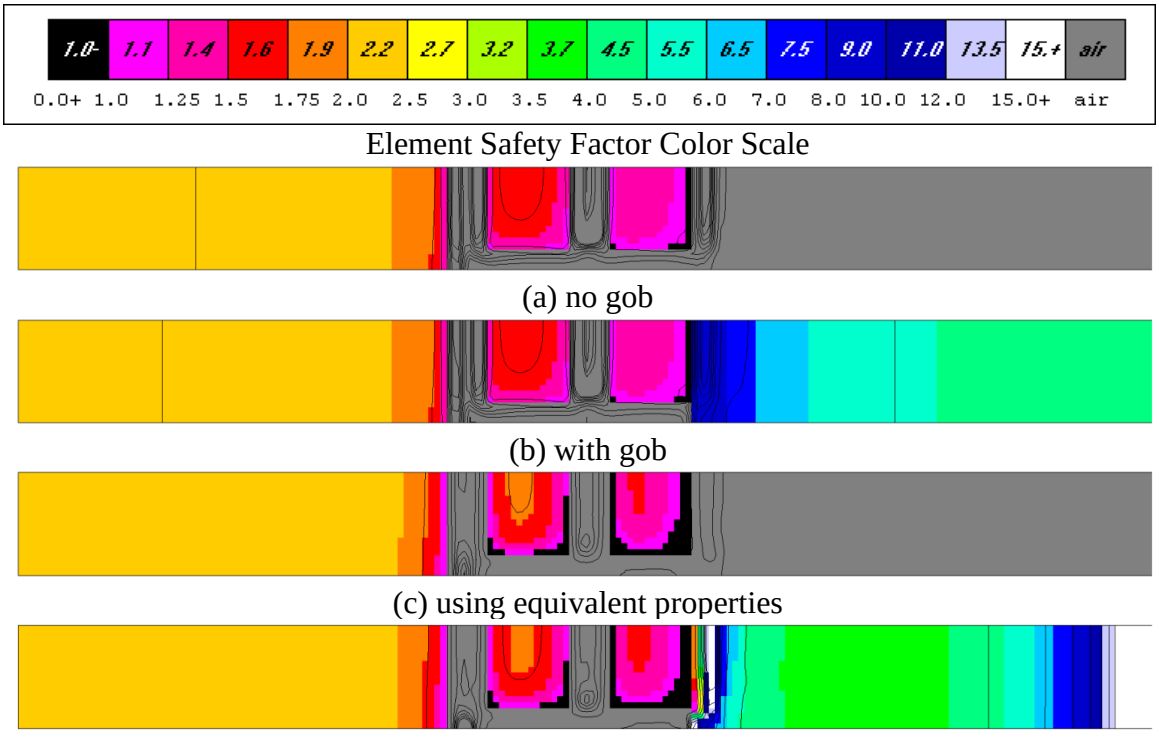


Figure 11 Element safety factor distributions in plan view at seam level in case a bleeder entry safety analyses: (a) no gob, (b) with gob, (c) using equivalent properties, (d) using equivalent properteis with gob. The coal seam is 10 ft (3 m) thick. Contours show gradation within color ranges.

Figure 12 provides for comparisons in vertical sections without gob and with gob and using equivalent properties of jointed rock relative to distributions of element safety factors near the bleeder entries. Again, the seam thickness (grey) is 10 ft (3 m). Elements are roughly 2.5 ft (0.75 m) cubes. There are four element "layers" through the seam which gives a reasonable stress distribution from roof to floor. This size is evident in the roof and floor elements especially over and below the mined panel to the right (grey). The pillar nearest the mined panel shows low safety factors (pink, red, 1.2, 1.4) while the pillar near the solid on the right hand side shows higher safety factors with the core in orange (2.2). In fact, the pillar near the mined panel shows some yielding in the right hand side (black) near the pillar corner (also seen in plan view). There is considerable yielding in the roof over the mined region and the floor as seen in the large black areas above and below the mined panel, more so in case of jointed rock. The gob makes little diffence in outcomes relative to bleeder entry safety whether using intact rock or equivalent properties of jointed rock. However, joints make a rock mass more compliant and weaker than intact rock as is evident in the figures. The gob also inhibits yielding in roof and floor strata above and below the mined panel both cases, without joints and with joints (equivalent properties).

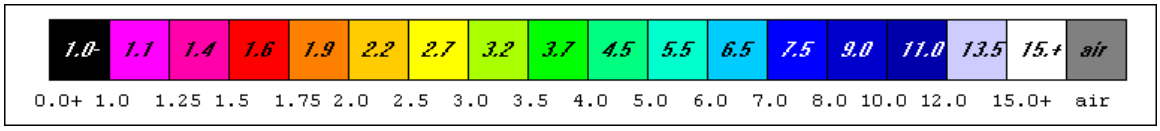


Element Safety Factor Color Scale

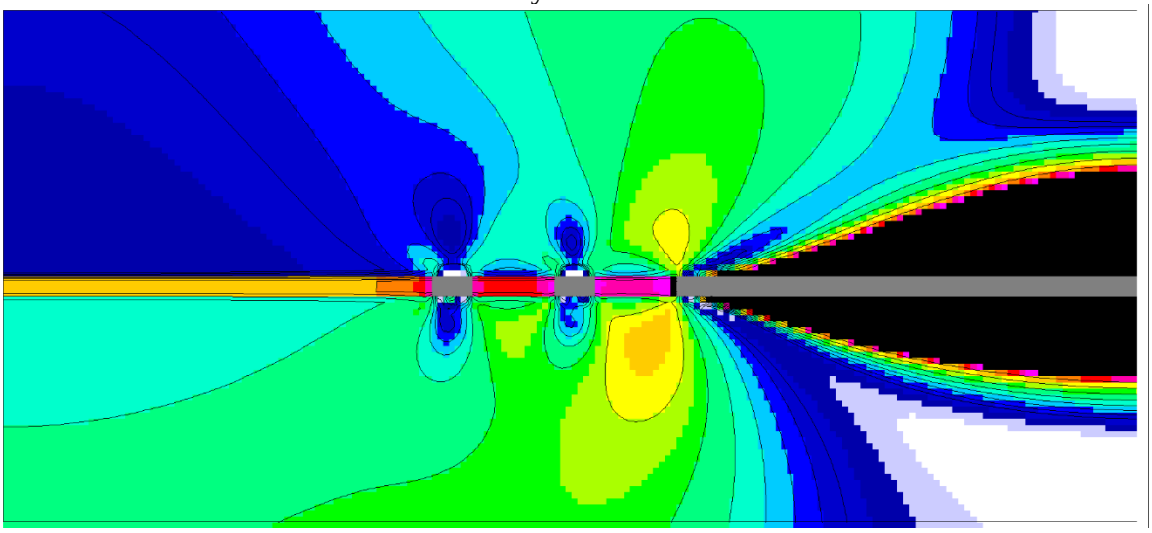

(a) no gob

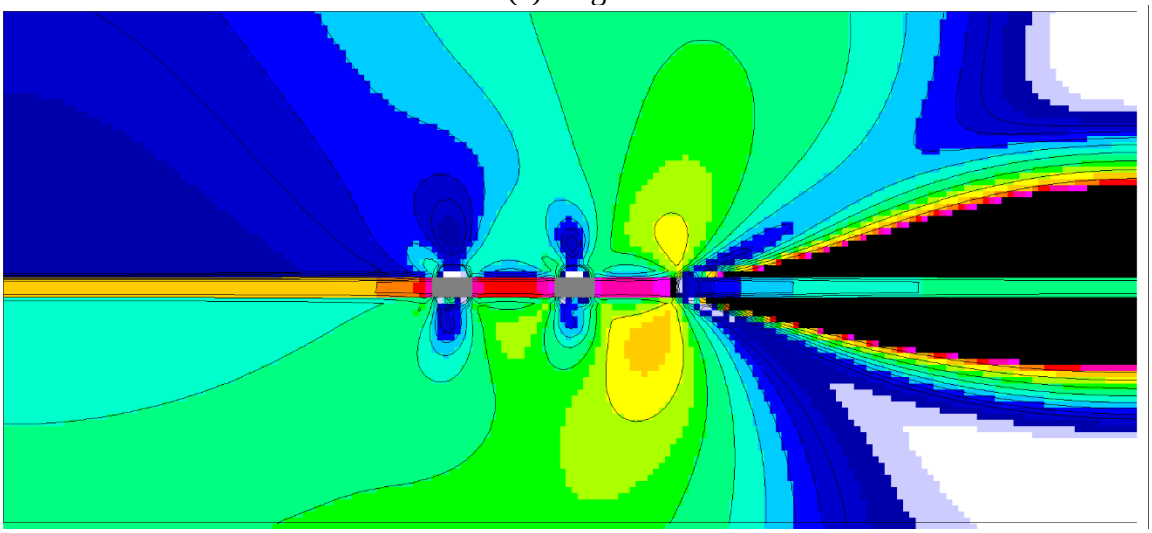

(b) with gob

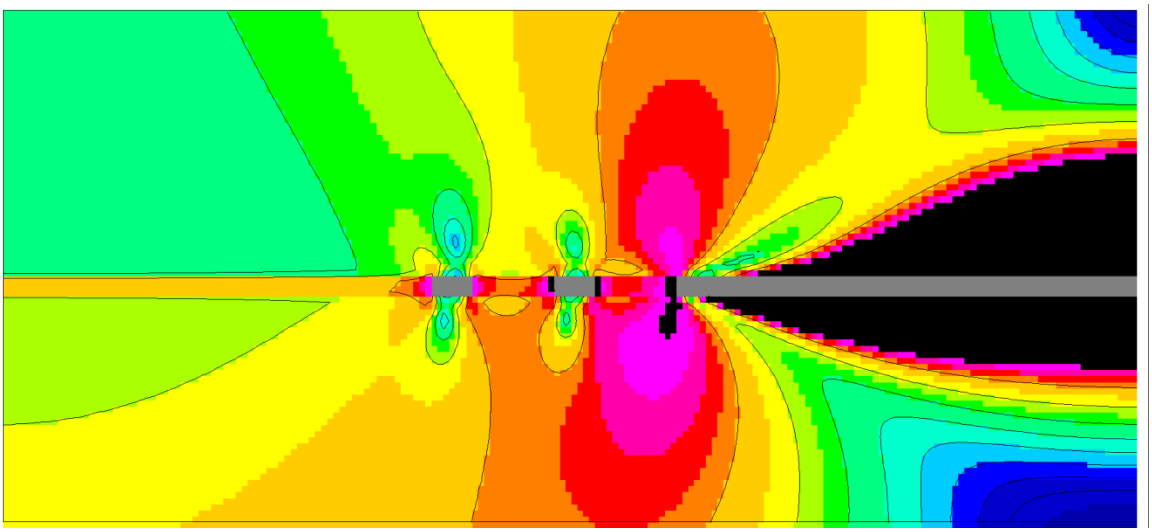

(c) using equivalent properties

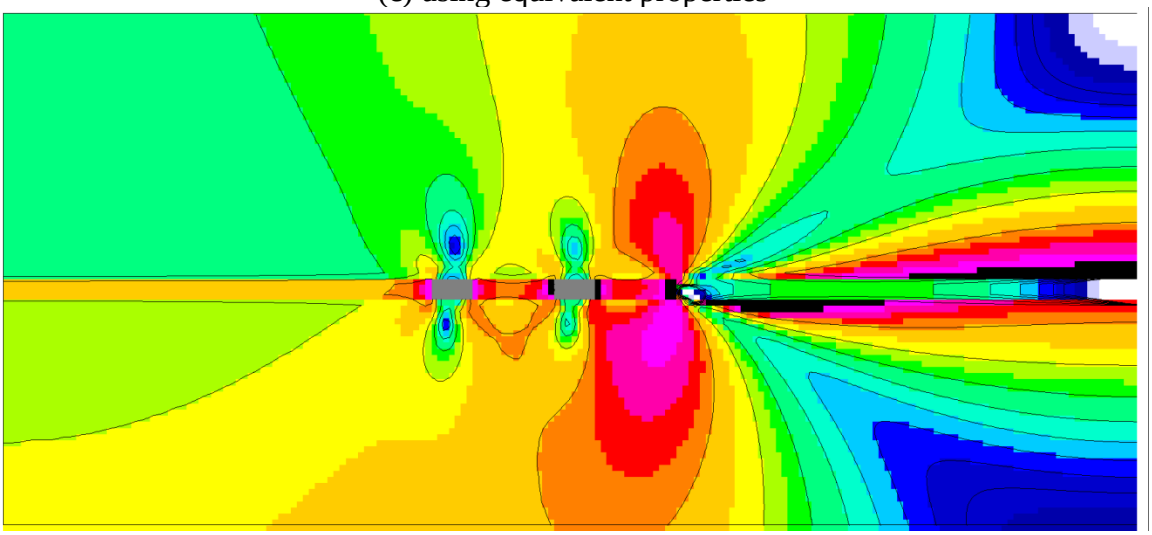

(d) using equivalent properties with gob

Figure 12 Element safety factor distributions without gob (a), with gob (b), using equivalent properties (c), and using equivalent properties with gob (d) in vertical sections in case of bleeder entry safety. The coal seam is 10 ft (3 m) thick.

**Problem 4** This example concerns *interpanel barrier pillars safety* and safety of associated panel entries, crosscuts and chain pillars in headgate and tailgates of a longwall panel. The mine is in the Wasatch Plateau coal field of central Utah and is relatively deep at 2707 ft (825 m). Details of are given in the User Manual in case of a rock mass without joints. The equivalent properties of a jointed rock mass are used here.

*Step 1 Preparation of a materials property file (stratigraphic column)* There are 11 layers in the geologic column; the 8$^{th}$ layer is the mined coal seam 11 ft (3.4 m) thick at a depth of 2,707 ft (825 m) which is the thinnest layer in the column. Order of strata is from the top down. As a

reminder, the last line of each stratum properties set gives the orientation (dip direction, dip), depth to the stratum top and stratum thickness as seen in Figure 13.

```
NLYRS =11
NSEAM = 8
1 North Horn         N=2
2.60E+06      2.60E+06      2.60E+06      0.26   0.26   0.26
1.75E+06      1.75E+06      1.75E+06     0.0      0.0   155.0
11803  11803  11803  696    696    696
1655   1655   1655
0      0      0      951
2 PRICE RIVER FRM
3.20E+06      3.20E+06      3.20E+06      0.26   0.26   0.26
2.17E+06      2.17E+06      2.17E+06     0.0      0.0   143.0
9976   9976   9976   377    377    377
1120   1120   1120
0      0      951    548
3 CASTLEGATE SANDSTONE
3.00E+06      3.00E+06      3.00E+06      0.22   0.22   0.22
1.92E+06      1.92E+06      1.92E+06     0.0      0.0   140.0
9585   9585   9585   435    435    435
1179   1179   1179
0      0      1499   568
4 SAND+SILTSTONE
3.10E+06      3.10E+06      3.10E+06      0.24   0.24   0.24
2.04E+06      2.04E+06      2.04E+06       0.0    0.0   142.0
13500  13500  13500  1189   1189   1189
2313   2313   2313
0      0      2067   344
5 ROOF SILTSTONE
2.80E+06      2.80E+06      2.80E+06      0.23   0.23   0.23
1.82E+06      1.82E+06      1.82E+06     0.0      0.0   142.0
12180  12180  12180  1291   1291   1291
2289   2289   2289
0      0      2411   138
6 ROOF SANDSTONE
3.39E+06      3.39E+06      3.39E+06      0.26   0.26   0.26
2.29E+06      2.29E+06      2.29E+06     0.0      0.0   140.0
14500  14500  14500  1088   1088   1088
2293   2293   2293
0      0      2549   150
7 ROOF SANDSTONE
3.39E+06      3.39E+06      3.39E+06      0.26   0.26   0.26
2.29E+06      2.29E+06      2.29E+06     0.0      0.0   140.0
14500  14500  14500  1088   1088   1088
2293   2293   2293
0      0      2699    8
8 COAL
4.06E+05      4.06E+05      4.06E+05      0.12   0.12   0.12
2.31E+05      2.31E+05      2.31E+05     0.0      0.0   78.0
4133   4133   4133   276    276    276
616    616    616
0      0      2707   11
9 FLOoR SANDSTONE
3.39E+06      3.39E+06      3.39E+06      0.26   0.26   0.26
2.29E+06      2.29E+06      2.29E+06     0.0      0.0   140.0
11716  11716  11716  1175   1175   1175
```

```
2142   2142   2142
0      0      2718     9
10 FLOoR SANDSTONE
3.39E+06      3.39E+06      3.39E+06      0.26   0.26   0.26
2.29E+06      2.29E+06      2.29E+06     0.0      0.0   140.0
11716  11716  11716  1175   1175   1175
2142   2142   2142
0      0      2727   200
11 MANCOS SHALE
2.20E+06      2.20E+06      2.20E+06      0.35   0.35   0.35
1.70E+06      1.70E+06      1.70E+06     0.0      0.0   145.0
10295  10295  10295  158    158    158
736    736    736
0      0      2927    171
```

Figure 13 Input strata properties file for interpanel barrier pillar mesh generation and computation of equivalent jointed rock mass properties. This file is *matABDg.txt*.

*Step 1j Preparation of an equivalent materials property file.* Equivalent material properties computation begins by preparing a runstream input for UT3PCJ as in the previous example problems. Thus,

```
Aberdeen deep w/ Joints 8/18/2022 3/22/2022 wgp
AB1.txt
celms.txt
ccrds.txt
none
none
cnsps.txt
aAB1
nelem =       1
nnode =       8
nspec =       8
nmat  =       4
ncut  =       1
ninc  =       1
nsigo =       0
inter =     100
maxit =    1000
nyeld =       2
nelcf =       0
ncave =       0
nfile =       1
npsi  =       1
nrstrt=       0
 error=    1.0000
 orf  =    1.8600
 xfac =   12.0000
 yfac =   12.0000
 zfac =   12.0000
 efac =    1.0000
 cfac =     100.0
 Aberdeen w/ Joints 3/22/2022 wgp
AB2.txt
celms.txt
ccrds.txt
```

```
none
none
cnsps.txt
aAB2
nelem =       1
nnode =       8
nspec =       8
nmat  =       4
ncut  =       1
ninc  =       1
nsigo =       0
inter =     100
maxit =    1000
nyeld =       2
nelcf =       0
ncave =       0
nfile =       2
npsi  =       1
nrstrt=       0
 error=    1.0000
 orf  =    1.8600
 xfac =   12.0000
 yfac =   12.0000
 zfac =   12.0000
 efac =    1.0000
 cfac =     100.0
```

and so on

```
Aberdeen w/ Joints 3/22/2022 wgp
AB11.txt
celms.txt
ccrds.txt
none
none
cnsps.txt
aAB11
nelem =       1
nnode =       8
nspec =       8
nmat  =       4
ncut  =       1
ninc  =       1
nsigo =       0
inter =     100
maxit =    1000
nyeld =       2
nelcf =       0
ncave =       0
nfile =      11
npsi  =       1
nrstrt=       0
 error=    1.0000
 orf  =    1.8600
 xfac =   12.0000
 yfac =   12.0000
 zfac =   12.0000
```

```
 efac =    1.0000
 cfac =     100.0
RUN END
```

To be sure, the jointing is the same as before (Figure 1) The result is EQ.txt. Thus,

```
NLYRS = 11
NSEAM =  8
  (1) North Horn  N=2 (DP2) & wt, 2000-11000, 1/16/2017
   0.285E+06   0.309E+06   0.354E+06        0.22        0.04        0.05
   0.777E+05   0.734E+05   0.948E+05        0.00        0.00      158.00
      3904.3      4069.8      4351.6       231.6       241.4       258.1
       549.0       572.3       611.9
         0.0         0.0         0.0       951.0
  2 PRICE RIVER FRM
   0.291E+06   0.317E+06   0.363E+06        0.22        0.03        0.04
   0.809E+05   0.761E+05   0.996E+05        0.00        0.00      143.00
      3006.9      3137.5      3360.9       113.6       118.6       127.0
       337.5       352.1       377.2
         0.0         0.0       951.0       548.0
3 CASTLEGATE SANDSTONE
   0.289E+06   0.314E+06   0.360E+06        0.21        0.03        0.04
   0.805E+05   0.758E+05   0.990E+05        0.00        0.00      140.00
      2974.7      3103.0      3322.3       135.0       140.8       150.8
       365.9       381.7       408.6
         0.0         0.0      1499.0       568.0
4 SAND+SILTSTONE
   0.290E+06   0.316E+06   0.362E+06        0.22        0.03        0.04
   0.807E+05   0.760E+05   0.993E+05        0.00        0.00      142.00
      4128.1      4306.8      4612.3       363.6       379.3       406.2
       707.3       737.9       790.3
         0.0         0.0      2067.0       344.0
5 ROOF SILTSTONE
   0.287E+06   0.312E+06   0.357E+06        0.21        0.03        0.04
   0.803E+05   0.756E+05   0.988E+05        0.00        0.00      142.00
      3899.1      4065.9      4350.6       413.3       431.0       461.1
       732.9       764.3       817.8
         0.0         0.0      2411.0       138.0
6 ROOF SANDSTONE
   0.292E+06   0.318E+06   0.366E+06        0.22        0.03        0.04
   0.810E+05   0.763E+05   0.999E+05        0.00        0.00      140.00
      4257.3      4443.4      4761.9       319.4       333.4       357.3
       673.3       702.7       753.1
         0.0         0.0      2549.0       150.0
7 ROOF SANDSTONE
   0.292E+06   0.318E+06   0.366E+06        0.22        0.03        0.04
   0.810E+05   0.763E+05   0.999E+05        0.00        0.00      140.00
      4257.3      4443.4      4761.9       319.4       333.4       357.3
       673.3       702.7       753.1
         0.0         0.0      2699.0         8.0
8 COAL
   0.178E+06   0.187E+06   0.201E+06        0.17        0.07        0.07
   0.621E+05   0.593E+05   0.720E+05        0.00        0.00       78.00
      2736.0      2802.7      2909.7       182.7       187.2       194.3
       408.2       418.2       434.1
         0.0         0.0      2707.0        11.0
9 FLOoR SANDSTONE
```

```
   0.292E+06   0.318E+06   0.366E+06        0.22        0.03        0.04
   0.810E+05   0.763E+05   0.999E+05        0.00        0.00      140.00
      3439.9      3590.2      3847.6       345.0       360.1       385.9
       628.9       656.4       703.5
         0.0         0.0      2718.0         9.0
10 FLOoR SANDSTONE
   0.292E+06   0.318E+06   0.366E+06        0.22        0.03        0.04
   0.810E+05   0.763E+05   0.999E+05        0.00        0.00      140.00
      3439.9      3590.2      3847.6       345.0       360.1       385.9
       628.9       656.4       703.5
         0.0         0.0      2727.0       200.0
11 MANCOS SHALE
   0.279E+06   0.303E+06   0.345E+06        0.23        0.06        0.07
   0.801E+05   0.754E+05   0.984E+05        0.00        0.00      145.00
      3665.7      3817.6      4074.4        56.3        58.6        62.5
       262.2       273.0       291.4
         0.0         0.0      2927.0       171.0
```

*Step 2 Mesh Generation* Mesh generation input is

| | |
|---|---|
| 1) the name of the material properties (stratigraphic column) file | *matABDg.txt* |
| 2) the number of panel entries (NES), | 3 |
| 3) entry and crosscut widths (WE, WC) | 20 20 (ft) |
| 4) pillar width and length (WP, LP) | 40 80 (ft) |
| 5) barrier pillar width | 300 (ft) |
| 6)longwall panel width | 750 (ft) |
| 7) element width, length, height (EX, EY, EZ) | 4 4 4 (ft) |
| 8) do gob effect? | Y or y=yes or Nor n=no |
| 9) add-in additional stresses Sxx, Syy, Szz, Tyz, Tzx, Txy? | Y or y=yes or Nor n=no |

*Step 3 FEM Execution and Results* The runstream file using equivalent properties after incorporating path names from the mesh generated output file and some minor editing is shown in Figure 14. Run time for this mesh was just under four hours. Vertical section views of the distribution of element safety factors are shown in Figure 15 in three cases: (a) without gob effect, (b) with gob effect, and (c) using equivalent properties. Element boundaries are not shown for clarity.

```
Interpanel Barrier ABD no gob jts 8/18/2022 wgp
F:\Visual Studio 2010\Projects\SPK\SPKJ\EQ.txt
F:\Visual Studio 2010\Projects\SPK\GMB3\belms
F:\Visual Studio 2010\Projects\SPK\GMB3\bcrds
F:\Visual Studio 2010\Projects\SPK\GMB3\brcte
F:\Visual Studio 2010\Projects\SPK\GMB3\bsigi
F:\Visual Studio 2010\Projects\SPK\GMB3\bnsps
aIPj
nelem =  347360
nnode =  378672
nspec =   59952
nmat  =      11
ncut  =      -1
ninc  =       5
nsigo =       1
inter =     200
```

```
maxit =    2000
nyeld =       2
nelcf =    4431
nsol  =       2
nprb  =       4
mgob  =       0
 error=    1.0000
 orf  =    1.8600
 xfac =   12.0000
 yfac =   12.0000
 zfac =   12.0000
 efac =    1.0000
 cfac =    1.0000
tolr% =    0.0100
ENDRUN
```

Figure 14 Runstream file for interpanel barrier pillar Problem 4 analysis using equivalent properties of a jointed rock mass.

The plan view in Figure 15 indicates yielding entry pillar ribs and pillar cores with low safety factors (*fs*<1.3). Indeed, the pillar adjacent to the longwall panel is yielding to the core. Entry ribs also show some yielding. The gob appears to reduce stress at a distance as seen in the somewhat higher safety factors in the rib of the entry adjacent to the interpanel barrier pillar. Stress is also reduced in the vicinity of the other two entries, although not enough to avoid yielding of the chain pillars between.

The effect of joints is evident in Figure 16 that shows results in vertical sections. Extensive yielding in roof and floor above the mined panel and above the bleeder entries is especially evident in Figure 16 (c) in case of equivalent properties. Again, joints do have adverse effects for ground control and safety and should be taken into proper account based on fundamental principles. Strong gob in conjunction with equivalent properties also has a noticeable effect as seen in comparing Figures 16 (c) and (d).

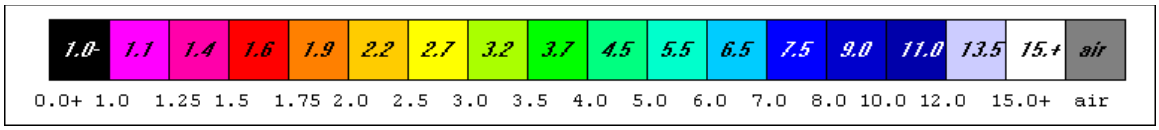


Safety Factor Color Scale

(a) no gob.

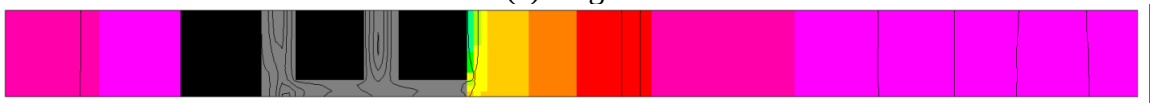

(b) with gob.

(c) using equivalent properties

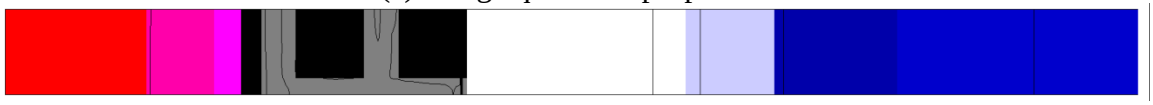

(d) using equivalent properties with gob

Figure 15 Plan view at seam level: interpanel barrier pillar (left), panel entries (3), longwall panel (right). (a) no gob, (b) with gob (c) using equivalent properties.

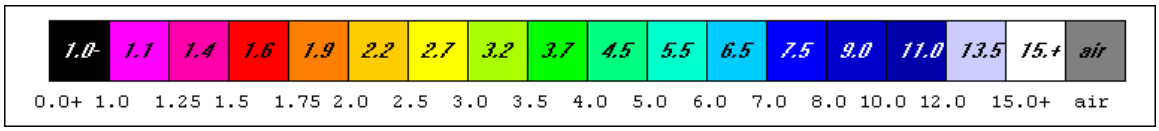


Safety Factor Color Scale

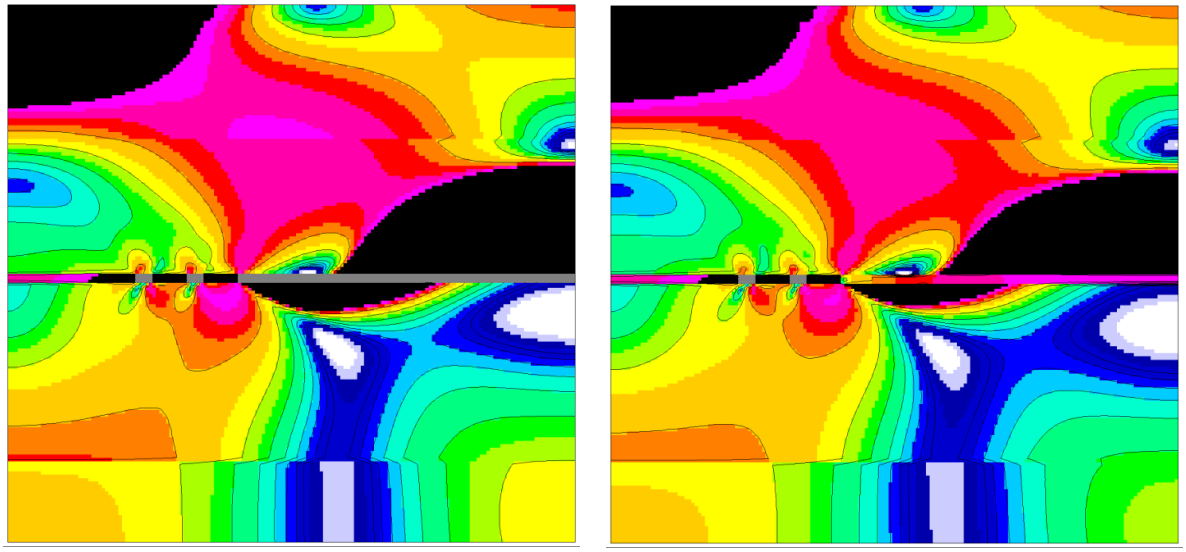

(a) no gob

(b) with gob

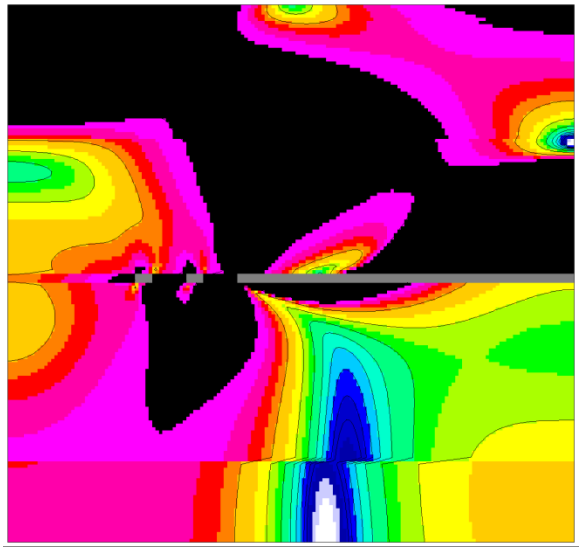

(c) using equivalent properties

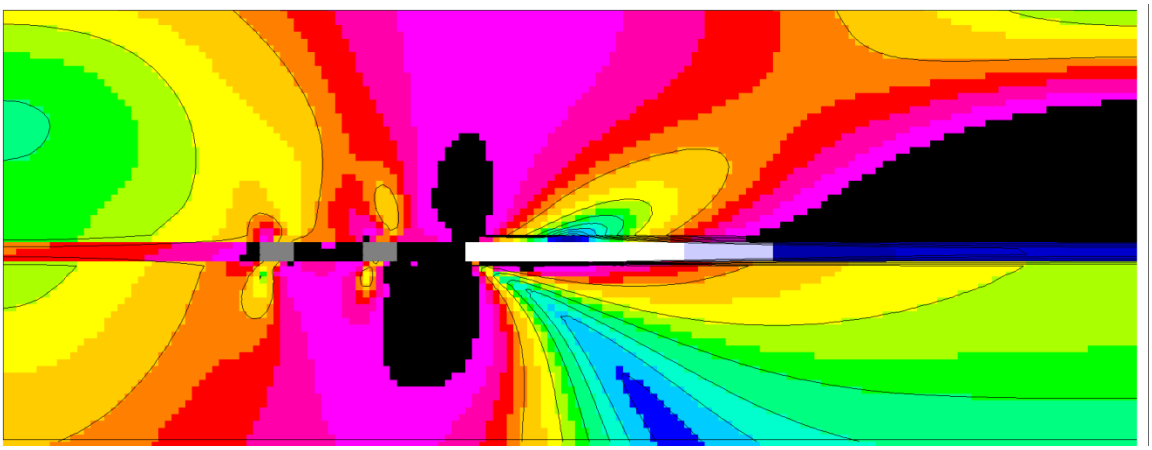

(d) using equivalent properties with gob

Figure 16 Vertical section showing interpanel barrier pillar (left hand side of plots) and a longwall panel (right hand side of plots) with three panel entries (a) no gob, (b) with gob, (c) using equivalent properties, (d) using equivalent properties with gob.

**Problem 5** Pillar safety in room and pillar mining is Problem 5 in the list of problems available for analysis upon execution of the mesh generator and completion of *Step 1j* in case of joints. Figure 17 is a plan view showing a typical pillar in an extensive array of similar pillars taken from the User Manual as a reminder. Symmetry is used to reduce mesh size; only the area in the red rectangle is contained in the mesh in plan view.

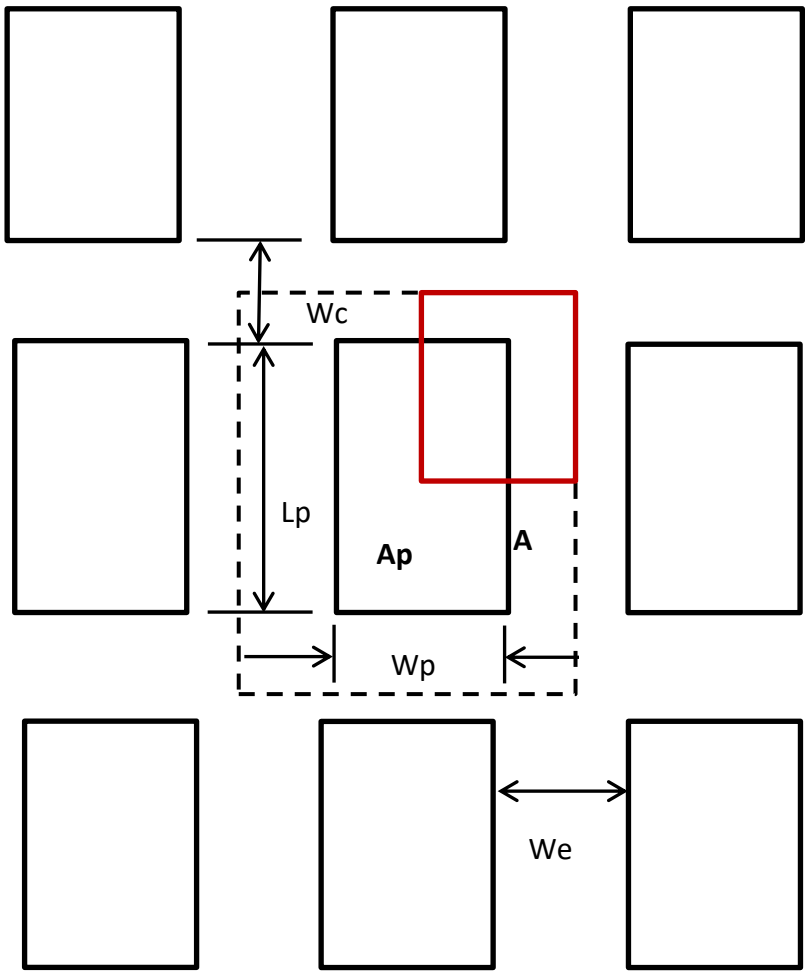


Figure 17 A typical pillar in a large array of pillars. Lp=pillar length, Wp=pillar width, We=entry width, Wc=cross cut width, Ap=area of pillar, A=total area (tributary area). Because of symmetry, only the region outlined by the red square in horizontal section is placed in the mesh. All four sides are planes of symmetry. The mesh extends above and below the bottom of the ore 1.5 times the mining width.

*Step 1 Preparation of a materials property file (stratigraphic column)* The intact rock properties are

```
NLYRS =12
NSEAM = 7
  (1) SHALE 1 N=2 (DP2) & spwts (pcf) dpth=m
  0.87e+06  0.87e+06  0.87e+06      0.22      0.22      0.22
  0.36e+06  0.36e+06  0.36e+06       0.0       0.0     144.0
    4922.0    4922.0   49220.0     520.0     520.0     520.0
     924.0     924.0     924.0
       0.0       0.0       0.0     62.0
  (2) MUDSTONE
  1.22e+06  1.22e+06  1.22e+06      0.20      0.20      0.20
  0.51e+06  0.51e+06  0.51e+06       0.0       0.0     134.0
    3580.0    3580.0    3580.0     497.0     497.0     497.0
```

```
   770.0     770.0     770.0
     0.0       0.0      62.0     148.0
(3) SANDSTONE 1
2.03e+06  2.03e+06  2.03e+06      0.23      0.23      0.23
0.82e+06  0.82e+06  0.82e+06       0.0       0.0     140.0
  6317.0    6317.0    6317.0     480.0     480.0     480.0
  1005.0    1005.0    1005.0
     0.0       0.0     210.0     249.0
(4) OIL SHALE 1
0.82e+06  0.82e+06  0.82e+06      0.33      0.33      0.33
0.31e+06  0.31e+06  0.31e+06       0.0       0.0     142.0
  5292.0    5292.0    5292.0     460.0     460.0     460.0
   908.0     908.0     908.0
     0.0       0.0     459.0     449.0
(5) SANDSTONE 2
1.22e+06  1.22e+06  1.22e+06      0.20      0.20      0.20
0.51e+06  0.51e+06  0.51e+06       0.0       0.0     134.0
  6317.0    6317.0    6317.0     480.0     480.0     480.0
  1005.0    1005.0    1005.0
     0.0       0.0     908.0     171.0
(6) SHALE 2
0.87e+06  0.87e+06  0.87e+06      0.22      0.22      0.22
0.36e+06  0.36e+06  0.36e+06       0.0       0.0     144.0
  5292.0    5292.0    5292.0     460.0     460.0     460.0
   908.0     908.0     908.0
     0.0       0.0    1079.0     420.0
(7) TRONA 1
4.08e+06  4.08e+06  4.08e+06      0.25      0.25      0.25
1.63e+06  1.63e+06  1.63e+06       0.0       0.0     134.0
  6804.0    6804.0    6804.0     410.0     410.0     410.0
  1021.0    1021.0    1021.0
     0.0       0.0    1499.0      10.0
(8) OIL SHALE 2
0.82e+06  0.82e+06  0.82e+06      0.33      0.33      0.33
0.31e+06  0.31e+06  0.31e+06       0.0       0.0     142.0
  5292.0    5292.0    5292.0     460.0     460.0     460.0
   908.0     908.0     908.0
     0.0       0.0    1509.0      89.0
(9) TRONA 2
4.08e+06  4.08e+06  4.08e+06      0.25      0.25      0.25
1.63e+06  1.63e+06  1.63e+06       0.0       0.0     134.0
  6804.0    6804.0    6804.0     410.0     410.0     410.0
  1021.0    1021.0    1021.0
     0.0       0.0    1598.0      10.0
(10) SHALE 3
0.87e+06  0.87e+06  0.87e+06      0.22      0.22      0.22
0.36e+06  0.36e+06  0.36e+06       0.0       0.0     144.0
  5292.0    5292.0    5292.0     460.0     460.0     460.0
   908.0     908.0     908.0
     0.0       0.0    1608.0    190.0
(11) SANDSTONE 3
2.03e+06  2.03e+06  2.03e+06      0.23      0.23      0.23
0.82e+06  0.82e+06  0.82e+06       0.0       0.0     140.0
  6317.0    6317.0    6317.0     480.0     480.0     480.0
  1005.0    1005.0    1005.0
     0.0       0.0    1798.0      49.0
(12) TIPTON FM
0.87e+06  0.87e+06  0.87e+06      0.22      0.22      0.22
```

```
  0.36e+06  0.36e+06  0.36e+06       0.0       0.0     144.0
    5292.0    5292.0    5292.0     460.0     460.0     460.0
     908.0     908.0     908.0
       0.0       0.0    1807.0    3313.0
```

*Step 1j Preparation of an equivalent materials property file* Equivalent material properties computation begins by preparing a runstream input for UT3PCJ as in the previous example problems. Thus, in case of mining trona

```
Trona deep w/ Joints 8/19/2022 3/22/2022 wgp
TR1prop.txt
celms.txt
ccrds.txt
none
none
cnsps.txt
aTR1
nelem =       1
nnode =       8
nspec =       8
nmat  =       6
ncut  =       1
ninc  =       1
nsigo =       0
inter =     100
maxit =    1000
nyeld =       2
nelcf =       0
ncave =       0
nfile =       1
npsi  =       1
nrstrt=       0
 error=    1.0000
 orf  =    1.8600
 xfac =   12.0000
 yfac =   12.0000
 zfac =   12.0000
 efac =    1.0000
 cfac =     100.0
inter =     100
maxit =    1000
nyeld =       2
nelcf =       0
ncave =       0
nfile =       3
npsi  =       1
nrstrt=       0
 error=    1.0000
 orf  =    1.8600
 xfac =   12.0000
 yfac =   12.0000
 zfac =   12.0000
 efac =    1.0000
 cfac =     100.0

and so on through 12 formations in the stratigraphic column
```

```
Trona deep w/ Joints 8/19/2022 3/22/2022 wgp
TR12prop.txt
celms.txt
ccrds.txt
none
none
cnsps.txt
aTR12
nelem =       1
nnode =       8
nspec =       8
nmat  =       6
ncut  =       1
ninc  =       1
nsigo =       0
inter =     100
maxit =    1000
nyeld =       2
nelcf =       0
ncave =       0
nfile =      12
npsi  =       1
nrstrt=       0
 error=    1.0000
 orf  =    1.8600
 xfac =   12.0000
 yfac =   12.0000
 zfac =   12.0000
 efac =    1.0000
 cfac =     100.0
RUN END

where TR1prop.txt is

   1 (1) joint  NS18/Jun/2015 wgp TRONA 5 jts 2/10/2022 3/16/2022
  1.25E+04  1.25E+04  1.25E+04      0.20      0.20      0.20
  0.52E+04  0.52E+04  0.52E+04       .00       .00        144.0
     35.80     35.80     35.80      4.97      4.97      4.97
      7.70      7.70      7.70
        90.00      90.0      30.0     -0.10
    2  --(2) joint EW N=2
  1.25E+04  1.25E+04  1.25E+04      0.20      0.20      0.20
  0.52E+04  0.52E+04  0.52E+04       .00       .00        144.0
     35.80     35.80     35.80      4.97      4.97      4.97
      7.70      7.70      7.70
       0.0      90.0      30.0     -0.10
    3  --(3) joint NESW N=2
  1.25E+04  1.25E+04  1.25E+04      0.20      0.20      0.20
  0.52E+04  0.52E+04  0.52E+04       .00       .00        144.0
     35.80     35.80     35.80      4.97      4.97      4.97
      7.70      7.70      7.70
      45.0      90.0      30.0     -0.10
    4  --(4) joint NWSE N=2
  1.25E+04  1.25E+04  1.25E+04      0.20      0.20      0.20
  0.52E+04  0.52E+04  0.52E+04       .00       .00        144.0
     35.80     35.80     35.80      4.97      4.97      4.97
      7.70      7.70      7.70
     -45.0       90.0     30.0     -0.10
```

```
    5  --(5) joint BEDDING PLANES N=2
  1.25E+04  1.25E+04  1.25E+04      0.20      0.20      0.20
  0.52E+04  0.52E+04  0.52E+04       .00       .00     144.0
     35.80     35.80     35.80      4.97      4.97      4.97
      7.70      7.70      7.70
       0.0       0.0       7.0     -0.10
   (1) SHALE 1 N=2 (DP2) & spwts (pcf) dpth=m
  0.87e+06  0.87e+06  0.87e+06      0.22      0.22      0.22
  0.36e+06  0.36e+06  0.36e+06       0.0       0.0     144.0
    4922.0    4922.0    4922.0     520.0     520.0     520.0
     924.0     924.0     924.0
       0.0       0.0       0.0     62.0

And so on through TR12prop.txt
```

The result is the file EQ.txt. Thus,

```
NLYRS =12
NSEAM = 7
   (1) SHALE 1 N=2 (DP2) & spwts (pcf) dpth=m AVERAGES 5/30/2015
   0.527E+06   0.527E+06   0.474E+06        0.25        0.14        0.12
   0.151E+06   0.151E+06   0.217E+06        0.00        0.00      144.00
      3830.3      3830.3      3634.0       404.7       404.7       383.9
       718.8       718.8       682.0
         0.0         0.0         0.0        62.0
  (2) MUDSTONE
   0.639E+06   0.639E+06   0.563E+06        0.25        0.11        0.10
   0.172E+06   0.172E+06   0.264E+06        0.00        0.00      144.00
      2590.5      2590.5      2431.0       359.6       359.6       337.5
       557.3       557.3       523.0
         0.0         0.0        62.0       148.0
  (3) SANDSTONE 1
   0.809E+06   0.809E+06   0.690E+06        0.28        0.10        0.08
   0.197E+06   0.197E+06   0.328E+06        0.00        0.00      144.00
      3988.6      3988.6      3682.4       303.1       303.1       279.8
       634.8       634.8       586.1
         0.0         0.0       210.0       249.0
  (4) OIL SHALE 1
   0.508E+06   0.508E+06   0.459E+06        0.32        0.21        0.19
   0.142E+06   0.142E+06   0.197E+06        0.00        0.00      144.00
      4164.8      4164.7      3957.5       362.0       362.0       344.0
       708.9       708.9       673.6
         0.0         0.0       459.0       449.0
  (5) SANDSTONE 2
   0.639E+06   0.639E+06   0.563E+06        0.25        0.11        0.10
   0.172E+06   0.172E+06   0.264E+06        0.00        0.00      144.00
      4571.0      4571.0      4289.6       347.3       347.3       326.0
       727.5       727.5       682.7
         0.0         0.0       908.0       171.0
  (6) SHALE 2
   0.527E+06   0.527E+06   0.474E+06        0.25        0.14        0.12
   0.151E+06   0.151E+06   0.217E+06        0.00        0.00      144.00
      4118.2      4118.2      3907.2       358.0       358.0       339.6
       701.0       701.0       665.1
         0.0         0.0      1079.0       420.0
  (7) TRONA 1
   0.101E+07   0.101E+07   0.832E+06        0.29        0.07        0.05
```

```
 0.223E+06   0.223E+06   0.411E+06        0.00        0.00      144.00
    3392.4      3392.4      3073.3       204.4       204.4       185.2
     480.8       480.8       435.6
       0.0         0.0      1499.0        10.0
(8) OIL SHALE 2
 0.508E+06   0.508E+06   0.459E+06        0.32        0.21        0.19
 0.142E+06   0.142E+06   0.197E+06        0.00        0.00      144.00
    4164.8      4164.7      3957.5       362.0       362.0       344.0
     708.9       708.9       673.6
       0.0         0.0      1509.0        89.0
(9) TRONA 2
 0.101E+07   0.101E+07   0.832E+06        0.29        0.07        0.05
 0.223E+06   0.223E+06   0.411E+06        0.00        0.00      144.00
    3392.4      3392.4      3073.3       204.4       204.4       185.2
     480.8       480.8       435.6
       0.0         0.0      1598.0        10.0
(10) SHALE 3
 0.527E+06   0.527E+06   0.474E+06        0.25        0.14        0.12
 0.151E+06   0.151E+06   0.217E+06        0.00        0.00      144.00
    4118.2      4118.2      3907.2       358.0       358.0       339.6
     701.0       701.0       665.1
       0.0         0.0      1608.0       190.0
(11) SANDSTONE 3
 0.809E+06   0.809E+06   0.690E+06        0.28        0.10        0.08
 0.197E+06   0.197E+06   0.328E+06        0.00        0.00      144.00
    3988.6      3988.6      3682.4       303.1       303.1       279.8
     634.8       634.8       586.1
       0.0         0.0      1798.0        49.0
(12) TIPTON FM
 0.527E+06   0.527E+06   0.474E+06        0.25        0.14        0.12
 0.151E+06   0.151E+06   0.217E+06        0.00        0.00      144.00
    4118.2      4118.2      3907.2       358.0       358.0       339.6
     701.0       701.0       665.1
       0.0         0.0      1847.0      3313.0
```

*Step 2 Mesh Generation* Mesh generation interactive input is echoed in part in an InData output file from mesh generation. Thus,

```
Input Data
 PILLARS
 Width of entries, WE (ft)  =     20.0
 Width of crosscuts, WC (ft)=   20.0
 Width of pillars, WP (ft)  =     30.0
 Length of pillars, LP (ft) =     90.0
 Height of pillars, HP (ft) =     10.0
 EX, EY, EZ, (ft)=      1.0      1.0      1.0
 Additional Sxx,Syy,Szz,Tyz,Tzx,Txy, tension +=
     0.0      0.0      0.0      0.0      0.0      0.0
```

Mesh generation also produces files for mesh plotting and plotting of element safety factor distributions (after a finite element analysis). A runstream file for finite element analysis is also produced as an output file from mesh generation. Thus,

```
R & P trona w/joints wp=30 90=lp wc=we=20 R=51% fine mesh
F:\Visual Studio 2010\Projects\SPK\SPKJ\EQ.txt
F:\Visual Studio 2010\Projects\SPK\GMB3\belms
F:\Visual Studio 2010\Projects\SPK\GMB3\bcrds
F:\Visual Studio 2010\Projects\SPK\GMB3\brcte
F:\Visual Studio 2010\Projects\SPK\GMB3\bsigi
F:\Visual Studio 2010\Projects\SPK\GMB3\bnsps
TReq
nelem =  618750
nnode =  656656
nspec =   73456
nmat  =      12
ncut  =      -1
ninc  =      10
nsigo =       1
inter =     200
maxit =    4000
nyeld =       2
nelcf =    7000
nsol  =       2
nprb  =       5
mgob  =       0
 error=    1.0000
 orf  =    1.8600
 xfac =   12.0000
 yfac =   12.0000
 zfac =   12.0000
 efac =    1.0000
 cfac =    1.0000
torl% =    0.0100
ENDRUN
```

*Step 3 FEM Execution and Results* Vertical section views of the distribution of element safety factors are shown in Figure 18 in three cases without gob effect and Figure 19 using equivalent properties. Element boundaries are not shown for clarity. Run time for this mesh was just under four hours.

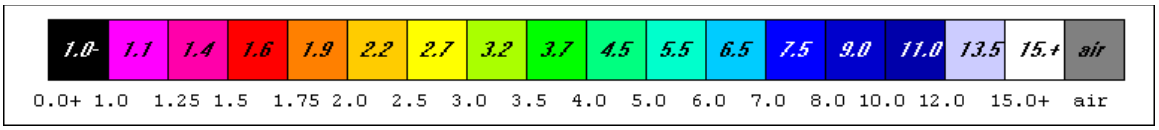


Safety Factor Color Scale

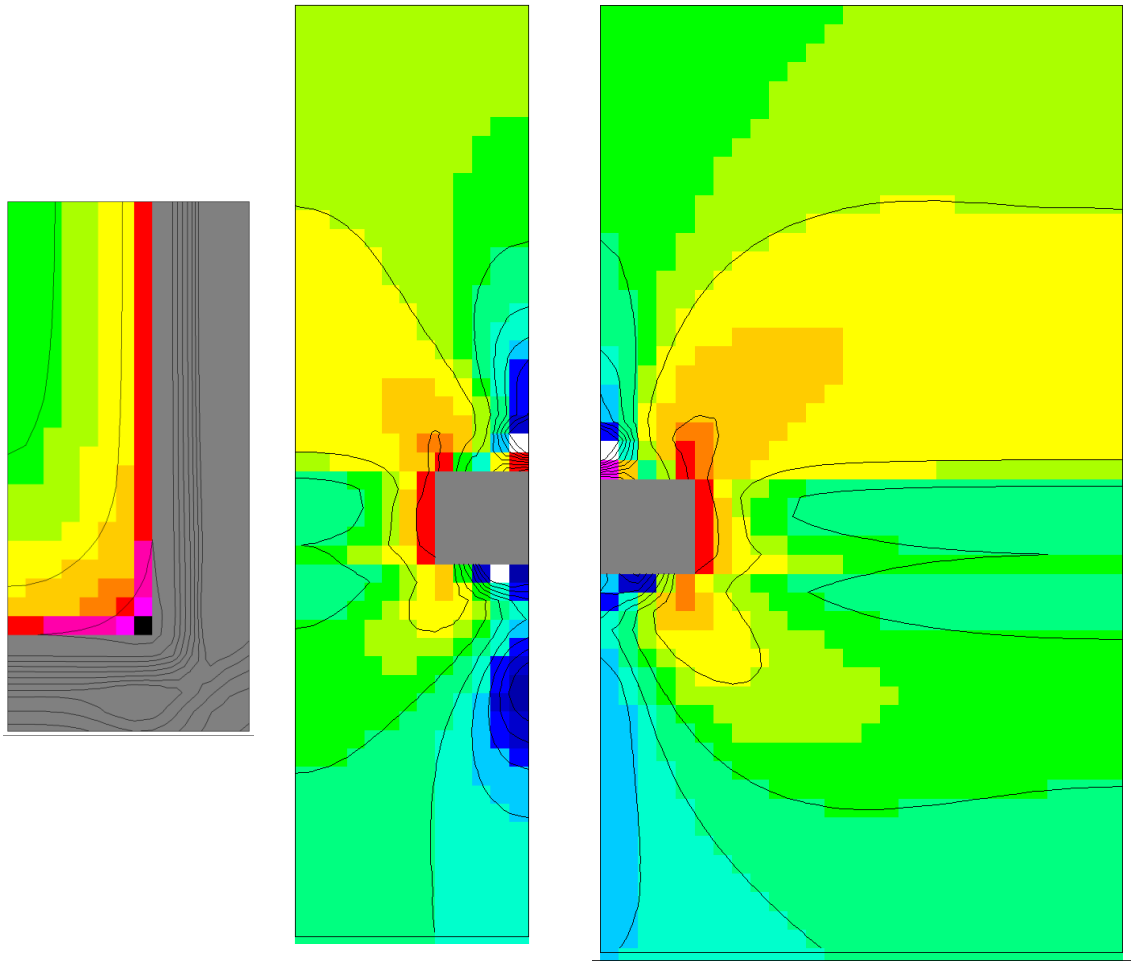

(a) Plan View (b) Vertical Narrow Section (c) Vertical Long Section

Figure 18 Plan and vertical sections show element safety factor distributions in case of a long pillar with and extraction ratio of 51 percent using intact rock properties. Gray=excavated entry and crosscut. Mining height is 10 ft (3 m). Entries and crosscuts are 20 ft (6.1 m) wide. Pillar is 30x90 ft (9.1x27.4 m).

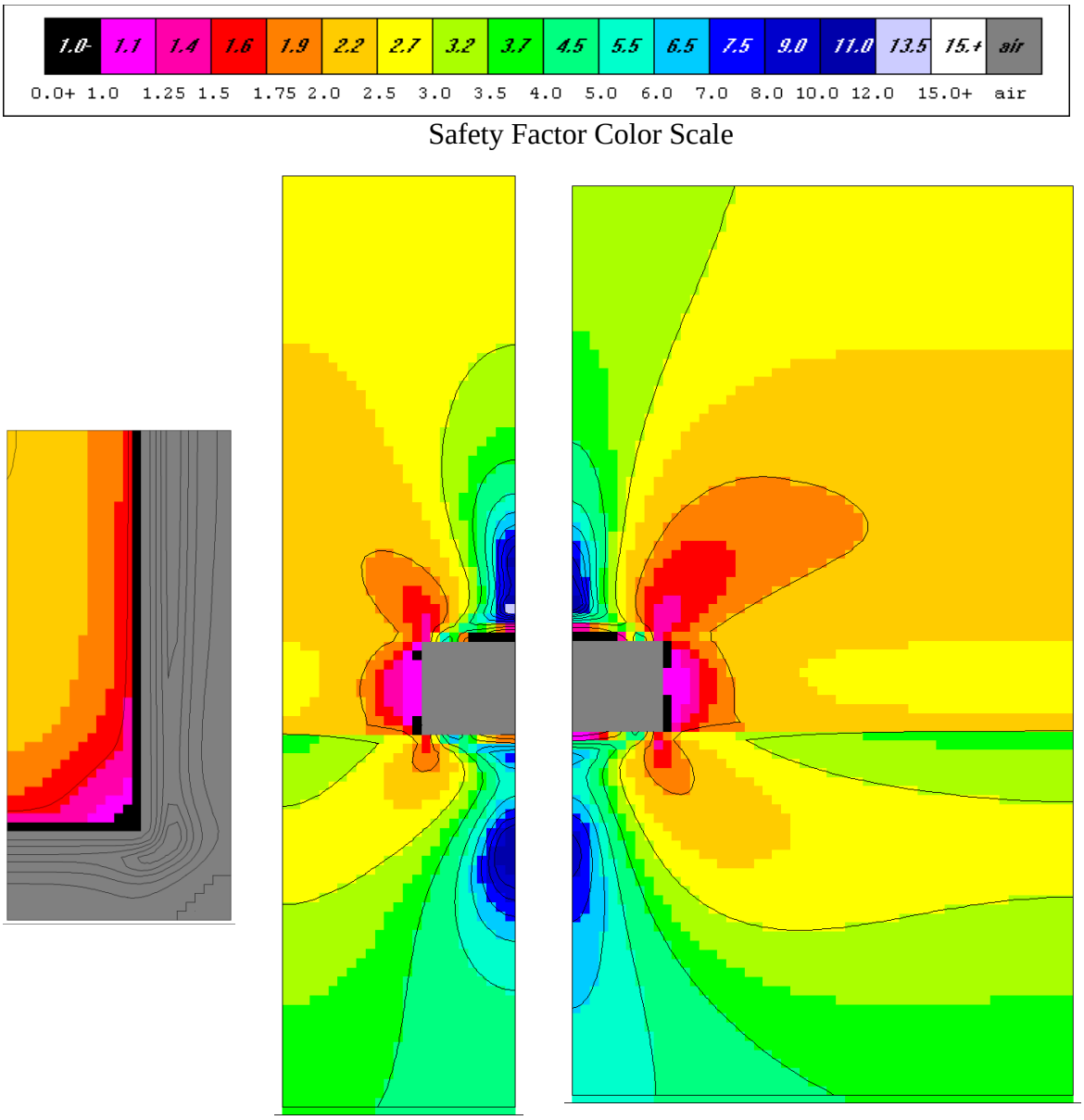


Safety Factor Color Scale

(a) Plan View (b) Vertical Narrow Section (c) Vertical Long Section

Figure 19 Plan and vertical sections show element safety factor distributions in case of a long pillar with and extraction ratio of 51 percent using *equivalent properties*. Gray=excavated entry and crosscut. Mining height is 10 ft (3 m). Entries and crosscuts are 20 ft (6.1 m) wide. Pillar is 30x90 ft (9.1x27.4 m).

Comparisons of results in Figure 19 (joints) with results in Figure 18 (no joints) clearly indicate that joints matter. More failures and lower safety factors occur in case of joints, not too surprisingly. These failures occur at points of peak stress concentration, near pillar edges, at entry and crosscut corners and near roof centers.

**Problem 6** *Shaft Safety* The first five problems of the seven problem types described in the User Manual for using UT3PC involve strata above and below the mining horizon and require a program run of UT3PCJ for each stratum during *Step1j0* calculations for equivalent properties. Problems six and seven involving shafts and tunnels are analyses of sections ("slabs") and may be in a single rock type and thus require just one program run in calculation of equivalent properties. However, thin formations that are inclined may appear in a section and thus require several runs for equivalent properties of the jointed formations present.

The example shaft safety problem concerns the Ross Shaft at the former Homestake Mine in Lead, South Dakota. The mine is now an underground research laboratory with great interest in the physics of neutrinos. In preparation for excavation of a very large underground cavern on the 4850 Level (4850 ft below surface), the Ross Shaft was rehabilitated as was the hoisting gear.

*Step 1 Specification of a material properties files* is

```
NLYRS = 3
NSEAM = 2
  (1) Poorman
  13.5e+06  13.7e+06  7.20e+06      0.23      0.22      0.15
   3.8e+06   5.6e+06  3.94e+06       0.0       0.0       0.0
   13630.0   12270.0   10000.0    2990.0    1910.0     820.0
    1500.0    1520.0    2800.0
      55.0      60.0    2900.0     560.0
  (2) Homestake
  12.8e+06   9.0e+06   9.3e+06      0.14      0.19      0.18
   4.8e+06   4.3e+06   3.9e+06       0.0       0.0       0.0
   20150.0   13270.0   11547.0    1378.0    1920.0    1139.0
    2025.0    2100.0    2470.0
      55.0      60.0    3460.0      80.0
 (3) Poorman
  13.5e+06  13.7e+06  7.20e+06      0.23      0.22      0.15
   3.8e+06   5.6e+06  3.94e+06       0.0       0.0       0.0
   13630.0   12270.0   10000.0    2990.0    1910.0     820.0
    1500.0    1520.0    2800.0
      55.0      60.0    3540.0     560.0
```

The Poorman formation is repeated because the formations are overturned. Depth to the center of the Homestake Formation is 3540 as seen in the file.

*Step 1j* begins with the geology of the shaft route above and below the depth of interest. The runstream for computing equivalent properties using UT3PCJ is

```
Homestake Shaft w/ Joints 8/21/2022 wgp
HM1.txt
celms.txt
ccrds.txt
none
none
cnsps.txt
aHM1
nelem =       1
```

```
nnode =       8
nspec =       8
nmat  =       3
ncut  =       1
ninc  =       1
nsigo =       0
inter =     100
maxit =    1000
nyeld =       2
nelcf =       0
ncave =       0
nfile =       1
npsi  =       1
nrstrt=       0
 error=    1.0000
 orf  =    1.8600
 xfac =   12.0000
 yfac =   12.0000
 zfac =   12.0000
 efac =    1.0000
 cfac =     100.0
Homestake  w/ Joints 8/21/2022 wgp
HM2.txt
celms.txt
ccrds.txt
none
none
cnsps.txt
aHM2
nelem =       1
nnode =       8
nspec =       8
nmat  =       3
ncut  =       1
ninc  =       1
nsigo =       0
inter =     100
maxit =    1000
nyeld =       2
nelcf =       0
ncave =       0
nfile =       2
npsi  =       1
nrstrt=       0
 error=    1.0000
 orf  =    1.8600
 xfac =   12.0000
 yfac =   12.0000
 zfac =   12.0000
 efac =    1.0000
 cfac =     100.0
Homestake w/ Joints 8/21/2022 wgp
HM3.txt
celms.txt
ccrds.txt
none
none
cnsps.txt
```

```
aHM3
nelem =       1
nnode =       8
nspec =       8
nmat  =       3
ncut  =       1
ninc  =       1
nsigo =       0
inter =     100
maxit =    1000
nyeld =       2
nelcf =       0
ncave =       0
nfile =       3
npsi  =       1
nrstrt=       0
 error=    1.0000
 orf  =    1.8600
 xfac =   12.0000
 yfac =   12.0000
 zfac =   12.0000
 efac =    1.0000
 cfac =     100.0
RUN END
```

where HM3 is

```
(3) joint N 261 E  02/11/2022  wgp 0.1 thik N=2
 15.80e+04 15.80e+04 15.80e+04      0.25      0.25      0.25
  6.32e+04  6.32e+04  6.32e+04       0.0       0.0       0.0
     286.0     286.0     286.0      16.0      16.0      16.0
     39.10     39.10     39.10
    261.00      74.0       2.4     -0.10
 (4) joint N 358 E N=2
 15.80e+04 15.80e+04 15.80e+04      0.25      0.25      0.25
  6.32e+04  6.32e+04  6.32e+04       0.0       0.0       0.0
     286.0     286.0     286.0      16.0      16.0      16.0
     39.10     39.10     39.10
     358.0      58.0       4.4     -0.10
 (3) Poorman
  13.5e+06  13.7e+06  7.20e+06      0.23      0.22      0.15
   3.8e+06   5.6e+06  3.94e+06       0.0       0.0       0.0
   13630.0   12270.0   10000.0    2990.0    1910.0     820.0
    1500.0    1520.0    2800.0      55.0      60.0    3540.0     560.0
```

and similarly for HM2 (Homestake) and HM1.

A schematic plot of the two joint sets is illustrated in Figure 20?

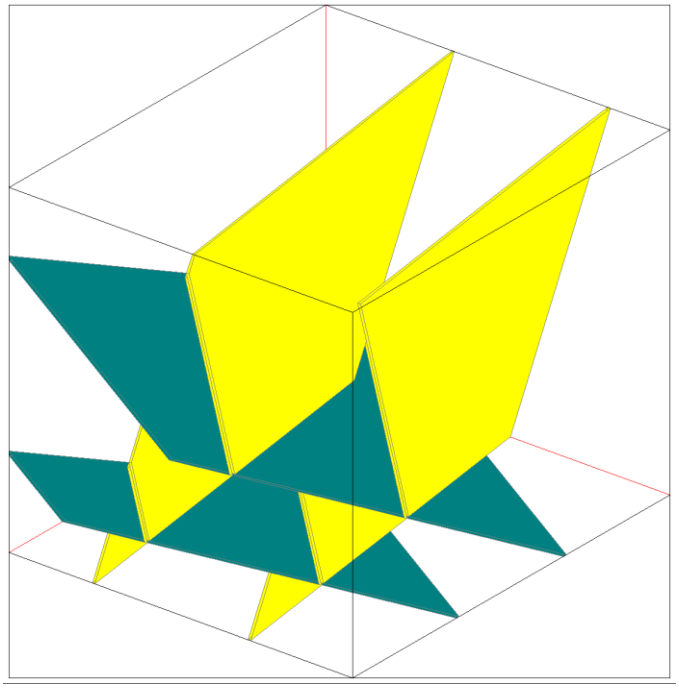

Figure 20 Schematic illustration of the two joint sets used in computing equivalent properties.

The resulting equivalent properties are

```
NLYRS =       3
NSEAM =       2
 (3) Poorman
   0.308E+07   0.405E+07   0.366E+07        0.14        0.28        0.18
   0.213E+07   0.123E+07   0.100E+07        0.00        0.00        0.00
      6511.0      6667.6      7128.2      1428.3      1037.9       584.5
      1760.7      1518.8      1178.5
        55.0        60.0      3540.0       560.0
  (2) Homestake
   0.301E+07   0.411E+07   0.414E+07        0.07        0.29        0.21
   0.204E+07   0.118E+07   0.984E+06        0.00        0.00        0.00
      9774.4      8964.5      7708.8       668.4      1297.0       760.4
      1475.8      1968.7      1397.8
        55.0        60.0      3460.0        80.0
   (3) Poorman
   0.308E+07   0.405E+07   0.366E+07        0.14        0.28        0.18
   0.213E+07   0.123E+07   0.100E+07        0.00        0.00        0.00
      6511.0      6667.6      7128.2      1428.3      1037.9       584.5
      1760.7      1518.8      1178.5
        55.0        60.0      3540.0       560.0
```

Again, repetition of the Poorman formation is a consequence of overturned folds.

*Step 2 Mesh Generation* leads to the mesh shown in Figure 21. Orientation of the formations is seen in the last line of equivalent properties as are depths and thicknesses.

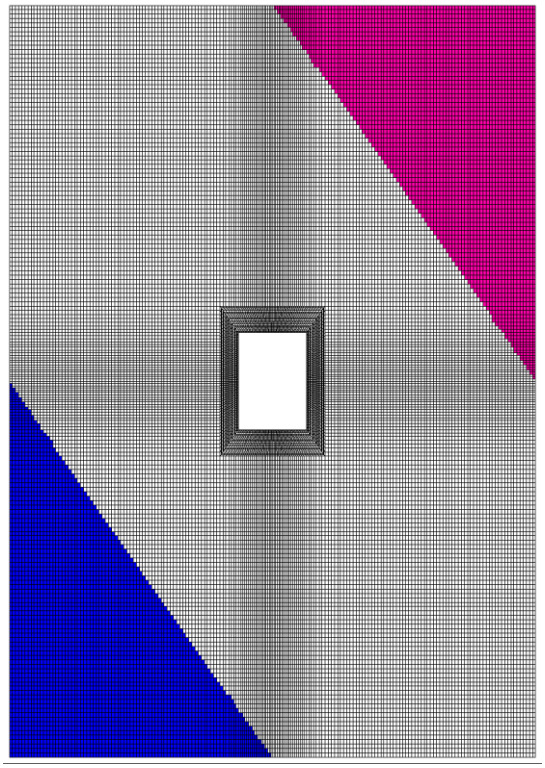

Figure 21 Mesh for problem 6 *Shaft Safety*. The shaft is 15 x 21 ft (4.6 x 6.4 m ). The mesh is a plan view.

Output files during mesh generation include an InData file, a runstream file, a mesh plot file, and a safety factor plot file. The InData file echoes some of the input. Thus,

```
Input Data
 SHAFT NPROB 6
 Shaft Shape = Rectangle
 Shaft System = Single Opening
 Shaft Width =      15.0
 Width/Height Ratio =       0.7
 Opening Height=      21.4
 Section Depth Seam Center (ft)   =    3500.0
 Additional Sxx,Syy,Szz,Tyz,Tzx,Txy, tension +=
   -3349.0   -2700.0   -4167.0       0.0       0.0     -88.0
 Shaft Stress Sxx,Syy,Szz,Tyz,Tzx,Txy, tension +=
   -3349.0   -2700.0   -4167.0       0.0       0.0     -88.0
```

where the additional stresses are just the preshaft stresses developed from formulas based on many stress measurements made at the mine. No separate gravity stresses are specified as seen in the absence of specific weights in the material property file EQ.txt.

*Step 3 Execution* uses the runstream file and the program UT3PC

```
HME RECTANGLE SHAFT 8/21/2022  01/26/2021 wgp
F:\Visual Studio 2010\Projects\SPK\SPKJ\EQ.txt
F:\Visual Studio 2010\Projects\SPK\GMB3\belms
F:\Visual Studio 2010\Projects\SPK\GMB3\bcrds
F:\Visual Studio 2010\Projects\SPK\GMB3\brcte
F:\Visual Studio 2010\Projects\SPK\GMB3\bsigi
F:\Visual Studio 2010\Projects\SPK\GMB3\bnsps
HMeq
nelem =   36384
nnode =   73728
nspec =   73728
nmat  =       3
ncut  =      -1
ninc  =       5
nsigo =       1
inter =     200
maxit =    2000
nyeld =       2
nelcf =     208
nsol  =       2
nprb  =       5
mgob  =       0
 error=    1.0000
 orf  =    1.8600
 xfac =   12.0000
 yfac =   12.0000
 zfac =   12.0000
 efac =       1.0
 cfac =       1.0
tolr% =    0.0100
ENDRUN
```

Results of interest are element safety factor distributions, especially in the immediate vicinity of the shaft. A comparison of distributions without and with joints is shown in Figure 22. Evidently jointing has little effect on shaft wall safety. In fact, the equivalent properties case appears to give a somewhat safer shaft wall, although a more irregular distribution of element safety factors.

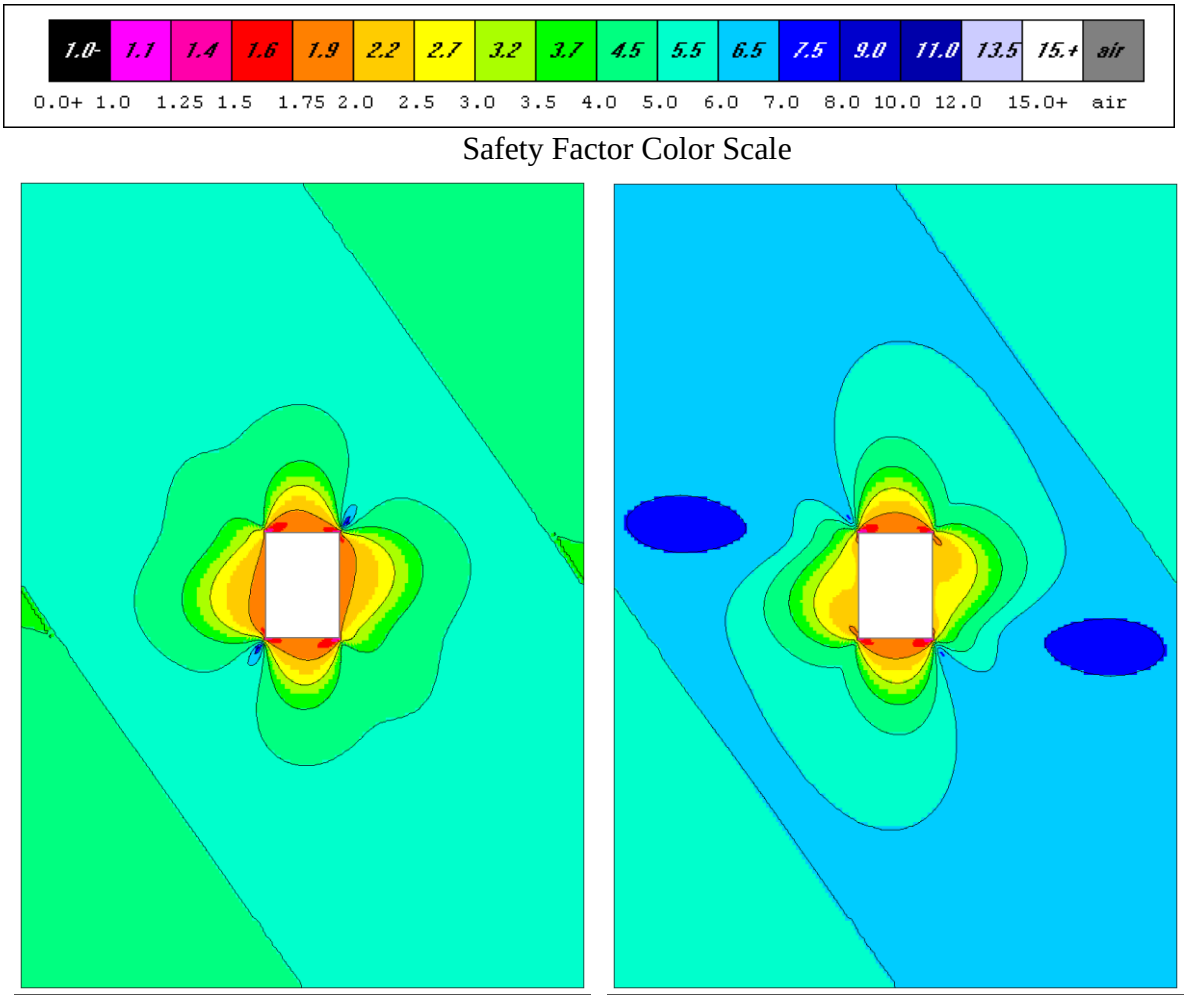


Figure 22 Element safety factor distributions without joints (a) and using equivalent jointed rock mass properties (b).

**Problem 7 Tunnels (drifts, crosscuts, adits)** The site for this example using equivalent properties of a jointed rock mass is the East Boulder Mine in the Stillwater complex of southwestern Montana. The example concerns twin circular tunnels developed as adits using a tunnel boring machine. Details are given in the User Manual where a strain to failure criterion is used for estimating equivalent strengths. The example here is different and uses an energy to failure criterion for strength estimation.

*Step 1 Preparation of a materials property file (stratigraphic column)* The material properties file for this example is

```
NLYRS = 1
NSEAM = 1
  (1) Gabbro Reef
  15.8e+06  15.8e+06  15.8e+06      0.25      0.25      0.25
  6.32e+06  6.32e+06  6.32e+06       0.0       0.0       0.0
   28000.0   28000.0   28000.0    1600.0    1600.0    1600.0
    3910.0    3910.0    3910.0
      90.0      90.0    2390.0     420.0
```

*Step 1j Preparation of an equivalent materials property file* Equivalent material properties computation begins by preparing a runstream input for UT3PCJ, as before. Thus,

```
Stillwater w/ Joints 8/24/2022 wgp
STMprop.txt
celms.txt
ccrds.txt
none
none
cnsps.txt
aSTM
nelem =       1
nnode =       8
nspec =       8
nmat  =       3
ncut  =       1
ninc  =       1
nsigo =       0
inter =     100
maxit =    1000
nyeld =       2
nelcf =       0
ncave =       0
nfile =       1
npsi  =       1
nrstrt=       0
 error=    1.0000
 orf  =    1.8600
 xfac =   12.0000
 yfac =   12.0000
 zfac =   12.0000
 efac =    1.0000
 cfac =     100.0
RUN END
```

The file STMprop.txt containing joint and intact rock properties is

```
(1) joint N 155 E  02/08/021 Stillwater wgp 0.1 thik N=2
 15.80e+04 15.80e+04 15.80e+04      0.25      0.25      0.25
  6.32e+04  6.32e+04  6.32e+04       0.0       0.0       0.0
    286.0     286.0     286.0      16.0      16.0      16.0
    39.10     39.10     39.10
         245.00      72.0       3.1     -0.10
 (2) joint N 81 E N=2
```

```
15.80e+04 15.80e+04 15.80e+04      0.25      0.25      0.25
 6.32e+04  6.32e+04  6.32e+04       0.0       0.0       0.0
    286.0     286.0     286.0      16.0      16.0      16.0
    39.10     39.10     39.10
    171.0      67.0       4.4     -0.10
(3) GABBRO  N=2 (DP2) & sp wts (pcf) z=vert 12/11/2017
15.80e+06 15.80e+06 15.80e+06      0.25      0.25      0.25
 6.32e+06  6.32e+06  6.32e+06       0.0       0.0       0.0
  28600.0   28600.0   28600.0    1600.0    1600.0    1600.0
   3910.0    3910.0    3910.0
    90.0      90.0    2390.0     420.0
```

A schematic of joints in the two joint sets is illustrated in Figure 23

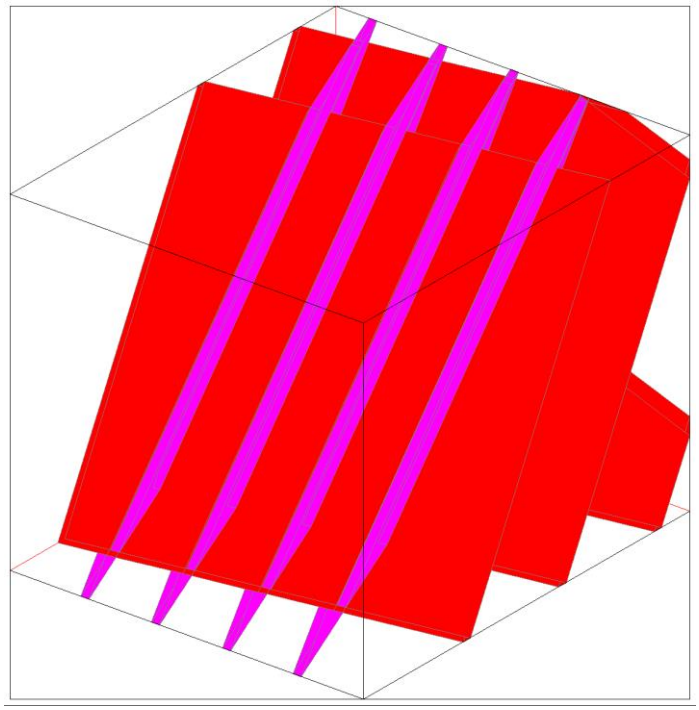

Figure 23 Schematic of two joint sets.  Pink=Set 1, Red=Set2.

*Step 2 Mesh Generation* Mesh generation input is given in part in the InData file developed during mesh generation:  Thus,

```
Input Data
 “TUNNEL” NPROB 7
 Tunnel Shape = Ellipse (including circle)
 Tunnel System = Twin Openings
 Tunnel Width =      15.0
 Width/Height Ratio =       1.0
 Pillar Width =      30.0
 Section Depth Seam Center (ft)   =    2600.0
 Additional Sxx,Syy,Szz,Tyz,Tzx,Txy, tension +=
   -5616.0   -3120.0   -4680.0       0.0       0.0       0.0
 Tunnel Stress Sxx,Syy,Szz,Tyz,Tzx,Txy, tension +=
   -5616.0   -3120.0   -4680.0       0.0       0.0       0.0
```

*Step 3 FEM Execution and Results* Figure 24 shows results in the form of a side by side comparison of distributions of element safety factors in case of intact rock properties and equivalent jointed rock properties. This example again clearly shows that joints matter.

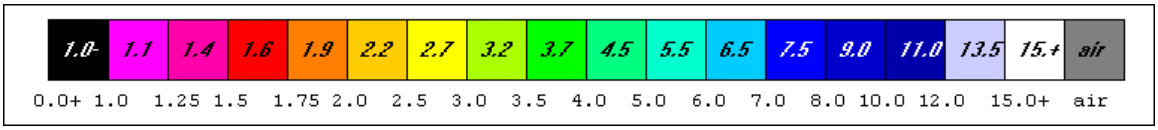


Factor of Safety Color Code

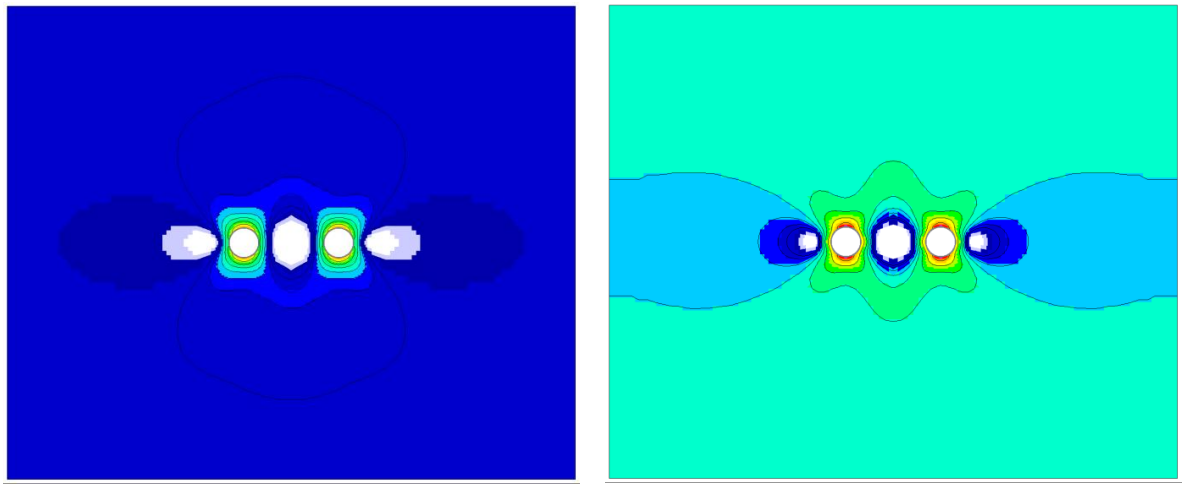

(a) (b)

Figure 24 Element safety factors about twin tunnels excavated by a tunnel boring machine at the Stillwater Mine (East Boulder) in intact rock. (a)No scaling of properties is done in this example. No joints are present in (a) where safety factors range from 2.7 (yellow) to over 15 (white). In (b) using equivalent jointed rock mass properties elements in back and floor are red indicating a local safety factor of 1.6. The pillar between tunnels appears secure.

**Summary** Computation of equivalent properties of jointed rock using the finite element program UT3PCJ requires a S*tep 1j* for generation of equivalent properties of jointed rock formations. This step follows *Step 1* for specification of intact formation properties.. The program UT3PCJ is used for generating equivalent properties. The output file from this step is a file of equivalent

jointed rock mass properties. Mesh generation (*Step 2*) may be done using either intact rock properties or equivalent rock properties. Finally *Step 3*, execution, is done for finite element analysis of the problem type selected from the seven choices available. The program UT3PC is used for analysis in all cases. Mesh plotting can be done after mesh generation and is recommended before program execution. Plotting of element safety factors for design guidance after program execution can be done in the usual manner.

## References - Jointed Rock Models


Hill, R. (1963) Elastic Properties of Reinforced Solids: Some Theoretical Principles. *J Mech Phys Solids*.Vol 11, pp 357-372.

Hudson, J. A. (1980) *The Excitation and Propagation of Elastic Waves*. Cambridge University Press.

Lekhnitiskii (1963) *Theory of Elasticity of an Anisotropic Elastic Body*. Holden-Day, San Francisco, pgs 404.

Pariseau, W. G. and H. Moon (1988) "Elastic Moduli of Well-jointed Rock Masses." *Numerical Methods in Geomechanics (Innsbruck,* Balkema, Rotterdam, pp 815-822.

Pariseau, W. G. (1993) "Equivalent Properties of a Jointed Biot Material", *Int'l. J. Rock Mech. Min. Sci. & Geomech. Abstr.*, Vol. 30, No. 7, pp 1151-1157.

Pariseau, W. G. (1995)"Non-representative Volume Element Modeling of Equivalent Jointed Rock Mass Properties". *Proc. Mechanics of Jointed and Faulted Rock – 2.* Balkema, Rotterdam, pp 563-568.

Pariseau, W. G. (1999) "An Equivalent Plasticity Theory for Jointed Rock Masses". *Int'l J. Rock Mech. Mng. Sci.*, Vol. 36, No.7, pp. 907-918.

Pariseau, W. G., D. Tesarik and T. Trancynger, (2012) "Rock Mechanics of the Davis Detector Cavern", SME Annual Meeting, Seattle, Washington, February 19-22, 2012, Preprint CD 12-022 and SME Transactions, Vol. 332, pp 2-20.

Pariseau, W. G. (2017) "Comparison of Underground Coal and Trona Mine Seismicity". Preprint 17-027, SME Annual Meeting & Exhibit, February 19-22, 2017 Denver, Colorado.

Pariseau, W. G. (2022) "User Manual **for a T**hree-dimensional Finite Element Program UT3PC (2nd edition) A Fundamental Approach to Design of Coal Mine Entries, Barrier Pillars, Bleeder Entries, Interpanel Barrier Pillars, Pillars and Rooms in Room and Pillar Mines, Shafts and Tunnels." Website UT3PC.net.

## APPENDIX IX MORE EXAMPLES of JOINT EFFECTS

This appendix presents more examples of joint effects using equivalent properties in analyses of the seven problem types addressed in this User Manual. Details of computations leading to equivalent properties, elastic moduli and strengths, are presented in APPENDIX VII. As in APPENDIX VIII concerning effects of jointed rock on excavation design, comparisons are made between intact and jointed rock to allow for assessment of joint effects on the distribution of element safety factors in the region of interest. Distributions of element safety factors in graphic form show whether yielding occurs and if so, the potential extent of yielding, thus presenting useful design guidance at a glance for a proposed excavation layout.

**Problem 1** This problem example concerns safety of main entries in a trona mine in southwestern Wyoming. The sequence of roof, seam and floor in trona mines is the reverse of the sequence in coal mines with respect to strength. In trona mines the seam is strong while the roof and floor are relatively compliant and weak. Just the opposite occurs in many coal mines where the coal seam is compliant and weak while the roof and floor are relatively stiff and strong. The problem is presented in detail when joints are absent in the User Manual (APPENDIX IV). In this example, *Step 1* and *Step 1j* for equivalent properties are already taken in a previous example problem involving safety in room and pillar mining in APPENDIX VIII. The equivalent properties are

```
NLYRS =12
NSEAM = 7
   (1) SHALE 1 N=2 (DP2) & spwts (pcf)
   0.527E+06   0.527E+06   0.474E+06        0.25        0.14        0.12
   0.151E+06   0.151E+06   0.217E+06        0.00        0.00      144.00
      3830.3      3830.3      3634.0       404.7       404.7       383.9
       718.8       718.8       682.0
         0.0         0.0         0.0        62.0
  (2) MUDSTONE
   0.639E+06   0.639E+06   0.563E+06        0.25        0.11        0.10
   0.172E+06   0.172E+06   0.264E+06        0.00        0.00      134.00
      2590.5      2590.5      2431.0       359.6       359.6       337.5
       557.3       557.3       523.0
         0.0         0.0        62.0       148.0
  (3) SANDSTONE 1
   0.809E+06   0.809E+06   0.690E+06        0.28        0.10        0.08
   0.197E+06   0.197E+06   0.328E+06        0.00        0.00      140.00
      3988.6      3988.6      3682.4       303.1       303.1       279.8
       634.8       634.8       586.1
         0.0         0.0       210.0       249.0
  (4) OIL SHALE 1
   0.508E+06   0.508E+06   0.459E+06        0.32        0.21        0.19
   0.142E+06   0.142E+06   0.197E+06        0.00        0.00      142.00
      4164.8      4164.7      3957.5       362.0       362.0       344.0
       708.9       708.9       673.6
         0.0         0.0       459.0       449.0
  (5) SANDSTONE 2
   0.639E+06   0.639E+06   0.563E+06        0.25        0.11        0.10
   0.172E+06   0.172E+06   0.264E+06        0.00        0.00      134.00
      4571.0      4571.0      4289.6       347.3       347.3       326.0
       727.5       727.5       682.7
         0.0         0.0       908.0       171.0
```

```
(6) SHALE 2
 0.527E+06   0.527E+06   0.474E+06        0.25        0.14        0.12
 0.151E+06   0.151E+06   0.217E+06        0.00        0.00      144.00
    4118.2      4118.2      3907.2       358.0       358.0       339.6
     701.0       701.0       665.1
       0.0         0.0      1079.0       420.0
(7) TRONA 1
 0.101E+07   0.101E+07   0.832E+06        0.29        0.07        0.05
 0.223E+06   0.223E+06   0.411E+06        0.00        0.00      134.00
    3392.4      3392.4      3073.3       204.4       204.4       185.2
     480.8       480.8       435.6
       0.0         0.0      1499.0        10.0
(8) OIL SHALE 2
 0.508E+06   0.508E+06   0.459E+06        0.32        0.21        0.19
 0.142E+06   0.142E+06   0.197E+06        0.00        0.00      142.00
    4164.8      4164.7      3957.5       362.0       362.0       344.0
     708.9       708.9       673.6
       0.0         0.0      1509.0        89.0
(9) TRONA 2
 0.101E+07   0.101E+07   0.832E+06        0.29        0.07        0.05
 0.223E+06   0.223E+06   0.411E+06        0.00        0.00      134.00
    3392.4      3392.4      3073.3       204.4       204.4       185.2
     480.8       480.8       435.6
       0.0         0.0      1598.0        10.0
(10) SHALE 3
 0.527E+06   0.527E+06   0.474E+06        0.25        0.14        0.12
 0.151E+06   0.151E+06   0.217E+06        0.00        0.00      144.00
    4118.2      4118.2      3907.2       358.0       358.0       339.6
     701.0       701.0       665.1
       0.0         0.0      1608.0       190.0
(11) SANDSTONE 3
 0.809E+06   0.809E+06   0.690E+06        0.28        0.10        0.08
 0.197E+06   0.197E+06   0.328E+06        0.00        0.00      140.00
    3988.6      3988.6      3682.4       303.1       303.1       279.8
     634.8       634.8       586.1
       0.0         0.0      1798.0        49.0
(12) TIPTON FM
 0.527E+06   0.527E+06   0.474E+06        0.25        0.14        0.12
 0.151E+06   0.151E+06   0.217E+06        0.00        0.00      144.00
    4118.2      4118.2      3907.2       358.0       358.0       339.6
     701.0       701.0       665.1
       0.0         0.0      1847.0      3313.0
```

These properties are based on intact rock properties and joints. Five joint sets are present and are illustrated in Figure 1.

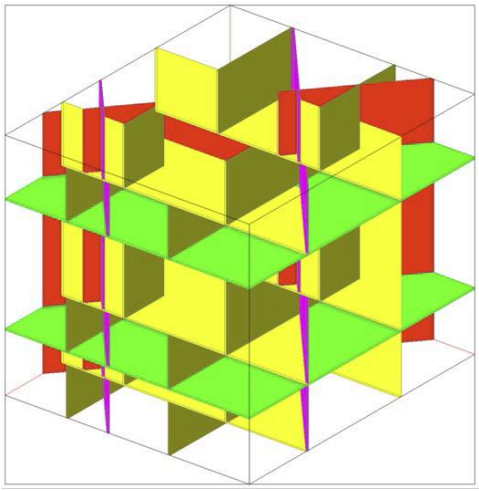

Figure 1 Five joint sets used in equivalent trona properties.

Mesh generation *Step 2* may be done next. Figure 2 shows plan and section views of the mesh.

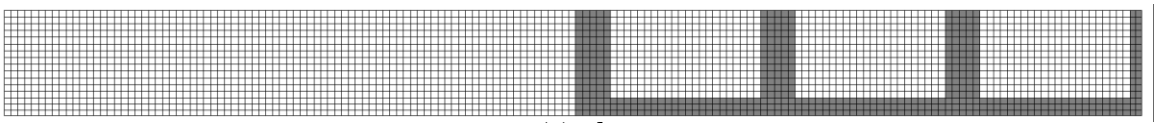

(a) plan view

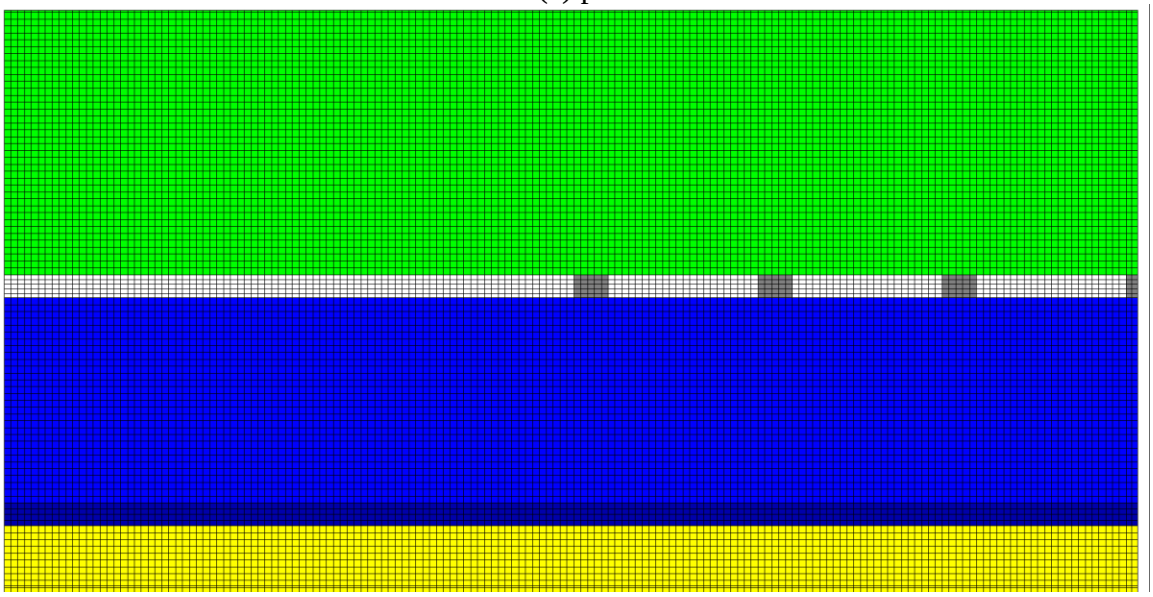

(b) vertical section

Figure 2 Mesh views for main entries in trona, (a) plan, (b) vertical section window. White=trona, Gray=entries, crosscuts. Depth is 1499 ft (457 m)

**Importantly**, generation of equivalent jointed rock mass properties is done using the finite element program UT3JPC, not UT3PC.

An analysis may be done (*Step 3*) following mesh generation (*Step 2*) using the equivalent material property file. Input data for mesh generation in this problem ("mains") is shown in Figure 3. The mesh generation input property file is EQ.txt.

Input Data
MAINS
Number of main entries, NMS = 7
Width of entries, WE (ft) = 15.0
Width of crosscuts, WC (ft) = 15.0
Width of pillars, WP (ft) = 65.0
Length of pillars LP (ft) = 76.0
EX, EY, EZ, (ft)= 3.0 3.0 2.0
Additional Sxx,Syy,Szz,Tyz,Tzx,Txy, tension +=

Figure 3 input/output data for mesh generation

The runstream for finite element analysis (*Step 3)* is

```
MAINS TRONA 2/2/2022 wgp w/jts 8/26/2022
F:\Visual Studio 2010\Projects\SPK\SPKJ\EQ.txt
F:\Visual Studio 2010\Projects\SPK\GMB3\belms
F:\Visual Studio 2010\Projects\SPK\GMB3\bcrds
F:\Visual Studio 2010\Projects\SPK\GMB3\brcte
F:\Visual Studio 2010\Projects\SPK\GMB3\bsigi
F:\Visual Studio 2010\Projects\SPK\GMB3\bnsps
aMTre
nelem = 1370736
nnode = 1467984
nspec =  190614
nmat  =      12
ncut  =      -1
ninc  =       5
nsigo =       1
inter =     100
maxit =    1000
nyeld =       2
nelcf =    2430
nsol  =       2
nprb  =       1
mgob  =       0
 error=    1.0000
 orf  =    1.8600
 xfac =   12.0000
 yfac =   12.0000
 zfac =   12.0000
 efac =    1.0000
 cfac =    1.0000
torl% =    0.0100
ENDRUN
```

and shows that the number of elements exceeds the suggested one million element guide. Fortunately, there is some tolerance in the guide line, so the runstream is executable. The run required 7-1/2 hours of computer time.

Results of analysis without joints and with joints (equivalent properties) are shown as element safety factor distributions in Figure 3. **Both are done using UT3PC**.

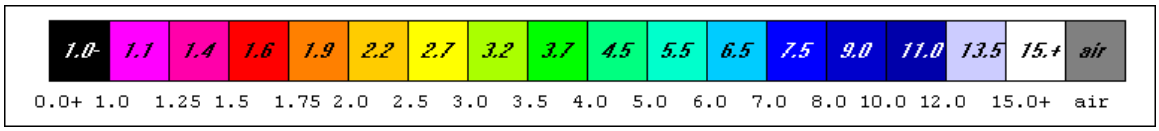


Element Safety Factor Color Scale

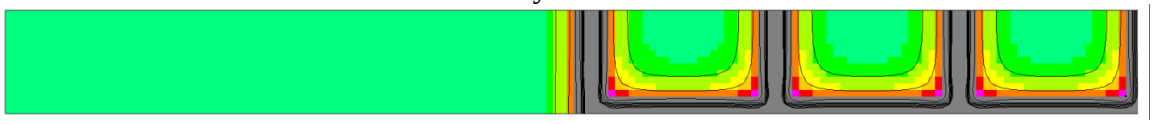

(a) Plan view of element safety factor distribution without joints

(b) Plan view of element safety factor distribution with equivalent properties

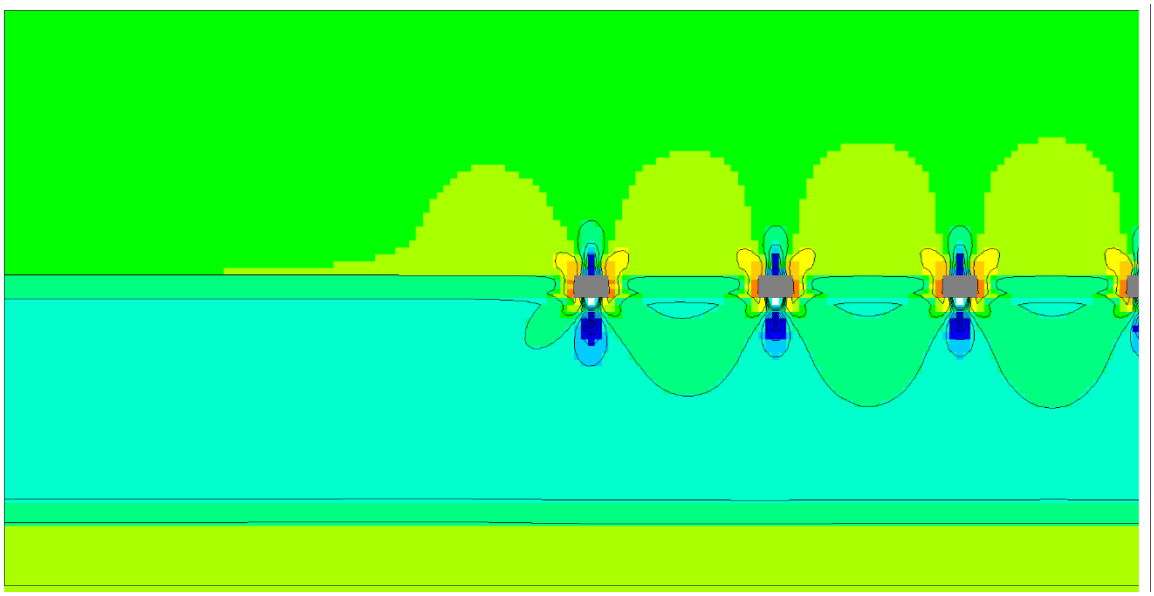

(c) Vertical section window through pillar centers showing element safety factor distribution without joints.

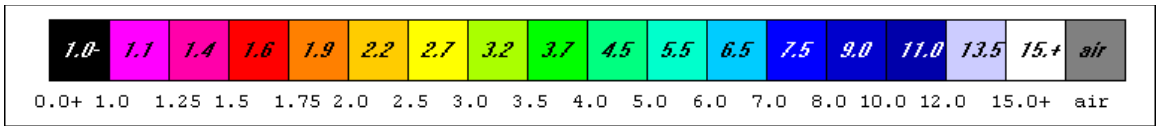


Element Safety Factor Color Scale

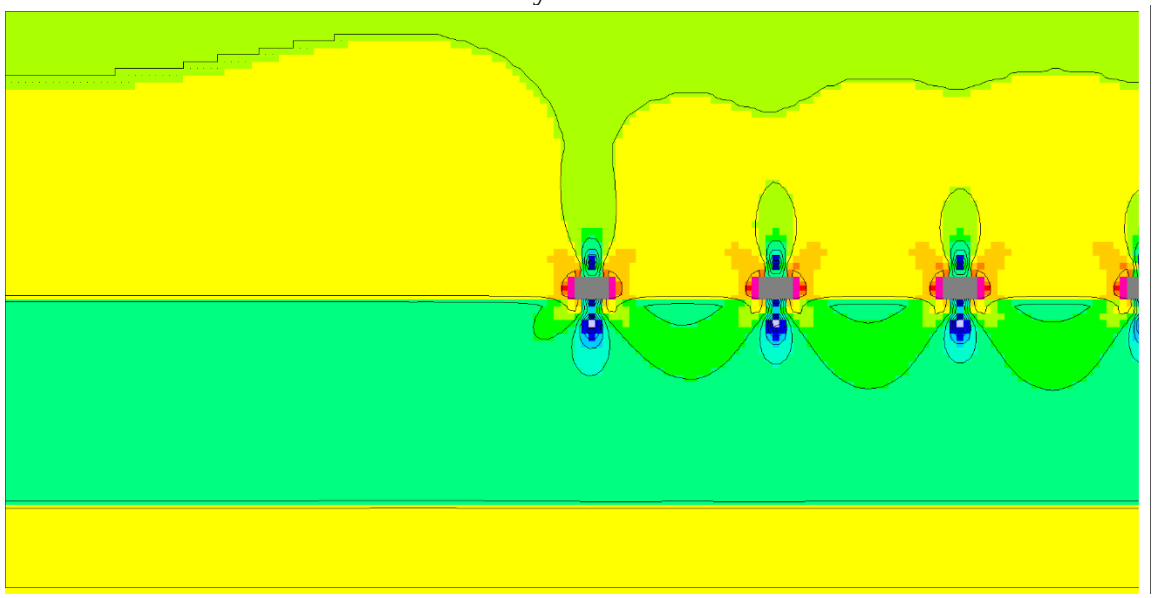

(d) Vertical section window through pillar centers showing element safety factor distribution using equivalent properties.

Figure 3 Element safety factor distributions in the case of seven main entries, Problem 1, in a deep trona mine.

Inspection of Figure 3 indicates a general reduction in element safety factors and some minor yielding at pillar corners. Pillar core safety factor decreases from 3.7 to 2.7 in case of joints as indicated by colors

**Problem 2** This problem relates to barrier pillar size for protection of main entries, crosscuts, and pillars from effects of adjacent longwall mining. An analysis that allows for gob effects is presented in the User Manual in the case where joints are absent. The three step process is again followed in the new analysis but is accompanied by *Step 1j* in case joints are present. An example of barrier pillar problem analysis (Problem 2 "barriers) follows in combination with the usual three-step process and the *Step1j* process.

*Step 1 Preparation of a materials property file (stratigraphic column).* The material property file for rock in this problem is the same as in **Problem 1**, "mains".

*Step 1j Computation of equivalent properties of jointed rock.* The equivalent jointed rock properties for this problem ("barriers") are the same used in the previous problem ("mains"). No additional computation is needed.

*Step 2 Mesh Generation*. Mesh generation input uses the same material properties for rock (and joints) as in the previous example.

*Step 3Execution* The new finite element runstream uses the same equivalent properties file used in the previous example. The runstream file is

```
BARRIER for mains, trona, 8/27/2022 wgp w/jts
F:\Visual Studio 2010\Projects\SPK\SPKJ\EQ.txt
F:\Visual Studio 2010\Projects\SPK\GMB3\belms
F:\Visual Studio 2010\Projects\SPK\GMB3\bcrds
F:\Visual Studio 2010\Projects\SPK\GMB3\brcte
F:\Visual Studio 2010\Projects\SPK\GMB3\bsigi
F:\Visual Studio 2010\Projects\SPK\GMB3\bnsps
aBT
nelem =  594432
nnode =  638435
nspec =   85025
nmat  =      12
ncut  =      -1
ninc  =       5
nsigo =       1
inter =     200
maxit =    2000
nyeld =       2
nelcf =    6655
nsol  =       2
nprb  =       2
mgob  =       0
 error=    1.0000
 orf  =    1.8600
 xfac =   12.0000
 yfac =   12.0000
 zfac =   12.0000
 efac =    1.0000
 cfac =    1.0000
torl% =    0.0100
ENDRUN
```

The Indata file generated as output during mesh generation is

```
Input Data
 BARRIER
 Number of main entries, NMS =   4
 Width of entries, WE (ft)    =      15.0
 Width of crosscuts, WC (ft)  =      15.0
 Width of pillars, WP (ft)    =      65.0
 Length of pillars, LP (ft)   =      76.0
 Barrier pillar width, WB (ft)=     100.0
 EX, EY, EZ, (ft)=       3.0       3.0       2.0
 Additional Sxx,Syy,Szz,Tyz,Tzx,Txy, tension +=
   0.0       0.0       0.0       0.0       0.0       0.0
 No gob effects
```

The finite element mesh is shown in Figure 4.

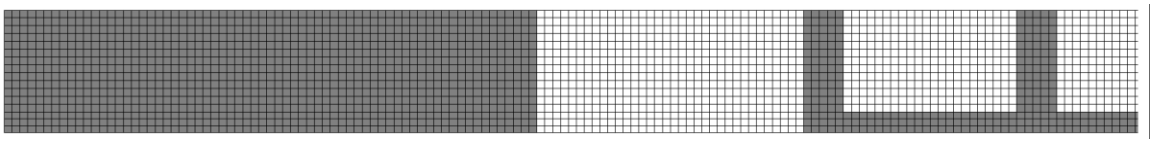

(a) plan view

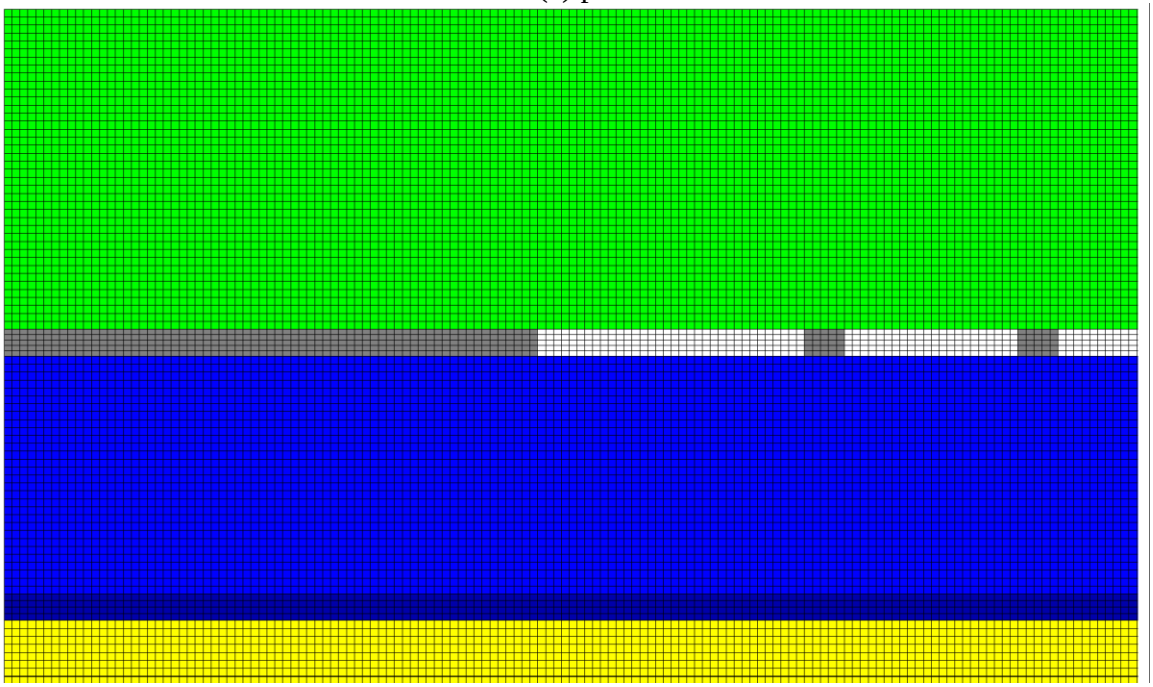

(b) vertical section close-up.

Figure 4 Plan and vertical section views of the mesh for a barrier pillar safety analysis. Only half of the four entry set is needed in the mesh. Grey elements define entry and crosscut regions, and longwall panel. White elements are trona. The barrier pillar is 100 ft (30 m) wide as seen in the Indata file.

Results in the form of element safety factor distributions without and with joints present are given in Figure 5 in plan view at seam level and in Figure 6 in vertical section.

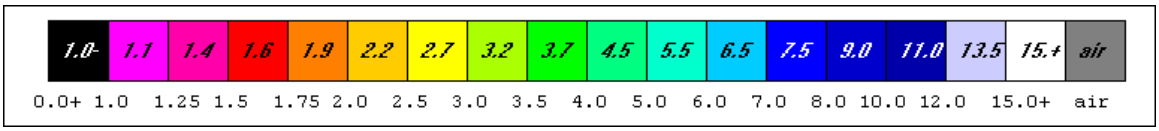


Element Safety Factor Color Scale

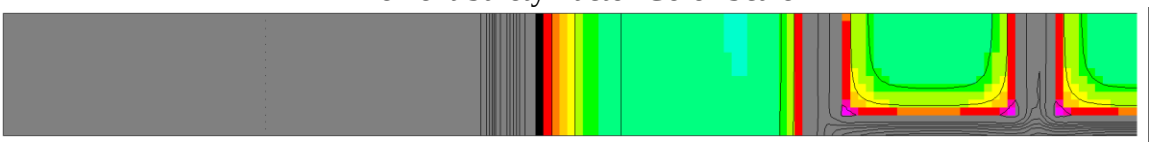

(a) without joints, no gob

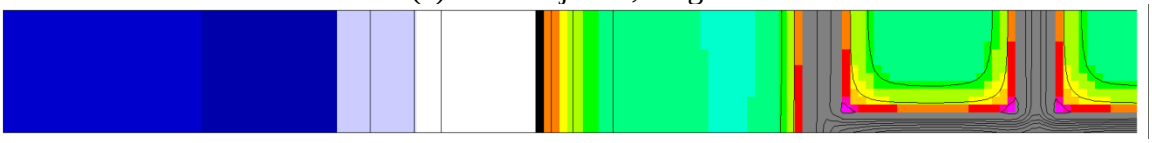

(b) without joints with strong gob

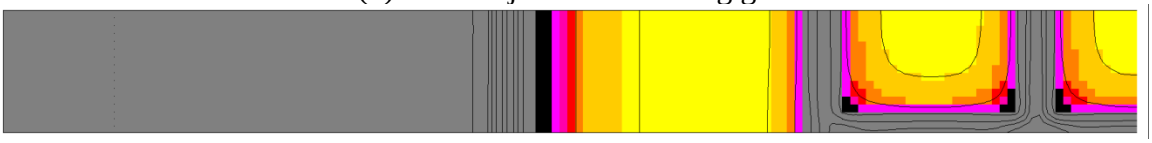

(c) using equivalent properties, no gob

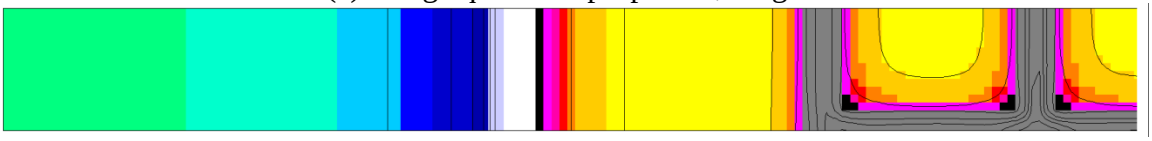

(d) using equivalent propetites with strong gob

Figure 5 Seam level element safety factor distributions.

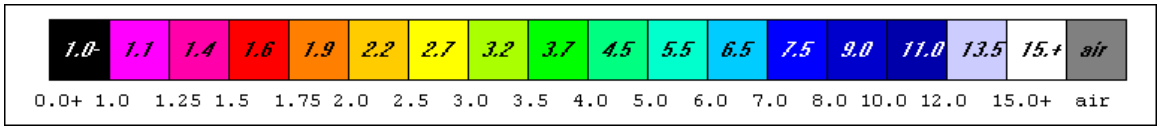


Element Safety Factor Color Scale

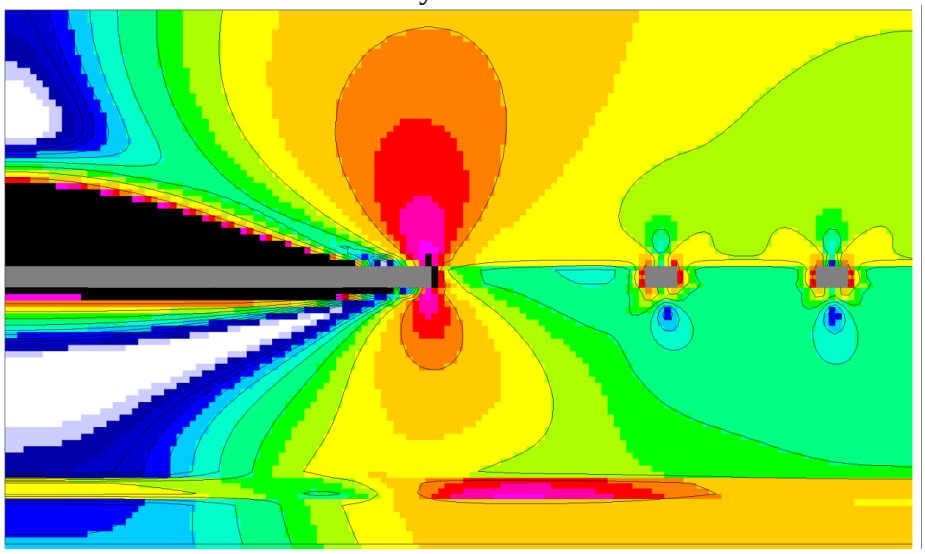

(a) no joints, no gob

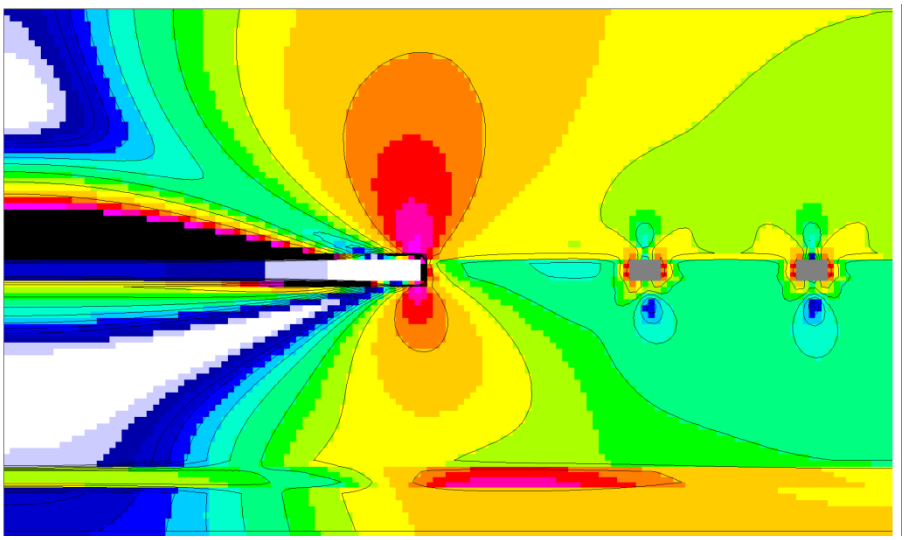

(b) without joints, with gob

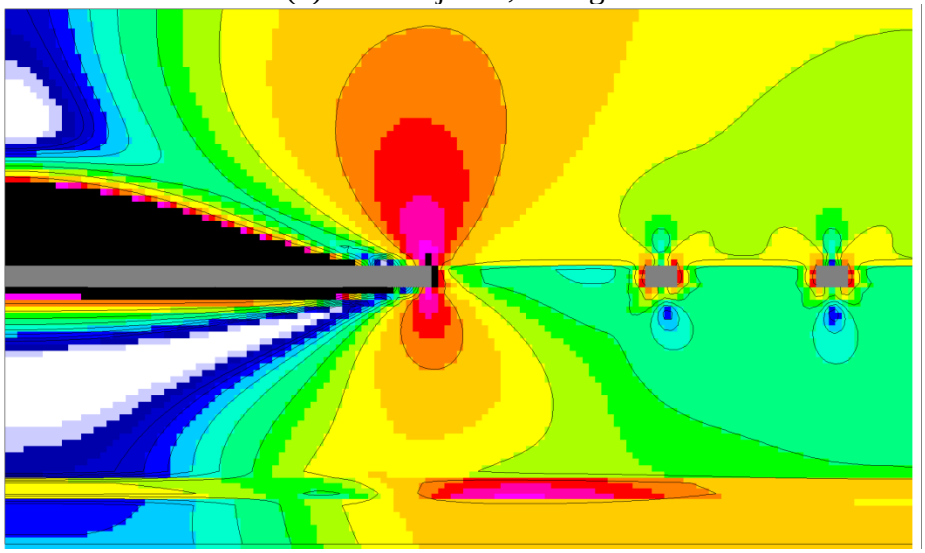

(c) using equivalent properties, no gob

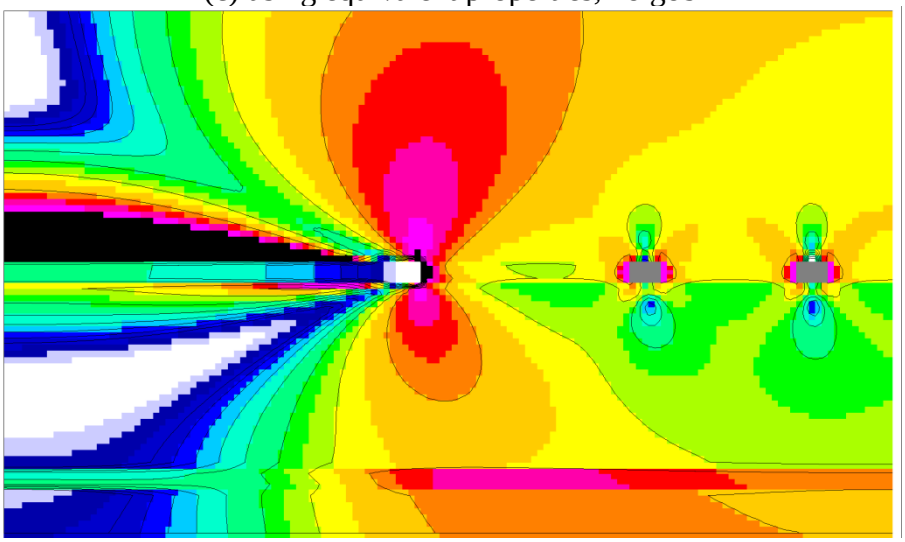

(d) using equivalent properties with strong gob

Figure 6 Element safety factors in vertical section.

The results in comparison show that joints have a noticeable effect as seen in element failures at the corners of pillars where crosscuts and entries meet in Figure 5. Figure 6 also shows more element failures in case of joints, especially near the barrier pillar wall adjacent to the mined region. This example indicates joints are important to barrier pillar design for defense of main entries.

**Problem 3** This problem concerns safety of bleeder entries and cross cuts used in longwall mining. Bleeder entries provide ventilation and a secondary escape route that must be maintained in a passable condition.

*Step 1 Preparation of a materials property file (stratigraphic column).* The material property file for rock in this problem is the same as in Problem 1 "mains" and Problem 2 "barriers".

*Step1j Computation of equivalent properties of jointed rock.* The equivalent jointed rock properties for this problem ("barriers") are the same used in the previous problem ("mains"). No additional computation is needed.

*Step 2 Mesh Generation*. Mesh generation input uses the same material properties for rock (and joints) as in the previous two examples. As always, mesh generation input is entered interactively and is

Input Data
BLEEDERS
Number of bleeder entries, NBS = 3
Width of entries, WE (ft) = 15.0
Width of crosscuts, WC (ft) = 15.0
Width of pillars, WP (ft) = 65.0
Length of pillars, LP (ft) = 76.0
EX, EY, EZ, (ft)= 3.0 3.0 2.0
Additional Sxx,Syy,Szz,Tyz,Tzx,Txy, tension +=
0.0 0.0 0.0 0.0 0.0 0.0
No gob effects

The runstream file for this analysis after some editing is shown in Figure 7 and the mesh is shown in Figure 8.

BLEEDERS trona, 8/28/2022 wgp no joints
F:\Visual Studio 2010\Projects\SPK\GMB3\TRprop.txt
F:\Visual Studio 2010\Projects\SPK\GMB3\belms

```
F:\Visual Studio 2010\Projects\SPK\GMB3\bcrds
F:\Visual Studio 2010\Projects\SPK\GMB3\brcte
F:\Visual Studio 2010\Projects\SPK\GMB3\bsigi
F:\Visual Studio 2010\Projects\SPK\GMB3\bnsps
aBLT
nelem = 1383680
nnode = 1480428
nspec =  188748
nmat  =      12
ncut  =      -1
ninc  =       5
nsigo =       1
inter =     200
maxit =    2000
nyeld =       2
nelcf =    8900
nsol  =       2
nprb  =       3
mgob  =       0
 error=    1.0000
 orf  =    1.8600
 xfac =   12.0000
 yfac =   12.0000
 zfac =   12.0000
 efac =    1.0000
 cfac =    1.0000
tolr% =    0.0100
ENDRUN
```

Figure 7 Runstream for Problem 3 “bleeders”.  Number of elements exceeds the recommended one million but there is leeway, so the mesh is acceptable.

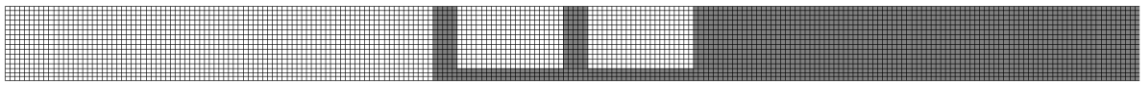

(a) plan view

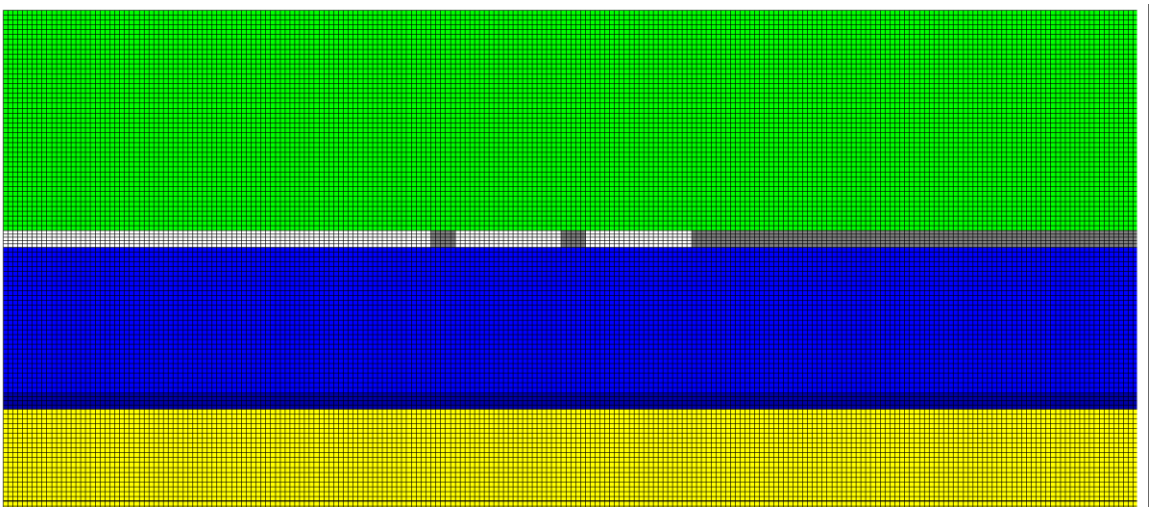

(b) vertical section window

Figure 8 Plan view and vertical sections of a three-dimensional mesh generated for bleeder entry safety analysis. White=trona, grey=excavated elements. Mining height is 10 ft (3 m). Depth is 1499 ft (457 m).

*Step 3 FEM Execution and Results*. Figure 9 shows element safety factor distributions in plan view at seam level. Element boundaries are removed in the plots for ease of viewing. The trona seam is 10 ft (3 m) thick. Depth is 1499 ft (457 m). Contours show gradation within color ranges. The zig-zag of some contours is caused by a change in formations.

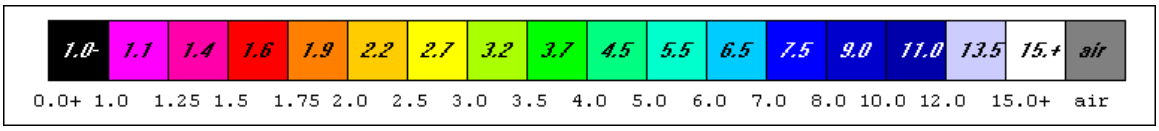


Element Safety Factor Color Scale

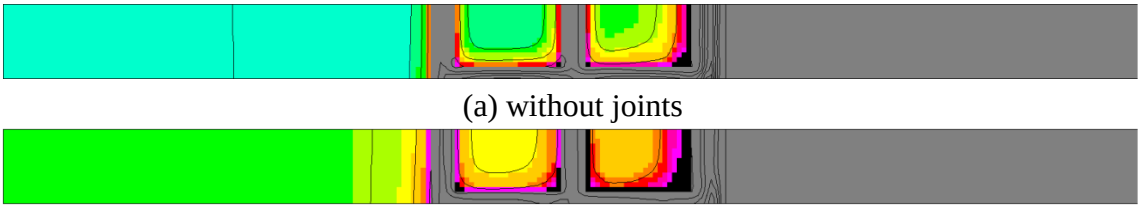

(a) without joints

(b) using equivalent properties

Figure 9 Element safety factor distributions in plan view at seam level in case of a bleeder entry safety analyses: (a) without joints, (b) using equivalent properties.

Figure 10 provide distributions of element safety factors without joints and using equivalent properties of jointed rock above and below the mined panel to the right (grey). The pillar nearest the mined panel shows low safety factors and some failure at the pillar wall while the pillar near the solid on the left hand side shows higher safety factors. There is considerable yielding in the roof over the mined region and in the floor as seen in the large black areas above and below the mined panel, more so in case of jointed rock.

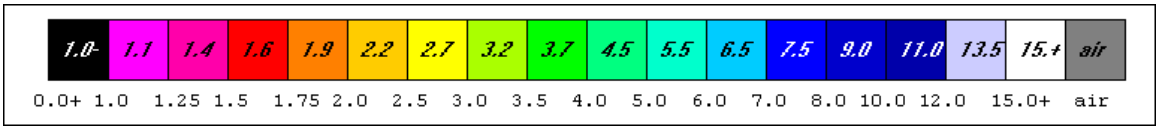


Element Safety Factor Color Scale

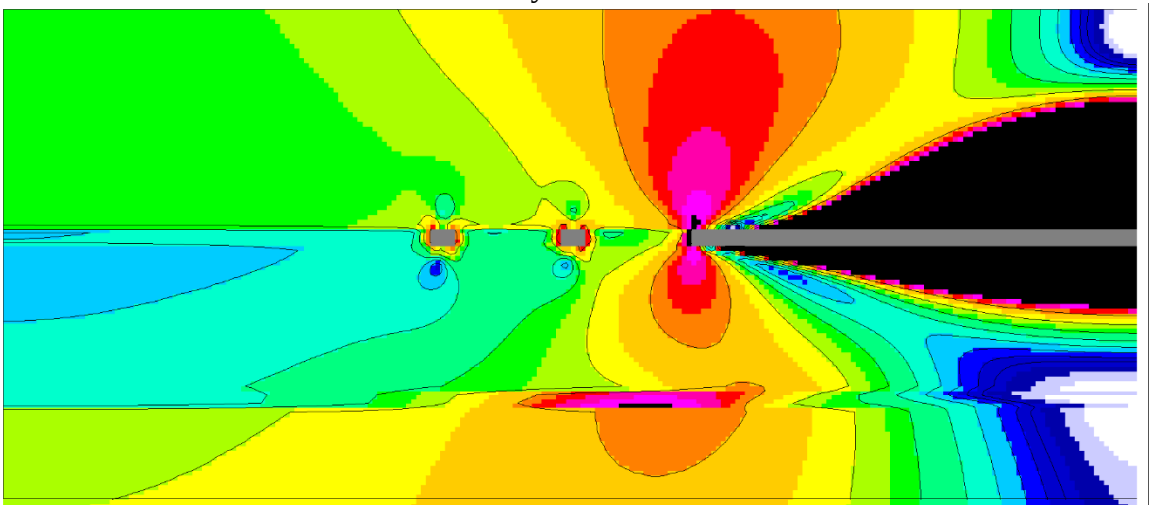

(a) without joints

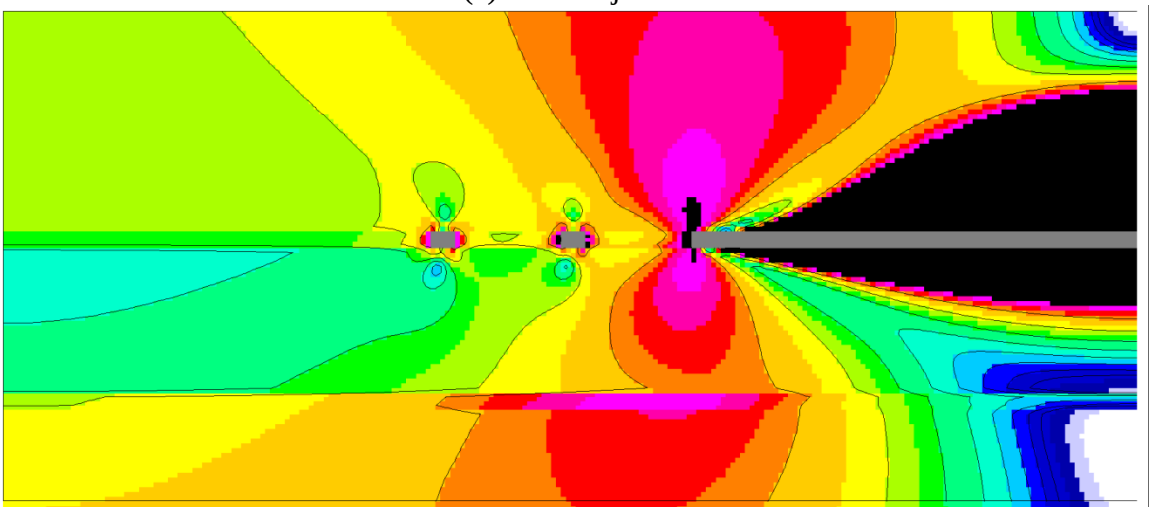

(b) using equivalent properties

Figure 10 Element safety factor distributions without joints (a) and using equivalent properties (b) in vertical sections in case of bleeder entry safety. The trona seam is 10 ft (3 m) thick. Depth is 1499 ft (457 m).

**Problem 4** This example concerns *interpanel barrier pillars safety* and safety of associated panel entries, crosscuts and chain pillars in headgates and tailgates of a longwall panel in a trona mine in southwestern Wyoming. Details are given in the User Manual in case of a rock mass without joints (APPENDIX V). Equivalent properties of a jointed rock mass are used here.

*Step 1 Preparation of a materials property file (stratigraphic column)* Again, formation properties are the same without joints and with joints. Either properties without joints or equivalent properties may be used for mesh generation in the next step.

*Step 1j Preparation of an equivalent materials property file* The equivalent properties are the same so there is no need to recompute.

*Step 2 Mesh Generation* Mesh generation input is

Input Data
INTERPANEL
Number of panel entries, NES = 3
Width of entries, WE (ft) = 20.0
Width of crosscuts, WC (ft) = 20.0
Width of pillars, WP (ft) = 40.0
Length of pillars, LP (ft) = 80.0
Longwall panel width, LPW (ft)= 750.0
Interpanel Barrier pillar width WBR (ft) = 300.0
EX, EY, EZ, (ft)= 4.0 4.0 4.0
Additional Sxx,Syy,Szz,Tyz,Tzx,Txy, tension +=
0.0 0.0 0.0 0.0 0.0 0.0
No gob effects

The mesh is shown in Figure 11 in plan and vertical section.

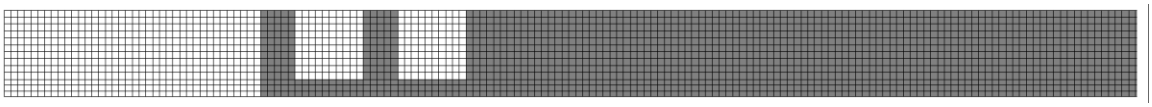

(a) plan view

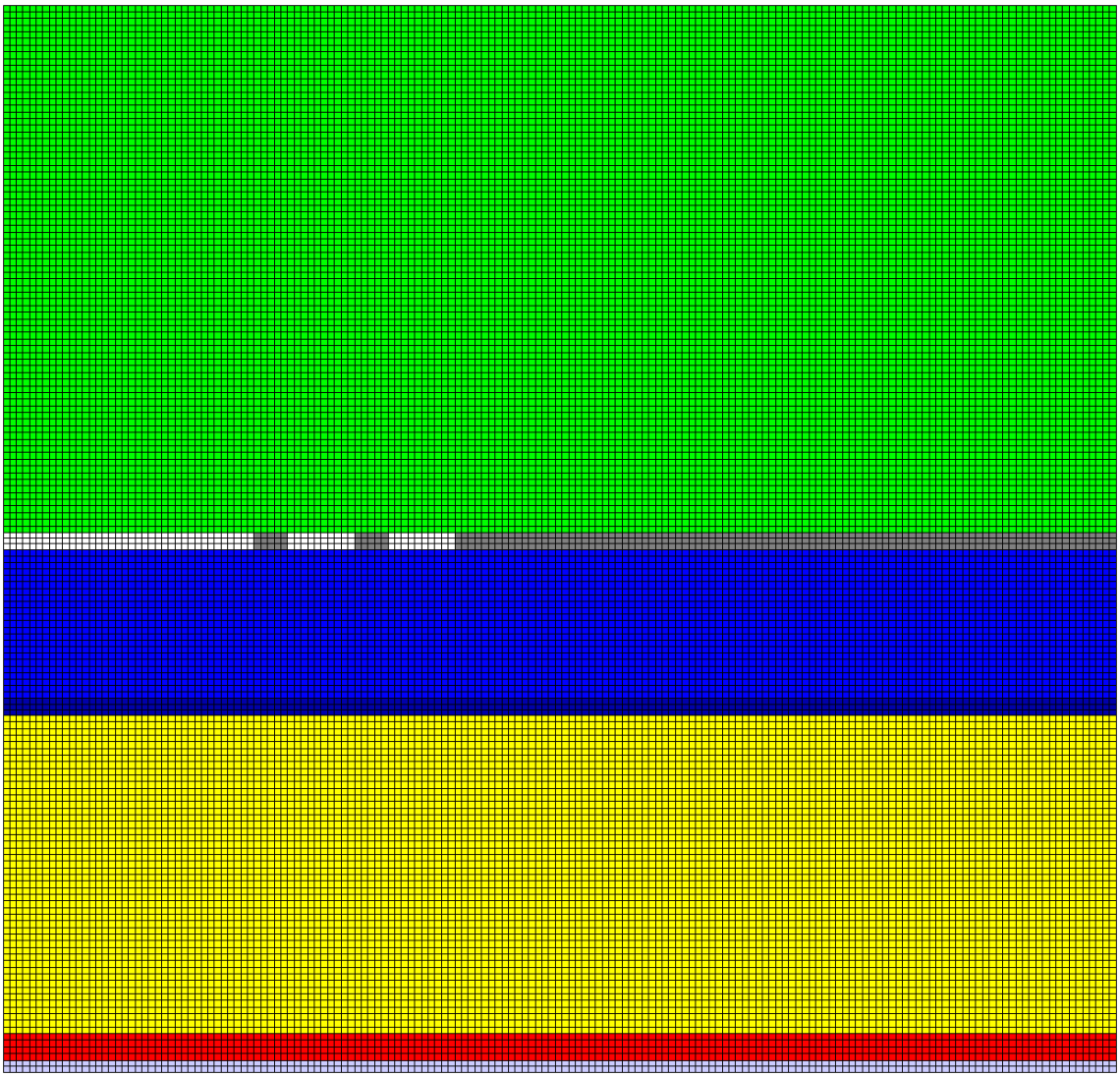

(b) vertical section

Figure 11 Mesh for interpanel barrier pillar analysis in a deep trona mine. Trona is white. Mined elements are grey. Mining height is 10 ft (3 m). Depth is 1499 ft (457 m).

*Step 3 FEM Execution and Results* The runstream file using equivalent properties after incorporating path names from the mesh generated output file and some minor editing is

```
Interpanel Barrier Trona no gob w/jts 8/30/2022 wgp
F:\Visual Studio 2010\Projects\SPK\SPKJ\EQ.txt
F:\Visual Studio 2010\Projects\SPK\GMB3\belms
F:\Visual Studio 2010\Projects\SPK\GMB3\bcrds
F:\Visual Studio 2010\Projects\SPK\GMB3\brcte
F:\Visual Studio 2010\Projects\SPK\GMB3\bsigi
F:\Visual Studio 2010\Projects\SPK\GMB3\bnsps
aIPj
nelem =  347360
```

```
nnode =  378672
nspec =   59952
nmat  =      11
ncut  =      -1
ninc  =       5
nsigo =       1
inter =     200
maxit =    2000
nyeld =       2
nelcf =    4431
nsol  =       2
nprb  =       4
mgob  =       0
 error=    1.0000
 orf  =    1.8600
 xfac =   12.0000
 yfac =   12.0000
 zfac =   12.0000
 efac =    1.0000
 cfac =    1.0000
tolr% =    0.0100
ENDRUN
```

Run time for this mesh was just under two hours.

Vertical section views of the distribution of element safety factors are shown in Figure 12 (a) without joints and (b) using equivalent properties. Element boundaries are not shown for clarity.

The plan view in Figure 12 indicates yielding entry pillar ribs and pillar cores with low safety factors ($fs$<1.3). Indeed, the pillar adjacent to the longwall panel is yielding almost to the core. Entry ribs also show some yielding.

The effect of joints is evident in Figure 13 that shows results in vertical sections. Extensive yielding in roof and floor above the mined panel and above the bleeder entries is especially evident in Figure 13 (b) in case of equivalent properties. Again, joints do have adverse effects for ground control and safety and should be taken into proper account based on fundamental principles. There are approximately 30 % more yielding elements in the case of joints than without joints. The pillars are also more threatened in case of joints (equivalent properties) as seen in the figures. Yielding in roof and floor over the mined panel is also more extensive in case of equivalent properties (joints).

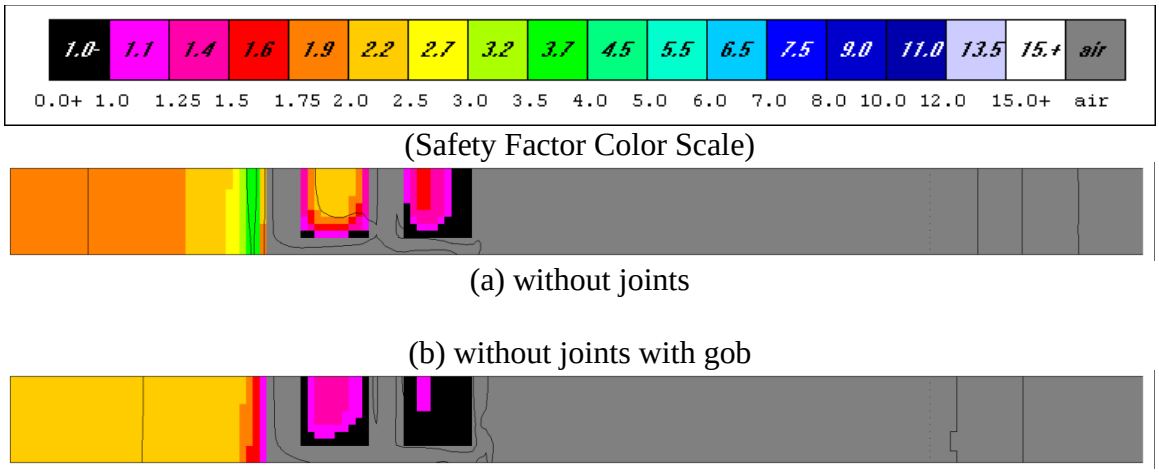


(Safety Factor Color Scale)

(a) without joints

(b) without joints with gob

(c) using equivalent properties

(d) using equivalent properties with gob

Figure 12 Plan view at seam level: interpanel barrier pillar (left), panel entries (3), longwall panel (right). (a) without joints, (b) using equivalent properties. Pillars are yielding (black) in both cases.

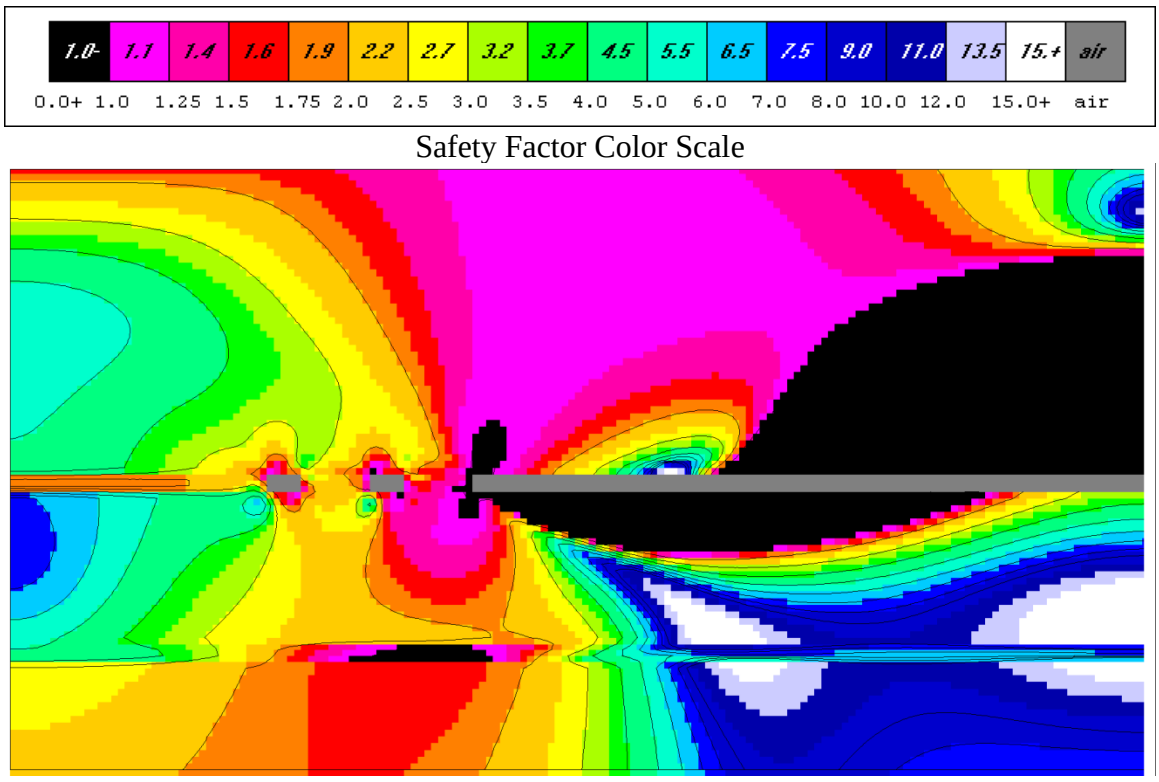


Safety Factor Color Scale

(a) without joins

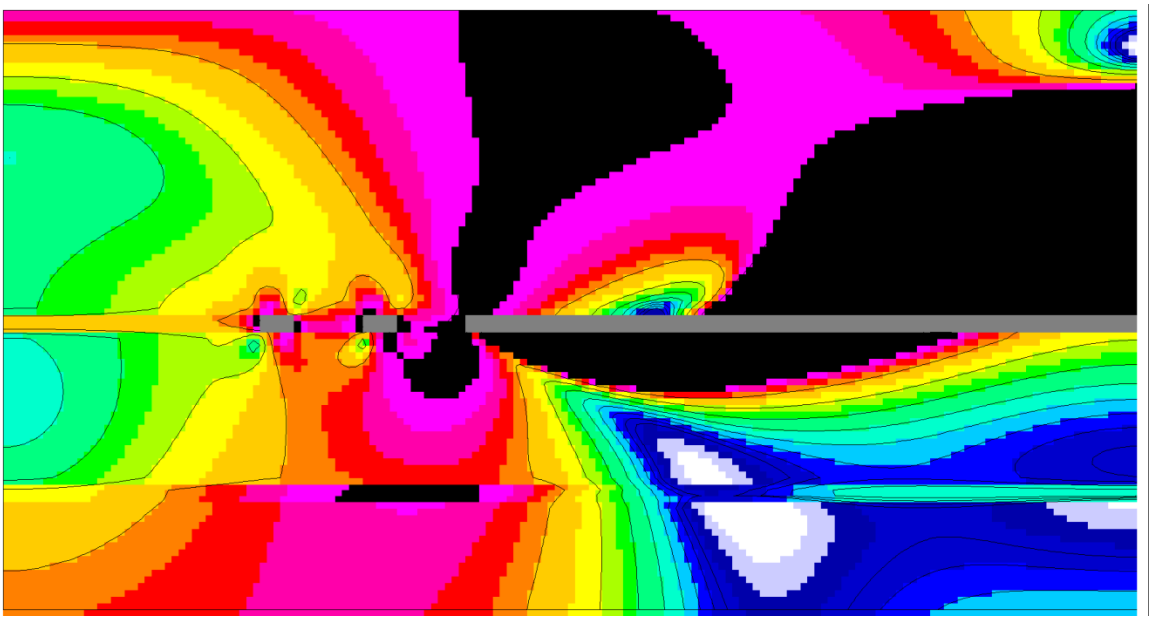

(b) using equivalent properties

Figure 13 Vertical sections: interpanel barrier pillar (left), panel entries (3), longwall panel (right). (a) without joints, (b) using equivalent properties. Pillars are near yielding (red) in both cases.

**Problem 5** Pillar safety in room and pillar mining is Problem 5 in the list of problems available for analysis. This example concerns an underground lead-zinc mine in southeast Missouri. The case without joints is addressed in the User Manual as a first example of analysis for safety in room and pillar mining. An update was done for comparisons in this example. The Indata files for both cases (without and with joints) are the same. Thus,

Input Data
PILLARS
Width of entries, WE (ft) = 30.0
Width of crosscuts, WC (ft)= 25.0
Width of pillars, WP (ft) = 25.0
Length of pillars, LP (ft) = 30.0
Height of pillars, HP (ft) = 30.0
EX, EY, EZ, (ft)= 2.0 2.0 2.0
Additional Sxx,Syy,Szz,Tyz,Tzx,Txy, tension +=
0.0 0.0 0.0 0.0 0.0 0.0

where no additional stresses are added to the gravity loads.

*Step 1 Preparation of a materials property file (stratigraphic column)* Figure 14 is a color schematic of the stratigraphic column from a mine in the New Lead Belt in southeast Missouri where room and pillar mining is used extensively. Mining often occurs on several levels and on occasion just a single level and over a restricted zone in the ore-bearing Bonneterre dolomite.

Although there are 13 formations in the figure, top and bottom ore are left, so the total is number of formations increases to 15.

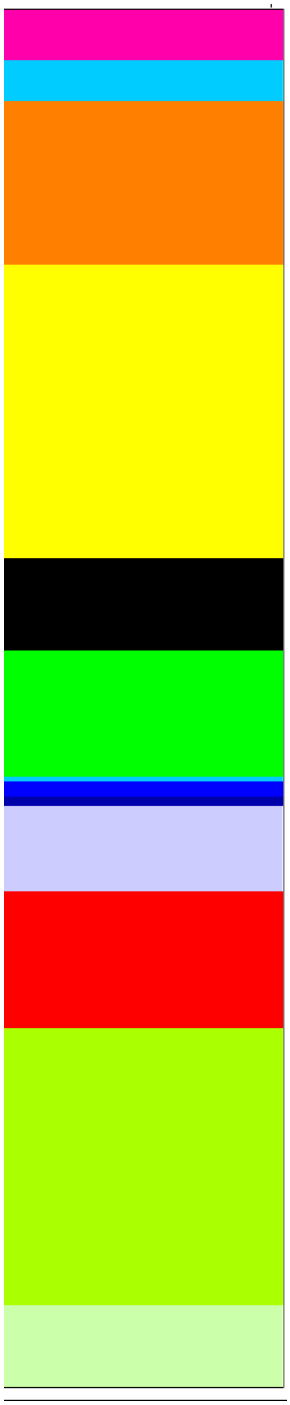


Figure 14 Stratigraphic column for example problems. Pillar is in Unit 10.

*Step 1j Preparation of an equivalent materials property file* Equivalent properties are generated using the runstream file which incorporates intact rock properties used in the case without joints. The joint sets are entirely fictitious and are only used for this example problem, although Sweeney et al indicate the presence of two vertical joint sets bearing N50E and N30W. Figure 15 is a schematic illustration of the assumed jointing intended to form blocky ground.

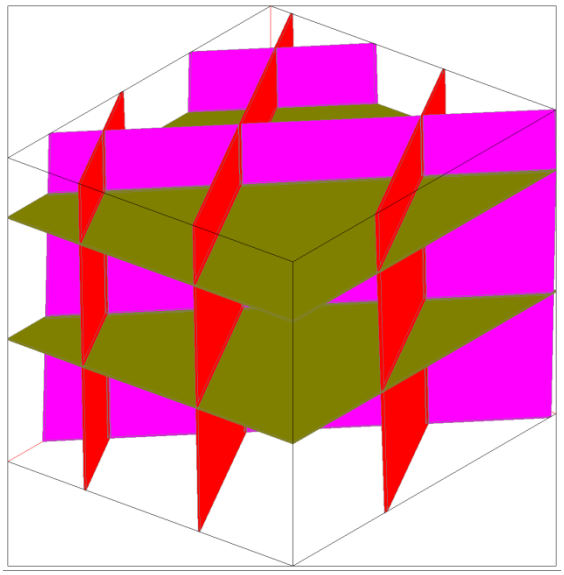

Figure 15 Schematic illustration of jointing assumed for this example problem. Horizontal joints are bedding planes.

he equivalent properties are

```
NLYRS =15
NSEAM =11
  (1) OVERBURDEN
   0.315E+04   0.344E+04   0.486E+04        0.41        0.13        0.20
   0.192E+04   0.179E+04   0.252E+04        0.00        0.00      130.00
      2510.5      2621.6      3119.2       125.5       131.1       156.0
       324.1       338.4       402.7
         0.0         0.0         0.0        60.0
    (2) GASCONADE DOLOMITE
   0.348E+07   0.382E+07   0.446E+07        0.29        0.19        0.23
   0.206E+07   0.187E+07   0.246E+07        0.00        0.00      163.00
      8444.8      8850.2      9557.3       832.4       872.4       942.1
      1530.8      1604.2      1732.4
         0.0         0.0        60.0        50.0
  (3) EMINENCE DOLOMITE
   0.423E+07   0.475E+07   0.580E+07        0.27        0.14        0.18
   0.235E+07   0.211E+07   0.291E+07        0.00        0.00      167.00
     10130.4     10735.7     11868.4       461.3       488.8       540.4
      1248.1      1322.6      1462.2
         0.0         0.0       110.0       195.0
 (4) POTOSI DOLOMITE
   0.443E+07   0.500E+07   0.620E+07        0.25        0.11        0.14
```

```
  0.239E+07   0.214E+07   0.297E+07        0.00        0.00      171.00
    16254.0     17277.2     19230.9       742.8       789.6       878.9
     2006.2      2132.4      2373.6
        0.0         0.0       305.0       350.0
 (5) DERBY-DOERUN DOLOMITE
  0.364E+07   0.401E+07   0.473E+07        0.28        0.18        0.21
  0.210E+07   0.191E+07   0.253E+07        0.00        0.00      162.00
    16459.8     17290.0     18762.4       890.2       935.1      1014.7
     2210.0      2321.5      2519.2
        0.0         0.0       655.0       110.0
 (6) DAVIS SHALE
  0.304E+07   0.329E+07   0.374E+07        0.22        0.14        0.16
  0.170E+07   0.157E+07   0.195E+07        0.00        0.00      161.00
    14771.8     15376.9     16401.8       907.7       944.9      1007.9
     2114.1      2200.7      2347.4
        0.0         0.0       765.0       150.0
 (7) BONNETERRE DOLOMIE
  0.344E+07   0.377E+07   0.439E+07        0.28        0.18        0.21
  0.200E+07   0.182E+07   0.238E+07        0.00        0.00      166.00
    20876.8     21864.0     23583.6       667.1       698.7       753.6
     2154.6      2256.5      2434.0
        0.0         0.0       915.0         6.0
(8) ORE
  0.389E+07   0.432E+07   0.517E+07        0.27        0.15        0.18
  0.219E+07   0.198E+07   0.267E+07        0.00        0.00      219.00
    12175.3     12836.6     14037.9       671.1       707.5       773.7
     1650.3      1739.9      1902.8
        0.0         0.0       921.0        18.0
(9) FALSE DAVIS SHALE
  0.246E+07   0.263E+07   0.290E+07        0.23        0.16        0.18
  0.142E+07   0.133E+07   0.159E+07        0.00        0.00      152.00
     4200.9      4336.8      4554.1       588.6       607.7       638.1
      907.9       937.2       984.2
        0.0         0.0       939.0        11.0
(10) TOP ORE
  0.389E+07   0.432E+07   0.517E+07        0.27        0.15        0.18
  0.219E+07   0.198E+07   0.267E+07        0.00        0.00      219.00
    12175.3     12836.6     14037.9       671.1       707.5       773.7
     1650.3      1739.9      1902.8
        0.0         0.0       950.0        10.0
 (4) (11) ORE
  0.389E+07   0.432E+07   0.517E+07        0.27        0.15        0.18
  0.219E+07   0.198E+07   0.267E+07        0.00        0.00      219.00
    12175.3     12836.6     14037.9       671.1       707.5       773.7
     1650.3      1739.9      1902.8
        0.0         0.0       960.0        30.0
 (12) BOTTOM ORE
  0.389E+07   0.432E+07   0.517E+07        0.27        0.15        0.18
  0.219E+07   0.198E+07   0.267E+07        0.00        0.00      219.00
    12175.3     12836.6     14037.9       671.1       707.5       773.7
     1650.3      1739.9      1902.8
        0.0         0.0       990.0        10.0
(13) BONNETERRE DOLOMITE
  0.344E+07   0.377E+07   0.439E+07        0.28        0.18        0.21
  0.200E+07   0.182E+07   0.238E+07        0.00        0.00      166.00
    20876.8     21864.0     23583.6       667.1       698.7       753.6
     2154.6      2256.5      2434.0
        0.0         0.0      1000.0       163.0
```

```
(14) LAMOTTE SANDSTONE
   0.252E+07   0.270E+07   0.298E+07        0.35        0.29        0.32
   0.168E+07   0.156E+07   0.194E+07        0.00        0.00      146.00
      8995.8      9298.1      9771.1       632.3       653.5       686.8
      1376.9      1423.2      1495.6
         0.0         0.0      1163.0       330.0
(15) PRECAMBIRAN FLESITES
   0.423E+07   0.475E+07   0.580E+07        0.27        0.14        0.18
   0.235E+07   0.211E+07   0.291E+07        0.00        0.00      167.00
     10130.4     10735.7     11868.4       461.3       488.8       540.4
      1248.1      1322.6      1462.2
         0.0         0.0      1493.0       100.0
```

As a reminder, the ratio of unconfined compressive strength to tensile strength is preserved as is the formula for shear strength in the computation of equivalent properties. The specific weight is not changed, of course. As usual, joint sets induce anisotropy in the equivalent properties.

*Step 2 Mesh Generation.* Mesh generation input is given in the InData file above entered interactively, as usual. Either the intact rock properties file or the equivalent properties file may be used for mesh generation. Symmetry of the problem allows for a relatively small number of elements and nodes. The runstream file from the mesh generator after some editing in case of equivalent properties is

```
Room & Pillar w/jts wgp  8/31/2022
F:\Visual Studio 2010\Projects\SPK\SPKJ\EQ.txt
F:\Visual Studio 2010\Projects\SPK\GMB3\belms
F:\Visual Studio 2010\Projects\SPK\GMB3\bcrds
F:\Visual Studio 2010\Projects\SPK\GMB3\brcte
F:\Visual Studio 2010\Projects\SPK\GMB3\bsigi
F:\Visual Studio 2010\Projects\SPK\GMB3\bnsps
aMAGj
nelem =  152325
nnode =  173568
nspec =   40876
nmat  =      15
ncut  =      -1
ninc  =       5
nsigo =       1
inter =     200
maxit =    2000
nyeld =       2
nelcf =    2535
nsol  =       2
nprb  =       5
mgob  =       0
 error=    1.0000
 orf  =    1.8600
 xfac =   12.0000
 yfac =   12.0000
 zfac =   12.0000
 efac =    1.0000
 cfac =    1.0000
torl% =    0.0100
ENDRUN
```

The mesh for pillar analysis is shown in Figure 16 in close-up views. Elements in the mesh are 2 ft (0.6 m) cubes. As the runstream file indicates, there are 152,325 elements in the mesh. The number of layers is equal to the number of material types which is 15 as also seen in the runstream file. Entry width is 30 ft (9 m); crosscut width is 25 ft (7.5 m). Pillar width is also 25 ft (7.5 m); pillar length is 30 ft (9 m). The vertical section in the figure is not full height which is at least 30 times pillar height. In this example, 30 times pillar height is 900 ft (270 m).

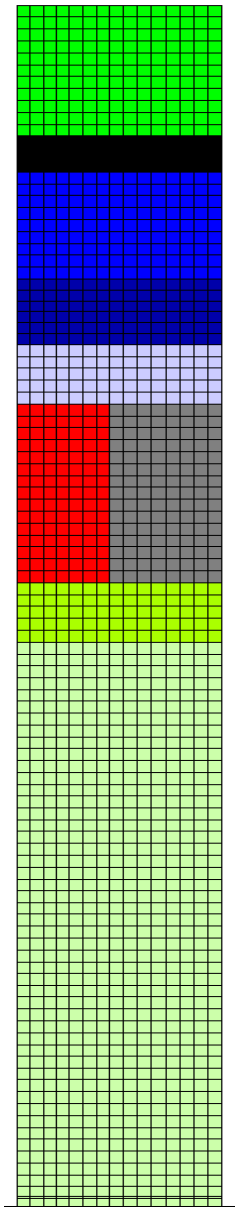

(a) vertical section

(b) plan view

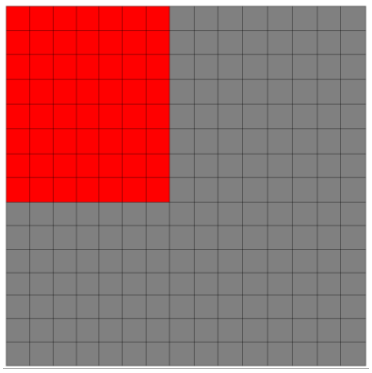

Figure 16 Vertical section (a) and plan view (b) of the finite element mesh for pillar analysis.

*Step 3 FEM Execution and Results*. Practical results for this problem are illustrated in Figure 17 which shows plan views at pillar mid-height and in Figure 18 which shows element safety factor

distributions in vertical sections. High stress concentration associated with relatively low safety factors (red, 1.40) at the room corners where roof and floor meet the pillar are evident. The pillar corner seen in plan view is also threatened in consideration of the low safety factor at the corner (pink, 1.1). Edges of the pillar extending from the corner are also in red (*fs*=1.4) and pose a concern for spalling. Overall, the pillar is safe at an area extraction ratio of approximately 75 percent. In this, regard the green in the pillar core indicates *fs*≈4 as does the tributary area formula for average *fs*.

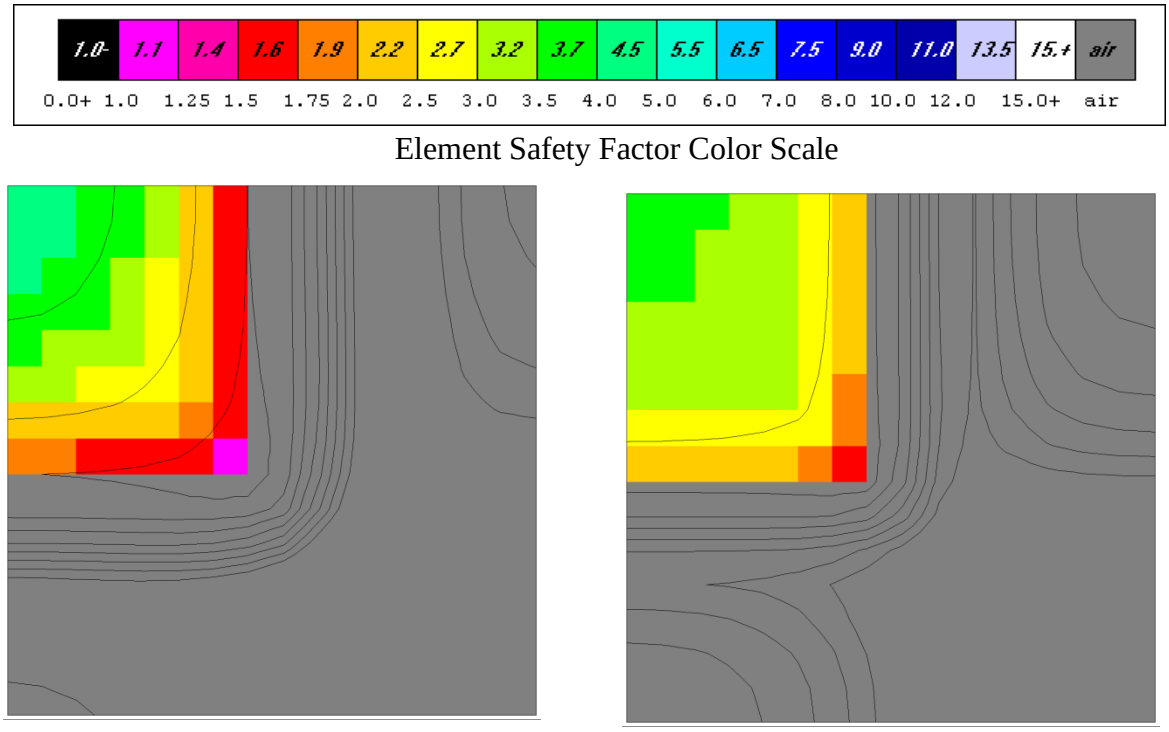


Element Safety Factor Color Scale

(a) without joints

(b) using equivalent properties

Figure 17 Plan views of element safety factor distributions.

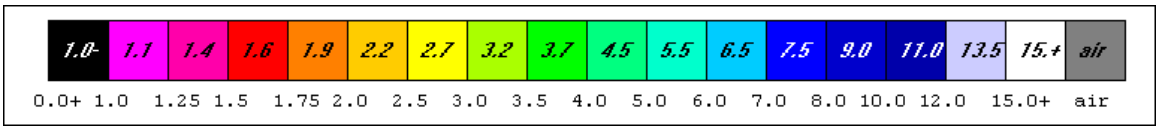


Element Safety Factor Color Scale

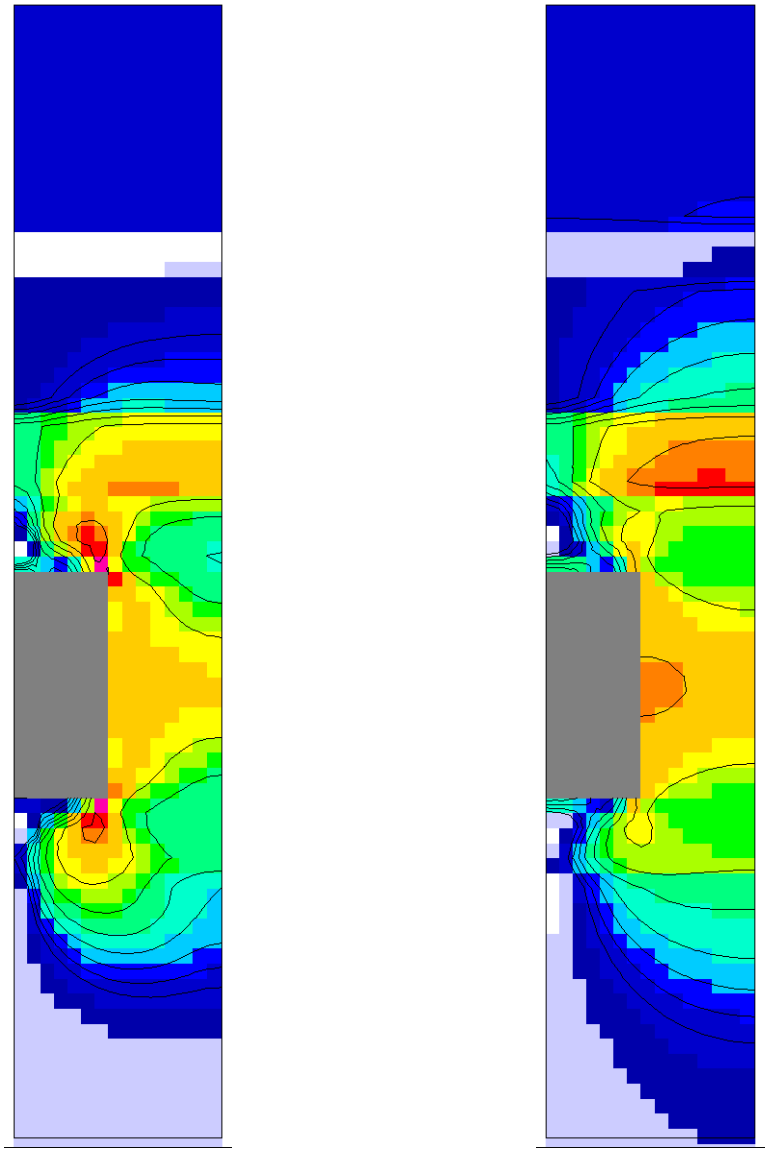

(a) without joints (b) using equivalent properties

Figure 18 Vertical section views of element safety factor distributions.

In this example there is little difference in the two cases. Thus, the assumed joint sets have no significant effect on room and pillar safety. Indeed, rooms and pillars are safe in both cases.

**Problem 6** *Shaft Safety* The first five problems of the seven problem types described in the User Manual for using UT3PC involve strata above and below the mining horizon and require a program run of UT3PCJ for each stratum during *Step 1j* calculations for equivalent properties. Problems six and seven involving shafts and tunnels are analyses of sections ("slabs") and may be in a single rock type and thus require just one program run in calculation of equivalent properties. However, thin formations that are inclined may appear in a section and thus require several runs for equivalent properties of the jointed formations present.

This example of shaft safety problem concerns twin rectangular shafts in the Silver Belt of the famous Coeur d'Alene mining district in northern Idaho. A finite element analysis without joints is discussed in the User Manual where background is given and references are cited. A new analysis without joints and one with joints using equivalent properties follows.

*Step 1* begins with the geology of the shaft route above and below the depth of interest. The three major formations present and properties are

```
NLYRS = 3
NSEAM = 2
  (1) Vitreous Quartzite
  6.1e+06   6.1e+06   6.1e+06      0.26      0.26      0.26
  2.4e+06   2.4e+06   2.4e+06       0.0       0.0       0.0
  24500.0   24500.0   24500.0    2800.0    2800.0    2800.0
   2400.0    2400.0    2400.0
    220.0      70.0    5800.0     180.0
  (2) Argillitic Quartzite
  4.2e+06   4.2e+06   1.8e+06      0.18      0.11      0.11
  1.1e+06   1.1e+06   1.8e+06       0.0       0.0       0.0
   8500.0    8500.0   12230.0    2790.0    2790.0    1080.0
   2820.0    2820.0    4400.0
    220.0      70.0    5980.0      40.0
  (3)  Sericitic Quartzite
  5.5e+06   5.5e+06   4.0e+06      0.21      0.20      0.20
  1.9e+06   1.9e+06   2.3e+06       0.0       0.0       0.0
  17470.0   17470.0   26040.0    2330.0    2330.0    1530.0
   3680.0    3680.0    3640.0
    220.0      70.0    6020.0     180.0
```

which is essentially *Step 1* in case of no joints present. Use of this file allows for mesh generation, although mesh generation can also be done following computation of equivalent properties

An assumed joint set is shown in Figure 19. This assumption is made for illustrating the role of joints in finite element analysis of shaft safety.

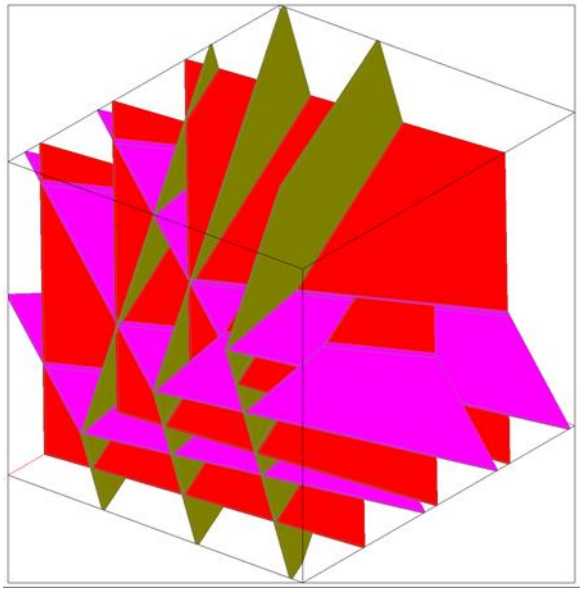

Figure 19 Schematic of assumed joint sets.  Steeply dipping joints are bedding planes

The runstream for computing equivalent properties using UT3J is

```
Caladay shaft w/ Joints 9/2/2022 wgp
CMS1.txt
celms.txt
ccrds.txt
none
none
cnsps.txt
aCM1
nelem =       1
nnode =       8
nspec =       8
nmat  =       4
ncut  =       1
ninc  =       1
nsigo =       0
inter =     100
maxit =    1000
nyeld =       2
nelcf =       0
ncave =       0
nfile =       1
npsi  =       1
nrstrt=       0
 error=    1.0000
```

orf = 1.8600
xfac = 12.0000
yfac = 12.0000
zfac = 12.0000
efac = 1.0000
cfac = 100.0
Caladay shaft w/ Joints 9/2/2022 wgp
CMS2.txt
celms.txt
ccrds.txt
none
none
cnsps.txt
aCM2
nelem = 1
nnode = 8
nspec = 8
nmat = 4
ncut = 1
ninc = 1
nsigo = 0
inter = 100
maxit = 1000
nyeld = 2
nelcf = 0
ncave = 0
nfile = 2
npsi = 1
nrstrt= 0
error= 1.0000
orf = 1.8600
xfac = 12.0000
yfac = 12.0000
zfac = 12.0000
efac = 1.0000
cfac = 100.0
Caladay shaft w/ Joints 9/2/2022 wgp
CMS3.txt
celms.txt
ccrds.txt
none
none
cnsps.txt
aCM3
nelem = 1
nnode = 8

```
nspec =       8
nmat  =       4
ncut  =       1
ninc  =       1
nsigo =       0
inter =     100
maxit =    1000
nyeld =       2
nelcf =       0
ncave =       0
nfile =       3
npsi  =       1
nrstrt=       0
 error=    1.0000
 orf  =    1.8600
 xfac =   12.0000
 yfac =   12.0000
 zfac =   12.0000
 efac =    1.0000
 cfac =     100.0
RUN END
```

where CMS1 is

```
(1) joint S70W 0.1 thik N=2
  4.2e+04   4.2e+04   1.8e+04      0.18      0.11      0.11
  1.1e+04   1.1e+04   1.8e+04       0.0       0.0       0.0
    850.0     850.0    1223.0     279.0     279.0     108.0
    282.0     282.0     210.0
          350.0      65.0       0.5      -0.10
 (2) joint  N=2
  4.2e+04   4.2e+04   1.8e+04      0.18      0.11      0.11
  1.1e+04   1.1e+04   1.8e+04       0.0       0.0       0.0
    850.0     850.0    1223.0     279.0     279.0     108.0
    282.0     282.0     210.0
    355.0      89.0       0.5     -0.10
 (3) joint bedding plane N=2
  4.2e+04   4.2e+04   1.8e+04      0.18      0.11      0.11
  1.1e+04   1.1e+04   1.8e+04       0.0       0.0       0.0
    850.0     850.0    1223.0     279.0     279.0     108.0
    282.0     282.0     210.0
    220.0      70.0       1.0     -0.10
  (1) Vitreous Quartzite N50W 70SW
  6.1e+06   6.1e+06   6.1e+06      0.26      0.26      0.26
  2.4e+06   2.4e+06   2.4e+06       0.0       0.0       0.0
  24500.0   24500.0   24500.0    2800.0    2800.0    2800.0
```

```
  2400.0    2400.0    2400.0
   220.0      70.0    5700.0     280.0
```

and similarly for CMS2 (Argillitic Quartzite) and CMS3 (Sericitic Quartzite).

The equivalent properties of the jointed rock mass are

```
NLYRS = 3
NSEAM = 2
  (1) Vitreous Quartzite N50W 70SW
  0.294E+06   0.620E+05   0.344E+06       0.10       0.00       0.19
  0.480E+05   0.163E+06   0.342E+05       0.00       0.00       0.00
     5377.8      2469.5      5816.8       614.6       282.2       664.8
     1049.6       482.0      1135.3
      220.0        70.0      5700.0       280.0
  (2) Argillitic Quartzite
  0.277E+06   0.616E+05   0.294E+06       0.12       0.00       0.17
  0.474E+05   0.153E+06   0.341E+05       0.00       0.00       0.00
     2184.1      1029.1      4941.6       716.9       337.8       436.4
      722.4       340.4       847.8
      220.0        70.0      5980.0        40.0
  (3)  Sericitic Quartzite
  0.290E+06   0.619E+05   0.331E+06       0.10       0.00       0.19
  0.479E+05   0.161E+06   0.342E+05       0.00       0.00       0.00
     4009.5      1853.0      7495.2       534.7       247.1       440.4
      845.4       390.7      1048.9
      220.0        70.0      6020.0       280.0
```

Completion of *Step1* and *Step 1j* allows for mesh generation. The mesh for the twin rectangular shafts is shown in Figure 20 in plan view. The Indata file with particulars including shaft depth of 6,000 ft (1,829 m) is

```
Input Data
 SHAFT NPROB 6
 Shaft Shape = Rectangle
 Shaft System = Twin Openings
 Shaft Width =      11.0
 Width/Height Ratio =       0.5
 Pillar Width =      22.0
 Section Depth Seam Center (ft)   =    6000.0
 Additional Sxx,Syy,Szz,Tyz,Tzx,Txy, tension +=
   -7571.0   -8441.0   -6688.0       0.0       0.0     927.0
 Shaft Stress Sxx,Syy,Szz,Tyz,Tzx,Txy, tension +=
   -7571.0   -8441.0   -6688.0       0.0       0.0     927.0
```

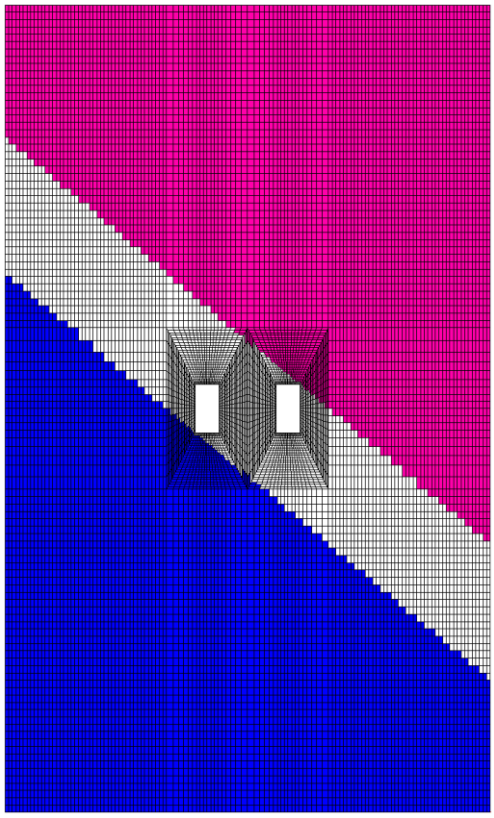

Figure 20 Mesh for twin rectangular shafts 11x22 ft (3.3x6.6 m) separated by a 22 ft (6.6 m) pillar. Inclination of the three formations present is evident in the figure.

The runstream for finite element analysis of shaft safety is

```
CALLADAY SHAFT twin rectangles 11 x 22 WP=22 ft 09/02/2022 4/17/21 02/01/2021 wgp
F:\Visual Studio 2010\Projects\SPK\SPKJ\EQ.txt
F:\Visual Studio 2010\Projects\SPK\GMB3\belms
F:\Visual Studio 2010\Projects\SPK\GMB3\bcrds
F:\Visual Studio 2010\Projects\SPK\GMB3\brcte
F:\Visual Studio 2010\Projects\SPK\GMB3\bsigi
F:\Visual Studio 2010\Projects\SPK\GMB3\bnsps
ACMfs
nelem =   15808
nnode =   32218
nspec =   32218
nmat  =       3
ncut  =      -1
ninc  =       5
nsigo =       1
inter =     200
maxit =    4000
nyeld =       2
nelcf =     144
nsol  =       2
nprb  =       6
mgob  =       0
```

```
 error=    1.0000
 orf  =    1.8600
 xfac =   12.0000
 yfac =   12.0000
 zfac =   12.0000
 efac =     1.000
 cfac =     1.000
tolr% =      0.01
ENDRUN
```

which shows a relatively small mesh of only 15,808 elements. Runtime is small, approximately five minutes.

Element safety factor distributions in the case without joints and in the case using equivalent properties are shown in Figure 21

The case without joints shows threatened shafts and pillar between in consideration of the orange and red color at the shaft walls indicating safety factors near 2 and 1.5, respectively. In case of joints using equivalent properties the black color indicates a yielding across the pillar and over much of the shaft wall. Thus, joints have a highly detrimental effect on shaft safety in this example.

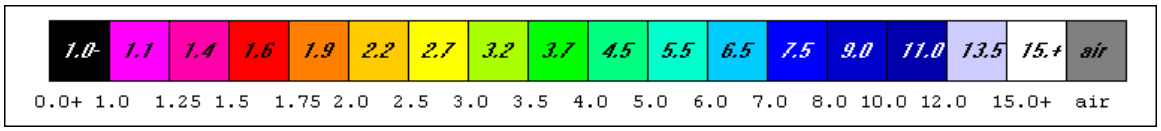


Element Safety Factor Color Scale

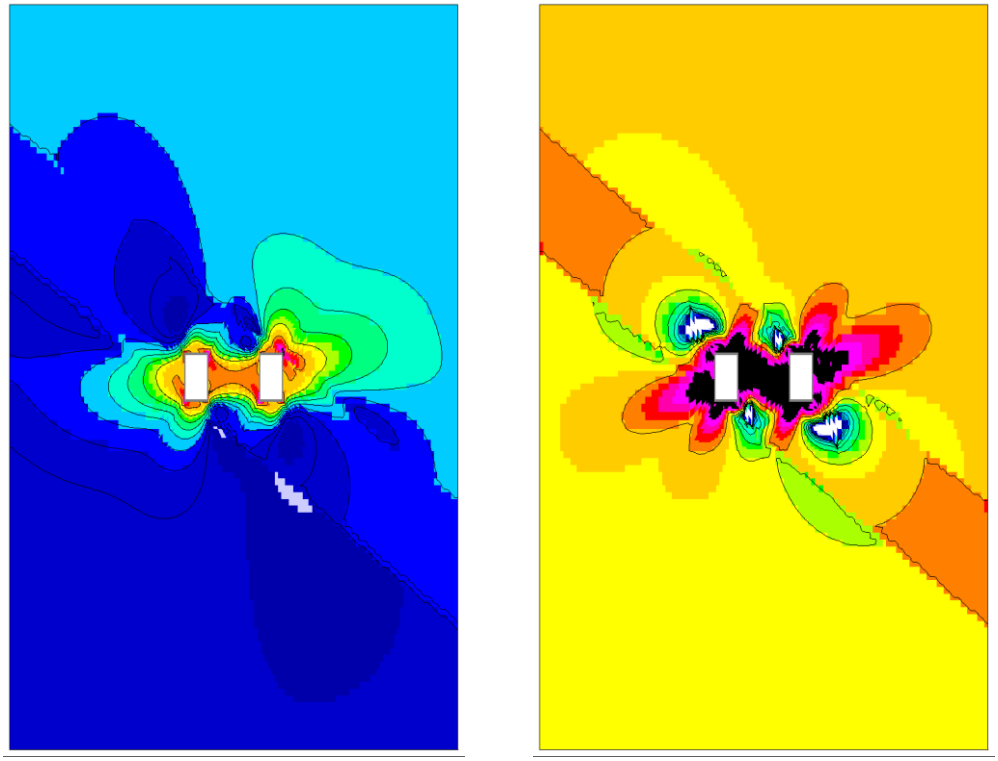

(a) without joints (b) using equivalent properties

Figure 21 Element safety factor distributions about twin rectangular shafts 11x22 ft (3.3x6.6 m) separated by a 22 ft (6.6 m) pillar.

**Problem 7 Tunnels (drifts, crosscuts, adits)** This example is inspired by a detailed study of a new mining method at the Carr Fork Mine (Pariseau et al 1984, Pariseau 1985), cited in the User Manual). The Carr Fork Mine was an underground copper mine in a contact metamorphic rock environment with an intended production of 10,000 short tons per day. Access was by vertical shaft in Pine Canyon near Tooele, Utah. Average depth in the vicinity of the new mining method study is 4,200 ft. Many measurements of stress and of Young's modulus in situ and other rock properties measured in the laboratory supported the study. Details are given in the User Manual.

The input material properties file is

```
NLYRS = 7
NSEAM = 2
 (4) Hornfels
 2.81e+06  2.81e+06  2.81e+06      0.27      0.27      0.27
 1.11e+06  1.11e+06  1.11e+06       0.0       0.0       0.0
  9200.0    9200.0    9200.0     800.0     800.0     800.0
  1566.0    1566.0    1566.0
     0.0      80.0    3800.0     350.0
 (5) Quartz Monzonite Porphyry
 2.17e+06  2.17e+06  2.17e+06      0.22      0.22      0.22
 0.89e+06  0.89e+06  0.89e+06       0.0       0.0       0.0
  7000.0    7000.0    7000.0     580.0     580.0     580.0
  1163.0    1163.0    1163.0
    55.0      60.0    4150.0     100.0
 (1) Garnetite Limestone
 3.56e+06  3/56e+06  3.56e+06      0.20      0.20      0.20
 1.48e+06  1.48e+06  1.48e+06       0.0       0.0       0.0
 11800.0   11800.0   11800.0     890.0     890.0     890.0
  1871.0    1871.0    1871.0
     0.0      80.0    4250.0     150.0
 (2) Garnetite Quartzite
 1.18e+06  1.18e+06  1.18e+06      0.22      0.22      0.22
 0.48e+06  0.48e+06  0.48e+06       0.0       0.0       0.0
  3600.0    3600.0    3600.0     270.0     270.0     270.0
   569.0     569.0     569.0
     0.0      80.0    4400.0      18.0
 (3) Hard Quartzite
 2.46e+06  2.46e+06  2.46e+06      0.25      0.25      0.25
 0.98e+06  0.98e+06  0.98e+06       0.0       0.0       0.0
  8000.0    8000.0    8000.0     720.0     720.0     720.0
```

```
  1385.0    1385.0    1385.0
    0.0      80.0    4418.0     122.0
 (6) Quartz Latite Porphyry
 1.30e+06  1.30e+06  1.30e+06      0.23      0.23      0.23
 0.53e+06  0.53e+06  0.53e+06       0.0       0.0       0.0
  4000.0    4000.0    4000.0     200.0     200.0     200.0
   516.0     516.0     516.0
    0.0      80.0    4540.0      20.0
 (4) Hornfels
 2.81e+06  2.81e+06  2.81e+06      0.27      0.27      0.27
 1.11e+06  1.11e+06  1.11e+06       0.0       0.0       0.0
  9200.0    9200.0    9200.0     800.0     800.0     800.0
  1566.0    1566.0    1566.0
    0.0      80.0    4560.0     160.0
```

where the NSEAM value of 2 indicates excavation in quartz monzonite porphyry.

A joint set is assumed that consists of joints from two sets and from bedding planes. Figure 22 illustrates the assumed joint sets that develops blocky ground.

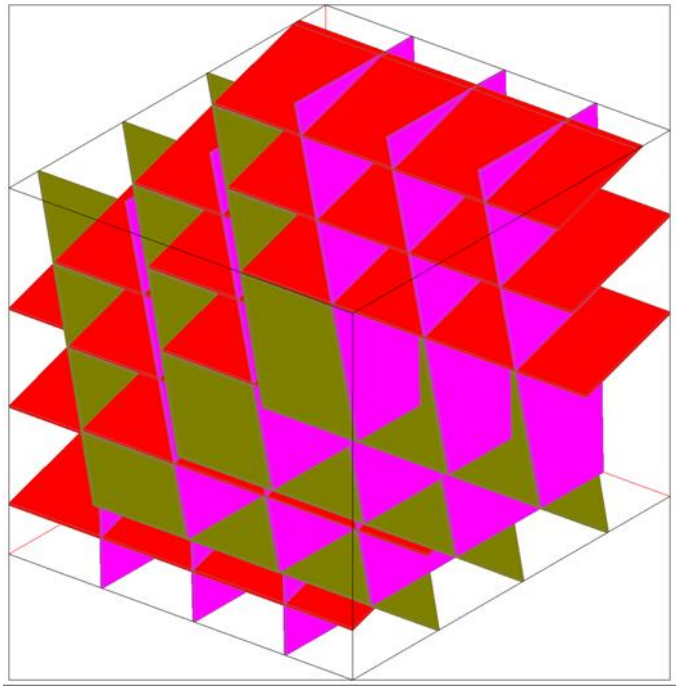

Figure 22 Schematic illustration of joints in three sets for tunnel analysis. Formations dip steeply and coincide with the dark bedding plane joints. Red joints are cross joints; pink joints are a third set.

The runstream file for computing equivalent properties in *Step1j* is

```
Carr Fork w/ Joints 09/03/2022 wgp
CR1.txt
celms.txt
ccrds.txt
none
none
cnsps.txt
aCR1
nelem =       1
nnode =       8
nspec =       8
nmat  =       4
ncut  =       1
ninc  =       1
nsigo =       0
inter =     100
maxit =    1000
nyeld =       2
nelcf =       0
ncave =       0
nfile =       1
npsi  =       1
nrstrt=       0
 error=    1.0000
 orf  =    1.8600
 xfac =   12.0000
 yfac =   12.0000
 zfac =   12.0000
 efac =    1.0000
 cfac =     100.0
error=    1.0000
 orf  =    1.8600
 xfac =   12.0000
 yfac =   12.0000
 zfac =   12.0000
 efac =    1.0000
 cfac =     100.0

….

Carr Fork w/ Joints 9/03/2022 wgp
CR7.txt
```

celms.txt
ccrds.txt
none
none
cnsps.txt
aCR7
nelem =  1
nnode =  8
nspec =  8
nmat  =  4
ncut  =  1
ninc  =  1
nsigo =  0
inter =  100
maxit =  1000
nyeld =  2
nelcf =  0
ncave =  0
nfile =  7
npsi  =  1
nrstrt=  0
error=  1.0000
orf  =  1.8600
xfac =  12.0000
yfac =  12.0000
zfac =  12.0000
efac =  1.0000
cfac =  100.0
RUN END

where CR1 is

(1) joint  N=2
2.17e+04  2.17e+04  2.17e+04  0.22  0.22  0.22
0.89e+04  0.89e+04  0.89e+04  0.0  0.0  0.0
70.0  70.0  70.0  5.80  5.80  5.80
11.63  11.63  11.63
90.0  89.0  3.0  -0.10
(2) joint  N=2  cross jts
2.17e+04  2.17e+04  2.17e+04  0.22  0.22  0.22
0.89e+04  0.89e+04  0.89e+04  0.0  0.0  0.0
70.0  70.0  70.0  5.80  5.80  5.80
11.63  11.63  11.63
180.0  20.0  4.0  -0.10
(3) joint bedding plane N=2
2.17e+04  2.17e+04  2.17e+04  0.22  0.22  0.22

```
 0.89e+04  0.89e+04  0.89e+04       0.0       0.0       0.0
    70.0      70.0      70.0      5.80      5.80      5.80
    11.63     11.63     11.63
     0.0      80.0       5.0     -0.10
 (4) Hornfels
 2.81e+06  2.81e+06  2.81e+06      0.27      0.27      0.27
 1.11e+06  1.11e+06  1.11e+06       0.0       0.0       0.0
  9200.0    9200.0    9200.0     800.0     800.0     800.0
  1566.0    1566.0    1566.0
     0.0      80.0    3800.0     350.0
```

and so on to CR7.

The equivalent properties file is

```
NLYRS = 7
NSEAM = 2
 (4) Hornfels
  0.551E+06   0.722E+06   0.732E+06       0.06       0.22       0.08
  0.219E+06   0.143E+06   0.142E+06       0.00       0.00       0.00
     4075.4      4663.9      4695.2       354.4      405.6      408.3
      693.8       794.0       799.4
        0.0        80.0      3800.0       350.0
 (5) Quartz Monzonite
  0.521E+06   0.670E+06   0.678E+06       0.06       0.20       0.08
  0.209E+06   0.139E+06   0.138E+06       0.00       0.00       0.00
     3430.3      3889.5      3913.5       284.2      322.3      324.3
      570.1       646.4       650.4
        0.0        80.0      4150.0       100.0
 (1) Garnetite Limestone
  0.576E+06   0.765E+06   0.776E+06       0.04       0.20       0.05
  0.230E+06   0.148E+06   0.147E+06       0.00       0.00       0.00
     4745.5      5470.2      5509.1       357.9      412.6      415.5
      752.4       867.4       873.5
        0.0        80.0      4250.0       150.0
 (2) Garnetite Quartzite
  0.433E+06   0.529E+06   0.534E+06       0.09       0.21       0.11
  0.174E+06   0.123E+06   0.122E+06       0.00       0.00       0.00
     2180.7      2410.1      2421.7       163.6      180.8      181.6
      344.8       381.1       382.9
        0.0        80.0      4400.0        18.0
 (3) Hard Quartzite
  0.536E+06   0.696E+06   0.705E+06       0.06       0.21       0.08
  0.213E+06   0.141E+06   0.140E+06       0.00       0.00       0.00
     3735.4      4255.2      4282.6       336.2      383.0      385.4
      647.0       737.0       741.8
```

```
      0.0       80.0      4418.0       122.0
 (6) Quartz Latite
 0.448E+06  0.552E+06  0.558E+06       0.09       0.21       0.11
 0.180E+06  0.126E+06  0.125E+06       0.00       0.00       0.00
    2348.8     2607.4     2620.5      117.4      130.4      131.0
     303.2      336.6      338.3
       0.0       80.0     4540.0       20.0
 (4) Hornfels
 0.551E+06  0.722E+06  0.732E+06       0.06       0.22       0.08
 0.219E+06  0.143E+06  0.142E+06       0.00       0.00       0.00
    4075.4     4663.9     4695.2      354.4      405.6      408.3
     693.8      794.0      799.4
       0.0       80.0     4560.0       160.0
```

*Step 2 Mesh Generation* Mesh generation input is given in the InData file that is developed during mesh generation: Thus,

```
Input Data
 "TUNNEL" NPROB 7
 Tunnel Shape = Arched Rectangle
 Tunnel System = Row of Openings
 Tunnel Width =      12.0
 Width/Height Ratio =       1.2
 Pillar Width =      38.0
 Section Depth Seam Center (ft)   =    4200.0
 Additional Sxx,Syy,Szz,Tyz,Tzx,Txy, tension +=
   -3880.0   -4620.0   -2495.0       0.0       0.0       0.0
 Tunnel Stress Sxx,Syy,Szz,Tyz,Tzx,Txy, tension +=
   -3880.0   -4620.0   -2495.0       0.0       0.0       0.0
```

A row of arched back crosscuts is specified to be 12 ft (3.6 m) wide by 10 ft (3 m) high in quartz monzonite porphyry at a depth of 4,200 ft (1,280 m). Separation is by a 38 ft (11.6 m) pillar. The premining stress state is computed from formulas developed from mine measurements.

Figure 23 (a) shows the mesh; Figure 23(b) shows the element safety factor distribution in the case without joints, and Figure 23(c) shows the case using equivalent properties. Evidently separation of crosscuts by the pillar between is sufficient to prevent interaction between crosscuts to the detriment of safety. When joints are present, the wall of the “tunnel” is yielding as seen in the black elements in Figure 23(c). A suitable ground control plan would be required for a safe design, of course.

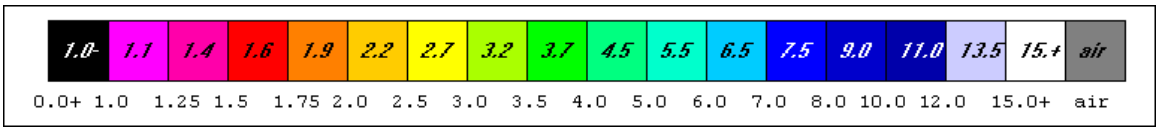


Element Safety Factor Color Scale

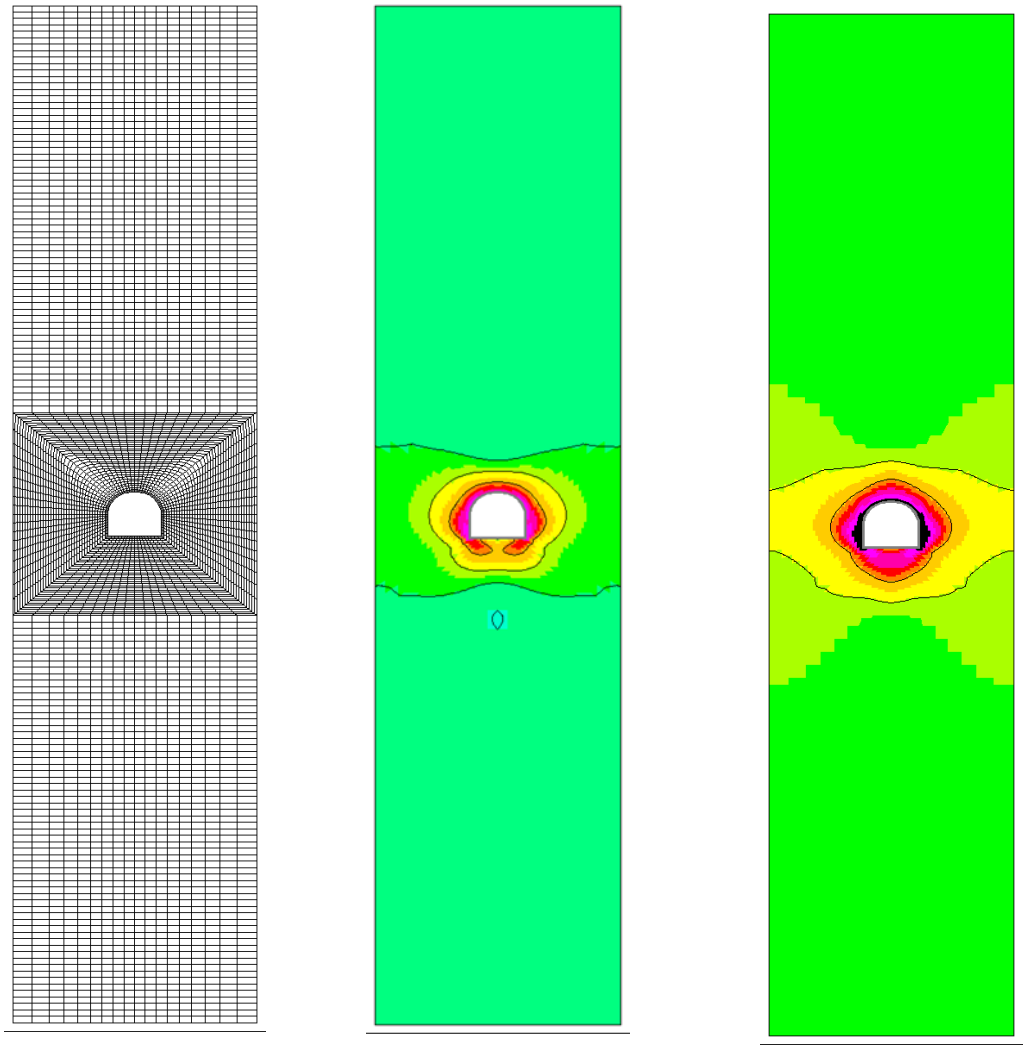

(a) mesh (b) without joints (c) equivalent properties

Figure 23 Arched back crosscut 12 ft (3.6 m) wide in a row of crosscuts, (a) mesh and (b), (c) element safety factors.

**Summary** Computation of equivalent properties of jointed rock using the finite element program UT3PCJ requires a S*tep1j* that follows the usual *Step 1* specifying intact formation properties. *Step1j* requires preparation of a jointed rock properties file that contains joint set and intact rock properties. The program UT3PCJ is used for generating equivalent properties in *Step 1j*. The output file from this step is a file of equivalent jointed rock mass properties EQ.txt. Mesh generation (*Step* 2) may be done using either intact rock properties or equivalent rock properties. Finally *Step* 3, execution, is done for finite element analysis of the problem type selected from the seven choices available using UTPC3. The program UT3PC is used in all problem types, without joints and using equivalent properties (with joints). Mesh plotting can be done after mesh generation and is recommended before program execution. Plotting of element safety factors for design guidance after program execution can be done in the usual manner. Thus, there are four computer programs used for User-friendly Design: (1) mesh generation, (2) computing equivalent properties of jointed rock formations, (3) plotting of meshes and element safety factors, and (4) finite element analysis for safe mine design.

## References - Jointed Rock Models

Hill, R. (1963) Elastic Properties of Reinforced Solids: Some Theoretical Principles. *J Mech Phys Solids*.Vol 11, pp 357-372.

Hudson, J. A. (1980) *The Excitation and Propagation of Elastic Waves*. Cambridge University Press.

Lekhnitiskii (1963) *Theory of Elasticity of an Anisotropic Elastic Body*. Holden-Day, San Francisco, pgs 404.

Pariseau, W. G., M. E. Fowler, J. C. Johnson, M. Poad and E. L. Corp (1984) "Geomechanics of the Carr Fork Mine Test Stope" *Geomechanics Applications in Underground hardrock Mining*, SME/AIME, New York, pp 3-38.

] Pariseau, W. G. (1985) "Research Study on Pillar Design for Vertical Crater Retreat." Final Report. U. S. Bureau of Mines Contract J0215043.

Pariseau, W. G. and H. Moon (1988) "Elastic Moduli of Well-jointed Rock Masses." *Numerical Methods in Geomechanics (Innsbruck,* Balkema, Rotterdam, pp 815-822.

Pariseau, W. G. (1993) "Equivalent Properties of a Jointed Biot Material", *Int'l. J. Rock Mech. Min. Sci. & Geomech. Abstr.,* Vol. 30, No. 7, pp 1151-1157.

Pariseau, W. G. (1995)"Non-representative Volume Element Modeling of Equivalent Jointed Rock Mass Properties". *Proc. Mechanics of Jointed and Faulted Rock – 2.* Balkema, Rotterdam, pp 563-568.

Pariseau, W. G. (1999) "An Equivalent Plasticity Theory for Jointed Rock Masses". *Int'l J. Rock Mech. Mng. Sci.,* Vol. 36, No.7, pp. 907-918.

Pariseau, W. G., D. Tesarik and T. Trancynger, (2012) “Rock Mechanics of the Davis Detector Cavern", SME Annual Meeting, Seattle, Washington, February 19-22, 2012, Preprint CD 12-022 and SME Transactions, Vol. 332, pp 2-20.

Pariseau, W. G. (2017) “Comparison of Underground Coal and Trona Mine Seismicity”. Preprint 17-027, SME Annual Meeting & Exhibit, February 19-22, 2017 Denver, Colorado.

Pariseau, W. G. (2022) “User Manual for a Three-dimensional Finite Element Program UT3PC (2nd edition) A Fundamental Approach to Design of Coal Mine Entries, Barrier Pillars, Bleeder Entries, Interpanel Barrier Pillars, Pillars and Rooms in Room and Pillar Mines, Shafts and Tunnels.” Website UT3PC.net.

Sweeney, P. H., E. D. Harrison, and M. Bradley (1977) Geology of the Magmont Mine, Viburnum Trend, Southeast Missouri, *Economic Geology*, Vol. 72, pp 365-377.

END

## APPENDIX X START TO FINISH

This appendix presents a user-friendly analysis from Step 1 at the start to Step 3 at the finish. Importantly, Step 1j is done in detail. As a reminder:

**Step 1** requires preparation of a material properties file including elastic moduli and strengths of intact rock which are usually obtained from laboratory tests.

**Step 1j** requires preparation of a jointed rock mass properties file in the form of *equivalent* elastic moduli and *equivalent* strengths. This step requires use of the finite element program UT3JPC.

**Step 2** involves mesh generation which is interactive and may be done following Step 1 or Step 1j. Mesh generation after Step1j is preferable. Mesh generation allows for seven problem types. Output includes a mesh plot file, an echo of input data, and a runstream file for finite element analysis.

**Step 3** involves execution of the finite element program UT3PC. Either intact rock properties or equivalent rock properties may be used. Doing both allows for comparisons and evaluation of joint effects on excavation safety. Plotting of element safety factor distributions provides for such comparisons and for evaluating the proposed excavation layout.

**Problem 6** *Shaft Safety* This example of a shaft safety problem concerns a hypothetical elliptical shaft in the Silver Belt of the famous Coeur d’Alene mining district in northern Idaho. Although the shaft geometry is hypothetical, the data are from mine measurements (reference [20] in the User Manual).

*Step 1* begins with the geology of the shaft route above and below the depth of interest. The three major formations present and **intact** rock properties are

NLYRS = 3 *Number of layers in the stratigraphic column*
NSEAM = 2 *Layer number of the stratum of interest*

(1) Vitreous Quartzite

| | | | | | | |
|---|---|---|---|---|---|---|
| 6.1e+06 | 6.1e+06 | 6.1e+06 | 0.26 | 0.26 | 0.26 | *E1 E2 E3 v12 v23 v31* |
| 2.4e+06 | 2.4e+06 | 2.4e+06 | 0.0 | 0.0 | 0.0 | *G12 G23 G31 γ1 γ2 γ3* |
| 24500.0 | 24500.0 | 24500.0 | 2800.0 | 2800.0 | 2800.0 | *C1 C2 C3 T1 T2 T3* |
| 2400.0 | 2400.0 | 2400.0 | | | | *R1 R2 R3* |
| 220.0 | 70.0 | 5800.0 | 180.0 | | | *α δ dpth thick* |

(2)Argillitic Quartzite

| | | | | | |
|---|---|---|---|---|---|
| 4.2e+06 | 4.2e+06 | 1.8e+06 | 0.18 | 0.11 | 0.11 |
| 1.1e+06 | 1.1e+06 | 1.8e+06 | 0.0 | 0.0 | 0.0 |
| 8500.0 | 8500.0 | 12230.0 | 2790.0 | 2790.0 | 1080.0 |
| 2820.0 | 2820.0 | 4400.0 | | | |
| 220.0 | 70.0 | 5980.0 | 40.0 | | |

(3) Sericitic Quartzite

| | | | | | |
|---|---|---|---|---|---|
| 5.5e+06 | 5.5e+06 | 4.0e+06 | 0.21 | 0.20 | 0.20 |
| 1.9e+06 | 1.9e+06 | 2.3e+06 | 0.0 | 0.0 | 0.0 |
| 17470.0 | 17470.0 | 26040.0 | 2330.0 | 2330.0 | 1530.0 |
| 3680.0 | 3680.0 | 3640.0 | | | |
| 220.0 | 70.0 | 6020.0 | 180.0 | | |

The italics are just a reminder of the notation. Details are given in the User Manual. The *E's, v's,* and *G's* are Young's moduli, Poisson ratios, and shear moduli, respectively. The *γ*'s are specific weights. The, *C's, T's* and *R's* are unconfined compressive, tensile and shear strengths, respectively. Elastic moduli and strengths are relative to the *a, b, c* directions of anisotropy which may be inclined to the *x, y, z* finite element axes as explained in detail in the User Manual. Dip direction (azimuth), dip, depth and thickness are *α, δ, dpth, and thick*, respectively.

*Step 1j* An assumed joint set is shown in Figure 1. This assumption is made for illustrating the role of joints in finite element analysis of shaft safety.

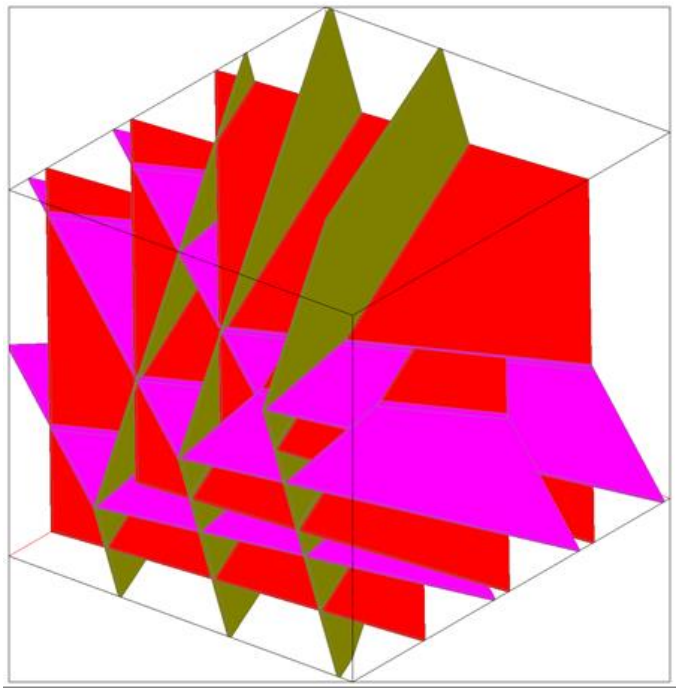

Figure 1 Schematic of assumed joint sets. Bedding planes are steeply dipping and dark colored. This cube is much larger than maximum joint spacing for illustrative purpose.

The runstream for computing equivalent properties using UT3JPC is

```
Elliptical Shaft w/ jts 11/11/2022 wgp
CMS1.txt
celms.txt
ccrds.txt
none
none
cnsps.txt
aCM1
nelem =       1
nnode =       8
nspec =       8
nmat  =       4
ncut  =       1
ninc  =       1
nsigo =       0
inter =     100
maxit =    1000
nyeld =       2
nelcf =       0
ncave =       0
```

nfile =  1
npsi  =  1
nrstrt=  0
 error=  1.0000
 orf  =  1.8600
 xfac =  12.0000
 yfac =  12.0000
 zfac =  12.0000
 efac =  1.0000
 cfac =  100.0
Elliptical Shaft w/ jts 11/11/2022
CMS2.txt
celms.txt
ccrds.txt
none
none
cnsps.txt
aCM2
nelem =  1
nnode =  8
nspec =  8
nmat  =  4
ncut  =  1
ninc  =  1
nsigo =  0
inter =  100
maxit =  1000
nyeld =  2
nelcf =  0
ncave =  0
nfile =  2
npsi  =  1
nrstrt=  0
 error=  1.0000
 orf  =  1.8600
 xfac =  12.0000
 yfac =  12.0000
 zfac =  12.0000
 efac =  1.0000
 cfac =  100.0
Elliptical Shaft w/ jts 11/11/2022
CMS3.txt
celms.txt
ccrds.txt
none
none

cnsps.txt
aCM3
nelem =  1
nnode =  8
nspec =  8
nmat  =  4B
ncut  =  1
ninc  =  1
nsigo =  0
inter =  100
maxit =  1000
nyeld =  2
nelcf =  0
ncave =  0
nfile =  3
npsi  =  1
nrstrt=  0
 error=  1.0000
 orf  =  1.8600
 xfac =  12.0000
 yfac =  12.0000
 zfac =  12.0000
 efac =  1.0000
 cfac =  100.0
RUN END

where CMS1 is

(1) joint S70W 0.1 thik N=2
  4.2e+04  4.2e+04  1.8e+04  0.18  0.11  0.11
  1.1e+04  1.1e+04  1.8e+04  0.0  0.0  0.0
   850.0  850.0  1223.0  279.0  279.0  108.0
   282.0  282.0  210.0
        350.0  65.0  0.5  -0.10
 (2) joint  N=2
  4.2e+04  4.2e+04  1.8e+04  0.18  0.11  0.11
  1.1e+04  1.1e+04  1.8e+04  0.0  0.0  0.0
   850.0  850.0  1223.0  279.0  279.0  108.0
   282.0  282.0  210.0
   355.0  89.0  0.5  -0.10
 (3) joint bedding plane N=2
  4.2e+04  4.2e+04  1.8e+04  0.18  0.11  0.11
  1.1e+04  1.1e+04  1.8e+04  0.0  0.0  0.0
   850.0  850.0  1223.0  279.0  279.0  108.0
   282.0  282.0  210.0
   220.0  70.0  1.0  -0.10

(1) Vitreous Quartzite N50W 70SW
6.1e+06 6.1e+06 6.1e+06 0.26 0.26 0.26
2.4e+06 2.4e+06 2.4e+06 0.0 0.0 0.0
24500.0 24500.0 24500.0 2800.0 2800.0 2800.0
2400.0 2400.0 2400.0
220.0 70.0 5700.0 280.0

and similarly for CMS2 (Argillitic Quartzite) and CMS3 (Sericitic Quartzite).

Note that the maximum joint spacing is 1 ft in the bedding plane joint set. This requires editing the coordinate file "ccrds.txt". Thus, after editing

crds file
1 0.000 0.0000 0.0000 2 1.0000 0.0000 0.0000
3 3.000 1.000 0.0000 4 0.000 1.0000 0.000
5 0.000 0.0000 1.0000 6 1.0000 0.0000 1.0000
7 1.0000 1.0000 1.0000 8 0.000 1.0000 1.0000

where the corners of the cube (nodes 1,…,8) are 1 ft apart, the maximum joint spacing.

The equivalent properties of the jointed rock mass appear in an output file **EQ.txt** of UT3JPC. Thus,

NLYRS = 3
NSEAM = 2
(1) Vitreous Quartzite N50W 70SW
0.295E+06 0.600E+05 0.355E+06 0.10 0.00 0.19
0.470E+05 0.166E+06 0.332E+05 0.00 0.00 0.00
5386.8 2429.5 5910.0 615.6 277.7 675.4
1051.4 474.2 1153.5
220.0 70.0 5700.0 280.0
(2) Argillitic Quartzite
0.278E+06 0.596E+05 0.301E+06 0.11 0.00 0.17
0.464E+05 0.156E+06 0.330E+05 0.00 0.00 0.00
2186.8 1012.6 5002.0 717.8 332.4 441.7
723.3 334.9 858.2
220.0 70.0 5980.0 40.0
(3) Sericitic Quartzite
0.291E+06 0.599E+05 0.341E+06 0.10 0.00 0.19
0.469E+05 0.164E+06 0.331E+05 0.00 0.00 0.00
4015.7 1823.1 7608.1 535.6 243.1 447.0
846.7 384.4 1064.7
220.0 70.0 6020.0 280.0

Jointing clearly induces directional properties (anisotropy) of elastic moduli and strengths as seen in this file. No specific weights are specified because the stress state is specified directly during mesh generation as *additional stresses* to gravity stress.

The **EQ.txt** file is easily saved under a more easily identified name, for instance, EQellipse.txt, in the present example. Saving this file within the mesh generator project (GMB3) is a convenient location and makes the next step quite easy.

There is a second output file from UT3JPC and that is CS.txt. This consists of elastic moduli and compliances and the product of the two which should be the identity matrix (6x6), thus providing a check on the computation of equivalent properties. No further use is made of this file.

*Step 2* Mesh generation is the next step. A sequential progression is to follow Step 1j. The InData file that echoes the input is

```
SHAFT NPROB 6
 Shaft Shape = Ellipse (including circle)
 Shaft System = Single Opening
 Shaft Width =      11.0
 Width/Height Ratio =       0.5
 Opening Height=      22.0
 Section Depth Seam Center (ft)   =    6000.0
 Additional Sxx,Syy,Szz,Tyz,Tzx,Txy, tension +=
   -7571.0   -8441.0   -6688.0       0.0       0.0     927.0
 Shaft Stress Sxx,Syy,Szz,Tyz,Tzx,Txy, tension +=
   -7571.0   -8441.0   -6688.0       0.0       0.0     927.0
```

The PlotMesh and PlotSfac files from mesh generation are

```
PlotShaft
NPROB =       6
NLYRS =       3
NSEAM =       2
Nelem =   36384
belms
Nnode =   73728
bcrds
none
Nelcf=     208
brcte
AMSH
```

and

```
PlotShaft
```

```
NPROB =       6
NLYRS =       3
NSEAM =       2
Nelem =   36384
belms
Nnode =   73728
bcrds
FEMfac.txt
Nelcf=     208
brcte
ASF
```

Both require minor editing before plotting.  The runstream output file from mesh generation is

```
runstream title
eqellipse.txt
belms
bcrds
brcte
bsigi
bnsps
bp1
nelem =   36384
nnode =   73728
nspec =   73728
nmat  =       3
ncut  =      -1
ninc  =       5
nsigo =       1
inter =     100
maxit =    1000
nyeld =       2
nelcf =     208
nsol  =       2
nprb  =       6
mgob  =       0
 error=    1.0000
 orf  =    1.8600
 xfac =   12.0000
 yfac =   12.0000
 zfac =   12.0000
 efac =    1.0000
 cfac =    1.0000
torl% =    0.0100
ENDRUN
```

which also requires minor editing before running. The editing required depends largely on the user's platform, of course.

Completion of *Step1* and *Step 1j* allows for mesh generation. The mesh for the shaft is shown in Figure 2 in plan view.

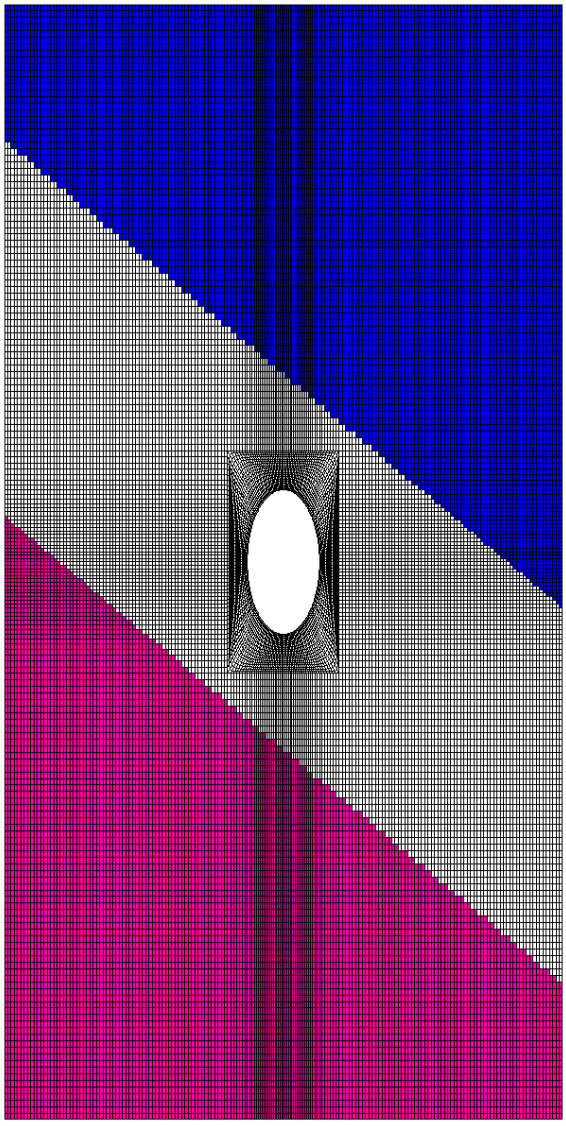

Figure 2 Mesh for an elliptical shaft 11x22 ft (3.3x6.6 m). Inclination of the three formations present is evident in the figure.

An element safety factor distribution in this example using equivalent properties is shown in Figure 3A where the long axis of the ellipse is parallel to the greatest compression in the plane of the shaft section. In Figure 3B, the long axis is perpendicular to the greatest compression. There is little difference between the two orientations with respect to element safety factor

distributions. Both indicate a redesign is needed. Additional trial designs are readily done with the convenience of the software used.

One redesign option is a circular shaft. If the diameter is 15.56 ft, then the area is equal to the area of either elliptical shaft. Figure 4 shows the safety factor distribution in case of a circular shaft.

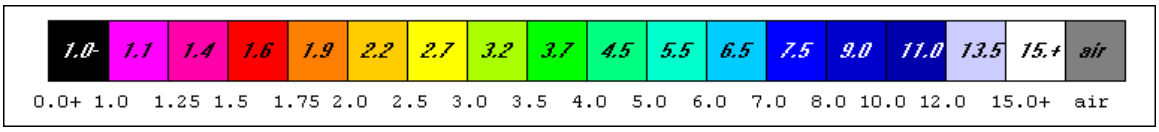


Element Safety Factor Color Scale

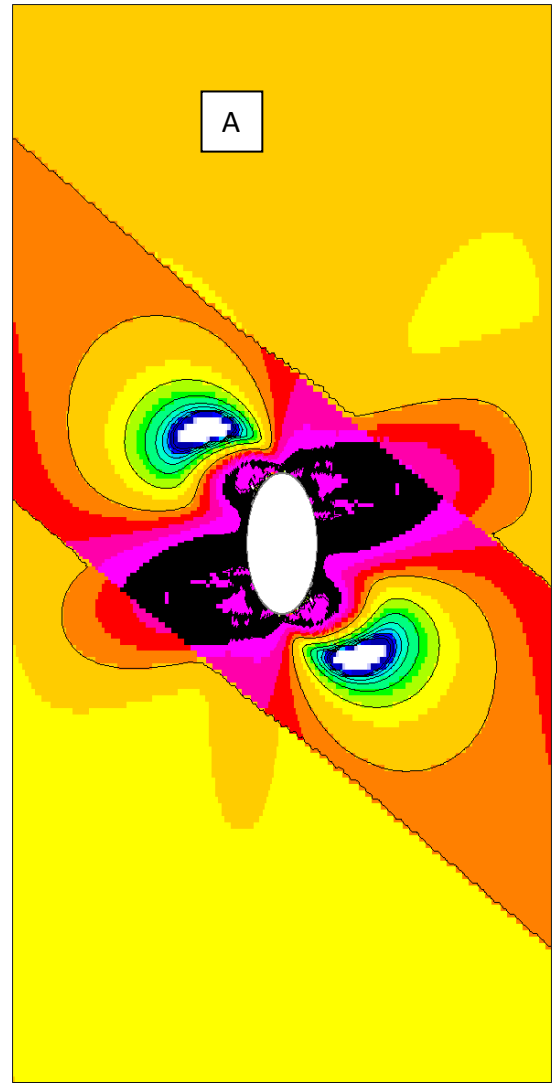

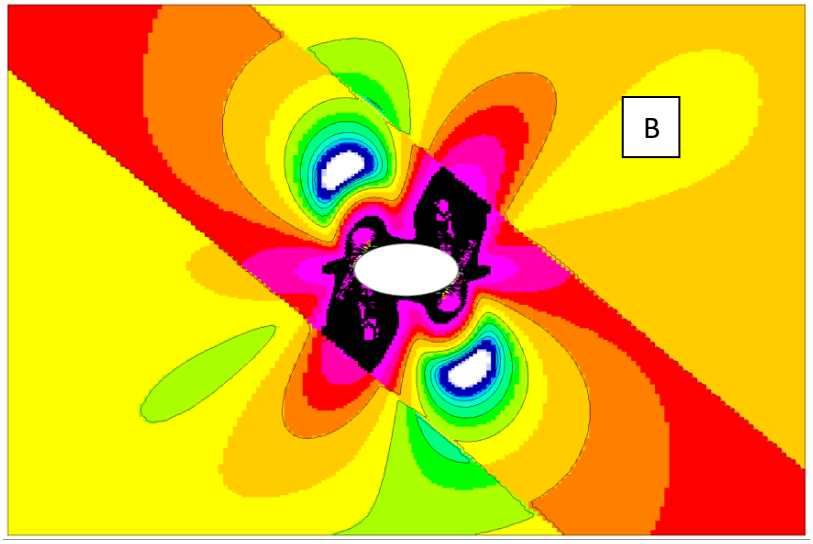


Figure 3 Element safety factor distribution in the case of an elliptical shaft: A=long axis parallel to the largest compression, B=long axis perpendicular to the largest compression.

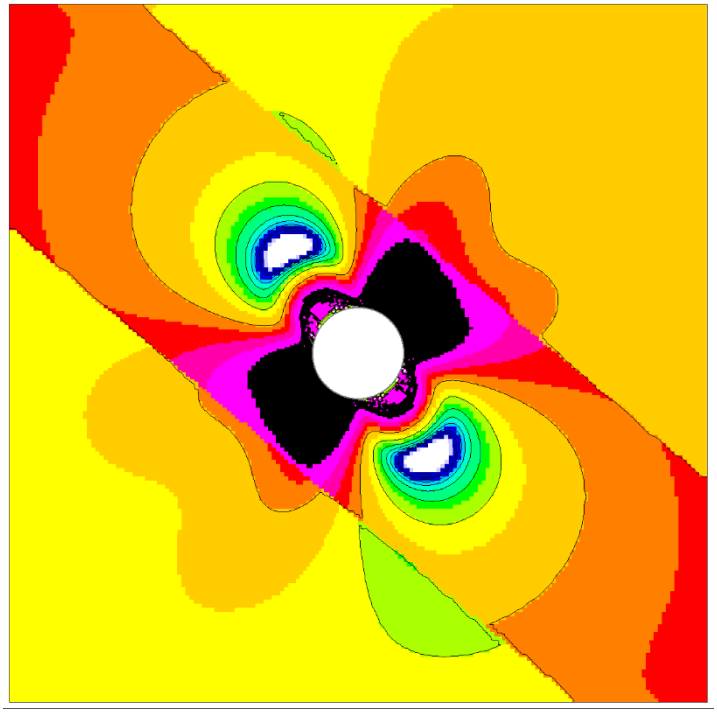

Figure 4 Element safety factor distribution in the case of a circular shaft with the same area as the two elliptical shafts.

The distribution of element failures in case of a circular shaft is not very different from distribution of element failures about the elliptical shafts. However, a circular shaft has a practical advantage in sinking and lining and perhaps would be the design choice. Of course,

further numerical design trials could be done, say, with different orientations of an elliptical section, perhaps with different ratios of semi-axes.

Figure 5 shows the distribution of element safety factors about the same circular shaft but without joints. A comparison with the case with joints in Figure 4 shows quite clearly that joints matter. Support and reinforcement of the jointed rock mass to increase "strength' is certainly needed.

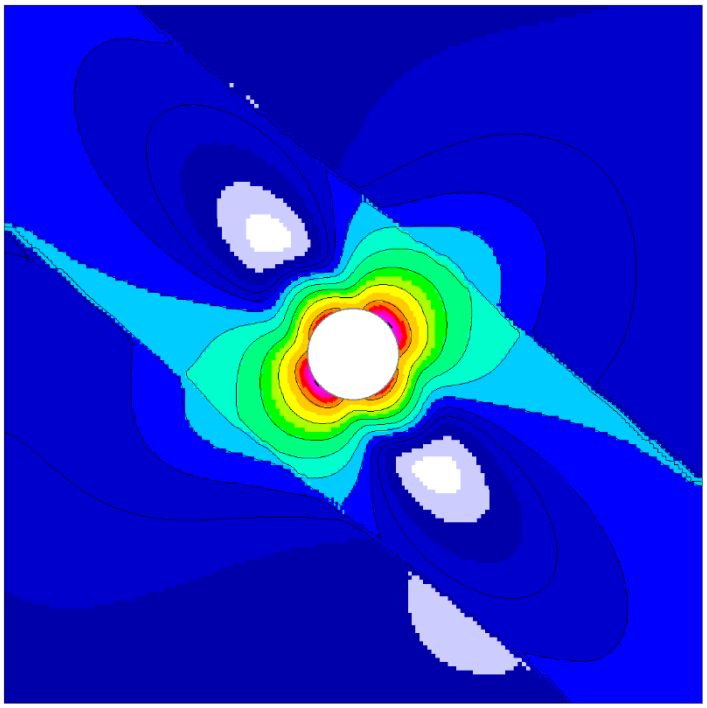

Figure 5 Element safety factor distribution in the case of a circular shaft with no joints, but with the same area as the two elliptical shafts.

This completes the example illustrating some details of the steps and intermediate editing of files needed from start to finish of an important example of the seven available problem types in underground mine design.

END